DIABLO CANYON
LONG TERM SEISMIC PROGRAM

PACIFIC GAS AND ELECTRIC COMPANY
Diablo Canyon Power Plant
Docket Nos. 50-275 and 50-323

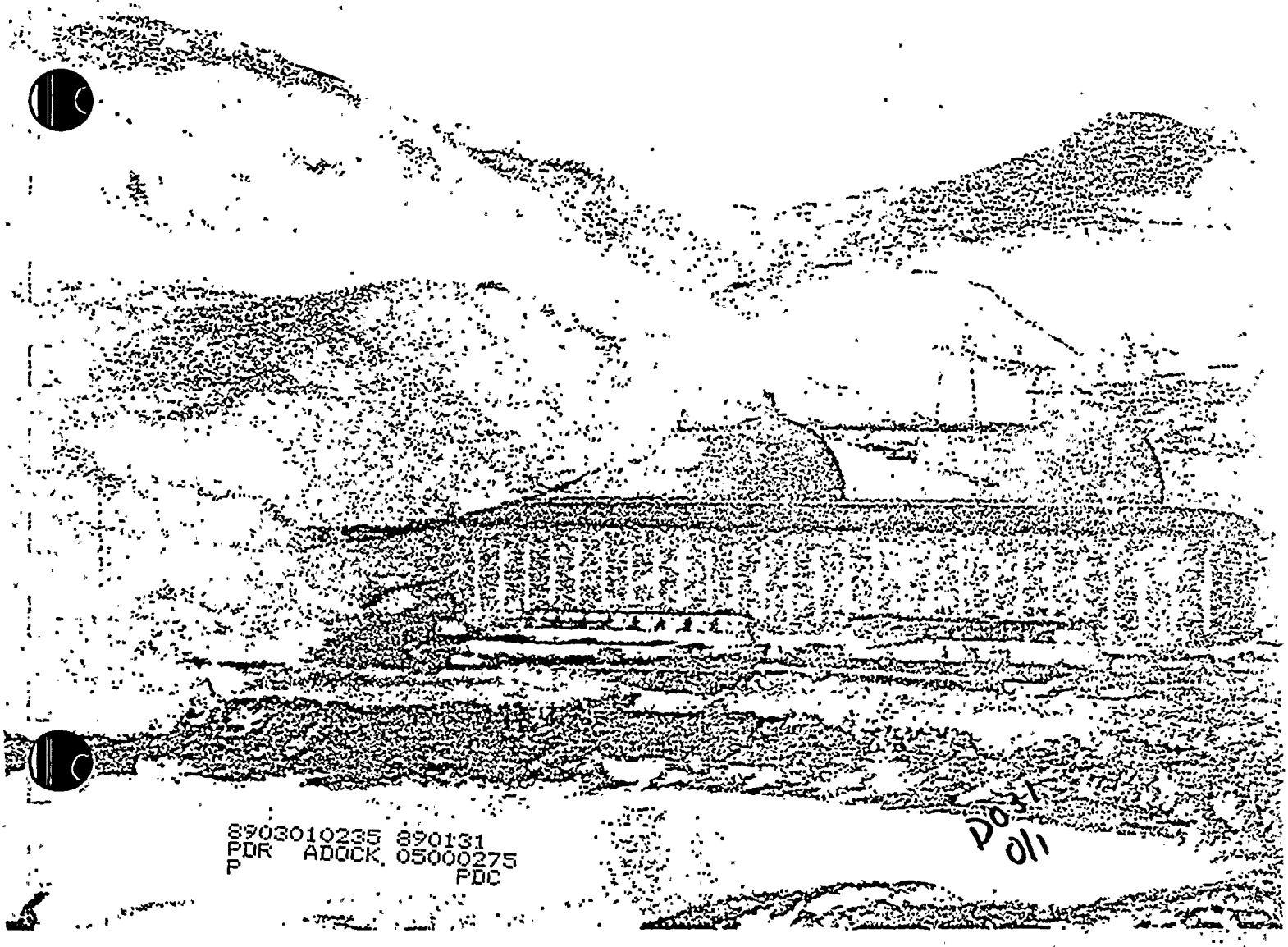

D031
011

RESPONSE TO QUESTION 1

January 1989

This volume is part of a set that responds to 47 questions asked of PG&E by the Nuclear Regulatory Commission (NRC) on December 13, 1988. The responses provide data requested to augment or clarify the Final Report of the Long Term Seismic Program submitted by PG&E to the NRC on July 31, 1988.

RESPONSE TO QUESTION 1a

QUESTION 1a

Provide the following deterministic comparisons of vertical ground motion estimates for Diablo Canyon and evaluate the significance of any differences:

a. The Hosgri 0.75 g Newmark response spectra with the LTSP 84% free field response spectra.

The 1977 Hosgri evaluation of the Diablo Canyon structures and components was performed using both Blume and Newmark ground response spectra anchored to a peak ground acceleration of 0.75 g for the horizontal response analysis. The response analysis in the vertical direction was done using a vertical spectrum resulting from scaling the Newmark horizontal spectrum by two-thirds. This provided a peak ground acceleration of 0.5 g for the 1977 Hosgri vertical ground response spectrum.

In the Long Term Seismic Program ground motion study, the frequency-dependent ratio of vertical to horizontal components of ground motion was developed by statistical analyses. This relationship was used to estimate the vertical component response spectrum from the results developed by regression of the horizontal spectrum. The resulting 84th percentile probability of nonexceedance vertical spectrum is shown in Figure Q1a-1. This is the same spectrum shown on Figure 4-23 of the Final Report.

The 1977 Hosgri evaluation vertical spectrum also is shown on Figure Q1a-1. As may be seen, the LTSP 84th percentile spectrum exceeds the Hosgri evaluation spectrum for frequencies greater than about 5.5 Hz. The LTSP 84th percentile motions were propagated through the structures and are depicted in the resulting floor response spectra. The exceedances have been considered in developing the fragility estimates of Plant structures and components as described in response to Question 1e. The fragility values are shown in Tables 6-23 and 6-24 of the Final Report.

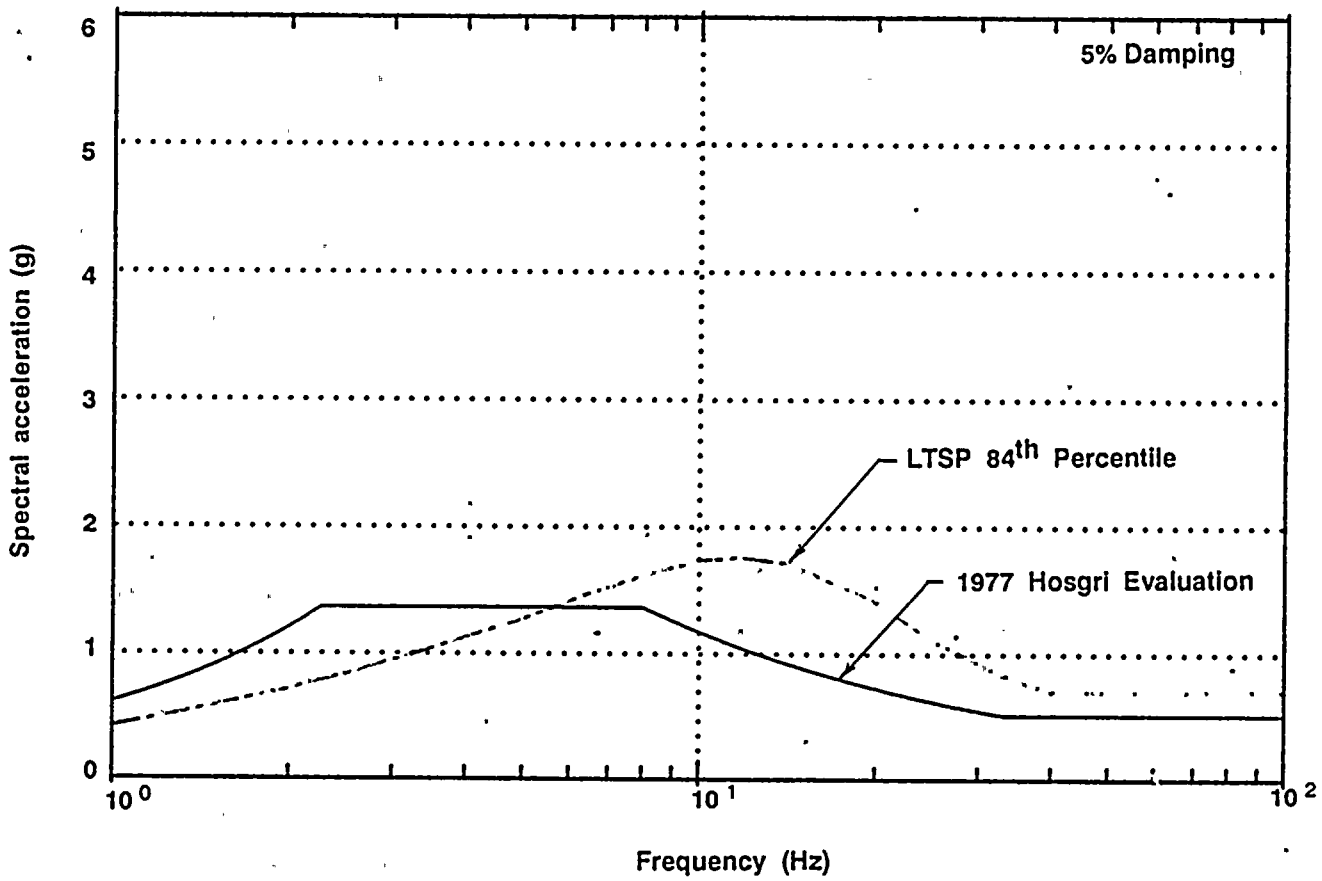

Figure Q1a-1

Comparison of the Long Term Seismic Program site-specific 84th percentile vertical response spectrum with the 1977 Hosgri evaluation response spectrum.

RESPONSE TO QUESTION 1b

QUESTION 1b

Provide the following deterministic comparisons of vertical ground motion estimates for Diablo Canyon and evaluate the significance of any differences:

b. The LTSP 84% free field response spectra with the LTSP basemat motions resulting from the soil-structure interaction analysis of the 84% free field ground motions.

In the Long Term Seismic Program, no soil/structure interaction analyses were performed in the vertical direction. Instead, the dynamic amplification factors of Plant structures in the vertical direction, as obtained from the fixed-base structural models in the Hosgri evaluation, were used. This was considered to be conservative, because the effect of soil/structure interaction would provide certain reductions in plant response due to radiation damping and spatial incoherency. Also, there would be little change, if any, in the soil/structure interaction frequency, because of the rock foundation. In the absence of any soil/structure interaction effect, the vertical motions at the basemats of the various structures were identical, and also the same as the free-field ground motions. The 5 percent damped spectrum for the vertical motions at both locations is shown in Figure Q1b-1.

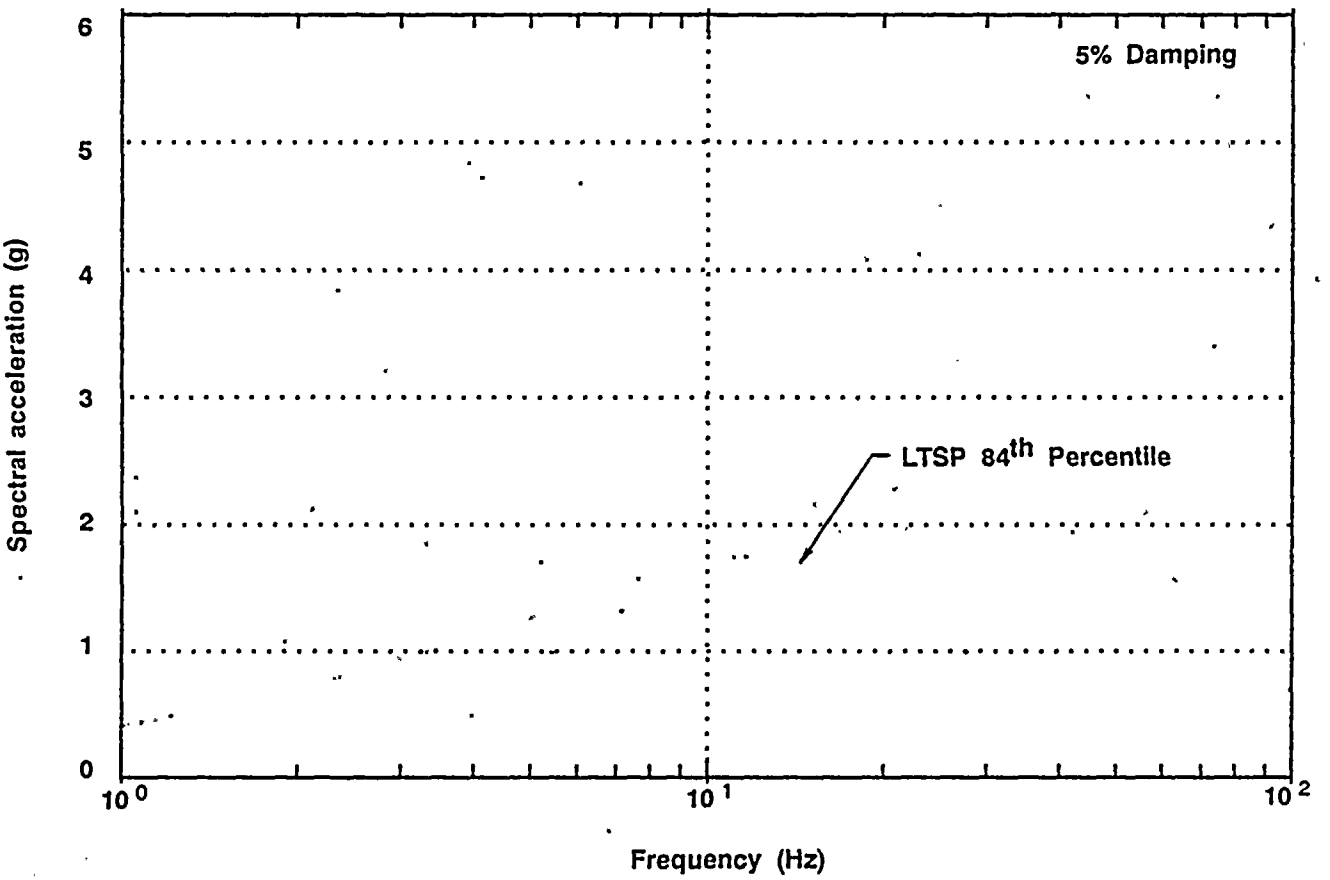

Figure 1b-1

Long Term Seismic Program vertical response spectrum both in the free-field and at the top of the basemats of the structures.

RESPONSE TO QUESTION 1c

QUESTION 1c

Provide the following deterministic comparisons of vertical ground motion estimates for Diablo Canyon and evaluate the significance of any differences:

c. *The LTSP 84% free field response spectra with the 84% free field response spectra modified for justified spatial incoherency.*

The spatial incoherence functions for ground motions developed in the ground motion study included the incoherency effects in both the horizontal and the vertical directions. However, because no Plant-specific vertical soil/structure interaction analyses were performed, the reduction in plant responses due to the effect of the vertical incoherency of ground motions was conservatively neglected. The vertical motions at the top of the basemats of various structures, therefore, remained unchanged from the free-field vertical ground motions.

RESPONSE TO QUESTION 1d

QUESTION 1d

Provide the following deterministic comparisons of vertical ground motion estimates for Diablo Canyon and evaluate the significance of any differences:

d. The Hosgri "Tau" reduced Newmark response spectra for different structures with the corresponding LTSP 84% free field response spectra modified by the soil-structure interaction analysis and justified incoherency effects.

During the 1977 Hosgri evaluation, the horizontal input motions for the various structures were derived by reducing the 0.75 g peak ground acceleration free-field ground motions by filtering factors, which were functions of the foundation dimensions of the respective structures. These factors were called "Tau" reduction factors. No such reductions were done for the vertical direction. The vertical input motion to the various structures, therefore, remained the same as the free-field motion anchored at 0.50 g peak ground acceleration.

RESPONSE TO QUESTION 1e

QUESTION 1e

Provide the following deterministic comparisons of vertical ground motion estimates for Diablo Canyon and evaluate the significance of any differences:

e. Hosgri reanalysis floor response spectra and other structural response parameters with corresponding parameters developed by the LTSP using 84% free field ground motions, soil-structure interaction analysis, justified spatial incoherency, and consistent structural parameters.

The only structural response parameter in the vertical direction that was considered to be significant to the studies was the vertical floor response spectrum developed for the evaluation of equipment in the applicable structures. As discussed on page 6-27 of the Final Report, the vertical floor spectra were established by scaling the Hosgri reevaluation vertical spectra using the spectral ratio method. The method is described below.

The vertical floor spectra were established by multiplying the unsmoothed and unbroadened 1977 Hosgri evaluation vertical spectral accelerations at the floor location of interest by the ratio of the 5 percent damped vertical ground spectrum (LTSP 84th percentile) to the 5 percent damped 1977 Hosgri evaluation vertical ground spectrum at different frequencies. For the vast majority of cases, the flexible floor slabs had single-mode responses and fundamental frequencies in the 25 to 30 Hz range (for example, the auxiliary building at elevation 140 feet, shown in Figure Q1e-1). Thus, for components having vertical fundamental frequencies less than the floor slab frequency, the ratio of the 84th percentile spectra to the 1977 Hosgri vertical spectra was evaluated at the component frequency; for components having vertical fundamental frequencies equal to or greater than the floor slab frequency, the ratio of the spectra was evaluated at the floor slab fundamental frequency. For a few cases (for example, the turbine building at elevation 119 feet, shown in Figure Q1e-2), the flexible floor slab has multiple-mode responses and relatively low fundamental frequencies, in the 7 to 8 Hz range. In these instances, for components having vertical frequencies equal to or greater than the floor slab fundamental frequency, the ratio of the 84th percentile spectra to the 1977 Hosgri vertical spectra was evaluated at the floor slab fundamental frequency and then increased to account for the effect of the higher frequency modes, as explained in the report by Kipp and others (1988).

The above factoring method was applied to generate vertical floor response spectra at the same locations in the structures as for the case of the horizontal floor response spectra described in Chapter 7 of the Final Report. These are shown in Figures Q1e-1 through Q1e-5. As can be seen in Figure Q1a-1, the 84th percentile spectrum possesses considerable enrichment in the high frequency range. Because most of the floors have their resonance frequencies in this range, the corresponding floor response spectra show a higher amplitude of spectral acceleration than the 1977 Hosgri vertical floor spectra. The 84th percentile floor response spectra, thus developed, have been used for the fragility evaluation of the essential Plant components. The process is explained fully, with actual examples demonstrating the inclusion of the vertical response, in Kipp and others (1988), Appendix D which follows as Attachment Q1e-1. This reference also provides a description of analyses made to validate the spectrum-factoring approach used for developing the in-structure vertical spectra. No allowance was made for either the soil/structure interaction or spatial incoherency effects in these evaluations.

References

Kipp, T. R., Wesley, D. A., Nakaki, D. K., 1988, Seismic fragilities of civil structures and equipment components at the Diablo Canyon Power Plant: NTS Engineering Report No. 1643-02.

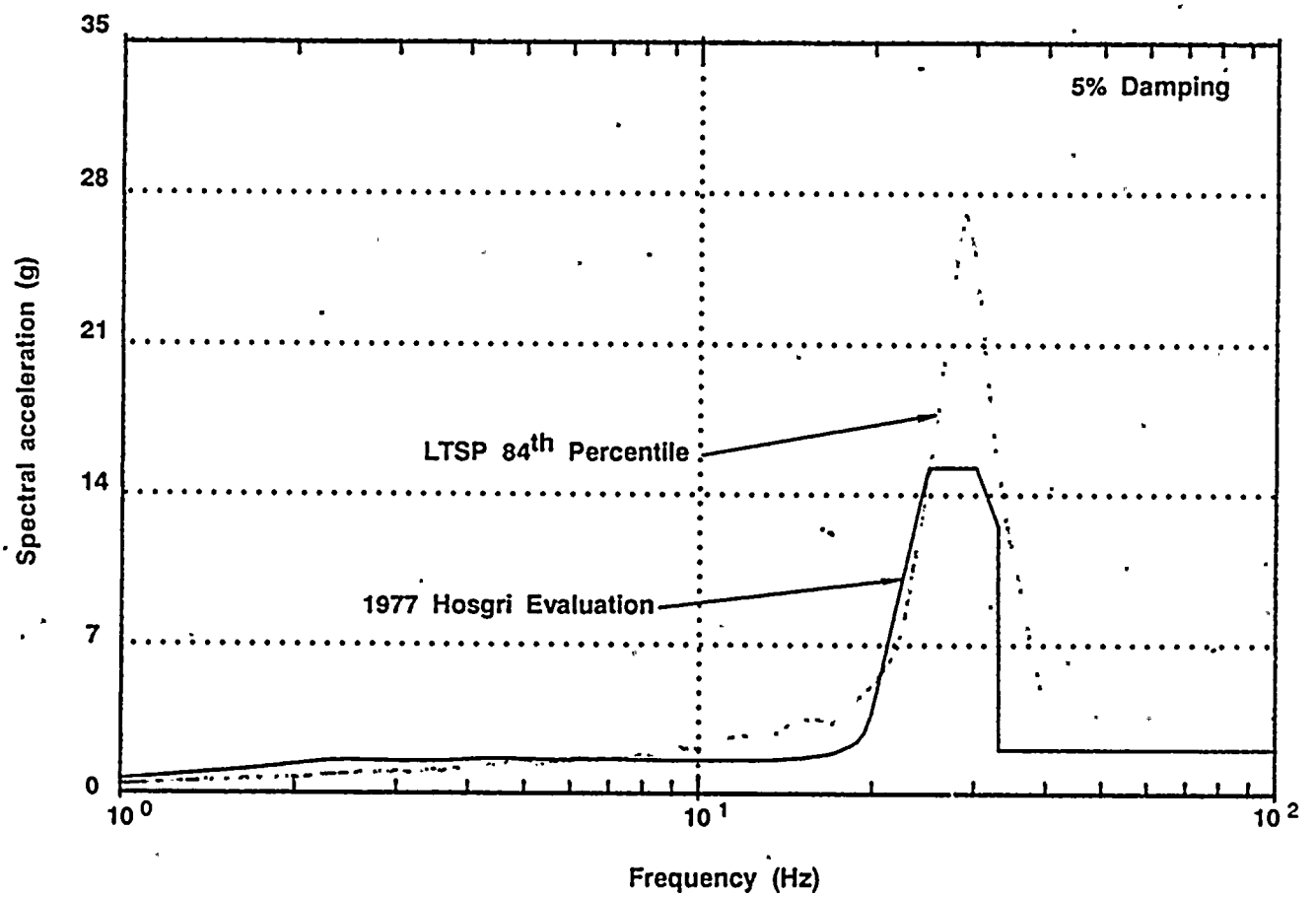

Figure Q1e-1

Comparison of vertical floor response spectra for the auxiliary building, elevation 140 feet, core west, flexible slab.

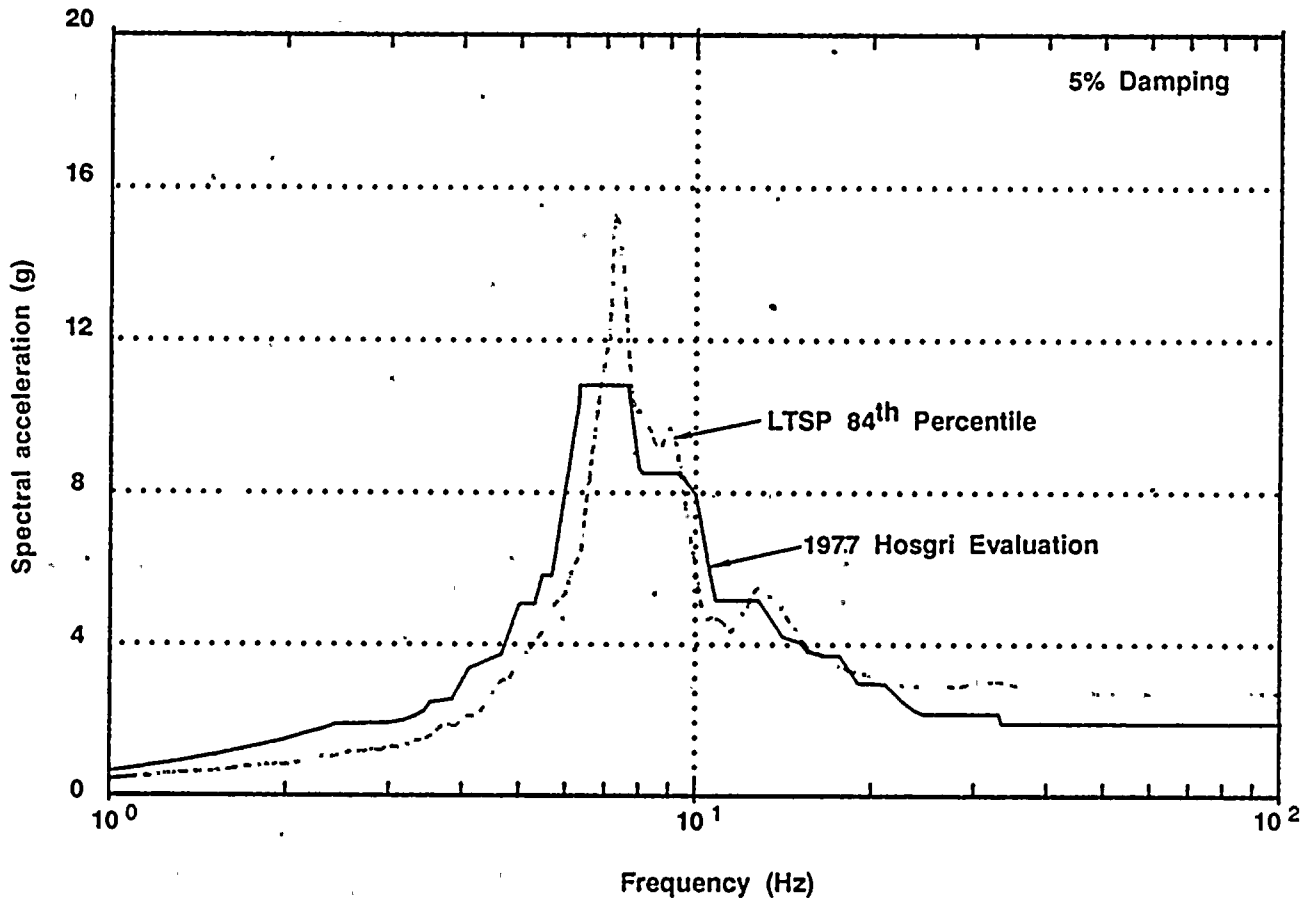

Figure Q1e-2

Comparison of vertical floor response spectra for the turbine building, elevation 119 feet, switchgear area.

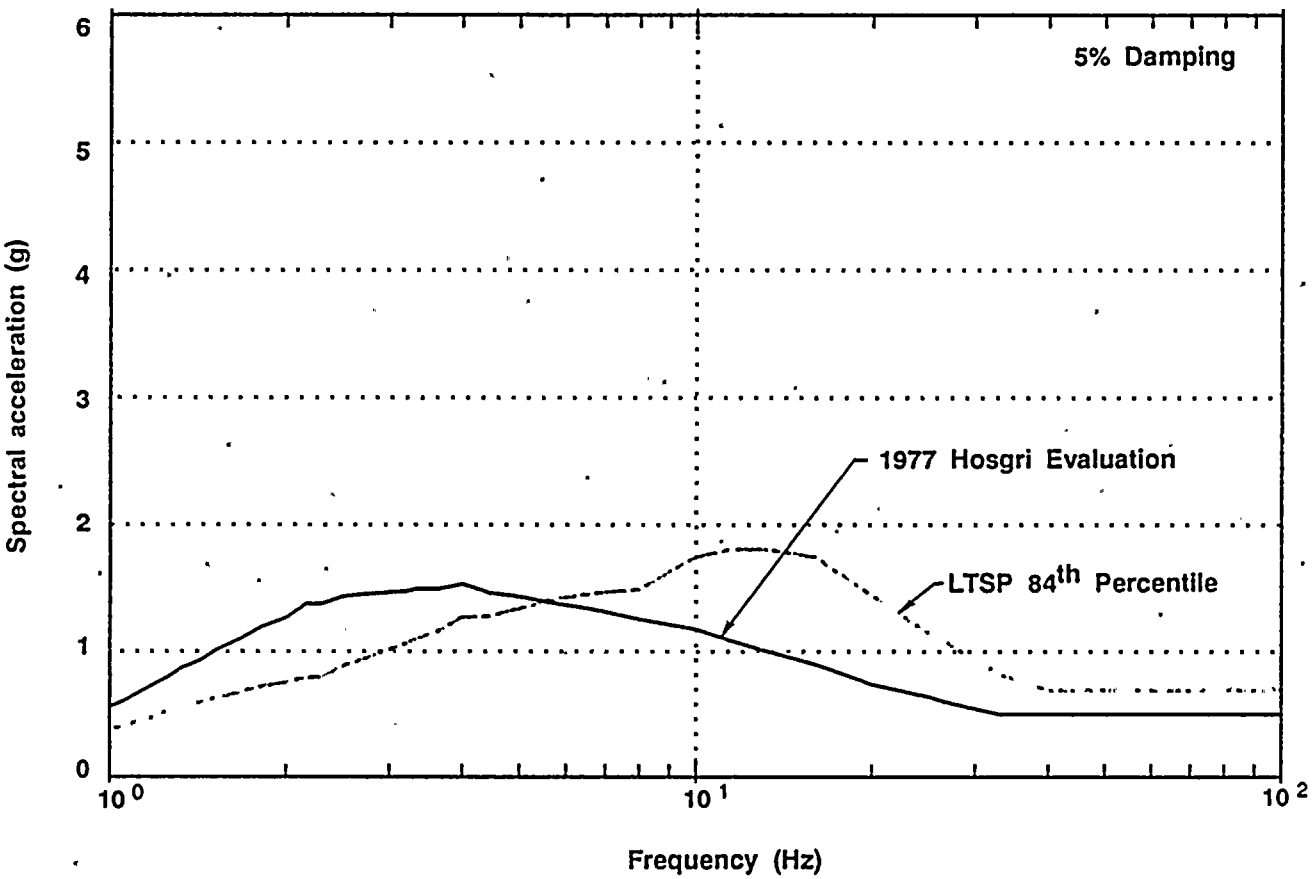

Figure Q1e-3

Comparison of vertical floor response spectra for the containment building, interior structure, elevation 140 feet.

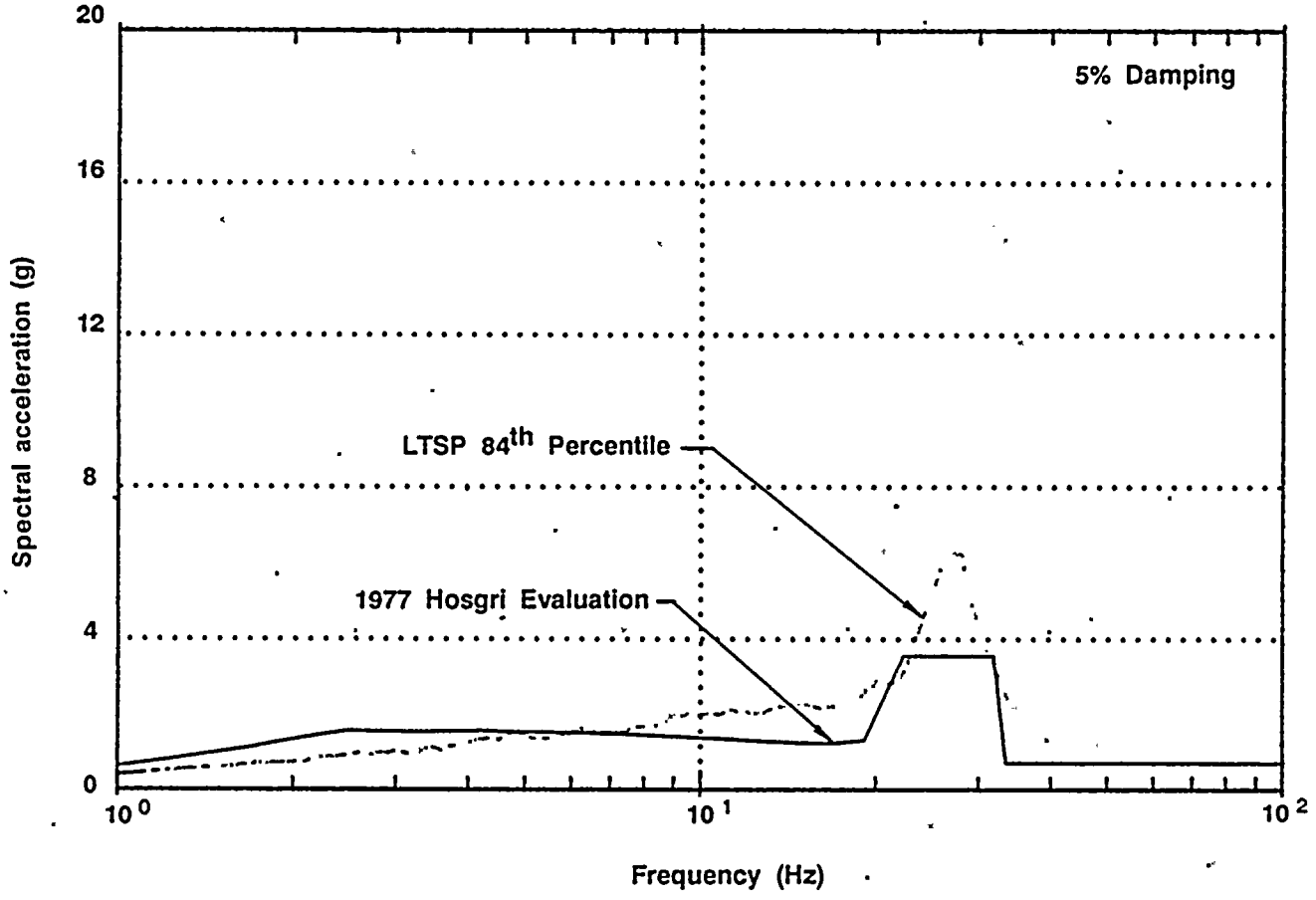

Figure Q1e-4

Comparison of vertical floor response spectra for the auxiliary building, elevation 100 feet, core west, flexible slab.

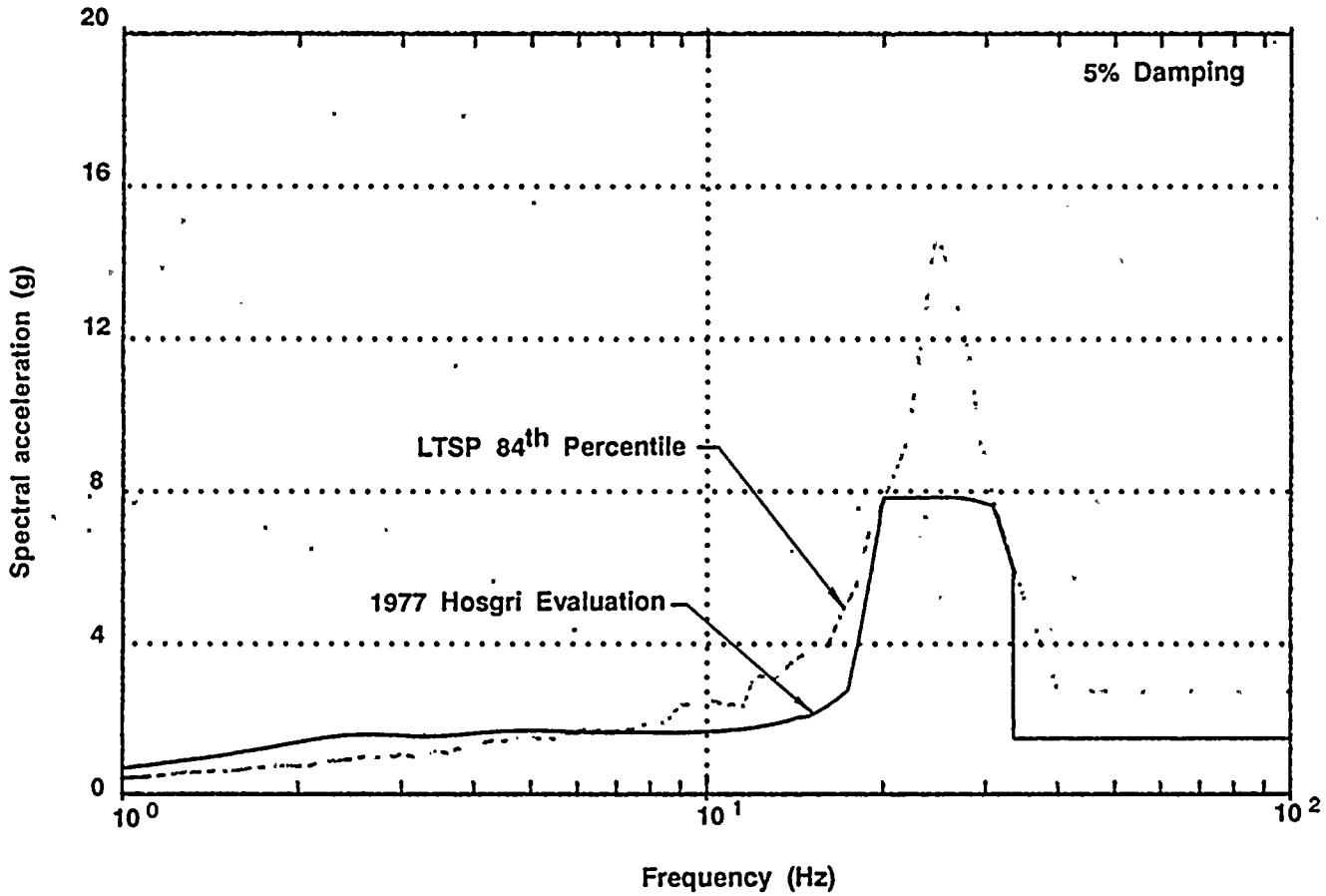

Figure Q1e-5

Comparison of vertical floor response spectra for the auxiliary building, elevation 115 feet, core west, flexible slab.

APPENDIX D

DEVELOPMENT OF VERTICAL FLOOR ACCELERATION INPUT FOR THE FRAGILITY EVALUATION OF DIABLO CANYON SAFETY RELATED EQUIPMENT

For virtually all previous Seismic Probabilistic Risk Assessments (SPRAs) of nuclear power facilities, design basis floor spectra were used to establish the equipment capacity and equipment response factors of safety. Structural response factors of safety were then estimated to account for conservatism or unconservatism in the generation of the design floor spectra. In contrast, for the Diablo Canyon SPRA, median-centered site-specific reference horizontal and vertical floor spectra were developed for use in the fragility evaluation of the important safety related equipment components. This report presents a discussion of the development of the reference floor response spectra with emphasis on the development of the vertical floor spectra and their use in the fragility evaluation. Three examples are also presented to illustrate the incorporation of the reference vertical response into the fragility capacity calculation. It must be understood that this Appendix only deals with the issue of the development and use of the increased median-centered reference vertical spectra in the Diablo Canyon SPRA fragility evaluation. All other details related to the fragility evaluation are addressed in the body of this report and Reference D-1.

Reference Ground Spectra

The important Diablo Canyon civil structures are founded on competent bedrock. The seismic Category I structures and most essential equipment within the structures were designed for the Double Design Earthquake (DDE) having a free-field horizontal ground response spectrum anchored to 0.40g. For the Hosgri reevaluation, both Blume and Newmark type horizontal ground response spectra anchored to 0.75g were used for the horizontal response analysis combined with structure dependent foundation filtering coefficients which reduced the effective horizontal base slab input. Newmark spectra anchored to 0.50g were used for the Hosgri vertical response analysis. In contrast to the horizontal direction, no foundation filtering was applied in the vertical direction such that the effective vertical acceleration remained at 0.50g. The Hosgri reevaluation vertical ground response spectra are shown in Figure D-1.

As part of the Diablo Canyon Long Term Seismic Program (LTSP) ground motion studies, site-specific median horizontal and vertical ground response spectra were developed. These spectra, shown in Figure D-2 for 5% damping, define the median spectral shape for the two earthquake components and depict the relative amplitude between the horizontal and vertical components on a frequency-by-frequency basis. It can be seen that the vertical ground acceleration component exceeds the horizontal component for frequencies between about 10 and 30 Hz.

As part of the effort in support of the Auxiliary Building Variability Study, documented in Appendix B of this report and also in Reference D-2, the 5% damped free-field horizontal ground response spectra shown in Figures D-3 and D-4 were developed. The variability study reference horizontal ground spectra were developed from an ensemble of 38 empirical and numerical time-history pairs, specifically assembled for the study as explained in Reference D-2. The time histories were scaled to an average spectral acceleration of 2.0g when averaged over the 4.8 to 14.7 Hz range. These scaled reference spectra formed the basis for the estimated Diablo Canyon civil structure fragilities.

The 5% damped vertical ground response spectrum, corresponding to the variability study scaled horizontal ground response spectra, was used as the vertical ground motion input for the structure and equipment fragility evaluations. This spectrum, was developed by scaling the average of the two variability study horizontal spectra (Figures D-3 and D-4) by the ratio of the site-specific vertical to horizontal median ground spectra amplitudes at various frequencies (Figure D-2). The resulting reference 5% damped vertical spectrum is compared with the corresponding Hosgri reevaluation vertical spectrum in Figure D-5.

Reference Floor Spectra

As noted in Reference D-2, median-centered reference horizontal floor spectra were generated for selected floors of the important Diablo Canyon civil structures corresponding to the location of important safety-related equipment. These were developed using median soil-structure interaction and building structural parameters.

Median-centered reference vertical floor spectra were not similarly generated. Reference vertical floor response was established by multiplying the unsmoothed and unbroadened Hosgri reevaluation vertical spectral acceleration at the floor location of interest by the ratio of the 5% damped reference vertical ground spectrum developed from the LTSP Variability Study horizontal ground spectrum to the 5% damped Hosgri reevaluation vertical ground spectrum (Figure D-5) over the appropriate frequency range. For the vast majority of cases, the flexible floor slabs exhibited single mode response with fundamental frequencies in the 25 to 30 Hz range (e.g., Auxiliary Building, El 100 feet, shown in Figure D-6). Thus, for components with vertical fundamental frequencies less than the floor slab frequency, the ratio of the reference to Hosgri vertical spectra was evaluated at the component frequency while for components with vertical fundamental frequencies equal to or greater than the floor slab frequency, the ratio of the spectra was evaluated at the floor slab fundamental frequency. For a few cases (e.g., Turbine

Building, El 119 feet, shown in Figure D-7), the flexible floor slab exhibits multiple mode response with relatively low fundamental frequencies in the 7 to 8 Hz range. In these instances, for components with vertical frequencies equal to or greater than the floor slab fundamental frequency, the ratio of the reference to Hosgri vertical spectra was evaluated at the floor slab fundamental frequency and then increased to account for the effect of the higher frequency modes. Illustrations of the development of the reference vertical floor spectra are given later in this Appendix.

Experience from the evaluation of numerous nuclear plants has shown that the horizontal excitation generally dominates the critical seismic response for typical plant equipment. Therefore, great care was taken in the Diablo Canyon SPRA effort to establish reasonable median-centered horizontal floor spectra. In contrast, the vertical excitation contribution to seismic response is generally small. This is due to the effect of the SRSS or 100/40/40 directional combination methods, to the fact that vertical frequencies of equipment tend to be high and thus, outside the power of the vertical floor spectrum, and to the fact that, in many cases, the effect of dead weight must be overcome before the critical element is exposed to a harmful stress condition from vertical excitation. Table D-1 lists each Diablo Canyon equipment component evaluated in support of the SPRA, its vertical fundamental frequency,

and the fraction of the governing response parameter value attributable to vertical excitation. The fractional contribution is calculated as follows depending upon the directional combination method used to determine total response.

SRSS $$1-\left(\frac{R_{H1}^2+R_{H2}^2}{R_{H1}^2+R_{H2}^2+R_V^2}\right)^{1/2}$$

100/40/40 $$\frac{.40R_V}{1.00R_{H1}+.40(R_{H2}+R_V)} \quad \text{or} \quad \frac{1.00R_V}{1.00R_V+.40(R_{H1}+R_{H2})}$$

The first 100/40/40 equation is applicable for the majority of cases where the excitation from one of the horizontal directions governs the critical response while the second 100/40/40 equation is applicable for those cases where the vertical excitation governs the critical response.

It can be seen from Table D-1 that most components have vertical frequencies greater than 33 Hz and that, except for piping or those components whose response is governed by piping loads, only one component (Pressurizer) has a vertical frequency less than 15 Hz. It can also be seen that the vertical excitation contribution to response, expressed as a fraction of total response, for the majority of the component failure modes is less than 0.10. With the exception of piping, conduit, and

HVAC duct supports, only the six (6) components listed below have failure modes in which the vertical excitation contribution is greater than 0.30.

1. Reactor Internals
2. Auxiliary Saltwater Pump
3. D.G. Fuel Oil Day Tank
4. 4.16kV Switchgear (Functional Failure)
5. 480V Breaker Panel
6. Main Control Board

Although the above are important components, only the functional failure of the 4.16kV Switchgear, which has been shown to be recoverable, has a lower seismic capacity than the Turbine Building which dominates the plant seismic risk (Reference D-2). Since vertical excitation is usually only a small contributor to the overall seismic response and has been shown to be unimportant with regard to plant seismic risk, the factoring method used for the generation of the reference vertical floor response is considered to be adequate for the estimation of median response.

Method Illustrations

In order to illustrate the assessment of the effects of vertical response in the fragility evaluation of important Diablo Canyon components, three examples are presented. The first is the Emergency Diesel Generator Control Panel whose fragility was based upon the results of the seismic qualification test for the postulated Hosgri event. The second example is the 4.16kV/480V Transformer whose fragility was based upon an analysis of the critical structural element for the reference seismic event. The third example is the 4.16kV Switchgear (functional failure mode) which exhibits the lowest seismic capacity of all components evaluated, is primarily sensitive to vertical excitation, and is located on a flexible floor slab with a relatively low fundamental frequency.

Diesel Generator Control Panel

The Diesel Generator Control Panel is located in the Turbine Building at the basemat elevation of 85 feet; thus, the reference ground spectra define the seismic response. The Control Panel is braced in the front-to-back direction (North/South) and therefore, the primary response is in the side-to-side and vertical directions with the side-to-side (East/West) direction strongly dominating the two. The fundamental

frequencies of the panel in the side-to-side and vertical directions are 7.9 and 22 Hz, respectively, and these are governed by the presence of the vibration isolators located at the base of the cabinet. The panel was qualified for the Hosgri seismic event by random, multifrequency, biaxial testing in which the horizontal and vertical Hosgri ground response spectra were enveloped by the corresponding Test Response Spectra (TRS). The test motion was analyzed at 3% damping resulting in the TRS curves given in Figures D-8 and D-9.

Based upon an interpolation of the 2% and 5% damped median spectra, the 5% damped reference ground spectra (Figures D-4 and D-5) were appropriately factored to establish the 3% damped response for a proper comparison of the TRS and the reference ground spectra over the frequency range of interest. Although the vertical fundamental frequency of the Control Panel was determined as part of the seismic qualification test, there is some uncertainty concerning the actual in-situ value. Estimating the uncertainty variability or the vertical frequency, β_f, to be 0.10, the frequency range of interest is 18.7 to 26.0 Hz which constitutes a $\pm 1.65\ \beta_f$ frequency variation about the central frequency of 22 Hz.

Comparing the vertical TRS with the adjusted reference vertical ground spectrum (Table D-2), shows that the reference vertical spectrum is

substantially higher than the qualification TRS over the frequency range of interest, resulting in a median overtest factor of only 0.53. This is primarily due to the fact that the vertical TRS was relatively low and only slightly bounded the Hosgri vertical ground spectrum. However, an evaluation of three critical structural elements of the Control Panel (5/8" hold down bolt, 1/2" vibration isolator anchor, and the worst case relay mounting screws) demonstrated that a substantial margin would have existed even if the qualification test vertical input had been approximately doubled such that the vertical overtest factor equalled the side-to-side overtest factor of 1.12. The evaluation of the three failure modes also showed that the vertical direction contribution to the critical response was less than 25% of the side-to-side direction contribution (21.3%, 20.9%, and 23.7%, respectively), and thus, increased the overall response by only about 3% when the directional contributions were combined by SRSS. This relationship between the horizontal and vertical contributions to overall response was also used to compute the randomness variability associated with earthquake component combination and to incorporate the uncertainty associated with the vertical response spectral shape as shown below.

Judging the absolute combination of the two directional responses to represent a 3β upper bound, the randomness variability for earthquake component combination is:

$$\beta_R = \frac{1}{3} \ln \frac{1.00 + .25}{(1.00^2 + 0.25^2)^{1/2}} = 0.06$$

Based upon the results of the variability and ground motion studies, the composite variability associated with spectral shape and earthquake component variation for the horizontal response is 0.28 at the cabinet horizontal fundamental frequency and the composite variability associated with spectral shape for the vertical response is 0.35 at the cabinet vertical fundamental frequency. Therefore, the overall composite variability for spectral shape is conservatively calculated as:

$$\beta_C = \left[\frac{(1.0 \times 0.28)^2 + (0.25 \times 0.35)^2}{1.0^2 + 0.25^2} \right]^{1/2} = 0.29$$

In summary, the horizontal side-to-side overtest factor was used as the basis for computing the Diesel Generator Control Panel fragility Capacity factor and the vertical excitation exceedance was addressed by using the reference ground spectrum in the evaluation of the three selected failure modes and demonstrating that the increased vertical response results in a very small increase in the overall response.

4.16kV/480V Transformer

The 4.16kV/480V Transformers are part of the 480V load centers and are located at elevation 100 feet in the Auxiliary Building. The three transformer coils (Figures D-10 through D-12) are mounted by means of bolted connections to heavy structural angles which are in turn welded to the base frame of the protective cabinet. The base frame is stitch welded to embedment plates placed in the floor slab. The critical failure mode is combined shear and tension in the 1/2 inch bolts which secure the support cross plate to the coil structural angle frame. The transformer coil assembly exhibits fundamental frequencies of 2.7 Hz, 2.7 Hz, and 13 Hz in the North/South, East/West, and vertical directions, respectively. All three directions contribute to critical response with the East/West (weak axis) direction being predominant. The total coil weight is 4560 lbs. with the coil center of gravity located approximately 26 inches above the top of the two structural angles.

The 4.16kV/480V Transformers are 1000KVA units that were originally qualified by similarity to larger 1500KVA units dynamically tested to input motion which enveloped the Hosgri floor spectra at this location. However, due to the increased vertical input and the uncertainty concerning the relative directional contribution to overall response, it

was necessary to reevaluate the Transformer for the reference input motion using a median-centered directional combination methodology.

The 5% damped reference horizontal floor response spectra, generated as part of the LTSP ground motion studies, are shown in Figures D-13 and D-14 and were used directly in the fragility capacity evaluation. The flexible slab response spectra for the Hosgri reevaluation are shown in Figure D-6 and indicate that the slab fundamental frequency is 27 - 28 Hz. Using the factoring approach described above, the 5% damped reference vertical spectrum for the Transformer was developed by scaling the 5% damped Hosgri vertical spectrum (Figure D-6) by the ratio of the 5% damped reference ground spectrum to the 5% damped Hosgri ground spectrum (Figure 5) on a frequency-by-frequency basis for all frequencies below 27.5 Hz and by the ratio at 27.5 Hz for all frequencies 27.5 Hz and greater. The resulting 5% damped reference vertical floor spectrum is shown in Figure D-15.

At the Transformer vertical fundamental frequency of 13 Hz, the estimated reference vertical spectral acceleration is 2.50g which was used in the fragility capacity evaluation. Based upon the recomputation of the critical element stresses for the reference input motion, the tensile forces in the 1/2" bolts due to East-West, North-South, and vertical excitation were found to be 6.34K, 1.66K, and 1.42K,

respectively. As a result, the vertical direction contribution to overall response is less than 3% using the above equation for SRSS response combination. In a manner similar to that described for the Diesel Generator Control Panel, the relationship between the three directional contributions was also used to compute the randomness variability associated with earthquake component combination, to prorate the uncertainties associated with response spectral shape, and to prorate the effect of ground motion incoherency.

Again judging the absolute sum combination to represent a 3β upper bound on response, the randomness variability for earthquake component combination is:

$$\beta_R = \frac{1}{3}\ln\left[\frac{6.34+1.66+1.42}{(6.34^2+1.66^2+1.42^2)^{1/2}}\right] = 0.11$$

At 2.7 Hz, the composite variability on spectral shape and earthquake component variation for both the East-West and North-South directions was found to be 0.24 while the composite variability on spectral shape and earthquake component variation is conservatively calculated as:

$$\beta_C = \left[\frac{(6.34\times0.24)^2+(1.66\times0.24)^2+(1.42\times0.36)^2}{6.34^2+1.66^2+1.42^2}\right]^{1/2} = 0.24$$

From the ground motion study, the factor of safety accounting for ground motion incoherency in the East-West and North-South directions were found to be 1.06 and 1.05, respectively for a frequency of 2.7 Hz. Therefore, the overall factor of safety for ground motion incoherency is computed as:

$$F_{GMI} = \frac{[(6.34 \times 1.06)^2 + (1.66 \times 1.05)^2 + (1.42 \times 1.00)^2]^{1/2}}{6.70} = 1.06$$

In summary, the vertical excitation exceedance for the 4.16kV/480V Transformer was addressed by recomputing the response for the reference event, including the higher vertical input. The analysis also demonstrated that the vertical response contributes only a small amount to the overall response.

4.16kV Switchgear

The 4.16 kV Switchgear are located at elevation 119 feet in the Turbine Building. The floor slab at this elevation is relatively flexible with a fundamental frequency of approximately 7.2 Hz and a number of modes below 33 Hz. The switchgear cabinets are welded to the floor embedment plates by means of intermittent fillet welds and puddle welds. The cabinets are also bolted together in strings of 9 cabinets and thus, they are well secured over a relatively large area of the floor slab.

As noted in Reference D-2, only two types of relays housed in the 4.16kV switchgear were found to be important in terms of the consequences of relay chatter. These were the Agastat 7012 timing relay and the General Electric IAC 53 protective relay. Both of these relays are primarily sensitive to vertical seismic input and both are normally in the de-energized state. The evaluation of the potential for chatter of these two relays formed the basis for the functional failure fragility for the 4.16kV Switchgear.

The Generic Equipment Ruggedness Spectra (GERS) for the 7012 and IAC 53 relays are 12.6g and 7.6g, respectively (Figures D-16 and D-17 taken from Reference D-3). Thus, the door mounted IAC 53 relay is the controlling element. Although the Diablo Canyon relays are pre-1974 vintage, they were subsequently upgraded to the post-1974 "Hi g" configuration which is the basis for the GERS. Comparison of the output from the vertical control accelerometer and the vertical response accelerometer placed on the back of one of the IAC 53 relays during the resonant search test shows virtually no amplification of the vertical input at less than 10 Hz and no cross-coupling of the horizontal input. further, the transmissibility plot shows a resonant frequency of the vertical door panel at approximately 20 Hz with amplification ranging from 1.0 to 2.65 over the $\pm 1.65\beta$ frequency range from 15.9 to 25.2 Hz (Modeling β_U =

0.14). Thus, the demand vertical acceleration at the relay was computed as the product of the median-centered reference floor response acceleration times the median door amplification determined from the dynamic test.

Using the factoring approach described above, the median-centered vertical floor response spectrum was established by scaling the unsmoothed and unbroadened Hosgri reevaluation vertical spectrum for the controlling floor location (Figure D-7) by the appropriate ratio of the 5% damped reference ground spectrum to the 5% damped Hosgri reevaluation ground spectrum (Figure D-5). For frequencies below the floor slab fundamental frequency of 7.2 Hz, the 5% damped Hosgri spectrum was scaled by the ratio established based upon a frequency-by-frequency comparison. For frequencies of 7.2 Hz and greater, the 5% damped Hosgri spectrum was scaled by the ratio of the ground spectra at 7.2 Hz (Ratio = 1.35) increased by 25% to account for higher frequency modes. Thus, the scale factor was 1.68 for frequencies of 7.2 Hz and greater. The resulting 5% damped reference vertical floor spectrum is shown in Figure D-18.

Since the response for this failure mode is 100% attributable to the vertical excitation, the fragility capacity factor is directly computed as shown in Table D-3 based upon the estimated response from the refer-

ence vertical input at the base of the cabinet. All variabilities are related to the vertical input alone and prorating variabilities by relative response contribution, illustrated in the two previous examples, is unnecessary.

In summary, the vertical excitation exceedance for the 4.16kV Switchgear functional failure mode was addressed by recomputing the vertical acceleration at the critical relay for the higher vertical input of the reference event and evaluating the functional failure fragility by comparison with the relay chatter GERS for the critical relay.

Validation of Hosgri Spectrum Factoring Approach

In order to validate the Hosgri spectrum factoring procedure for the generation of median-centered reference vertical spectra, as used in the three examples, a 50 percentile vertical floor spectrum for the controlling location in the 4.16kV Switchgear area was developed by the factoring approach to correspond to the LTSP 84 percentile vertical ground motion spectrum. A modified time history corresponding to the LTSP 84 percentile vertical ground spectrum was also input into the multi-mode Turbine Building elevation 119 feet floor slab model and the resulting vertical floor response spectrum was generated. The 5% damped vertical spectra generated by the two approacnes are compared in Figure D-19 showing good agreement in terms of general shape and amplitude.

The 4.16kV Switchgear area was selected for the method comparison since the multiple mode character of the Hosgri reevaluation spectrum at this location provided the most difficult test for the factoring procedure. Comparison for the LTSP 84 percentile vertical ground motion was chosen since the modified time history was readily available from other studies and was not substantially different in shape from the reference vertical ground spectrum.

Conclusions

The increased vertical input associated with the median vertical spectral shape for the Diablo Canyon site was incorporated into all equipment fragilities as illustrated by the three examples given above. The factoring method used to develop the reference event vertical floor spectra was shown to produce floor spectra in good agreement with those generated by time-history analysis, even for the multi-mode Turbine Building slabs. Further, the fraction of the total critical response attributable to vertical excitation was shown to be small for the vast majority of components evaluated and was found to be unimportant in terms of plant seismic risk. Therefore, the incorporation of the vertical ground input by the Hosgri factoring method described is judged to be adequate.

References

D-1. Kennedy, R.P., D.A. Wesley, and W.H. Tong, "Probabilistic Evaluation of the Diablo Canyon Turbine Building Seismic Capacity Using Nonlinear Time History Analyses," NTS Engineering Report 1643.01, Revision 0, December, 1988.

D-2. Pacific Gas and Electric Company, "Final Report of the Diablo Canyon Long Term Seismic Program," July, 1988, Docket Numbers 50-275 and 50-323.

D-3. Smith, C.B. and K.L. Merz, "Generic Seismic Ruggedness of Power Plant Equipment," EPRI Report NP-5223, ANCO Engineers, Inc., May 1987.

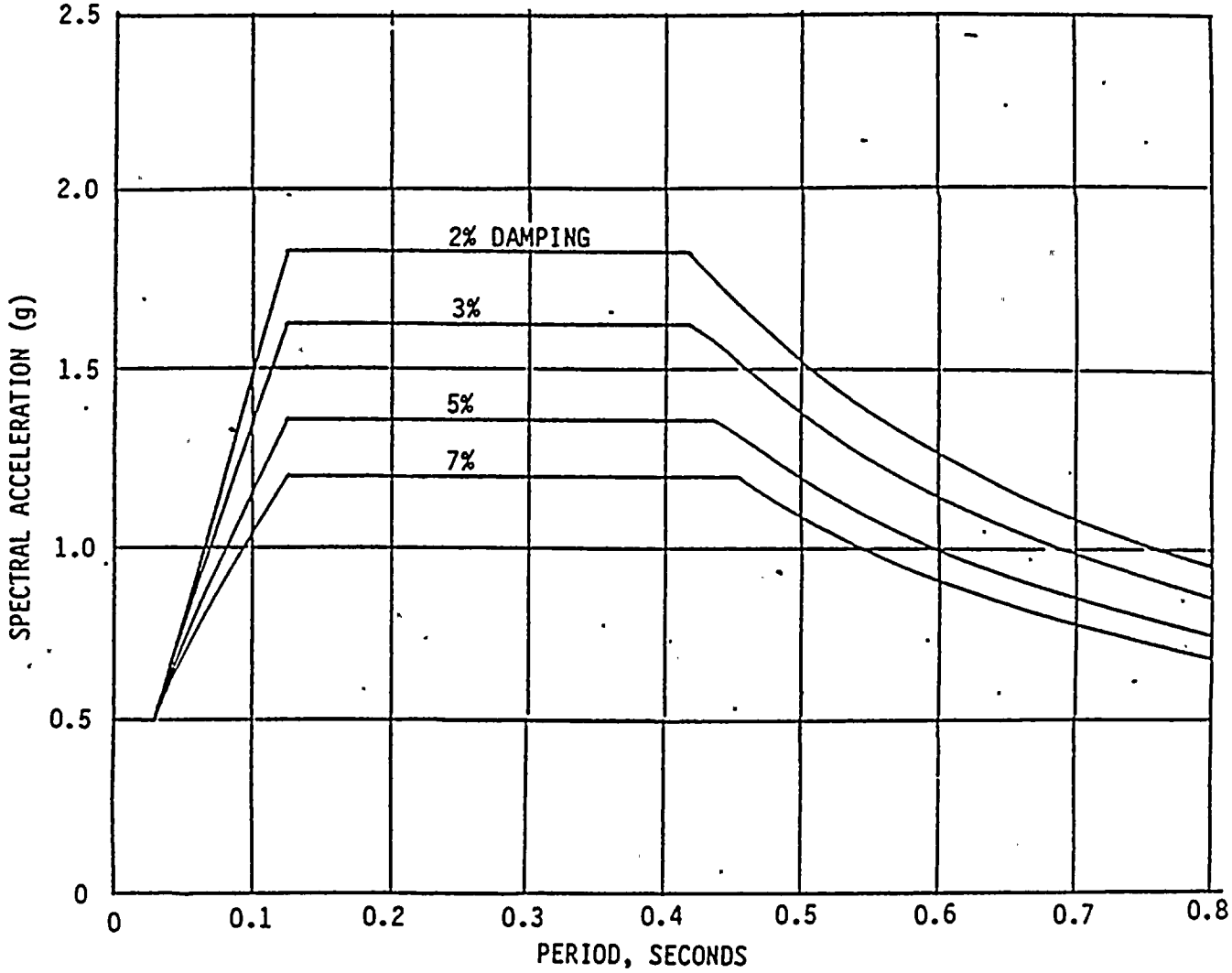

Figure D-1. Hosgri Reevaluation Vertical Response Spectra at Foundations of All Buildings

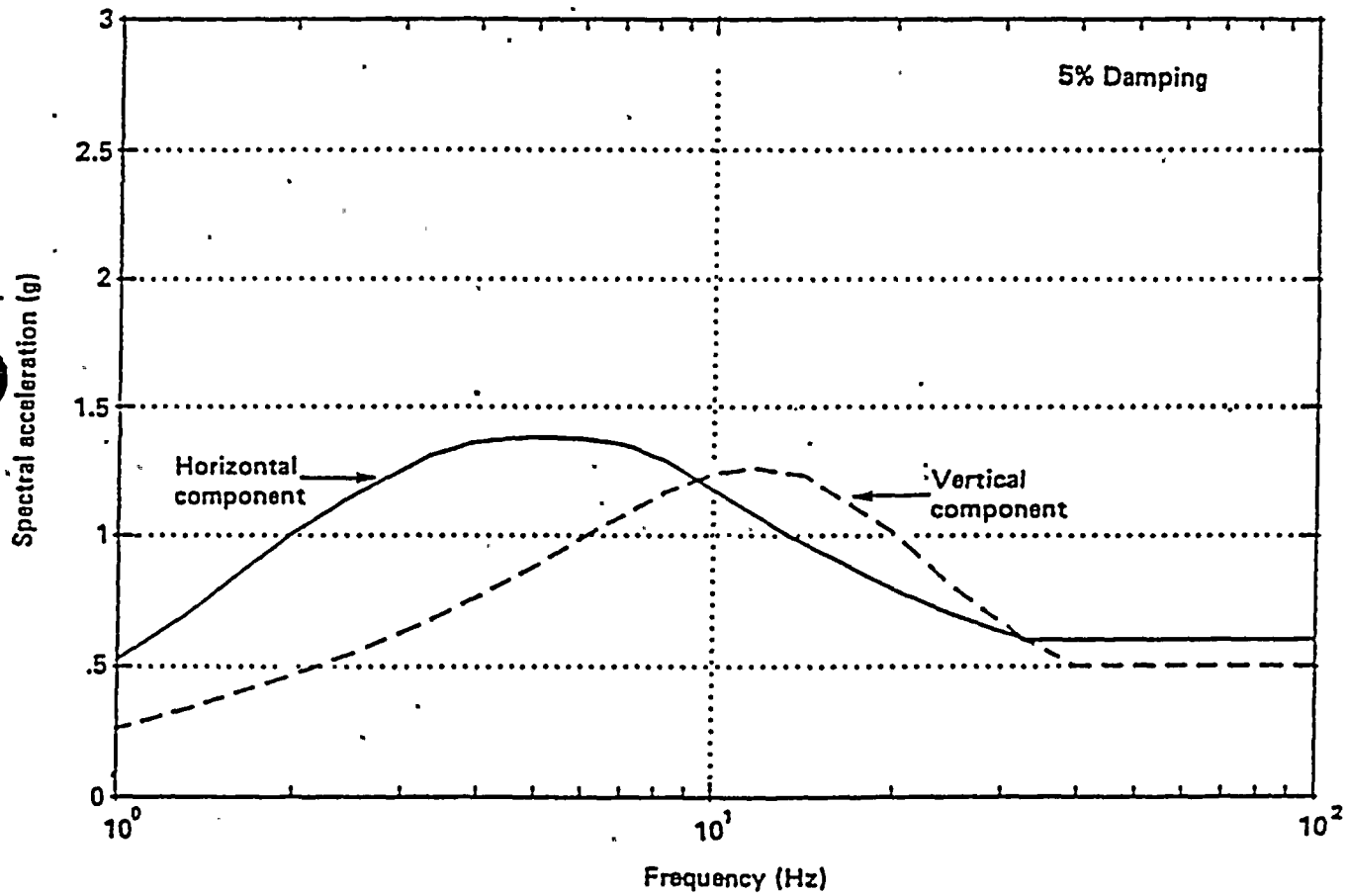

Figure D-2. Diablo Canyon Site-Specific Median Ground Motion Acceleration Response Spectra

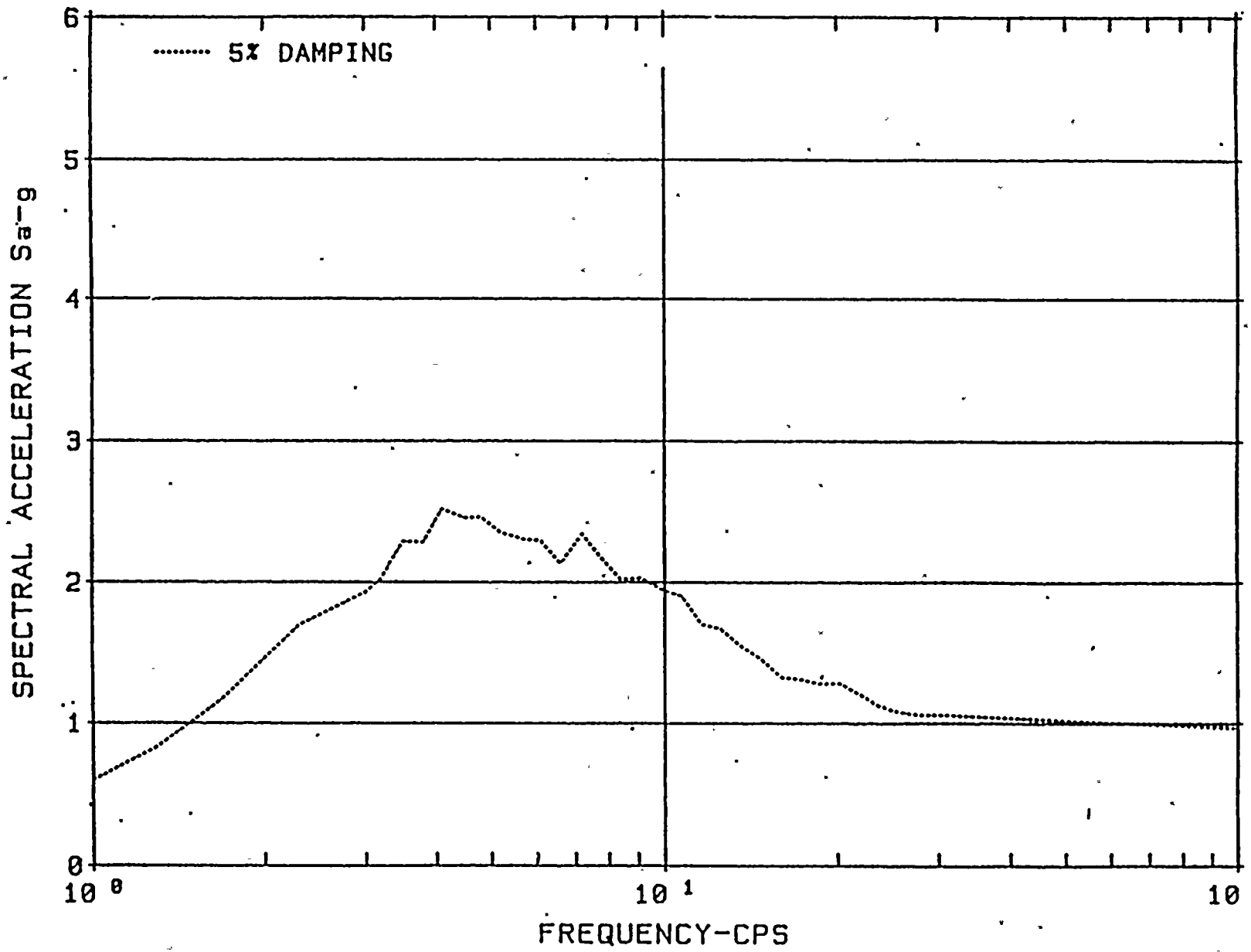

Figure D-3. North-South 50 Percentile Ground Response Spectrum for Empirical and Numerical Time-Histories

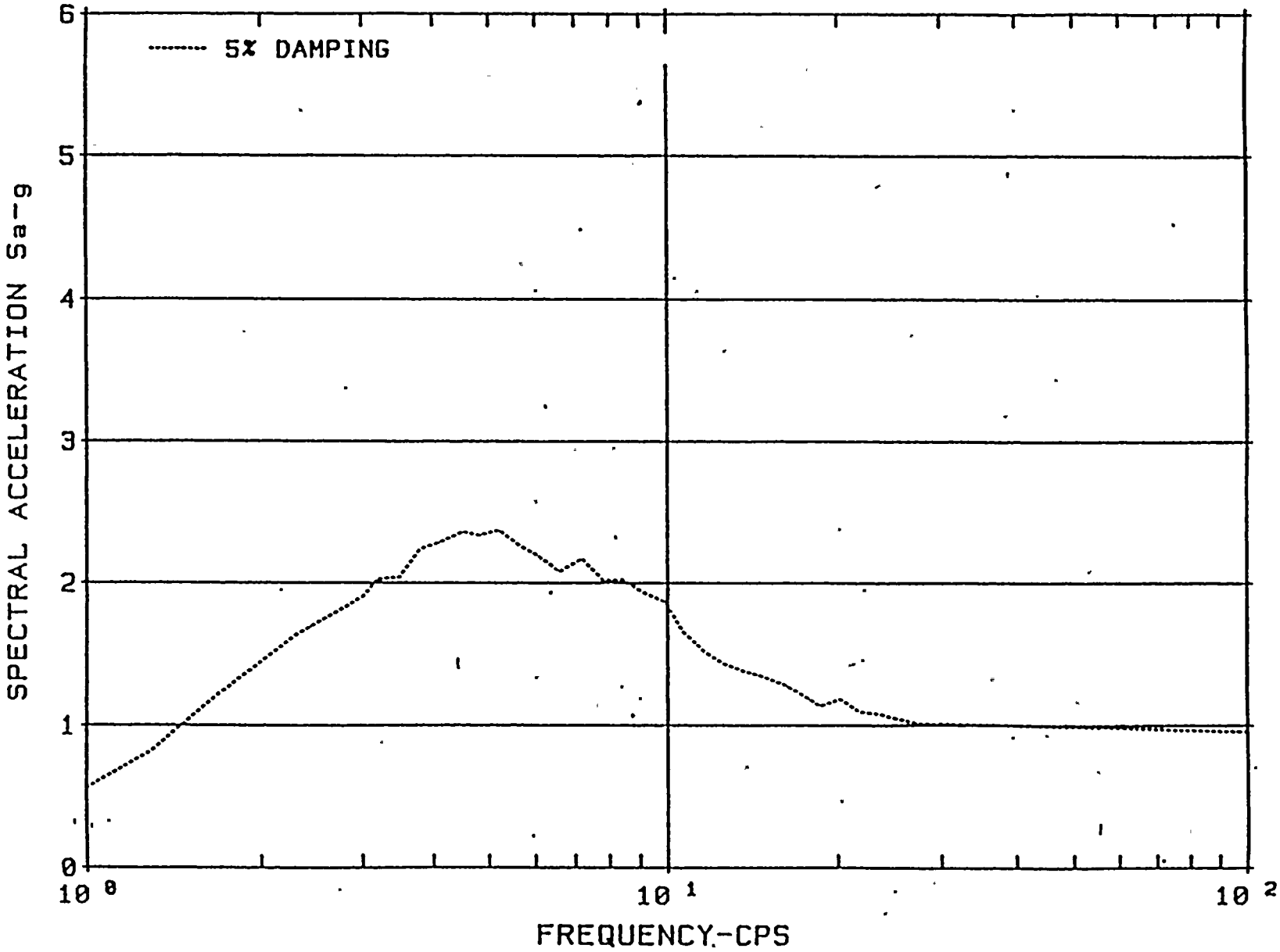

Figure D-4. East-West 50 Percentile Ground Response Spectrum for Empirical and Numerical Time Histories

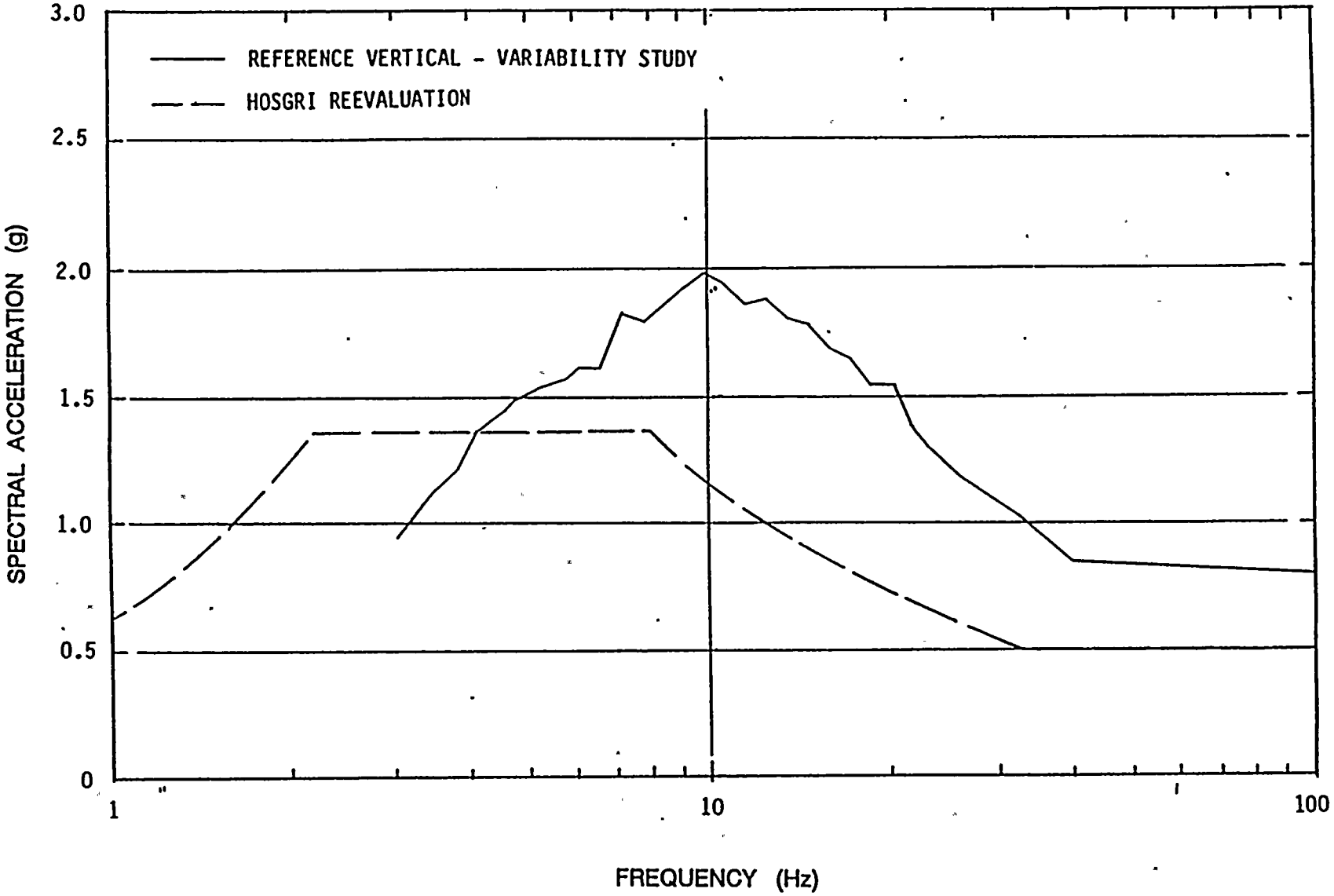

Figure D-5. Comparison of 5% Damped Vertical Ground Response Spectra

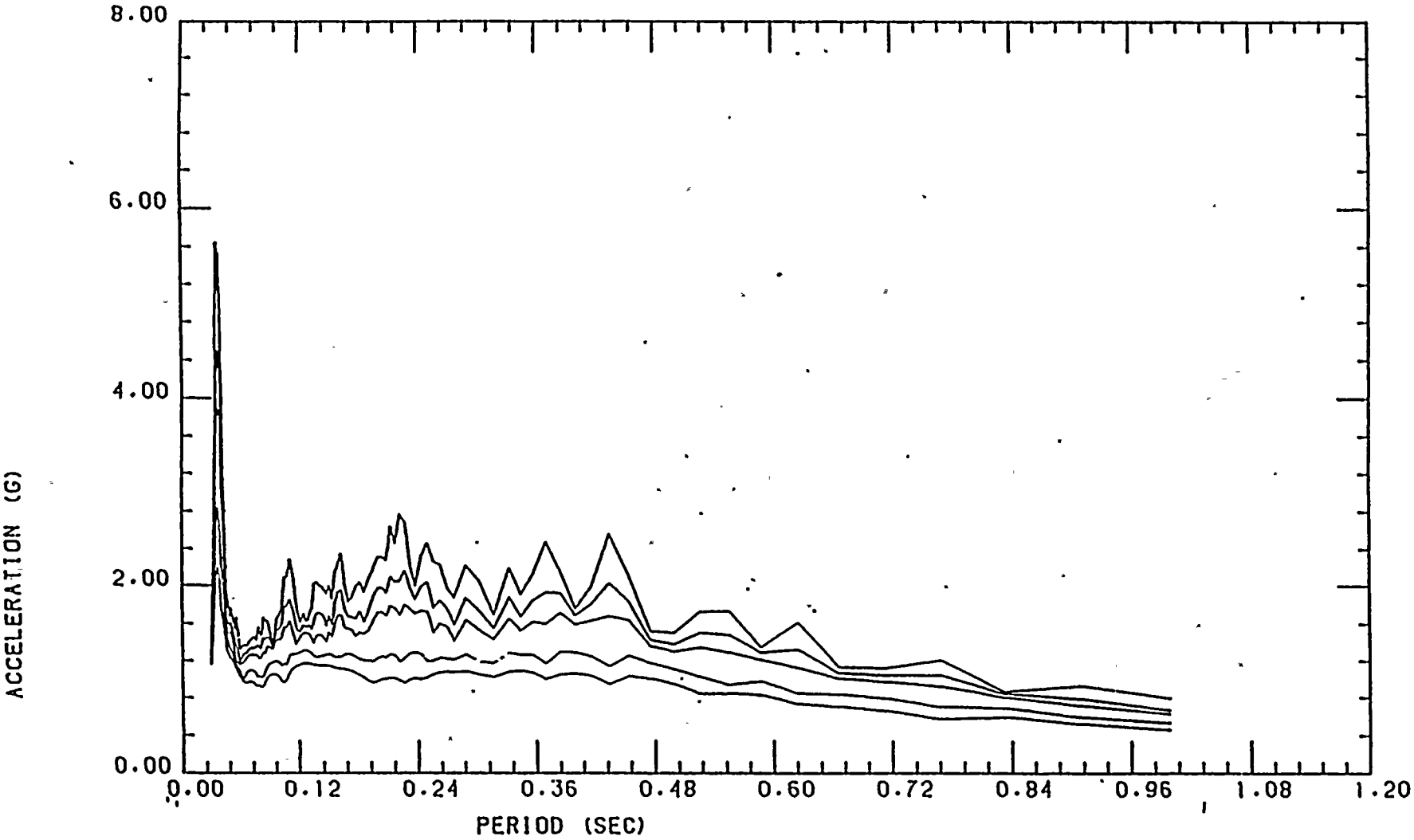

Figure D-6. Hosgri Reevaluation Vertical Floor Response Spectra for the Auxiliary Building, Elevation 100', Slab 2, Node 161 (2,3,4,7, and 10% Damping)

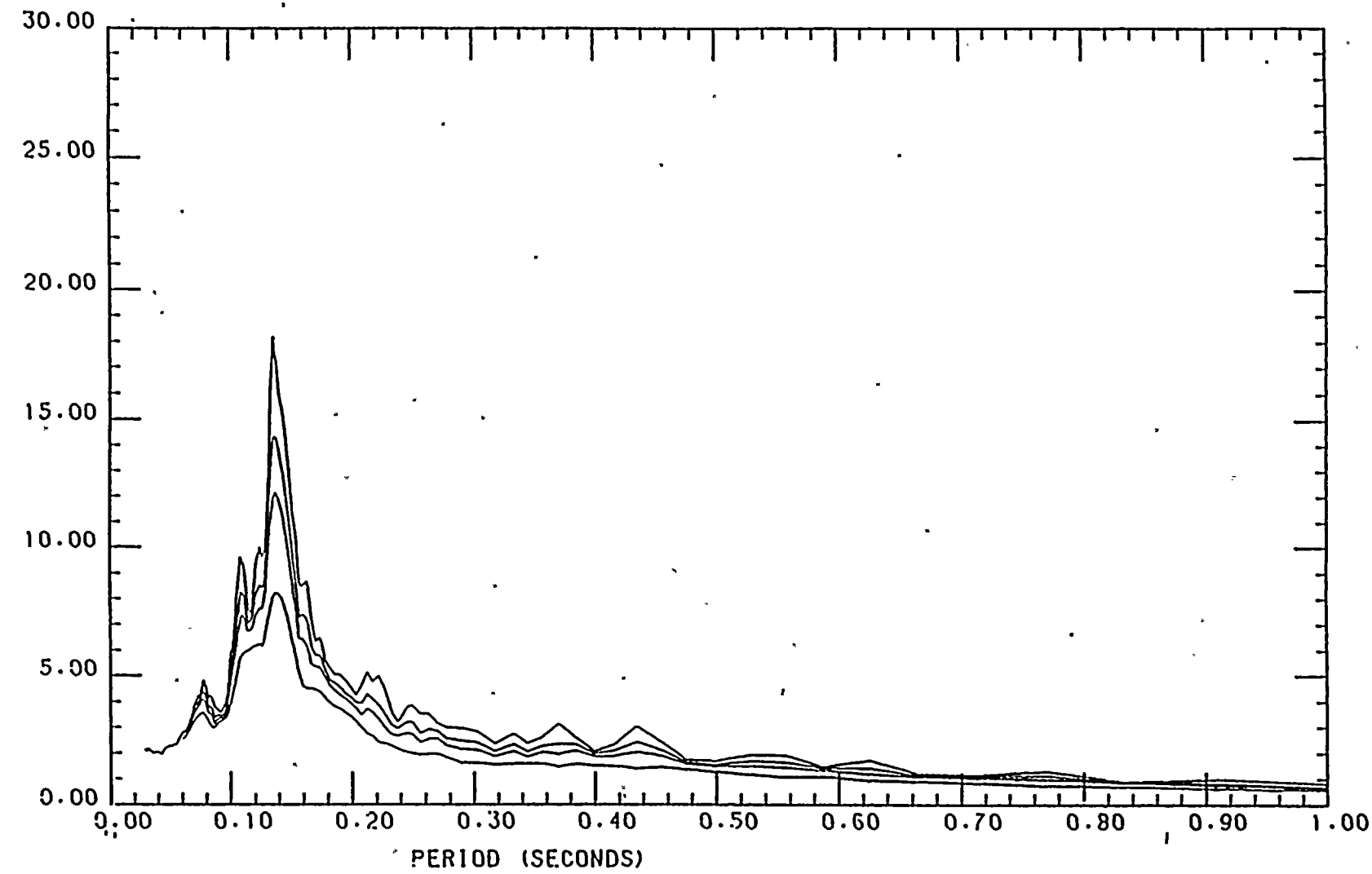

Figure D-7. Hosgri Reevaluation Vertical Floor Response Spectra for the Turbine Building, Elevation 119', Switchgear Area, Node 451 (2,3,4, and 7% Damping)

Full Scale 10 g Accel. No. 1 Control (✓) Response ( )

Operator MEEHAN Specimen GEN. CON. PANEL & PRESS. SWITCHES.

Date 12-7-78 Damping 7 % Axis of Test HORIZ 55.V 1ST SSE

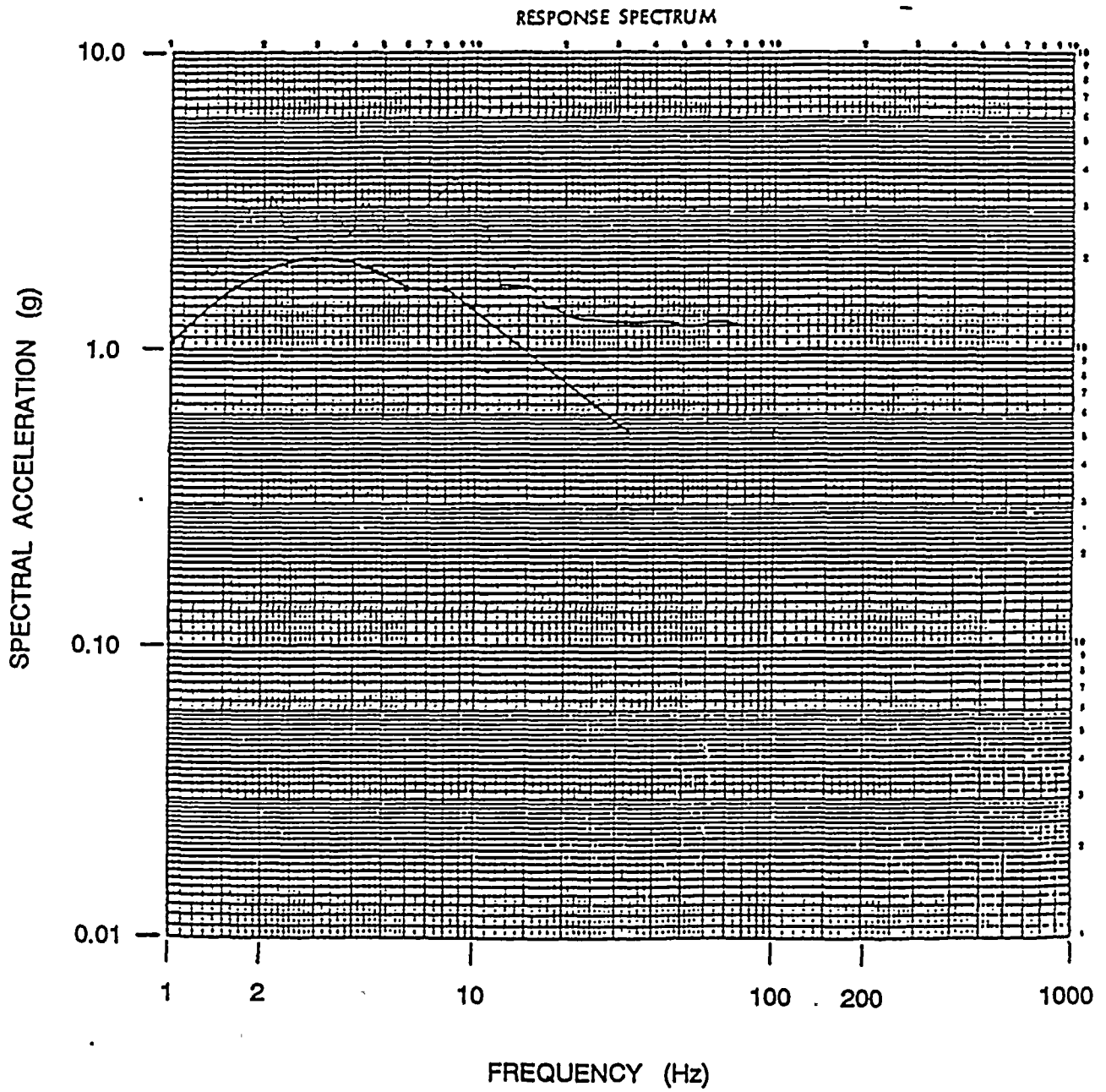

Figure D-8. Diesel Generator Control Panel - Horizontal Test Response Spectrum (3% Damping)

Full Scale 10 g Accel. No. 2 Control (✓) Response ( )

Operator MEEHAN Specimen GEN. CON. PANEL 8' PROBS. SWITCHES

Date 12-7-78 Damping 3 % Axis of Test VERT 55-J
2ND SSE

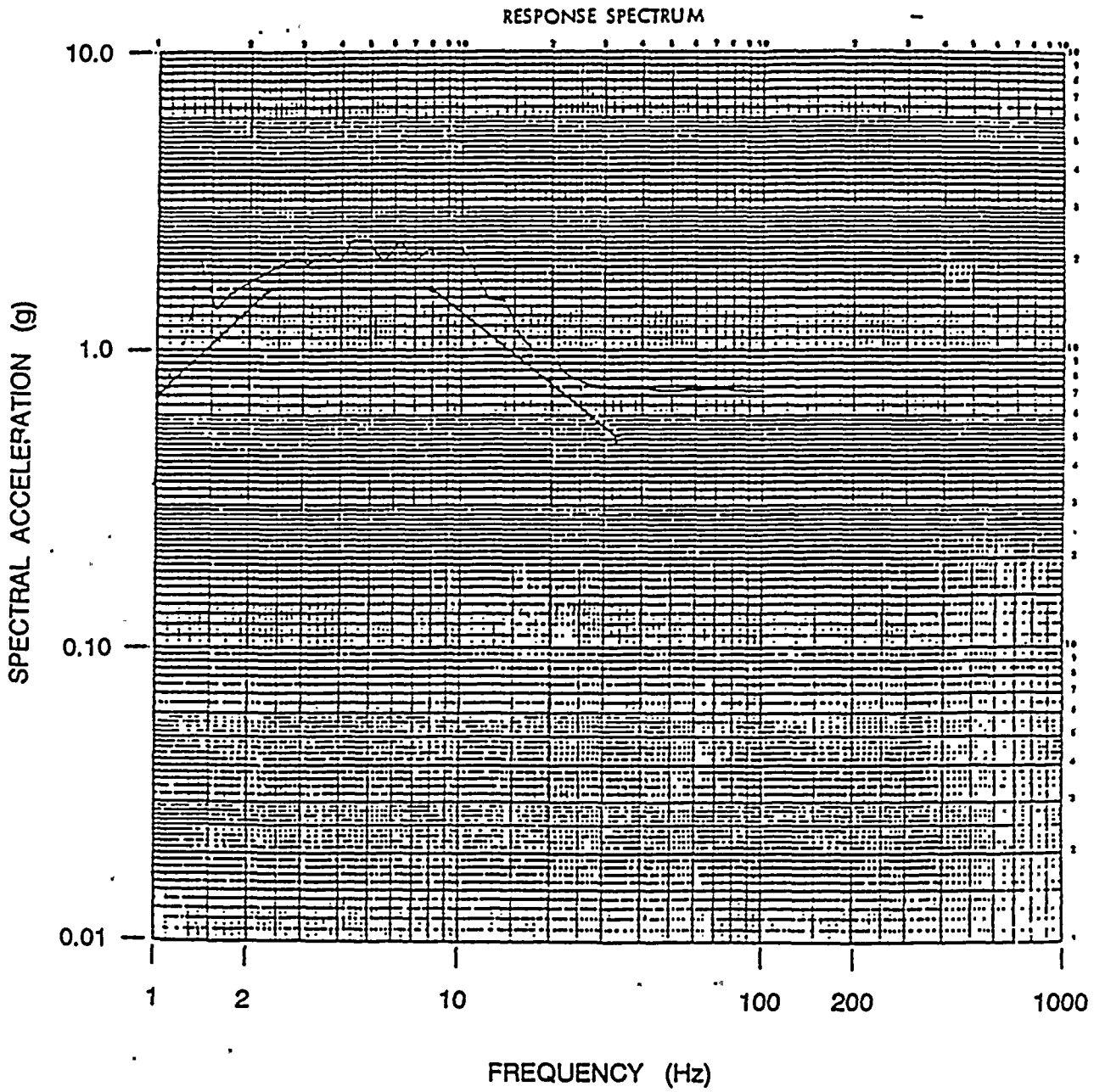

Figure D-9. Diesel Generator Control Panel - Vertical Test Response Spectrum (3% Damping)

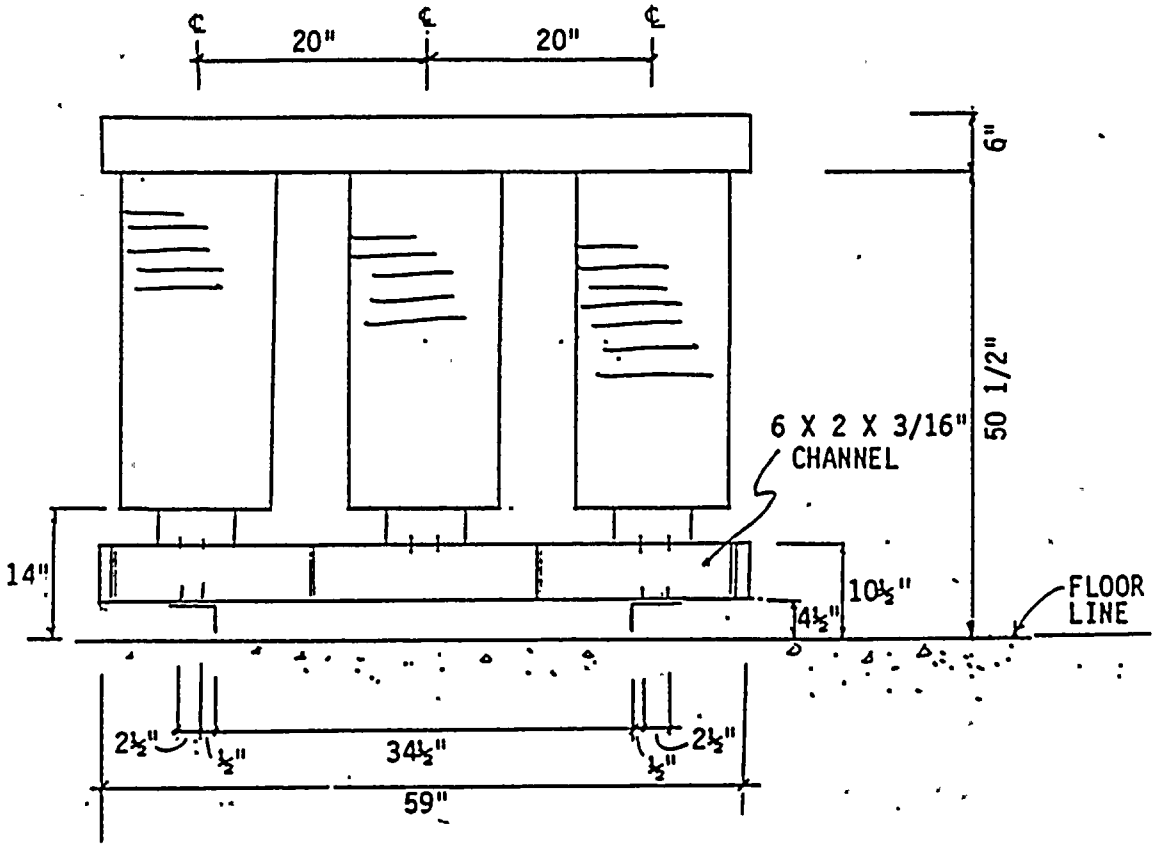

EAST ELEV

NOT TO SCALE

TOTAL WT OF COILS = 4560#

TOTAL CABINET WT = 5350#

Figure D-10. 4.16kV/480V Transformer Coils and Supports - East Elevation

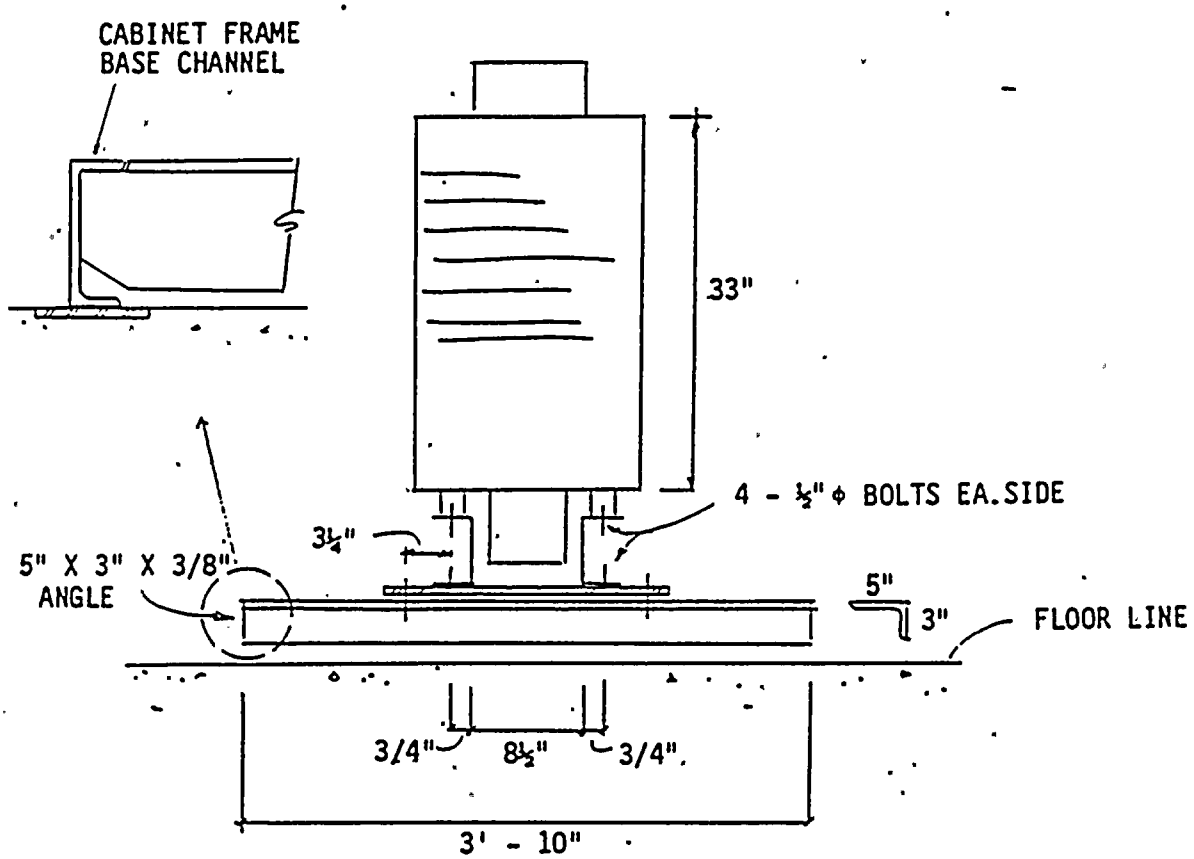

NORTH ELEV. NOT TO SCALE

THE ENDS OF THE L5 X 3 X 3/8 ARE WELDED TO THE CHANNEL AT THE BASE OF THE CABINET FRAME

Figure D-11. 4.16kV/480V Transformer Coils and Supports - North Elevation

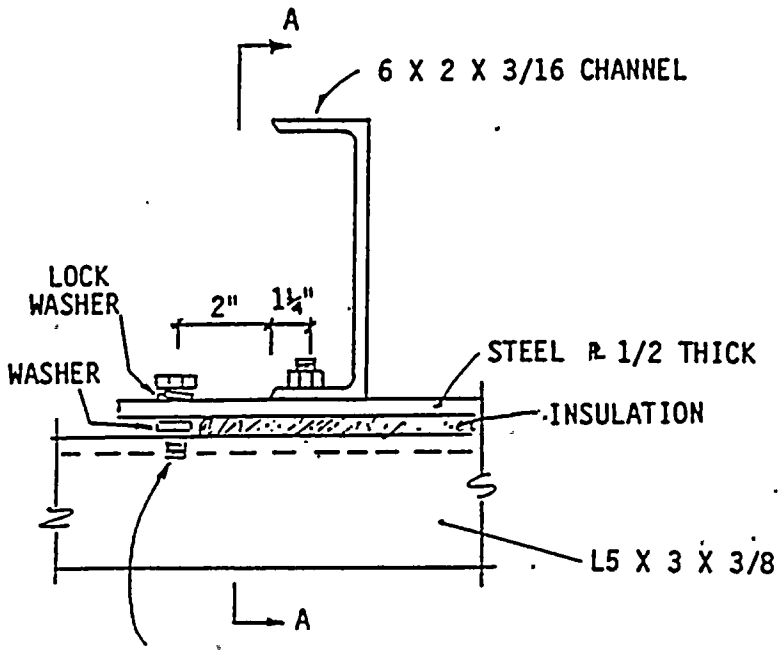

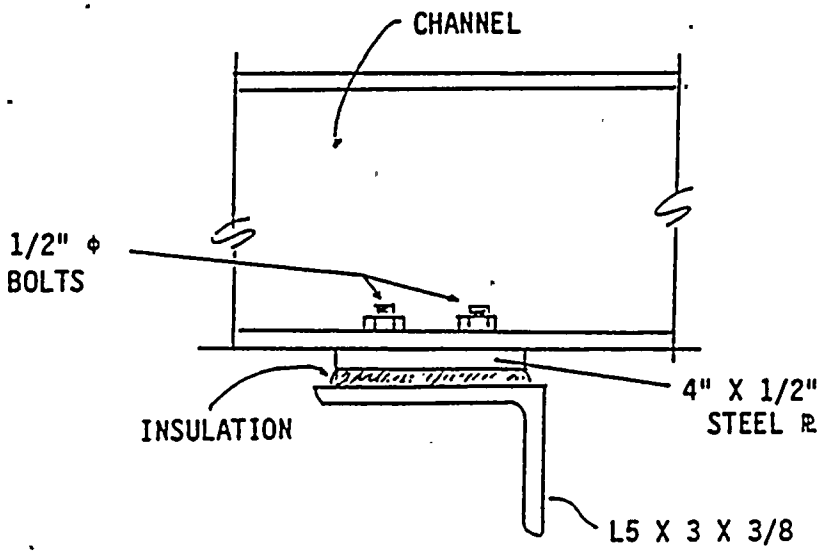

NOT TO SCALE

SECTION A-A

Figure D-12. 4.16kV/480V Transformer Coil Support Anchorage Detail

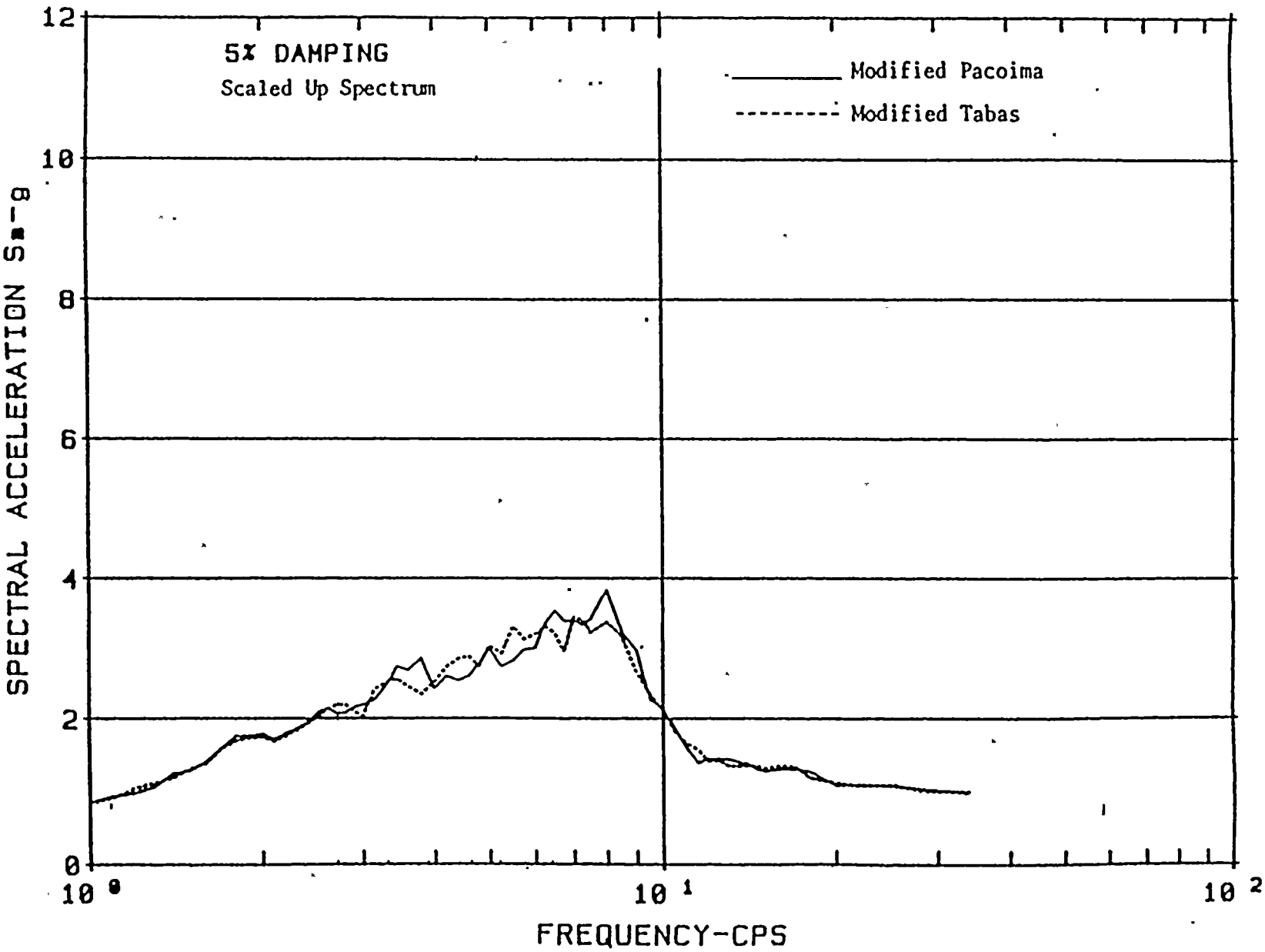

Figure D-13. North-South Reference Floor Response Spectra for the Auxiliary Building, Core West, Elevation 100'

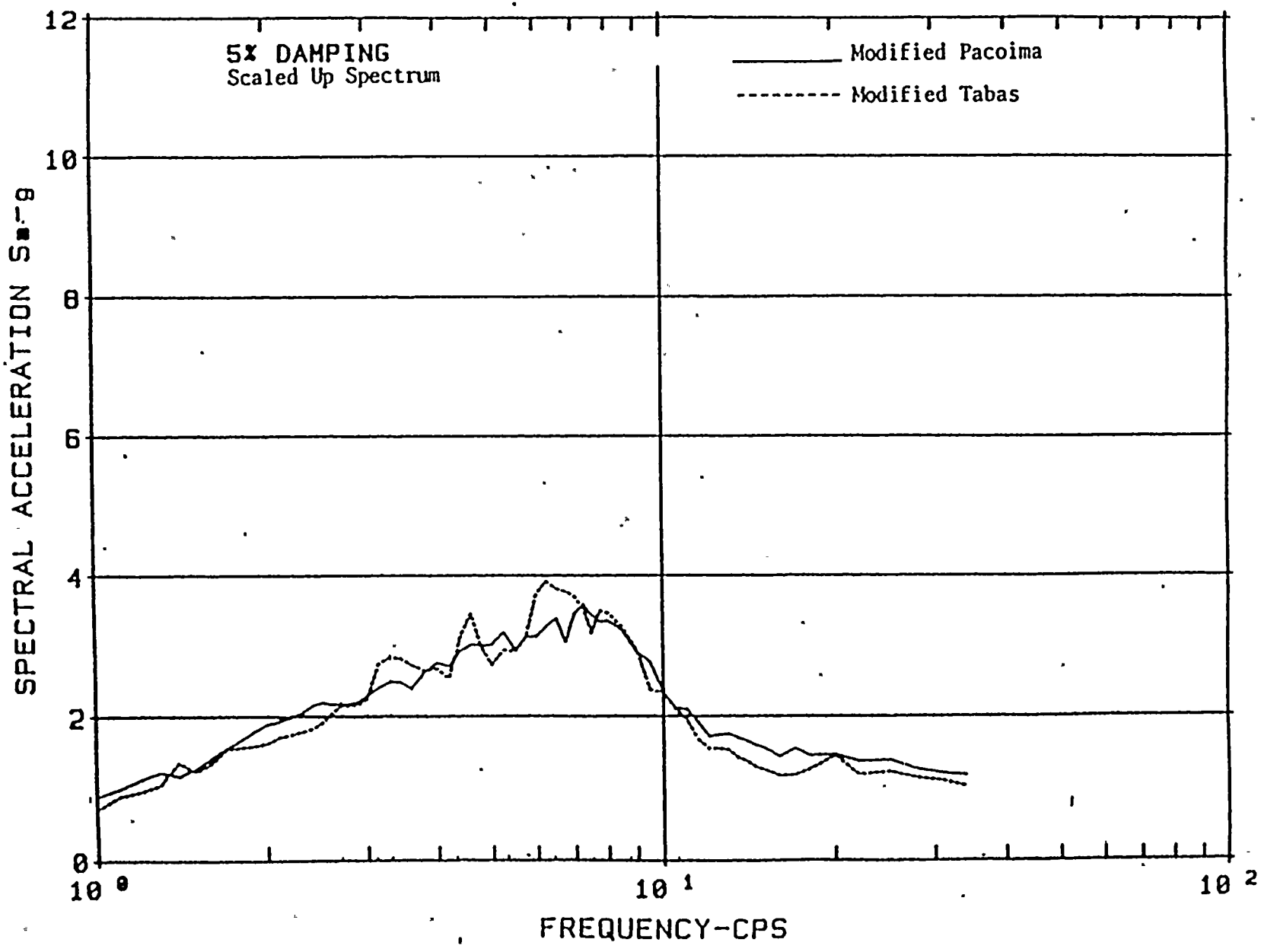

Figure D-14. East-West Reference Floor Response Spectra for the Auxiliary Building, Core West, Elevation 100'

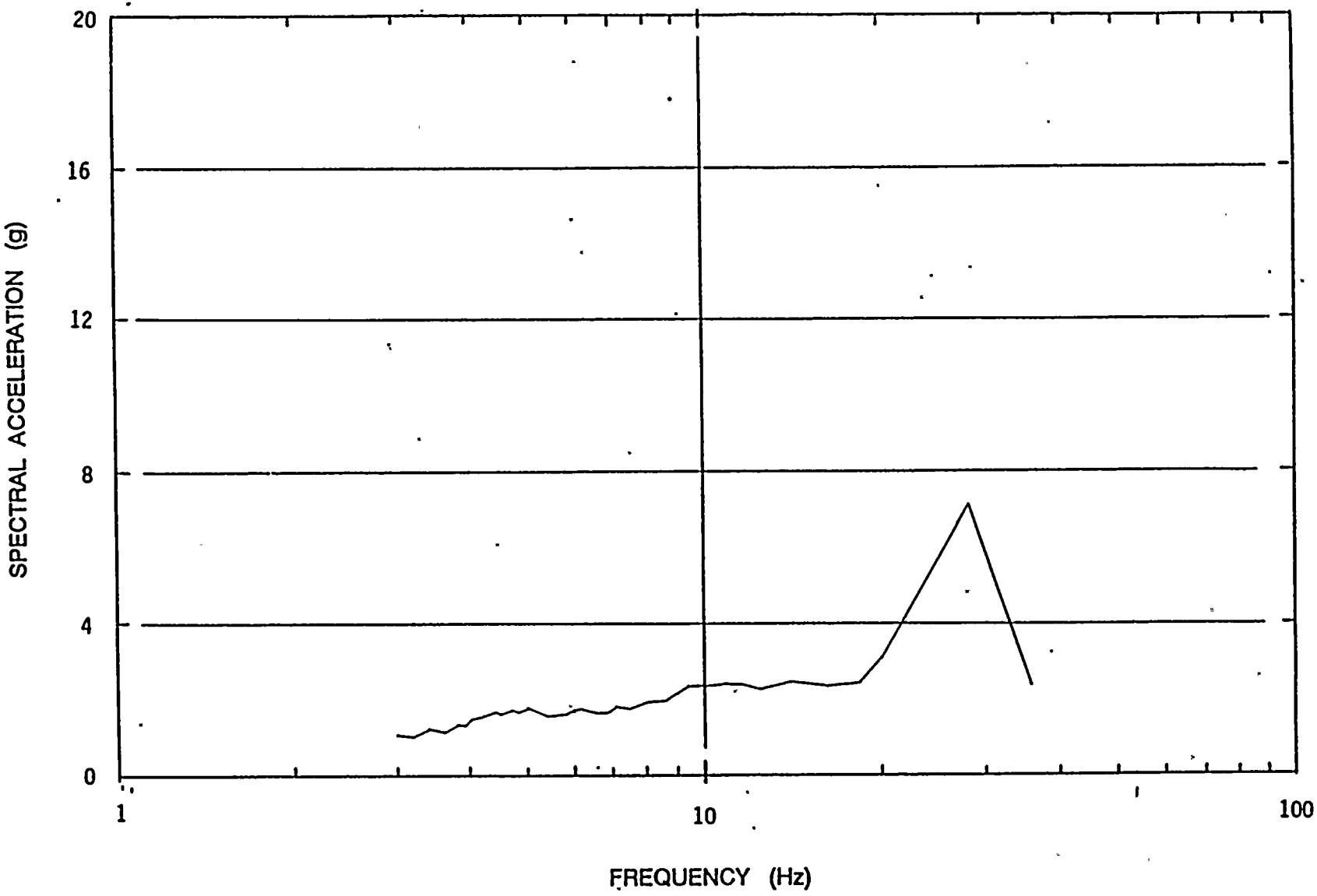

Figure D-15. 5% Damped Reference Vertical Floor Response Spectrum for the Auxiliary Building, Elevation 100', Slab 2, Node 161

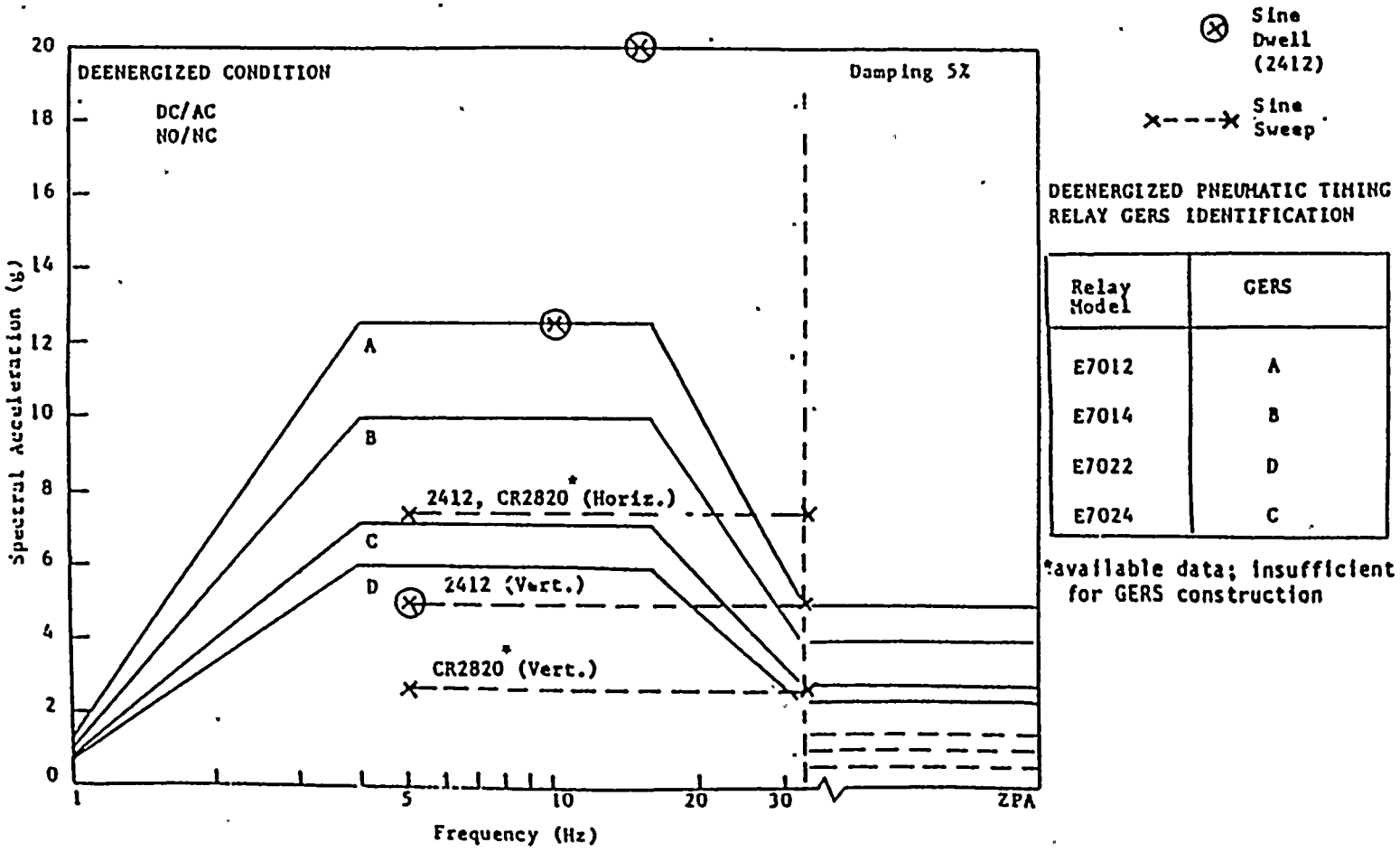

Figure D-16. GERS and Available Data for Pneumatic Timing Relays (Deenergized)

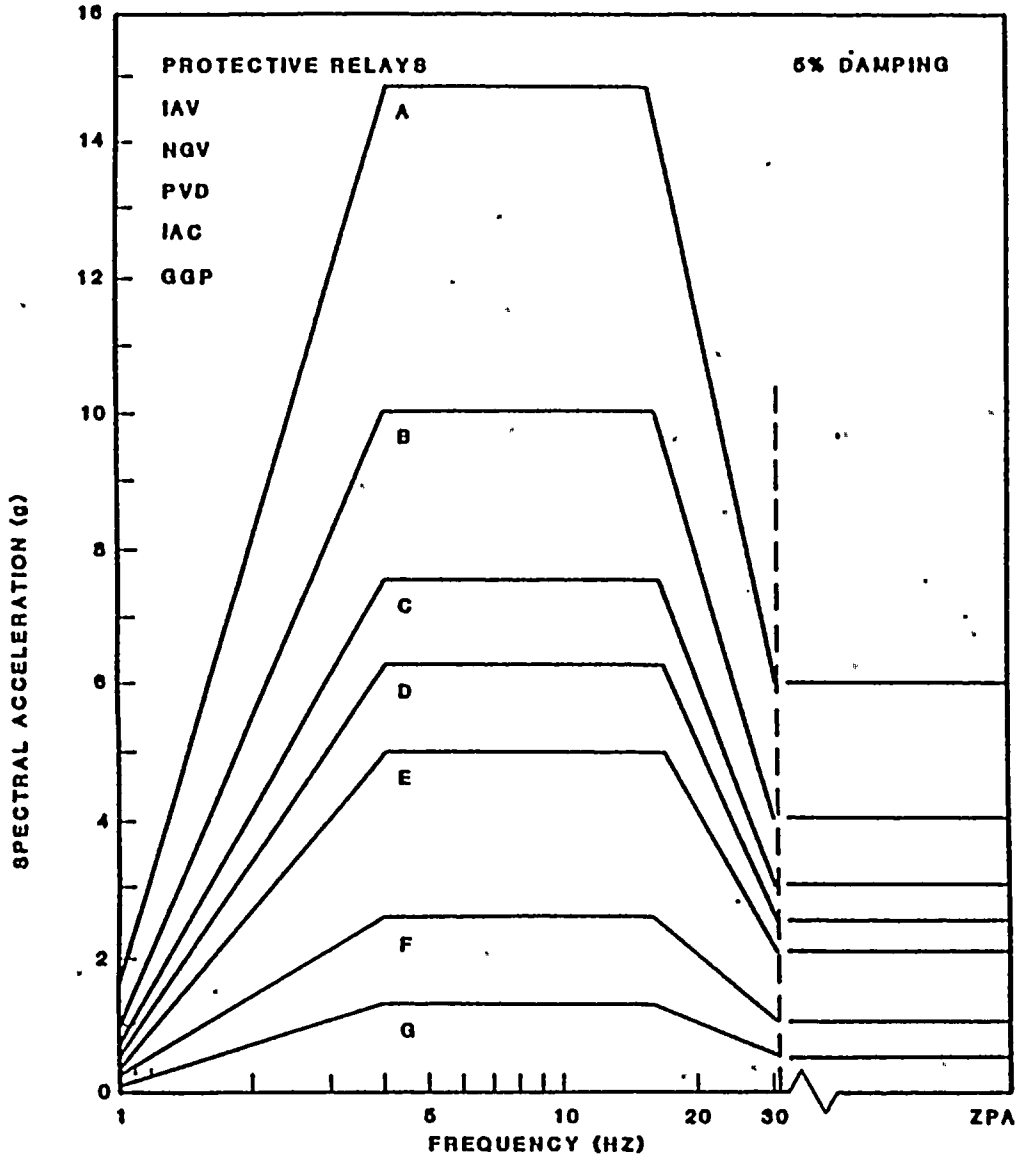

GERS IDENTIFICATION

MODEL	OPERATE STATE	NON-OPERATE STATE
IAV 55	A (NC)	C (NC)
53	A (NO) G (NC)	D (NO) A (NC)
NGV 11-23	A	A
29	D	D
PVD 21	E	C
11	A	F
IAC	B	C
GGP	A	E

Figure D-17. GERS for Protective Relays

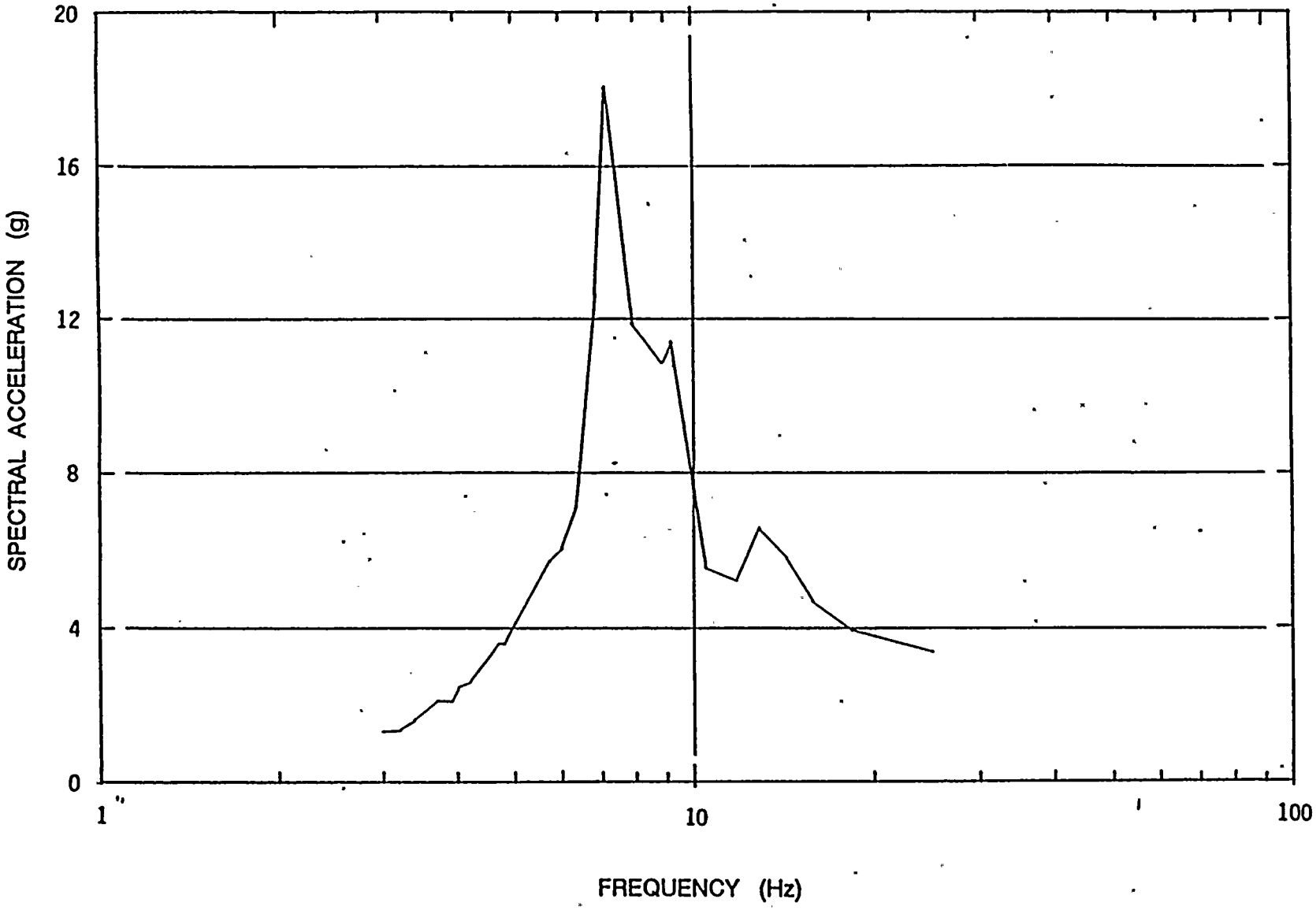

Figure D-18. 5% Damped Reference Vertical Floor Response Spectrum for the Turbine Building, Elevation 119', Switchgear Area

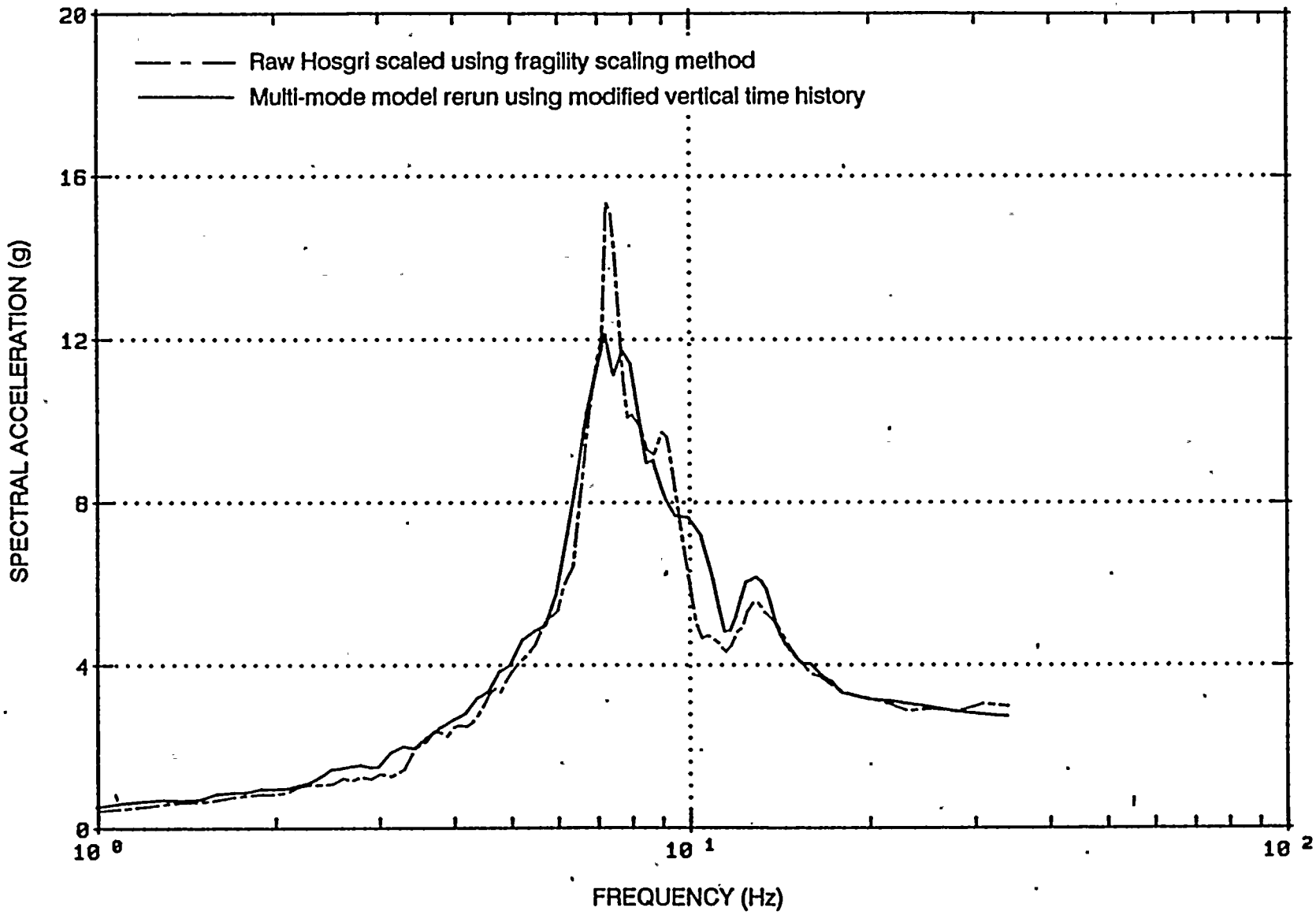

Figure D-19. 5% Damped LTSP 84 Percentile Vertical Floor Response Spectrum for Turbine Building Elevation 119', Switchgear Area, Node 451

Table D-1. Influence of Vertical Accelerations on Diablo Canyon Equipment

COMPONENT	VERTICAL FREQUENCY (Hz)	VERTICAL EXCITATION CONTRIBUTION	COMMENT
1. REACTOR PRESSURE VESSEL	16 - 20	Negligible	
2. REACTOR INTERNALS	16 - 20	1.00	
3. STEAM GENERATOR	23	Negligible	
4. PRESSURIZER	11	Negligible	
5. PRESSURIZER SAFETY VALVE	Piping	Negligible	
6. PRESSURIZER RELIEF VALVE	Piping	Negligible	
7. REACTOR COOLANT PUMP	20.6	0.01	
8. CONTROL ROD DRIVE	> 35	Negligible	
9. NSSS PIPING	7 - 9	Unknown**	
10. RHR PUMP	Piping 12 - 18	0.05	
11. RHR HEAT EXCHANGER	90	0.02	
12. SI ACCUMULATOR	65 - 79	0.05	
13. SI PUMP	> 33	0.30	
14. BORON INJECTION TANK	68 -84	Negligible	
15. CCW PUMP	Piping 14 - 20	Negligible	
16. CCW HEAT EXCHANGER	17.6 & 34.3	0.06	
17. CCW SURGE TANK	44.4	0.10	
18. CENTRIFUGAL CHARGING PUMP	> 33	0.10	
19. RECIPROCAL CHARGING PUMP	> 33	Unknown**	
20. AUXILIARY SALTWATER PUMP	48.6	0.36	
21. CONTAINMENT SPRAY PUMP	> 33	0.07	
22. SPRAY ADDITIVE TANK	51	0.06	
23. MAIN STEAM ISOLATION VALVE	Piping	0.04	
24. MAIN STEAM SAFETY VALVE	Piping	Negligible	
25. MAIN STEAM PORV	Piping 10 - 20	Negligible	
26. AUX. FEEDWATER PUMP (Motor Driven)	> 33	Unknown**	
27. AUX. FEEDWATER PUMP (Turbine Driven)	> 33	0.02	
28. D.G. FUEL OIL DAY TANK	10.4	1.00	
29. D.G. FUEL OIL PUMP/FILTER	Piping 14 - 20	0.12	
30. D.G. FUEL OIL SHUTOFF VALVE	Piping	Negligible	
31. D.G. AIR START COMPRESSOR	> 33	0.12	
32. D.G. AIR START RECEIVER	> 33	0.08	
33. DIESEL GENERATOR	25.7	0.08	
34. D.G. RADIATOR/WATER PUMP	> 33	0.02	
35. D.G. INLET SILENCER/AIR FILTER	55.6	Negligible	
36. D.G. EXCITATION CUBICLE	> 33	0.02	

Table D-1. Influence of Vertical Accelerations on Diablo Canyon Equipment (Cont.)

COMPONENT	VERTICAL FREQUENCY (Hz)	VERTICAL EXCITATION CONTRIBUTION	COMMENT
37. D.G. CONTROL PANEL	22	0.03	Structural
		Negligible	Functional
38. D.G. MAIN LEAD TERMINAL BOX	24	0.07	
39. CONTAINMENT FAN COOLER	66	0.05	
40. CONTROL ROOM VENTILATION SUPPLY FAN	> 33	0.05	
41. CONTROL ROOM VENTILATION AIR CONDITIONING UNIT/COMPRESSOR	> 33	0.13	
42. CONTROL ROOM VENTILATION CONTROL CABINET	28	0.05	
43. VITAL ELECTRICAL ROOM SUPPLY/RETURN FANS	> 33	0.03	
44. VITAL ELECTRICAL ROOM BACKDRAFT & SHUTOFF DAMPERS	> 33	Negligible	
45. 4.16 kV SWITCHGEAR	> 33	Negligible	Structural
	19 - 21	1.00	Functional
46. 4.16 kV POTENTIAL TRANSFORMER	33.7	0.02	Bus F
	> 50	0.02	Bus G & H
47. SAFEGUARD RELAY PANEL	50	0.01	Structural
		0.02	Functional
48. 125V DC BATTERIES	72	Negligible	
49. 125V DC BATTERY RACK	72	0.07	
50. 125V DC BATTERY CHARGER	> 35	0.10	
51. 125V DC SWITCHGEAR/BREAKER PANEL	> 35	0.02	
52. 120V AC INSTRUMENT BREAKER PANEL	> 33	Negligible	
53. 120V AC INVERTER	> 33	0.01	
54. 4.16kV/480V TRANSFORMER	13	0.02	
55. 480V BREAKER PANEL	> 35	0.73	
56. AUXILIARY RELAY PANEL	> 33	0.09	
57. MAIN CONTROL BOARD	> 33	< 0.35	
58. HOT SHUTDOWN PANEL	> 33	0.03	Structural
		Negligible	Functional
59. AUXILIARY SAFEGUARDS CABINET	> 33	0.02	
60. PROCESS CONTROL & PROTECTION CABINET	> 33	0.05	
61. SOLID STATE PROTECTION SYSTEM	> 33	Negligible	
62. REACTOR TRIP SWITCHGEAR	> 33	0.02	

Table D-1. Influence of Vertical Accelerations on Diablo Canyon Equipment (Cont.)

COMPONENT	VERTICAL FREQUENCY (Hz)	VERTICAL EXCITATION CONTRIBUTION	COMMENT
63. RESISTANCE & TEMPERATURE DETECTORS	Not Specified*	Negligible	
64. PRESSURE AND Δ P TRANSMITTER	> 33	Negligible	
65. AUXILIARY RELAY RACK	> 35	0.08	
66. LOCAL STARTER BOARD	32	0.11	
67. MOLDED CASE CIRCUIT BREAKER	> 33	0.03	
68. VALVE LIMIT SWITCH	> 35	Location Dependent	
69. IMPULSE LINE	5 - 20	Location Dependent	
70. CONTAINMENT PURGE VALVE	> 35	0.07	
71. OFF-SITE POWER	Various	Location Dependent	
72. PENETRATION/PENETRATION BOX	28	0.06	
73. BOP PIPING & SUPPORTS	Various 6 - 20	Up to 1.00	
74. BOP RELIEF & CHECK VALVES	Piping	0.06	
75. AIR & MOTOR OPERATED VALVES	Piping	Negligible	
76. CONDUIT, CABLE TRAYS & SUPPORTS	Various 6 - 35	Up to 0.95	
77. HVAC DUCTS & SUPPORTS	Various > 15	Up to 1.00	

* Fragility based on Incore Thermocouple Cabinet estimated to have a vertical frequency of approximately 30 Hz.

** Response information provided was insufficient to establish directional contribution fractions.

Table D-2. Calculation of Vertical Overtest Factor for the Diesel Generator Control Pad

Median vertical frequency = 22 Hz $\beta_f = 0.10$

Center Prob.	.n β	Frequency (Hz)	S_{av} (3%) (g)	TRS (3%) (g)	TRS/RRS	
0.05	-1.65	18.7	1.83	1.00	0.55	
0.15	-1.04	19.8	1.83	1.00	0.55	
0.25	-0.68	20.6	1.77	0.93	0.52	
0.35	-0.39	21.2	1.64	0.87	0.53	
0.45	-0.13	21.7	1.60	0.85	0.53	Median
0.55	+0.13	22.3	1.56	0.83	0.53	0.53
0.65	+0.39	22.9	1.54	0.81	0.53	
0.75	+0.68	23.6	1.50	0.80	0.53	
0.85	+1.04	24.4	1.45	0.80	0.55	
0.95	+1.65	26.0	1.39	0.77	0.55	

(15 - 20 Hz) $S_{av}^{3\%} = 1.20 S_{av}^{5\%}$

(20 - 26 Hz) $S_{av}^{3\%} = 1.17 S_{av}^{5\%}$

Table D-3. Calculation of Capacity Strength Factor for 4.16kV Switchgear Functional Failure Mode

Median vertical frequency = 20 Hz $\beta_f = 0.14$

Center Prob.	n β	Frequency (Hz)	S_{av} (g)	Amp.	F_s	
0.05	-1.65	15.9	4.75	1.00	1.84	
0.15	-1.04	17.3	4.35	1.03	1.95	
0.25	-0.68	18.2	4.12	1.40	1.52	
0.35	-0.39	18.9	3.95	1.52	1.46	
0.45	-0.13	19.6	3.85	1.65	1.38	Median
0.55	+0.13	20.4	3.73	2.65	0.88	1.57
0.65	+0.39	21.1	3.65	1.80	1.33	
0.75	+0.68	22.0	3.60	1.50	1.62	
0.85	+1.04	23.1	3.54	1.40	1.76	
0.95	+1.65	25.2	3.44	1.00	2.54	

$$F_s = \frac{1.15 x GERS}{Amp x S_{av}}$$

RESPONSE TO QUESTION 2a
Volume 1 of 2

January 1989

This volume is part of a set that responds to 47 questions asked of PG&E by the Nuclear Regulatory Commission (NRC) on December 13, 1988. The responses provide data requested to augment or clarify the Final Report of the Long Term Seismic Program submitted by PG&E to the NRC on July 31, 1988.

RESPONSE TO QUESTION 2a

QUESTION 2a

Provide copies of the following reports referenced in the LTSP Final Report:

a. *Bechtel Power Corporation, 1988, "CLASSI" Computer Program: Theoretical Manual, User's Manual, and Validation Report.*

The CLASSIF Computer Program Theoretical Manual (Attachment Q2a-1), User's Manual (Attachment Q2a-2) and Validation Manual (Attachment Q2a-3) follow. The "Description of Validation Test Problems and Results," Appendix A of the Validation Manual (Attachment Q2a-4) contains information proprietary to Bechtel Power Corporation. This attachment has been submitted to the NRC separately, with an Application for Withholding Proprietary Information from Public Disclosure, in accordance with 10 CFR 2.790 of the Commission's regulations.

ATTACHMENT Q2a-1

CONTINUUM
LINEAR
ANALYSIS FOR
SOIL
STRUCTURE
INTERACTION
-VERSION

CLASSIF THEORETICAL MANUAL

JULY 1988

CE934

BECHTEL POWER CORPORATION

CLASSIF

COMPUTER PROGRAM CLASSIF
THEORETICAL MANUAL

Prepared
for

Diablo Canyon
Long Term Seismic Program
Pacific Gas & Electric Company
San Francisco, California

by

Bechtel Western Power Corporation
San Francisco, California

July 27, 1988

PREFACE

CLASSI (Continuum Linear Analysis for Soil-Structure Interaction) is a linear three-dimensional, seismic soil-structure interaction (SSI) analysis program developed by Luco and Wong in 1976 at the University of California, San Diego. Since then, the CLASSI program has been continuously upgraded to expand its capabilities and efficiency from those of its initial development. Thus, various versions of the CLASSI program exist in the industry, each covering somewhat different analysis capabilities. The CLASSIF program is a Bechtel version of CLASSI program originally developed in 1978, and recently modified by Wong and Luco in 1985. During the course of installation, testing, and validation of the CLASSIF program on the Bechtel UNIVAC system, some modifications and enhancements were made to the code to improve its performance. These include: implement new algorithms for computing and inverting the Green's functions; add a capability for computing SSI responses to steady-state force excitation applied on the structure., add a capability for computing the relative displacement between two locations in the structure; add a capability for calculating the traction vectors used for a restart of analysis for new wave inputs, add a capability for calculating the transfer function between the SSI response motion and the scattered foundation input motions, implement a subroutine for reading in the fixed-based modal properties of structures generated from the BSAP-DYNAM program (a post processor for the Bechtel Structural Analysis Program); implement a free format for the input data and improve the printed output format, correct the option for generating foundation symmetry about one axis; correct the option for calculating the transfer function due to external forcing function, correct the option for calculating the SSI response to include contribution from more than one mode of response; implement the option to bypass a zero-mean baseline correction for calculating the time history response due to ground motion input.

This report has been prepared by Bechtel Power Corporation and has been reviewed following the Bechtel Standard Engineering Department Procedure for nuclear projects. This report has been prepared for incorporating the

published technical papers and reports by Luco and Wong relating to the theoretical formulations of the substructuring method used in CLASSI for solving the SSI problem. References to their papers and reports are acknowledged, wherever appropriate, in various sections of the report, and the list of references is provided.

This report was prepared under a contract agreement between PG&E and Bechtel and is intended for exclusive use by PG&E only. Except for copies that may be required for the Nuclear Regulatory Commission (NRC) in satisfying a regulatory requirement, no copy should be distributed outside of PG&E without prior written consent from Bechtel.

DISCLAIMER

Every reasonable effort was made to provide a comprehensive and flexible computer program. However, the computer program itself and associated documentation are supplied without representation of warranty, expressed or implied, as to its content, accuracy, or freedom from defects or errors.

TABLE OF CONTENTS

TABLE OF CONTENTS (Continued)

1. INTRODUCTION

This report presents the theoretical bases for the computer program CLASSIF which is a computer program for linear three-dimensional seismic soil-structure interaction (SSI) analyses using the halfspace continuum approach. The program solves the SSI problem in frequency domain using the Fast Fourier Transform technique. CLASSIF is comprised of three program modules (GLAYER, CLAF, and SSIF) developed to solve the SSI problem in separate steps; the results of individual steps by different modules are combined in the final interaction analysis module so as to satisfy the interaction conditions at the structural base. The GLAYER module computes the Green's functions of the displacement at the surface of horizontal soil layers over a halfspace. The CLAF module computes the foundation impedance functions and the scattered foundation input motions based on the Green's functions computed from the GLAYER module. The SSIF module forms the equations of motion of the SSI system and then computes the SSI responses of the system using the impedance functions and scattered foundation input motions as input.

The CLASSIF formulation of the SSI problem is presented in Section 2. The Green's functions for a layered halfspace are described in Section 3. In Section 4, the calculations of impedance and compliance function for rigid surface foundations using the Green's functions are presented in Section 3. The general wave fields for characterization of the free-field input motions to CLASSIF are presented in Section 5. Section 6 presents the procedure for the calculation of scattered foundation input motions. The equations of motion and solution procedure for the SSI problem are presented in Section 8. References are provided in Section 9.

2. FORMULATION OF THE SOIL-STRUCTURE INTERACTION PROBLEM

To provide a frame work for presenting the CLASSIF theory, the formulation of the soil-structure interaction problem for the case of an isolated structure on a rigid foundation supported on a layered viscoelastic medium as illustrated in Figure 2-1 is first described (Ref. 1). Based on the assumed linearity of the model, the response of the soil-structure system may be obtained in two stages. In the first stage, the frequency response of the system for harmonic excitation of the type $\exp(i\omega t)$ is obtained in the frequency domain. The second stage is to the evaluation of the corresponding time history response in the time domain by means of the Fourier synthesis given by:

$$U(t) = (1/2\pi) \int_{-\infty}^{\infty} U(\omega)\, e^{i\omega t}\, d\omega \qquad (2\text{-}1)$$

In this equation, $U(t)$ denotes the time history response; and $U(\ )$ represents the corresponding frequency response. The Fourier synthesis described by Eq. (2-1) is achieved numerically by the use of the Fast Fourier Transform algorithm (Ref. 2).

The approach used to obtain the frequency response for the complete soil-structure system is based on the substructuring technique as illustrated in Figure 2-2. The technique consists of subdividing the complete interaction problem into a series of simpler basic problems that can be solved independently. Once the solution for each of the basic problems is known, the response of the complete soil-structure system can then be obtained by combining the solutions to the basic problems.

The first basic problem that needs to be solved in the evaluation of the free-field response motion, i.e., the determination of the response of the soil deposit for a given incident seismic wave before the cavity for the foundation has been excavated. For a uniform or horizontally layered soil deposits and for plane incident waves, the free-field motion on the soil

surface may be characterized by: (1) the three-component displacement vector $\{U_g\}e^{i\omega t}$ at a reference point; (2) the wave field and azimuthal angle of direction of propagation of the incident wave, and (3) the vertical angle of incidence or the apparent horizontal velocity c of the incident wave. For a given seismic excitation characterized by prescribed wave fields, the three components of the free-field motions at the ground surface $\{U_g\}$ may not be independent. In addition, for surface wave excitations in a layered soil model, the apparent horizontal velocity c is frequency dependent. The characteristics of the free-field motion are discussed in Section 5.

The second basic problem is the evaluation of the frequency response of the rigid foundation bonded to the soil and subjected to harmonic incident seismic waves in absence of the superstructure. In this step, the foundation is assumed massless, the inertia of the foundation being incorporated at a later stage. The presence of the rigid imposes constraints and foundation modifies the free-field motions. The resulting response of the massless foundation, called scattered foundation input motion, is represented by a six-component vector

$$\{U_o^*\} = (\Delta_x^*, \Delta_y^*, \Delta_z^*, \theta_x^*, \theta_y^*, \theta_z^*)$$

in which Δ^*_x, Δ^*_y, and Δ^*_z, represent the translational components while θ^*_x, θ^*_y, and θ^*_z represent the rotational components of the response about the x, y, and z axes of the scattered foundation input motion at a reference point of the rigid foundation, respectively. The foundation input motion $\{U^*_o\}$ is a function of the frequency of the excitation, geometry of the foundation, characteristics of the soil deposit, and the type of seismic excitation wave field. The foundation input motion is related to the free-field motion through a transfer function matrix called the scattering matrix $[S(\omega)]$, as shown in block 2 of Figure 2-2. The determination of the scattered foundation input motion is discussed in Section 6.

When the inertias of the foundation and the presence of the superstructure are taken into account in the interaction, the total response $\{U_o\} = (\Delta_x, \Delta_y, \Delta_z, \theta_x, \theta_y, \theta_z)^T$ at a reference point of the rigid foundation may be written in the form

$$\{U_o\} = \{U_o^*\} + \{U_s\} \tag{2-3}$$

in which the 6 x 1 vector $\{U_s\}$ represents the additional response motion of the foundation resulting from the deformation of the soil caused by the inertial forces and moments that exert on the soil medium through the foundation. These forces and moments can be represented by the 6 x 1 vector $\{F_s\} = (F_{xs}, F_{ys}, F_{zs}, M_{xs}, M_{zs}, M_{zs},)^T$, in which F_{xs}, F_{ys}, and F_{zs} represent the resultant force components, while M_{xs}, M_{ys}, and M_{zs} denote the resultant moment components about the reference point in the foundation.

The response motion $\{U_s\}$ of the foundation caused by the inertias of the structure and foundation can be related to the generalized forces $\{F_s\}$ by the relation:

$$\{U_s\} = [C(\omega)]\{F_s\} \tag{2-4}$$

where $[C(\omega)]$ is the 6 x 6 foundation compliance matrix associated with the rigid foundation. Thus, the third basic problem is to evaluate the foundation compliance matrix associated with the rigid foundation. The evaluation of the foundation compliance matrix is described in Section 4. The compliance matrix is a function of the frequency of the excitation, the geometry of the foundation, and the characteristics of the underlying soil deposit, and can be derived from the point force solution for a halfspace called Green's function. This will be described in Section 3.

Let $\{F_b\} = (F_{xb}, F_{yb}, F_{zb}, M_{xb}, M_{yb}, M_{zb})^T$ represents the resultant forces and moments of the superstructure acting on the foundation, the equation of motion for the rigid foundation can be written in the form

$$\{F_s\} = \omega^2 [M_0] \{U_0\} + \{F_b\} \quad (2\text{-}5)$$

where $[M_0]$ is the 6 x 6 mass matrix for the rigid foundation.

The generalized inertia force $\{F_b\}$ of the superstructure acting on the foundation can be expressed in terms of the product of the total response motion of the foundation $\{U_0\}$ and the equivalent mass of the superstructure through the relation

$$\{F_b\} = \omega^2 [M_b(\omega)]\{U_0\} \quad (2\text{-}6)$$

where $[M_b(\omega)]$ plays the role of a 6 x 6 frequency-dependent equivalent mass matrix. This matrix can be derived from the geometry, mass distribution and elastic properties of the superstructure. Thus the fourth basic problem is the derivation of this equivalent mass matrix $[M_b(\omega)]$. This derivation will be discussed in Section 7.

Once the basic problems as described previously have been solved, the total response motion $\{U_0\}$ of the foundation, including the soil structure interaction effects, can be obtained by elimination $\{F_b\}$, $\{F_s\}$ and $\{U_s\}$ from Eqs. (2-3) through (2-6). The resulting expression is

$$\{U_0\} = ([I]-\omega^2 [C(\omega)] ([M_0] + [M_b(\omega)]))^{-1} \{U_0^*\} \quad (2\text{-}7)$$

in which [I] denotes the 6 x 6 identity matrix. The various terms in equation (2-7) represents the different interaction effects. The effects of scattering of the incident seismic waves by the rigid foundation are included in the scattered foundation input motion vector $\{U_0^*\}$. The interaction effects between the superstructure, foundation and soil are represented in Eq. (2-7) by the term $[C(\omega)]([M_0] + [M_b(\omega)])$. The total motion of the foundation $\{U_0\}$ results from a combination of both types of effects as shown in the feedback block diagram of Figure 2-2.

Once the total motion of the foundation has been obtained, the response at any location in the superstructure can be easily obtained by the back substitution technique (Section 7).

The formulation described above for the SSI problem involving a single structure can be readily extended to the case involving several independent structures interacting through the soil. In this case, the foundation response vector $\{U_0\}$ includes six degrees of freedom for each of the N foundations, and the matrices $[M_0]$ and $[M_b(\omega)]$ are block diagonal of dimensions 6N x 6N. The coupling between foundations is incorporated in the compliance matrix $[C(\omega)]$ and in the foundation input motion $\{U_0^*\}$.

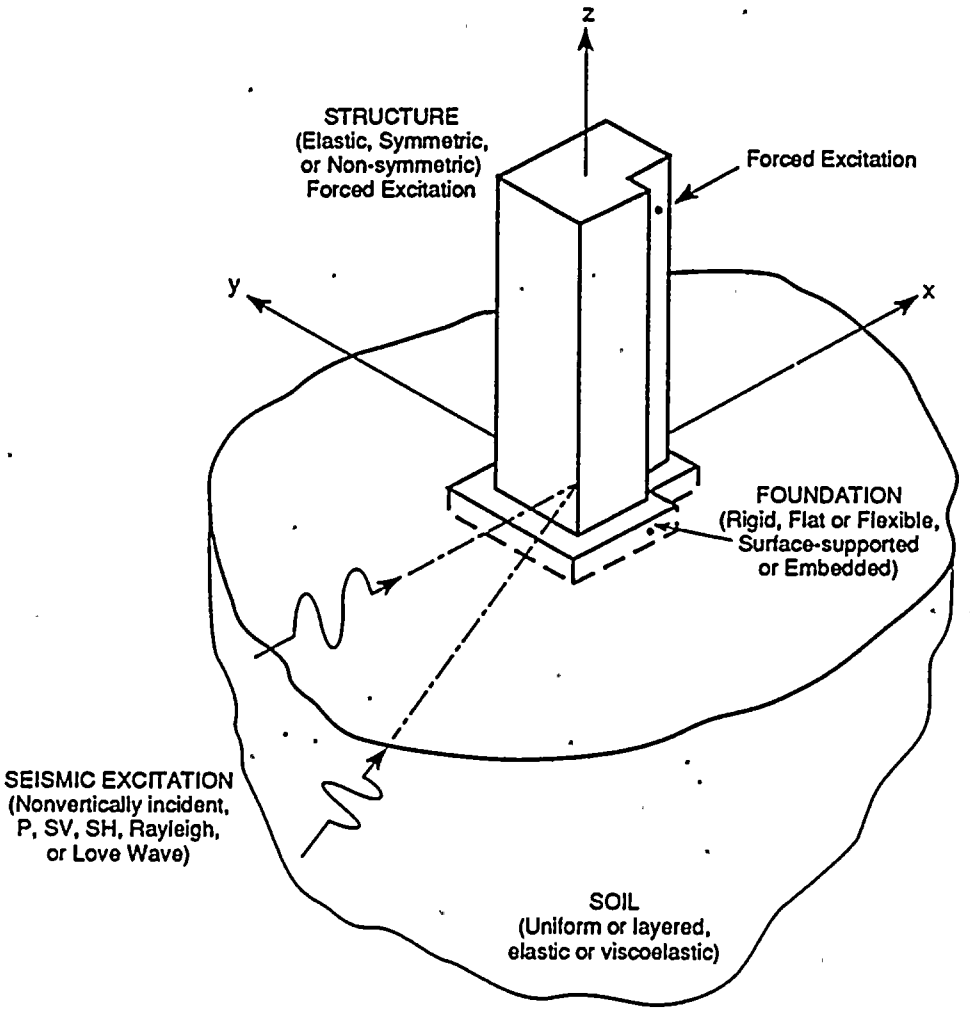

Figure 2-1. Description of the Soil-Structure System

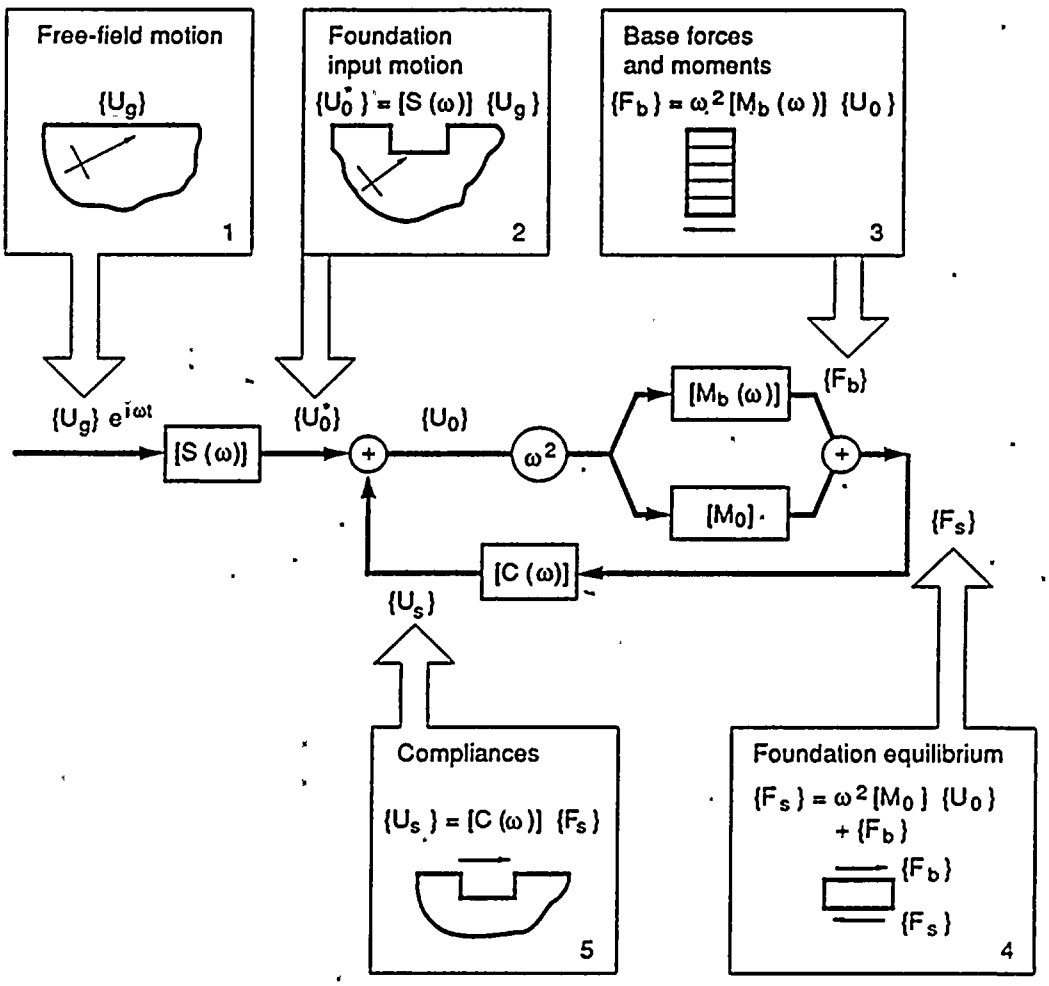

Figure 2-2. Interaction Block Diagram

3. GREEN'S FUNCTIONS FOR A LAYERED HALFSPACE

Using the principle of superposition in linear elastodynamic theory, the displacement and stress fields generated by point forces can be used to calculate similar fields generated by an arbitrary stress distribution. These point force solutions, called Green's functions, can be derived for any medium theoretically. Consider the set of harmonic point load, with amplitudes, $\underset{\sim}{P} = (P_x, P_y, P_z)^T$, acting at the source point $\underset{\sim}{r}_o = (x_o, y_o, 0)^T$ on the free surface of a soil medium, the harmonic displacements, with amplitudes, $\underset{\sim}{U} = (U_x, U_y, U_z)^T$, at the observation point $\underset{\sim}{r} = (x, y, 0)^T$ are related to the point load by the 3 x 3 Green's function matrix [G] as

$$\underset{\sim}{U}\, e^{i\omega t} = [G(\omega, \underset{\sim}{r} - \underset{\sim}{r}_o, \underset{\sim}{p})]\, \underset{\sim}{P}\, e^{i\omega t} \qquad (3\text{-}1)$$

in which ω is the excitation frequency, and $\underset{\sim}{p}$ is a symbolic representation of the material properties of the underlying soil medium. The notation is such that z is the component normal to the soil surface, while x and y are the tangential components in the X and Y directions, respectively.

As shown in Eq. (3-1), [G] is a function of the excitation frequency ω, the relative position of $\underset{\sim}{r}$ and $\underset{\sim}{r}_o$, and the property vector $\underset{\sim}{p}$. There are many properties of an inhomogeneous soil medium that can influence the Green's function; in particular, the vector $\underset{\sim}{p}$ for a horizontally layered medium is

$$\underset{\sim}{p} = \{n;\ \mu_1, \mu_2, \ldots, \mu_n;\ \beta_1, \beta_2, \ldots, \beta_n;\ \rho_1, \rho_2, \ldots, \rho_n;\ h_1, h_2, \ldots, h_n;\ \nu_1, \nu_2, \ldots, \nu_n;\ \xi_1, \xi_2, \ldots, \xi_n\} \qquad (3\text{-}2)$$

where n = the number of layers,
μ_i = the shear modulus of the i^{th} layer,
β_i = the shear wave velocity of the i^{th} layer,
ρ_i = the mass density of the i^{th} layer,
h_i = the thickness of the i^{th} layer,
ν_i = the Poisson's ratio of the i^{th} layer, and
ξ_i = the critical damping factor of the i^{th} layer

To account for all the parameters, the Green's function calculation requires a lengthy numerical integration of the Hankel transform-type integral representation as presented by Luco and Apsel in Refs (3) and (4). Furthermore, [G] in Eq. (3-1) must be calculated repeatedly for different frequencies during numerical integration to obtain the foundation impedance matrix, as will be described in Section 4, thus, the cost of the computation increases dramatically. To reduce overlapping calculations, the program CLAF has adopted a scheme which interpolates the values of [G] from a precalculated table using a numerical solution technique that will be described in Section 8.

For a given $\underset{\sim}{p}$ and ω, [G] is a function of $\underset{\sim}{r} - \underset{\sim}{r}_0 = (x - x_0, y - y_0, 0)^T$, a total of two spatial variables. The number of independent variables, however, can be reduced to one for the horizontal homogeneous layered soil medium if the polar coordinate system (R,ψ,z'), shown in Figure 3-1, is used. To separate the singularities from [G] and to render [G] dimensionless, a new matrix [G'] may be defined as

$$[G(\omega, \underset{\sim}{r}-\underset{\sim}{r}_0, \underset{\sim}{p})] = [G'(b_0, \psi, \underset{\sim}{p}')]/\mu R \qquad (3\text{-}3)$$

where

$$R = |r-r_0| = \sqrt{(x-x_0)^2+(y-y_0)^2}$$

$$\psi = \arg(\underset{\sim}{r}-\underset{\sim}{r}_0) = -\tan^{-1}((y-y_0)/(x-x_0))$$

$$b_0 = \omega R/\beta$$

$$\underset{\sim}{p}' = (n,; \mu_1/\mu, \mu_2/\mu, \text{--}, \mu_n/\mu; \beta_1/\beta, \beta_2/\beta, \text{--}, \beta_n/\beta;$$
$$\rho_1/\rho, \rho_2/\rho, \text{--}, \rho_n/\rho; h_1/h, h_2/h, \text{--}, h_n/h;$$
$$\nu_1, \nu_2, \text{--}, \nu_n; \xi_1, \xi_2, \text{--}, \xi_n)$$

The reference values of μ, β, and ρ, used to normalize p' and [G'], are usually taken to be those of the top layer.

Using the reciprocity relationships, the off-diagonal terms of [G'] can be related as

$$g'_{xy} = g'_{yx}$$
$$g'_{xz} = -g'_{zx} \qquad (3\text{-}4)$$
$$g'_{yz} = -g'_{zy}$$

leaving only 6 independent elements in [G']. But a simpler form of [G'] can be obtained by using the cylindrical coordinate system. Since the point forces are axisymmetric, hence, the general displacement-force relationship in cylindrical coordinates can be written in a form of a 3 x 2 matrix as

$$\mu R \begin{Bmatrix} U_r(\underset{\sim}{r}) \\ U_\psi(\underset{\sim}{r}) \\ U_z'(\underset{\sim}{r}) \end{Bmatrix} = \begin{bmatrix} f_{rr}\cos(\psi-\psi_o) & f_{rz}' \\ f_{\psi r}\sin(\psi-\psi_o) & f_{\psi z}' \\ f_{z'r}\cos(\psi-\psi_o) & f_{z'z'} \end{bmatrix} \begin{Bmatrix} P_r(\psi_o) \\ P_z' \end{Bmatrix} \qquad (3\text{-}5)$$

in which, $f_{z'r} = -f_{rz}'$, $f_{\psi z}' = 0$, $\sin\psi = -(y-y_o)/R$, $\cos\psi = (x-x_o)/R$. The four independent functions, f_{rr}, $f_{\psi r}$, $f_{z'r}$, and $f_{z'z'}$ are functions of the dimensionless frequency, b_o.

To calculate the Green's function [G'] in the cartesian coordinate system, the following mappings for the forces and displacements may be used.

$$\begin{Bmatrix} P_x(\underset{\sim}{r}_o) \\ P_y(\underset{\sim}{r}_o) \\ P_z(\underset{\sim}{r}_o) \end{Bmatrix} = \begin{Bmatrix} P_r(o) \\ P_r(-\pi/2) \\ -P_z' \end{Bmatrix} \qquad (3\text{-}6)$$

and

$$\begin{Bmatrix} U_x(\underset{\sim}{r}) \\ U_y(\underset{\sim}{r}) \\ U_z(\underset{\sim}{r}) \end{Bmatrix} = \begin{bmatrix} \cos\psi & -\sin\psi & 0 \\ -\sin\psi & -\cos\psi & 0 \\ 0 & 0 & -1 \end{bmatrix} \begin{Bmatrix} U_r(\underset{\sim}{r}) \\ U_\psi(\underset{\sim}{r}) \\ U_z'(\underset{\sim}{r}) \end{Bmatrix} \qquad (3\text{-}7)$$

Eq. (3-6) can be used with Eq. (3-5) to relate the displacement in polar coordinates to the force in cartesian coordinates as

$$\mu R \begin{Bmatrix} U_r(\underset{\sim}{r}) \\ U_\psi(\underset{\sim}{r}) \\ U_z'(\underset{\sim}{r}) \end{Bmatrix} = \begin{bmatrix} f_{rr}\cos\psi & f_{rr}\cos(\psi+\pi/2) & -f_{rz}' \\ f_{\psi r}\sin\psi & f_{\psi r}\sin(\psi+\pi/2) & 0 \\ -f_{rz}'\cos\psi & -f_{rz}'\cos(\psi+\pi/2) & -f_{z'z'} \end{bmatrix} \begin{Bmatrix} P_x(\underset{\sim}{r}_o) \\ P_y(\underset{\sim}{r}_o) \\ P_z(\underset{\sim}{r}_o) \end{Bmatrix} \qquad (3\text{-}8)$$

Eq. (3-7) can relate the displacements and the forces, both in the cartesian coordinates as

$$\begin{Bmatrix} U_x(\underset{\sim}{r}) \\ U_y(\underset{\sim}{r}) \\ U_z(\underset{\sim}{r}) \end{Bmatrix} =$$

$$\frac{1}{\mu R} \begin{bmatrix} f_{rr}\cos^2\psi - f_{\psi r}\sin^2\psi & -(f_{rr}+f_{\psi r})\sin\psi\cos\psi & -f_{rz}'\cos\psi \\ -(f_{rr}+f_{\psi r})\sin\psi\cos\psi & f_{rr}\sin^2\psi - f_{\psi r}\cos^2\psi & f_{rz}'\sin\psi \\ f_{rz}'\cos\psi & -f_{rz}'\sin\psi & f_{z'z'} \end{bmatrix} \begin{Bmatrix} P_x(\underset{\sim}{r}_o) \\ P_y(\underset{\sim}{r}_o) \\ P_z(\underset{\sim}{r}_o) \end{Bmatrix} \qquad (3\text{-}9)$$

Using the definition of Eq. (3-3), the elements of matrix [G'] are defined as

$$\begin{aligned} g'_{xx}(b_o, \psi, \underset{\sim}{P}') &= f_{rr}(b_o, \underset{\sim}{P}')\cos^2\psi - f_{\psi r}(b_o, \underset{\sim}{P}')\sin^2\psi \\ g'_{xy}(b_o, \psi, \underset{\sim}{P}') &= -[f_{rr}(b_o, \underset{\sim}{P}') + f_{\psi r}(b_o, \underset{\sim}{P}')]\sin\psi\cos\psi \\ g'_{xz}(b_o, \psi, \underset{\sim}{P}') &= -f_{rz}'(b_o, \underset{\sim}{P}')\cos\psi \\ g'_{yy}(b_o, \psi, \underset{\sim}{P}') &= f_{rr}(b_o, \underset{\sim}{P}')\sin^2\psi - f_{\psi r}(b_o, \underset{\sim}{P}')\cos^2\psi \\ g'_{yz}(b_o, \psi, \underset{\sim}{P}') &= f_{rz}'(b_o, \underset{\sim}{P}')\sin\psi \\ g'_{zz}(b_o, \psi, \underset{\sim}{P}') &= f_{z'z'}(b_o, \underset{\sim}{P}') \\ g'_{yx} &= g'_{xy} \; ; \; g'_{zx} = -g'_{xz} \; ; \; g'_{zy} = -g'_{yz} \end{aligned} \qquad (3\text{-}10)$$

where f_{rr}, $f_{\psi r}$, f_{rz}', and $f_{z'z'}$ are the Green's functions in polar coordinates multiplied by μR. For a given $\underset{\sim}{p}'$, the functions f are dependent on only one dimensionless variable b_o, thus the Green's function table generated from GLAYER as input into CLAF requires only four complex functions tabulated versus b_o. The range of the table should begin at $b_o = 0$ and end at $b_o = \omega \ell_{max}/\beta$, with ℓ_{max} being the maximum possible length of the foundation mat. The six independent elements listed above are in the most convenient forms for numerical calculation using the integration method derived by Apsel and Luco (Ref. 4) to calculate f_{rr}, $f_{\psi r}$, f_{rz}' and $f_{z'z'}$.

For a given layered stratum, a Green's function table must be calculated for each frequency. For a homogeneous half-space, however, one table is sufficient for all frequencies because p' is not a function of frequency (no finite thicknesses). The limit of the Green's function table for the latter case should be extended to $b_o = \omega_{max}\, \ell_{max}/\beta$ in order to accommodate all frequencies of interest below ω_{max}.

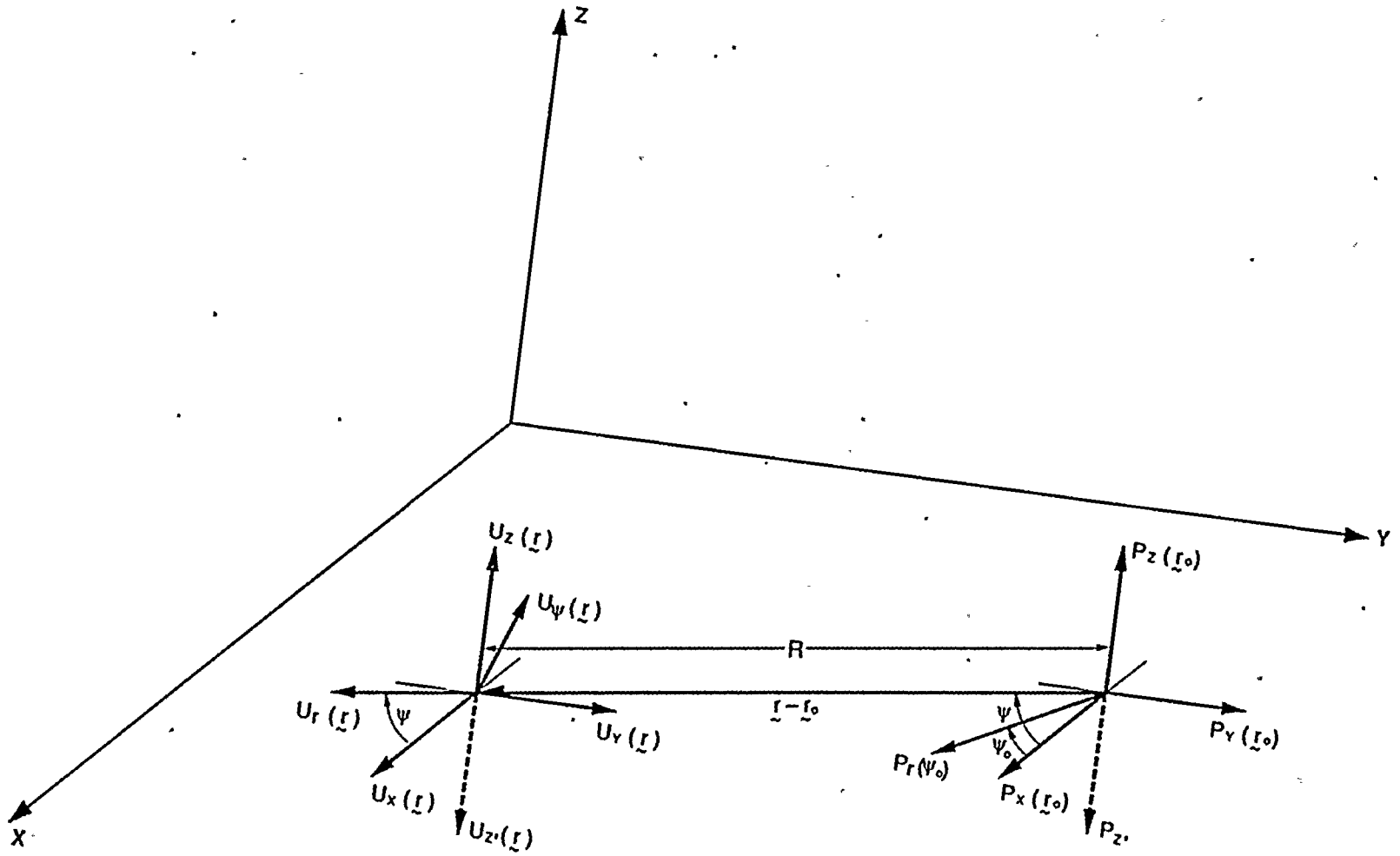

Figure 3-1. Polar Coordinate System of Green's Function

4. IMPEDANCE AND COMPLIANCE MATRICES

One of the key elements in the characterization of the soil-structure interaction system is the impedance matrix for the foundation. For rigid foundations, the impedance matrix relates the harmonic generalized force that the foundation exerts on the soil to the harmonic generalized displacement of the foundation. The compliance function is defined as the inverse of the impedance matrix.

To evaluate these dynamic force-displacement relationships numerically for a rigid foundation of arbitrary shape placed on the surface of a soil deposit, the contact area between the rigid foundation and the soil medium is discretized into a number of small rectangular subregions over which the contact tractions are assumed to be uniform. Using the Green's functions generated, the displacements generated by the uniform tractions of unknown magnitudes in these subregions can be formulated and by invoking the displacement boundary conditions of a rigid foundation, a system of linear algebraic equations in the variables of the unknown contact tractions in each subregion is obtained. Once these equations are solved for the contact tractions, the total forces and moments acting on the rigid massless foundation can be computed by direct integrations, giving the desired dynamic force-displacement relationship for the foundation.

Considering the general case of multiple-foundation model as illustrated in Figure 4-1, which involves N independent massless rigid foundations of arbitrary shape bonded to the surface of a common layered viscoelastic halfspace. The foundations are subjected to harmonic external forces and moments and to harmonic seismic waves excitations. The response of each rigid foundation can be described by three translational and three rotational degrees of freedom as shown in Figure 4-1.

The desired dynamic force-displacement relation for the N foundations including the through-soil coupling effects can be written in the frequency domain as follows:

$$F_S = [K] \cdot (\{U_O\} - \{U_O^*\}) \qquad (4\text{-}1)$$

in which $\{F_S\}$ is the 6N vector of harmonic generalized external forces acting on the N foundations including 3N forces and 3N moments; [K] is the 6N x 6N impedance (or dynamic stiffness) matrix for the system of N foundations; $\{U_O\}$ is the 6N x 6N harmonic generalized displacement vector for the foundations and $\{U_O^*\}$ is the 6N x 6N generalized scattered foundation input motion vector induced by the seismic excitation in absence of external forces. Both $\{U_O\}$ and $\{U_O^*\}$ include 3N translational and 3N rotational components. The vector $\{F_O^*\}$ defined by:

$$\{F_O^*\} = [K]\{U_O^*\} \qquad (4\text{-}2)$$

is the generalized seismic driving force vector which represents the forces and moments that the soil exerts on the foundations when the foundations are held fixed under the action of the seismic wave excitation in the soil medium.

The components of the vectors $\{F_S\}$ and $\{U_O\}$ are arranged in the form

$$\{F_S\}^T = (\{F_{S1}\}^T, \{F_{S2}\}^T, \text{--}, \{F_{SN}\}^T) \qquad (4\text{-}3)$$

$$\{U_O\}^T = (\{U_{O1}\}^T, \{U_{O2}\}^T, \text{--}, \{U_{ON}\}^T) \qquad (4\text{-}4)$$

in which the vector $\{F_{Si}\}$ defined by

$$\{F_{Si}\} = (F^i_{SX}, F^i_{Sy}, F^i_{Sz}, M^i_{SX}/a, M^i_{Sy}/a, M^i_{Sz}/a)^T \quad , \quad i=1,\ldots, N$$

includes the resultant external force $(F^i_{SX}, F^i_{Sy}, F^i_{Sz})$ and the resultant external moment $(M^i_{SX}, M^i_{Sy}, M^i_{Sz})$ about a point of reference $(x_i, y_i, 0)$ acting on the ith foundation. The components of the resultant moment are normalized by a reference length of a. The vector $\{U_{Oi}\}$ defined by

$$\{U_{Oi}\} = (U^i_{Ox}, U^i_{Oy}, U^i_{Oz}, a\theta^i_{Ox}, a\theta^i_{Oy}, a\theta^i_{Oz})^T \quad , \quad i=1,\ldots, N$$

includes the displacement (U^i_{ox}, U^i_{oy}, U^i_{oz}) at the point of reference (x_i, y_i, 0) and the rotation vector (θ^i_{ox}, θ^i_{oy}, θ^i_{oz}) normalized by the length of reference a. The components of $\{F_o^*\}$ and $\{U_o^*\}$ are arranged similarly.

To obtain the impedance matrix [K], it is necessary to solve a mixed boundary-value problem in which vanishing tractions are imposed on the portion of the surface z = 0 not covered by the rigid foundations while displacement constraints in the form of rigid-body displacements are imposed on the foundation contact areas. The problem can be formulated by means of the integral representation as follows:

$$\{U(\vec{x})\} = \sum_{j=1}^{N} \int_{S_j} [G(\omega, \vec{x}-\vec{\zeta}, \underset{\sim}{P})] \; T_j(\vec{\zeta}) \; dS_j(\vec{\zeta}) + \{U_g(\vec{x})\} \quad (4\text{-}5)$$

in which $\{U(\vec{x})\} = (U_x, U_y, U_z)^T$ represents the displacement vector at a point $\vec{x}$ on the soil surface; $T_j(\vec{\zeta})$ the vector of tractions that the jth foundation exerts on the soil; [G] is the 3 x 3 matrix of Green's functions; S_j is the area of the jth foundation; and $\{U_g(\vec{x})\}$ is the free-field motion on the ground surface. For numerical computations each of the N foundations is discretized into smaller rectangular subregions over which the tractions are assumed to be uniform. Based on this discretization, the discrete form of Eq. (4-5) becomes

$$\{\bar{U}_{ik}\} = \sum_{j=1}^{N} \sum_{\ell=1}^{n_j} [G_{ij}^{k\ell}]\{R_{j\ell}\} + \{\bar{U}_{gik}\} \quad (4\text{-}6)$$

in which $\{\bar{U}_{ik}\}$ represents the vector of averaged displacement over the kth subregion of the ith foundation and $\{\bar{U}_{gik}\}$ the corresponding averaged free-field motion. The vector $\{R_{j\ell}\}$ represents the resultant of the traction vector over the ℓth subregion of the jth foundation and n_j is the number of subdivision of the jth foundation. The matrix $[G_{ij}^{k\ell}]$ is defined by

$$[G_{ij}^{k\ell}] = \frac{1}{S_{ik}S_{j\ell}} \int_{S_{ik}} \int_{S_{j\ell}} [G(\omega, \vec{x}-\vec{\zeta}, \underset{\sim}{P})]\, dS_{ik}(\vec{x})\, dS_{j\ell}(\vec{\zeta}) \qquad (4\text{-}7)$$

in which S_{ik} represents the area of the kth subregion of the ith foundation. The numerical integration procedure for calculating the Green's functions for a layered half-space appearing in Eq. (4-7) are described by Apsel and Luco in Ref. (4). The procedure uses separate integration schemes for the singularities and the regular part of the integrand. The singularities of the integrand, contained in the static Green's functions for a uniform half-space, are integrated analytically. The remaining non-singular part of the integrand is integrated by Gaussian quadrature.

In matrix notation, Eq. (4-6) can be written in the form

$$\begin{Bmatrix} \bar{U}_1 \\ \bar{U}_2 \\ \vdots \\ \bar{U}_N \end{Bmatrix} = \begin{bmatrix} G_{11} & G_{12} & \cdots \\ G_{21} & G_{22} & \cdots \\ \vdots & \vdots & \\ & & G_{NN} \end{bmatrix} \begin{Bmatrix} R_1 \\ R_2 \\ \vdots \\ R_N \end{Bmatrix} + \begin{Bmatrix} \bar{U}_{g1} \\ \bar{U}_{g2} \\ \vdots \\ \bar{U}_{gN} \end{Bmatrix} \qquad (4\text{-}8)$$

in which the vectors $\{\bar{U}_i\}$ and $\{R_i\}$ represent the average displacement and the resultant forces over each of the subregions of the ith foundation, respectively. The vectors $\{\bar{U}_{gi}\}$ and the submatrices $[G_{ij}]$ are defined similarly. Since the subregion are rectangular in shape, the average value is assumed to be the value at the center of the subregion in CLAF.

The displacement boundary condition on S_i, averaged over each subregion of S_i, is given by

$$\{\bar{U}_i\} = [\alpha_{ii}]\, \{U_{oi}\} \qquad (4\text{-}9)$$

where $\{U_{oi}\}$ is the 6 x 1 vector of generalized displacements for the ith foundation and $[\alpha_{ii}]$ is a $3n_i$ x 6 matrix connecting the motion of the center of area of each subregion with each of the rigid-body degrees of freedom of the ith foundation, and is given by

$$[\alpha_{ij}]^T = \begin{bmatrix} 1 & 0 & 0 & \cdot & 1 & 0 & 0 & \cdot \\ 0 & 1 & 0 & \cdot & 0 & 1 & 0 & \cdot \\ 0 & 0 & 1 & \cdot & 0 & 0 & 1 & \cdot \\ 0 & 0 & \bar{y}_{i1}/a & \cdot & 0 & 0 & \bar{y}_{i2}/a & \cdot \\ 0 & 0 & -\bar{x}_{i1}/a & \cdot & 0 & 0 & -\bar{x}_{i2}/a & \cdot \\ -\bar{y}_{i1}/a & \bar{x}_{i1}/a & 0 & \cdot & -\bar{y}_{i2}/a & \bar{x}_{i2}/a & 0 & \cdot \end{bmatrix} \quad (4\text{-}10)$$

in which $(\bar{x}_{ik}, \bar{y}_{ik})$ are the coordinates of the center of area of the kth subregion of the ith foundation. The displacement boundary condition for all N foundations can then be written in the form

$$\{\bar{U}\} = [\alpha]\{U_0\} \quad (4\text{-}11)$$

in which $\{\bar{U}\} = (\{\bar{U}_1\}^T, \{\bar{U}_2\}^T, \ldots, \{\bar{U}_N\}^T)^T$, $\{U_0\}$ is the generalized displacement vector for the N foundations and $[\alpha]$ is a block diagonal matrix of $[\alpha_{ij}]$.

Substitution from Eq. (4-11) into Eq. (4-8) and solving for $\{R\} = (\{R_1\}^T, \{R_2\}^T, \ldots, \{R_N\}^T)^T$ leads to

$$\{R\} = [G]^{-1}[\alpha]\{U_0\} - [G]^{-1}\{\bar{U}_g\} \quad (4\text{-}12)$$

in which [G] is the matrix of Green's function appearing in Eq. (4-8) and $\{\bar{U}_g\} = (\{\bar{U}_{g1}\}^T, \{\bar{U}_{g2}\}^T, \ldots \{\bar{U}_{gN}\}^T)^T$.

The generalized force $\{F_{si}\}$ that the ith foundation exerts on the soil is given by

$$\{F_{si}\} = [\alpha_{ii}]^T \{R_i\} \quad (4\text{-}13)$$

considering all N foundations, Eq. (4-13) becomes

$$\{F_s\} = [\alpha]^T \{R\} \quad (4\text{-}14)$$

in which $\{F_s\}$ is the generalized force vector for the N foundations.

Substitution from Eq. (4-12) into Eq. (4-14) and comparison with Eqs. (4-1) and (4-2) leads to

$$[K] = [\Gamma]^T [\alpha] \tag{4-15}$$

and

$$\{F_o^*\} = [\Gamma]^T \{U_g\} \tag{4-16}$$

where

$$[\Gamma] = [G]^{-1} [\alpha] \tag{4-17}$$

Eqs. (4-15) and (4-16) indicate that both the impedance matrix and the driving force vector can be easily calculated once the matrix $[\Gamma]$ has been obtained. The columns of the matrix $[\Gamma]$ represent the contact tractions on all the subregions for unit rigid body motions of the foundations in the order (U^1_{ox}, U^1_{oy}, U^1_{oz}, a θ^1_{ox}, a θ^1_{oy}, a θ^1_{oz}, U^2_{ox}, U^2_{oy}, ...).

When the number of foundations is large, the order 3M x 3M ($M = \sum_{j=1}^{N} n_j$) of the complex matrix [G] appearing in Eq. (4-17) is large and the direct solution of the matrix equation required to calculate [G] can become costly. Recognizing that the dominant terms of [G] are block diagonal, a special iterative solution scheme which circumvents the costly direct solution is described in Section 8.

Let [C] represent the compliance matrix for the foundations. By definition of the compliance matrix,

$$[C] = [K]^{-1} \tag{4-18}$$

By substituting [K] from Eq. (4-15) into Eq. (4-18), [C] can be calculated by

$$[C] = ([\Gamma]^T [\alpha])^{-1} = [\alpha]^T [G] [\alpha] \qquad (4\text{-}19)$$

where $[\Gamma]$ and $[\alpha]$ are as defined in Eqs. (4-17) and (4-10), respectively.

Once the compliance matrix and the traction matrix are known, the scattered foundation input motion vector can be easily obtained as described in Section 6.

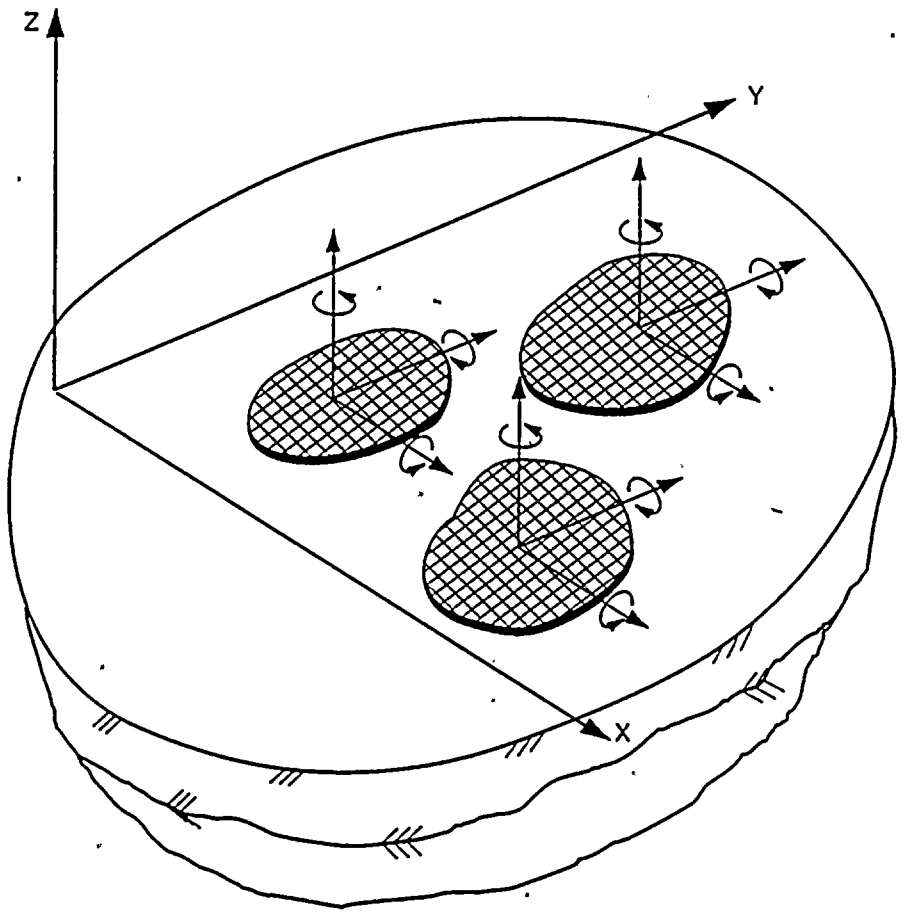

Fig. 4-1. Description of the Model and Coordinate System

5. FREE-FIELD MOTION

The characterization of free-field motion in CLASSIF requires the specification of the three time history components of motion at a point, two equivalent phase velocities, the incidence angle of wave propagation direction and the incident wave type. The free-field surface motion derived from this model has a uniform amplitude of motion but with phase differences at different points on the ground surface.

In order to avoid using too many parameters for describing each incident wave field, the free-field motions prescribed on the ground surface are represented in CLASSIF by the following general wave form:

$$\begin{Bmatrix} u_L(\omega) \\ u_T(\omega) \\ u_V(\omega) \end{Bmatrix} = \begin{Bmatrix} \hat{u}_L \\ \hat{u}_T \\ \hat{u}_V \end{Bmatrix} e^{-i(\omega/c(\omega))x'} F(\omega) \qquad (5\text{-}1)$$

in which $x' = x\cos\theta + y\sin\theta$,

θ = the direction of wave propagation measured counter-clockwise to the x-axis,

$F(\omega)$ = Fourier transform of the free-field ground motion,

$c(\omega)$ = the apparent wave propagation velocity,

$\hat{u}_L, \hat{u}_T, \hat{u}_V$ = the complex amplitude of the longitudinal, transverse, and vertical components, respectively, as shown in Figure 5-1.

The general wave field described in the form of Eq. (5-1) is intended to separate the more complex frequency function of the motion pertaining to the time history of the motion from the more smooth frequency function that describes the wave field characteristics of the soil medium. The form has the advantage that for many idealized simple wave fields, at least one of the parameters $\hat{u}_L$, $\hat{u}_T$, and $\hat{u}_V$ can be prescribed as a constant over frequency. For example, only the $u_T(\omega)$ component is nonzero for SH or Love waves; therefore, by setting $\hat{u}_T = 1$, and $F(\omega) = u_T(\omega)$ at $x' = 0$, Eq. (5-1) has effectively separated the seismic frequency content from the wave form. For P, SV, or Rayleigh waves in a layered medium, the $u_L(\omega)$

and $u_\gamma(\omega)$ components are coupled; the best method is to make $\hat{u}_L = 1$, $\hat{u}_\gamma(\omega) = u_\gamma(\omega)/u_L(\omega)$ and $F(\omega) = u_L(\omega)$ at $x' = 0$. The ratio $\hat{u}_\gamma(w)$ for this case is still a function of frequency (except for a uniform half-space), but it is a smooth frequency function in the form of the impedance matrix $[K(\omega)]$ because the seismic frequency contents are represented by $F(\omega)$. Alternatively, the same motions can be prescribed by setting $\hat{u}_\gamma = 1$, $\hat{u}_L(\omega) = u_L(\omega)/u_\gamma(\omega)$, and $F(\omega) = u_\gamma(\omega)$ at $x' = 0$.

The phase term $e^{-i(\omega/c(\omega))x'}$ in Eq. (5-1) describes the variation of phase along the direction of propagation x'. The apparent velocity of wave propagation, $c(\omega)$, determines the wavelength on the surface and is therefore instrumental in determining the amount of wave scattering from the foundation. For body waves in an elastic medium, $c(\omega)$ is a constant and is related to the angle of wave incidence. For example, the apparent velocity is infinite ($c \rightarrow \infty$) for vertically incident S or P waves because the phase is identical for all points on the surface. For other angles of incidence, $c = 1/\cos\theta_\gamma$, where θ_γ is an angle measured with respect to the horizontal axis x'.

For surface waves in a layered medium, $c(\omega)$ is a function of frequency (except for a Rayleigh wave in a uniform half-space) and it is equal to the phase velocity of the surface waves. The variation of velocity $c(\omega)$ with frequency is different for each mode of surface waves; furthermore, some modes do not exist below a critical frequency. Thus, the normalized amplitudes $\hat{u}_L$, $\hat{u}_T$, or $\hat{u}_\gamma$ should be set to zero for frequencies lower than the critical frequency.

Using the representation of Eq. (5-1), free-field motions that are comprised of "N_W" plane wave fields such that the ith plane wave has a frequency content $F_i(\omega)$, a propagation velocity $c_i(\omega)$, and a direction of propagation, θ_i, can be represented in CLASSIF by the following general form:

$$\{U_g\} = [\hat{W}]\{F(\omega)\} \qquad (5\text{-}2)$$

where $\{U_g\}^T = (U_{gx}, U_{gy}, U_{gz})^T$, and $[\hat{W}]$ is the normalized wave form matrix given by

$$[\hat{W}] = \begin{bmatrix} \cdots \hat{u}^i_L(\omega)\cos\theta_i - \hat{u}^i_T \sin\theta_i \cdots \\ \cdots \hat{u}^i_L(\omega)\sin\theta_i + \hat{u}^i_T \cos\theta_i \cdots \\ \cdots \qquad \hat{u}^i_y(\omega) \qquad \cdots \end{bmatrix} \tag{5-3}$$

and $x'_i = x\cos\theta_i + y\sin\theta_i$.

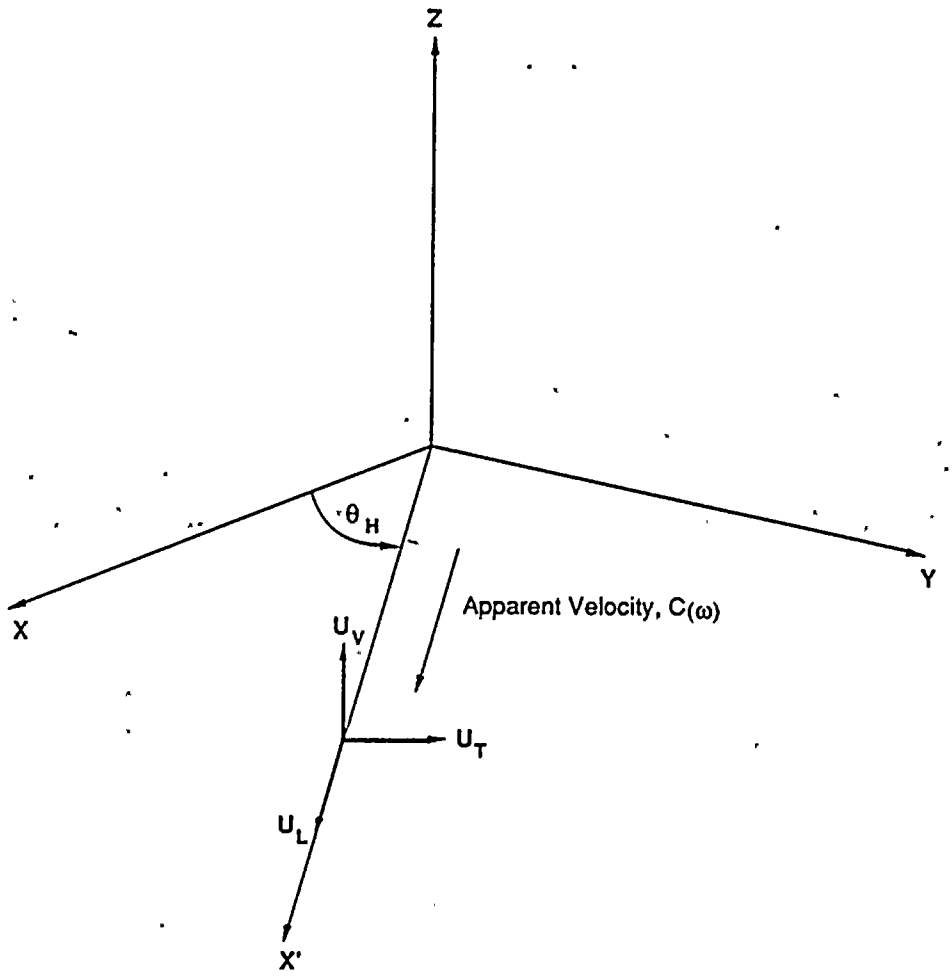

Figure 5-1. Incident Plane Wave Propagation

6. SCATTERED FOUNDATION INPUT MOTIONS

The problem of determining the response of a rigid massless foundation subjected to seismic waves is a mixed boundary-value problem in elastodynamics, as described in Section 4. On the free surface of the ground the condition of zero tractions is imposed, while at the interface between the foundation and the soil, displacement conditions are prescribed. The displacement on the interface must correspond to a rigid-body motion of the foundation and the resultant force and moment of the contact tractions must be zero. Furthermore, as the foundation tends to infinity the total displacement field must tend to the free-field motion. In CLASSIF, the formulation is obtained by introducing the concept of seismic driving forces. Referring to Eqs. (4-1) and (4-18), the total response $\{U_0\}$ of a rigid massless foundation subjected to seismic excitation and to external forces $\{F_S\}$ is given by

$$\{U_0\} = \{U_0^*\} + [C(\omega)]\ \{F_S\} \tag{6-1}$$

where $\{U_0^*\}$ is the foundation input motion and $[C(\omega)]$ is the compliance matrix for the foundation, Eq. (6-1) can also be written in the form

$$\{U_0\} = [C(\omega)]\ (\{F_S\} + \{F_0^*\}) \tag{6-2}$$

where the driving force vector $\{F_0^*\}$ is such that (see also Eq. (4.2))

$$\{U_0^*\} = [C(\omega)]\ \{F_0^*\} \tag{6-3}$$

The physical meaning of the driving force vector $\{F_0^*\}$ can be obtained by inspection of Eq. (6-2). In particular, if the foundation is held fixed under the action of the seismic excitation, then $\{U_0\} = 0$ and $\{F_S\} = -\{F_0^*\}$, i.e. the external forces required to keep the foundation fixed are of equal amplitude and opposite direction to the driving forces. The driving force vector, thus, represents the forces and moments that the soil exerts on the foundation when the foundation is held fixed while subjected to the seismic excitation.

Substituting the driving force vector in Eq. (4-16) into Eq. (6-3) gives

$$\{U_o^*\} = [C(\omega)]\,[\Gamma]^T\,\{\bar{U}_g\} \tag{6-4}$$

which indicates that the scattered foundation input motion corresponds to a weighted average of the free-field motion along the contact area between the foundation and the soil. The weight factors are the contact tractions induced by each mode of the six rigid-body motion degrees-of-freedom.

Define the scattering matrix $[S(\omega)]$ as the transfer function between the free-field motion and the scattered foundation input motion as follows,

$$[S(\omega)] = [C(\omega)]\,[\Gamma]^T \tag{6-5}$$

Thus, by substituting Eq.. (6-5) into Eq. (6-4), the scattered foundation input motions can be rewritten as

$$\{U_o^*\} = [S(\omega)]\,\{\bar{U}_g\} \tag{6-6}$$

For the free-field motion that is represented by "N_w" plane wave in the form of Eq. (5-2), Eq. (6-6) can be combined with Eq. (5-2) to give

$$\{U_o^*\} = [\hat{S}(\omega)]\,\{F(\omega)\} \tag{6-7}$$

where $[\hat{S}(\omega)]$ = the normalized scattering matrix = $[S(\omega)][\hat{W}]$. It should be noted that the scattered foundations input motion $\{U_o^*\}$ generally contains the irregular frequency content of the seismic motion, and is not suited for interpolations. However, by expressing $\{U_o^*\}$ in the form of Eq. (6-7), $[\hat{S}(\omega)]$ is a matrix of smooth frequency functions for which interpolations are more suitable. The representation by Eq. (6-7) also has the advantage that $\{F(\omega)\}$ which relates to the input seismic time history, can be changed without affecting $[\hat{S}(\omega)]$ which is strictly a function of the wave form and the geometry of the foundation-soil system. The numerical scheme used in the program for interpolating both $[\hat{S}(\omega)]$ and $[K]$ is described in Section 8.

7. EQUATIONS OF MOTION AND SOLUTION PROCEDURE

7.1 Equations of Motion

The equations of motion expression for the dynamic equilibrium of the SSI system at the base can be written in the time domain as follows:

$$\{F\} - [M_o]\{\ddot{U}_o\} = 0 \qquad (7\text{-}1)$$

in which $\{F\}$ represents the 6Nx1 force vector acting on the N foundations, $[M_o]$ represents the 6Nx6N block diagonal mass matrix composed of the foundation mass and mass moment of inertia, and $\{\ddot{U}_o\}$ represents the 6Nx1 acceleration response vector of the N foundations.

In the frequency domain, Eq. (7-1) can be rewritten as follows:

$$\{F\} + \omega^2[M_o]\{U_o\} = 0 \qquad (7\text{-}2)$$

in which ω is the circular frequency, $\{\ddot{U}_o\} = -\omega^2\{U_o\}$, and $\{U_o\}$ = the unknown 6Nx1 displacement vector of the N foundations that are to be determined.

The forces acting on the foundations subjected to seismic input motions and external forced vibration can be written as

$$\{F\} = \{F_b\} + \{F_e\} - \{F_s\} \qquad (7\text{-}3)$$

in which $\{F_e\}$ is the external force vector acting on the foundations, $\{F_s\}$ is the generalized interaction force vector acting on the foundations as given by Eq. (4-1), $\{F_b\}$ is the generalized force vector that the structures exert on the foundations which can be determined as follows.

Consider the equations of motion for one of the structure which can be written as follows:

$$-\omega^2 [M] \{U_T\} + i\omega[C_S] \{U\} + [K_S] \{U\} = \{F_E\} \qquad (7\text{-}4)$$

in which [M] is the structural mass matrix, $[C_S]$ is the structural damping matrix, {U} is the structural relative displacement vector, $[K_S]$ is the structural stiffness matrix, $\{F_E\}$ is the external force vector applied on the structure, i is equal to $\sqrt{-1}$, and $\{U_T\}$ is the total structural displacement vector which can be written as

$$\{U_T\} = [\alpha_S] \{U_O\} + \{U\} \qquad (7\text{-}5)$$

where $[\alpha_S]$ is the rigid-body transformation matrix of the structure which is given by

$$[\alpha_S] = \begin{bmatrix} \\ \\ \\ \\ [\alpha_S^j] \\ \\ \\ \\ \\ \end{bmatrix} = \left[\begin{array}{ccc|ccc} & & & & & \\ & & & & & \\ & & & & & \\ 1 & 0 & 0 & 0 & z^j & -y^j \\ 0 & 1 & 0 & -z^j & 0 & x^j \\ 0 & 0 & 1 & y^j & -x^j & 0 \\ -- & -- & -- & -- & -- & -- \\ 0 & 0 & 0 & 1 & 0 & 0 \\ 0 & 0 & 0 & 0 & 1 & 0 \\ 0 & 0 & 0 & 0 & 0 & 1 \\ & & & & & \\ & & & & & \\ & & & & & \end{array}\right] \qquad (7\text{-}6)$$

in which (x^j, y^j, z^j) are the jth nodal coordinates of the structure.

Substituting Eq. (7-5) into Eq. (7-4) yields

$$(-\omega^2[M] + i\omega[C_S] + [K_S])\ \{U\} = \omega^2[M]\ [\alpha_S]\ \{U_O\} + \{F_E\} \qquad (7\text{-}7)$$

Assuming that the structure possesses classical normal modes, the generalized displacements of structure can be transformed into the normal displacements as follows,

$$\{U\} = [\phi]\ \{n\} \tag{7-8}$$

in which $[\phi]$ is the mode shape matrix and $[n]$ is the normal displacement vector. Substituting Eq. (7-8) into Eq. (7-7), and then premultiplying Eq. (7-7) by $[\phi]^T$ and invoking the following orthogonal properties of normal modes

$$\begin{aligned} [\phi]^T [M] [\phi] &= [I]_2 \\ [\phi]^T [K_S] [\phi] &= [\ \omega_r^2\ ] \\ [\phi]^T [C_S] [\phi] &= [\ 2\omega_r \xi_r\ ] \end{aligned} \tag{7-9}$$

in which ω_r is the rth modal frequency and ξ_r is the rth modal damping, Eq. (7-7) can be rewritten as follows,

$$[-\omega^2 + 2i\omega\omega_r\xi_r + \omega_r^2]\ \{n\} = \omega^2[\gamma]\ \{U_0\} + [\phi]^T\ \{F_E\} \tag{7-10}$$

where γ is the modal participation matrix given by

$$[\gamma] = [\phi]^T\ [M]\ [\alpha_S] \tag{7-11}$$

The normal displacement $[n]$ can be solved from Eq. (7-10) as follows:

$$\{n\} = [D(\omega)]\ ([\gamma]\ \{U_0\} + (1/\omega^2)\ [\phi]^T\ \{F_E\}) \tag{7-12}$$

in which $[D(\omega)]$ is the modal amplification matrix given by

$$[D(\omega)] = \left[\ \frac{(\omega/\omega_r)^2}{1 + (\omega/\omega_r)^2 + 2i\,\xi_r\,(\omega/\omega_r)}\ \right] \tag{7-13}$$

The total displacement of the structure in Eq. (7-5) can then be obtained from using Eqs. (7-12) and (7-8) as follows

$$\{U_T\} = ([\alpha_S] + [\phi][D(\omega)][\gamma])\{U_0\} + (1/\omega^2)[\phi][D(\omega)][\phi]^T\{F_E\} \tag{7-14}$$

The forces that the structure exerts on the foundation are given by

$$\{Fb\} = [\alpha_s]^T (\{F_E\} + \omega^2[M] \{U_T\}) \quad (7\text{-}15)$$

Substituting Eq. (7-14) into Eq. (7-15) and rearranging the terms, the forces $\{F_b\}$ can then be expressed in terms of the unknown $\{U_o\}$ as follows,

$$\{F_b\} = \omega^2[M_b(\omega)] \{U_o\} + [\gamma_b^*] \{F_E\} \quad (7\text{-}16)$$

in which $[\gamma_b^*]$ is the forced modal participation factor matrix given by

$$[\gamma_b^*] = [\alpha_s]^T + [\gamma]^T [D(\omega)] [\phi]^T \quad (7\text{-}17)$$

and $[M_b(\omega)]$ is the equivalent mass matrix given by

$$[M_b(\omega)] = [M_{bo}] + [\gamma]^T [D(\omega)] [\gamma] \quad (7\text{-}18)$$

in which

$$[M_{bo}] = [\alpha_s]^T [M] [\alpha_s] \quad (7\text{-}19)$$

corresponds to the 6 x 6 mass matrix of the superstructure for rigid translations and rotations about the point of reference on the foundation.

It is of interest to observe the behavior of the equivalent mass matrix $[M_b(\omega)]$ as the frequency ω tends to infinity. From Eq. (7-13), it can be seen that $[D(\omega)] \rightarrow [I]$ as $\omega \rightarrow \infty$. Eq. (7-18) indicates, then, that

$$[M_b(\omega)] \rightarrow [M_{bo}] - [\gamma]^T [\gamma] \quad \text{as } \omega \rightarrow \infty \quad (7\text{-}20)$$

If the set of fixed-base modes is complete, it can be shown that

$$[\alpha_s] = [\phi] [\gamma] \quad (7\text{-}21)$$

$$[M_{bo}] = [\gamma]^T [\gamma] \qquad (7\text{-}22)$$

Eqs. (7-20) and (7-22) reveal that if the set of fixed base modes is complete, $[M_b(\omega)] \rightarrow o$ as $\omega \rightarrow \infty$. Referring to Eq. (2-7), it may be seen that at sufficiently high frequencies, the total response of the foundation $\{U_o\}$ becomes essentially independent of the properties of the superstructure.

If the set of modes is not complete, $[M_b(\omega)]$ will not tend to zero as $\omega \rightarrow \infty$, but to a residual mass matrix which represents the contribution to the base forces and moments of the modes excluded.

For most practical applications, not all fixed-base modes need to be considered. If the first m modes of vibration are included, then the matrices $[\phi]$, $[\gamma]$, and $[D(\omega)]$ will have dimensions 6N x m, 6 x m, and m x m, respectively. One of the advantages of the formulation is that the contributions of the missing modes, i.e., the modes higher than the m th mode, to the base forces and moments are still approximately represented in the equivalent mass matrix $[M_b(\omega)]$ through the matrix $[M_{bo}]$.

Another advantage of the procedure described to obtain the equivalent mass matrix is that the fixed-base mode shapes, natural frequencies, modal damping ratios, and participation factors can be obtained by the method most appropriate to the particular structure being analyzed. For complex structures, these quantities may be obtained by use of a finite element model; in other cases, simplified lumped mass or continuous representations may be adequate.

With $\{F_b\}$ given in Eq. (7-16), the next step is to determine $\{U_o\}$ in Eq. (7-2). This can be achieved by substituting $\{F_b\}$ in Eq. (7-16) into Eq. (7-2) as follows:

$$\{U_o\} = ([K] - \omega^2([M_o] + [M_b(\omega)]))^{-1} (\{F_e\} + [\gamma_b^*] \{F_E\} + \{F_o^*\}) \qquad (7\text{-}23)$$

It is of interest to note that $\{U_o\}$ in Eq. (7-23) can be further simplified for the following special cases when the SSI system is excited by only the seismic input motion or the external force excitation.

Case (a): Seismic Input Motion

For a special case of seismic input motions only, i.e., $\{F_e\} = \{F_E\} = \{0\}$, $\{U_o\}$ in Eq. (7-23) can be simplified, after substituting $\{F_o^*\}$ from Eq. (4-2) into Eq. (7-23), as follows,

$$\{U_o\} = [H^*_o(\omega)] \{U_o^*\} \tag{7-24}$$

in which $[H^*_o(\omega)]$ is the transfer function between scattered foundation input motions and foundation interaction motions, and is given by

$$[H^*_o(\omega)] = ([I] - \omega^2[C] ([M_o] + [M_b(\omega)]))^{-1} \tag{7-25}$$

It can be noted that $\{U_o\}$ given by Eq. (7-24) is identical with that previous given by Eq. (2-7) in Section 2. Substituting Eq. (6-6) into Eq. (7-24) gives

$$\{U_o\} = [H_{go}(\omega)] \{U_g\} \tag{7-26}$$

in which $[H_{go}(\omega)]$ is the transfer function between free-field ground motions and foundation interaction motions, and is given by

$$[H_{go}(\omega)] = [H^*_o(\omega)] [S(\omega)] \tag{7-27}$$

in which $[S(\omega)]$ is the scattering matrix as previously defined in Eq. (6-5). For the purpose of numerical computation as discussed in Section 6, it is more convenient to use Eq. (6-7) rather than Eq. (6-6) for $\{U_o^*\}$. As a result, $\{U_o^*\}$ in Eq. (7-26) can be rewritten in the form suitable for numerical computation as follows,

$$\{U_o\} = [\hat{H}_{go}(\omega)]\{F(\omega)\} \quad (7\text{-}28)$$

in which $[\hat{H}_{go}(\omega)]$ is the normalized transfer function of $[H_{go}(\omega)]$, i.e., $[\hat{H}_{go}(\omega)] = [H^*_o(\omega)][\hat{S}(\omega)]$, and $[F(\omega)]$ is as defined in Eq. (5-2).

Once $\{U_o\}$ is determined, the total structure displacement response $\{U_T\}$ can readily be obtained from substituting Eq. (7-26) into Eq. (7-14) as follows,

$$\{U_T\} = [H_{gs}(\omega)]\{\bar{U}_g\} \quad (7\text{-}29)$$

in which $[H_{gs}(\omega)]$ is the transfer function between free-field ground motions and structural responses, and is given by

$$[H_{gs}(\omega)] = [H_{os}(\omega)][H_{go}(\omega)] \quad (7\text{-}30)$$

in which $[H_{go}(\omega)]$ is as defined in Eq. (7-27), and $[H_{os}(\omega)]$ is the transfer function between foundation interaction motions and structural responses, and is given by

$$[H_{os}(\omega)] = [\alpha_s] + [\phi][D(\omega)][\gamma] \quad (7\text{-}31)$$

It follows that the absolute acceleration responses of structure can simply be obtained from Eq. (7-29) as

$$\{\ddot{U}_T\} = -\omega^2\{U_T\} \quad (7\text{-}32)$$

in which $\{U_T\}$ is as given by Eq. (7-29).

Case (b): External Force Excitation

For a special case of external force excitation, i.e., $\{F_o^*\} = 0$, $\{U_o\}$ in Eq. (7-23) can be reduced to

$$\{U_o\} = [H_{eo}(\omega)]\{F_e\} + [H_{Eo}(\omega)]\{F_E\} \quad (7\text{-}33)$$

in which $[H_{eo}(\omega)]$ is the transfer function between the external forces applied at the foundation base and the foundation interaction motion, and is given by

$$[H_{eo}(\omega)] = ([K] - \omega^2([M_o] + [M_b(\omega)]))^{-1} \quad (7\text{-}34)$$

and $[H_{Eo}(\omega)]$ is the transfer function between the external forces applied on the structures and the foundation interaction motions, and is given by

$$[H_{Eo}(\omega)] = [H_{eo}(\omega)][\gamma_b^*] \quad (7\text{-}35)$$

in which $[H_{eo}(\omega)]$ and $[\gamma_b^*]$ are as defined in Eq. (7-34) and (7-17), respectively.

To obtain the total structural displacement response $\{U_T\}$ for this case, Eq. (7-33) is substituted into Eq. (7-14) to give

$$\{U_T\} = [H_{es}(\omega)]\{Fe\} + [H_{Es}(\omega)]\{FE\} \quad (7\text{-}36)$$

in which $[H_{es}(\omega)]$ is the transfer function between external forces applied at the foundation base and structural responses, and is given by

$$[H_{es}(\omega)] = [H_{os}(\omega)][H_{eo}(\omega)] \quad (7\text{-}37)$$

in which $[H_{eo}(\omega)]$ and $[H_{os}(\omega)]$ are as defined in Eqs. (7-34) and (7-31), respectively; and $[H_{Es}(\omega)]$ is the transfer function between external forces applied on the structure and structural responses, and is given by

$$[H_{Es}(\omega)] = [H_{os}(\omega)][H_{Eo}(\omega)] + [H_{Es}^*(\omega)] \quad (7\text{-}38)$$

in which $[H_{Es}^*(\omega)]$ is the transfer function between external forces applied on the structure and foundation interaction motions, and is given by

$$[H^*_{Es}(\omega)] = (1/\omega^2)\,[\phi]\,[D(\omega)]\,[\phi]^T \qquad (7\text{-}39)$$

Once $\{U_T\}$ is determined from Eq. (7-36), the corresponding $\{\ddot{U}_T\}$ can, again, be easily obtained using Eq. (7-32).

7.2 Solution Procedure

The equations of motion of the SSI problem formulated in the frequency domain in Section 7.1 can be solved in the frequency domain for the frequency response function. To obtain the time history (transient) response from the frequency response of the SSI system, the following solution procedure is used in the CLASSIF program.

(1) Let $g(t)$ be the input time history for either the seismic free-field ground motion or the external forcing function. Then, the Fourier transform of $g(t)$ is computed from

$$F(\omega) = \int_{-\infty}^{\infty} g(t)\, e^{-i\omega t}\, dt \qquad (7\text{-}40)$$

in which $F(\omega)$ is the Fourier transform of $g(t)$, ω is the circular frequency, t is time, and $i = \sqrt{-1}$.

(2) Using $F(\omega)$ computed from step (1), the foundation interaction motion $\{U_0\}$ can be computed from Eq. (7-28) for seismic motion input, or from Eq. (7-33) for forcing function input.

(3) The time history response of the foundation interaction motion $\{U_0(t)\}$ can be obtained from performing the inverse Fourier transform of $\{U_0\}$ as follows

$$\{U_0(t)\} = (1/2\pi) \int_{-\infty}^{\infty} \{U_0\} e^{i\omega t}\, d\omega \qquad (7\text{-}41)$$

(4) To obtain the time history response of the structure, the frequency response of the structure $\{U_T\}$ can similarly be computed using Eq. (7-29) for seismic motion input, or using Eq. (7-36) for forcing function input.

(5) Once $\{U_T\}$ is determined from step (4), the time history response of the structure $\{U_T(t)\}$ can, again, be obtained from performing the inverse Fourier transform of $\{U_T\}$ as follows

$$\{U_T(t)\} = (1/2\pi) \int_{-\infty}^{\infty} \{U_T\} e^{i\omega t} \, d\omega \qquad (7\text{-}42)$$

8. NUMERICAL SOLUTION TECHNIQUES

In this section, the numerical solution techniques used in the CLASSIF program for computing integration, interpolation, and inversion of Green's functions are presented. The numerical criterion for discretization of foundation subregions is also presented.

8.1 Numerical Integration Scheme for Computing Green's Functions

The technique for the numerical integration of Green's functions has been developed and presented by Apsel and Luco in Ref. 4. This paper is reproduced in Appendix A for easy reference. The numerical integration scheme used in CLASSIF uses the method of quadrature which is based on the local representation of the function by a fourth order (quartric) polynomial, as given by Eq. (8) in Ref. 4. A five-point sampling of the Green's function kernel is applied to check the adequacy of the representation locally by the quartric polynomial in the wave number domain. The sampling points is a given wave number interval are selected according to an error criterion, as given by Eq. (16) in Ref. 4, which requires that the contribution of the fifth order term in the polynomial expansion of the Green's function kernal to the Green's function integral over the interval be significantly smaller than the integral. This numerical integration scheme includes an automatic checking procedure that, if the prescribed tolerance of the error criterion is not satisfied, a new sampling point is automatically inserted between the two points with the largest spacing. The sequence of points is then renumbered and integration including the new point sampled is performed. This process is repeated until the prescribed tolerance (set to be 0.002 in the program) is satisfied. Thus, the accuracy of the numerical integration scheme for Green's function is automatically ensured to within the set tolerance with this automatic checking procedure.

8.2 Spatial Interpolation Scheme for Computing Green's Functions

As indicated in Section 3, it is more economical to obtain the Green's function matrix needed for impedance calculations described in Section 4 by interpolation from the precalculated Green's function table because of the large number of points at which the Green' functions must be calculated. It has been shown in Eq. (3-10) that for a frequency, ω, and a set of soil properties, p, the Green's functions depend on only the parameter $b_0 = \omega R/\beta$. Thus, the Green's function matrix are calculated by program module GLAYER for a selected set of values of b_0, and the matrices for all other values of b_0 are obtained by interpolation using the table of calculated values. To minimize the errors created by the interpolation, an optimal increment, Δb_0, for the Green's function table must be chosen small enough so that a prescribed accuracy can be obtained; on the other hand, Δb_0 should be chosen sufficiently large so that the number of points in the table is reasonable. This optimal increment is generally dependent on the frequency and the soil properties; it is therefore not easily predicted before the calculation. An algorithm for setting up interpolation tables for the four functions (f_{rr}, $f_{\psi r}$, $f_{rz'}$, and $f_{z'z'}$) is described here. Using this method, the increment size is determined automatically by the computer program and the complete set of tables (one for each frequency) are calculated using a minimum number of frequencies.

The interpolation of Green's function values for each specified frequency is performed using a second order polynomial with three equally spaced points as follows,

$$f(x_0+qh) = (1/2)q(q-1)\ f(x_0-h) + (1+q^2)f(x_0) + (1/2)q(q+1)f(x_0+h) \qquad (8\text{-}1)$$

in which $q = (x-x_0)/h$, h is an equally spaced increment, and f(x) is a function of one spatial variable. The interpolation is initiated by calculating a set of Green's function values with a relatively

coarse increment, then the increments are halved and new values at the half increments are calculated using Eq. (8-1). Following the new calculations, accuracy tests are performed by comparing the exact calculated values with the interpolated values at several check points based on the following criterion

$$E_k = |(f_k^* - f_k)/f_k| \leq \varepsilon \quad , \quad k = 1, 2, \cdots, n_c \qquad (8\text{-}2)$$

in which ε_k is the relative error of the calculated value at the k th check point, f_k is the exact value at the kth check point, f_k^* is the interpolated value at the kth check point calculated from Eq. (8-1), ε is the allowable relative error which has been set in GLAYER as 2%, n_c is the total number of check points. If the accuracy of the interpolated values tested at the check points does not satisfy the criterion given by Eq. (8-2), another set of half increments between all previous points are established and the new Green's function values are calculated. The process is then repeated until the prescribed accuracy is reached.

For example, consider the initial table of Green's function values consisting of points 1, 3, 5, 7 and 9. The second set of points at locations in between the first five, i.e., 2, 4, 6 and 8, are then interpolated from the initial points using Eq. (8-1). At this time, it is possible to use some of the initial points for accuracy check; i.e., f_3^*, calculated from points 2, 4 and 6 by the equation

$$f_3^* = (3/8)\, f_2 + (3/4)\, f_4 - (1/8)\, f_6 \qquad (8\text{-}3)$$

Eq. (8-3) is obtained from Eq. (8-1) by using point number 4 as x_o, $h = x_4 - x_2 = x_6 - x_4$, and $q = (x_3 - x_4)/h = -1/2$.

The accuracy of the interpolation can simply be estimated from the criterion given in Eq. (8-2), i.e.,

$$|(f_3^* - f_3)/f_3| \leq \varepsilon \qquad (8\text{-}4)$$

Using a similar scheme as Eq. (8-3), f_5^* can be calculated by either

$$f_5^* = (3/8)\ f_4 + (3/4)\ f_6 - (1/8)\ f_8 \qquad (8\text{-}5)$$

or

$$f_5^* = -(1/8)\ f_2 + (3/4)\ f_4 + (3/8)\ f_6 \qquad (8\text{-}6)$$

However, to be consistent with CLAF, f_5^* is always interpolated with $q<0$; i.e., Eq. (8-5), where the index of the interpolated point is always between the indices of the first two of the three given points.

If the error computed by Eq. (8-4) is not within the desired tolerance, the table must be further refined by calculating values at the "1/2" points; i.e., $x_{1.5}$, $x_{2.5}$, ..., etc. Following the latest calculations, a new estimate of f_3^* can be interpolated from $f_{2.5}$, $f_{3.5}$, and $f_{4.5}$ as

$$f_3^* = (3/8)\ f_{2.5} + (3/4)\ f_{3.5} - (1/8)\ f_{4.5} \qquad (8\text{-}7)$$

in which Eq. (8-7) is obtained by substituting $x_0 = x_{3.5}$, $h = x_{4.5} - x_{3.5}$, and $q = -1/2$ into Eq. (8-1). The new value of f_3^* given by Eq. (8-7) should be a better estimate of f_3, the error is of order $(\Delta x)^3$ each time the increment Δx is halved. This process is repeated until the prescribed accuracy is reached. Thus, the accuracy of spatial interpolation of Green's function is automatically ensured to within the set tolerance with this automatic checking procedure.

8.3 Numerical Iterative Scheme for Inverting Green's Functions

As presented in Section 4, for multiple foundations interacting through soil, when the number of foundations is large, the order of

the matrix [G] in Eq. (4-17) can be large and the required inversion of this matrix to generate impedance for foundations for each frequency can become costly. This is particularly true at high frequencies when each foundation has to be divided into a large number of subregions. To avoid this problem Wong and Luco (Ref. 5) has developed an interactive solution procedure based on the observation that the diagonal blocks of the compliance matrix are only slightly affected by the presence of adjacent foundations. To describe this procedure, it is convenient to write the matrix [G] in the form,

$$[G] = [G_0]([I] - [G_0]^{-1}\,[B]) \tag{8-8}$$

in which [I] is the 3M x 3M identity matrix, M is the total number of foundation subregions, $[G_0]$ is the block diagonal matrix defined by

$$[G_0] = \begin{bmatrix} G_{11} & 0 & 0 & 0 \\ 0 & G_{22} & 0 & 0. \\ : & : & : & : \\ 0 & 0 & 0 & G_{NN} \end{bmatrix} \tag{8-9}$$

and

$$[B] = \begin{bmatrix} 0 & G_{12} & G_{13} & \cdot & \cdot \\ G_{21} & 0 & G_{23} & \cdot & \cdot \\ G_{31} & G_{32} & 0 & \cdot & \cdot \\ : & : & : & & \end{bmatrix} \tag{8-10}$$

The inverse of [G] is given by

$$[G]^{-1} = ([I] - [G_0]^{-1}\,[B])^{-1}\,[G_0]^{-1} \tag{8-11}$$

which upon expansion in powers of $[G_0]^{-1}\,[B]$ leads to

$$[G]^{-1}=[G_0]^{-1}+[G_0]^{-1}[B][G_0]^{-1}+[G_0]^{-1}[B][G_0]^{-1}[B][G_0]^{-1}+\ldots \tag{8-12}$$

Substitution from Eq. (8-12) into Eq. (4-17) results in

$$[\Gamma] = \sum_{n=0}^{\infty} [\Gamma_n] \qquad (8\text{-}13)$$

in which

$$[\Gamma_0] = [G_0]^{-1} [\alpha] \qquad (8\text{-}14)$$

and

$$[\Gamma_n] = [G_0]^{-1} [B] [\Gamma_{n-1}] \quad , \quad n \geq 1 \qquad (8\text{-}15)$$

The successive terms in Eq. (8-13) have an interesting physical interpretation. The term $[\Gamma_0]$ represents the resultant of the contact tractions on each of the subregions for the case that each of the rigid foundations is considered as an isolated foundation. The term $[\Gamma_1]$ represents the contact tractions on the various subregions when the foundations are held fixed under the wave displacement field created by $[\Gamma_0]$. In the calculation of $[\Gamma_1]$ each foundation is considered to be isolated. Thus $[\Gamma_1]$ represents a first order correction to the contact tractions due to the fact that the wave field created by the tractions $[\Gamma_0]$ is such that the waves radiating from the ith foundation satisfy the rigid-body motion displacement condition on that foundation but not on the others. The terms $[\Gamma_2]$, $[\Gamma_3]$, ... have similar interpretations and represent successive corrections to the contact tractions.

The iterative approach has a number of computational advantages over the direct approach. These advantages are discussed in the Appendix of Ref. 5. In particular, for a large number of foundations N all subdivided into the same number of subdivisions n_0, the ratio of the number of complex operations after k interactions in the iterative approach to that in the direct approach can be approximated by

$18k/(3n_0 + 18)$. For k = 10 iterations and $n_0 = 10 \times 10 = 100$, the ratio is 0.566 indicating a considerable saving. For a small number of foundations (N = 2) the savings in the number of operations are not as significant.

8.4 Numerical Criterion for Discretization of Foundation Subregions

The convergence and accuracy of the iterative approach for inverting Green's functions in Section 8.3 have been tested for a wide frequency range and complete numerical results describing the effects of the separation between two square rigid foundations on the impedance functions have been presented by Wong and Luco in Ref. 5. It was found that for small separations the calculated impedances are markedly affected by the particular choice of discretization of the foundations. The criterion for the discretization of the foundation was also studied and established for the impedance calculation. The criterion requires that the foundation be discretized with finer subregions at the foundation perimeter where the stress gradient is the highest. As an example, if the foundation of dimension 2ax2a is subdivided into 10x10 perpendicular grids, the center points of these grids which are used for the integration of Green's functions, are required to be separated with the distance Δ times the factors $(1, \alpha, \alpha^2, \alpha^3, \alpha^4, \alpha^4, \alpha^3, \alpha^2, \alpha, 1)$, in which $\Delta = a\,(\alpha - 1)/(\alpha^5 - 1)$, and $\alpha \leq 1$. Ref. 5 has demonstrated that $\alpha = 2.0$ gives a sufficient accuracy for the impedance calculation. The adequacy of this criterion for impedance calculation has also been demonstrated by the extensive benchmarking studies performed in the CLASSIF Validation Report (Ref. 6).

9. REFERENCES

1. Luco, J. E., "Linear Soil-Structure Interaction," Seismic Safety Margins Program (Phase 1), Lawrence Livermore Laboratory, UCRL-15272, July 1980.

2. Liu, S. C., and L. W. Fagel, "Earthquake Interaction by Fast Fourier Transform," Journal of Engineering Mechanics, ASCE, 97, EM4, 1971.

3. Luco, J. E., and R. J. Apsel, "On the Green's Functions for a Layered Half-Space: Part I," Bulletin of the Seismological Society of America, Vol. 73, No. 4, August 1983.

4. Apsel, R. J., and J. E. Luco, "On the Green's Functions for a Layered Half-Space: Part II," Bulletin of the Seismological Society of America, Vol. 73, No. 4, August 1983

5. Wong, H. L., and J. E. Luco, "Dynamic Interaction Between Rigid Foundations in a Layered Half-Space," Soil Dynamics and Earthquake Engineering, Vol. 5, No. 3, 1986.

6. "Computer Program CLASSIF: Validation Report," Prepared for PG&E by Bechtel Power Corporation, July 27, 1988.

Appendix A:

A copy of Paper by Apsel, R. J., and J. E. Luco, "On the Green's Functions for a Layered Half-Space. Part II.," Bulletin of the Seismological Society of America, Vol. 73, No. 4, August 1983.

Bulletin of the Seismological Society of America, Vol. 74, No. 4, pp. 931–951, August 1984

ON THE GREEN'S FUNCTIONS FOR A LAYERED HALF-SPACE. PART II

By Randy J. Apsel and J. Enrique Luco

Abstract

A numerical procedure to obtain the dynamic Green's functions for layered viscoelastic media is presented. The procedure is based on numerical evaluation of certain Hankel-type integrals which appear in an integral representation derived previously by the authors. Comparisons illustrating the accuracy and flexibility of the approach are made with a number of solutions obtained by other methods.

Introduction

In a companion paper (Luco and Apsel, 1983), the authors have presented an integral representation for the complete three-dimensional response of a layered viscoelastic half-space for an arbitrary buried source. In this method, the different Fourier components (with respect to azimuth) of the response, in the frequency domain, are expressed in terms of semi-infinite Hankel-type integrals with respect to horizontal wavenumber. The numerical evaluation of the response requires the development of an efficient and accurate technique to compute such integrals. The numerical technique should be stable for the extreme conditions involved in applications to problems in seismology and earthquake engineering which are characterized by a wide range of frequencies, source-to-observer distances, and earth or soil stratigraphic models. The first part of this study is addressed to the description of a numerical technique to accomplish these purposes.

The second objective of the study is to validate the complete representation as well as the method of numerical integration by comparison with complete or partial solutions obtained by other methods. These comparisons also illustrate the flexibility of the proposed method to evaluate the dynamic response of a layered viscoelastic half-space under various conditions.

Method of Integration

Integral representation. In a companion paper (Luco and Apsel, 1983) we obtained an integral representation for the displacement and stress fields in a layered viscoelastic medium for a distribution of body forces per unit volume given, in cylindrical coordinates, by

$$\begin{Bmatrix} F_r^j(r,\theta,z;\omega) \\ F_\theta^j(r,\theta,z;\omega) \\ F_z^j(r,\theta,z;\omega) \end{Bmatrix} = \frac{\delta_{jl}}{4\pi}\left(\frac{r_0}{r}\right)^3 \sum_{n=0}^{\infty} Q_n \begin{Bmatrix} F_{1n}^j(r_0,z_0)\cos(n\theta-\theta_{0n}) \\ F_{2n}^j(r_0,z_0)\sin(n\theta-\theta_{0n}) \\ F_{3n}^j(r_0,z_0)\cos(n\theta-\theta_{0n}) \end{Bmatrix} \qquad (1)$$

where j indicates the layer number, δ_{jl} is the Kronecker delta, Q_n are constants with dimensions of force, and, F_{1n}^j, F_{2n}^j, F_{3n}^j are given functions of the dimensionless variables $r_0 = \omega r/\beta$ and $z_0 = \omega z/\beta$ in which ω is the frequency, and β is a shear wave velocity of reference. In writing equation (1), it has been assumed that the body forces are concentrated in the lth layer. In this case, the solution for the diplacement and stress fields in the jth medium can be written in the form

$$4\pi(\tilde{\mu}ru_r', r^2\sigma_{rr}', r^2\sigma_{rz}') = \sum_{n=0} Q_n(r_0U_{rn}', r_0^2\Sigma_{rn}', r_0^2\Sigma_{zn}')\cos(n\theta - \theta_{0n})$$

$$4\pi(\tilde{\mu}ru_\theta', r^2\sigma_{r\theta}', r^2\sigma_{z\theta}') = \sum_{n=0} Q_n(r_0U_{\theta n}', r_0^2\Sigma_{\theta n}', r_0^2\Sigma_{\theta n}')\sin(n\theta - \theta_{0n})$$

$$4\pi(\tilde{\mu}ru_z', r^2\sigma_{rz}', r^2\sigma_{zz}') = \sum_{n=0} Q_n(r_0U_{zn}', r_0^2\Sigma_{zn}', r_0^2\Sigma_{zn}')\cos(n\theta - \theta_{0n}) \quad (2)$$

where $\tilde{\mu}$ represents a shear modulus of reference. The terms $U_{rn}', \ldots, \Sigma_{rn}', \ldots$, appearing in equation (2) are functions of r_0 and z_0, and are obtained from the following Hankel transform-type integrals

$$\begin{Bmatrix} U_{rn}' \pm U_{\theta n}' \\ \Sigma_{rn}' \pm \Sigma_{\theta n}' \end{Bmatrix} = \int_0^\infty \begin{Bmatrix} \pm u_{1n}' + u_{3n}' \\ \pm\sigma_{11n}' + \sigma_{13n}' \end{Bmatrix} kJ_{n\pm1}(kr_0)\,dk \quad (3)$$

$$\left(U_{rn}', \Sigma_{rn}', \Sigma_{\theta n}', \Sigma_{zn}' + \frac{2c_f}{d_f r_0}(U_{rn}' + nU_{\theta n}'), \Sigma_{\theta n}' + \frac{2c_f}{d_f r_0}(nU_{rn}' + U_{\theta n}')\right) = \int_0^\infty (u_{2n}', \sigma_{12n}', \sigma_{32n}', \sigma_{12n}', \sigma_{32n}')kJ_n(kr_0)\,dk \quad (4)$$

where $u_{1n}', \ldots, \sigma_{1n}'$, are functions of the dimensionless wavenumber k and of z_0. In equations (3) and (4), $c_f = (\beta_f/\tilde{\beta})^2$, $\beta_f = (\mu_f/\rho_f)^{1/2}$, $d_f = \tilde{\rho}/\rho_f$, and $\tilde{\rho} = \tilde{\mu}/\tilde{\beta}^2$ is a density of reference. The terms $u_{1n}', u_{2n}', \sigma_{11n}', \sigma_{12n}', \sigma_{32n}'$, and σ_{33n}' are associated with waves which in the far field are polarized in vertical planes (P, SV, and Rayleigh waves), while u_{3n}', σ_{13n}', and σ_{31n}' are associated with waves polarized in horizontal planes (SH and Love waves). An efficient method to evaluate the functions $u_{1n}', \ldots, \sigma_{11n}', \ldots$, for point and ring loads in a layered medium has been presented by the authors (Luco and Apsel, 1983). These functions of the dimensionless wavenumber k depend on the characteristics of the layered medium, on frequency, and on the depth of the source, z_0', and observer z_0.

Equations (2) to (4) indicate that, to obtain the response in the frequency domain for concentrated loads applied at a point of coordinates $(0, z')$, it is necessary to evaluate integrals of the form

$$I_n(r_0, z_0, z_0') = \int_0^\infty F(k, z_0, z_0')J_n(kr_0)\,dk \quad (5)$$

where n takes values 0, 1, and 2. For ring loads of radius a located at a depth z', the form of the corresponding integral is given by

$$I_{mn}(r_0, z_0, z_0') = \int_0^\infty F(k, z_0, z_0')J_m(ka_0)J_n(kr_0)\,dk \quad (6)$$

where $a_0 = \omega a/\tilde{\beta}$ and n takes the values $m - 1$, m, and $m + 1$ (Luco and Apsel, 1983). The difficulty in evaluating integrals of the type given by equations (5) and (6) stems from the oscillatory nature of both the Bessel functions and the kernel $F(k, z_0, z_0')$.

Description of the kernel $F(k, z_0, z_0')$. Before proceeding with the description of the method of integration employed to evaluate integrals of the type given by equations (5) and (6), it is convenient to illustrate the characteristics of the kernels

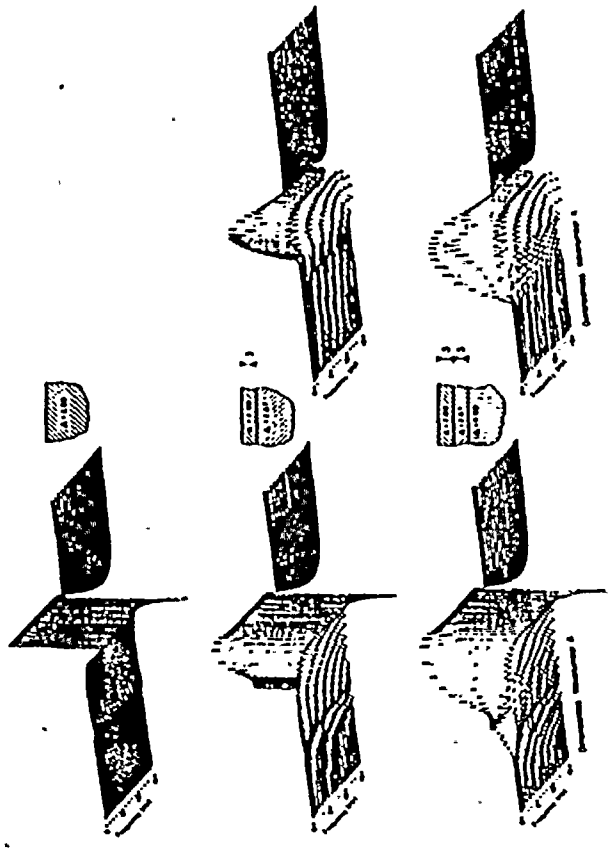

FIG. 1. Real parts of the free-surface displacement components in the frequency-wavenumber domain due to a concentrated force at the free surface of a uniform half-space. In each three-dimensional figure, dimensionless wavenumbers from 0 to 2 run from *left to right*; frequencies from 15 to 0 Hz run from *front to back*.

$F(k, z_o, z_o')$ as a function of the dimensionless wavenumber k. The real parts of two representative F integrands are pictured in Figure 1 for the simple structures also shown in the figure. The three-dimensional plots in the left-hand column represent the real part of the F integrands for the vertical displacement at the free surface due to a concentrated vertical point force at the free surface (viz. u_{zz}^1); the plots in the right-hand column represent the real part of the F integrands for the tangential displacement due to a concentrated horizontal point force (viz. u_{xx}^1). The axes running from left to right correspond to the dimensionless wavenumber k which is inversely proportional to the phase velocity (the range from $k = 0$ to $k = 2$ is shown in the plots). High frequency is in the foreground, and low frequency is in the background. The poles of the F integrands have been shifted off the real k axis by introducing material attenuation for both shear (Q_β) and compressional (Q_α) waves. This not only facilitates implementation of an integration scheme for real k values, but at the same time models physically realizable attenuation in the Earth. The plots on the left involve P, SV, and Rayleigh waves while those on the right involve SH-Love waves.

For a uniform half-space with source and receiver at the surface, the functions F are frequency independent as is apparent in the upper left plot of Figure 1. The large undispersed oscillation corresponds to the Rayleigh wave for the half-space, and the small inflection represents the compressional wave. For a layer overlying a half-space, higher surface wave modes appear as the frequency is increased as depicted in the center plots. All the surface waves are normally dispersed since on a given mode, the phase velocity decreases as the frequency in increased. In the lower plots, the two layers which overlie a half-space have the same properties (velocities, density, attenuation factors, and thickness) as used in the center model. Thereby, at sufficiently high frequencies, when the waves become insensitive to the underlying half-space, the most fundamental surface wave modes should match those for the center model.

Figure 1 illustrates the oscillatory nature of the kernels $F(k, z_o, z_o')$. For more detailed earth structures, the variation of F with k is even more pronounced than that shown in Figure 1 (Apsel, 1979). The plots shown also reveal that the F integrands are well behaved at large wavenumbers indicating that the tail ends of the wavenumber integrals can be evaluated without difficulty.

Upper limit of integration. For numerical evaluation, the upper limit of integration appearing in equations (5) and (6) must be truncated to a finite value k_2. If the source and the observer are located at different depths, the exponential decay of the kernel $F(k, z_o, z_o')$, which for sufficiently large values of k depends on $k\omega|z - z'|/\beta$, is sufficient to guarantee that the truncated integral gives an accurate estimate to the total integral if k_2 is selected such that $k_2\omega|z - z'|/\beta \gg 1$.

An alternative procedure is obtained by considering that, for high values of the dimensionless wavenumber k, the F integrands for any frequency tend to the values of the F integrands in the static case. Taking advantage of this property, the integral in equation (5) can be written schematically in the form

$$I_n(\omega) \simeq I_n(0) + \int_0^{k_2} [F(\omega) - F(0)] J_n(kr_o)\, dk \tag{7}$$

in which $F(0)$ represents the static ($\omega = 0$) F integrands, and $I_n(0)$ represents the corresponding static ($\omega = 0$) integrals. The upper limit of integration, k_2, is thereby defined in this case by the convergence of the dynamic integrands to the static integrands.

The procedure of equation (7) is particularly useful when source and receiver are at the same depth, in which case the decay of the kernel F as a function of k is slow. In equation (7), the static F integrands and integrals may be replaced by the static integrands and integrals for a uniform half-space with the properties of the layer containing the source-receiver pair. Although the dynamic F integrands may converge more slowly to the half-space static F integrands, the advantage is that analytic expressions are available for the half-space static integrands and integrals (Apsel, 1979).

Method of integration. The method of quadrature is based on sampling the kernel $F(k, z_o, z_o')$ in such a way that it can be represented locally by a quartic polynomial

$$F(k, z_o, z_o') = \sum_{m=1}^{5} A_m(z_o, z_o') \left(\frac{k - k_1}{\Delta k}\right)^{m-1}, \quad k_1 \le k \le k_5. \tag{8}$$

The coefficients $A_m(z_o, z_o')$ $(m = 1, \ldots, 5)$ are determined by imposing equation (8) at five points $k_j (j = 1, 5)$ in the interval (k_1, k_5). The normalization constant Δk appearing in equation (8) is defined by $\Delta k = k_5 - k_1$. The coefficients A_m can be written in the form

$$A_m = \sum_{j=1}^{5} C_{mj} F_j \tag{9}$$

where F_j represents $F(k_j, z_o, z_o')$ and C_{mj} are functions of the spacing of the sampling points $k_j (j = 1, 5)$ (Appendix I).

The contribution of the interval (k_1, k_5) to the total integral indicated by equations (5) or (7) is given by

$$\Delta I = \sum_{j=1}^{5} F_j \sum_{m=1}^{5} C_{mj} \int_{k_1}^{k_5} \left(\frac{k - k_1}{\Delta k}\right)^{m-1} J_n(kr_o)\, dk. \tag{10}$$

Although the integrals appearing in equation (10) can be expressed in terms of Bessel functions, it is more efficient to consider an alternative approach which depends on the argument kr_o of the Bessel function. For values of kr_o such that $k_1 r_o > \hat{x} \gg 1$, the Bessel function $J_n(kr_o)$ can be represented by an asymptotic expansion of the form

$$J_n(kr_o) = \hat{P}(n, kr_o)\cos(kr_o) - \hat{Q}(n, kr_o)\sin(kr_o) \tag{11}$$

in which

$$\hat{P}(n, kr_o) = \sqrt{\frac{2}{\pi kr_o}} \left\{ P(n, kr_o)\cos\left[(2n+1)\frac{\pi}{4}\right] + Q(n, kr_o)\sin\left[(2n+1)\frac{\pi}{4}\right] \right\},$$

$$\hat{Q}(n, kr_o) = \sqrt{\frac{2}{\pi kr_o}} \left\{ Q(n, kr_o)\cos\left[(2n+1)\frac{\pi}{4}\right] - P(n, kr_o)\sin\left[(2n+1)\frac{\pi}{4}\right] \right\} \tag{12}$$

where

$$P(n, kr_o) = 1 - \frac{(s-1)(s-9)}{2!(8kr_o)^2} + \frac{(s-1)(s-9)(s-25)(s-49)}{4!(8kr_o)^4} - \cdots$$

$$Q(n, kr_o) = \frac{s-1}{8kr_o} - \frac{(s-1)(s-9)(s-25)}{3!(8kr_o)^3} + \cdots \tag{13}$$

and $s = 4n^2$. Since $\hat{P}(n, kr_0)$ and $\hat{Q}(n, kr_0)$ are smoothly varying functions of kr_0, the products $F\hat{P}$ and $F\hat{Q}$ can be represented locally by quartic polynomials and the contribution of the interval (k_1, k_4) to the total integral can be approximated by

$$\Delta I = \sum_{j=1}^{5} F_j \hat{P}(n, k_j r_0) \sum_{m=1}^{5} C_{mj} \int_{k_1}^{k_4} \left(\frac{k - k_1}{\Delta k}\right)^{m-1} \cos(kr_0)\, dk$$

$$- \sum_{j=1}^{5} F_j \hat{Q}(n, k_j r_0) \sum_{m=1}^{5} C_{mj} \int_{k_1}^{k_4} \left(\frac{k - k_1}{\Delta k}\right)^{m-1} \sin(kr_0)\, dk, \quad (k_1 r_0 > \hat{x}) \tag{14}$$

in which the integrals involving sine and cosine can be evaluated analytically (Appendix II).

For values of kr_0 such that $k_5 r_0 < \hat{x}$, it is sufficient to require that the sampling be fine enough ($\Delta k r_0 < \Delta \hat{x} \ll 2\pi$) to insure that the Bessel functions are properly represented by the sampling within the interval (k_1, k_5). In this case, the product $F(k, z_0, z_0^*) J_n(kr_0)$ can be represented locally by a quartic polynomial and the contribution of the interval (k_1, k_4) to the total integral can be approximated by

$$\Delta I = \sum_{j=1}^{5} F_j J_n(k_j r_0) \sum_{m=1}^{5} \frac{C_{mj} \Delta k}{m}. \tag{15}$$

The sampling points $k_j (j = 1, 5)$ in a given interval are selected according to an error criterium. One possible error criterium is to require that

$$\left(\frac{\Delta k}{5} \sum_{j=1}^{5} C_{5j} F_j\right) \ll \left(\Delta k \sum_{j=1}^{5} \left(\sum_{m=1}^{5} \frac{C_{mj}}{m}\right) F_j\right). \tag{16}$$

which corresponds to the condition that the contribution of the fifth order term in the polynomial expansion of $F(k, z_0, z_0^*)$ to the integral over the interval (k_1, k_4) be significantly smaller than that integral (neglecting the effect of the Bessel function). If the error criterium is not satisfied, a new sampling point is inserted between the two points with the largest spacing, the sequence of points is renumbered and the process is repeated. The total integral in the truncated interval $(0, k_t)$ is evaluated by adding the contributions given by equation (14) or (15) for each interval. For the first interval, $k_1 = 0$, and the contribution to the total integral from the interval (k_1, k_4) is given by equation (15) after substitution of $\Delta k/m$ by $\Delta k[1 - (-k_1/\Delta k)^m]/m$.

For integrals of the type given by equation (6), a similar method of quadrature is employed. In this case, it is necessary to consider three situations depending on the values of the arguments ka_0 and kr_0 of the Bessel functions. If both arguments are less than $\hat{x}$, the product $FJ_n(ka_0) J_n(kr)$ is locally represented by a quartic polynomial. If both aguments are larger than $\hat{x}$, then both Bessel functions are represented by their asymptotic expansions, and the smoothly varying portions of the integrand are represented by quartic polynomials. If one of the arguments is larger than $\hat{x}$ while the other is less than $\hat{x}$, then the asymptotic representation is used only for one of the Bessel functions.

Various other sampling and interpolation schemes have been considered (Apsel, 1979), and it has been found that the scheme described above is sufficiently accurate and efficient for most engineering and seismological applications. In cases in which the response in the time domain is required, the integrations described above for each frequency are followed by a Fourier synthesis

$$I(r, z, z^*; t) = \frac{1}{2\pi} \int_{-\infty}^{\infty} I(r_0, z_0, z_0^*) e^{i\omega t}\, d\omega. \tag{17}$$

performed by the discrete Fast Fourier Transform algorithm.

Validation and Comparisons

The complexity of the numerical procedure used to evaluate the Green's functions suggests the need for an exhaustive set of validation calculations prior to employing the method in actual applications. A suite of five external checks is presented for such a purpose in the form of comparisons with known solutions. The first three tests validate the reliability of the numerical procedure when considering a uniform half-space, whereas the final two tests include a finite number of layers. Finally, comparisons with partial solutions obtained by a generalized ray technique and a normal mode technique are made.

Comparison with contour integration approach (Wong, 1975). As a first test, the complex displacement components on the surface ($z = 0$) of a uniform half-space are evaluated as a function of dimensionless source-receiver distance $r_0 = \omega r/\beta$. The source is a harmonic point force acting on the free surface ($z^* = 0$) of a half-space defined by a reference shear wave velocity β and a Poisson's ratio of 0.33.

The complex displacement components for a perfectly elastic half-space (0 per cent damping) obtained by Wong (1975) using contour integration are tabulated in Table 1 for values of r_0 from 0 to 5 5. The displacements in the first two columns are for a vertical point force while those in the last two columns are for a horizontal point force. It should be noted that $U_{zz}^1(r_0, 0) = U_{rz}^1(r_0, 0)$. The corresponding results for a nearly elastic half-space (0.01 per cent damping, or material attenuation coefficients $Q_\alpha = Q_\beta = 5000$) obtained using the present approach are also listed in Table 1 and match Wong's results with reasonable accuracy given the differences in attenuation models.

Comparison with the results of Pekeris and Lifson (1957). The comparison with results obtained by Pekeris and Lifson (1957) extends the validation to the case of a concentrated vertical force applied at a depth z, in a uniform half-space. The time dependence of the applied force is represented by the Heaviside step function and Poisson's ratio is taken to be 0.25. Pekeris and Lifson obtained the exact motion of the surface of the elastic half-space in the time domain through use of a method similar to that of Cagniard. The validation test is consequently performed in the time domain with the present results generated through Fourier synthesis as described by equation (17).

The left-hand side of Figure 2 displays the results of Pekeris and Lifson for the vertical component of displacement on the free surface at various radial distances, r. The results are presented as a function of the dimensionless time $\tau = \beta t/\sqrt{r^2 + z_0^2}$. The arrivals marked P, S, and R correspond to the compressional, shear, and Rayleigh waves, respectively; the arrivals marked SP correspond to the diffracted wave which starts as S and upon reaching the surface is converted into P (for radial distances beyond the critical distance of $z_0/\sqrt{2}$). The high-frequency prominence of the Rayleigh wave for large values of r/z_0 is deceptively exaggerated

by the reduced time scale. The corresponding results obtained with the present method for a nearly elastic half-space ($Q_\alpha = 1000$, $Q_\beta = 500$) are shown, at a different scale, on the right-hand side of Figure 2. Due to the reduced time parameter, it was necessary to continue the calculations out to extremely high frequencies to match the resolution for radial distances less than $5z_s$. The agreement between the two sets of results is excellent.

Comparison with Cagniard de Hoop approach (Johnson, 1974) In this test, the free surface displacements due to a double couple buried in a uniform half-space

TABLE 1

COMPARISON OF THE PRESENT SOLUTION WITH THE CONTOUR INTEGRATION SOLUTION FOR THE RESPONSE OF A UNIFORM HALF-SPACE TO A CONCENTRATED POINT FORCE ACTING AT THE FREE SURFACE

Wong's (1975) Results with 0% Damping				
00	−0.027, 0.000	0.106, 0.000	0.159, 0.000	−0.106, 0.000
05	−0.032, 0.007	0.067, −0.062	0.146, −0.058	−0.089, 0.058
10	−0.033, 0.025	0.037, −0.102	0.112, −0.105	−0.045, 0.099
15	−0.020, 0.047	−0.029, −0.108	0.063, −0.133	0.015, 0.112
20	0.006, 0.060	−0.087, −0.077	0.011, −0.137	0.075, 0.093
25	0.041, 0.058	−0.120, −0.017	−0.034, −0.120	0.118, 0.045
30	0.074, 0.035	−0.114, 0.053	−0.064, −0.090	0.132, −0.020
35	0.092, −0.005	−0.070, 0.110	−0.076, −0.054	0.111, −0.084
40	0.087, −0.054	−0.001, 0.134	−0.075, −0.024	0.069, −0.132
45	0.056, −0.096	0.072, 0.118	−0.065, −0.004	−0.014, −0.144
50	0.005, −0.120	0.127, 0.064	−0.054, 0.004	−0.088, −0.129
55	−0.054, −0.116	0.144, −0.013	−0.048, 0.033	−0.145, −0.077
Present Results with 0.01% Damping ($Q_\alpha = Q_\beta = 5000$)				
00	−0.027, 0.000	0.106, 0.000	0.159, 0.000	−0.106, 0.000
05	−0.032, 0.007	0.068, −0.061	0.146, −0.058	−0.090, 0.058
10	−0.033, 0.025	0.037, −0.102	0.112, −0.105	−0.046, 0.099
15	−0.021, 0.046	−0.028, −0.108	0.062, −0.133	0.013, 0.112
20	0.006, 0.060	−0.087, −0.077	0.009, −0.137	0.073, 0.093
25	0.041, 0.057	−0.120, −0.017	−0.037, −0.120	0.115, 0.045
30	0.073, 0.035	−0.114, 0.053	−0.068, −0.090	0.128, −0.020
35	0.092, −0.006	−0.071, 0.109	−0.081, −0.055	0.107, −0.084
40	0.087, −0.054	−0.002, 0.134	−0.078, −0.024	0.066, −0.131
45	0.057, −0.096	0.072, 0.117	−0.066, −0.004	−0.015, −0.149
50	0.006, −0.120	0.127, 0.063	−0.052, 0.004	−0.087, −0.129
55	−0.054, −0.115	0.145, −0.013	−0.044, 0.033	−0.142, −0.077

obtained by the present method are compared with the complete solution obtained by the Cagniard-de Hoop method (Johnson, 1974). It should be noted that in the present approach, the surface motion due to a buried dislocation can be obtained by use of reciprocity theorems in the form of suitable combination of stress components evaluated at the depth of the source for a point force acting on the free surface.

The source-time dependence is represented by an 8-sec ramp function, and Poisson's ratio is taken to be 0.25. The attenuation factors used in the present solution are the same as in the previous validation study. The depth of the point dislocation is 5 km, and the epicentral distance is 20 km. The surface displacements are evaluated at an observation azimuth of 22.5° from the strike of the fault, and are normalized by the shear modulus $\bar{\mu}$ times 10^{20} cm^2 divided by the source moment M_o.

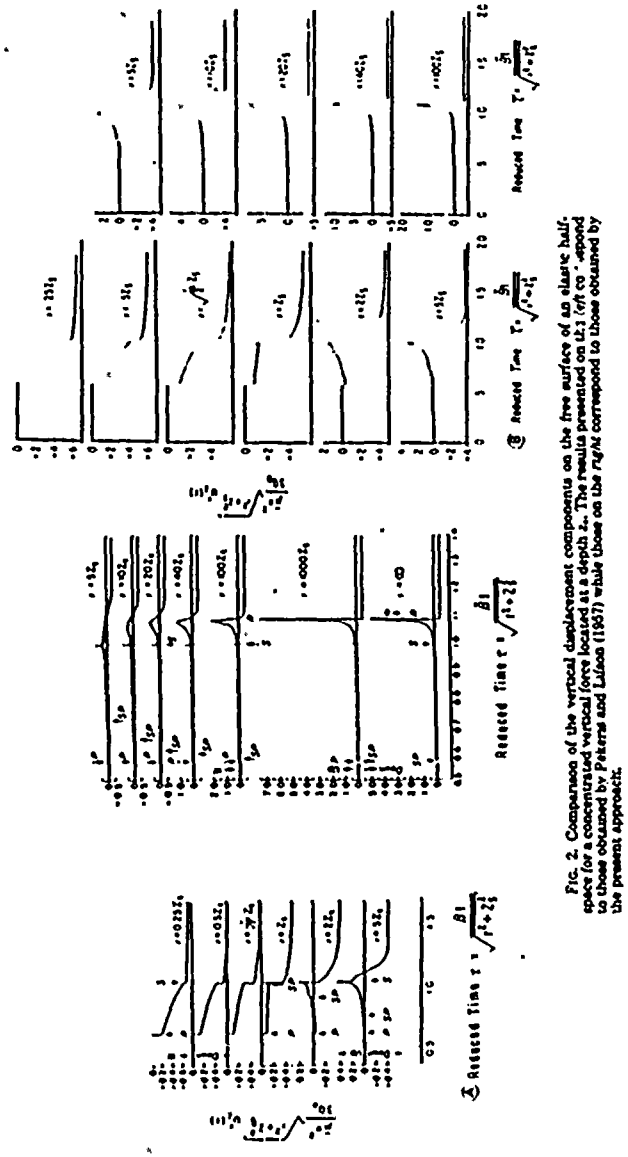

FIG. 2. Comparison of the vertical displacement components on the free surface of an elastic half-space for a concentrated vertical force located at a depth z_s. The results presented on the left correspond to those obtained by Pekeris and Lifson (1957) while those on the right correspond to those obtained by the present approach.

Six different fundamental orientations of the buried point dislocation corresponding to dip and rake angles (δ, γ) of (90°, 0°), (90°, 90°), (45°, 0°), (45°, 90°), (0°, 0°), and (0°, 90°) were considered. A typical comparison is shown in Figure 3. The upper, center, and lower curves in Figure 3 correspond, respectively, to the horizontal displacement component along the direction of the nodal plane, the vertical displacement component, and the horizontal displacement component 90° from the nodal plane. The three displacement components are plotted to the scale appearing on the left and are displayed as a function of real time. The agreement obtained for all components and all fault slip prescriptions is good. The differences at long times result from having to doubly integrate the present results (i.e., to convolve with the ramp source function), whereas Johnson's results are obtained directly for the ramp time dependence.

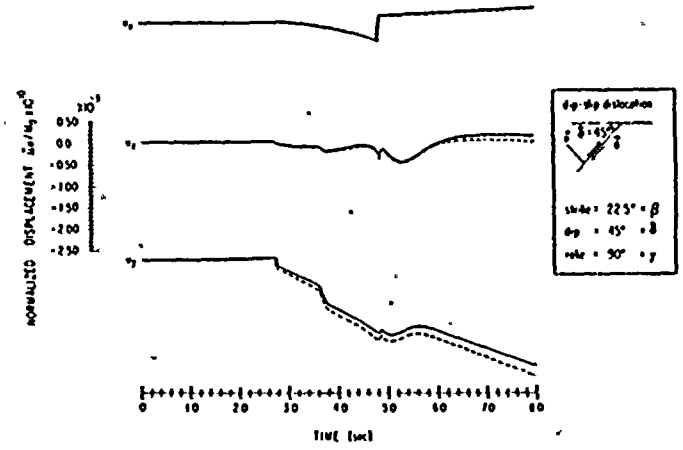

FIG. 3. Comparison of the present solution with the Cagniard de Hoop solution (Johnson, 1974) for the response of a uniform half space to a buried dip slip dislocation with 45° dip

In summary thus far, the comparisons with Wong (1975) and Pekeris and Lifson (1957) verify the accuracy of the displacements in a uniform half-space and the comparison with Johnson (1974) verifies the accuracy of the stresses in a uniform half-space. The following two subsections serve to substantiate the accuracy of the present solution for horizontally layered media.

Comparison with finite element approach (Day, 1977). The free surface displacements resulting from the action of a buried double-couple source are tested once again, but now for the case of a horizontally layered Earth model. The model consists of two layers overlying a semi-infinite half-space as shown in Figure 4, where the individual parameters characterizing the layers are defined. The attenuation factors apply only to the present solution since the finite element solution (Day, 1977) contains no material attenuation.

Source depths of 5 and 1 km are considered and the source time-dependence is represented by a ramp of 1-sec duration in both cases. The source corresponds to a

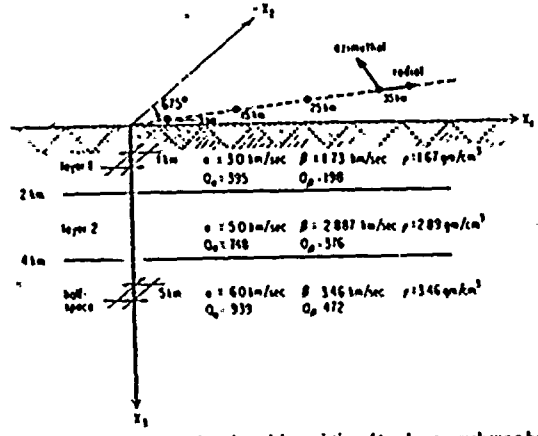

FIG. 4. Source receiver geometry and earth model, consisting of two layers overlying a half space, for use in comparison with the finite element solution

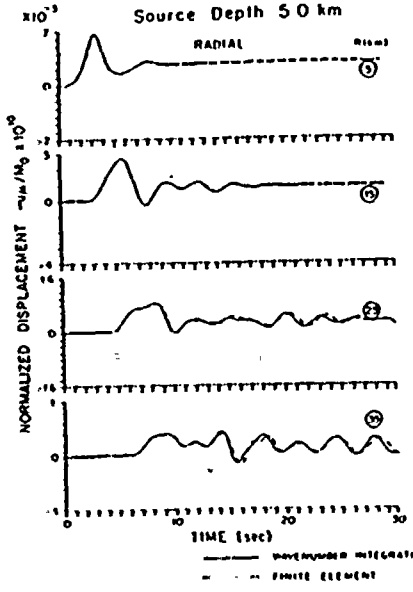

FIG. 5. Comparison of the present solution with the finite element solution (Day, 1977) for the radial displacement component at the free surface due to a vertical strike slip dislocation buried at a depth of 5 km in the earth model depicted in Figure 4

vertical strike-slip dislocation, and the receivers are located at epicentral distances of 5, 15, 25, and 35 km on an azimuth of 22.5° from the strike of the fault (in a dilatational quadrant). The ground motion is normalized by the ratio of the shear modulus in the source layer, μ, times 10_{20} cm^3 to the source moment, M_0. The finite element results have been low-pass filtered down to 0.5 Hz to remove spurious numerical ringing; the present results are computed up to 5 Hz and passed through the same filter in order to maintain consistency in the comparisons.

The comparison to Day's (1977) finite element results for the radial component

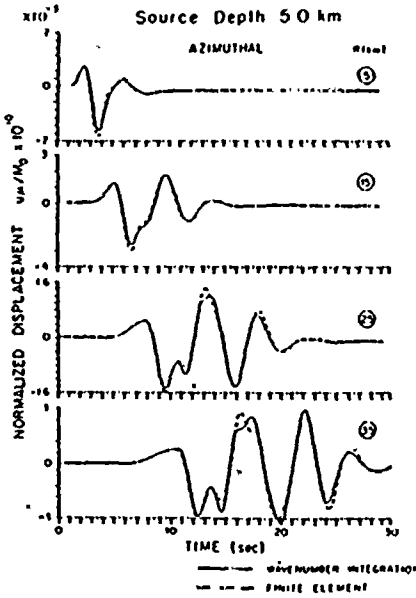

FIG. 6. Corresponding comparison to Figure 5 for the azimuthal displacement component with the source buried at 5 km

of ground motion for the deeper source is shown in Figure 5 at all four epicentral distances. The agreement is remarkable, especially in light of the vast differences between the two solution techniques. The slight deviations in phase have periods much lower than the expected resolution of 2 sec (0.5 Hz). The comparison for the corresponding azimuthal component of motion is shown in Figure 6.

Comparison with discrete wavenumber/finite element approach (Olson, 1978). In this final validation study, the results for the model shown in Figure 4 and for the source described in the previous comparison are compared with those obtained by the discrete wavenumber/finite element method (Olson, 1978). Comparisons for all three components of ground motion at epicentral distances of 5, 15, 25, and 35 km

for a source at a depth of 5 km were made. A typical comparison is presented in Figure 7. Once again, the agreement is excellent and the phase coherence is nearly perfect.

Olson's discrete wavenumber/finite element method more closely resembles the present method than Day's finite method in that the radial dependence is handled analytically through separation of variables. The major differences are: (1) the dependence with depth is calculated using a one-dimensional finite element treatment instead of the closed form factorization of the present method; (2) the response

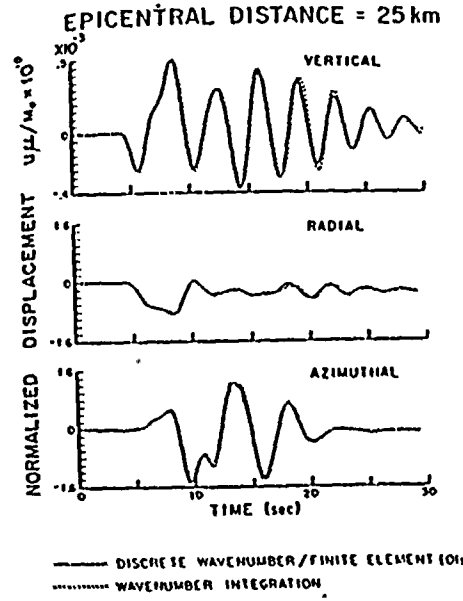

FIG. 7. Comparison of the present solution with the discrete wavenumber/finite element solution (Olson, 1978) for the free surface displacement components at an epicentral distance of 25 km due to a vertical strike-slip dislocation buried at a depth of 5 km in the earth model depicted in Figure 4

is transformed out of the wavenumber domain through Bessel series rather than direct integration; and (3) the procedure is performed explicitly in the time domain with no provision for material attenuation. When the wavelengths of interest are shorter than the changes in the geology as a function of depth, then Olson's method becomes less efficient than the present direct integration method.

Comparison to generalized ray techniques (Helmberger, 1974). In the generalized ray technique, the time-dependent wave field for a layered medium is decomposed into contributions attributed to an infinite set of rays traveling from the source to an individual receiver. Each ray contribution can be evaluated exactly

by the Cagniard-de Hoop technique. However, the number of rays selected is invariably limited by the computational difficulties associated with finding the separate Cagniard paths for every point on the contour and for each kinematic group (rays with same travel time), for all source-receiver pairs. To reduce the cost, certain approximations are used in connection with the Bessel functions causing the generalized ray results to be least reliable at short distances and long periods. Also, differences can be expected in the decay of certain waves with distance since the generalized ray results include no material attenuation.

The earth model employed for the comparison consists of a single layer overlying

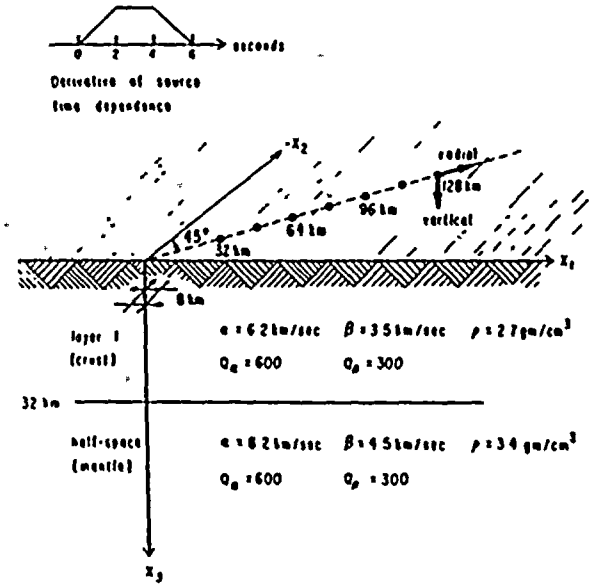

FIG. 8. Source-receiver geometry and earth model consisting of a 32 km thick crust overlying a half-space for use in comparison with the generalized ray solution.

a half-space as shown in Figure 8, where the individual parameters characterizing the layers are defined (the specific attenuation factors apply only to the present solution). It is hoped that by representing the 32-km-thick crust by a single layer, the generalized ray technique will be able to include a sufficient number of multiple reflections and interconversions to converge to the complete solution generated by the present approach.

The source depth is 8 km and the source time-dependence is a quadratic ramp defined by the time integral of the function appearing at the top of Figure 8. The source is equivalent to a vertical strike-slip dislocation; receivers are located at epicentral distances of 32, 48, 64, 80, 96, 112, and 128 km at an azimuth of 45° from the strike (SH mode) for the vertical and radial displacements.

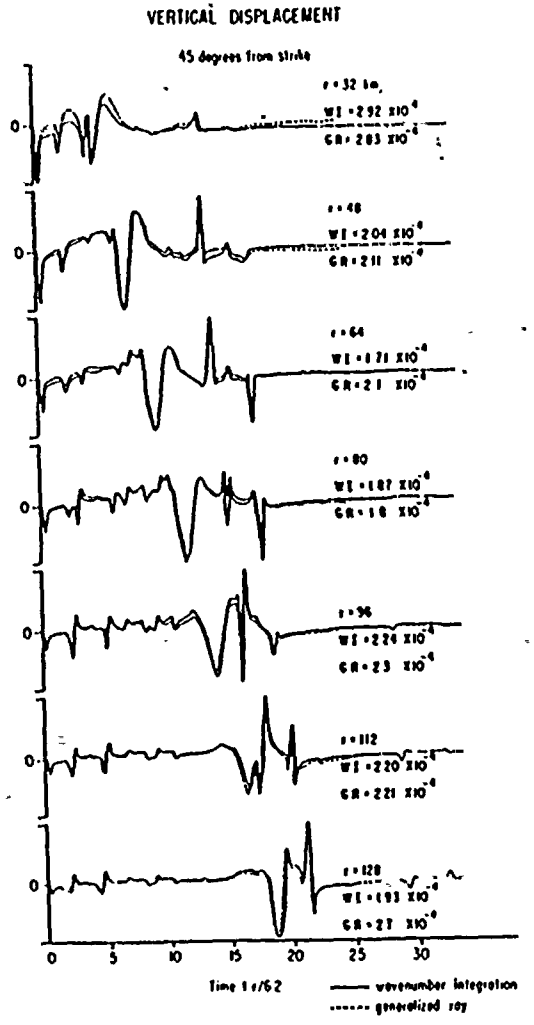

FIG. 9. Comparison of the present solution with the generalized ray solution (Helmberger, 1974) for the vertical displacement component on the free surface due to a vertical strike-slip dislocation buried at a depth of 8 km in the earth model depicted in Figure 8.

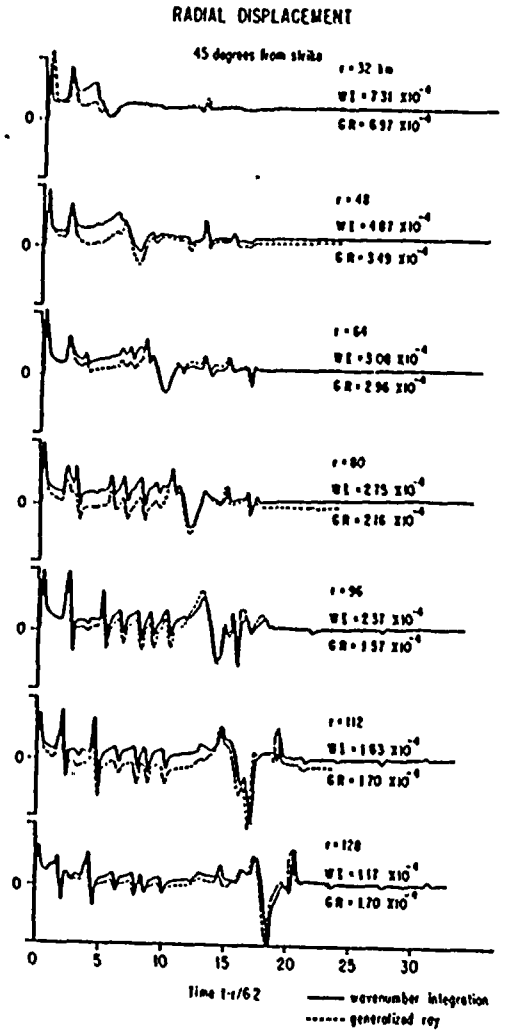

FIG. 10. Corresponding comparison to Figure 9 for the radial displacement component.

The generalized ray results (provided by D. Helmberger) are compared to the present results in Figures 9 and 10 for the vertical and radial displacement components, respectively. The ground displacements are normalized by the ratio of the shear modulus in the source layer times 10^{20} cm^2 divided by the scalar moment of the source. The maximum amplitudes obtained by the respective techniques are self-scaled to fit within the same height on each figure and are shown above and below each seismogram. The time scales are shifted by a time corresponding to the direct compressional arrival at each epicentral distance. The phase coherence is nearly perfect at all epicentral distances considered. Combined with the excellent overall agreement in amplitude, these results lend confidence in the generalized ray

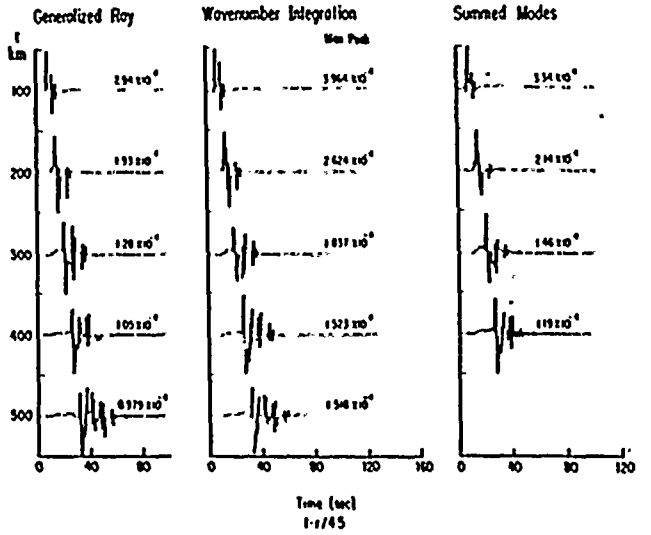

FIG. 11. Comparison of the present solution with the normal mode solution (Harkrider, 1964) and the generalized ray solution (Helmberger, 1974) for the azimuthal displacement component at epicentral distances between 100 and 500 km due to a vertical strike-slip dislocation buried at a depth of 8 km in the earth model depicted in Figure 8

technique and further validate the present method. The deficiencies in amplitude at short distances in the generalized ray results are due to the approximations used in connection with the Bessel functions. The discrepancies in amplitude at the larger distances are probably related to the differences between using an elastic model versus a nearly elastic model (material attenuation factor of $Q_\beta = 300$ included in the present solution). Also, the convergence of the generalized ray expansion is impaired by the increased number of contributing rays at the larger epicentral distances. Finally, the discrepancies at long periods in the generalized ray technique are enhanced by the approximations made for the Bessel functions in the generalized ray calculation (especially in the radial displacements).

Comparison to normal mode technique (Harkrider, 1964, 1970). The previous comparisons are extended to the case of epicentral distances in the range between 100 and 1000 km. The layered earth structure is the same as that depicted in Figure 8 except that attenuation factors of $Q_\beta = 10{,}000$ and $Q_\alpha = 20{,}000$ are used in the present solution so as to eliminate the predominant effects of damping for comparative purposes. The source is also the same as shown in Figure 8 except that the duration is 1.5 sec instead of 0.6 sec.

In addition to comparing with the generalized ray solution (Helmberger, 1974) at these larger distances, the present solution is matched against a solution constructed by superposition of surface-wave modes (Harkrider, 1964, 1970). Similar to the

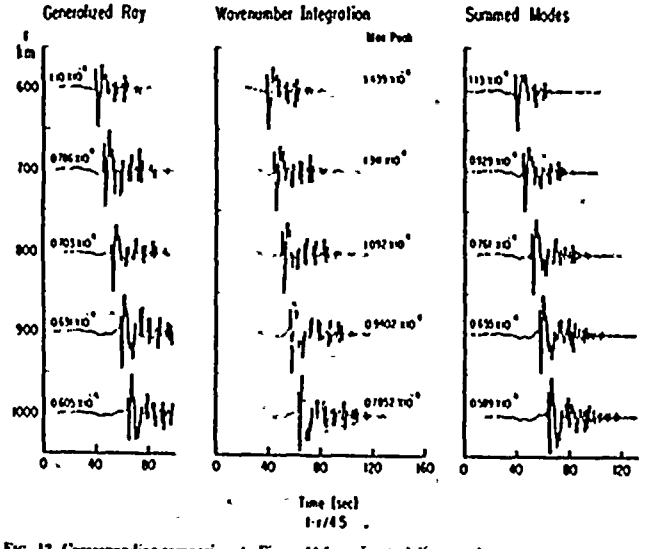

FIG. 12. Corresponding comparison to Figure 11 for epicentral distances between 600 and 1000 km.

present method, the normal mode technique operates first in the frequency domain so that the number of layers offers no limitations. However, the increase in number of contributing modes with frequency restricts the practicability of the normal mode technique to frequencies lower than about 1 or 2 Hz. For this problem, however, the normal mode solution is expected to provide a closer match to the complete wavenumber integration solution than the generalized ray solution since surface waves will tend to dominate the ground motion at periods greater than 1 or 2 sec.

The transverse displacements (*SH*-Love waves) are shown in Figure 11 for epicentral distances in the range between 100 and 500 km and in Figure 12 for epicentral distances between 600 and 1000 km. The ground displacements for all three methods are normalized by the ratio of the shear modulus in the source layer times 10^{20} cm^2 divided by the scalar moment of the source. The maximum amplitudes obtained by the respective techniques are self-scaled to fit within the same height

on each figure and are shown above each seismogram. The time scales are reduced by a time corresponding to the epicentral distance divided by the shear-wave velocity of the mantle, so as to align zero time with the first possible critically reflected arrival. (The generalized ray and normal mode results are courtesy of D. Helmberger and D. Harkrider, respectively.)

As in the match to the generalized ray results at closer epicentral distances, the phase coherence and amplitude agreement is excellent. The somewhat larger time step in the normal mode calculations and the inadequate number of rays in the generalized ray calculation accounts for some of the amplitude discrepancies. Also, the modal superposition only includes the first five surface wave modes.

Summary

A numerical procedure to evaluate the Green's functions for a layered viscoelastic half-space has been presented. The accuracy of the numerical procedure and the associated computer programs has been tested by comparisons with solutions obtained by other methods. In particular, the results obtained by the present approach for the surface displacements on an elastic half-space for concentrated surface forces, concentrated buried sources and buried point dislocations have been compared with the results obtained by Pekeris and Lifson (1957), Johnson (1974), and Wong (1975), respectively. For layered media, the surface displacements generated by a buried point dislocation and calculated by the present approach were compared with those obtained by use of the finite element method (Day, 1977) and the discrete wavenumber-finite-element method (Olson, 1978). Additional comparisons with the results obtained by the generalized ray approach (Helmberger, 1974) and the normal mode technique (Harkrider, 1964, 1970) were also made for the case of a point dislocation buried in an elastic layer overlying an elastic half-space. The excellent agreement obtained for a wide range of frequencies, epicentral distances, and earth or soil structures indicate the reliability and flexibility of the proposed method.

The computer time required to perform the calculations depends on the desired accuracy and the number of source and observer depths, epicentral distances, and layers considered. In a case involving a source located on the surface of a half-space consisting of 10 layers, the computation of the displacement and stress fields at an array of observation stations at five depths and 100 radial distances took 2 to 3 min/frequency in a PRIME 750 computer. When the number of radial distances was reduced to 10, the computer time was reduced to 30 sec/frequency. Calculations of the Green's functions for 20 ring loads and 40 observation points buried in a layered half-space consisting of 6 layers took 2.5 min/frequency in a CDC-7600 computer.

Acknowledgments

The authors would like to thank S. Day, D. Harkrider, S. Hartzell, D. Helmberger, S. Olson, J. Orcutt, and D. Wong for their generous assistance in pursuing the validation comparisons described in the text. The contributions of R. Wiggins and J. Frazier to the development of the sampling technique used are also acknowledged. This study was supported by Grants NSF 77-23829 and NSF PFR 79 08006 from the National Science Foundation.

References

Apsel, R. J. (1979). Dynamic Green's functions for layered media and applications to boundary-value problems, *Ph.D. Thesis*, University of California, San Diego, La Jolla, California.

Day, S. M. (1977). Finite element analysis of seismic scattering problems, *Ph.D. Thesis*, University of California at San Diego, La Jolla, California.

Harkrider, D. G. (1964). Surface waves in multilayered elastic media, Part I. Rayleigh and Lovewaves from buried sources in a multilayered elastic half space, *Bull. Seism. Soc. Am.* **54**, 627-680.
Harkrider, D. G. (1970). Surface waves in multilayered elastic media, Part II. Higher mode spectra and spectral ratios from point sources in plane layered earth models, *Bull. Seism. Soc. Am.* **60**, 377-393.
Helmberger, D. V. (1974). Generalized ray theory for shear dislocations, *Bull. Seism. Soc. Am.* **64**, 45-64.
Johnson, L. R. (1974). Green's function for Lamb's problem, *Geophys. J. R. Astr. Soc.* **37**, 99-131.
Luco, J. E. and R. J. Apsel (1983). On the Green's functions for a layered half space, Part I, *Bull. Seism. Soc. Am.* **73**, 909-929.
Olson, A. (1978). Synthesizing ground motion using a discrete wave-number/finite element representation (abstract), *EOS, Trans. Am. Geophys. Union* **59**, 1128.
Pekeris, C. L. and H. Lifson (1957). Motion on the surface of a uniform elastic half space produced by a buried pulse, *J. Acoust. Soc. Am.* **29**, 1233-1238.
Wong, H. L. (1975). Dynamic soil structure interaction, Report EERL-75-01, Earthquake Engineering Research Laboratory, California Institute of Technology, Pasadena, California.

SIERRA GEOPHYSICS, INC.
15446 BEL-RED ROAD, SUITE 400
REDMOND, WASHINGTON 98052 (R.J.A.)

DEPARTMENT OF APPLIED MECHANICS AND ENGINEERING SCIENCES
UNIVERSITY OF CALIFORNIA AT SAN DIEGO
LA JOLLA, CALIFORNIA 92093 (J.E.L.)

Manuscript received 16 September 1982

APPENDIX I: COEFFICIENTS IN QUARTIC POLYNOMIALS

The coefficients $C_{mj}(m = 1, 5; j = 1, 5)$ appearing in equation (9) are given by

$$(C_{11}, C_{21}, C_{31}, C_{41}, C_{51}) = (0, -bcd, b(c+d)+cd, -(b+c+d), 1)/a(a-b)(a-c)(a-d) \quad (A1)$$

$$(C_{12}, C_{22}, C_{32}, C_{42}, C_{52}) = (1, -a(bc+bd+cd)-bcd, a(b+c+d)+b(c+d)+cd, -(a+b+c+d), 1)/abcd \quad (A2)$$

$$(C_{13}, C_{23}, C_{33}, C_{43}, C_{53}) = (0, acd, -a(c+d)-cd, a+c+d, -1)/b(a-b)(b-c)(b-d) \quad (A3)$$

$$(C_{14}, C_{24}, C_{34}, C_{44}, C_{54}) = (0, -abd, a(b+d)+bd, -(a+b+d), 1)/c(a-c)(b-c)(c-d) \quad (A4)$$

$$(C_{15}, C_{25}, C_{35}, C_{45}, C_{55}) = (0, abc, -a(b+c)-bc, (a+b+c), -1)/d(a-d)(b-d)(c-d) \quad (A5)$$

where

$$a = (k_1 - k_t)/\Delta k, \quad b = (k_2 - k_t)/\Delta k,$$
$$c = (k_4 - k_t)/\Delta k, \quad d = (k_5 - k_t)/\Delta k. \quad (A6)$$

APPENDIX II: AUXILIARY INTEGRALS

The integrals appearing in equation (14) can be written in the form

$$\int_{k_t}^{k_2} \begin{matrix}\cos\\ \sin\end{matrix}(kr_0)\,dk = \Delta k S\left(\frac{\Delta x}{2}\right)\begin{Bmatrix}\cos\\ \sin\end{Bmatrix}(\bar{x}) \quad (A7)$$

$$\int_{k_t}^{k_4}\left(\frac{k-k_t}{\Delta k}\right)\begin{matrix}\cos\\ \sin\end{matrix}(kr_0)\,dk = -\Delta k\left\{\frac{1}{2}S\left(\frac{\Delta x}{2}\right)\begin{matrix}\cos\\ \sin\end{matrix}(\bar{x}) \mp \frac{1}{\Delta x}\left[S\left(\frac{\Delta x}{2}\right)-\cos\left(\frac{\Delta x}{2}\right)\right]\begin{matrix}\sin\\ \cos\end{matrix}(\bar{x})\right\} \quad (A8)$$

$$\int_{k_t}^{k_4}\left(\frac{k-k_t}{\Delta k}\right)^2\begin{matrix}\cos\\ \sin\end{matrix}(kr_0)\,dk = -\Delta k\left\{\frac{1}{2}\left[S\left(\frac{\Delta x}{2}\right)-\frac{4}{(\Delta x)^2}\left(S\left(\frac{\Delta x}{2}\right)-\cos\left(\frac{\Delta x}{2}\right)\right)\right]\begin{matrix}\cos\\ \sin\end{matrix}(\bar{x}) \mp \frac{1}{\Delta x}\left[S\left(\frac{\Delta x}{2}\right)-\cos\left(\frac{\Delta x}{2}\right)\right]\begin{matrix}\sin\\ \cos\end{matrix}(\bar{x})\right\} \quad (A9)$$

$$\int_{k_t}^{k_4}\left(\frac{k-k_t}{\Delta k}\right)^3\begin{matrix}\cos\\ \sin\end{matrix}(kr_0)\,dk = -\Delta k\left\{\frac{1}{2}\left[S\left(\frac{\Delta x}{2}\right)-\frac{6}{(\Delta x)^2}\left(S\left(\frac{\Delta x}{2}\right)-\cos\left(\frac{\Delta x}{2}\right)\right)\right]\begin{matrix}\cos\\ \sin\end{matrix}(\bar{x}) \mp \frac{1}{\Delta x}\left[\left(\frac{3}{2}S\left(\frac{\Delta x}{2}\right)-\cos\left(\frac{\Delta x}{2}\right)\right)-\frac{6}{(\Delta x)^2}\left(S\left(\frac{\Delta x}{2}\right)-\cos\left(\frac{\Delta x}{2}\right)\right)\right]\begin{matrix}\sin\\ \cos\end{matrix}(\bar{x})\right\} \quad (A10)$$

$$\int_{k_t}^{k_4}\left(\frac{k-k_t}{\Delta k}\right)^4\begin{matrix}\cos\\ \sin\end{matrix}(kr_0)\,dk = -\Delta k\left\{\frac{1}{2}\left[S\left(\frac{\Delta x}{2}\right)-\frac{8}{(\Delta x)^2}\left(\frac{3}{2}S\left(\frac{\Delta x}{2}\right)-\cos\left(\frac{\Delta x}{2}\right)\right)+\frac{48}{(\Delta x)^4}\left(S\left(\frac{\Delta x}{2}\right)-\cos\left(\frac{\Delta x}{2}\right)\right)\right]\begin{matrix}\cos\\ \sin\end{matrix}(\bar{x}) \mp \frac{1}{\Delta x}\left[\left(2S\left(\frac{\Delta x}{2}\right)-\cos\left(\frac{\Delta x}{2}\right)\right)-\frac{12}{(\Delta x)^2}\left(S\left(\frac{\Delta x}{2}\right)-\cos\left(\frac{\Delta x}{2}\right)\right)\right]\begin{matrix}\sin\\ \cos\end{matrix}(\bar{x})\right\} \quad (A11)$$

in which

$$\Delta k = k_4 - k_t, \quad \Delta x = \Delta k r_0, \quad S\left(\frac{\Delta x}{2}\right) = \frac{\sin(\Delta x/2)}{(\Delta x/2)}, \quad \bar{x} = \left(\frac{k_t + k_4}{2}\right)r_0. \quad (A12)$$

ATTACHMENT Q2a-2

CONTINUUM LINEAR ANALYSIS FOR SOIL STRUCTURE INTERACTION -VERSION

CLASSIF USER'S MANUAL

JULY 1988

CE934

BECHTEL POWER CORPORATION

CLASSIF

COMPUTER PROGRAM CLASSIF
USER'S MANUAL

Prepared for

Diablo Canyon
Long Term Seismic Program
Pacific Gas & Electric Company
San Francisco, California

by

Bechtel Western Power Corporation
San Francisco, California

July 27, 1988

PREFACE

CLASSI (Continuum Linear Analysis for Soil-Structure Interaction) is a linear three-dimensional, seismic soil-structure interaction (SSI) analysis program developed by Luco and Wong in 1976 at the University of California, San Diego. Since then, the CLASSI program has been continuously upgraded to expand its capabilities and efficiency from those of its initial development. Thus, various versions of the CLASSI program exist in the industry, each covering somewhat different analysis capabilities. The CLASSIF program is a Bechtel version of CLASSI program originally developed in 1978, and recently modified by Wong and Luco in 1985. During the course of installation, testing, and validation of the CLASSIF program on the Bechtel UNIVAC system, some modifications and enhancements were made to the code to improve its performance. These include: implement new algorithms for computing and inverting the Green's function; add a capability for computing SSI responses to steady-state forced vibration applied on the structure; add a capability for computing the relative displacement between two locations in the structure; add a capability for calculating the traction vectors used for a restart of analysis for new wave inputs; add a capability for calculating the transfer function between the SSI response motion and the scattered foundation input motions; implement subroutines for reading in the fixed-based modal properties of structures generated from the BSAP-DYNAM program (a post processor for the Bechtel Structural Analysis Program); implement a free format for the input data and improve the printed output format; correct the option for generating foundation symmetry about one axis; correct the option for calculating the transfer function due to external forcing function; correct the option for calculating the SSI response to include contribution from more than one mode of response; implement the option to bypass a zero-mean baseline correction for calculating the time history response due to ground motion input.

This report has been prepared by Bechtel Power Corporation and has been reviewed following the Bechtel Standard Engineering Department Procedure for nuclear projects.

This report was prepared under a contract agreement between PG&E and Bechtel and is intended for exclusive use by PG&E only. Except for copies that may be required for the Nuclear Regulatory Commission (NRC) in satisfying a regulatory requirement, no copy should be distributed outside of PG&E without prior written consent from Bechtel.

DISCLAIMER

Every reasonable effort was made to provide a comprehensive and flexible computer program. However, the computer program itself and associated documentation are supplied without representation of warranty, expressed or implied, as to its content, accuracy, or freedom from defects or errors.

TABLE OF CONTENTS

TABLE OF CONTENTS

2. PROGRAM DESCRIPTION

2.1 General

CLASSIF is a linear 3-D computer program for seismic soil-structure interaction (SSI) analysis using a continuum halfspace model for representing the foundation medium. The program is a Bechtel version of CLASSI (Continuum Linear Analysis for Soil-Structure Interaction) developed by Luco and Wong since 1976 at the University of California, San Diego. The program is based on the substructuring method and uses the Fast Fourier Transform (FFT) technique to solve the SSI problem in the frequency domain.

Basically, the substructuring method used by CLASSIF separates the analysis of kinematic interaction from that of inertial interaction in two successive analysis steps. Consider, for example, a typical structure on a rigid foundation supported on a soil medium as shown in Fig. 2-1. The substructuring method applied to this soil-structure system is schematically shown in Fig. 2-2. The analysis of kinematic interaction as shown in block I of Fig. 2-2, is handled by first deriving the so-called seismic wave scattering matrix, which is then used to transform a given free-field seismic ground wave field into a set of seismic motions associated with the structural base motion degrees-of-freedom. The analysis of inertial interaction is handled by first deriving the foundation impedance matrix using an integral equation method and Green's functions of a continuum halfspace. The foundation impedances are then combined with the fixed-base structural impedances to form the SSI system, as shown in block II of Figure 2-2. Finally, the interaction response is calculated as shown in block III of Figure 2-2 by subjecting the SSI system to the motions at the structure base resulting from the kinematic interaction from block I as the input seismic excitation. Further details on the theoretical bases of the substructuring method are provided in the CLASSIF theoretical report (Ref. 1).

Based on the substructuring method as described, the CLASSIF program is comprised of three separate program modules consisting of GLAYER, CLAF and SSIF modules. These three program modules solve the SSI problem in separate steps; the results of individual steps by different modules are combined in the final interaction analysis module so as to satisfy the interaction condition at the base. Functionally, the GLAYER module computes the Green's function matrix which relates the harmonic point loads acting at source points and the harmonic displacements at observation points on the surface of horizontal soil layers over a halfspace. Then, the CLAF module computes the foundation impedance matrix and the scattered foundation input motion matrix induced by incident plane waves of arbitrary direction and amplitudes, using the Green's function computed from the GLAYER module as input. The impedance matrix describes the harmonic force-displacement relationship of the foundation mats while the scattered foundation input motion describes the motion of a rigid, massless foundation mats induced by the incident wave. Finally, the SSIF module completes the substructuring process by combining the foundation impedance matrix and the scattered foundation input motion matrix computed from CLAF, and the fixed-base modal properties of structures computed independently from a structural dynamic analysis program to determine the interaction motions at the foundation mats, and then computes the SSI responses at the requested locations in the structures resulting from the foundation interaction motions.

2.2 Program Capabilities and Limitations

The CLASSIF program has the following capabilities and the limitations:

- The underlying soil medium can be simulated as an elastic or viscoelastic (constant hysteretic damping), uniform or horizontally-layered halfspace. There is no restriction on neither number of layers nor their thicknesses.

- The foundation basemat must be rigid, flat, and supported on the surface of halfspace. They can be of any arbitrary planar shape and multiple structural foundations can also be accommodated.

- Free-field seismic ground motions can be specified as a seismic wave field composed of arbitrary incident plane P, SV, or SH body waves, or Rayleigh and Love surface waves, or any combination thereof.

- The effect of foundation embedment can only be approximately evaluated using the embedment foundation impedance modification factors.

- The analysis procedure utilizes the frequency domain solution method. Therefore, non-linear strain-dependent soil properties cannot be directly considered. It requires separate analyses to determine the strain-compatible equivalent linear soil properties for input to the program.

- The fixed-base modal properties of structures required as input to CLASSIF need to be extracted form other structural dynamic analysis programs. Either finite element models or lumped parameter models can be used as the structure model.

- The program has the capability to interface with the Bechtel BSAP-DYNAM program to extract the fixed-base modal properties for input to SSI analysis.

- CLASSIF program uses the modal superposition to calculate the dynamic response at any point within the structure. The truncated higher modes are included as rigid masses at the reference level and there is no loss in effective mass from the superstructures.

- Externally-applied transient or steady state forced vibration dynamic loads can be prescribed either on the structure or on the foundation.

- The program can be used to calculate the response time history (accelerogram) as well as the complex frequency response (transfer functions).

- The effect of surface-supported, mutliple-structure-to-structure interaction can be rigorously evaluated.

2.3 Capabilities Validated

The computer program CLASSIF was tested in Ref. (2) for a set of eighteen validation test problems to validate the various analysis capabilities available in the program; broadly classified as, impedance analysis, wave scattering analysis, seismic SSI analysis and forced vibration analysis. The capabilities that were validated by these test problems are shown in Table 2.3-1.

Table 2.3-1

List of Capabilities Tested for CLASSIF

CAPABILITIES TESTED	VALIDATION TEST PROBLEM NO.
1 IMPEDANCE ANALYSIS	
1.1 Foundation on Uniform Halfspace	
1.1.1 Circular Foundation	1, 11
1.1.2 Square Foundation	8
1.1.3 Strip Foundation	9, 10
1.1.4 Ring Foundation	12
1.2 Foundation on Layered System	
1.2.1 Circular Foundation	2, 4
1.2.2 Strip Foundation	10
1.3 Multiple Foundations	5
2 SCATTERING ANALYSIS	
2.1 Inclined Body Waves	3
2.2 Surface Waves	6
3 SSI ANALYSIS	
3.1 Seismic Response	1, 4, 7, 13, 14, 17, 18
3.2 External Force Vibration	15, 16

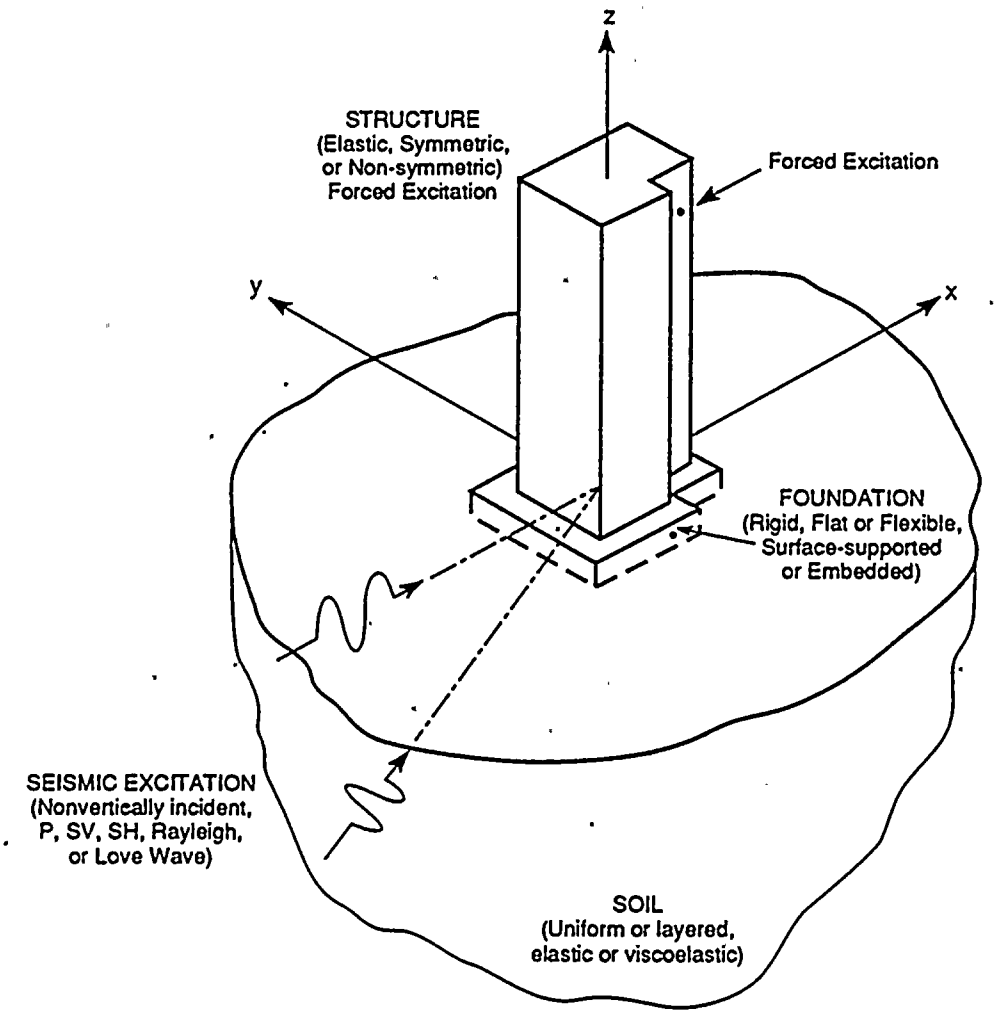

Figure 2-1. Description of the Soil-Structure System

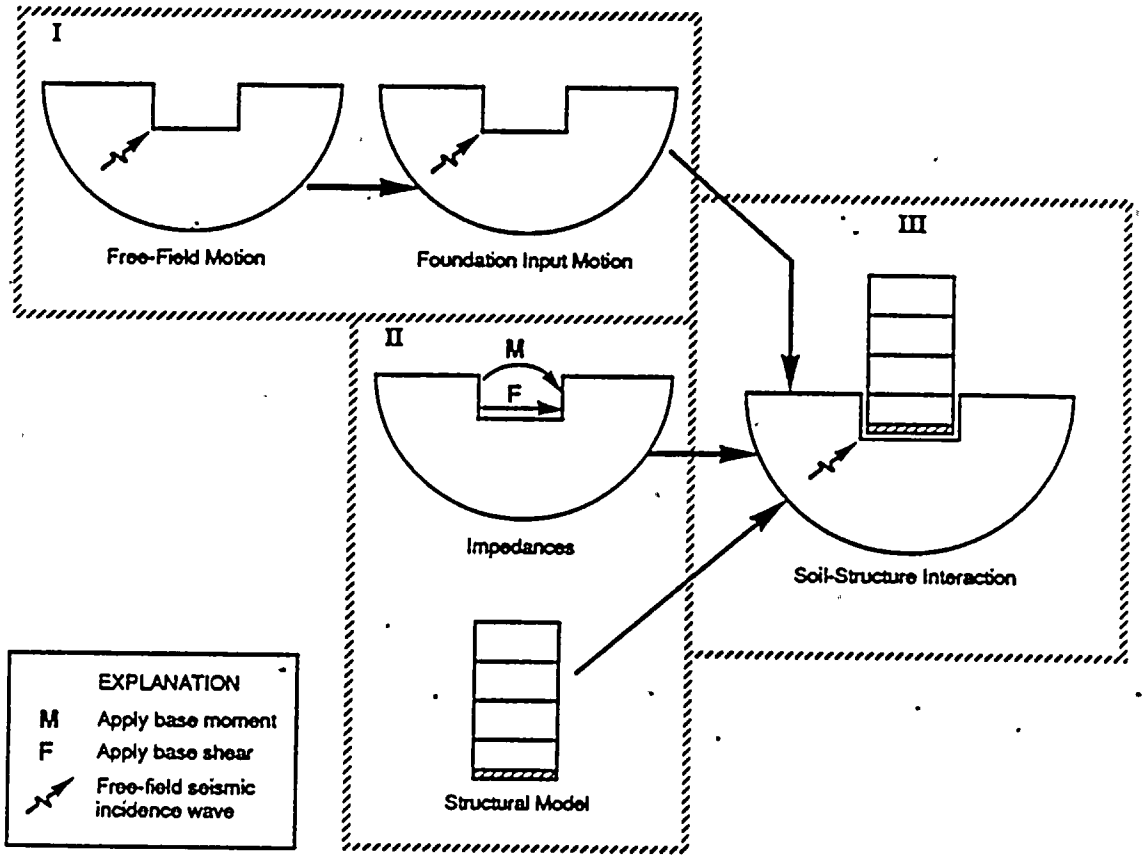

Figure 2-2. CLASSIF Substructuring Technique for SSI Analysis

3. PROGRAM ORGANIZATION

3.1 Program Structure

The CLASSIF program is organized to suit the substructuring process of SSI analysis, as described in Section 2. The program is thus subdivided into three separate program modules GLAYER, CLAF and SSIF for separate steps of analyses. These three program modules are interfaced with each other through the output files generated from the previous step of analysis. The flow charts showing the interface relationship between these modules for the impedance and scattering analysis, seismic SSI analysis, and forced vibration analysis are depicted in Figs. 3.1-1 through 3.1-3, respectively. The basic input data required for these modules and the output results generated from these modules are also shown in these figures. For seismic SSI analysis or forced vibration analysis, the fixed-base modal properties of structures generated from an independent analysis using a standard structural dynamic analysis computer program, e.g., Bechtel standard computer program BSAP, are also required as part of the input to the SSIF program module, as shown in Figs. 3.1-2 and 3.1-3, respectively.

3.2 File Structure

The flow charts showing the file structures are depicted in Fig. 3.1-4 for the impedance and scattering analysis, and in Fig. 3.1-5 for both the seismic SSI analysis and forced vibration analysis. The descriptions of the file formats and contents generated from the program modules GLAYER, CLAF and SSIF for these analyses are provided as shown in Table 3.1-1.

Table 3.1-1

Description of Files Generated from CLASSIF Program Modules

File Name	Format	Generated by	Contents
File 7	Binary	GLAYER	Green's function table, control parameters, dimensionless frequencies.
File 8	Binary	CLAF	Foundation impedance matrix, dimensionless frequencies.
File 9	Binary	CLAF	Foundation input motion vector, dimensionless frequencies.
File 11	Binary	CLAF	Foundation contact traction matrix, dimensionless frequencies.
File 15	Binary	SSIF	Response time histories or transfer functions.

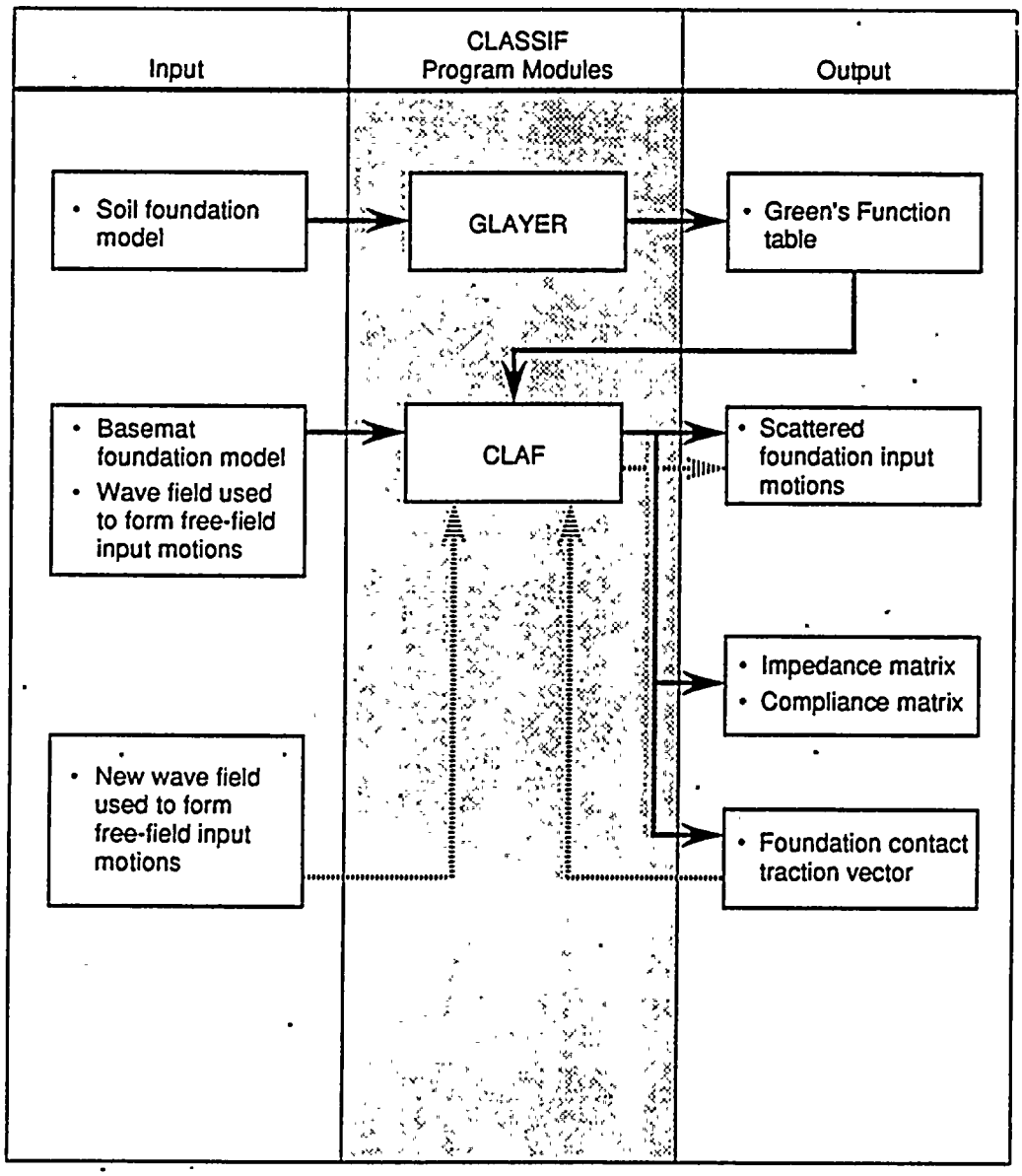

Figure 3.1-1. Flow Chart Showing Program Module Interfaces for Scattering Analysis

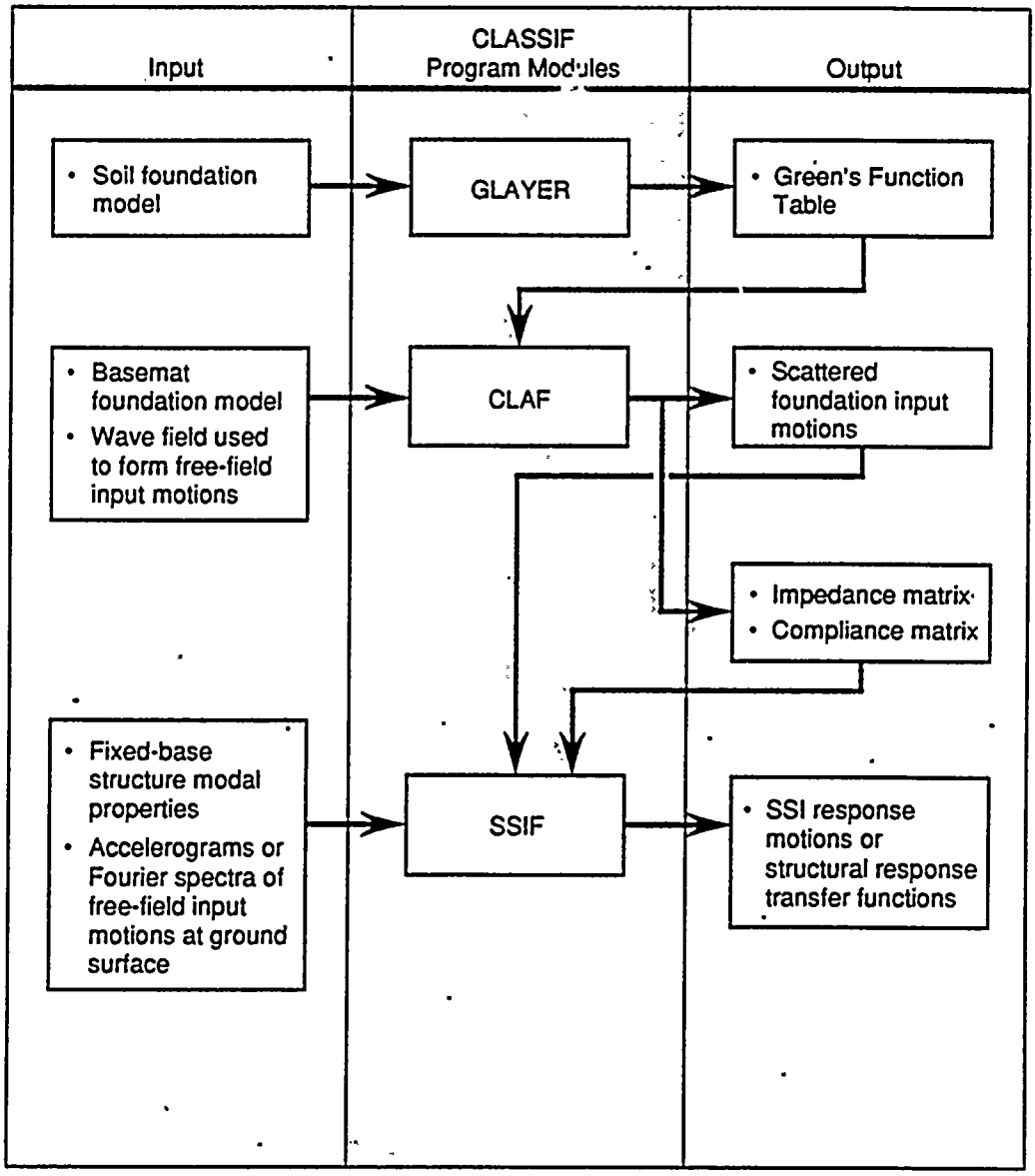

Figure 3.1-2. Flow Chart Showing Program Module Interface for Seismic SSI Analysis

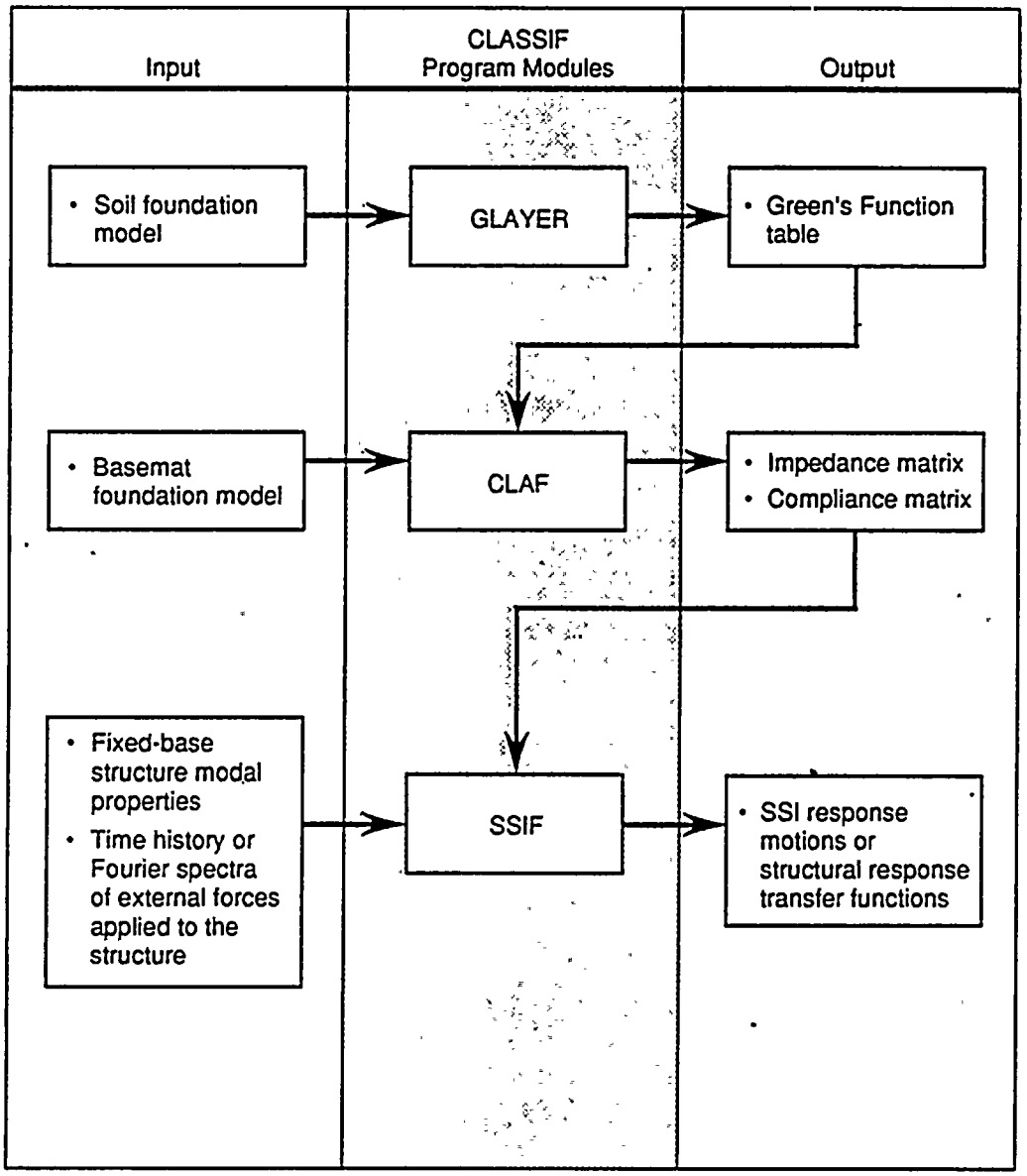

Figure 3.1-3. Flow Chart Showing Program Module Interfaces for Forced Vibration SSI Analysis

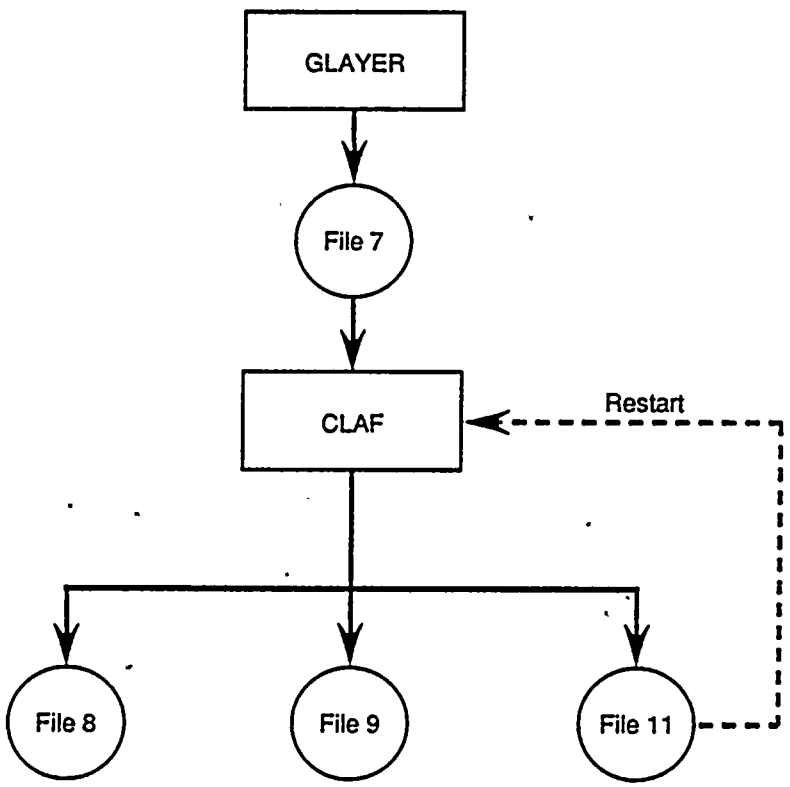

Figure 3.1-4. Flow Chart Showing File Structure for Scattering Analysis

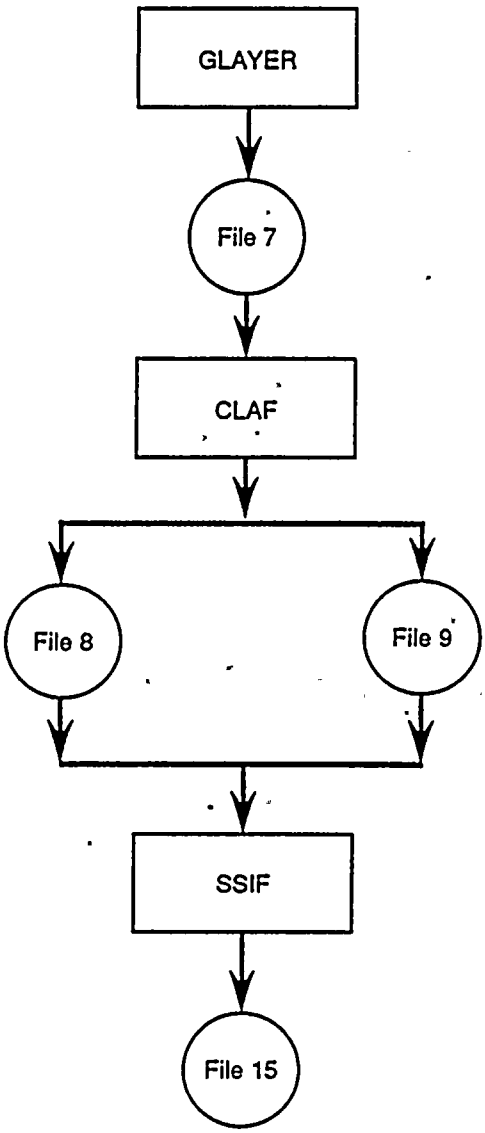

Figure 3.1-5. Flow Chart Showing File Structure for Seismic SSI Analysis or Forced Vibration Analysis

4. NUMERICAL STABILITY CRITERIA

The CLASSIF program uses numerical schemes for interpolation and integration of Green's functions for layered soil media. To ensure the accuracy of the numerical results, criteria for those numerical schemes have been established and implemented into the programs, as described in this section. In addition, the criterion for the discretization of foundation area for the impedance calculation is described.

(a) Criterion for the numerical integration scheme for computing Green's functions for layered media.

The criterion for the numerical integration of Green's functions has been studied and established by Apsel and Luco (Ref. 3). The numerical integration scheme used in CLASSIF uses the method of quadrature which is based on the local representation of the function by a fourth order (quartic) polynomial. A five-point sampling of the Green's function kernel is applied to check the adequacy of the representation locally by the quartric polynomial in the wave number domain. The sampling points in a given wave number interval are selected according to an error criterion which requires that the contribution of the fifth order term in the polynomial expansion of the Green's function kernal to the Green's function integral over the interval be significantly smaller than the integral. This numerical integration scheme includes an automatic checking procedure that, if the prescribed tolerance of the error criterion is not satisfied, a new sampling point is automatically inserted between the two points with the largest spacing. The sequence of points is then renumbered and integration including the new point sampled is peformed. This process is repeated until the prescribed tolerance (set to be 0.002 in the program) is satisfied. Thus, the accuracy of the numerical integration scheme for Geen's function is automatically ensured to within the set tolerance with this automatic checking procedure.

(b) Criterion for the spatial interpolation of Green's function to generate impedances.

For each specified frequency, the generation of impedance from calculated Green's functions in the CLASSIF program uses a second order polynomial with three equally spaced points (Ref. 1) for interpolating the Green's functions for spatial variable. This interpolation scheme includes an automatic accuracy checking procedure in the program by comparing the exact calculated values with the interpolated values at several check points. This automatic checking procedure works by first calculating an intial table of Green's function values for a set of relatively coarse increments, then the increments are halved and new values at the half increments are calculated. Accuracy tests are then performed at these half increment points to determine whether the accuracy of the interpolated values are within a prescribed tolerance (set to be .02 in the program). If the accuracy is not sufficient, another set of half increments is established and the new values are calculated. This process is repeated until the prescribed accuracy is reached. Thus, the accuracy of spatial interpolation of Green's function is automatically ensured to within the set tolerance with this automatic checking procedure.

(c) Criterion for the discretization of foundation area.

The criterion for the discretization of CLASSIF foundation area for Green's function integration to generate impedances has been studied and established by Wong and Luco (Ref. 4). The criterion requires that the foundation be discretized with finer subregions at the foundation perimeter where the stress gradient is the highest. As an example, if the foundation of dimension 2ax2a is to be subdivided into 10x10 perpendicular grids, the center points of these grids which are used for the integration of Green's functions, are required to be separated with the distances times the factors (1,

α^2, α^3, α^4, α^4, α^3, α^2, 1), in which $\Delta = a\ (\alpha - 1)/(\alpha^5 - 1)$, and $\alpha \geq 1$. Ref. 3 has demonstrated that $\alpha = 2.0$ gives a sufficient accuracy for the impedance calculation. The adequacy of the criterion for impedance calculation has also been demonstrated by the extensive benchmarking studies performed in the CLASSIF Validation Report (Ref. 2).

5. APPLICATION GUIDELINES

This section provides the users with guidelines on effective usage of the CLASSIF program to solve the SSI problem. The application of the program requires the following analysis steps.

Step 1: The dynamic characteristics of the super-structure such as the mass, stiffness, and damping matrices are modelled using a standard structural dynamic analysis program and the fixed based modal properties (natural frequencies, mode shapes, modal damping ratios, and modal participation factors) are computed and used for input to the CLASSIF program.

Step 2: The mass and mass moments of inertia of the structural foundation are separately computed.

Step 3: The area of the foundation assumed to be rigid is discretized into small subregions. Finer subdivisions are used near the foundation perimeter where the stress gradient of the foundation interface stresses is the largest. Then, the program module GLAYER is executed to obtain the Green's functions which are frequency dependent.

Step 4: The program module CLAF is executed to integrate the Green's functions over the discretized foundation area to obtain the foundation impedance functions which are frequency dependent. For forced excitations, the driving force vector is directly formed. For seismic excitations, the seismic incidence wave field (wave type, azimuth, and incidence angle) is specified, and the seismic driving force vector normalized to unit input amplitude is computed.

Step 5: The forcing function or the control ground motion time histories are input to program module SSIF. The module forms the system equations of motion in the frequency domain by assembling the

fixed-base modal properties of the structures from Step 1, the foundation base inertia properties from Step 2, the foundation impedance matrix and driving force vectors from Step 4. The equations of motion are solved for SSI response transfer functions which are used finally to convolve with the Fourier transforms of the input time histories to give the response motion time histories at desired locations.

Step 6: The response time histories of the structural foundation are used as input to re-excite the fixed-base structural model of Step 1 to compute the time history response of internal stresses, forces, and moments in the structure.

To aid the users on preparations of the input data for each of the three CLASSIF program modules, i.e., GLAYER, CLAF and SSIF modules, guidelines are provided in Subsection 5.1. Furthermore, guidelines are also provided for specifications of some of the input parameters for these program modules in Subsection 5.2.

5.1 Preparations of Input Data

The input data for GLAYER, CLAF and SSIF are organized into modules of input data, which can be entered in a free format. The units of input data are in consistent units. To help detect possible errors in the input data, each data module starts with a "Module Identification Line" consisting of a bracket with 2-digit module number followed by comments after Column 4. The program module will only read the integer located at Columns 2 and 3 to check if each module starts at the correct place. If the previous module contains the wrong number of data lines, the incorrect offset of the module identification line will cause an error and stop the program to warn the user. The spaces after Column 4 of the Module Identification Line can be used for comments; they are however, ignored by the program.

GLAYER Module

The data modules for GLAYER consist of 11 modules of input data which are provided in Subsection 6.1. The flow chart showing these modules of input data is schematically depicted in Fig. 5-1. It also identifies the modules of input data associated with the option which allows the user to manually or automatically determine the increment of radius to be used for Green's function calculation. If the user selects the option IFITER=0 in Module No. (02), the user needs to specify the increment of radius for the Green's function, and prepare the input data for Module Nos. (00) through (03) and Module Nos. (05) through (10), as shown in Fig. 5-1. However, if the user selects the option IFITER = 1, the program will automatically determine the optimal increment of radius for the Green's function, and the user needs only to prepare the input data for Modules Nos (00) through (02) and Module Nos. (04) through (10), as shown in Fig. 5-1.

CLAF Module

The data modules for CLAF consist of 7 modules of input data which are provided in Subsection 6.2. The flow chart showing these modules of input data is schematically depicted in Figure 5-2. In this figure, the modules of input data associated with the restart option (IPASS) and the option for calculating impedance and wave scattering matrices (NCASE) are identified for the user to prepare the input data for CLAF. All data modules, i.e., Module Nos. (00) through (06), need to be prepared for the impedance and scattering analyses, as shown in Fig. 5-2. For impedance matrix calculation for mutliple foundations, the input data for Module No. (03) need to be repeated for each of these foundations, as indicated in Fig. 5.2. For a layered soil medium, the input data for Module No. (06) also need to repeated for each of excitation frequencies. If only the impedance calculation is requested, i.e., NCASE=0, only excitation frequencies need to be specified as input data for Module

No. (06). However, if both impedance and wave scattering calculations are requested, i.e., NCASE≠0, both excitation frequencies and incident plane waves need to be specified as input for Module No. (06). The guidelines on how to specify the input data for different types of incident plane waves are described in Subsection 5.2.

SSIF Module

The data modules for SSIF consist of 13 modules of input data which are provided in Subsection 6.3. The flow chart showing these modules of input data is schematically depicted in Fig. 5-3. As can be seen from this figure, only 11 of 13 data modules, i.e., Module Nos. (00) through (04) and Module Nos. (07) through (12) are currently available for input data preparation in this version of CLASSIF. The two data modules tha are currently not available are Module Nos. (05) and (06). Module No. (06) is associated with the option for flexible foundation (METHOD=2), and Module No. (05) is associated with the option for read-in the rigid mass matrix and modal participation factor matrix for the structure (IFCAL=0), as shown in Fig. 5-3.

If there are more than one structure resting on a foundation, the input data for Module Nos. (03) and (04) need to be repeated NSTR times for each of NSTR structures, as shown in Fig. 5-3. Similarly, if there are more than one foundation, the input data for Module No. (07) need to be repeated NFDN times for each of NFDN foundations.

Fig. 5-3 shows that the option NEXFOR=0 in Module No. (03) should be selected for seismic SSI analysis, and the option NEXFOR=N, where N is total number of points at which external forces are applied, should be selected for forced vibration analysis. The relative displacement response can be obtained from using the input parameter NREL in Module No. (08) to indicate the number of relative displacement components to be calculated. No relative displacement

will be calculated if NREL=0, and, by default, only the absolute acceleration response will be calculated at the indicated dynamic degrees of freedom.

For a time history analysis the input parameter LFT=1 should be specified in Module No. (09), and the input data need to be prepared for Module Nos. (10) and (12), as shown in Fig. 5-2. For a frequency analysis, however, the input parameter LFT=2 should be specified in Module No. (09), and the input data need to be prepared for Module Nos. (11) and (12), as shown in Fig. 5-2.

5.2 Specifications of Input Parameters

In this subsection, guidelines on specifications of some of the input parameters contained in the data modules for GLAYER, CLAF and SSIF are outlined to aid the user in prescribing these input parameters.

GLAYER Module

(i) The optimal increment of radius used in the Green's function calculation, i.e., the parameter DR, must be chosen small enough so that a prescribed accuracy of the interpolated values of Green's function can be obtained, but should not be too large so that the number of points in the Green's function table is reasonable. This optimal increment, however, is not easily predicted before calculation, since it is dependent on frequency and on the soil properties. Recognizing this difficulty, the GLAYER module has provided the user with the option IFITER=1 in data Module No. (02) which will automatically selected the optimal DR, and check the interpolated Green's function values to ensure that the accuracy of the interpolated values are within the set tolerance as per the criterion described in Section 4(b).

Therefore, it is recommended that the user should select the option IFITER=1 rather than the option IFITER=0 in prescribing the input parameter DR.

(ii) For a uniform halfspace (NLY=1), the user needs to specify only one frequency of analysis (NFRQ=1) which corresponds to the maximum frequency for the FRQ parameter, at which the Green's Function Table is to be calculated. This maximum frequency is usually specified to be about 34 cps, which covers the frequency range practically used for the SSI analysis.

(iii) For a layered soil medium (NLY>1), a Green's Function Table must be calculated for each frequency. Thus, the user should specify the total number of frequencies for the NFRQ parameter and the frequencies must be input in the ascending order. These frequencies should cover the frequency up to about 34 cps, including the predominant frequencies of the SSI system.

CLAF Module

(i) Since the accuracy of the foundation impedance function depends on proper discretization of the foundation area, the user should follow the foundation discretization criterion for impedance calculation as described in Section 4(c), when discretizing the foundation subregions. It should be noted that the foundation areas can only be discretized as square or rectangular subregions; other shapes of subregions are not permitted by CLAF.

(ii) For a symmetrical foundation, the user should take advantage of the symmetrical conditions of the foundation to reduce computing costs of impedance calculation. The input

parameters IFSX and IFSY can be used for this purpose to indicate the foundation symmetry about x-axis and y-axis, respectively.

(iii) The user should save the traction vector on File 11 using the input parameter IPASS=1, for a restart calculation of scattered foundation input motions due to new incident wave inputs. This restart calculation option can substantially reduce computing costs of calculating the new scattered input motions especially for a large foundation or multiple foundations.

(iv) The user can specify the incident plane wave using the input parameters BOC, TH, ULR, ULI, UTR, UTI, UVR, and UVI in CLAF data Module No. (06). These input parameters are related to the general wave form used in CLAF for the incident plane wave propagating along the x'-axis, as shown in Figure 5-4, as follows:

$$\begin{Bmatrix} U_L(\omega) \\ U_T(\omega) \\ U_V(\omega) \end{Bmatrix} = \begin{Bmatrix} \hat{U}_L \\ \hat{U}_T \\ \hat{U}_V \end{Bmatrix} e^{-i(\omega/c(\omega))x'} U_g(\omega)$$

in which $U_L(\omega)$, $U_T(\omega)$ and $U_V(\omega)$ are the longitudinal, transverse and vertical components, respectively, of the plane wave depicted in Figure 5-4, ω is circular frequency in radian/second, $\hat{U}_L$ = (ULR) + i(ULI), $\hat{U}_T$ = (UTR) + i(UTI), $\hat{U}_V$ = (UVR) + i(UVI), $\cos\theta_V = \beta/c$ = BOC, $c(\omega)$ = the apparent wave velocity, β = the shear wave velocity of the top soil layer, θ_V = the vertical incident wave angle measured with respect to the horizontal x'-axis, $i = \sqrt{-1}$, $x' = x\cos\theta_H + Y\sin\theta_H$, θ_H = the horizontal wave angle measured counterclockwise with

respect to the x-axis, as shown in Figure 5-4, $U_g(\omega)$ is the Fourier amplitude of the free-field motion at the center of the foundation.

With the above form of incident plane wave, U_L, U_T and U_V can be specified such that at least one of them is a constant over frequency. For example, only the $U_T(\omega)$ is non-zero for SH or Love waves; therefore, the user can set $\hat{U}_T = 1$, and $Ug(\omega) = U_T(\omega)$ at $x' = 0$. For P, SV or Rayleigh waves in a layered medium, the $U_L(\omega)$ and $U_V(\omega)$ components are coupled; the best method is to make $\hat{U}_L = 1$, $\hat{U}_V = U_V(\omega)/U_L(\omega)$, and $U_g(\omega) = U_L(\omega)$ at $x' = 0$. The ratio $\hat{U}_V$ is still a function of frequency (except for a halfspace). Alternatively, the same motion can be prescribed by setting $\hat{U}_V = 1$, $\hat{U}_L = U_L(\omega)/U_V(\omega)$, and $U_g(\omega) = U_V(\omega)$ at $x' = 0$.

The phase $e^{-i(\omega/c(\omega))x'}$ in the above equation describes the variation of phase along the direction of propagation x'. The apparent velocity of wave propagation, $c(\omega)$, determines the wavelength on the surface and is therefore instrumental in determining the amount of wave scattering from the foundation. For body waves in an elastic medium, $c(\omega)$ is a constant and is related to the angle of wave incident. For example, the apparent velocity is infinite ($c \rightarrow \infty$) for vertically incident S or P waves because the phase is identical for all points on the surface. For other angles of incidence, $c = \beta/\cos\theta_V$, where θ_V is an angle measured with respect to the horizontal axis x'.

For surface waves in a layered medium, $c(\omega)$ is a function of frequency (except for a Rayleigh wave in a uniform halfspace) and it is equal to the phase velocity of the surface waves. The variation of velocity $c(\omega)$ with frequency is different for each mode of surface waves; furthermore, some modes do

not exist at low frequencies. Thus, the normalized amplitudes $\hat{U}_L$, $\hat{U}_T$ or $\hat{U}_V$ should be set to zero for frequencies lower than the critical frequency.

SSIF Module

(i) The program requires that the coordinate system of the structure must be oriented such that the z-axis represents the vertical axis of the structure.

(ii) The program has options for the user to transform the foundation impedance matrix and scattered input motion vector, the mass matrix of the rigid foundation, and the structural matrix, from their local coordinate systems to the reference coordinate system, using the input parameters X, Y, Z and Q. The translational angle Q are measured counterclockwise in radians from the X-axis as shown in Figure 5-5. To illustrate the coordinate transformation option, an example consisting of a foundation and a structure that is eccentric is shown in Figure 5-5. Since the impedance matrix and the scattered input motion vector are calculated for the bottom of the foundation mat where the origin of the foundation coordinate system (X_F, Y_F, Z_F) is located, and the foundation motion is to be calculated at the reference coordinate system (X_R, Y_R, Z_R), a transformation is needed. As illustrated in Figure 5-5, $X_F = 0$, $Y_F = 0$, $Q_F = 0$ and Z_F is a negative number. Z_F is negative because of the origin of the (X_F, Y_F, Z_F) system is below the reference system. As an additional example for defining the transformation coordinates X, Y, Z and Q, the building coordinate system (X_B, Y_B, Z_B) is considered. As illustrated in Figure 3.1, $X_B < 0$, $Y_B > 0$, $Z_B = 0$ and $Q_B > 0$.

In the program transformations are allowed only if all six degrees of freedom are considered. This restriction is important because a symmetrical structure placed eccentrically about a foundation can cause torsion, rocking and translations in all directions; hence, all six components are required.

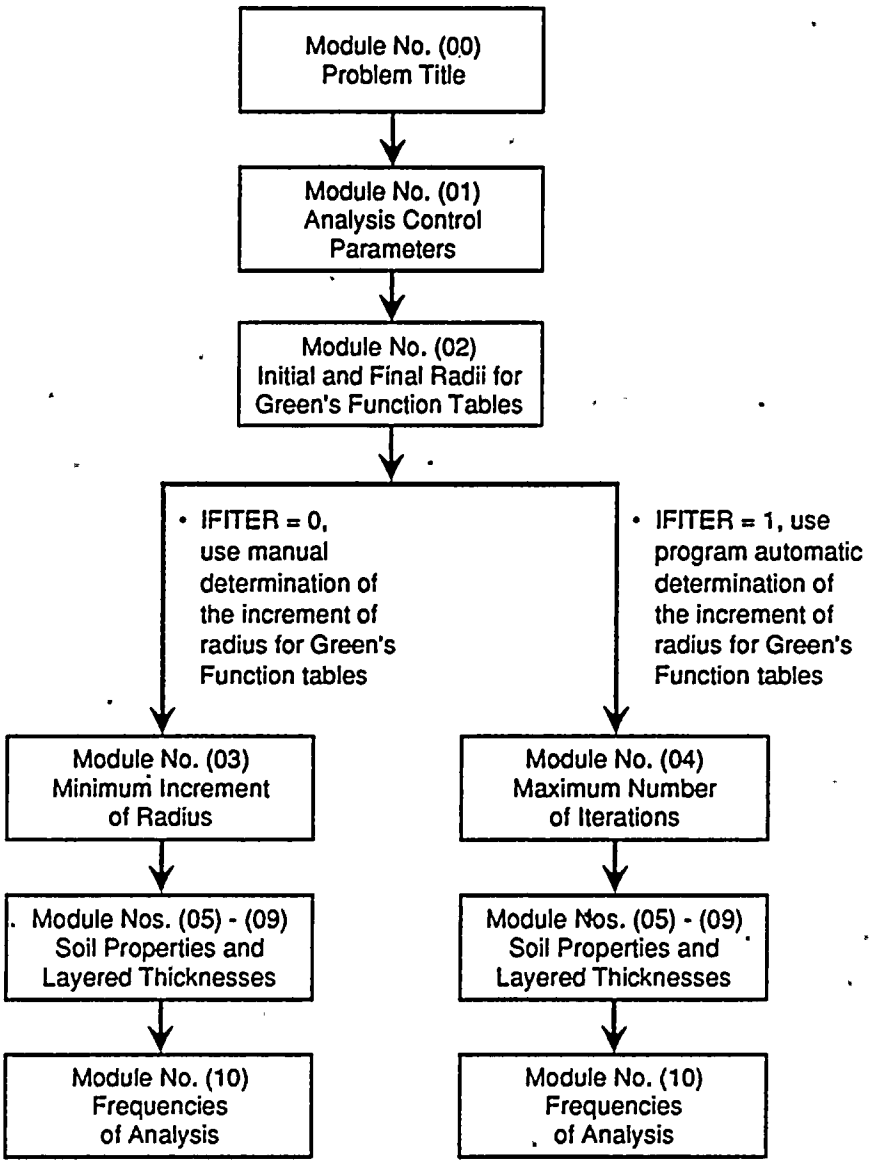

Figure 5-1. Flow Chart Showing Modules of Input Data for GLAYER Program Module

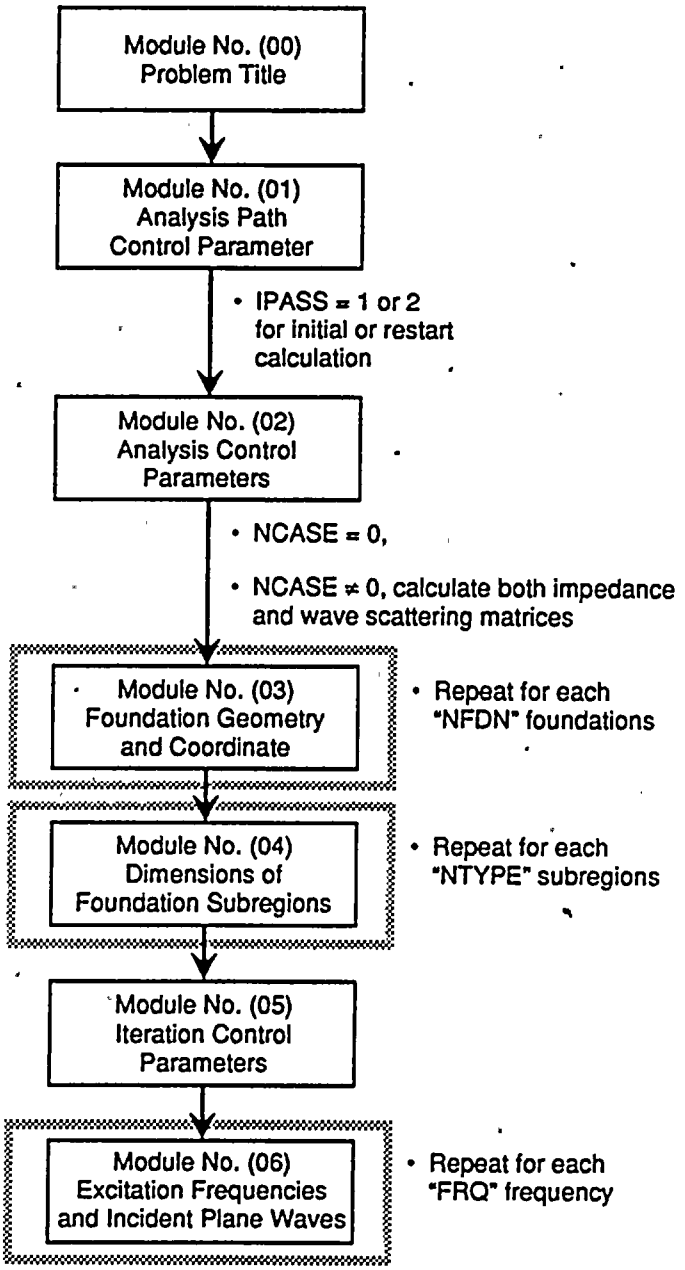

Figure 5-2. Flow Chart Showing Modules of Input Data for CLAF Program Module

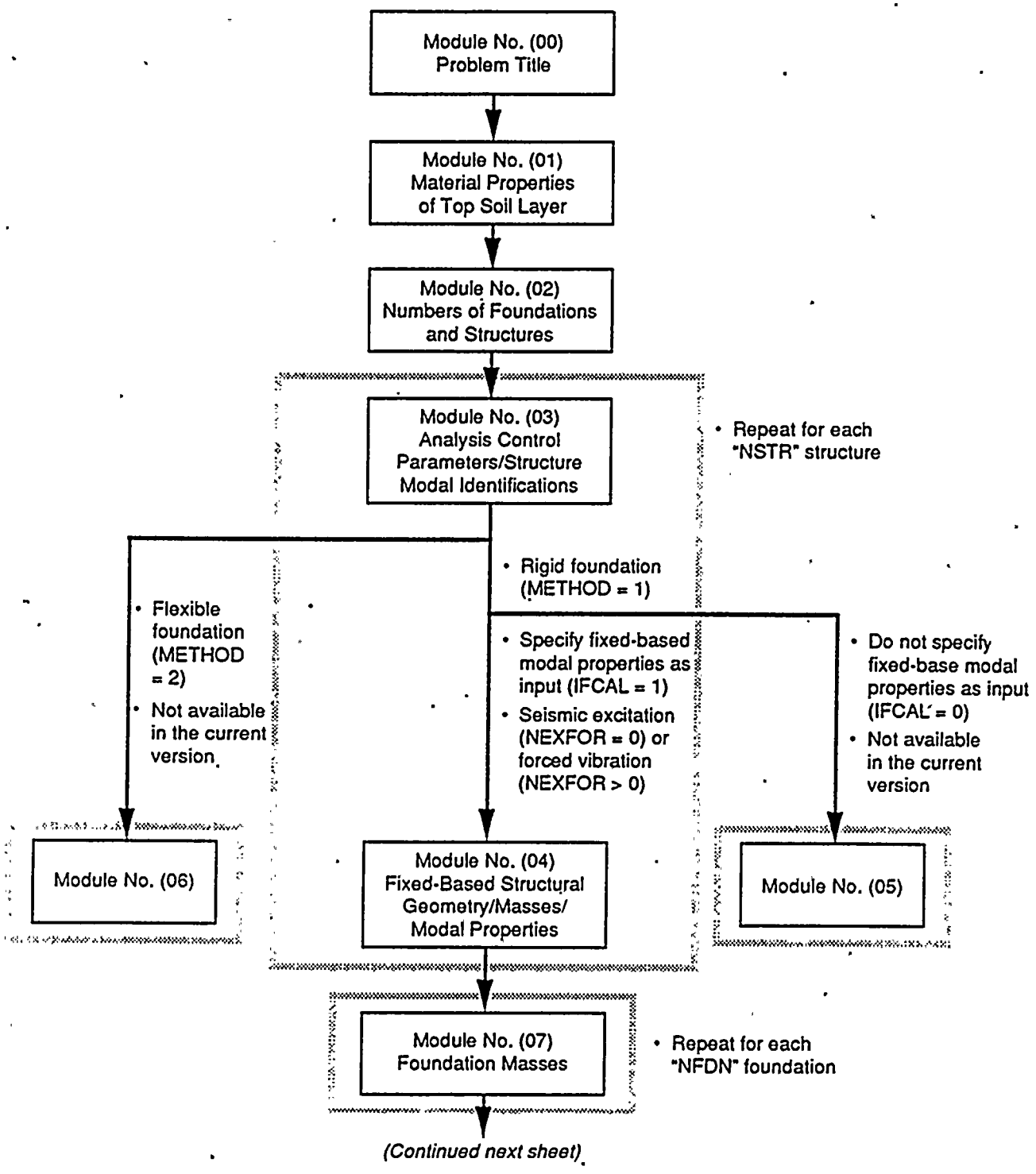

Figure 5-3. Flow Chart Showing Modules of Input Data for SSIF Program Module

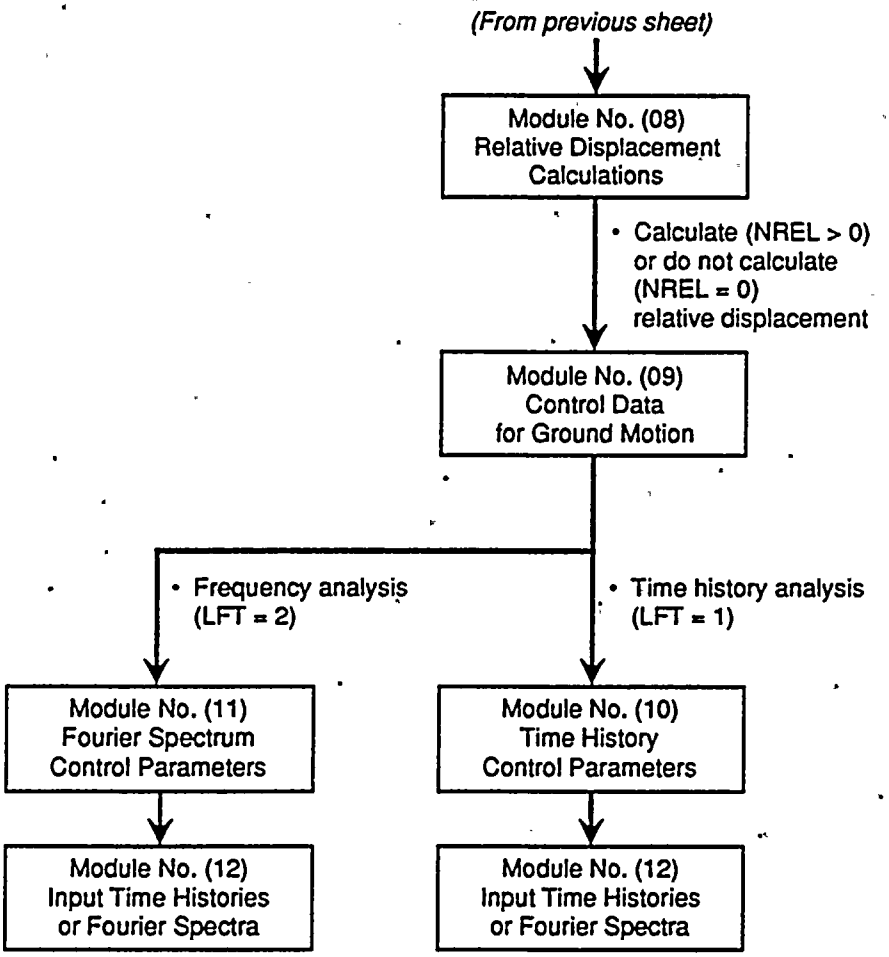

Figure 5-3. (Cont'd)

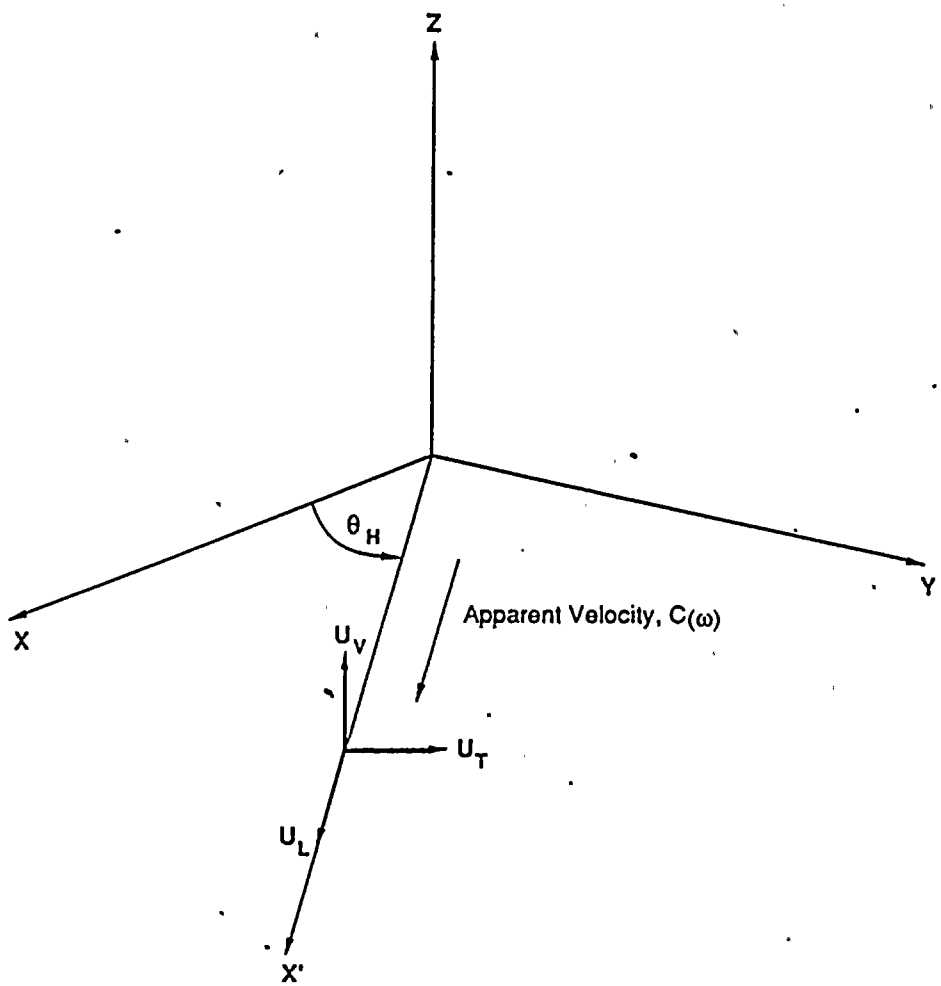

Figure 5-4. Incident Plane Wave Propagation

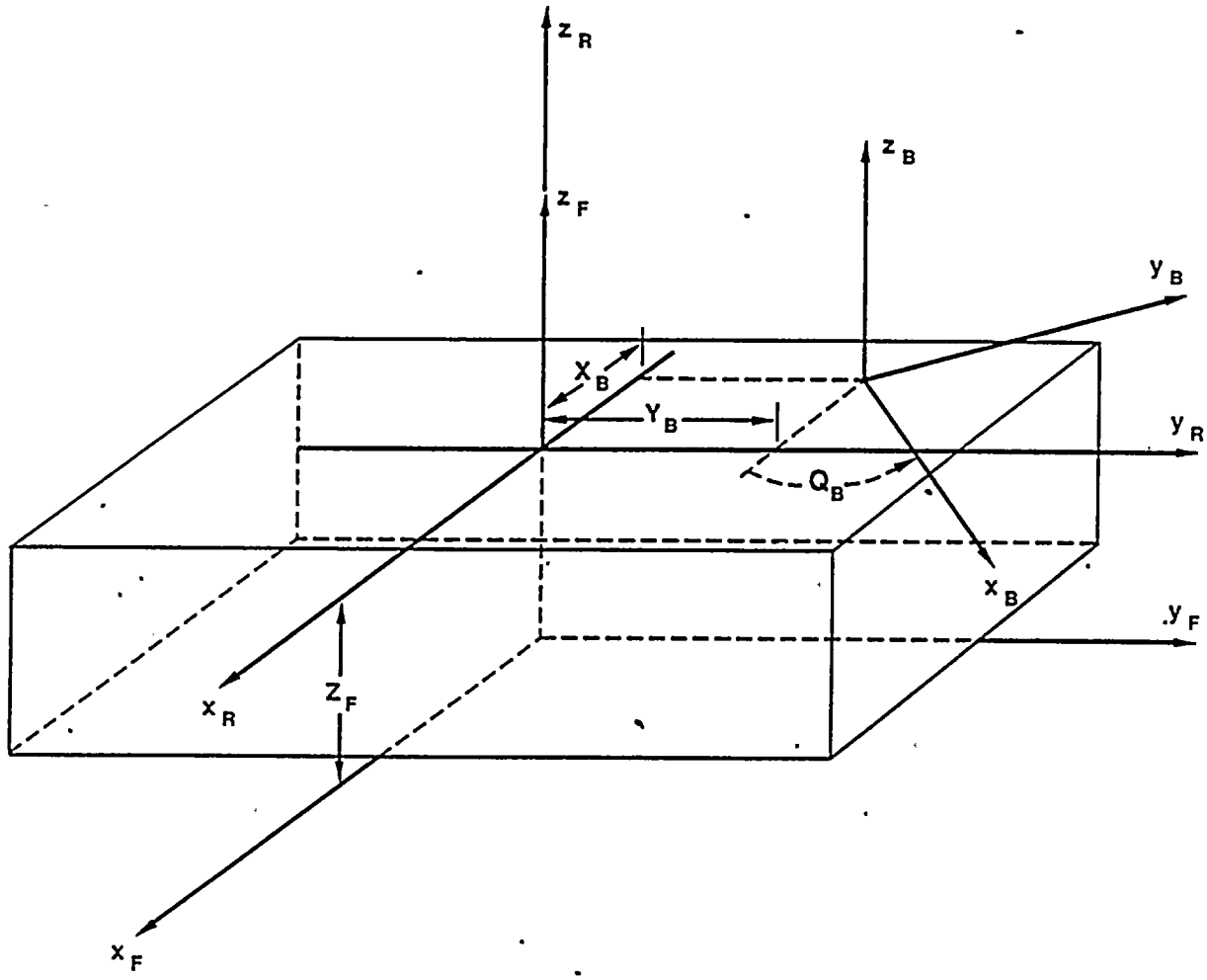

Figure 5-5. Example of Coordinate Transformations for Structure and Foundation

6. INPUT DATA

6.1 GLAYER Module

Module No. (00) - Problem Title

Card 1 - Module Identification Line (See note below.)

Card 2 - TITLE

TITLE - Any combination of up to 80 alpha/numerical characters.

Note: Module Identification Line consists of a parenthesis with a 2-digit module number followed by comments after column 5.

Module No. (01) - Analysis Control Parameters

Card 1 - Module Identification Line (see note in Module No. (00)).

Card 2 - NFRQ, NLY, IFITER, LLLL, IPRNT

NFRQ - The total number of frequencies required to yield impedance functions that are suitable for interpolation (for a uniform halfspace, a special case, set NFRQ = 1).

NLY - The total number of layers in the soil medium including the underlying halfspace.

IFITER - A control parameter to allow manual or automatic determination of the increment of radius, DR, for the Green's Function Table.

0 - Program uses the prescribed "DR" in Module No. (10) as the increment of radius for the output Green's Function Table. This option is for users who are experienced in choosing the optimum increment, DR, and is much faster than the iterative procedure.

1 - Program calculates the Green's Function Table by iteration. The optimal value of "DR" is set automatically by the program as the initial value and is bisected after each iteration until the values of the Green's Function Table pass the interpolation tests. The iterative procedure is terminated when the interpolated values at the test points fall within a certain threshold of the previous interpolated values. This option is more convenient to use than the other option but will require more computer time.

LLLL - The initial number of points in the Green's Function table before the iterations begin. This parameter is used only when "IFITER" is equal to 1. To avoid a large number of iterations (the most time consuming procedure), it is recommended to choose a larger value of LLLL for high frequencies and a lower one for low frequencies. The recommended values are LLLL = 64 for low frequencies, and LLLL = 256 or larger for high frequencies.

IPRNT - A control parameter for printing the Green's Function Tables.

0 - Do not print the Green's Function Table.

1 - Print the Green's Function Table.

Module No. (02) - Initial and Final Radii for Green's Function Table

Card 1 - Module Identification Line (see note in Module No. (00)).

Card 2 - RI, RE

RI - The initial radius for all the Green's Function Table.

RE - The final radius for all the Green's Function Table.

Note: Usually, "RI" is zero and "RE" is the maximum distance between two points on any mats within the multi-foundation system. With this extended range defined, all Green's Functions for the integral equation formulation can be obtained by interpolations.

Module No. (03) - Minimum Increment of Radius

This module is required only if IFITER = 0 in Module No. (01), otherwise skip to the next data module.

Card 1 - Module Identification Line (see note in Module No. (00)).

Card 2 - DRMIN

DRMIN - The minimum increment of "DR" used among all the Green's Function Tables (one for each frequency). Generally, DR is the smallest for the highest frequency case. The only purpose of this parameter is to determine the memory size required to store the largest Green's Function Table.

Module No. (04) - Maximum Number of Iterations

This module is required only if IFITER = 1 in Module No. (01).

Card 1 - Module Identification Line (see note in Module No. (00)).

Card 2 - NITER

NITER - The maximum number of iterations allowed. "NITER" is used to prevent possible nonconvergent iterations and to determine the maximum memory size required to store the largest Green's Function Table. The recommended value for NITER is 6.

Module No. (05) - Shear Wave Velocities of Layered Soil Medium

Card 1 - Module Identification Line (see note in Module No. (00)).

Card 2 - BETA

BETA - The shear wave velocity of each layer in the soil medium. They must be specified in a consecutive order starting from the top layer to the bottom layer for the halfspace.

Module No. (06) - Mass Densities of Layered Soil Medium

Card 1 - Module Identification Line

Card 2 - RHO

RHO - The mass density of each layer in the soil medium. They must be specified in a consecutive order starting from the top layer to the bottom layer for the halfspace.

Module No. (07) - Poisson's Ratios of Layered Soil Medium.

Card 1 - Module Identification Line (see note in Module No. (00)).

Card 2 - POISON

POISON - The Poisson's ratio of each layer in the soil medium. They must be specified in a consecutive order starting from the top layer to the bottom layer for the halfspace.

Module No. (08) - Damping Coefficients of Layered Soil Medium

Card 1 - Module Identification Line (see note in Module No. (00)).

Card 2 - DAMP

DAMP - The damping coefficient of each layer in the soil medium. They must be specified in a consecutive order starting from the top layer to the bottom layer for the halfspace.

Module No. (09) - Soil Layered Thicknesses

Card 1 - Module Identification Line (see note in Module No. (00)).

Card 2 - TH

TH - The thickness of each layer in the soil medium. They must be specified in a consecutive order starting from the top layer to the bottom layer which represents the halfspace. The thickness for the halfspace can be specified as any finite value of thickness. The physical unit of the soil layered thickness must be consistent with those of shear wave velocity and mass density as specified in Module Nos. (05) and (06).

Module No. (10) - Frequencies of Analysis

Card 1 - Module Identification Line (see note in Module No. (00)).

IF IFITER = 0 in Module No. (01), specify the following input data for Card 2. Otherwise, skip to the next input data for Card 2.

Card 2 - FRQ, DR

FRQ - Frequencies (cycle/sec) for which the Green's Function Table are created. The input frequencies must be in ascending order and the total number of frequencies should equal to "NFRQ" as specified in Module No. (01). It

should be noted that if the lowest frequency is set to zero, a substitute value of FRQ = 0.01 cycle/sec will be used.

For the special case of a uniform halfspace (NLY=1), only the maximum frequency needs to be entered because the Green's Function of lower frequencies can be interpolated from the same table by simply scaling the dimensionless frequency argument.

DR - The increment of radius to be used in the Green's function table. The value of DR must be chosen for each frequency so that the interpolated values will have adequate accuracy At higher frequencies, i.e., shorter wave lengths, DR must be smaller. DR must also be greater or equal to DRMIN as specified in Module No. (03) for all frequencies.

IF IFITER = 1 in Module No. (01), specify the following input data for Card 2.

Card 2 - FRQ

FRQ - See above description for FRQ.

6.2 CLAF Module

Module No. (00) - Problem Title

Card 1 - Module Identification Line (See note below).

Card 2 - TITLE

TITLE - Any combination of up to 80 alpha-numerical characters.

Note: Module Identification line consists of a parenthesis with a 2 digit module number followed by comments after column 5.

Module No. (01) - Analysis Path Control Parameter

Card 1 - Module Identification Line (see note in Module No. (00)).

Card 2 - IPASS

1 - Initial calculation; program performs the initial calculation of the foundation impedance matrix, the traction vector, the driving force vector, and the scattered input motion vector.

2 - Restart calculation; program uses the calculated traction vector from the initial calculation and new incident wave input to restart the calculation for the new driving force and scattered input motion vectors.

Module No. (02) - Reference Parameters

Card 1 - Module Identification Line (see note in Module No. (00)).

Card 2 - G, VS, CL

G - The reference shear modulus of the soil medium (first layer).

VS - The reference shear wave velocity of the soil medium (first layer).

CL - The characteristic length of the foundation mat.

Note: G, VS and CL are used as the normalized parameters. G is used to normalize the dimensionless impedance and wave scattering matrices. VS is used to normalize the dimensionless frequency a_0. CL is used to normalize the dimensionless frequency, impedance and wave scattering matrices. CL should be selected to represent a dimension of a typical mat in the foundation system, e.g., the radius if the mat is circular; the width or half-width, if the mat is rectangular. Using this normalization procedure, the normalized impedance functions will generally be in the order of "1" or "10".

Card 3 - NUMFRQ, NLAYER, NGRN

NUMFRQ - The number of frequencies at which the impedance and scattering matrices are to be calculated.

NLAYER - The number of layers in the soil medium including the underlying halfspace. If NLAYER = 1 (halfspace), only one Green's function Table will be read in. Otherwise, a new table will be read in for each of the NUMFRQ frequencies.

NGRN - The maximum number of points among all the Green's function Tables calculated by GLAYER. The only purpose of this parameter is to allocate the memory size required to store the largest Green's Function Table.

Card 4 - NFDN, NTYPE, SCALE

NFDN - The number of foundation mats in the soil-foundation system.

NTYPE - The number of rectangular subregions of different dimension used in the analysis. To classify two subregions as the same type, both the X and Y dimensions of the subregions must be identical.

SCALE - A scale factor for the convenience of input. The values of XC, YC, XB, YB, XH and YH in Module No. (03) will be divided by this factor.

Card 5 - NCASE, IFCVAR

NCASE - The number of incident wave forms considered in the analysis. If NCASE is set to zero, only the impedance matrix will be calculated.

IFCVAR - A control parameter to indicate whether the incident wave parameters BOC on Module No. (06), i.e., ULR, ULI, UTR, UTI, UVR and UVI, are frequency dependent.

0 - Wave form is frequency independent

1 - Wave form is frequency dependent

Module No. (03) - Foundation Geometry/Coordinate

Card 1 - Module Identification (see note in Module No. (00)).

Card 2 - NP(N), IFSX, IFSY, NREP(N)

NP(N) - The number of rectangular subregions required to approximate the N^{th} foundation surface. For foundation mat with 2-fold of 4-fold symmetry use the value of NP(N)/2 or NP(N)/4, respectively.

IFSX - A control parameter to indicate the symmetry about the X-axis of the N^{th} foundation mat.

0 - The N^{th} foundation mat is not symmetrical about the X-axis.

1 - The N^{th} foundation mat is symmetrical about the X-axis.

IFSY - A control parameter to indicate the symmetry about Y-axis of the N^{th} foundation mat.

0 - The N^{th} foundation mat is not symmetrical about the Y-axis.

1 - The N^{th} foundation mat is symmetrical about the Y-axis.

NREP(N) - A control parameter to indicate whether the geometry of the N^{th} foundation mat is identical to the $N-1^{th}$ foundation mat.

0 - The geometry of the N^{th} foundation mat is not a repetition of the $N-1^{th}$ foundation mat. (Note: NREP(1) must be set to 0).

1 - The geometry of the N^{th} foundation mat is a repetition of the $N-1^{th}$ foundation mat.

Card 3 - XC(N), YC(N)

XC(N) - The X-coordinate of the local system origin, usually located at the centroid of the N^{th} foundation measured with respect to the reference coordinate system, and expressed as a fraction of CL.

YC(N) - The Y-coordinate of the local system origin, usually located at the centroid of the N^{th} foundation measured with respect to the reference coordinate system, and expressed as a fraction of CL.

Note: For example, if CL = 90 m, and the X-coordinate from the reference origin of the entire foundation system in 300 m, then XC = 3.333 if SCALE = 1.0 or XC = 10.00 if SCALE = 3.0. XC and YC may be expressed in physical units if SCALE is CL expressed in physical units.

Card 4 - B(I), YB(I), LET(I)

This card is required to be repeated for NP(N) times only if NREP(N) = 0.

XB(I) - The X-coordinate of I^{th} subregion centroid measured with respect to the local coordinate system of the N^{th} foundation.

YB(I) - The Y-coordinate of I^{th} subregion centroid measured with respect to the local coordinate system of the N^{th} foundation.

LET(I) - An integer pointer of subregion type number which defines the dimension of subregion.

Note: Repeat Module No. (03) for NFDN times.

Module No. (04) - Dimensions of Foundation Subregions

Card 1 - Module Identification Line (see note in Module No. (00)).

Card 2 - XH(J), YH(J)

This card is required to be repeated for NTYPE times.

XH(J) - The X-dimensions of J^{th} type subregion, expressed as a fraction of CL.

YH(J) - The Y-dimension of J^{th} type subregion, expressed as a fraction of CL.

Module No. (05) - Iteration Control Parameters

Card 1 - Module Identification Line (see note in Module No. (00)).

Card 2 - IPDF, IPCMPL

IPDF - Control parameter for printing the driving force vector.

0 - Do not print the driving force vector.

1 - Print the driving force vector.

IPCMPL - Control parameter for calculating and printing the compliance matrix.

0 - Do not calculate the compliance matrix.

1 - Calculate and print the compliance matrix.

Card 3 - NITER, TOLER

NITER - The maximum number of iterations to be performed in obtaining the impedance matrix. (Default = 20 iterations)

TOLER - Tolerance of convergence during iteration (expressed in terms of fraction, e.g., 0.05).

Module No. (06) - Excitation Frequencies and Incident Plane Waves

Card 1 - Module Identification (see note in Module No. (00)).

Card 2 - FRQ (see Note 1)

FRQ - The excitation frequencies at which the impedance matrix and wave scattering matrices are to be calculated. The results for the entire spectrum may be obtained during one or several computer runs. For the latter, a post-processor must be written to combine the results stored in the separate binary files.

Card 3 - BOC(J), TH(J), ULR(J), ULI(J), UTR(J), UTI(J), UVR(J), UVI(J) (See Notes 2 and 3)

BOC(J) - Ratio of the shear wave velocity to the apparent wave velocity for the Jth incident wave. For vertically incident waves, BOC is 0 because the apparent velocity is infinite.

TH(J) - The horizontal angle for the J^{th} incident wave measured counterclockwise with respect to the reference X-axis in degrees.

ULR(J), ULI(J) - The complex longitudinal of the J^{th} incident wave.

ULR - Real part of the complex amplitude.
ULI - Imaginary part of the complex amplitude.

UTR(J), UTI(J) - The complex transverse amplitude of the Jth incident wave.

UTR - Real part of the complex amplitude.
UTI - Imaginary part of the complex amplitude.

UVR(J), UVI(J) - The complex vertical amplitude of the Jth incident wave.

UVR - Real part of the complex amplitude.
UVI - Imaginary part of the complex amplitude.

Notes: 1. For a special case of a uniform halfspace (NLAYER = 1), the results for the entire range of frequencies of analysis can be obtained by specifying only the highest frequency for the FRQ parameter. However,

for a layered soil medium, the input excitation frequencies FRQ must be specified to be the same set of frequencies as that used for Green's function calculation.

2. For NCASE≠0 and IFCVAR=0, the incident wave is not frequency dependent. The parameters BOC, TH, ULR, ULI, UTR, UTI, UVR and UVI need only be input once. For NCASE ≠ 0 and IFCVAR = 1, the incident wave is frequency dependent. The parameters on Card 3 must be provided for each excitation frequency requested. (Repeat Card 2 and Card 3 as a set for NUMFRQ times).

3. For NCASE = 0, skip Card 3 input data.

6.3 SSIF Module

Module No. (00) - Problem Title

Card 1.- Module Identification Line (see note below)

Card 2 - TITLE

TITLE - Any combination of up to 80 alpha-numerical characters.

Note: Module Identification Line consists of a parenthesis with a 2-digit module number followed by comments after column 5.

Module No. (01) - Reference Parameters

Card 1 - Module Identification Line (see note in Module No. (00)).

Card 2 - G, VS, CL

G - The reference shear modulus of the soil medium (first layer).

VS - Shear wave velocity of the soil medium (first layer).

CL - The characteristic length of the foundation mat. (See note in Module No. (02) of CLAF program module for description of CL.)

Module No. (02) - Numbers of Foundations and Structures

Card 1 - Module Identification Line (see note in Module No. (00)).

Card 2 - NFDN, NTSTR

NFDN - The number of foundation mats in the interaction system.

NTSTR - The number of structures in the interaction system (NTSTR can be larger than NFDN because there can be two or more superstructures placed on top of each foundation mat).

Card 3 - IFTIMP(J), XF(J), YF(J), ZF(J), QF(J)

IFTIMP(J) - Conditional flag for transforming the impedance and scattering matrices to the reference coordinate system.

0 - Do not perform the transformation.

1 - Perform the transformation on all the 6x6 blocks of the impedance and scattering matrices which are coupled with the Jth foundation using translational parameters XF(J), YF(J), ZF(J) and rotational parameter QF(J).

XF(J), YF(J), ZF(J) - The coordinates of the local system origin measured with respect to the reference coordinate system of the J^{th} foundation. These transformation coordinates are in the physical unit of length.

QF(J) - The horizontal angle of the local system measured counterclockwise from the reference system of the J^{th} foundation. It has the unit of radians.

(Repeat Card 3 for NFDN times)

Module No. (03) - Analysis Control Parameters

Card 1 - Module Identification Line (see note in Module No. (00)).

Card 2 - METHOD(I), NMODE(I), NDOF(I), IFNPTR(I), IFCAL

METHOD(I) - The method to be used for structure to calculate the condensed structure matrix:

1 - Use the assumption of rigid foundation mats

2 - Use the assumption of flexible foundation with each rigid footing having 6 degrees of freedom. (This option is currently not available in the program).

NMODE(I) - The number of structural modes to be considered for the I^{th} structure. There should be enough modes to adequately cover the frequency band of interest.

NDOF(I) - The number of dynamic degree of freedom that the I^{th} structure possesses after all dynamic properties have been condensed to the foundation level. NDOF(I) may be less than or equal to 6.

IFNPTR(I) - The foundation mat pointer for the I^{th} structure. It indicates which foundation mat that the I^{th} superstructure will be placed. This parameter is not used for the METHOD = 2 option.

IFCAL - Conditional flag to determine whether the input data is of the form of mode shapes or modal participation factor.

0 - Do not calculate the $[M_{bo}]$ and $[\gamma]$ matrices, they have been calculated externally to the program and should be provided in the input data. This option is useful for simple analytical models or experimental results. (This option, however, is currently not available in the program).

1 - Calculate (M_{bo}) and [γ] matrices from the structure data [ϕ], [α_s], and [M]. This option is convenient for discrete models.

Note: $[M_{bo}]$ is the rigid body mass matrix of the i^{th} structure defined as $[M_{bo}] = [\alpha_s]^T [M] [\alpha_s]$, in which $[\alpha_s]$ = the structural geometry matrix, and [M] is the structural mass matrix. [γ] is the modal participation factor matrix defined as $[\phi]^T [M] [\alpha_s].[\phi]$ is the mode shape matrix.

Card 3 - IDOF

IDOF - The dynamic degree of freedom indicator for the I^{th} structure: 1-X, 2-Y, 3-Z, 4-XX, 5-YY, and 6-ZZ. For example, if the structure is a plane strain model in the X-Z plane, the NDOF(i) would be 3 and the IDOF array has 3 components; 1, 3, and 5.

Card 4 - IFTRAN, X, Y, Z, Q

IFRAN - Conditional flag for transforming the matrices of the I^{th} structure to the newly defined reference coordinate system.

0 - Do not transform the structural matrices.

1 - Transform the structural matrices with parameters X, Y, Z, and Q.

X,Y,Z,Q - Transformation parameters for the structural matrices (see Module No. (02) for detailed description).

Card 5 - NKEEP(I), NEXFOR(I)

NKEEP(I) - The total number of dynamic degrees of freedom in the I^{th} structure (other than those of the foundation motion) at which the structural response calculation is desired.

NEXFOR(I) - The total number of dynamic degrees of freedom in the I^{th} structure at which external forces are applied. Thus, NEXFOR > 0 indicates force excitation, and NEXFOR = 0 indicates seismic excitation.

Module No. (03) - Structural Node Identifications

Card 1 - Module Identification Line (see note in Module No. (00)).

Card 2 - ND, NNODES, NBAND

ND - The number of unconstrained dynamic degrees of freedom in the I^{th} structure. (Note: The structural nodes at the foundation level are fixed.)

NNODES - The number of mass points in the I^{th} structure consisting of ND dynamic degrees of freedom.

NBAND - The one-half band width of the global mass matrix for the I^{th} structure. For a lumped mass system, set NBAND = 1.

Card 3 - NCARD

This card is required if NKEEP ≠ 0; otherwise, skip this card.

NCARD - The number of mass points in the I^{th} structure at which the structure response calculation is desired.

Card 4 - NOID, ISEL(L)

This card is required to be repeated for NCARD times.

NOID - Nodal identification for the I^{th} structure at which the structural response calculation is desired.

ISEL(L) - A 6-column array represents the six dynamic degrees of freedom at each node: 1-X, 2-Y, 3-Z, 4-XX, 5-YY and 6-ZZ. Set each column to 0 or 1 to indicate whether the structural response is desired.

0 - A structural response calculation is not desired at this dynamic degree of freedom.

1 - A structural response calculation is desired at this dynamic degree of freedom.

Card 5 - NCARD

This card is required if NEXFOR ≠ 0; otherwise, skip this card.

NCARD - The number of nodal points in the I^{th} structure at which external forces are applied.

Card 6 - NOID, ISEL(L)

NOID - Nodal identification for the I^{th} structure at which external forces are applied.

ISEL(L) - A 6-column array represents the six dynamic degrees of freedom at each node; 1-X, 2-Y, 3-Z, 4-XX, 5-YY and 6-ZZ. Set each column to 0 or 1 to indicate whether the external forcing function is applied.

0 - No external forcing function is applied at this dynamic degree of freedom.

1 - An external forcing function is applied at this dynamic degree of freedom.

Module No. (04) - Fixed-Base Structural Geometry

This module is required if METHOD = 1 and IFCAL = 1; otherwise, skip to Module No. (05).

Card 1 - Module Identification Line (see note in Module No. (00)).

Card 2 - NODEID, X, Y, Z, IFCOOR

This card is required to be repeated for NNODES times.

NODEID - Structural node identification.

X,Y,Z - Global cartesian coordinate of the structural node.

IFCOOR - A 6-column array represents the six degrees of freedom of each node; 1-X, 2-Y, 3-Z, 4-XX, 5-YY, and 6-ZZ. Set each column to 0 or 1 to indicate whether it is a dynamic degree of freedom.

0 - This degree of freedom is a dynamic degree of freedom.

1 - This degree of freedom is not a dynamic degree of freedom.

Module No. (04) - Fixed-Base Structural Masses

This module is required if METHOD = 1 and IFCAL = 1; otherwise, skip to Module No. (05).

Card 1 - Module Identification Line (see Note in Module No. (00)).

Card 2 - MMX

MMX - The global mass matrix of the structure, [M]. Since [M] has a symmetrical band, SSIF will read [M] one diagonal at a time starting at the center diagonal. The free-formatted read statement expects (NBAND * ND) numbers. Since the diagonal become shorter as they move away from the center, they should be filled with zero at the end to make each diagonal the same length (ND numbers).

Module No. (04) - Fixed-Base Structural Modal Properties

This module is required if METHOD = 1 and IFCAL = 1; otherwise, skip to Module No. (05).

Card 1 - Module Identification Line (see note in Module No. (00)).

Card 2 - WN(I), DAMP(I), T

WN(I) - The I^{th} modal frequency in rad/sec.

DAMP(I) - The I^{th} modal damping coefficient in fraction (e.g., 0.01 = 1%).

Card 3 - T

T - The mode shape of the structure. T is a temporary array, it will be erased after the pertinent information has been extracted. The free-formatted read statement expects ND numbers. (Note: ND should equal to the total number of zeroes (active dynamic degree of freedom) given in the IFCOOR arrays).

(Repeat Cards 2 and 3 for NMODE times).

(Repeat Module Nos. (03) and (04) for each of NTSTR structure).

Module No. (05) - The read in option for Method = 1 and IFCAL = 0

(This option is currently not available).

Module No. (06) - The flexible foundation option, Method = 2.

(This option is currently not available).

Module No. (07) - Foundation Masses

Card 1 - Module Identification Line (see note in Module No. (00)).

Card 2 - FMI

FMI - The 6x6 mass matrix of the rigid foundation mat. It is read in 6 lines (row by row) with 6 numbers on each line.

Card 3 - IFTR, X, Y, Z, Q

IFTR - Conditional flag for tranforming the foundation mass matrix to the reference coordinate system.

0 - Do not perform the transformation.

1 - Perform the transformation.

X, Y, Z, Q - Transformation parameters for the foundation mass matrix (see Module No. (02) for detailed description).

(Repeat Module No. (07) for NFDN times).

Module No. (08) - Relative Displacement Calculations

Card 1 - Module Identification Line (see note in Module No. (00)).

Card 2 - NREL

NREL - The number of relative displacement components to be calculated. For each component, a pair of points: J and K, must be specified. The relative displacement is defined as U(J) - U(K). If NREL = 0, no relative displacement is calculated.

Card 3 - JWST(I), JWKEEP(I), KWST(I), KWKEEP(I)

This card is required if NREL $\neq$ 0; otherwise, skip this card.

JWST(I) - This integer indicates which structure that the "J"-point is located for the Ith pair.

JWKEEP(I) - This integer indicates which of the NKEEP degrees of freedom is to be used as the "J" component within the structure defined by JWST(I).

KWST(I) - This integer indicates which structure that the "K"-point is located for the I^{th} pair.

KWKEEP(I) - This integer indicates which of the NKEEP degrees of freedom is to be used as the "K" component within the structure defined by JWST(I).

(Repeat Card 3 for NREL times.)

Module No. (09) - Control Data for Input Ground Motion

Card 1 - Module Identification Line (see note in Module No. (00).)

Card 2 - LFT, NCOM, NCASE, FMIN, FMAX

LFT - Conditional flag to select the type of analysis.

1 - Time history analysis, input "NCOM" components of accelerograms, one for each plane wave. The results written in FORTRAN Unit 15 are also in the form of accelerograms.

2 - Frequency analysis, input "NCOM" components of real or complex Fourier spectra, One for each plane wave. The results written in FORTRAN Unit 15 are complex Fourier spectra.

NCOM - The number of plane waves, Nw, used to form the free-field motion.

NCASE - A parameter used in the CLAF program, it is the number of wave forms calculated in the Scattering Matrix, [S(ω)]. The number of columns in [S(ω)], i.e., NCASE, can be larger than NCOM because not all the columns have to be used in a given analysis.

FMIN, FMAX - The minimum and maximum frequencies (in cycles/sec) of the impedance or scattering matrix table. These two values indicate to SSIF what range of frequency the interpolation tables cover. Using the Fast Fourier Transform, the maximum frequency of SSIF will calculate response from 0 to 1./(2*DT) cycles/sec. For a FMAX that is less than the Nyquist frequency, SSI will fill the responses with zeros for f > FMAX.

Module No. (10) - Time History Control Parameters

This module is required if LFT = 1, otherwise, skip to Module No. (11).

Card 2 - DT, NPOINT, NFFT

DT - The time increment of the input accelerograms in seconds.

NPOINT - The number of points in the accelerograms. SSIF requires the same number of points for each accelerograms.

NFFT - An integer equaling a positive integral power of 2, e.g., 4096. NFFT is the number of points to be used in the Fast Fourier Transformation. If NFFT $\leq$ NPOINT, zeros will be used to fill the end of the accelerograms; if NFFT > NPOINT, the accelerogram will be truncated with "NFFT" points.

Module No. (11) - Fourier Spectrum Control Parameters

This module is required if LFT = 2.

Card 1 - Module Identification Line (see note in Module No. (00).)

Card 2 - DW, NFRQ, IFCMPX, IFCNST

DW - The circular frequency increment in rad/sec.

NFRQ - The number of frequencies in the analysis. The range of frequency covered is from 0 to (NFRQ-1)*DW.

IFCMPX - Conditional flag for identifying the input Fourier spectra.

1 - The input Fourier spectra are real.

2 - The input Fourier spectra are complex.

IFCNST - Conditional flag for identifying the constant Fourier spectra.

1 - The input Fourier spectra are constant over frequency. This option is useful along with IFCMPX=1 for determining the transfer functions of the soil-structure interaction system if the free-field spectrum amplitude is set to unity.

0 - The input Fourier spectra are not constant over frequency. The spectra must be read in all NFRQ points.

Module No. (12) - Input Time Histories or Fourier Spectra

Card 1 - Module Identification Line (see note in Module No. (00).)

Card 2 - FORM

FORM - A character variable of length 40 or less. It is to receive the format of the input time histories or forcing functions, e.g., (8F9.6) if there are 8 numbers per line. (Note: the parenthesis is required.)

Card 3 - ISWITCH

ISWITCH - A parameter to switch the time history input from card to file input.

0 - Read in time histories or Fourier spectra from card.

1 - Read in time histories or Fourier spectra from file using I/O unit 16.

Card 4 - IWTYPE(NC), IWFS(NC), IWCOL(NC), MEAN

IWTYPE(NC) - An integer of value 0, 1 or 2 to indicate which type of time history or transfer function that the NC^{th} component is (see notes below).

IWFS(NC) - An integer to indicate which foundation or structure that the NC^{th} component is associated with (see notes below).

IWCOL(NC) - An integer to indicate which column of the appropriate matrix that the NC^{th} component is associated with (see notes below).

MEAN - Flag for performing baseline correction on the input time histories.

0 - Perform baseline correction on the input time histories.

1 - Do not perform baseline correction on the input time histories.

Notes: The following notes explain the use of combinations of IWTYPE, IWFS and IWCOL for various types of SSI analysis.

IWTYPE(NC)=0 Seismic waves incident at the foundation system.

IWFS: Not applicable for this case, set it to 0.

IWCOL: Identifies which column of the Scattering Matrix is this component associated with.

IWTYPE(NC)=1 External force applied at one of the foundations.

IWFS: Indicates which foundation that this component of force is applied at.

IWCOL: Indicates which dynamic degree of freedom of the foundation labeled by IWFS that this component of force is associated with.

IWTYPE(NC)=2 External force applied at a node of a superstructure.

IWFS: Indicates which superstructure that this component of force is associated with.

IWCOL: Indicates which column of the matrix that this component of force is associated with.

Card 5 - SCALE

SCALE - A factor used to multiply each point in input time history or Fourier spectrum.

Card 6 - ACC

ACC - An array to store the input time history or foreing function. Its length is NP, and NP is defined as follows:

LFT=1 (time history analysis)
NP = the small of NPOINT or NFFT+2

LFT=2 (frequency analysis)
IFCMPX=1, IFCNST=0 : NP = NFRQ
IFCMPX=2, IFCNST=0 : NP = 2*NFRQ
IFCMPX=1, IFCNST=1 : NP = 1
IFCMPX=2, IFCNST=1 : NP = 2

A note of caution concerning the case where LFT=1 and NPOINT is greater than NFFT, the read statement will read in only NFFT+2 numbers, leaving a set of numbers unread. If the next time history follows the present time history in the same data file, SSIF will not be able to skip forward to the correct starting point for the next time history. This problem will not occur if each file only contains one time history. Also, for the case where LFT=2 and IFCMPLX=2, the real part occupies the odd while the imaginary part occupies the even positions of the array ACC.

7. JOB CONTROL LANGUAGE

In this section, the Job Control Language (JCL) statements to run the three program modules of CLASSIF, i.e., GLAYER, CLAF and SSIF, on Bechtel's UNIVAC BEC90B computer are provided.

7.1 GLAYER Module

To run the GLAYER program module, use the following JCL statements:

```
Col.
1

@Run,priority/R userid,charge-to,CE934,time,pages/cards
@Passwd         password
@ASG,A          T$*CE934.
@Delete,c       Output Green's Function Filename.
@ASG,up         Output Green's Function Filename.
@Use       7.,  Output Green's Function Filename.
@XQT            T$*CE934.GLAYER
     (Input Data)
@Fin
```

7.2 CLAF Module

To run the CLAF program module with the initial pass, i.e., IPASS = 1, use the following JCL statements:

```
Col
1

@Run,priority/R userid,charge-to,CE934,time,pages/cards
@Passwd         password
@ASG, A         T$*CE934.
```

```
@ASG, A        Input Green's Function Filename.
@Delete, C     Impedance Output Filename.
@Delete, C     Scattering Output Filename.
@Delete, C     Traction Output Filename.
@ASG, UP       Impedance Output Filename.
@ASG, UP       Scattering Output Filename.
@ASG, UP       Traction Output Filename., F///10000
@Use       7., Input Green's Function Filename.
@Use       8., Impedance Output Filename.
@Use       9., Scattering Output Filename.
@Use      11., Traction Output Filename.
@XQT            T$*CE934.CLAF
     (Input Data)
@Fin
```

To run the CLAF program module with the restart option, i.e., IPASS = 1, use the following JCL statements:

```
Col
.1

@Run, priority/R userid,charge-to,CE934,time,pages/cards
@Passwd        password
@ASG,A         T$*CE934.
@ASG,A         Input Traction Filename.
@Delete,C      Output Scattering Filename.
@ASG,UP        Output Scattering Filename.
@Use       9., Output Scattering Filename.
@Use      12., Input Traction Filename.
@XQT            T$*CE934.CLAF
     (Input Data)
@Fin
```

7.3 SSIF Module

To run the SSIF program module, use the following JCL statements:

```
Col
1

@Run, priority/R userid,charge-to,CE934,time,page
@Passwd          password
@ASG, A          T$*CE934.
@ASG, A          Input Impedance Filename.
@ASG, A          Input Scattering Filename.
@ASG, A          Input Time History Filename. (optional)
@Delete,C        Output Time History Filename.
@ASG,UP          Output Time History Filename.
@Use             8., Input Impedance Filename.
@Use             9., Input Scattering Filename.
@Use             15., Output Time History/Transfer Function Filename.
@Use             16., Input Time History Filename. (optional)
@XQT             T$*CE934.SSIF
     (Input Data)
@Fin
```

8. OUTPUT DESCRIPTION

This section provides brief descriptions of computer printed outputs from GLAYER, CLAF and SSIF program modules.

8.1 GLAYER Module

(1) User support information.
(2) Echoprint of input data.
(3) Banner page.
(4) Print problem description and control parameters.
(5) Print a table of soil properties.
(6) Print the Green's Function table for each frequency of analysis (optional). Each table consists of four independent complex components of Green's function at the surface of soil medium tabulated at equal dimensionless intervals.

8.2 CLAF Module

(1) User support information.
(2) Echoprint of input data.
(3) Banner page.
(4) Print problem description and control parameters.
(5) Print a table of the centroids of foundation subregions.
(6) Print a table of the dimensions of subregion types.
(7) Print control parameters for analysis.
(8) Print a table of input incident wave data.
(9) Print the normalized foundation impedance matrix, driving force vector (optional), scattered input motion vector, and foundation compliance matrix (optional) for each dimensionless frequency of analysis.

The normalized foundation impedances are given in the form of A + i B. Thus, the foundation stiffness and damping imnpedances can be calculated from the normalized foundation impedances as follows:

$$K_{TT} = G \times CL \times A \quad ; \quad C_{TT} = G \times CL \times B/\omega$$

$$K_{RR} = G \times (CL)^3 \times A \quad ; \quad C_{RR} = G \times (CL)^3 \times B/\omega$$

$$K_{TR} = G \times (CL)^2 \times A \quad ; \quad C_{TR} = G \times (CL)^2 \times B/\omega$$

where K = foundation stiffness, C = foundation damping, the subscripts T and R indicate the translational and rotational components, respectively, G = shear modulus of top soil layer, CL = characteristic length, and ω = circular frequency in radian/second.

8.3 SSIF Module

(1) User support information.
(2) Echoprint of input data.
(3) Banner page.
(4) Print problem description and control parameters.
(5) Print fixed-base modal properties of structure.
(6) Print a table of requested output response locations.
(7) Print a table of foundation mass matrices.
(8) Print the normalized foundation impedance matrices.
(9) Print the scattered input motion vectors.
(10) Print control parameters for response calculation.
(11) Print control parameters for time history/frequency analysis.
(12) Print input time histories/forcing functions.
(13) Print maximum SSI responses.

9. APPLICATION EXAMPLE

To demonstrate the application of CLASSIF program to seismic SSI analysis, a typical containment structure subjected to a vertically propagating shear (SV) wave excitation is considered. The listing of the input data of this application example for GLAYER, CLAF and SSIF modules prepared according to Figs. 5-1 through 5-3, respectively, are provided in Appendix A.

The containment structure consisting of containment shell and internal structure is represented by a two lumped-mass stick model, as shown in Fig. 9-1. The stick model consists of 11 massess for the containment shell and 6 masses for the internal structure. The lumped masses and beam properties of the model are provided in Table 9-1. The fixed-base modal properties of the containment structure are shown in Table 9-2. The foundation model of the containment circular basemat resting on a viscoelastic halfspace is shown in Fig. 9-2. The soil properties of the supporting halfspace medium are also shown in this figure. The foundation model used in the analysis is represented by a quarter model of the circular basemat. The foundation quarter model is discretized into 37 rectangular subregions, with the finer ones concentrated around the edge of the foundation where the stress gradient is the highest, as shown in Fig. 9-3. The discretizations of these foundation subregions are based on the criterion for impedance calculations given in Section 4, and are good up to about 25 cps.

The 1940 EL Centro earthquake time history scaled to 0.1 g is specified at the ground surface for the free-field input motion in the form of a vertically propagating SV wave. The input motion and 2% damping response spectrum scaled up to 1.0 g are plotted as shown in Figs. 9-4 and 9-5, respectively. The duration of the input motion is 10.24 seconds with a time increment of .005 second.

Following the application guidelines provided in Section 5, the SSI analysis of the containment structure subjected to a vertically

propagating SV wave excitation, as shown in Fig. 9-1, is performed using CLASSIF in three separate analysis runs as follows:

Step 1. Run GLAYER to compute the Green's functions for the halfspace soil medium shown in Fig. 9-2, and save them on file 7.

Step 2. Using the Green's function of the halfspace saved on file 7 as input, run CLAF to compute the normalized foundation impedance for the rigid containment basemat shown in Fig. 9-2, and the scattered foundation input motion due to the vertically propagating SV wave, and saved them on files 8 and 9, respectively, as shown in Fig. 3.1-4.

Step 3. Using the normalized foundation impedance saved on file 8, the scattered foundation input motion saved on file 9, and the fixed-base structural modal properties generated from an independent analysis as input, run SSIF to compute the SSI response motions at the tops of foundation, containment and internal structures, as shown in Fig. 3.1-5.

The analysis results obtained from CLASSIF are presented in Figs. 9-6 through 9-10. The foundation stiffness and damping impedances for the horizontal and rocking components shown in Figs. 9-6 and 9-7, respectively, are calculated from the corresponding normalized foundation impedances obtained from CLAF run by using the equations given in Section 8.2. Also shown in Figs. 9-6 and 9-7 are the results obtained by Luco in Ref. (5). As can be seen from these figures, the horizontal and rocking foundation impedances from CLASSIF are in good agreement with those obtained by Luco. The 2% damping response spectra of response motions obtained from SSIF are computed and plotted in Fig. 9-8 for the top of foundation, Fig. 9-9 for the top of containment shell, and in Fig. 9-10 for the top of internal structure. Similar results obtained from using the response motions generated from FASS computer program (Ref. 6) are also shown in Figs. 9-8 through 9-10. As can be seen from these figures, the results from CLASSIF are compared closely with those from FASS.

Table 9-1

Properties of the Containment Structural Model

(Concrete Modulus E = 6.9×10^5ksf, G = 2.7×10^5ksf)

Joint Properties				Member Properties			
Mass No.	Weight (kips)	Rotatory Inertia		Location Between Joint No.	Area (ft^2)	Shear Area (ft^2)	Moment of Inertia ($10^6 \times ft^4$)
base	2000	21.1×10^6					
1	4600	-		base to 1	1400	700	2.8
2	4200	-		1 to 2	1400	700	2.8
3	4200	-	C	2 to 3	1400	700	2.8
4	4200	-	O	3 to 4	1400	700	2.8
5	4200	-	N	4 to 5	1400	700	2.8
6	4200	-	T	5 to 6	1400	700	2.8
7	4610	-	A	6 to 7	1400	700	2.8
8	3020	-	I	7 to 8	990	500	1.9
9	2470	-	N	8 to 9	990	500	1.5
10	2120	-	M	9 to 10	990	500	0.8
11	190	-	E	10 to 11	990	500	0.2
12	2800	-	N	base to 12	2000	1320	1.1
13	2510	-	T	12 to 13	2560	1560	1.2
14	6290	-	I	13 to 14	2210	1460	1.2
15	3760	-	N	14 to 15	1960	730	1.3
16	8540	-	E	15 to 16	1740	600	0.9
17	1220	-	R	16 to 17	780	360	0.2
18	820	-	N	17 to 18	190	70	0.004
			A				
			L				
			S				

Table 9-2

Fixed-Base Modal Properties of the Containment Structure

Mode No.	Frequency (cps)	Participation Factor	Damping Ratio
1*	5.27	-30.406	.02
2#	11.97	13.5	.02
3*	16.28	-13.9	.02
4#	17.53	-20.5	.02
5*	29.26	6.9	.02

Notes:

(*) Containment mode
(#) Internal structure mode

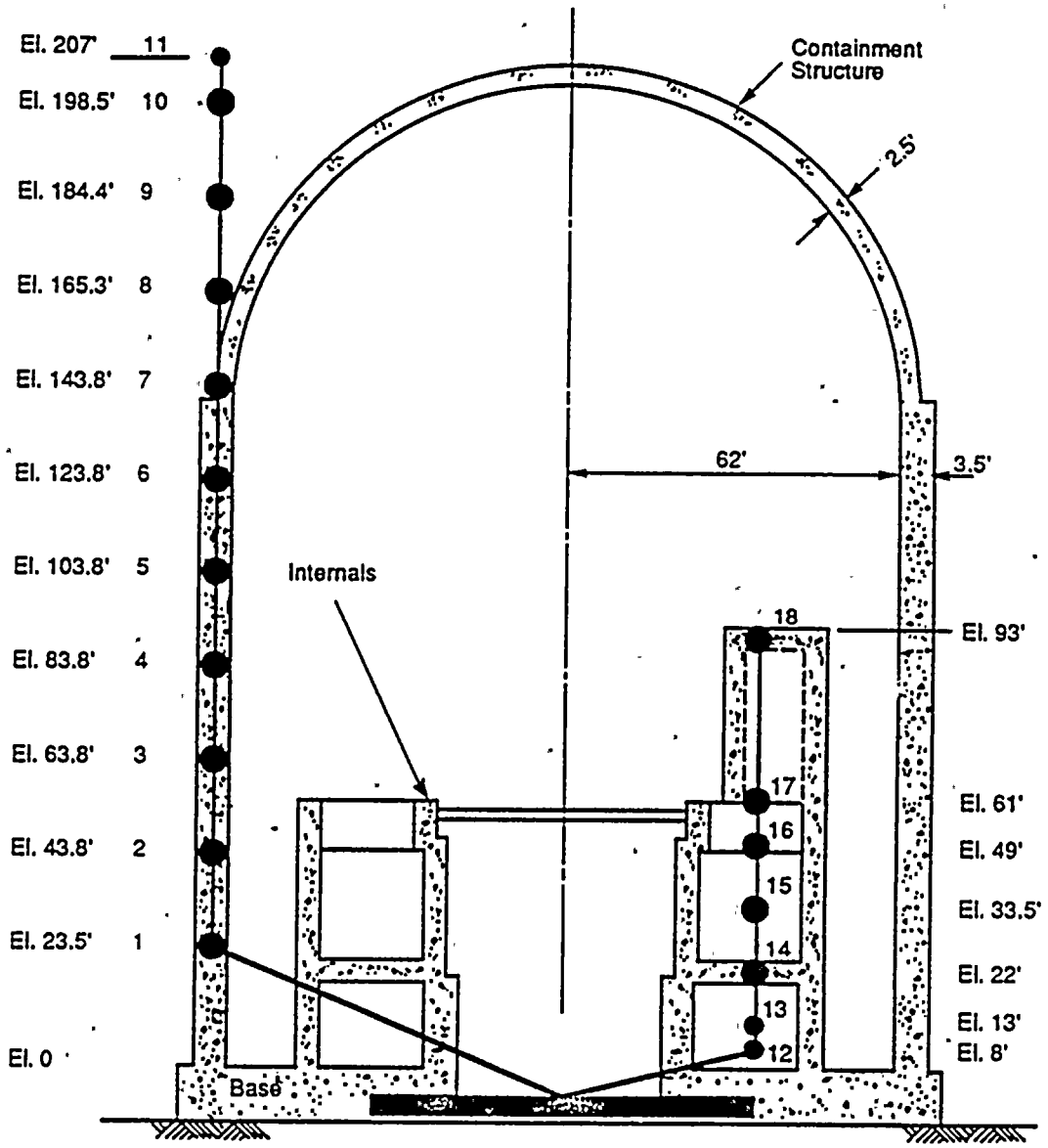

Figure 9-1. Lumped-Mass Stick Models of the Containment and Internal Structures

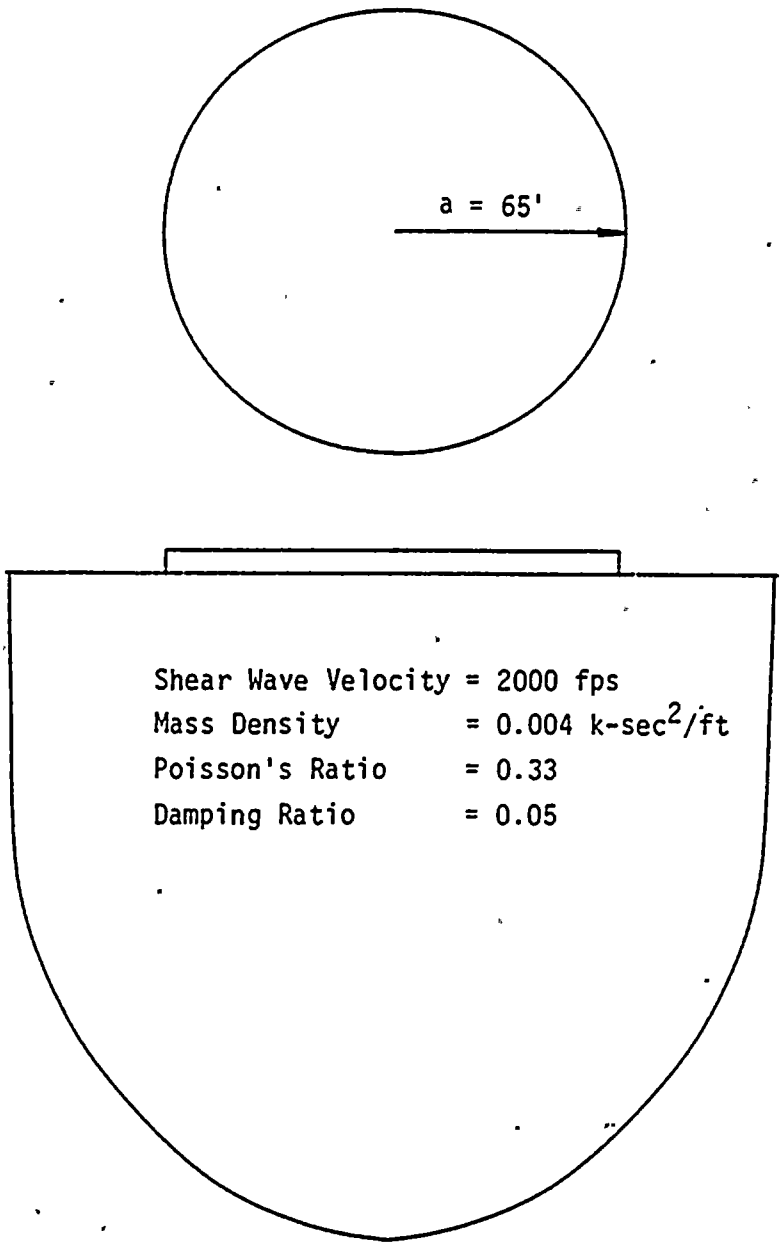

Figure 9-2. Circular Foundation on Viscoelastic Halfspace

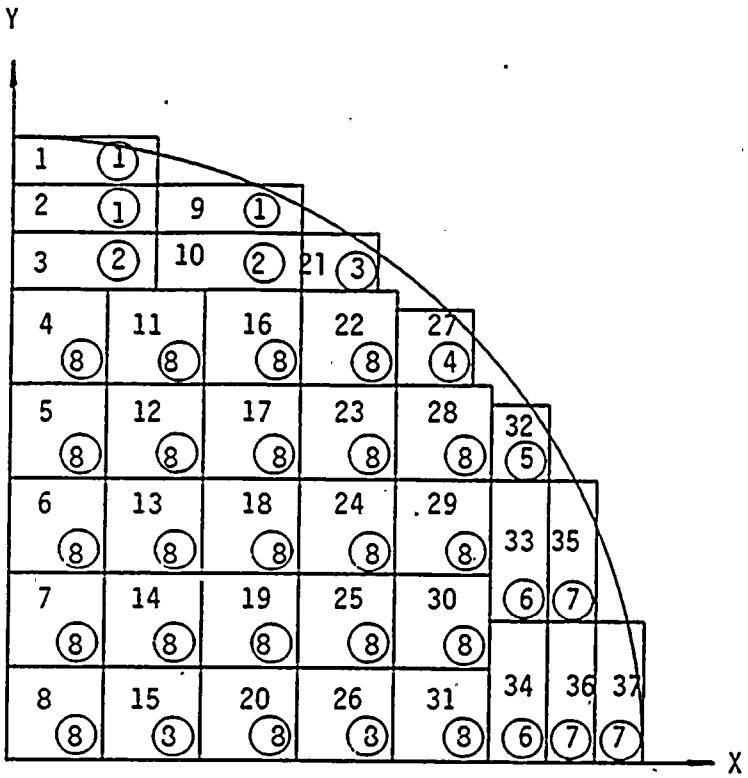

65' RADIUS

SUBREGION TYPE	X-DIM	Y-DIM
1	15	4.4
2	15	6
3	8.2	6
4	8	8
5	6	8.2
6	6	15
7	4.4	15
8	10	10

Figure 9-3. Foundation Quarter Model

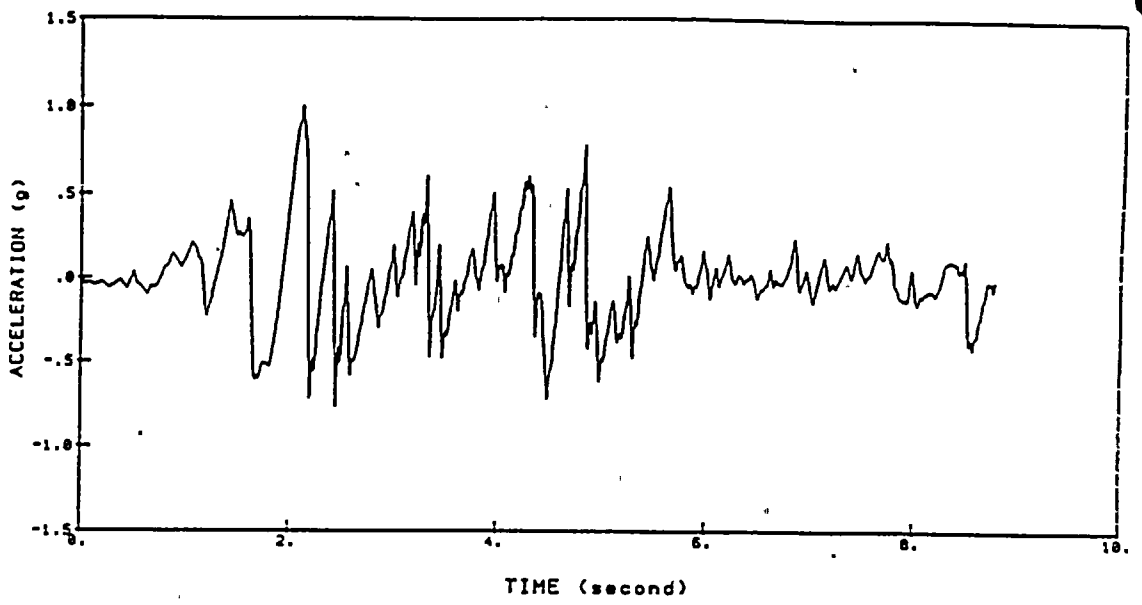

Figure 9-4. 1940 El Centro Earthquake Time History Scaled to 1.0 g

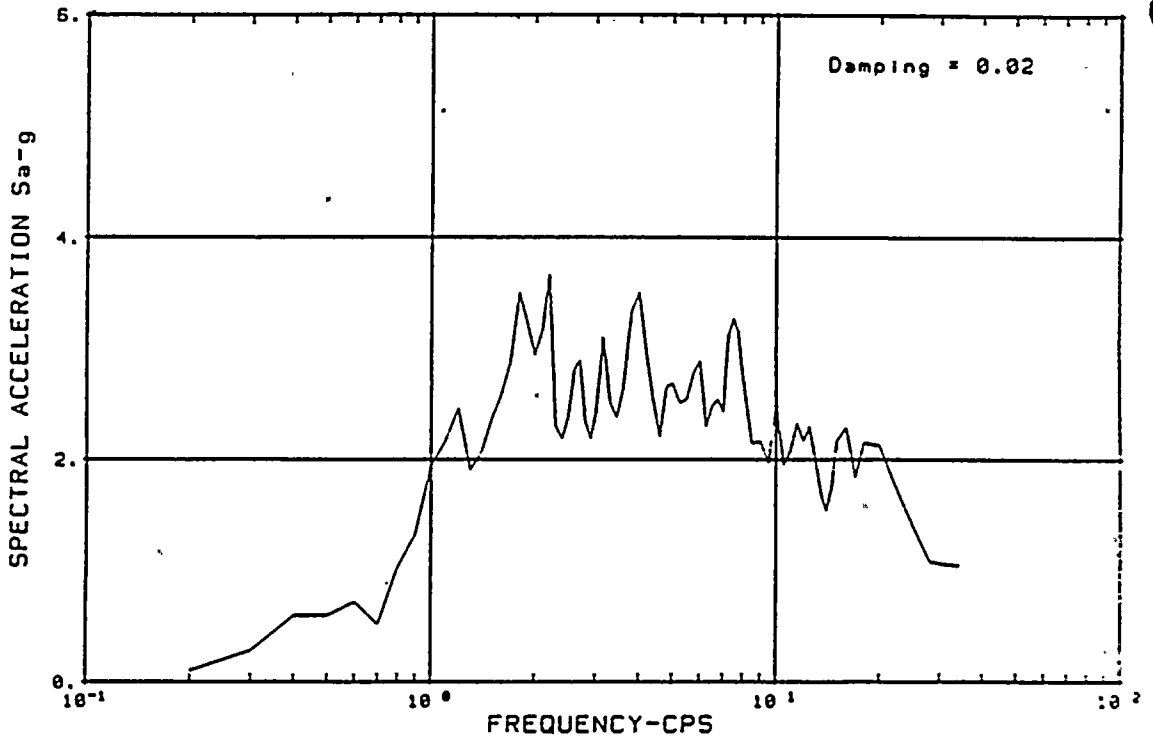

Figure 9-5. Response Spectrum of 1940 El Centro Earthquake Time History Scaled to 1.0 g

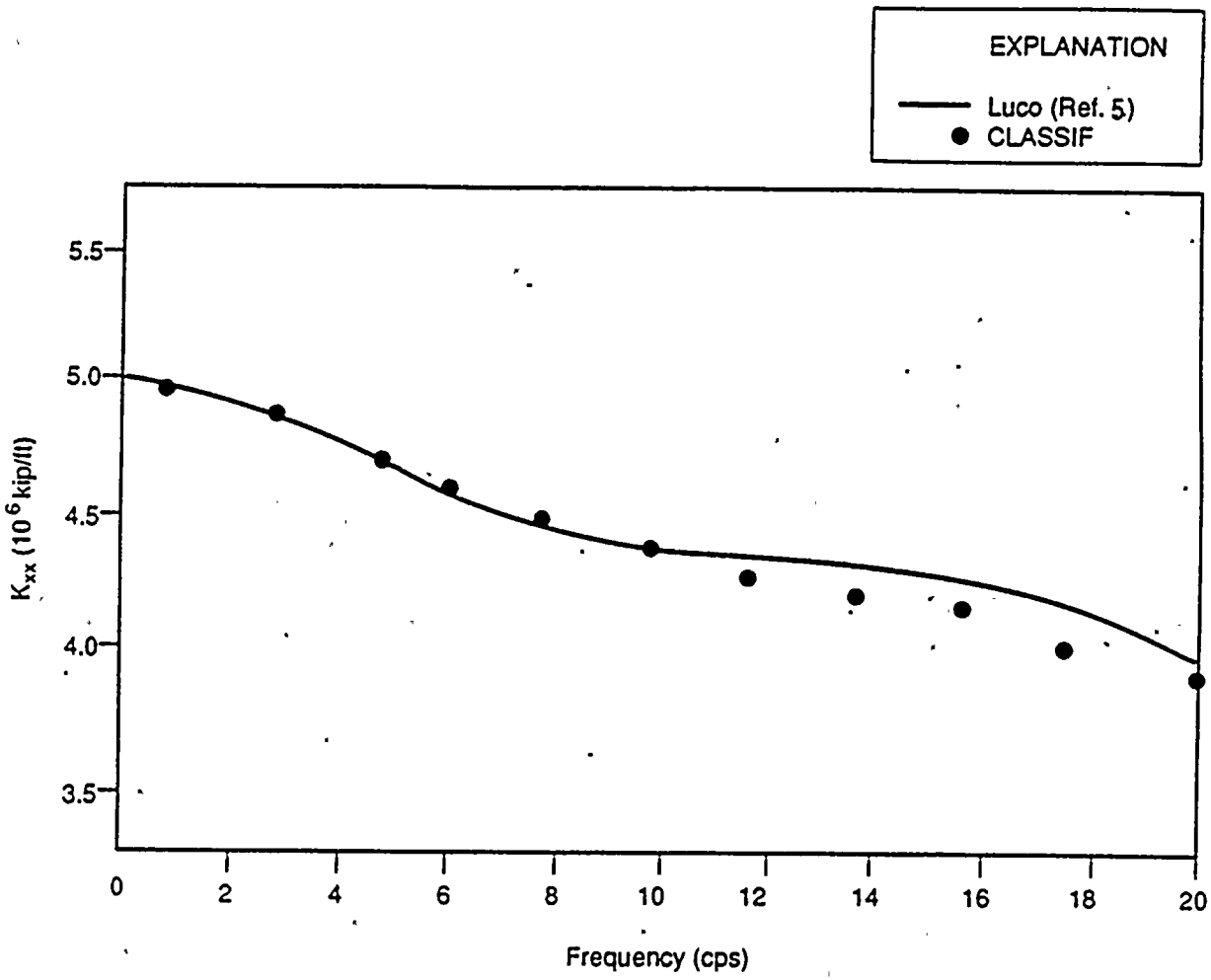

Figure 9-6(a). Horizontal Stiffness Impedance for a Circular Foundation

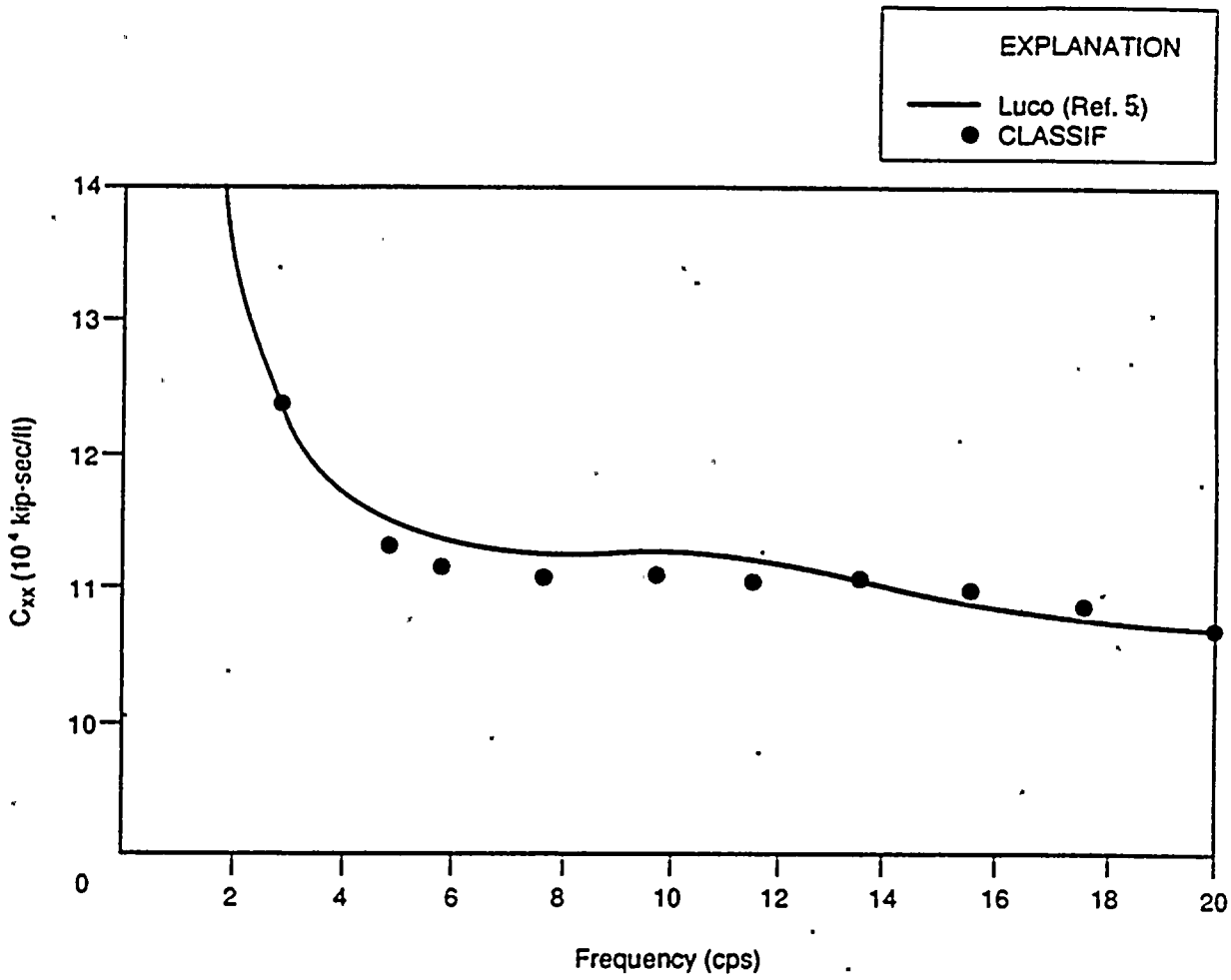

Figure 9-6(b). Horizontal Damping Impedance for a Circular Foundation

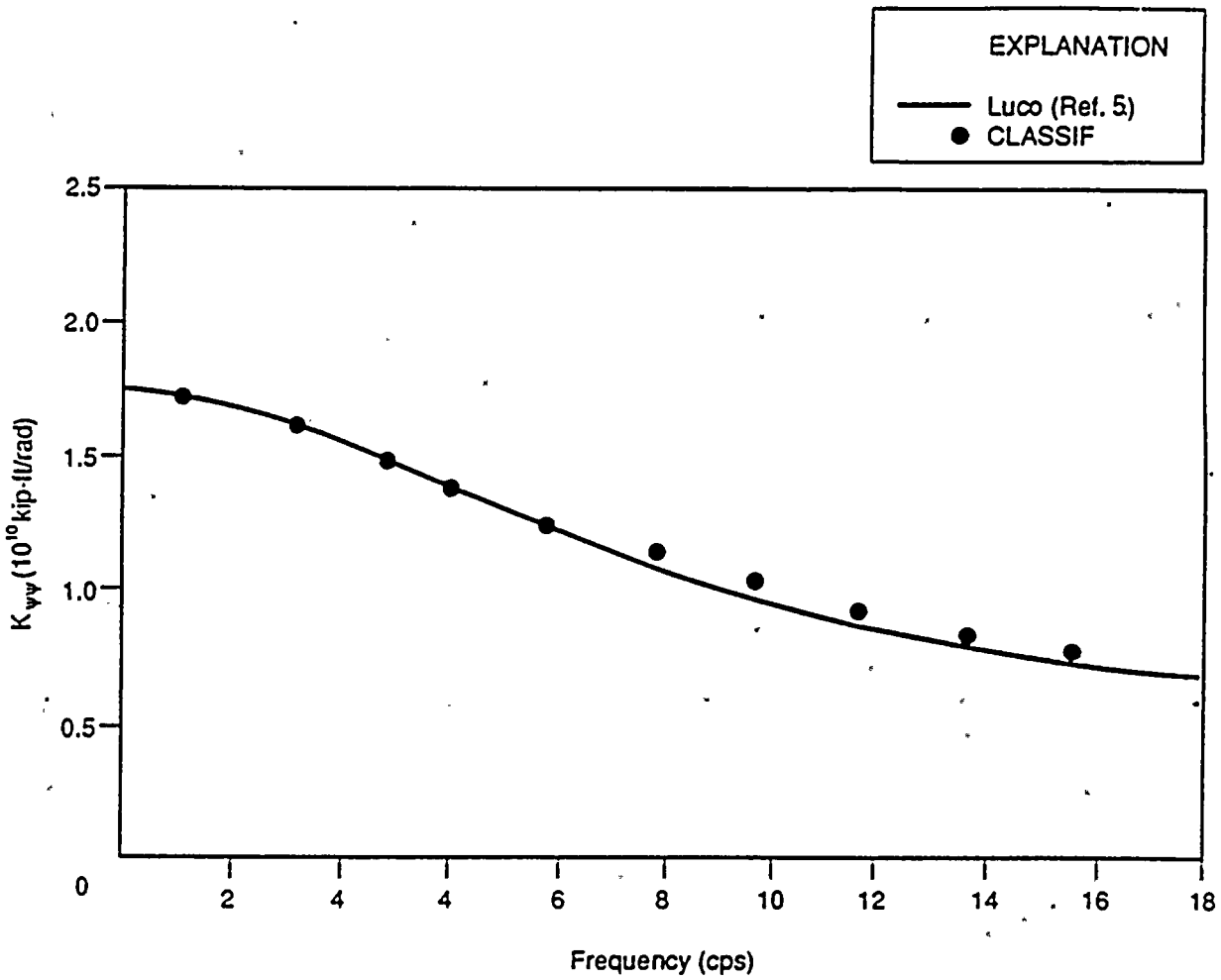

Figure 9-7(a). Rocking Stiffness Impedance for a Circular Foundation

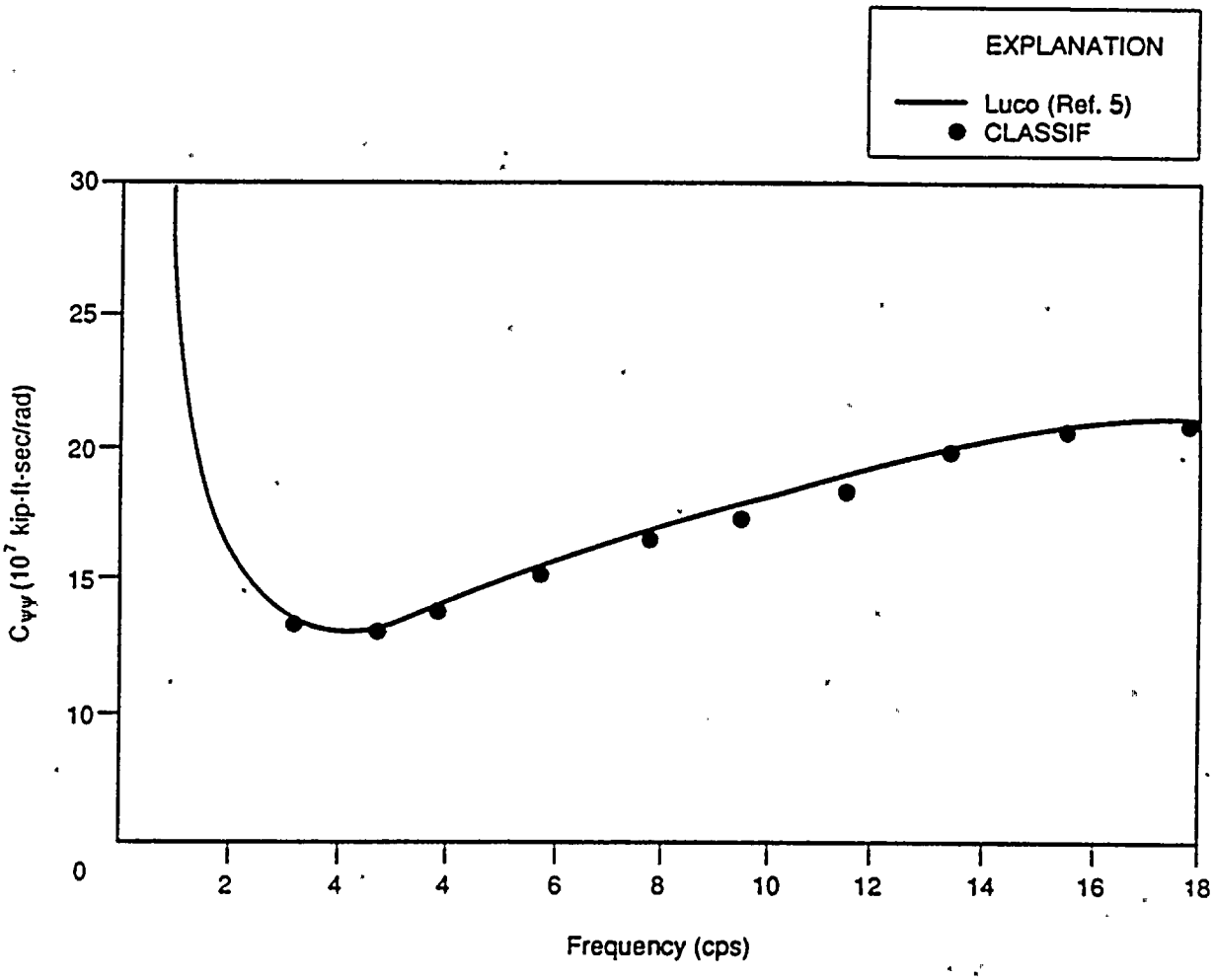

Figure 9-7(b). Rocking Damping Impedance for a Circular Foundation

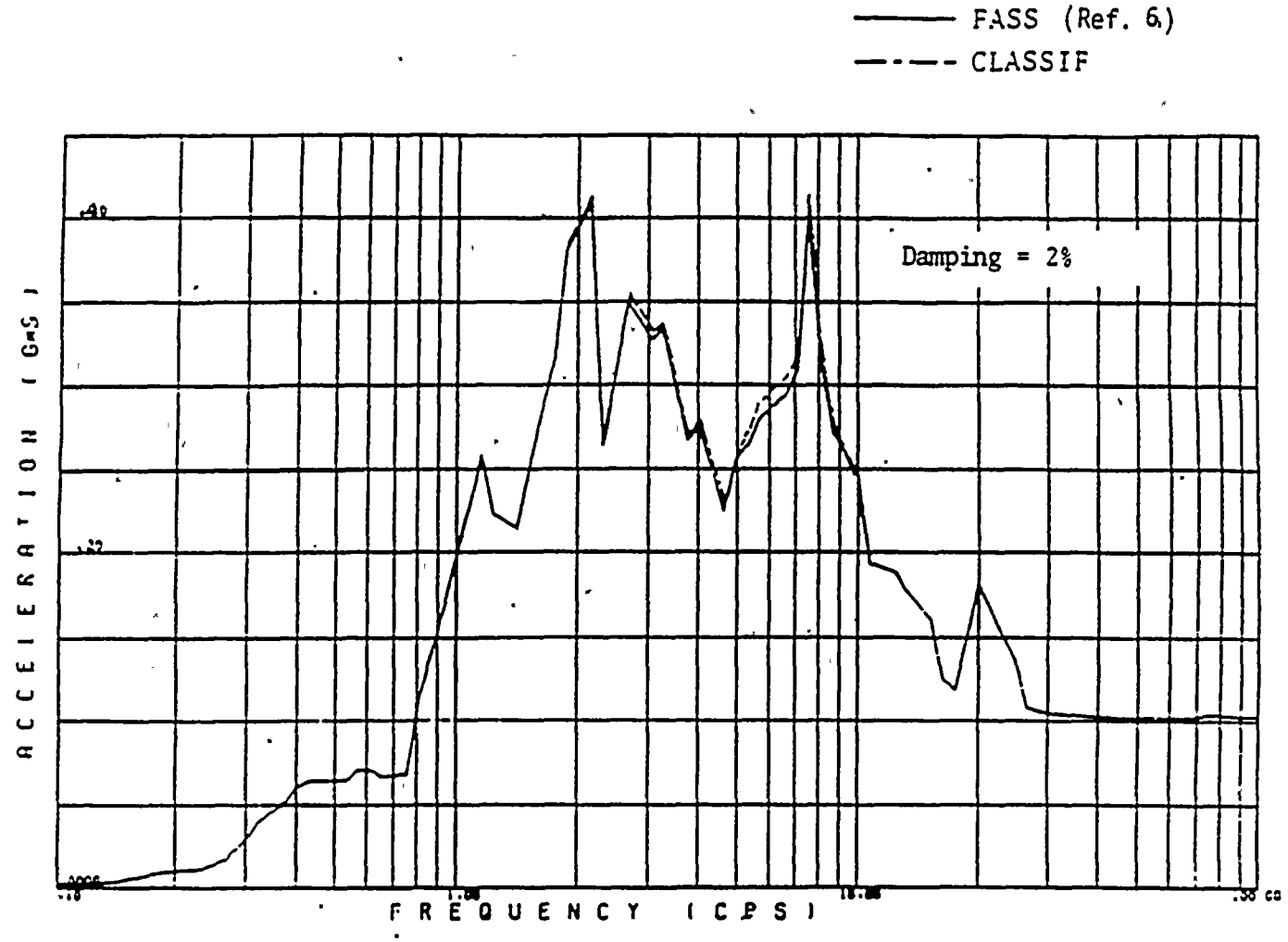

Figure 9-8. Response Spectrum at the Top of the Foundation Basemat

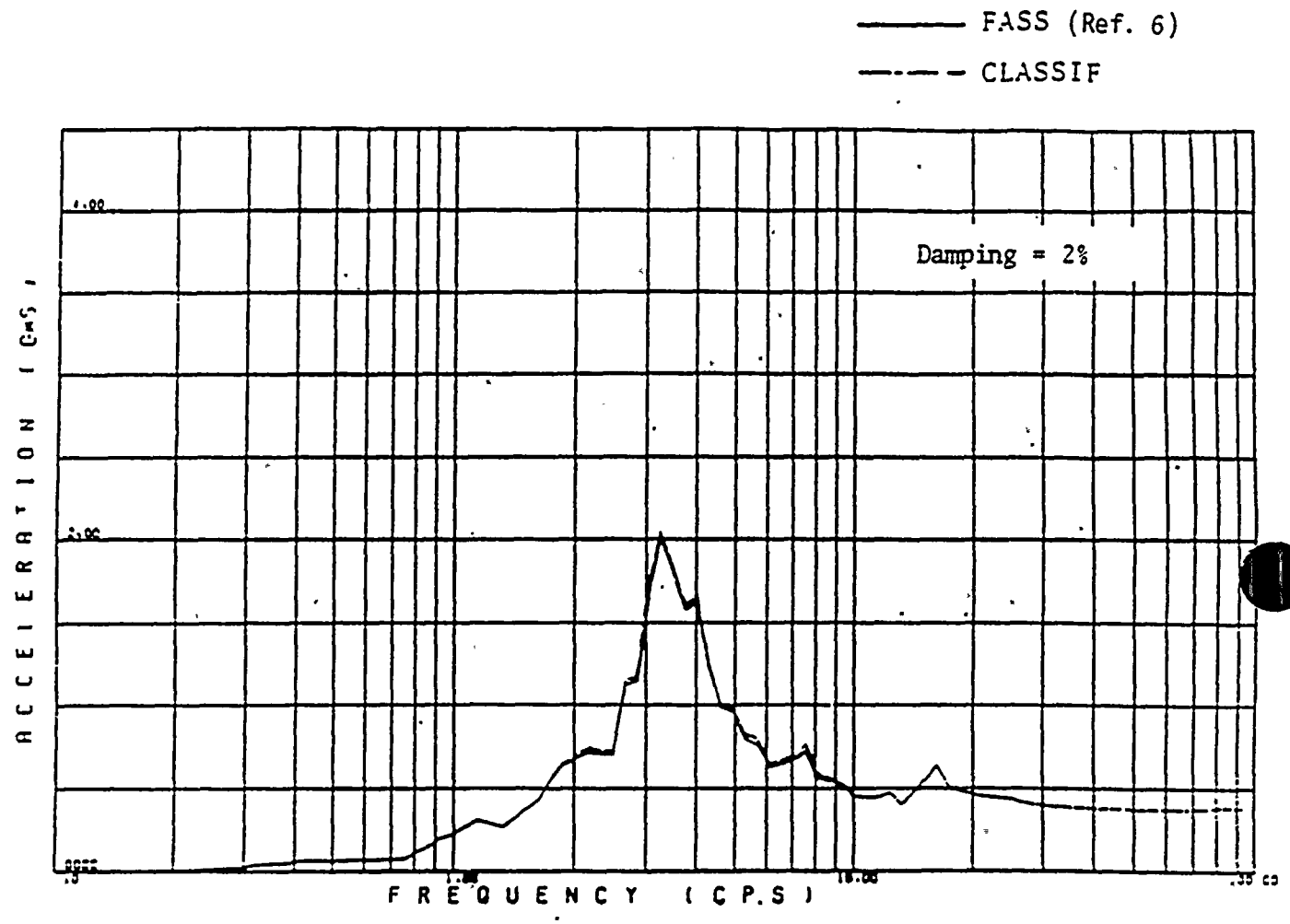

Figure 9-9. Response Spectrum at the Top of Containment Structure

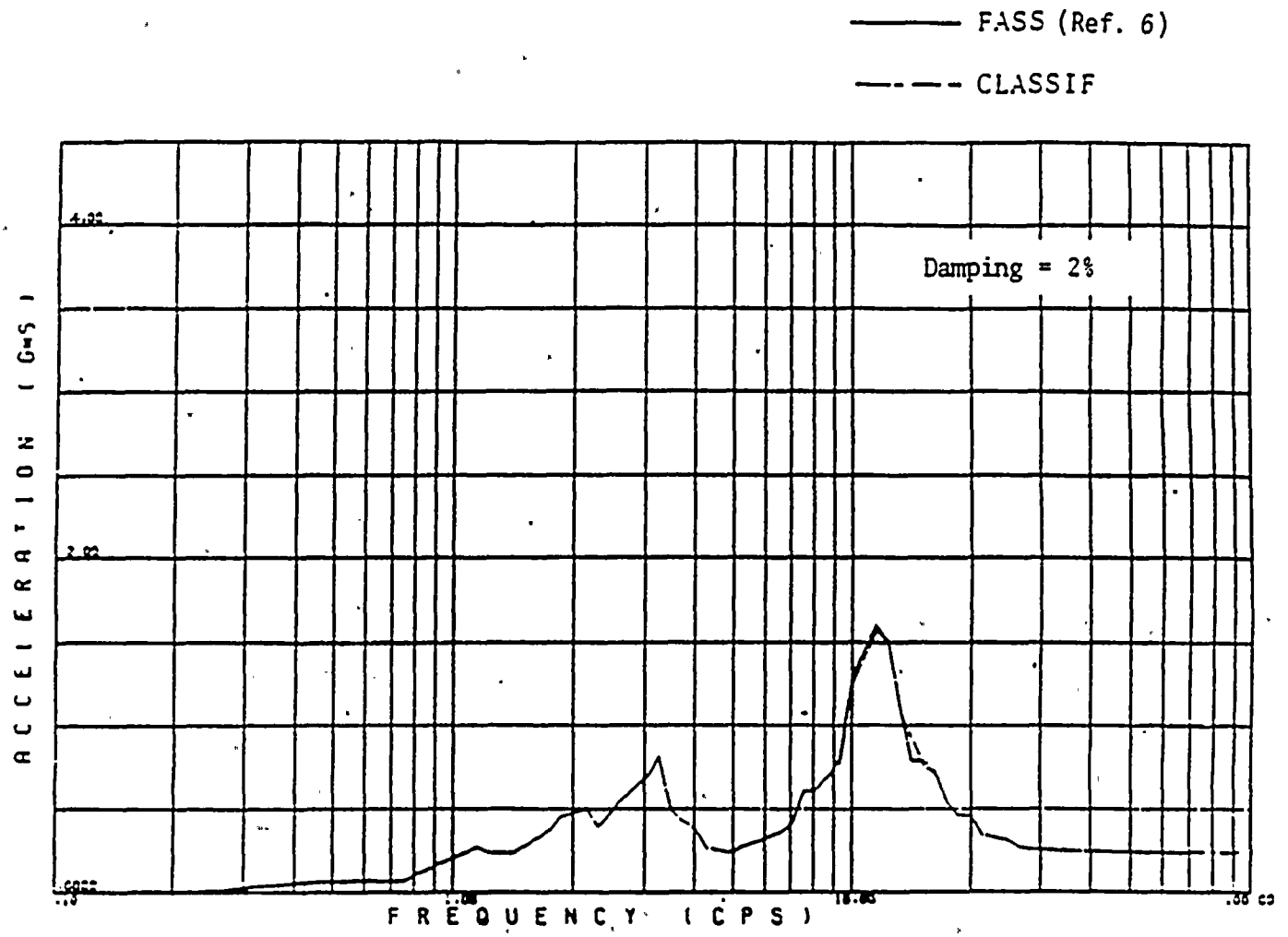

Figure 9-10. Response Spectrum at the Top of Internal Structure

10. REFERENCES

1. "Computer Program CLASSIF: Theoretical Report," Prepared for PG&E by Bechtel Power Corporation, July 27, 1988.

2. "Computer Program CLASSIF: Validation Report," Prepared for PG&E by Bechtel Power Corporation, July 27, 1988.

3. Apsel, R. J., and J. E. Luco, "On the Green's Functions for a Layered Halfspace: Part II," Bulletin of the Seismological Society of America, Vol. 73, No. 4, August 1983.

4. Wong, H. L., and J. E. Luco, "Dynamic Interaction Between Rigid Foundations in a Layered Halfspace," Soil Dynamics and Earthquake Engineering, Vol. 5, No. 3, 1986.

5. Luco, J.E., "Vibration of a Rigid Disc on a Layered Viscoelastic Medium," Nuclear Engineering and Design, 36, 1976.

6. Tseng, W. S., Computer Program FASS (CE933, Version B1), Bechtel Power Corporation, 1986.

APPENDIX A

Listing of Input Data for Application Example

A.1 Listing of Input Data for GLAYER Module

```
(00) TITLE
     EXAMPLE PROBLEM NO. 1, GLAYER - GREENS FUNCTION CALCULATION
(01) NFRQ, NLY, IFITER, LLLL, IPRNT
   1     1     1  300     1
(02) RI, RE
   0.0       150.0
(04) NITER
     6
(05) SHEAR WAVE VELOCITY
   2000.
(06) SOIL MASS DENSITY
   0.004
(07) SOIL POISON'S RATIO
   0.33
(08) SOIL DAMPING
   0.05
(09) LAYER THICKNESS
   50.0
(10) FREQ
   26.
```

A.2 Listing of Input Data for CLAF Module

```
(00) TITLE
     EXAMPLE PROBLEM NO. 1, CLAF - FOUNDATION IMPEDANCE CALCULATION
(01) ANALYSIS PATH (1=INITIAL CALC, 2=RESTART CALC)
     1
(02) PARAMETERS /G,VS,CL/NFRQ,NLAYER,NGRN/NFDN,NTYPE,SCALE/NCASE,IFCVAR
  16149.0    2000.    65.0
   13    1   1000
    1    8    65.
    1    0
(03) FOUNDATION # 1 / NPI,IFSX,IFSY,NREP(IPDN) / X0,Y0 / XB,YB,LET
   37    1    1    0
   0.0       0.0
   7.5      62.6        1
   7.5      58.2        1
   7.5      53.0        2
   5.0      45.0        8
   5.0      35.0        8
   5.0      25.0        8
   5.0      15.0        8
   5.0       5.0        8
  22.5      58.2        1
  22.5      53.0        2
  15.0      45.0        8
  15.0      35.0        8
  15.0      25.0        8
  15.0      15.0        8
  15.0       5.0        8
  25.0      45.0        8
  25.0      35.0        8
  25.0      25.0        8
  25.0      15.0        8
  25.0       5.0        8
  34.1      53.0        3
  35.0      45.0        8
  35.0      35.0        8
  35.0      25.0        8
  35.0      15.0        8
  35.0       5.0        8
  44.0      44.0        4
  45.0      35.0        8
  45.0      25.0        8
  45.0      15.0        8
  45.0       5.0        8
  53.0      34.1        5
  53.0      22.5        6
  53.0       7.5        6
  58.2      22.5        7
  58.2       7.5        7
  62.6       7.5        7
(04) SUBREGION DIMENSIONS / XH ,YH
  15.0       4.4
  15.0       6.0
   8.2       6.0
   8.0       8.0
   6.0       8.2
   6.0      15.0
   4.4      15.0
  10.0      10.0
(05 PRINTOUT & ITERATION CONTROL / IPDF,IPCMPL / NITER,TOLER
   1    1
```

```
   20    0.05
(06) FREQ. IN CPS AND INCIDENT WAVE FORM
   0.9766
    0.0       0.00       1.0       0.0       0.0       0.0       0.0       0.0
   2.9297
   4.8828
   5.8594
   7.8125
   9.7656
  11.7188
  13.6719
  15.6250
  17.5781
  20.5078
  22.4609
  25.3906
```

A.3 Listing of Input Data for SSIF Module

```
(00) TITLE
     EXAMPLE PROBLEM NO. 1, SSIF - SSI CALCULATION
(01) PARAMETERS : G, VS, CL
 16149.0   2000.       65.0
(02) PARAMETERS : NFDN, NTSTR / IFTIMP, XF, YF, ZF, QF
    1     1
    0     0.0         0.0         0.0         0.0
(03) P-B STR # 1 : METHOD,NMODE,NDOF,IFNPTR,IFCAL
    1     5     6     1     1
    1     2     3     4     5     6
    0     0.0         0.0         0.0         0.0
    6     0
(03) PARAMETERS : ND, NNODES, NBAND/ NCARD / RCKEEP
   18    18     1
    6
    1     1     0     0     0     0     0
    7     1     0     0     0     0     0
   11     1     0     0     0     0     0
   12     1     0     0     0     0     0
   15     1     0     0     0     0     0
   18     1     0     0     0     0     0
(04)    NODAL COORDINATE AND ACTIVE DDOF
    1          .0000         .0000       23.5000         0  1  1  1  1  1
    2          .0000         .0000       43.8000         0  1  1  1  1  1
    3          .0000         .0000       63.8000         0  1  1  1  1  1
    4          .0000         .0000       83.8000         0  1  1  1  1  1
    5          .0000         .0000      103.8000         0  1  1  1  1  1
    6          .0000         .0000      123.8000         0  1  1  1  1  1
    7          .0000         .0000      143.8000         0  1  1  1  1  1
    8          .0000         .0000      165.3000         0  1  1  1  1  1
    9          .0000         .0000      184.4000         0  1  1  1  1  1
   10          .0000         .0000      198.5000         0  1  1  1  1  1
   11          .0000         .0000      207.0000         0  1  1  1  1  1
   12          .0000         .0000        8.0000         0  1  1  1  1  1
   13          .0000         .0000       13.0000         0  1  1  1  1  1
   14          .0000         .0000       22.0000         0  1  1  1  1  1
   15          .0000         .0000       33.5000         0  1  1  1  1  1
   16          .0000         .0000       49.0000         0  1  1  1  1  1
   17          .0000         .0000       61.0000         0  1  1  1  1  1
   18          .0000         .0000       93.0000         0  1  1  1  1  1
(04)    MASS MATRIX
   .14286+003  .13043+003  .13043+003  .13043+003  .13043+003  .13043+003
   .14317+003  .93789+002  .76708+002  .65839+002  .59006+001  .86957+002
   .77950+002  .19534+003  .11677+003  .26522+003  .37888+002  .25466+002
(04)    FREQ ,DAMPING, AND MODE SHAPES
     33.13880       .02000
  -.46754-002 -.94814-002 -.14697-001 -.20181-001 -.25734-001 -.31163-001
  -.36296-001 -.41847-001 -.46246-001 -.49110-001 -.50617-001  .00000
   .00000      .00000       .00000      .00000      .00000      .00000
     75.22960       .02000
   .00000      .00000       .00000      .00000      .00000      .00000
   .00000      .00000       .00000      .00000      .00000      .18835-002
   .30553-002  .55107-002  .10832-001  .19072-001  .25719-001  .18353+000
    102.31630       .02000
  -.17955-001 -.30042-001 -.36607-001 -.36577-001 -.29840-001 -.17448-001
  -.14306-002  .21080-001  .38805-001  .48851-001  .52827-001  .00000
```

```
  .00000       .00000       .00000       .00000       .00000       .00000
    1 0.13470       .02000
  .00000       .00000       .00000       .00000       .00000       .00000
  .00000       .00000       .00000       .00000       .00000      -.58937-002
 -.92813-002 -.15964-001 -.29586-001 -.47669-001 -.50004-001  .74378-001
   183.86770       .02000
  .29065-001  .38748-001  .29499-001  .60466-002 -.19944-001 -.35529-001
 -.32923-001 -.21563-002  .27771-001  .42928-001  .46161-001  .00000
  .00000       .00000       .00000       .00000       .00000       .00000
(07) FOUNDATION # 1 : MASS MATRIX (6 X 6)
  621.          0.           0.           0.           0.           0.
    0.        621.           0.           0.           0.           0.
    0.          0.         621.           0.           0.           0.
    0.          0.           0.      655279.           0.           0.
    0.          0.           0.           0.      655279.           0.
    0.          0.           0.           0.           0.      655279.
    0        0.0          0.0          0.0          0.0
(08) NO RELATIVE DISPL REQUESTED
    0
(09) IMPEDANCE CONTR PARAMETERS : LFT, NCOM, NCASE, FMIN, FMAX
    1     1     1    0.9766    25.3906
(10) REAL TIME ANALYSIS : DT, NPOINT, NFFT
 .005        2048     4096
(12) TIME HIST : FORMAT/ISWITCH /IWTYPE,IWFS,IWCOL,MEAN/SCALE /ACCEL
  (8F9.6)
    1
    0    0    1    0
  0.1
```

ATTACHMENT Q2a-3

CONTINUUM
LINEAR
ANALYSIS FOR
SOIL
STRUCTURE
INTERACTION
F-VERSION

CLASSIF VALIDATION MANUAL

JULY 1988

CE934

BECHTEL POWER CORPORATION

CLASSIF

COMPUTER PROGRAM CLASSIF
VALIDATION REPORT

Prepared
for

Diablo Canyon
Long Term Seismic Program
Pacific Gas & Electric Company
San Francisco, California

by

Bechtel Western Power Corporation
San Francisco, California

July 27, 1988

PREFACE

CLASSI (Continuum Linear Analysis for Soil-Structure Interaction) is a linear three-dimensional, seismic soil-structure interaction (SSI) analysis program developed by Luco and Wong in 1976 at the University of California, San Diego. Since then, the CLASSI program has been continuously upgraded to expand its capabilities and efficiency from those of its initial development. Thus, various versions of the CLASSI program exist in the industry, each covering somewhat different analysis capabilities. The CLASSIF program is a Bechtel version of CLASSI program originally developed in 1978, and recently modified by Wong and Luco in 1985. During the course of installation, testing, and validation of the CLASSIF program on the Bechtel UNIVAC system, some modifications and enhancements were made to the code to improve its performance. These include: implement new algorithms for computing and inverting the Green's function; add a capability for computing SSI responses to steady-state forced vibration applied on the structure; add a capability for computing the relative displacement between two locations in the structure; add a capability for calculating the traction vectors used for a restart of analysis for new wave inputs; add a capability for calculating the transfer function between the SSI response motion and the scattered foundation input motions; implement subroutines for reading in the fixed-based modal properties of structures generated from the BSAP-DYNAM program (a post processor for the Bechtel Structural Analysis Program); implement a free format for the input data and improve the printed output format; correct the option for generating foundation symmetry about one axis; correct the option for calculating the transfer function due to external forcing function; correct the option for calculating the SSI response to include contribution from more than one mode of response; implement the option to bypass a zero-mean baseline correction for calculating the time history response due to ground motion input.

This report has been prepared by Bechtel Power Corporation and has been reviewed following the Bechtel Standard Engineering Department Procedure for nuclear projects.

This report was prepared under a contract agreement between PG&E and Bechtel and is intended for exclusive use by PG&E only. Appendix A of this report contains technical information proprietary to Bechtel Power Corporation. Except for copies that may be required for the Nuclear Regulatory Commission (NRC) in satisfying a regulatory requirement, no copy should be distributed outside of PG&E without prior written consent from Bechtel.

DISCLAIMER

Every reasonable effort was made to provide a comprehensive and flexible computer program. However, the computer program itself and associated documentation are supplied without representation of warranty, expressed or implied, as to its content, accuracy, or freedom from defects or errors.

TABLE OF CONTENTS

TABLE OF CONTENTS (Cont'd)

1 INTRODUCTION

This report presents the validation test problems used and the results of tests obtained for validating computer program CLASSIF which is a Bechtel version of the CLASSI computer program for linear three-dimensional seismic soil-structure interaction (SSI) analysis using the halfspace continuum approach. The program solves the SSI problem in frequency domain using the Fast Fourier Transform technique. CLASSIF is comprised of three program modules (GLAYER, CLAF, and SSIF) developed to solve the SSI problem in separate steps; the results of individual steps by different modules are combined in the final interaction analysis module so as to satisfy the interaction conditions at the structural base. The GLAYER module computes the Green's functions at the surface of horizontal soil layers over a halfspace. The CLAF module computes the foundation impedance functions and the scattered foundation input motions using the Green's function computed from GLAYER module as input. The SSIF module forms the system equations of motion and then computes the SSI responses of structure using the impedance functions and scattered foundation input motions as input. More detailed theoretical bases of the program is presented in the programs theoretical manual.

The description of the program is provided in Section 2. The validation methods and scopes are described in Section 3. The of validation test problems and results of comparisons between CLASSIF results and the benchmark solutions are summarized in Section 4. Conclusions are provided in Section 5. References for the benchmark solutions are provided in Section 6.

2 PROGRAM DESCRIPTION

CLASSI (Continuum Linear Analysis for Soil-Structure Interaction) is a linear three-dimensional seismic SSI analysis program developed by Luco and Wong since 1976 at the University of California, San Diegeo. The program solves the SSI problem in frequency domain using the Fast Fourier Transforms technique. CLASSI is comprised of program modules developed to solve the SSI problems in separate steps, the results of individual steps by different modules are combined in the final interaction analysis module to satisfy the interaction conditions at the structural base. The methodology and computer program have been continuously upgraded to expand the capabilities since their initial development. Thus; various versions of the CLASSI program exist in the industry, each covering somewhat different analysis capabilities. The CLASSIF program is a Bechtel version of CLASSI program originally developed in 1978, and recently modified by Wong and Luco in 1985. This version has the following capabilities and limitations:

- The foundation medium is assumed to be elastic or viscoelastic, uniform or horizontally layered continuum halfspace. Damping in the foundation medium can be specified as constant hysteresis damping ratios for different soil layers.

- The structural foundation is assumed to be rigid and bonded on the surface of the foundation medium. The basic Green's function for the continuum halfspace adopts the solutions by Apsel.

- Multiple structural foundations can be analyzed. Improved numerical algorithm has been implemented for increasing the accuracy of impedance and scattering calculations for multiple foundations.

- 3-D forced-vibration analysis capabilities have been implemented which can accommodate forced excitations on the foundation as well as in the structures.

- o 3-D seismic incidence wave environment in the form of vertical or inclined P, SV and SH body waves and the R and L surface waves, and the combination thereof, can be specified as the seismic input.

- o Due to the limitation of surface foundation, the scattering of seismic waves considers only the horizontal variation of input motion. The vertical variation of ground motion is not recognized..

- o The program is a linear analysis program; thus, the strain-dependency of soil properties cannot be directly considered. It requires separate analyses to obtain the strain-compatible equivalent linear soil properties for input to the analysis.

The CLASSIF computer program consists of three distinct program modules: GLAYER, CLAF, and SSIF. The application of the program requires the following analysis steps.

Step 1: The dynamic characteristics of the super-structure such as the mass, stiffness, and damping matrices are modelled using a standard structural dynamic analysis program and the fixed-base modal properties (natural frequencies, mode shapes, modal damping ratios, and modal participation factors) are computed and used for input to the CLASSIF program.

Step 2: The mass and mass moments of inertia of the structural foundation are separately computed.

Step 3: The area of the foundation assumed to be rigid is discretized into small subregions. Finer subdivisions are used near the foundation perimeter where the stress gradient of the foundation interface stresses is the largest. Then, the program module GLAYER is executed to obtain the Green's functions which are frequency dependent.

Step 4: The program module CLAF is executed to integrate the Green's functions over the discretized foundation area to obtain the foundation impedance functions which are frequency dependent. For forced excitations, the driving force vector is directly formed. For seismic excitations, the seismic incidence wave field (wave type, azimuth, and incidence angle) is specified, and the seismic driving force vector normalized to unit input amplitude is computed.

Step 5: The forcing function or the control ground motion time histories are input to program module SSIF. The module forms the system equations of motion in the frequency domain by assembling the fixed-base modal properties of the structures from Step 1, the foundation base inertia properties from Step 2, the foundation impedance matrix and driving force vectors from Step 4. The equations of motion are solved for SSI response transfer functions which are used finally to convolve with the Fourier transforms of the input time histories to give the response motion time histories at desired locations.

Step 6: The response time histories of the structural foundation are used as input to re-excite the fixed-base structural model of Step 1 to compute the time history response of internal stresses, forces, and moments in the structure.

3 VALIDATION METHODS AND SCOPE

3.1 Validation Methods

The methods used to validate the capabilities of CLASSIF are in accordance with the methods used in the nuclear industry. Typically, for any validation test problem selected, the problem is modelled and analyzed using CLASSIF. The CLASSIF solution is then compared with the benchmark solution (basis of comparison) to assess the validity and accuracy of CLASSIF results. The basis of comparison is provided by one or more of the following methods:

a. Hand calculations are used for simple problems to provide the solution for cross-checking the results. The calculations when used are fully described.

b. Bechtel standard computer programs or comparable validated public domain programs are used to provide the solution for comparison. If Bechtel in-house program is used, the reference in made accordingly and the results are transferred from the in-house validation report. If an already validated public domain program is used, the analysis model is described and the results are transferred from the applicable validation report.

c. The analytical solutions obtained from the technical literature are used as the basis of comparison. This validation method is most extensively used for CLASSIF validations. An extensive effort is made to locate and select reference solutions from the literature for CLASSIF validations.

3.2 Capabilities Validated

The computer program CLASSIF was tested for a set of eighteen validation test problems described in Section 4 to validate the various analysis capabilities available in the program; broadly classified as, impedance analysis, wave scattering analysis, seismic SSI analysis and forced vibration analysis. The capabilities that were validated by these test problems are shown in Table 3-1. The corresponding benchmark solutions for these validation test problems, that were used as the bases of comparisons against CLASSIF results, are identified in Table 3-1.

Table 3-1

List of Capabilities Tested for CLASSIF

CAPABILITIES TESTED	VALIDATION TEST PROBLEM NO.	BENCHMARK SOLUTIONS*
1 IMPEDANCE ANALYSIS		
1.1 Foundation on Uniform Halfspace		
1.1.1 Circular Foundation	1, 11	2, 14-16,
1.1.2 Square Foundation	8	11
1.1.3 Strip Foundation	9, 10	12, 13
1.1.4 Ring Foundation	12	17
1.2 Foundation on Layered System		
1.2.1 Circular Foundation	2, 4	4, 6
1.2.2 Strip Foundation	10	13
1.3 Multiple Foundations	5	8
2 SCATTERING ANALYSIS		
2.1 Inclined Body Waves	3	5
2.2 Surface Waves	6	9
3 SSI ANALYSIS		
3.1 Seismic Response	1, 4, 7, 13, 14, 17, 18	3, 7, 10, 18, 3
3.2 External Force Vibration	15, 16	19, 20-21

*Note: List of references for benchmark solutions is given in Section 6.

4. SUMMARY OF VALIDATION TEST PROBLEMS AND RESULTS

Eighteen validation test problems are used to test the capabilities of computer program CLASSIF, as shown in Table 3-1. Briefed descriptions and results of these problems are summarized in this section. Comparisons of the CLASSIF results with the benchmark solutions are also described. For more detailed presentation of these validation test problems, the readers are referred to Appendices A.1 through A.18 for Validation Test Problem Nos. 1 through 18, respectively.

4.1 Validation Test Problem No. 1

Description

The seismic SSI responses of a typical pressurized water reactor (PWR) containment structure (Ref. 1), as shown in Fig. 4.1-1, are considered in this problem. The containment circular basemat is founded on a viscoelastic halfspace as shown in Fig. 4.1-2. The containment structure resting on a viscoelastic halfspace is subjected to the horizontal seismic input motion consisting of a vertically propagating SV wave. The 1940 El Centro earthquake time history scaled to 0.1 g maximum acceleration is specified as the free-field input motion at the ground surface. The input motion and its 2% damping response spectrum scaled up to 1.0 g are shown in Fig. 4.1-3. To evaluate the accuracy of the CLASSIF results, the foundation impedance functions and the SSI responses computed from CLASSIF are compared with those obtained from Luco (Ref. 2) and computer program FASS (Ref. 3), respectively.

Results

The horizontal stiffness and damping impedances computed from CLASSIF are plotted as shown in Figs. 4.1-4 and 4.1-5, and the rocking stiffness and damping impedances are plotted as shown in Figs. 4.1-6 and 4.1-7. For comparison, the corresponding stiffness and damping

impedances obtained by Luco (Ref. 2) are also plotted on these figures. As can be seen from these figures, the CLASSIF results are in good agreement with the Luco's results.

The 2% damping response spectra of the SSI response motions obtained from CLASSIF for the tops of the foundation, containment shell, and internal structure are plotted as shown in Figs. 4.1-8 through 4.1-10, respectively. To evaluate the accuracy of the CLASSIF results, the SSI response motions at these locations in the containment structure are also computed using computer program FASS (CE933), (Ref. 3). The 2% damping response spectra of the SSI motions computed from FASS are also plotted in Figs. 4.1-8 through 4.1-10. As can be seen from these figures, the CLASSIF results compare very well with the FASS results.

Thus, it can be concluded that CLASSIF can be used accurately for computing the foundation impedance functions, and the SSI response of a containment structure resting on a viscoelastic halfspace.

4.2 Validation Test Problem No. 2

The impedance functions for a circular foundation resting on a two layered soil medium are analyzed. The foundation model and the soil layered properties are shown in Fig. 4.2-1. The impedance functions computed from CLASSIF are compared with those reported by Luco in Ref. 4.

Results

The horizontal, vertical, and rocking components of the normalized stiffness and damping coefficients obtained from CLASSIF are plotted in Figs. 4.2-2 through 4.2-4, respectively, against the dimensionless frequency a_0. ($a_0 = \omega\ a/V_S$, in which ω = circular frequency a = foundation radius = 65 ft, and V_S = 2,000 fps). To evaluate the accuracy of the CLASSIF results, the analytical impedance functions reported by Luco in Ref. 4 are also plotted for comparison in these

figures. Comparing the CLASSIF results with the Luco's results for a ratio of h/a = 1.0, in which h is the thickness of top soil layer, i.e., 65 ft, shows that the CLASSIF results generally compare well with the Luco's results for $a_0 \leq 5$ which corresponds to frequency of less than about 25 cps. The difference which occurs beyond this frequency range practically used in the SSI response analysis, may be attributed to the different techniques used in obtaining the impedance functions.

Thus, it can be concluded that CLASSIF can be used with sufficient accuracy for computing the impedance functions for a circular foundation resting on a soil layered system.

4.3 Validation Test Problem No. 3

Description

A square foundation resting on a uniform halfspace subjected to inclined body wave excitation, as shown in Fig. 4.3-1, is analyzed. Three types of inclined body wave; namely, P, SV and SH waves, are considered in this problem. The inclined body waves impinge the foundation with an incident wave angles θ_V measured with respect to the horizontal axis. The following cases of analysis due to different inclined body waves are considered; (a) SH wave with θ_V = 45°, (b) SV wave with θ_V = 60°, and (c) P wave with θ_V = 60°. The scattered foundation responses to these inclined body waves are computed using CLASSIF and the results are compared with those obtained by Wong and Luco (Ref. 5).

Results

The results obtained from CLASSIF are presented in terms of the elements of the wave scattering matrix of the foundation input motions, which are the coefficients relating the free-field input motions to the response motions of the rigid, massless foundation.

The computed scattering elements due to the inclined SH, SV and P waves impinged the foundation with the incident wave angles of θ_V = 45°, 60° and 60°, respectively, are plotted against the dimensionless frequency a_0 in Figs. 4.3-2 and 4.3-3. The symbols S and R labelled on these figures indicate the translational and rocking components of the foundation scattering element, respectively. The subscripts x, y, and z on S and R indicate the directions of the foundation response with respect to the coordinate system shown in Fig. 4.3-2. To evaluate the CLASSIF results, the results obtained by Wong and Luco (Ref. 5) are also plotted in Figs. 4.3-2 and 4.3-3. As can be seen from these figures, the CLASSIF results are almost identical to the Wong and Luco's results.

It can thus be concluded that the scattered foundation input motions to inclined body wave excitations can be accurately computed using CLASSIF.

4.4 Validation Test Problem No. 4

Description

The SSI model of a containment structure, as shown in Fig. 4.4-1, is subjected to the vertically propagating SV+P wave excitation, and to the horizontally propagating R (Rayleigh) wave excitation. This model is similar to that used in Seed and Lysmer's report (Ref. 6). The soil profile and the soil-layered properties are as shown in Fig. 4.4-2. The free-field input motion with 0.75 g maximum acceleration is specified at the ground surface in the form of SV+P wave and R wave. The 2% damping response spectrum of the free-field input motion is shown in Fig. 4.4-3. For the R wave input excitation, it is further specified that the R wave is horizontally propagating in the positive direction, and that the free-field input motion is located at the center of the foundation. To evaluate the CLASSIF results, the SSI responses computed from CLASSIF are compared with those obtained from computer program SASSI (Ref. 7).

Results

The 2% damping response spectra of horizontal SSI response motions at the tops of foundation and containment shell due to the SV+P wave excitation are shown in Figs. 4.4-4 and 4.4-5, respectively. To evaluate the CLASSIF results, the corresponding response spectra obtained from SASSI (Ref. 7) are also plotted in these figures. As can be seen from Figs. 4.4-4 and 4.4-5, the CLASSIF results compare reasonably well with those obtained from SASSI. Similar comparisons of response spectra obtained from CLASSIF and SASSI are also made in Figs. 4.4-6 and 4.4-7 for horizontal SSI responses to R wave excitation. As can be seen from these figures, the CLASSIF results are also in reasonably good agreement with the corresponding SASSI results.

Based on the comparison results, it can be concluded that both CLASSIF and SASSI analyses yield responses which are consistent with each other. This consistency contributes to confidence on both results.

4.5 Validation Test Problem No. 5

The impedance functions for two adjacent square foundations resting on a viscoelastic halfspace soil medium are analyzed using CLASSIF. Both foundations have dimensions 2a x 2a of 104' x 104', and they are separated by a clear distance "d" of 26'. The foundation model considered is shown in Fig. 4.5-1. The soil properties of the halfspace are shown in Fig. 4.5-2. To evaluate the accuracy of the CLASSIF results, the foundation impedance functions computed from CLASSIF are compared with those obtained by Wong and Luco (Ref. 8).

Results

The computed impedance functions for these foundations are grouped into two sets of uncoupled foundation deformation modes. The first set involves generalized coordinate directions 1, 3 and 5, while the

second set involves generalized coordinate directions 2, 4 and 6. The impedance functions for the first set are shown in Figs. 4.5-3 and 4.5-4 and those for the second set are shown in Figs. 4.5-5 and 4.5-6. The impedance functions are plotted in these figures as a function of dimensionless frequency a_0 for d/a of 0.5. Also shown in these figures are the impedance functions obtained by Wong and Luco (Ref. 8) for the same d/a ratio of 0.5. As can be seen from these figures, the impedance functions obtained from CLASSIF for d/a of 0.5 are essentially identical to those obtained by Wong and Luco.

Thus, it is concluded that CLASSIF can be accurately used for computing the impedance functions for two foundations interactive with each other through the soil medium.

4.6 Validation Test Problem No. 6

Description

The scattered responses of a square foundation resting on an elastic halfspace to Rayleigh wave excitation are analyzed using CLASSIF. The foundation model and the soil properties are shown in Fig. 4.6-1. The foundation as shown in this figure is a square foundation with dimensions of 104'x104'. The free-field control motion in the form of Rayleigh wave propagating in the horizontal direction is specified at the center of the foundation. The scattered foundation responses obtained from CLASSIF are compared with those obtained by Wong and Luco (Ref. 9).

Results

The scattered response of a square foundation to the Rayleigh wave excitation propagating in X_1-direction consists of three components; (1) the longitudinal component (U_1^*), (2) the vertical component (U_3^*), and (3) the rocking component about X_2 axis (ϕ_2^*). The computed U_1^* and U_3^* normalized with respect to the horizontal Rayleigh wave amplitude R_H are plotted as a function of dimensionless

frequency a_0 in Fig. 4.6-2. The normalized rocking response, expressed as $a\phi_2^*$ normalized with respect to R_H, is also plotted against the dimensionless frequency a_0, as shown in Fig. 4.6-2. To evaluate the CLASSIF results, the three components of the foundation response are compared with those obtained by Wong and Luco in Ref. 9. It can be seen from the comparison that the CLASSIF results are in very good agreement with the Wong and Luco's results.

Thus, it is concluded that CLASSIF can be accurately used for computing the scattered foundation response foundation to Rayleigh wave excitation, as considered in this validation test problem.

4.7 Validation Test Problem No. 7

Description

Two identical structures resting on a layered-soil medium, as shown in Fig. 4.7-1, is subjected to a horizontal seismic input motion. The foundation model and the soil properties are also shown in this figure. The free-field input motion in the form of a vertically propagating SV wave is specified at the ground surface. The 1% damping response spectrum of this input motion is shown in Fig. 4.7-2. To evaluate the accuracy of the CLASSIF results, the SSI response obtained from CLASSIF is compared with that obtained from computer program FLUSH (Ref. 10).

Results

The 1% damping response spectrum of the horizontal SSI response motion at the top of the structure is shown in Fig. 4.7-3. For comparison purposes, the corresponding response spectrum obtained from the FLUSH computer program are also shown in this figure. As can be seen from Fig. 4.7-3, the CLASSIF results are closely compared with the FLUSH results.

Thus, it can be concluded that CLASSIF can be accurately used for computing the SSI response of two structures interactive with each other through the layered soil medium.

4.8 Validation Test Problem No 8

A square plate foundation resting on an elastic halfspace soil medium is analyzed using CLASSIF to compute the foundation impedance functions. The foundation model and the soil properties used in this test problem are shown in Fig. 4.8-1. The dimensions of the foundation are 104'x104'. To evaluate the accuracy of the CLASSIF results, the foundation impedance functions computed from CLASSIF are compared with those obtained by Dominguez (Ref. 11).

Results

The horizontal, vertical, rocking and torsional foundation impedance functions obtained from CLASSIF are normalized with respect to their corresponding static values. These normalized impedance functions are plotted as a function of the dimensionless frequency parameter a_0, as shown in Figs. 4.8-2 through 4.8-5, respectively. Also shown in these figures are the corresponding impedance functions obtained by Dominguez (Ref. 11). As can be seen from these figures, the normalized impedance functions from CLASSIF are in close agreement with those obtained by Dominguez.

Thus, it can be concluded that CLASSIF can be accurately used for computing the impedance functions of a square plate foundation resting on an elastic halfspace

4.9 Validation Test Problem No. 9

Description

A rectangular foundation resting on a uniform halfspace soil medium

is analyzed using CLASSIF to compute the foundation compliance functions. The rectangular foundation is proportioned to closely resemble a strip foundation with the foundation length being ten times the foundation width, giving the rectangular foundation with dimensions of 10.4'x104', as shown in Fig. 4.9-1. The soil properties of the halfspace are also shown in Fig. 4.9-1. To evaluate the accuracy of the CLASSIF results, the foundation compliance functions computed from CLASSIF are compared with those obtained by Luco and Westmann (Ref. 12).

Results

The foundation compliance functions obtained from CLASSIF are plotted against the dimensionless frequency a_0 in Figs. 4.9-2 through 4.9-4 for the vertical, horizontal, and rocking components, respectively. Also shown in these figures are the corresponding foundation compliance functions of a strip foundation obtained by Luco and Westman. As can be seen from these figures, the foundation compliance functions obtained from CLASSIF are compared very well with those reported by Luco and Westmann in Ref. (12).

Thus, the compliance functions for a strip foundation resting on a uniform halfspace soil medium can be accurately computed by CLASSIF.

4.10 Validation Test Problem No. 10

Description

The vertical compliance functions for a rigid strip foundation resting on two different soil media are analyzed using CLASSIF. The strip foundation is modelled as the rectangular foundation with dimension of 20'x320'. Two cases of soil media considered in this problem are as follows: Case (a) a two layered viscoelastic soil medium; and Case (b) a viscoelastic halfspace. The soil properties specified for Cases (a) and (b) are shown in Figs. 4.10-1 and

4.10-2, respectively. The accuracy of the compliance functions obtained from CLASSIF for both Cases (a) and (b) are validated by comparing with those obtained by Gazetas and Roessett in Ref. 13.

Results

The vertical foundation compliance functions obtained from CLASSIF for Cases (a) and (b) are plotted against the dimensionless frequency a_0, as shown in Figs. 4.10-3 and 4.10-4, respectively. Also shown in these figures are the corresponding vertical foundation compliance functions obtained by Gazetas and Roessett in Ref. 13. The comparisons of results in Figs. 4.10-3 and 4.10-4 show that the CLASSIF results generally agree well with the Gazetas and Roessett's results except for Case (a) when $a_0 > 1.5$, which corresponds to frequency greater than about 24 cps. This difference which occurs around the frequency range where the impedance values are apparently sensitive to numerical analysis techniques, may be attributed to the different techniques used in obtaining the impedance functions.

Based on the above results of comparison, it is concluded that CLASSIF can be used with sufficient accuracy for computing the compliance functions of a strip foundation resting on a layered viscoelastic or viscoelastic halfspace soil medium.

4.11 Validation Test Problem No. 11

Description

The impedance functions for a circular foundation resting on an elastic halfspace soil medium is analyzed using CLASSIF. The foundation model and the soil properties of the halfspace are shown in Figure 4.11-1. The foundation impedance functions computed from CLASSIF are compared with those obtained by Veletsos, et al (Refs. 14-16).

Results

The foundation impedance functions obtained from CLASSIF are plotted as a function of the dimensionless frequency parameter a_0 in Fig. 4.11-2 for the horizontal, rocking and the coupling between horizontal and rocking components; Fig. 4.11-3 for the vertical component; and Fig. 4.11-4 for the torsional component. Also shown in these figures are the results obtained by Veletsos, et al (Refs. 14-16). As can be seen from these figures, the foundation impedance functions obtained from CLASSIF are in close agreement with those obtained by Veletsos, et al.

Thus, it is concluded that CLASSIF can be accurately used for computing the impedance functions for a circular foundation resting on an elastic halfspace soil medium.

4.12 Validation Test Problem No. 12

Description

A rigid ring foundation resting on an elastic halfspace soil medium is analyzed using CLASSIF to compute the vertical foundation impedance functions. The foundation model and soil properties used for the analysis are as shown in Figure 4.12-1. The foundation has an inside radius (R_i) of 90' and outside radius (R_o) of 100'. The ratio of the width of the ring foundation to the outside radius of foundation $\Delta R/R_o$ is 0.1. The vertical foundation impedance function computed from CLASSIF is compared with those obtained by Veletsos and Tang (Ref. 17).

Results

The vertical impedance function obtained from CLASSIF is plotted as a function of the dimensionless frequency a_0, as shown in Figure 4.12-2. Also shown in these figures are the corresponding impedance

functions obtained by Veletsos and Tang (Ref. 17) for $\Delta R/R_0$ = 0.02, 0.1, 0.2, 0.5 and 1.0. As can be seen from this figures, the impedance function obtained from CLASSIF is in close agreement with that obtained by Veletsos and Tang.

Thus, it can be concluded that CLASSIF can be accurately used for computing the impedance function for a rigid ring foundation resting on an elastic halfspace soil medium.

4.13 Validation Test Problem No. 13

Description

The SSI model of a containment structure used in this problem is the same as that used in Validation Test Problem No. 1, as shown in Figures 4.1-1 and 4.1-2. This model is also subjected to the same input motion as in Validation Test Problem No. 1. The relative displacement response motion between the tops of containment shell and internal structure is computed directly using CLASSIF. To evaluate the accuracy of the CLASSIF results, the computed maximum relative displacement response is compared with that obtained from computer program DATAN (Ref. 18).

Results

The maximum relative displacement response motion between the tops of containment shell and internal structure computed from CLASSIF is shown in Table 4.13-1. To evaluate the accuracy of the CLASSIF results, this relative displacement response motion is also computed using computer program DATAN to double integrate its relative acceleration response resulted from subtracting the absolute acceleration response at the top of containment shell from that at the top of internal structure. The resulted maximum relative displacement response computed from DATAN is also shown in Table 4.13-1. As can be seen from this table, the maximum relative displacement response obtained from CLASSIF closely compares with that obtained from DATAN.

Thus, it is concluded that CLASSIF can be accurately used to directly compute the relative displacement response between two locations in the structure.

4.14 Validation Test Problem No. 14

Description

The SSI model of a containment structure used in this problem is the same as that used in Validation Test Problem No. 1, as shown in Figures 4.1-1 and 4.1-2. The CLASSIF computer program is used to compute the transfer functions for the responses at the tops of containment shell and internal structure relative to the horizontal free-field ground motion input. To evaluate the accuracy of the CLASSIF results, the calculated response transfer functions from CLASSIF are compared with those obtained from computer program FASS (Ref. 3).

Results

The transfer functions for the responses at the tops of containment shell and internal structure relative to the ground motion input computed from CLASSIF are plotted in Figs. 4.14-1 and 4.14-2, respectively. For comparison, the corresponding structural response transfer functions obtained from computer program FASS (Ref. 3) are also computed and plotted as shown in these figures. As can be seen from these figures, the CLASSIF results are essentially identical to those obtained from FASS.

Thus, it is concluded that CLASSIF can be accurately used to compute the transfer functions for structural responses relative to the ground motion input.

4.15 Validation Test Problem No. 15

Description

A rigid circular disk resting on a uniform halfspace soil medium is subjected to a trapezoidal pulse excitation in the vertical direction as shown in Figure 4.15-1. The trapezoidal pulse excitation has a duration of 1.0 second with a time increment of 0.005 second. The foundation model and the properties of the halfspace are also shown in this figure. To evaluate the accuracy of the CLASSIF results, the foundation response is compared against the analytical solution obtained by Lysmer in Ref. 19.

Results

The vertical displacement response time history of the circular disk obtained from CLASSIF is plotted as shown in Figure 4.15-2. For comparison, the corresponding Lysmer's solution (Ref. 19) is also shown in this figure. As can be seen from this figure, the vertical displacement response time history obtained from CLASSIF is in close agreement with that obtained by Lysmer.

Thus, it is concluded that CLASSIF can be accurately used for computing the displacement response time history of a circular foundation subjected to a dynamic forced excitation.

4.16 Validation Test Problem No. 16

Description

A three lumped-mass stick model of the scaled down experimental reactor building model is shown in Figure 4.16-1. The model is subjected to a vertical external forced vibration applied at node 2, as shown in Fig. 4.16-1. Using the experimental test impedance functions obtained from Refs. 20 - 22, as shown in Figures 4.16-2

and 4.16-3, as input for soil springs and dampers, the transfer function between the displacement response at node 2 and the forced excitation is computed using the computer program CLASSIF. To evaluate the accuracy of the CLASSIF results, the response transfer function computed from CLASSIF is compared with that obtained from the experimental test results reported in Refs. 20 and 21.

Results

The displacement response transfer function amplitude obtained from CLASSIF for node 2 is plotted against frequency as shown in Figure 4.16-4. The corresponding experimental test results obtained from Refs. 20 - 22 are also plotted in this figure. As can be seen from this figure, the CLASSIF result is correlated well with that obtained from tests.

Thus, it is concluded that CLASSIF can be accurately used to compute the displacement response transfer function for a soil-structure system subjected to an external dynamic forced excitation.

4.17 Validation Test Problem No. 17

Description

The SSI responses of a structure to a vertically propagating SV wave excitation are analyzed using computer program CLASSIF. Two cases of SSI analysis are performed as follows: Case (a) SSI analysis is performed with no transformation on coordinate systems of the foundation and structure; Case (b) SSI analysis is performed with transformations on coordinate systems of the foundation and structure. The foundation and structure models used for both analysis cases are identical to each other, except for the locations and orientations of their coordinate systems. The lumped-mass stick models of the structures and their coordinate systems for Cases (a) and (b) are shown in Figs. 4.17-1 and 4.17-2, respectively. The

foundation models and their coordinate systems for Cases (a) and (b) are shown in Figs. 4.17-3 and 4.17-4, respectively. To evaluate the accuracy of the SSI responses resulting from transforming the coordinate systems of both the foundation and structure to the reference coordinate system, the CLASSIF results obtained from Case (b) are compared with those obtained from Case (a).

Results

The maximum response accelerations computed from CLASSIF for both Cases (a) and (b) are tabulated in Table 4.17-1. As can be seen from this table, the SSI analysis results obtained from Case (b) are identical to those obtained from Case (a). Thus, it can be concluded that CLASSIF can be accurately used to compute the SSI responses resulting from transforming the coordinate systems of both the foundation and structure.

4.18 Validation Test Problem No. 18

Description

The SSI responses of a containment structure to combined input motions comprised of SV+P waves and R (Rayleigh) wave are analyzed using computer program CLASSIF. The SSI model of the containment structure used in this problem is the same as that used in Validation Test Problem No. 4. The free-field input motion, scaled to 0.03g, is specified at the ground surface for both SV+P waves. To evaluate the accuracy of the SSI responses to combined input motions, the SSI responses due to SV+P+R waves are compared with the combined SSI responses due to separate inputs of SV+P waves and R wave in Validation Test Problem No. 4.

Results

The 2% damping response spectra of the SSI response motions due to SV+P+R waves are compared with those of the combined SSI response motions due to separate inputs of SV+P waves and R wave in Fig. 4.18-1 for the top of foundation, Fig. 4.18-2 for the top of containment shell, and in Fig. 4.18-3 for the top of internal structure. As can be seen from the results of comparisons shown in these figures, they are essentially identical to each other. Thus, it is concluded that CLASSIF can be accurately used for computing the SSI responses to combined input motions comprised of multiple plane waves.

Table 4.13-1

Comparison of Maximum Response Relative Displacement

Computer Program	Max Relative Displacement ($X10^{-3}$ ft)	Time (sec)
CLASSIF	0.467	2.465
DATAN	0.461	2.465

Table 4.17-1

Comparison of Maximum Horizontal Response Accelerations

Node No.	Max. Acceleration (g) Case 17(a)	Case 17(b)
1	.2577	.2577
2	.1527	.1527
3	.0986	.0986

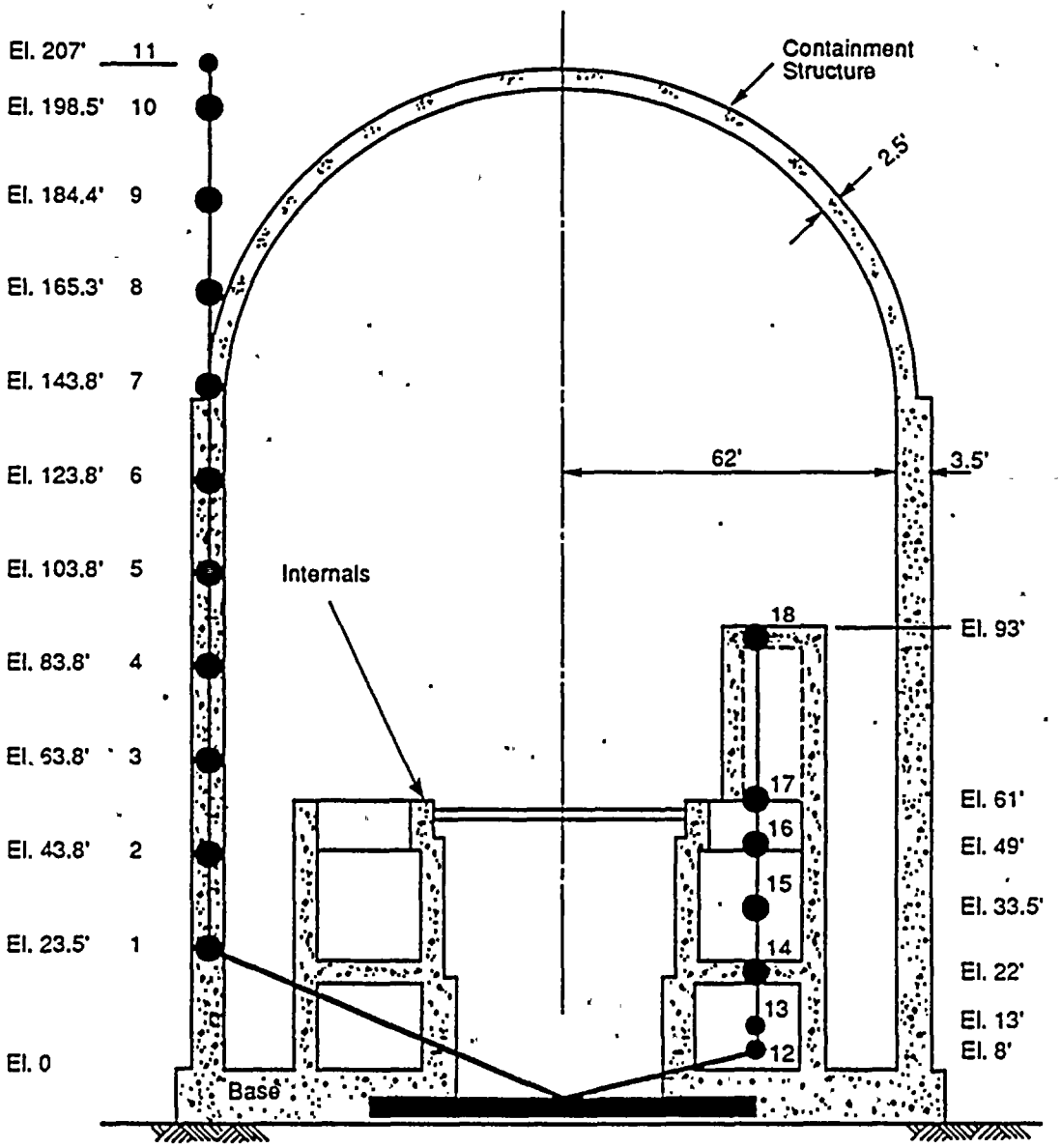

Figure 4.1-1. Lumped-Mass Stick Models of the Containment and Internal Structures

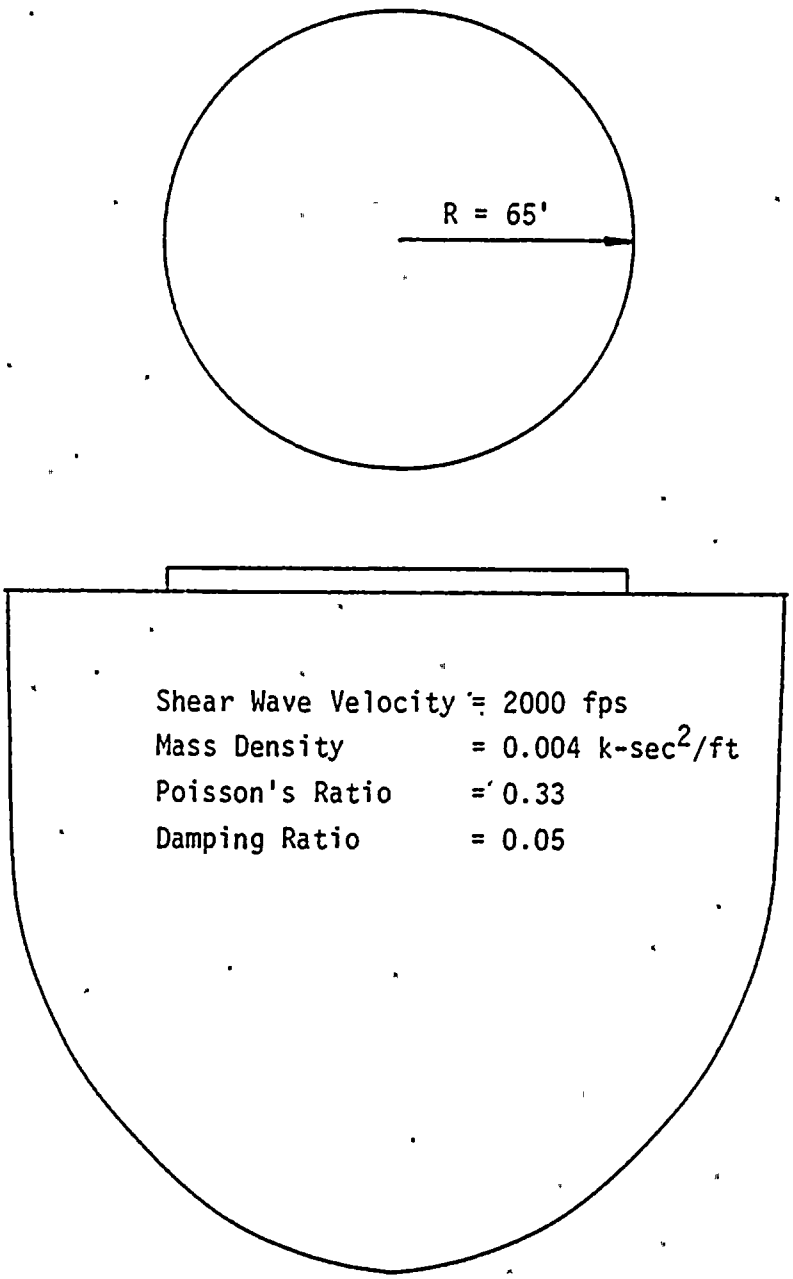

Figure 4.1-2. Circular Foundation on Viscoelastic Halfspace

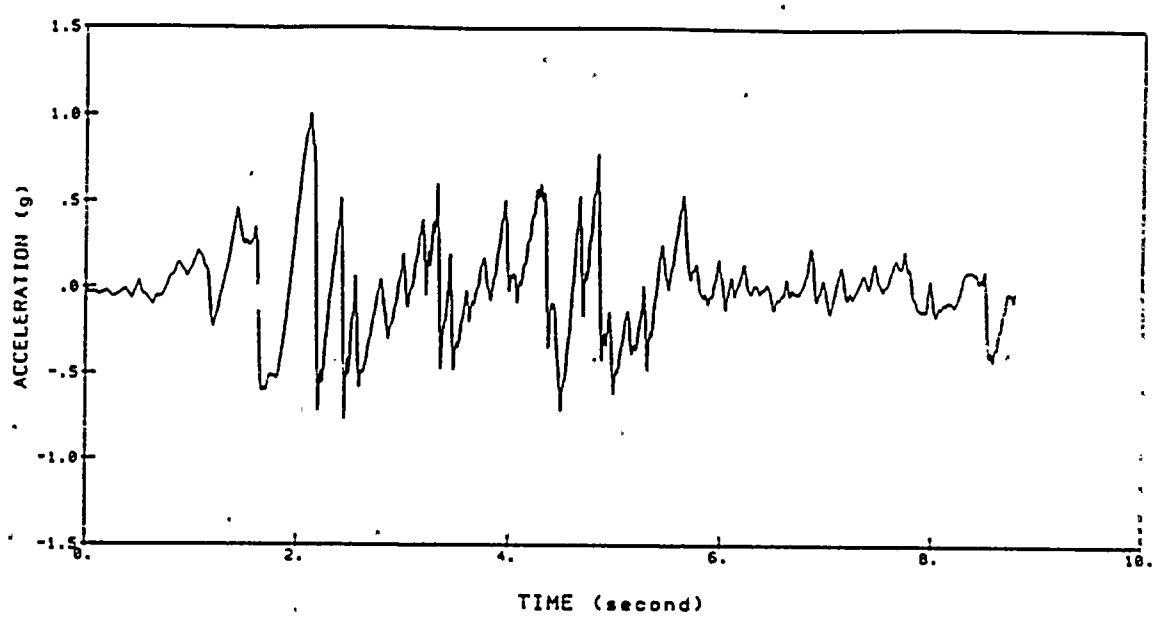

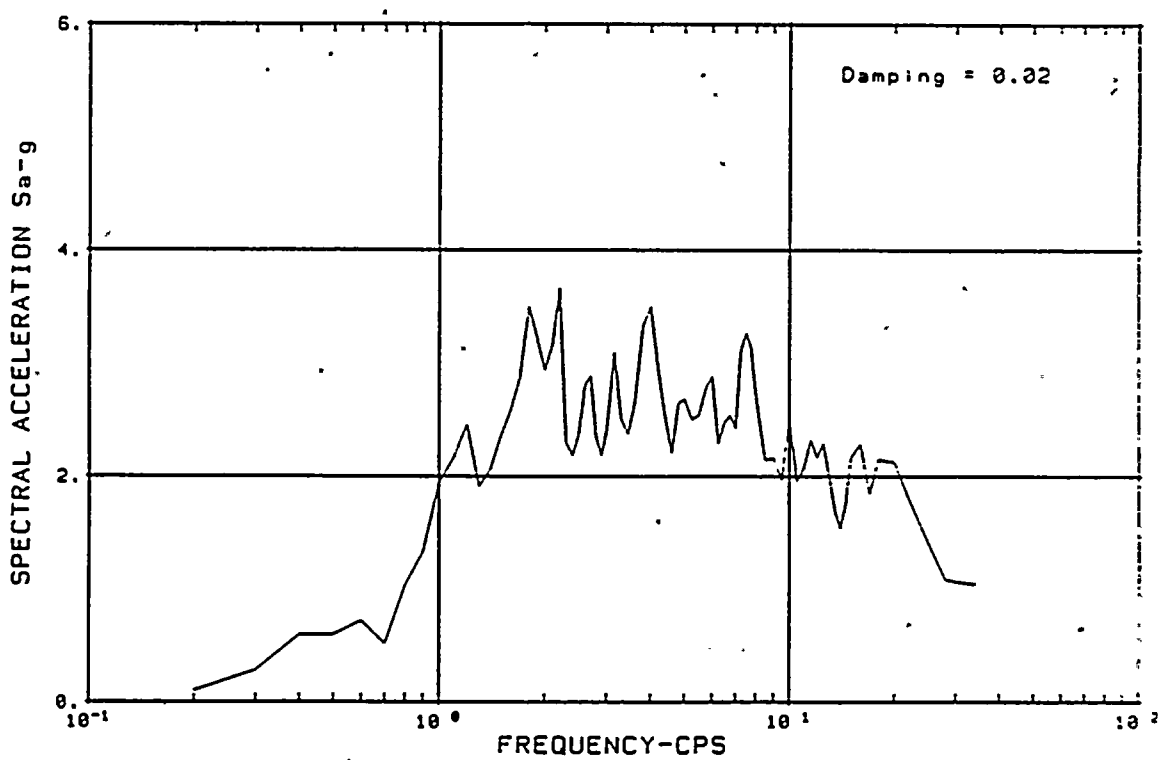

Figure 4.1-3. Acceleration Time History and Response Spectrum of 1940 El Centro Time History Scaled to 1.0 g

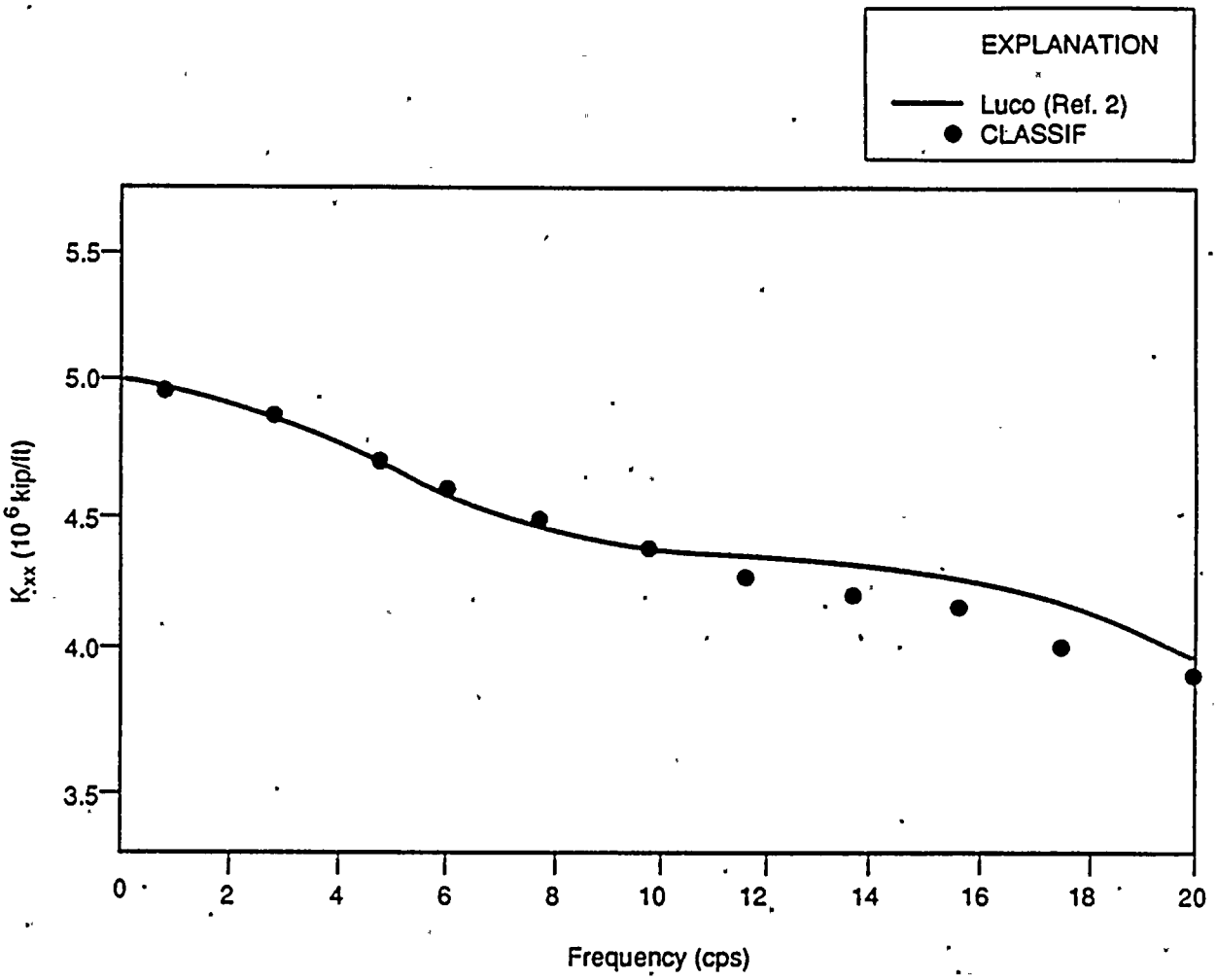

Figure 4.1-4. Horizontal Stiffness Impedance for a Circular Foundation

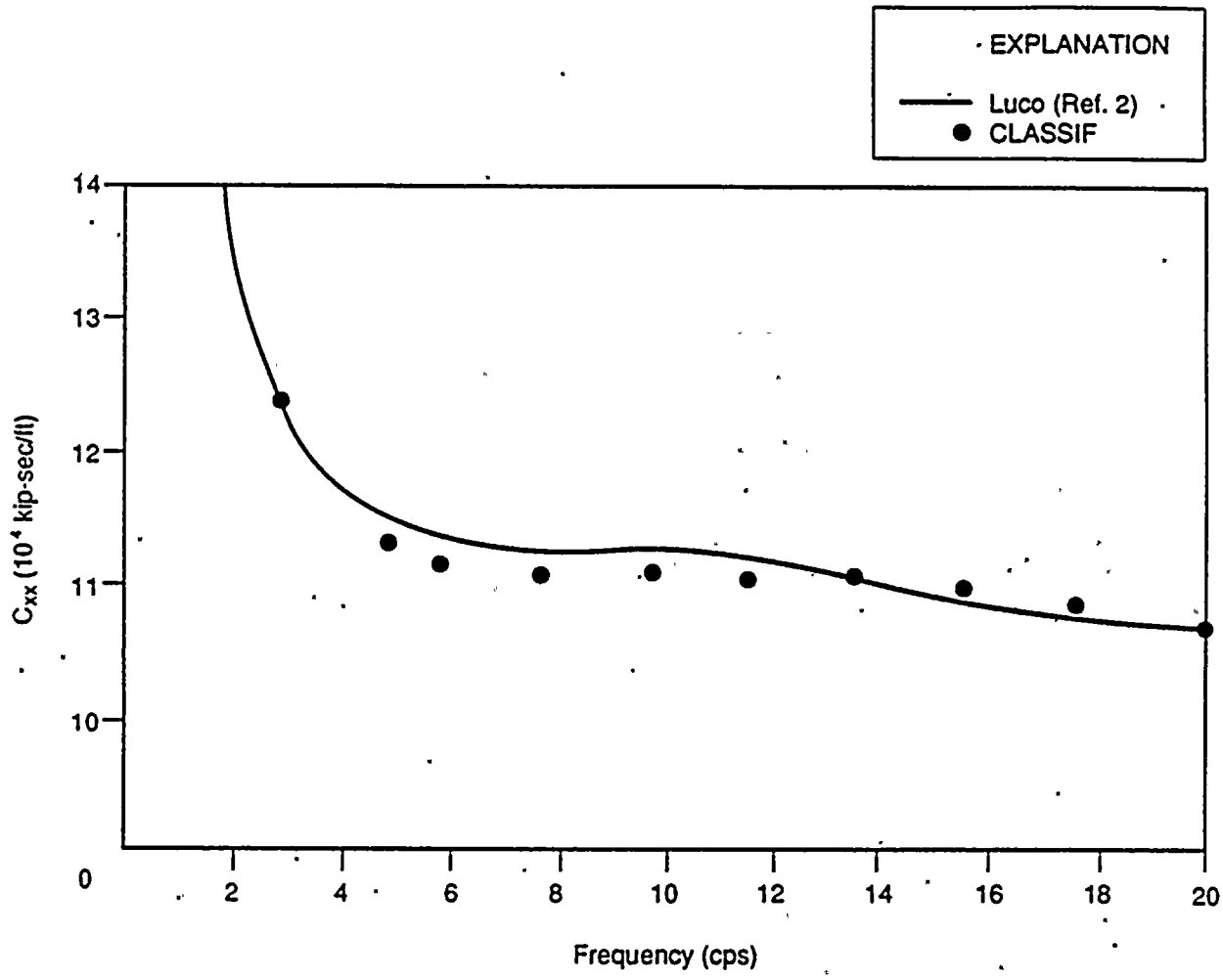

Figure 4.1-5. Horizontal Damping Impedance for a Circular Foundation

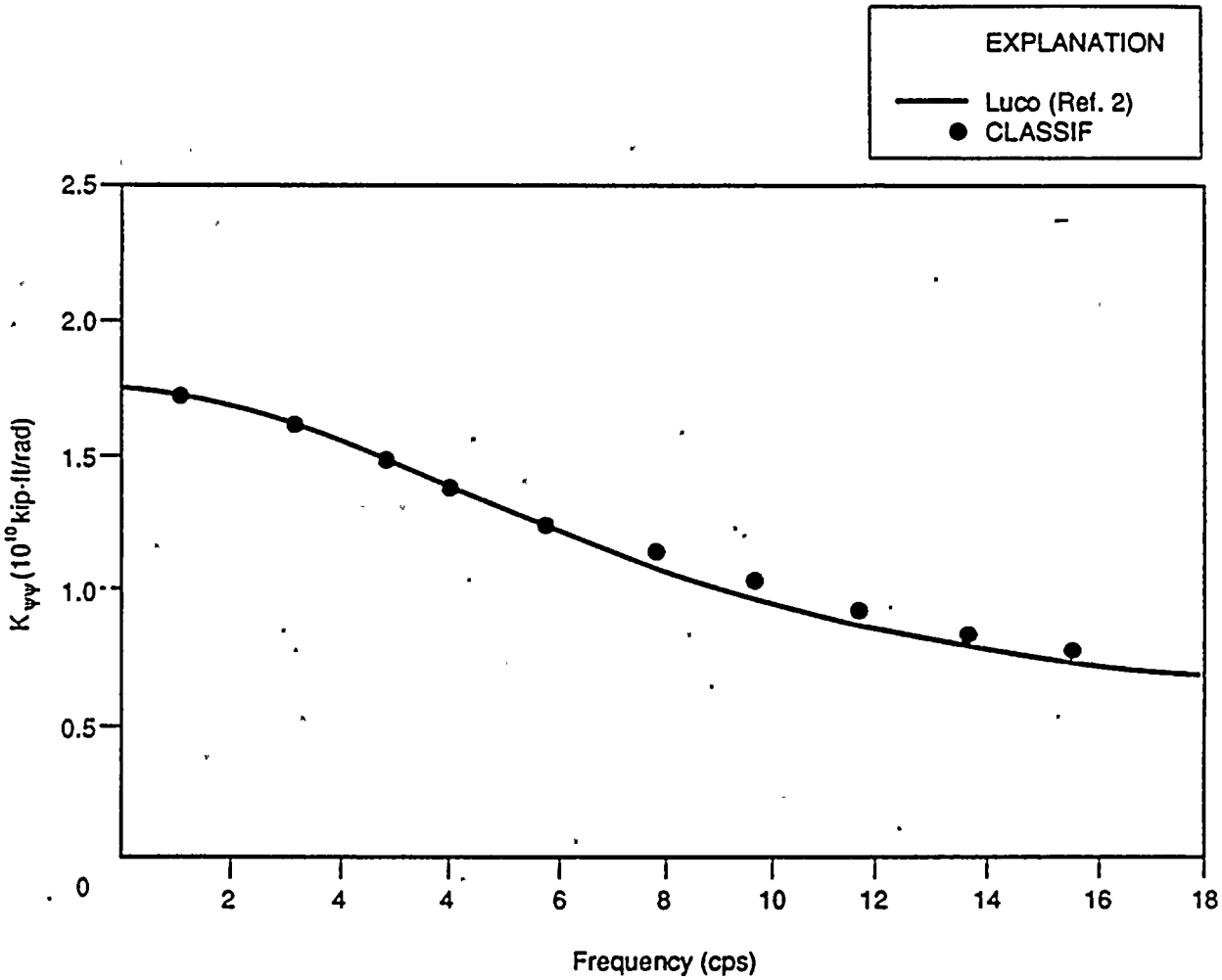

Figure 4.1-6. Rocking Stiffness Impedance for a Circular Foundation

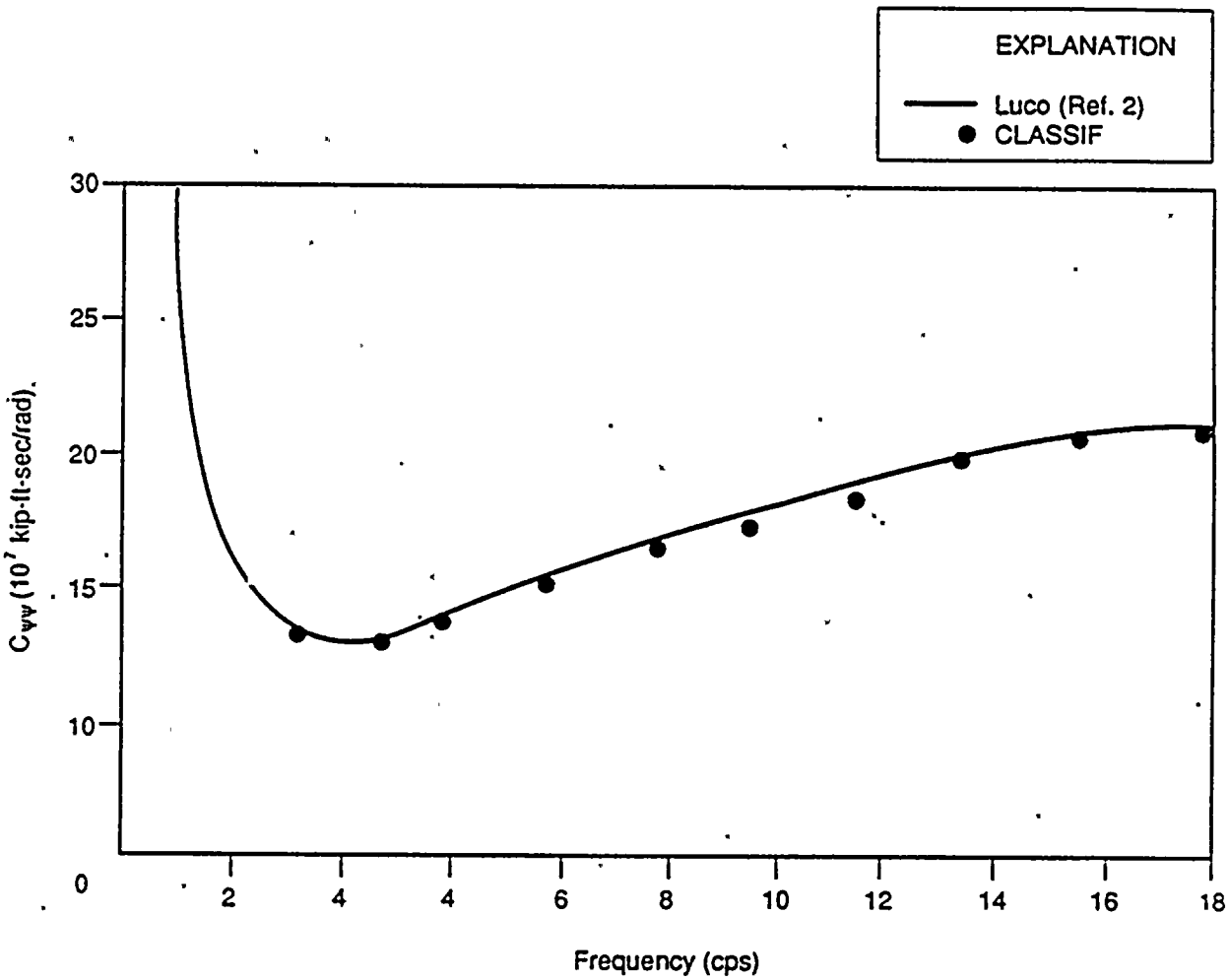

Figure 4.1-7. Rocking Damping Impedance for a Circular Foundation

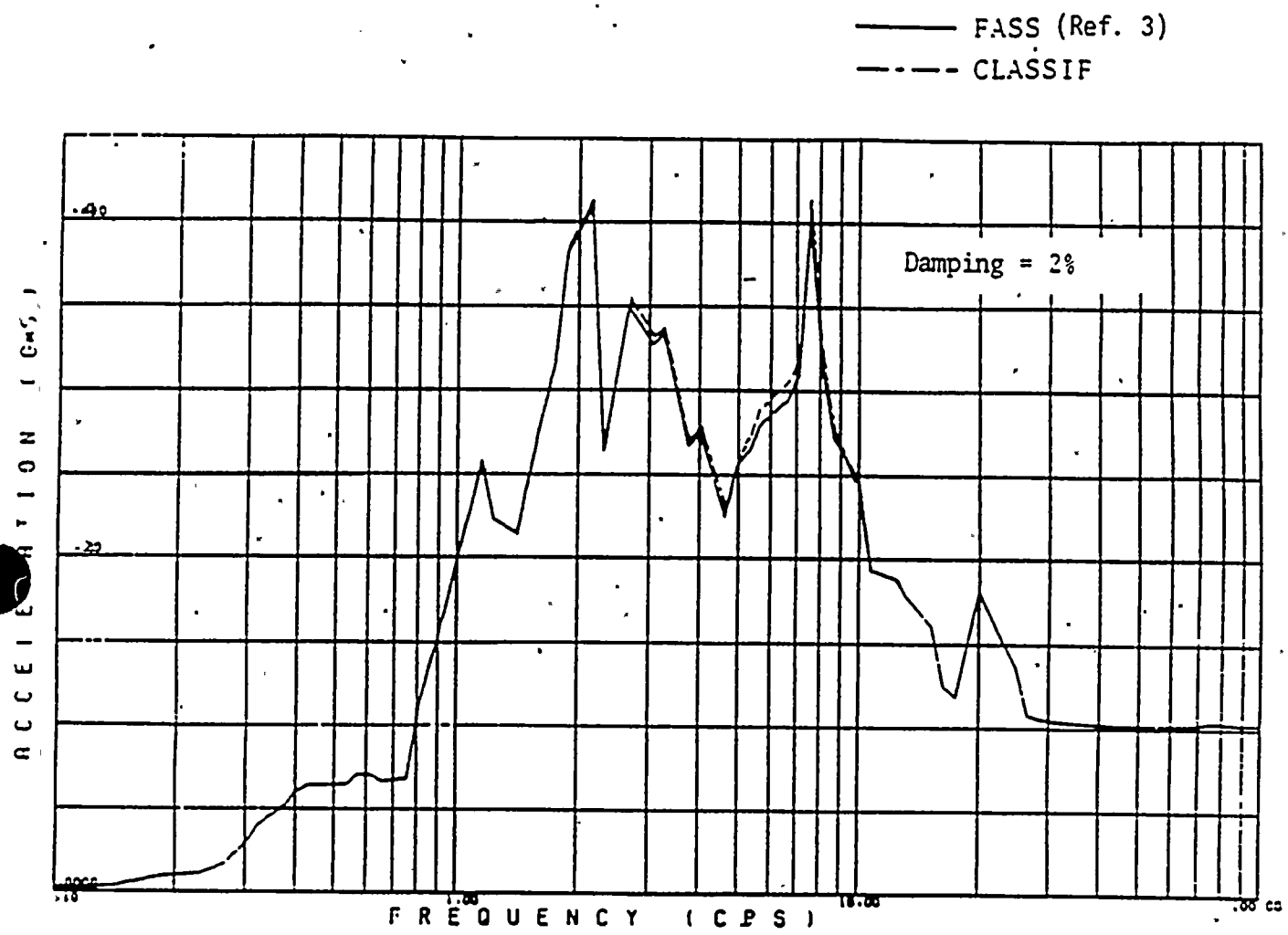

Figure 4.1-8. Absolute Acceleration Response Spectrum at the Top of the Foundation

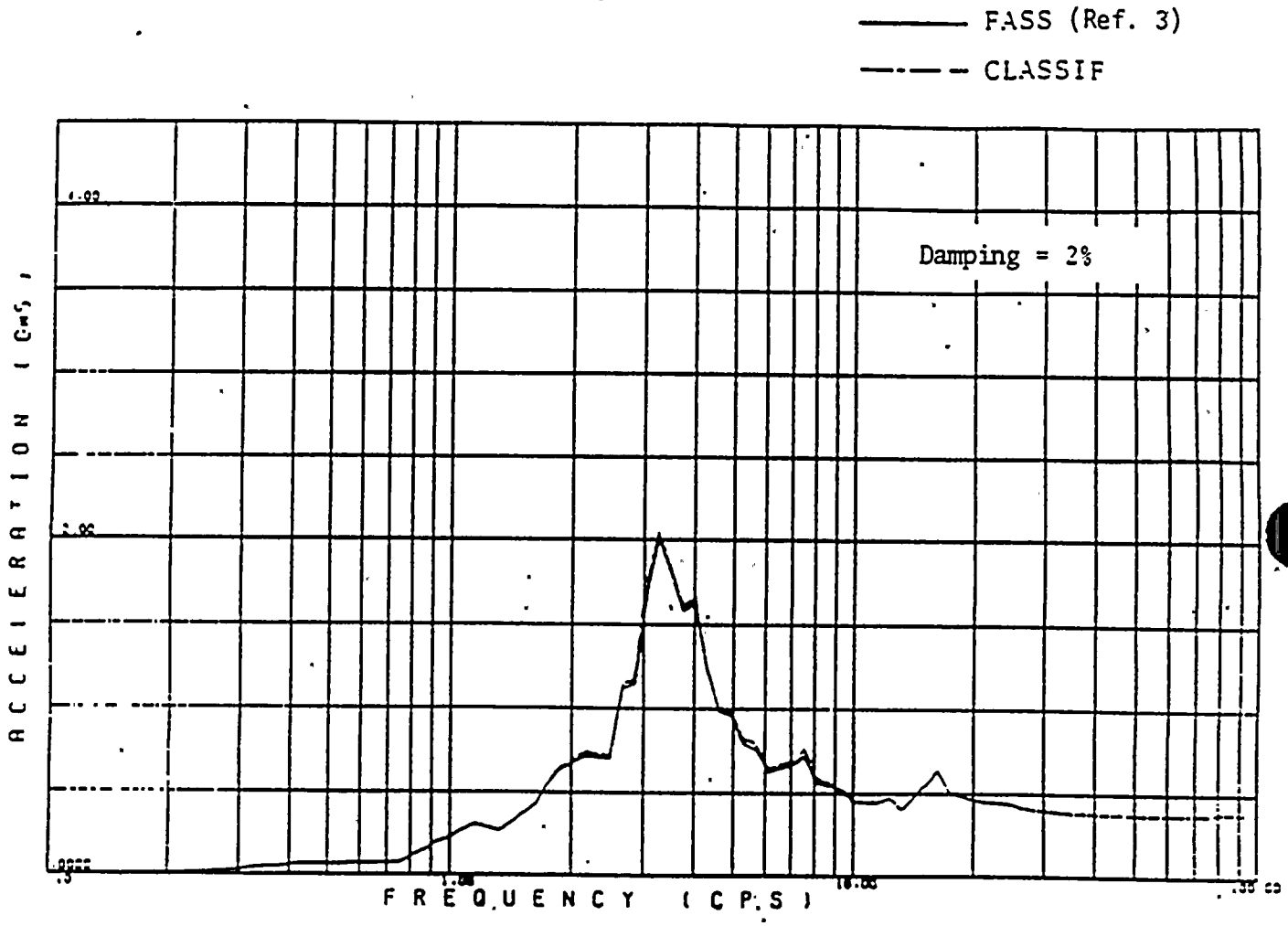

Figure 4.1-9. Absolute Acceleration Response Spectrum at the Top of Containment Building

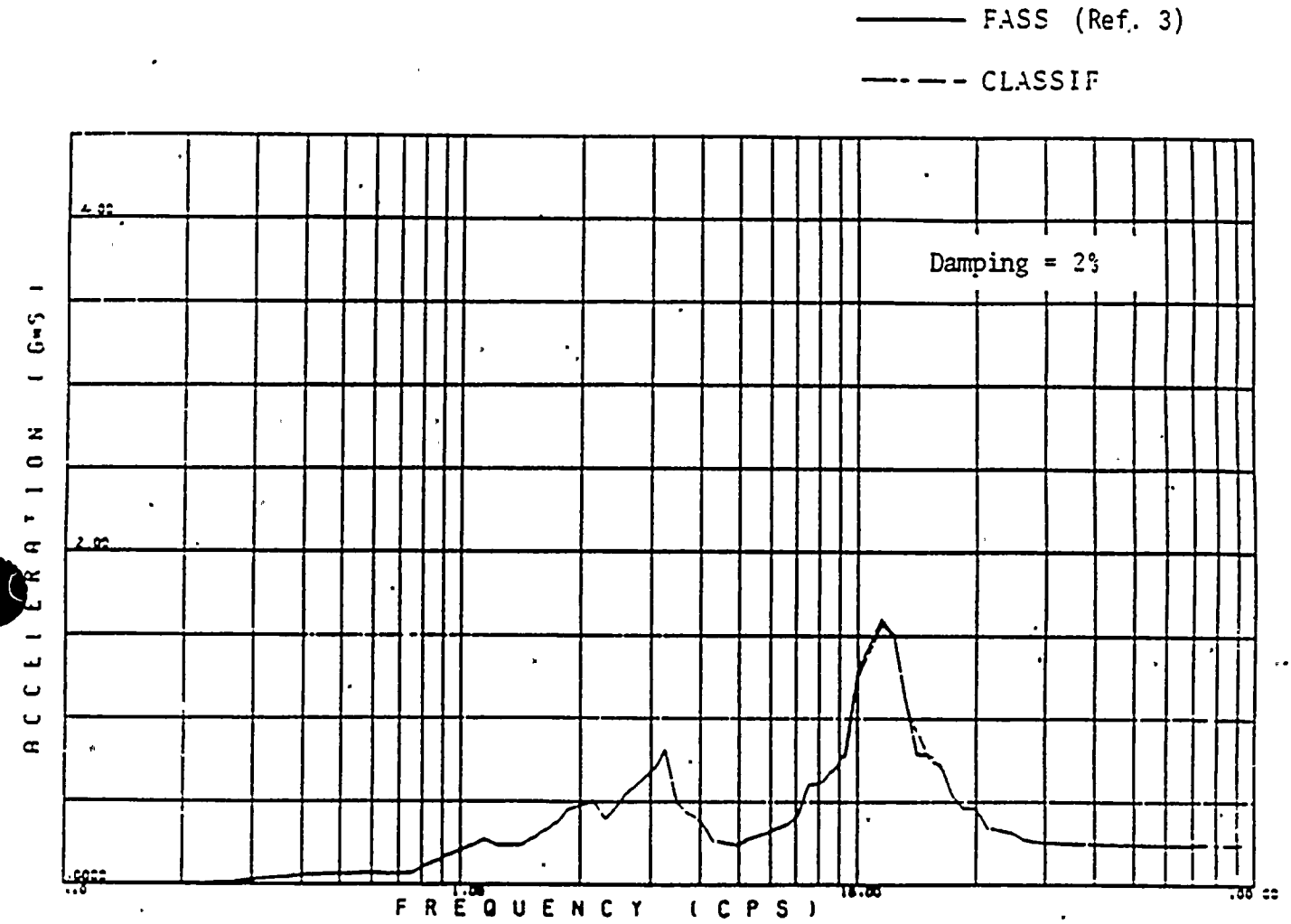

Figure 4.1-10. Absolute Acceleration Response Spectrum at the Top of Internal Structure

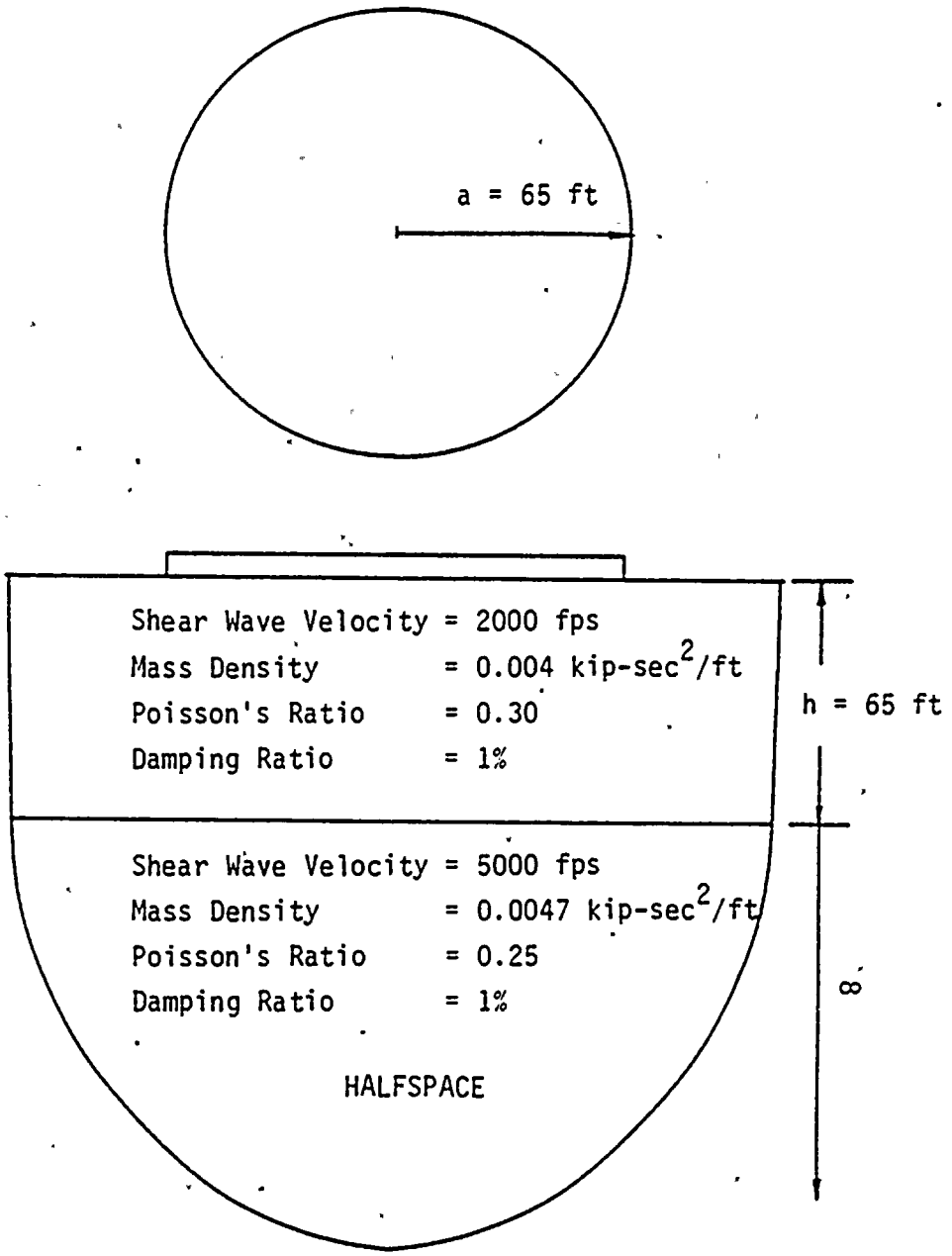

Figure 4.2-1. Circular Foundation on Two Soil Layered System

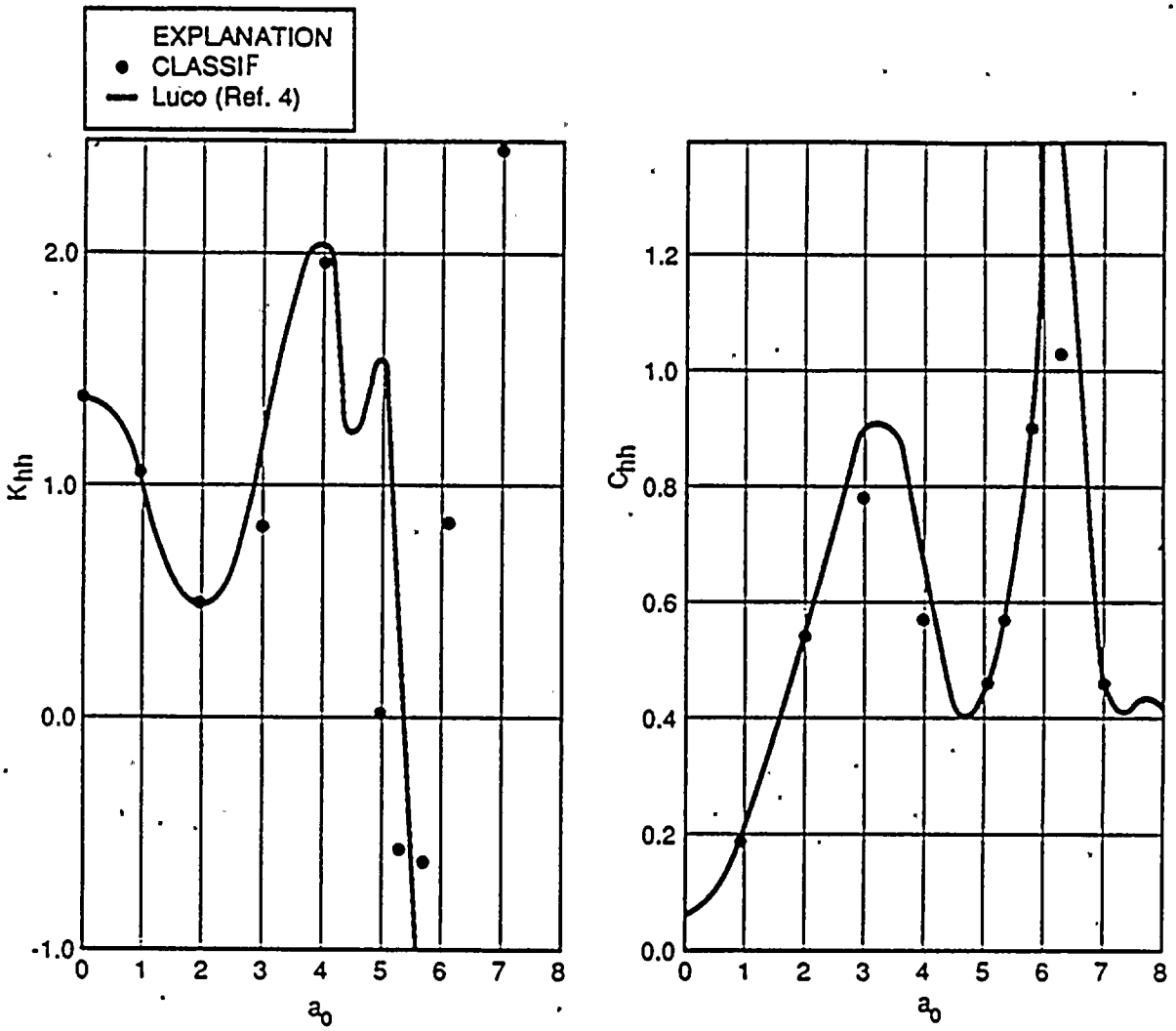

Figure 4.2-2. Horizontal Stiffness and Damping Coefficients

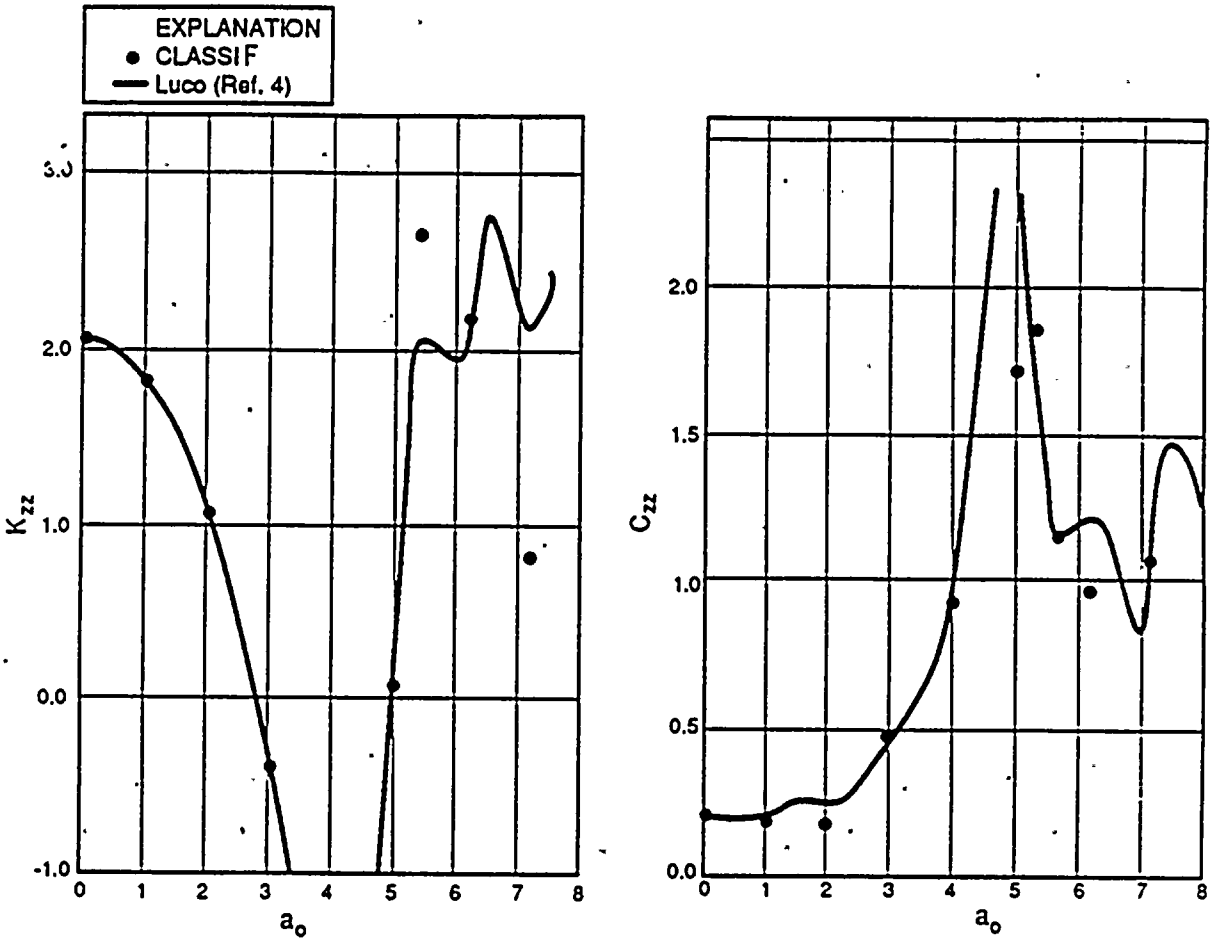

Figure 4.2-3. Vertical Stiffness and Damping Coefficients

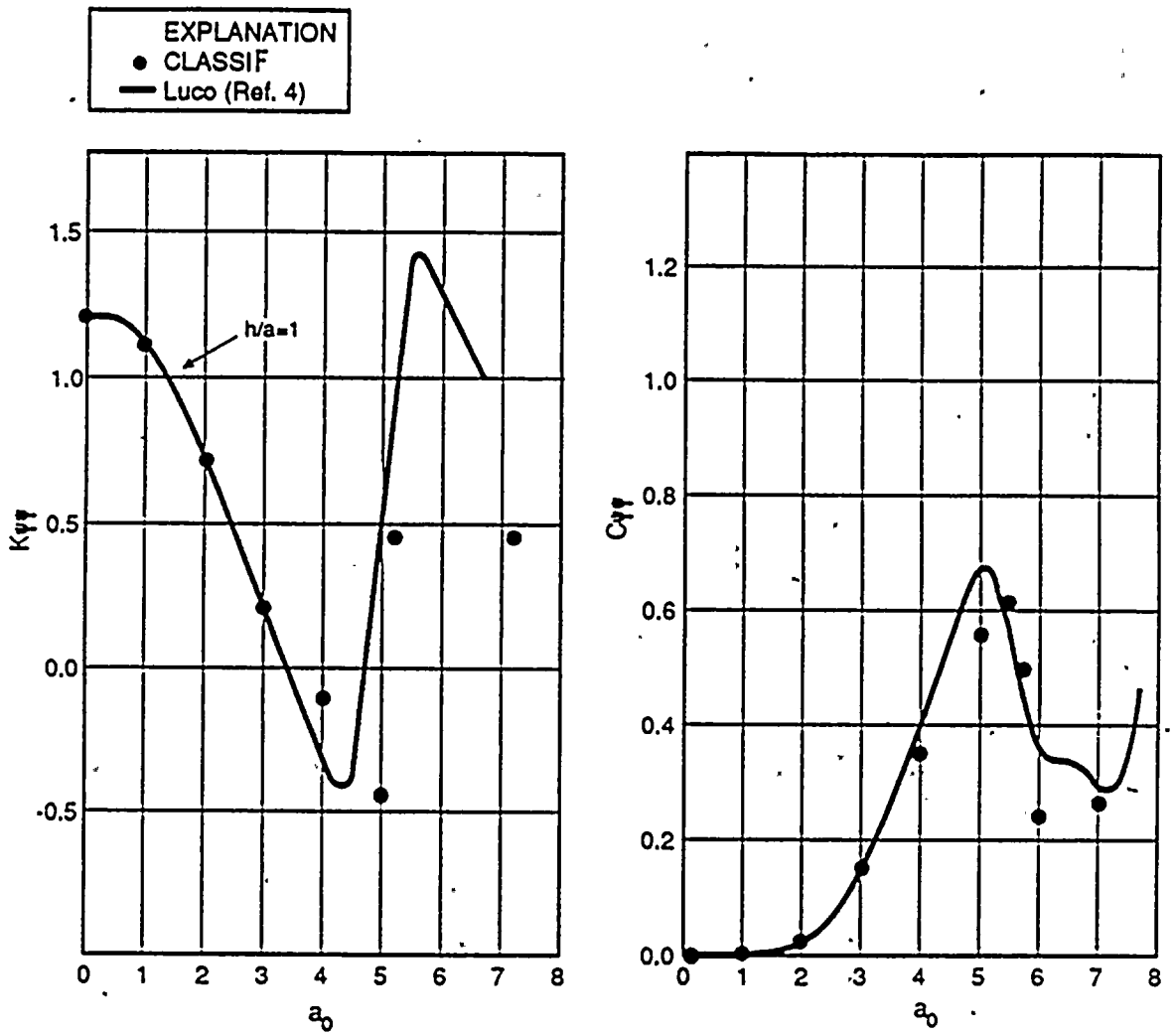

Figure 4.2-4. Rocking Stiffness and Damping Coefficients

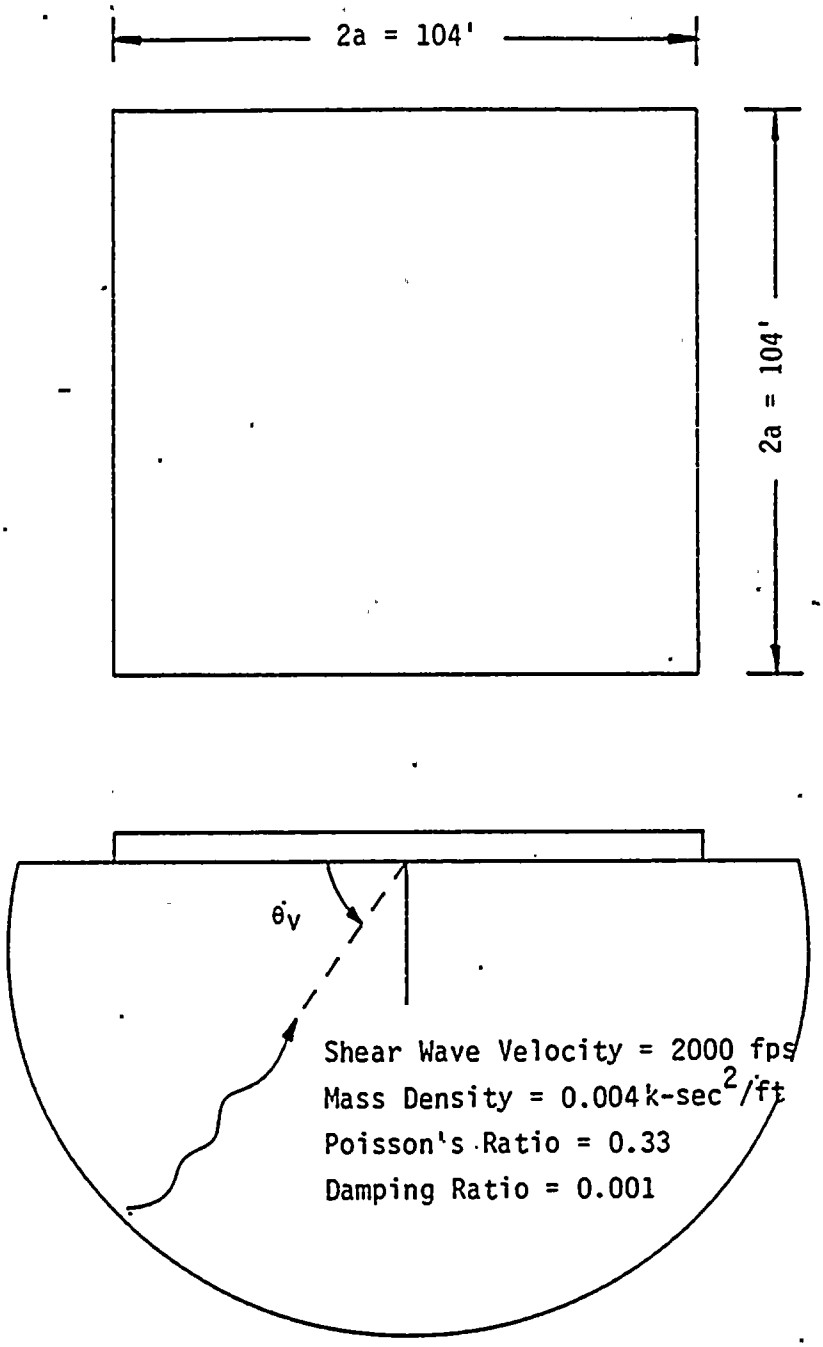

Figure 4.3-1. Square Foundation on Elastic Halfspace

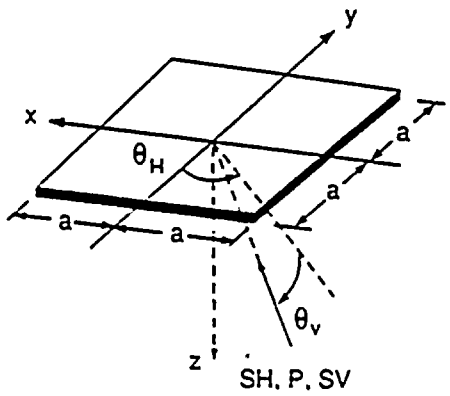

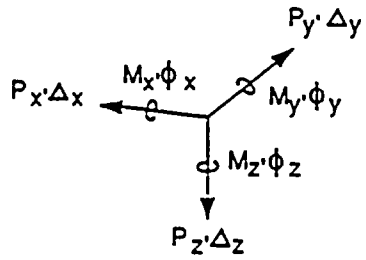

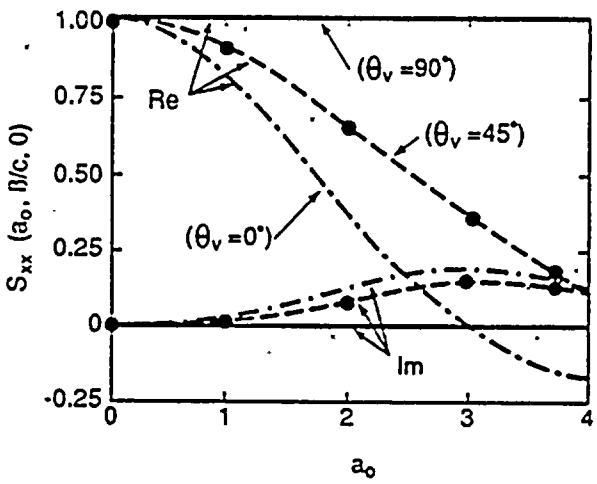

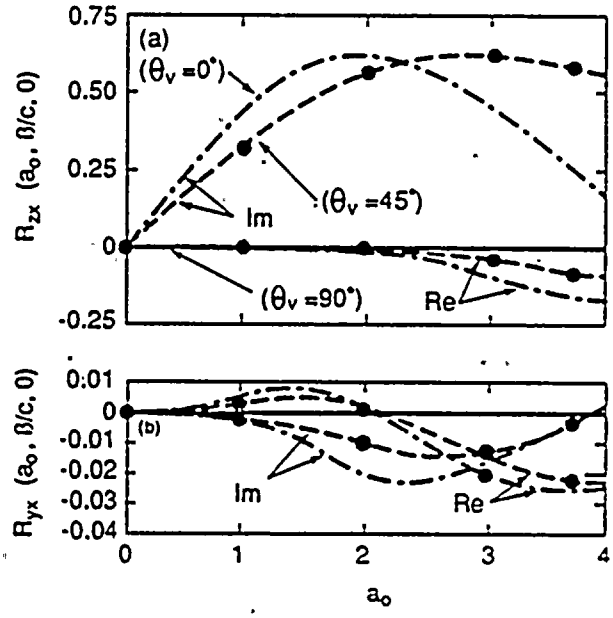

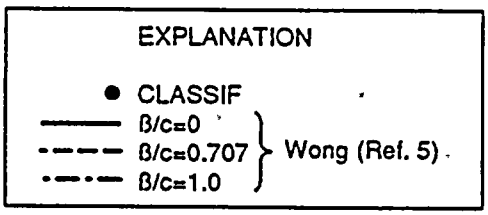

Figure 4.3-2. Scattering Elements for Inclined SH-Wave

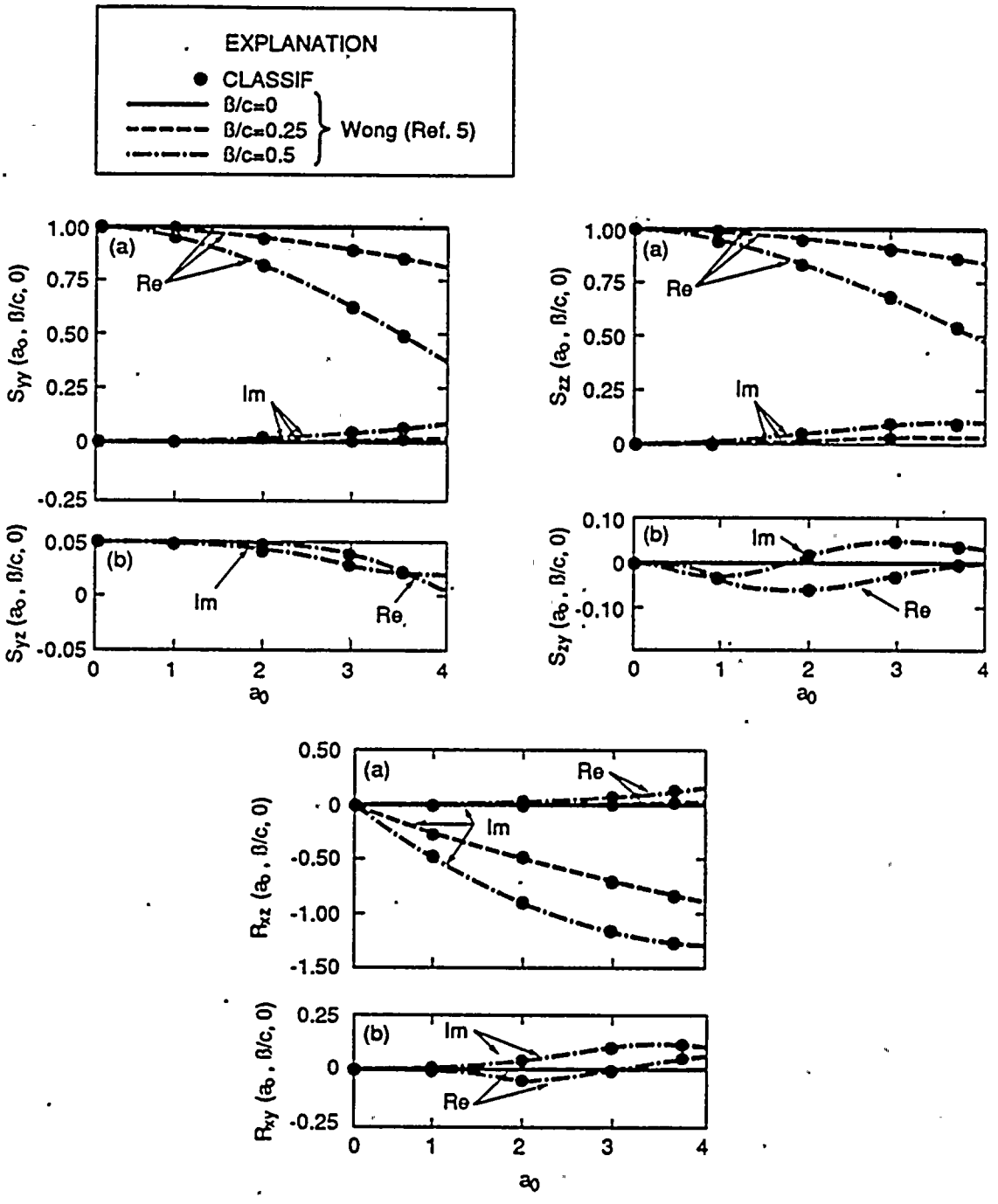

Figure 4.3-3. Scattering Elements for Inclined SV- and P-Waves

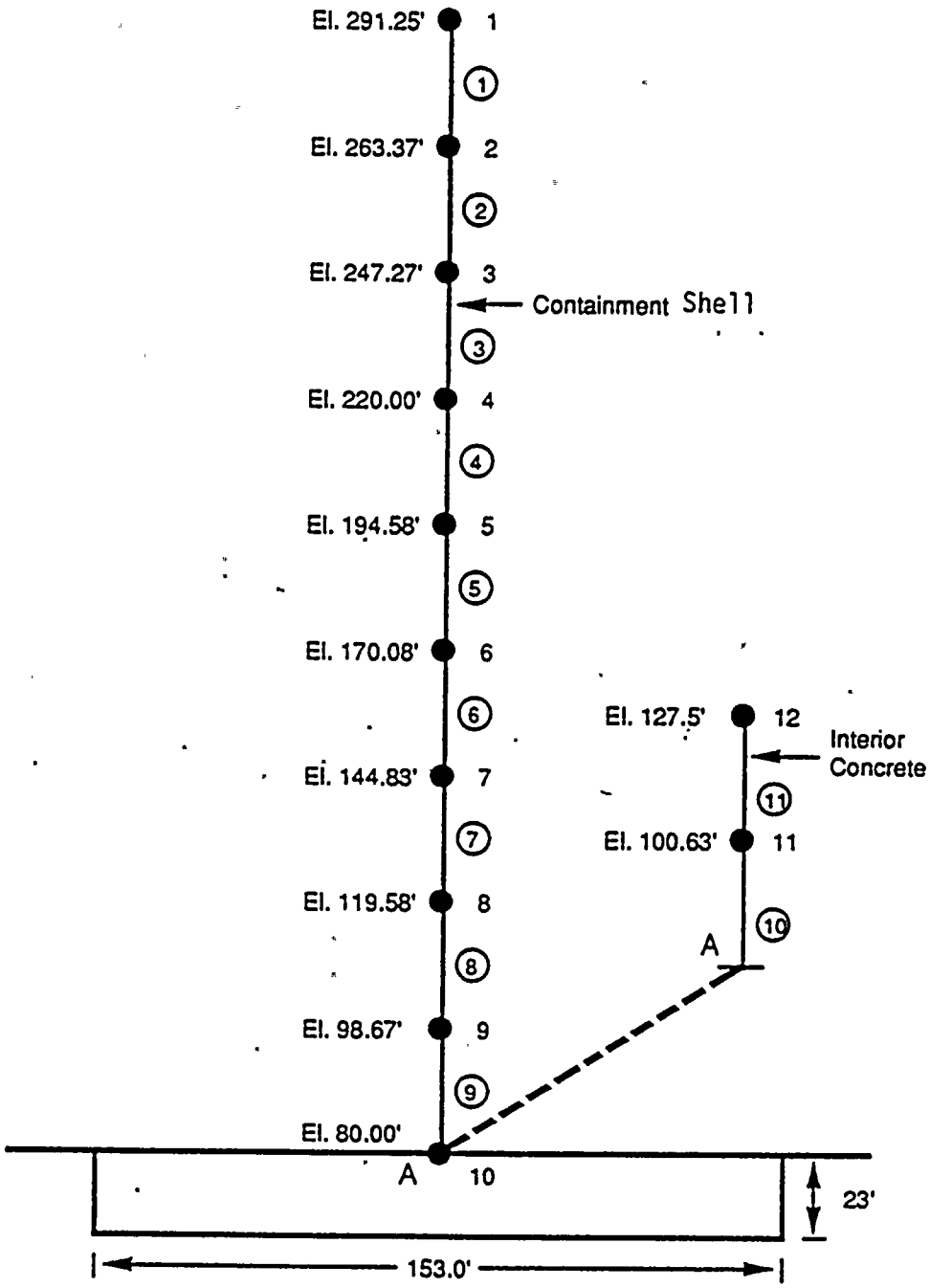

Figure 4.4-1. Lumped-Mass Stick Model of the Containment Structure

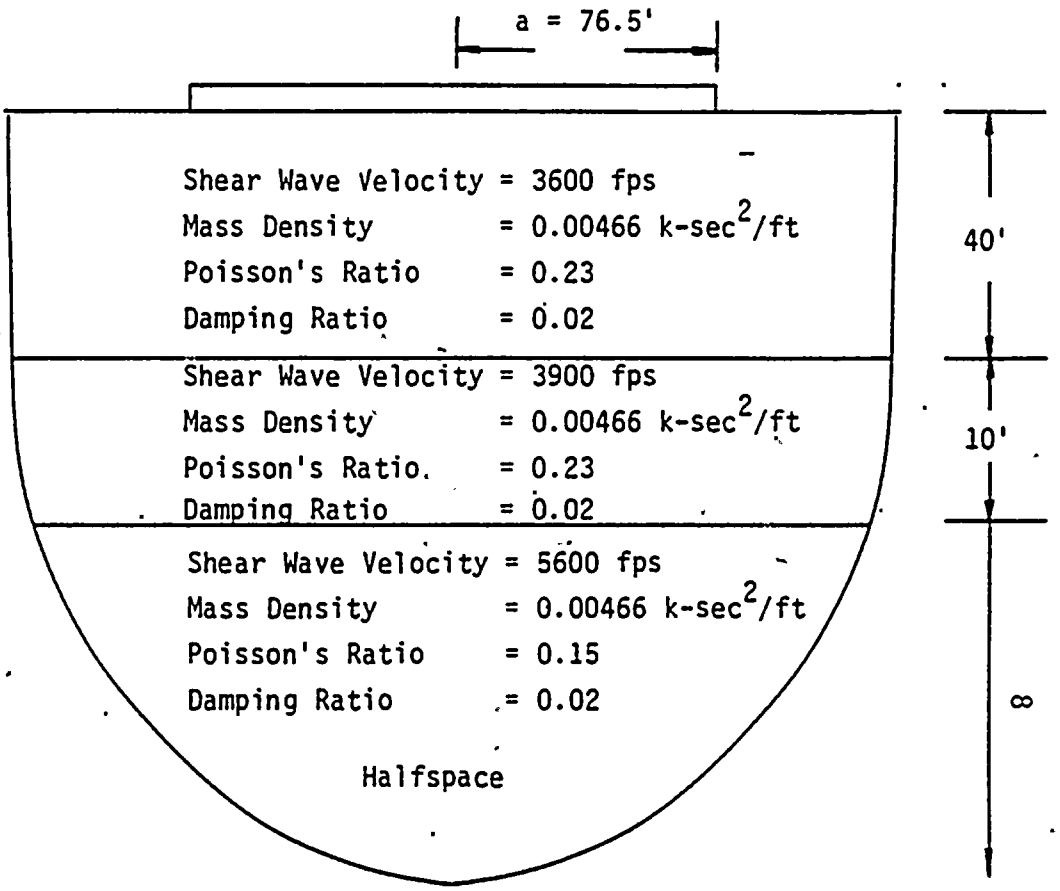

Figure 4.4-2. Circular Foundation on Viscoelastic Layered Soil

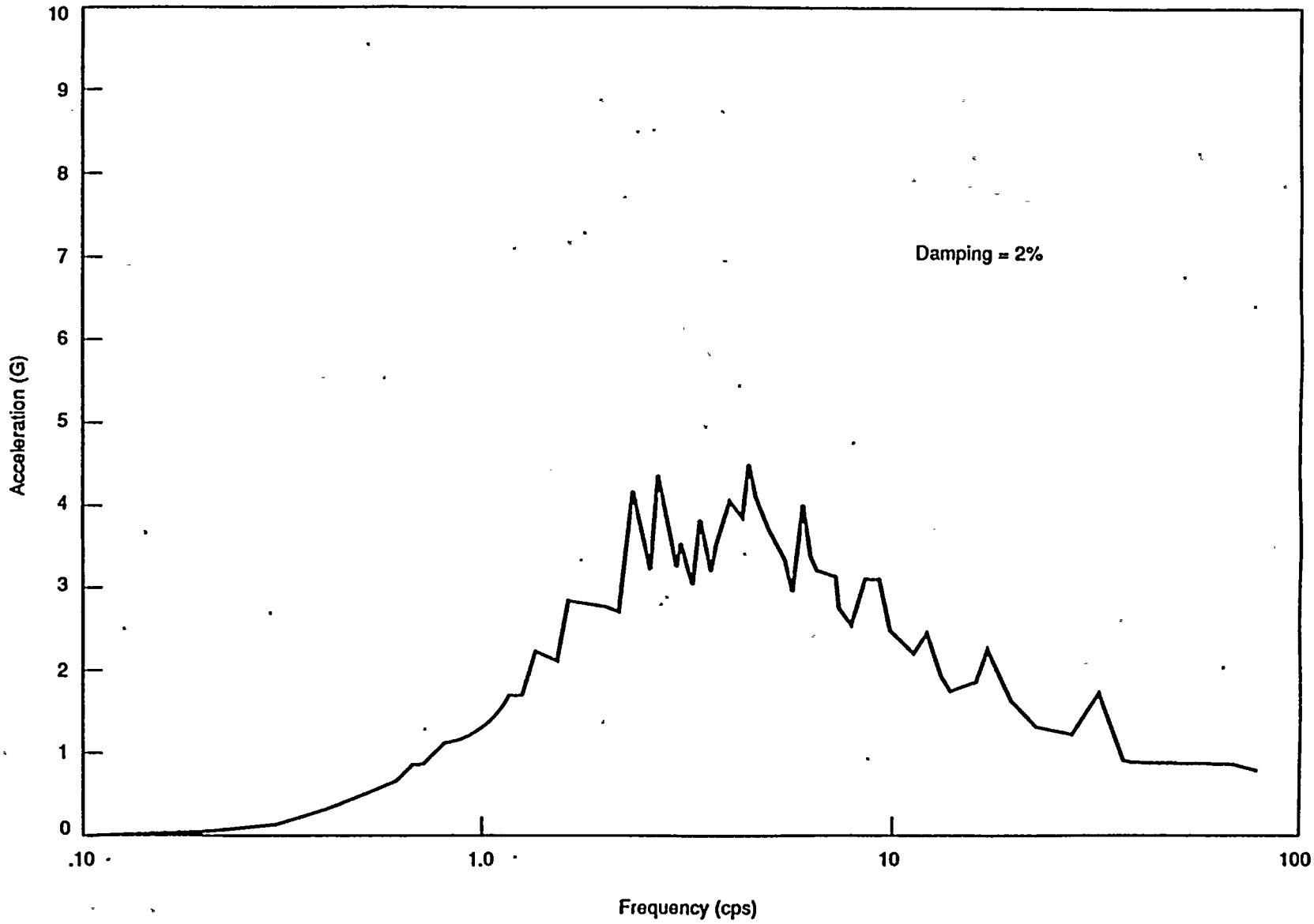

Figure 4.4-3. Acceleration Response Spectrum of Input Motion

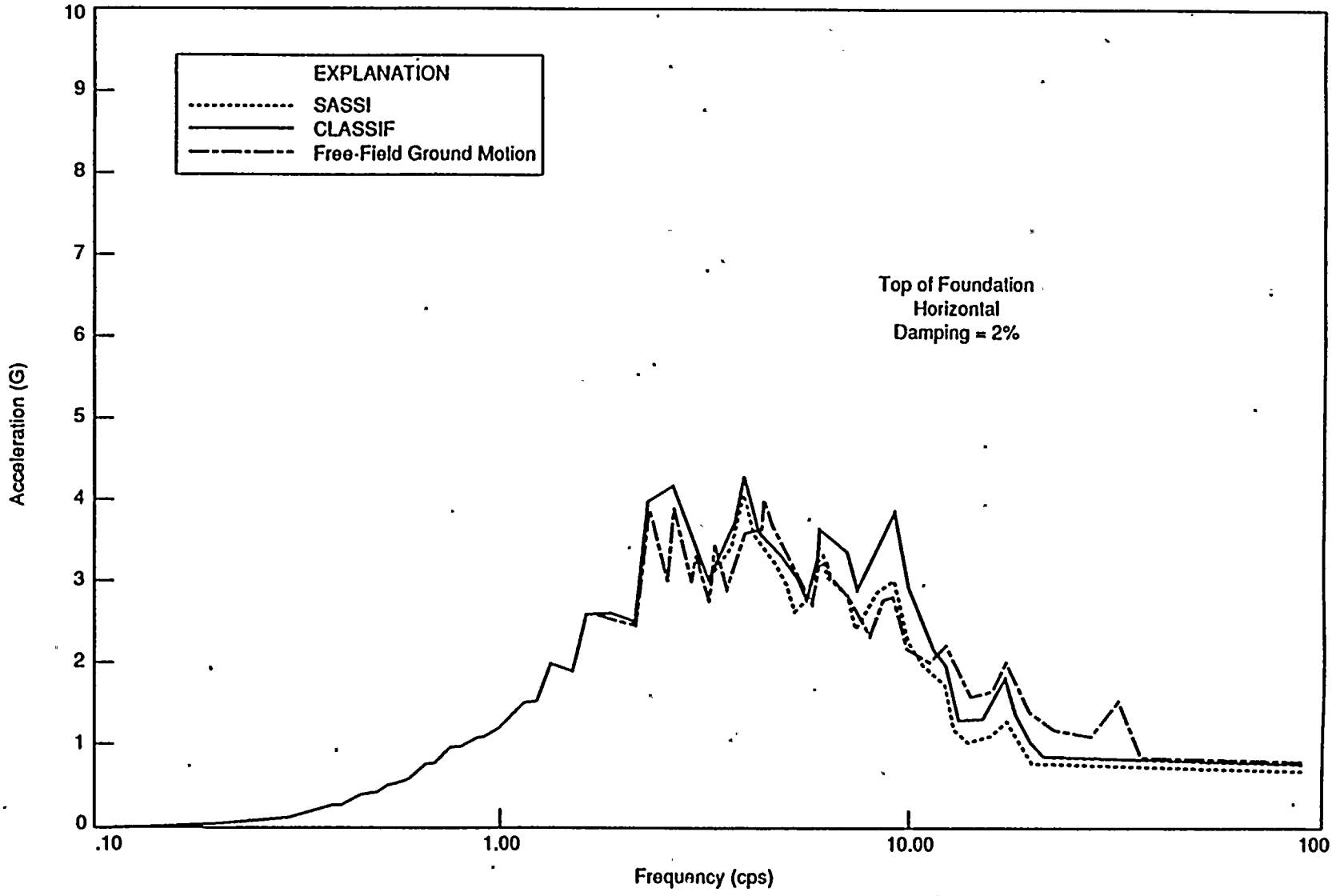

Figure 4.4-4. Horizontal Acceleration Response Spectrum at the Top of Foundation (SV+P Wave Case)

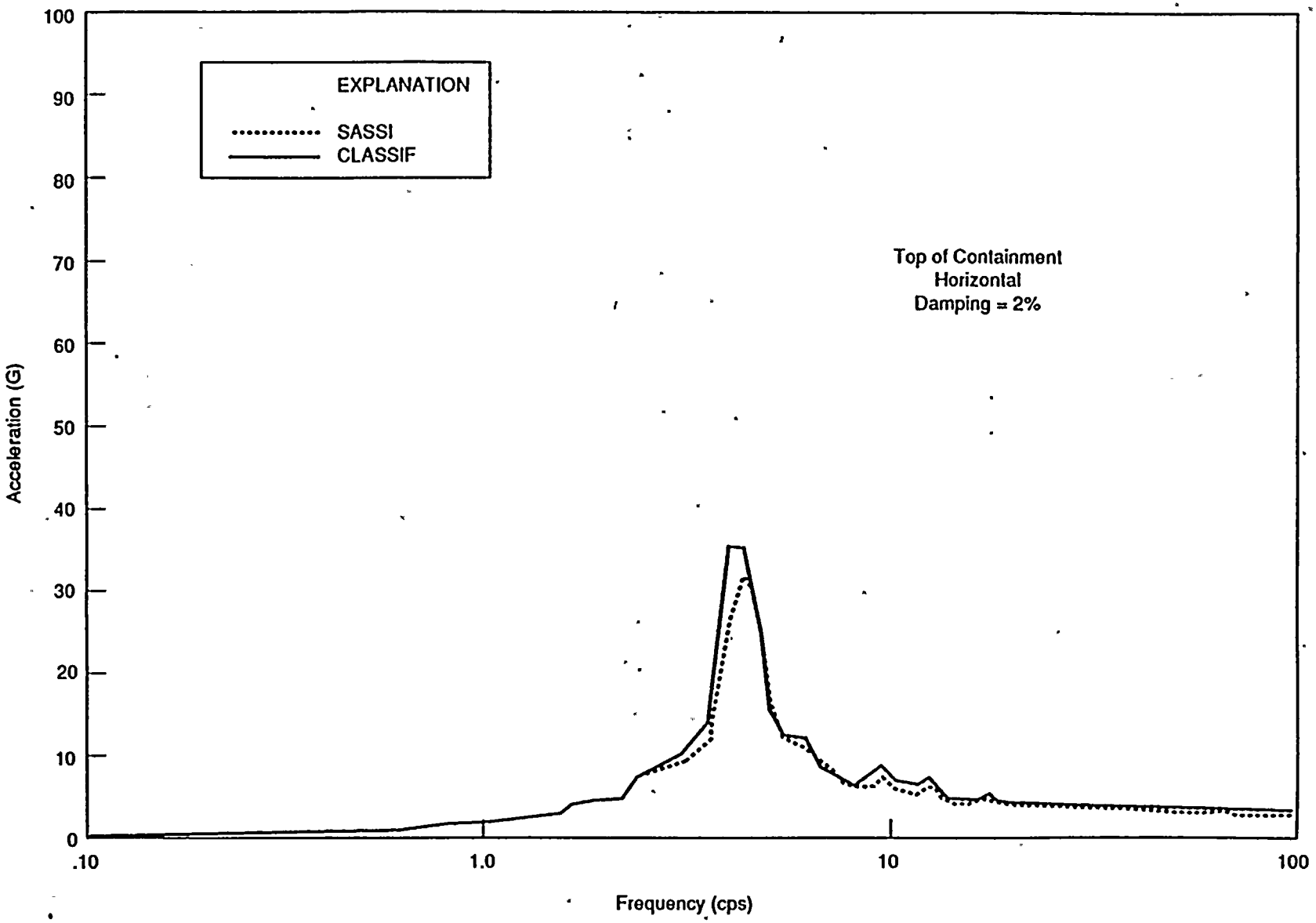

Figure 4.4-5. Horizontal Acceleration Response Spectrum at the Top of Containment (SV+P Wave Case)

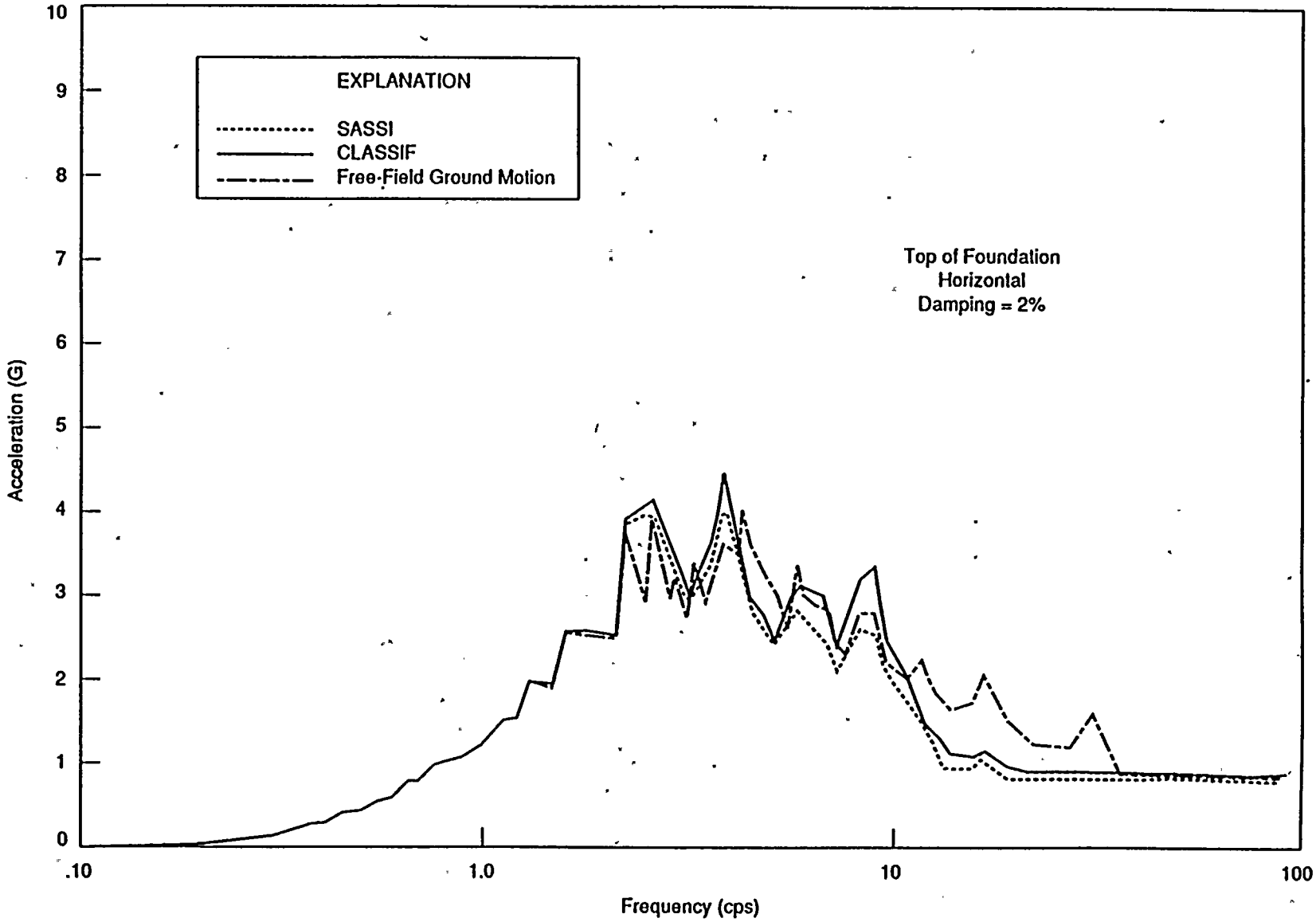

Figure 4.4-6. Acceleration Response Spectrum at the Top of the Foundation (Rayleigh Wave Case)

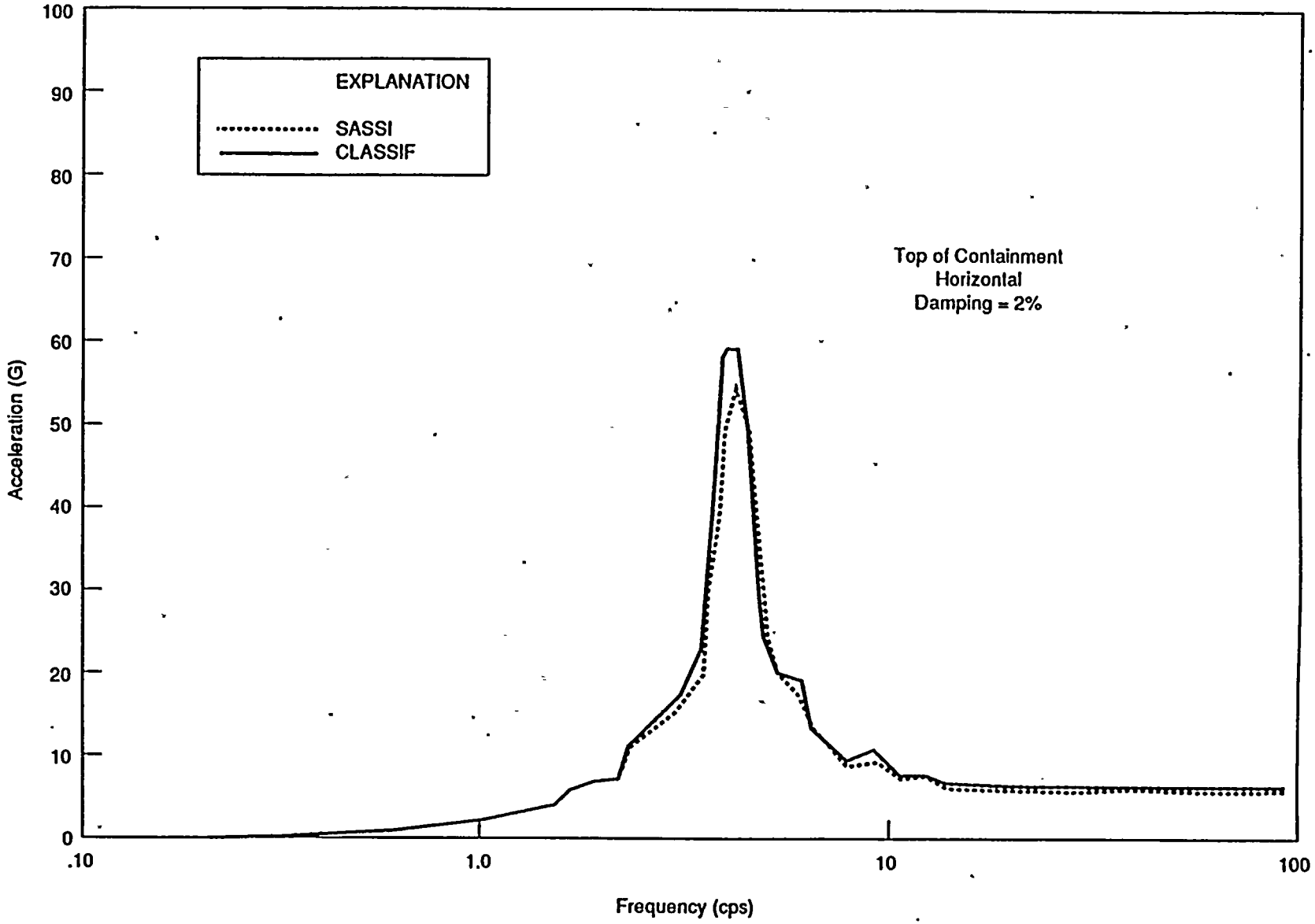

Figure 4.4-7. Horizontal Acceleration Response Spectrum at the Top of Containment (Rayleigh Wave Case)

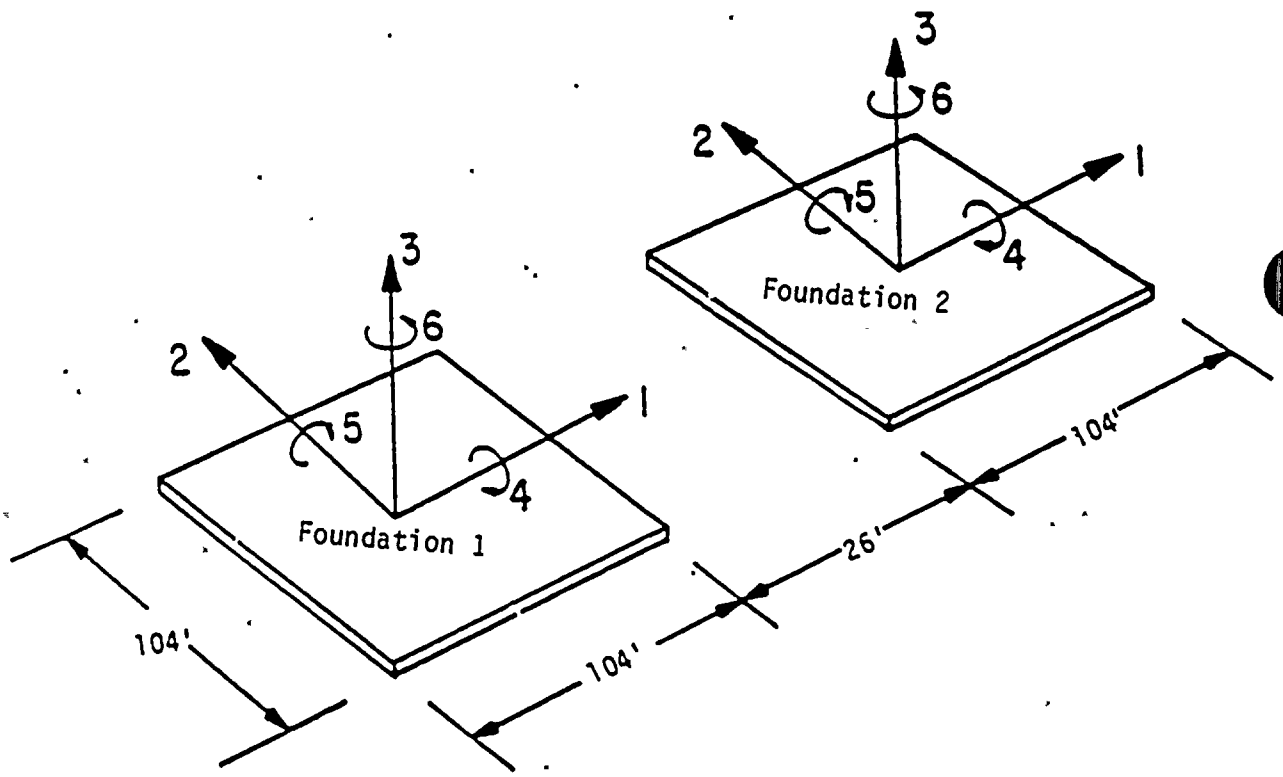

Figure 4.5-1. Coordinate Systems for Two-Foundation Model

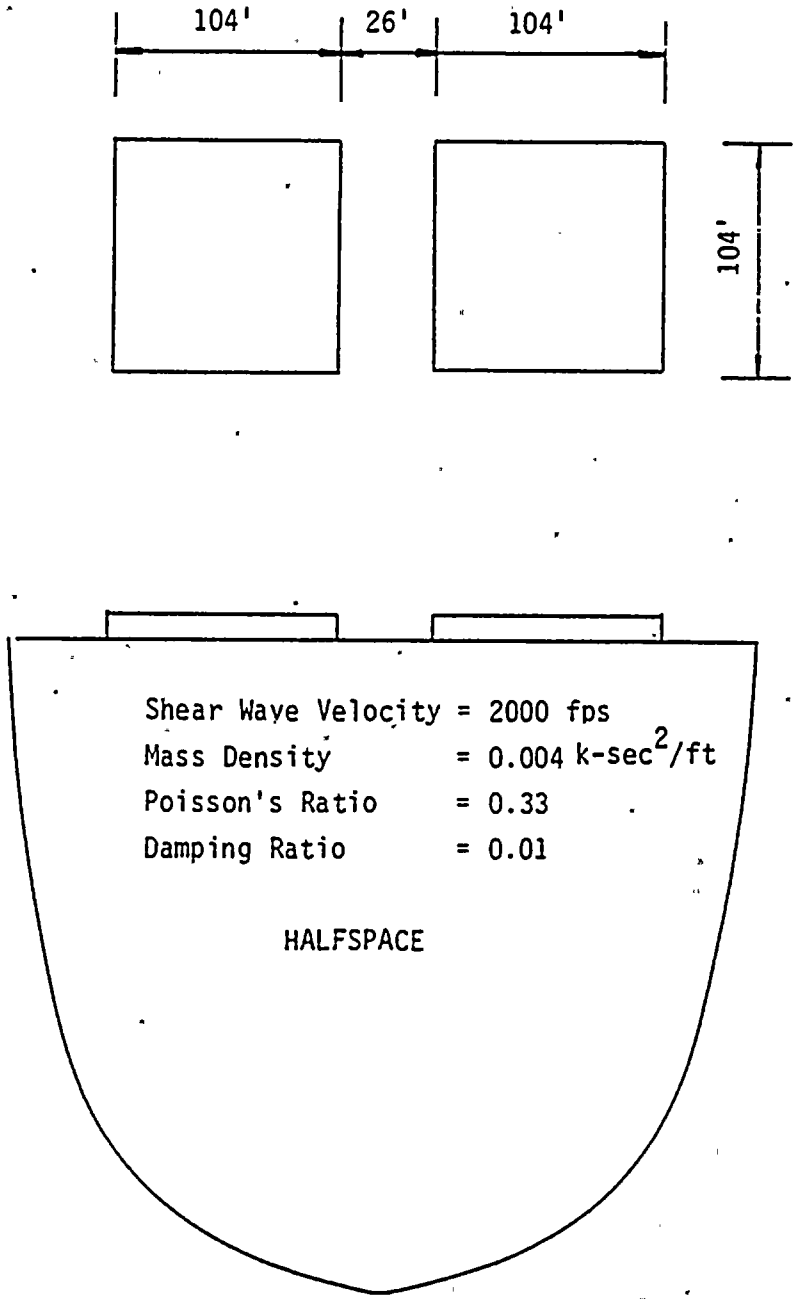

Figure 4.5-2. Two Adjacent Square Foundations on Halfspace

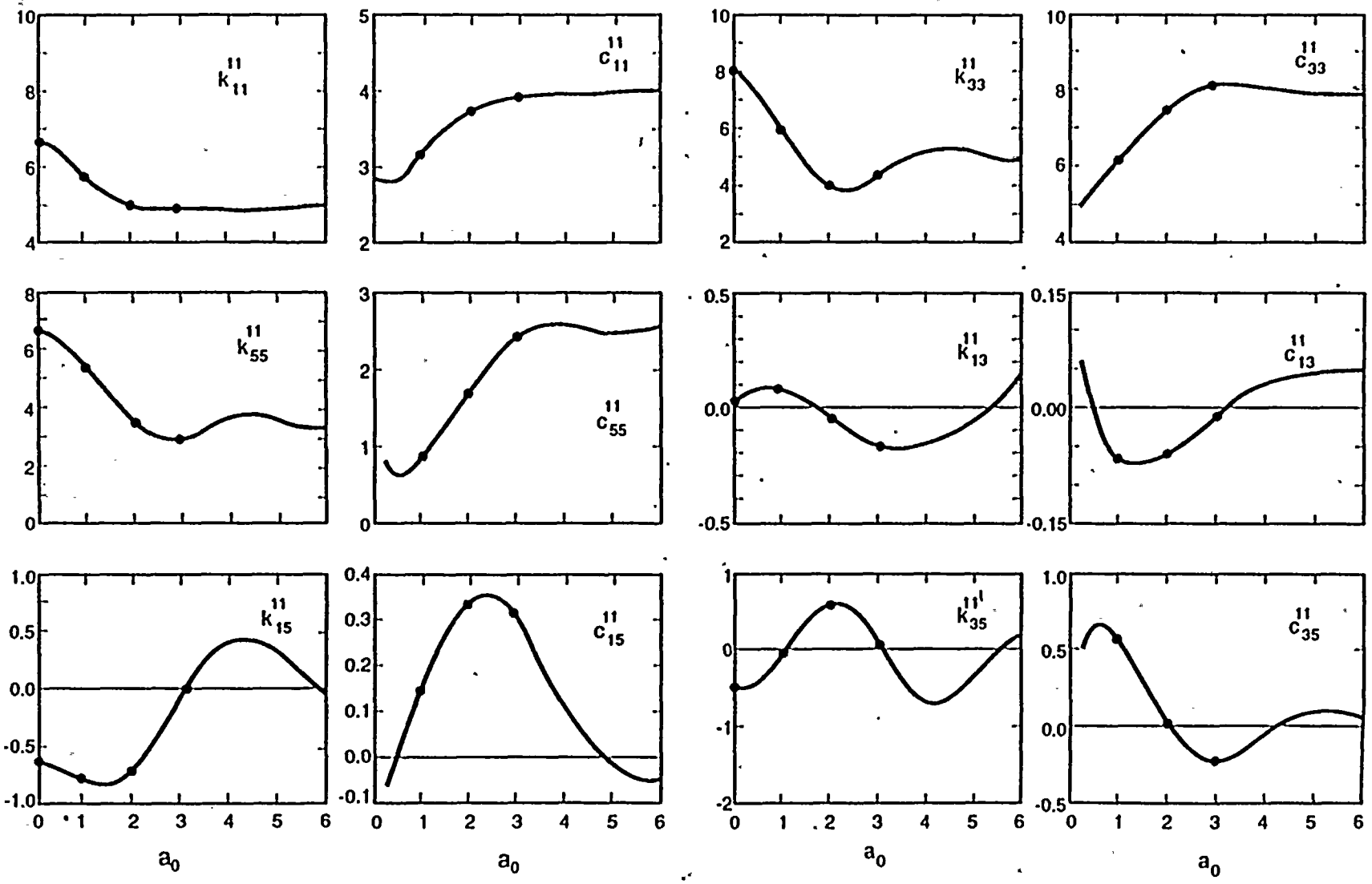

Figure 4.5-3. Impedance Functions for Foundation No. 1 Associated with DOFs in Coordinate Directions 1, 3, and 5

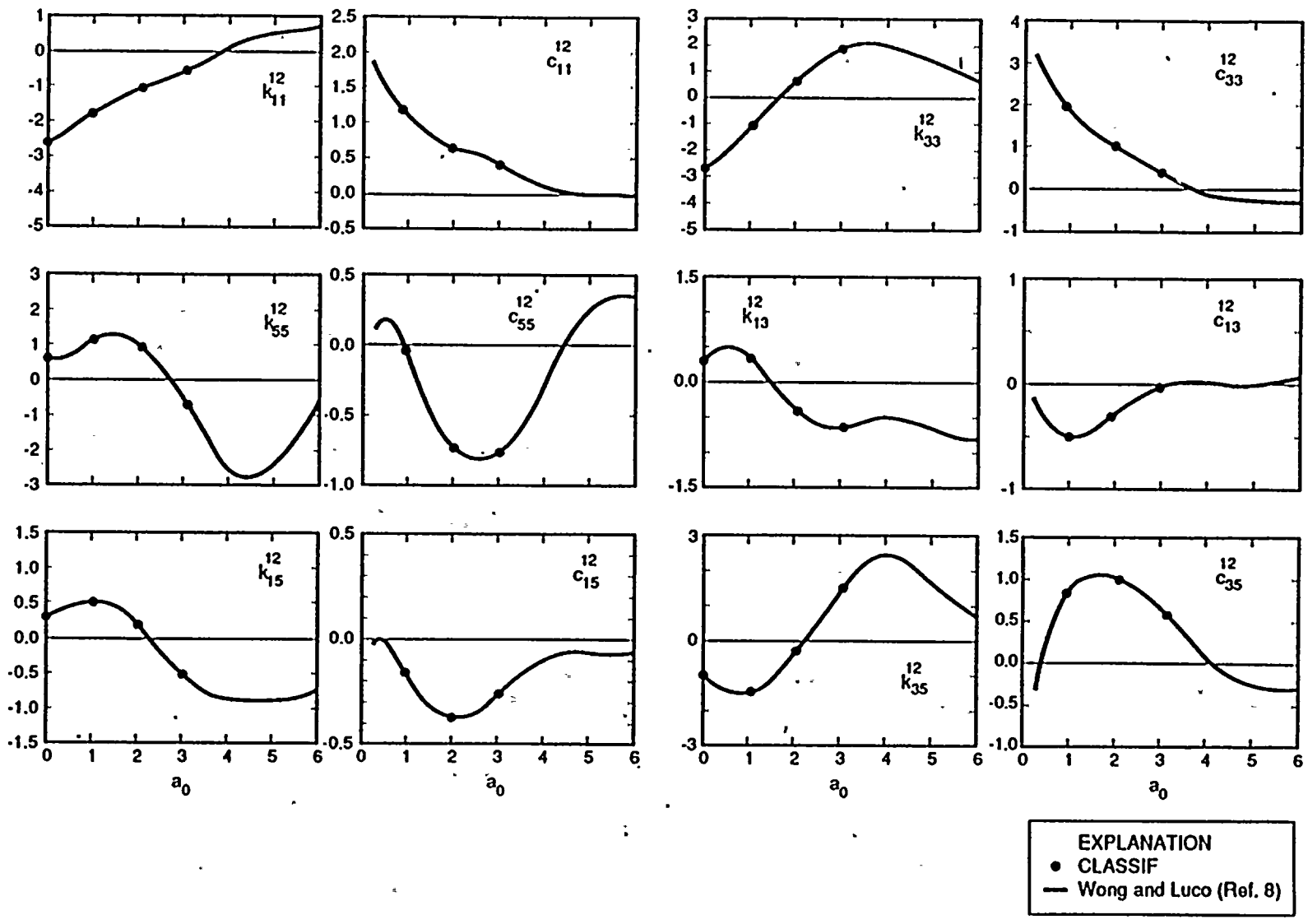

Figure 4.5-4. Impedance Functions for Foundation No. 1 due to Coupling from Foundation No. 2 for DOFs in Coordinate Directions 1, 3, and 5

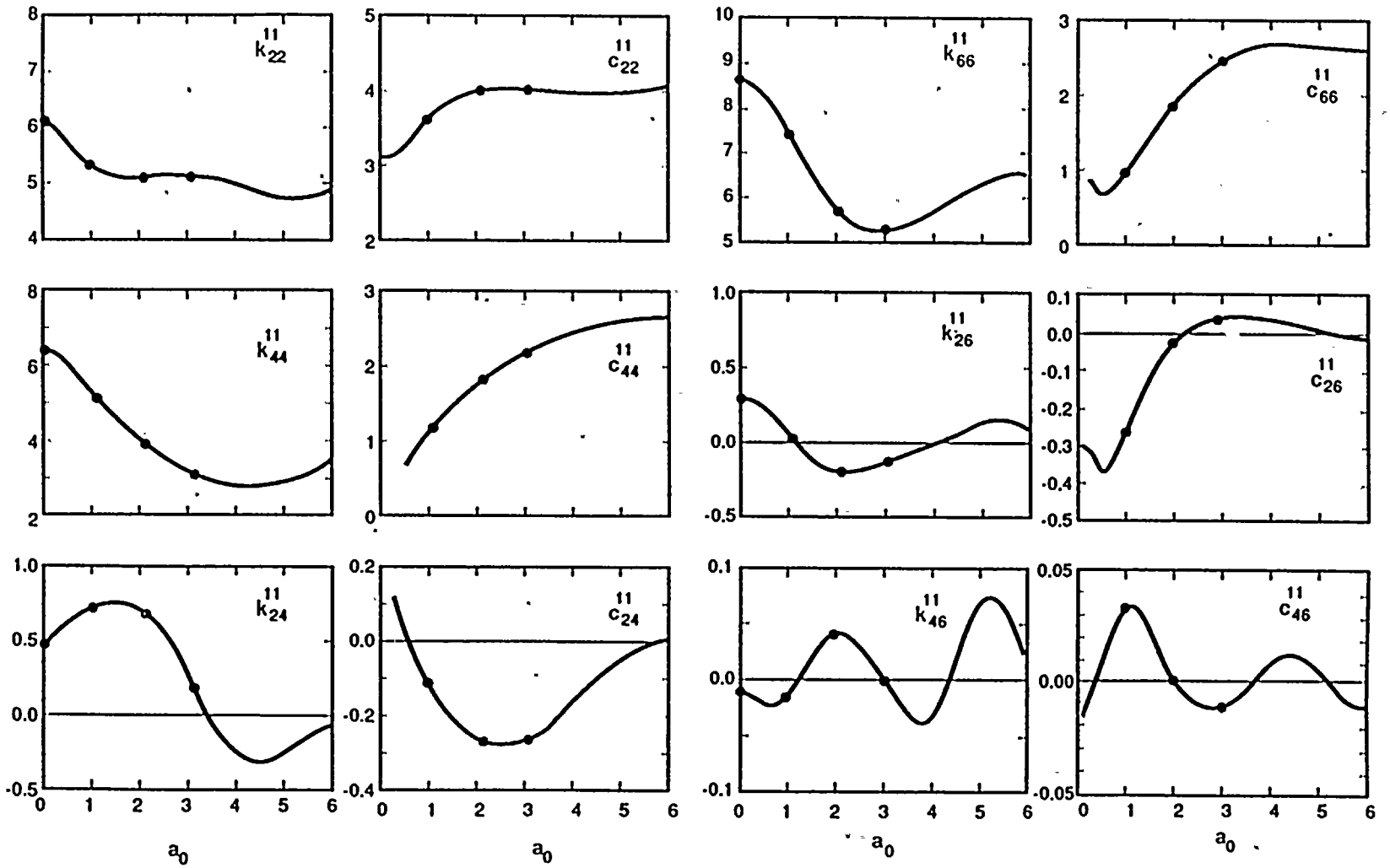

Figure 4.5-5. Impedance Functions for Foundation No. 1 Associated with DOFs in Coordinate Directions 1, 3, and 5

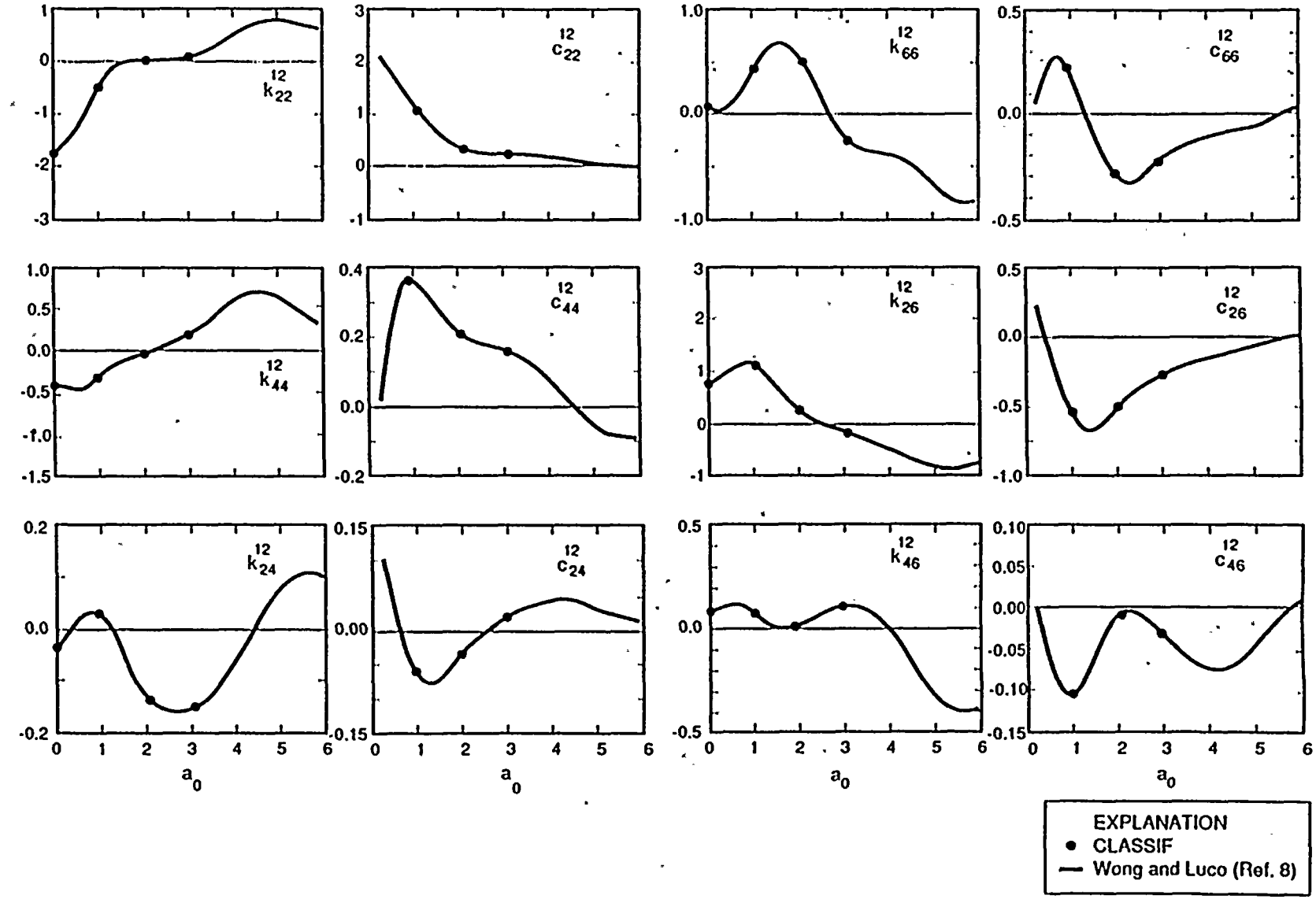

Figure 4.5-6. Impedance Functions for Foundation No. 1 due to Coupling from Foundation No. 2 for DOFs in Coordinate Directions 1, 3, and 5

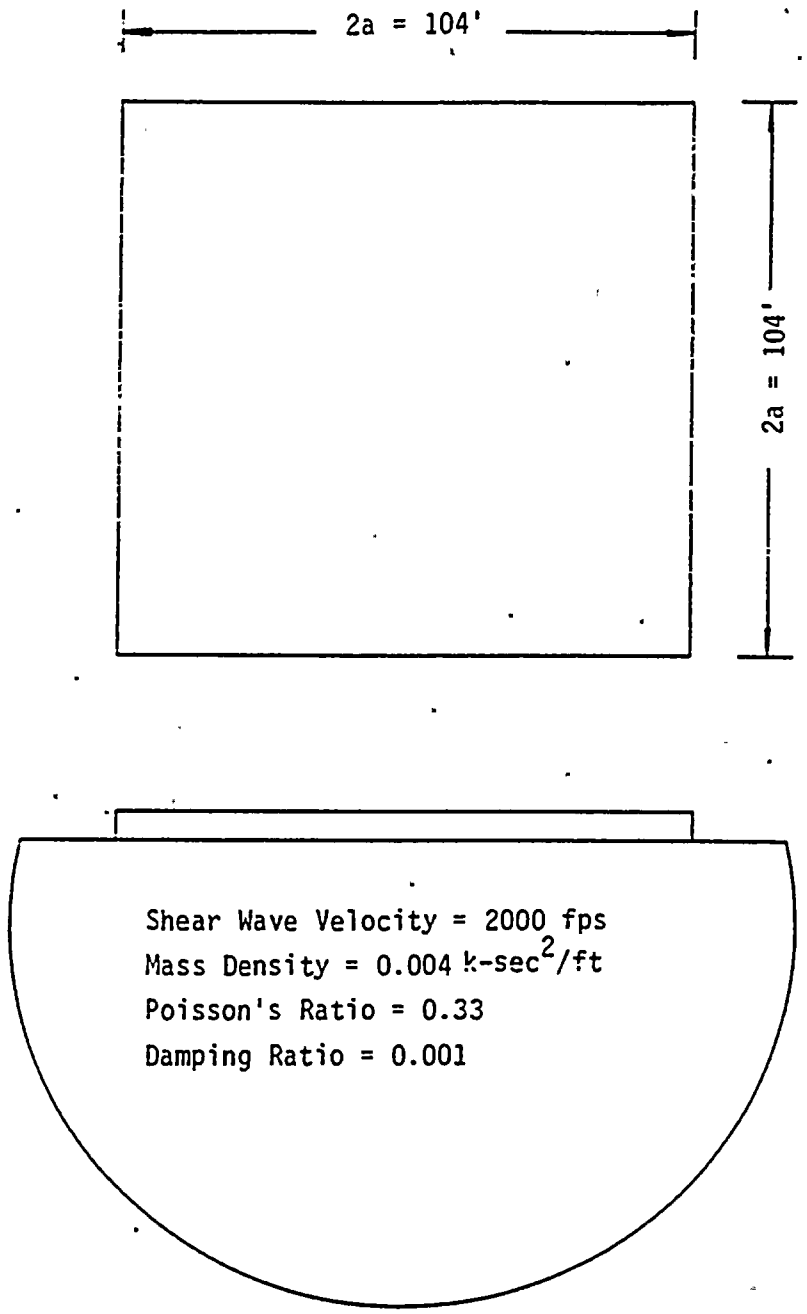

Figure 4.6-1. Square Foundation on Elastic Halfspace

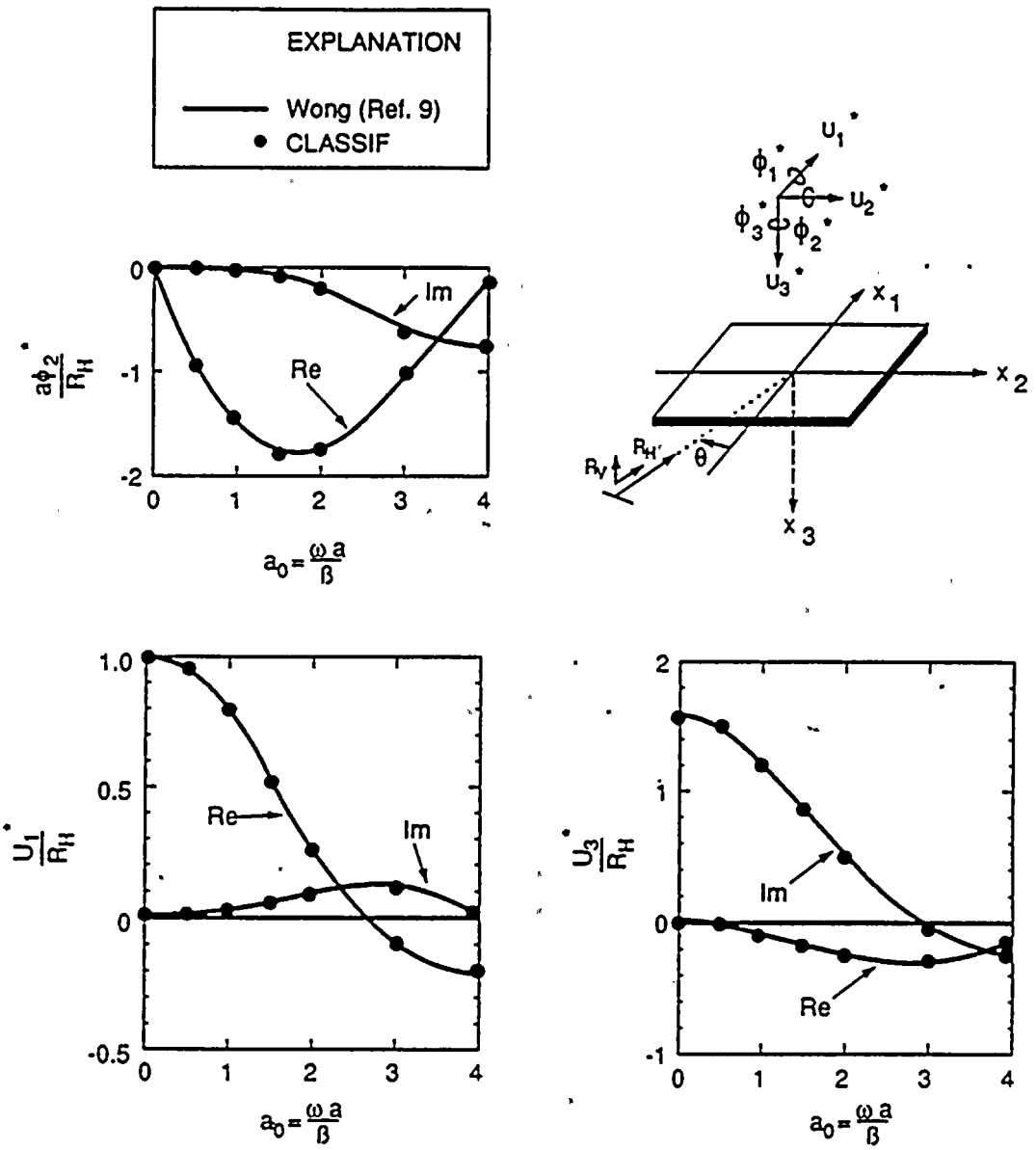

Figure 4.6-2. Response to Rayleigh Wave

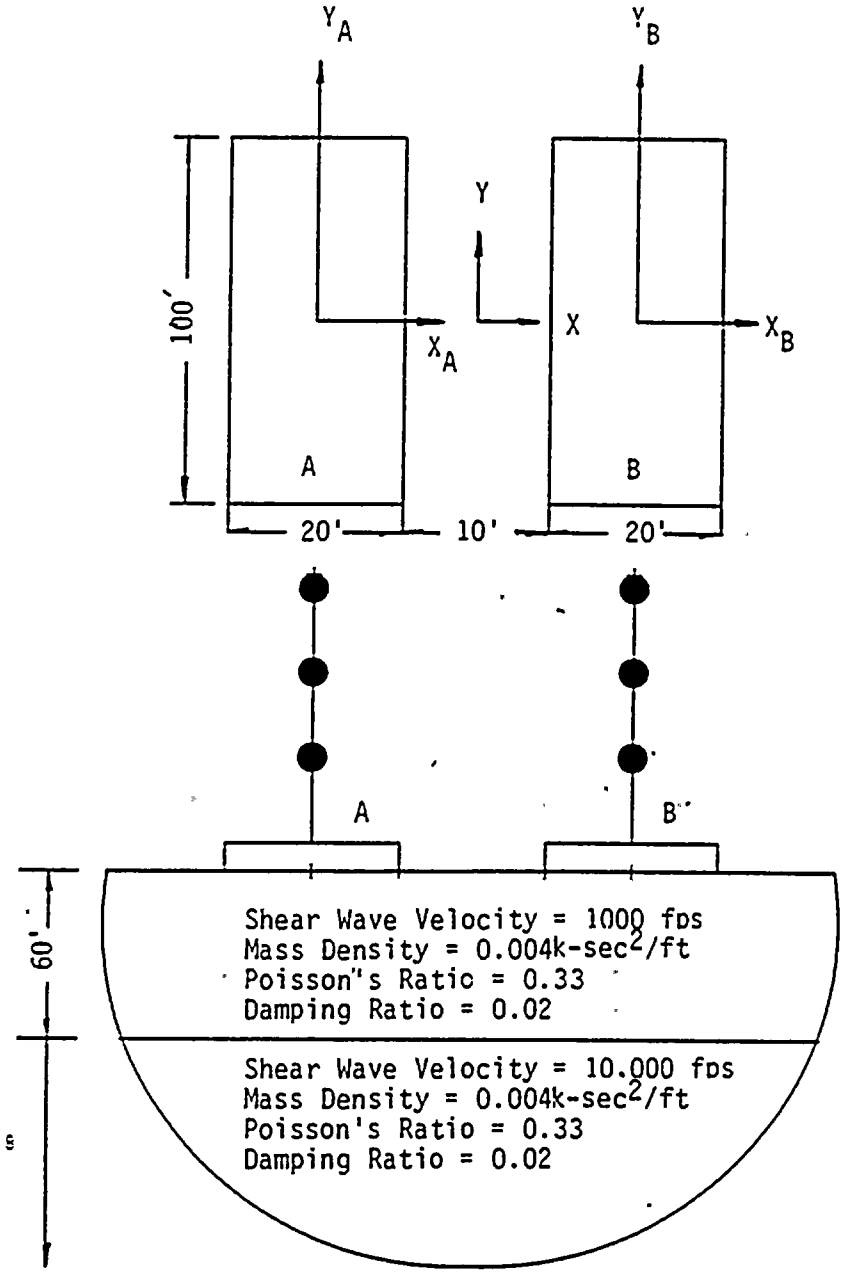

Figure 4.7-1. Soil-Foundation Model

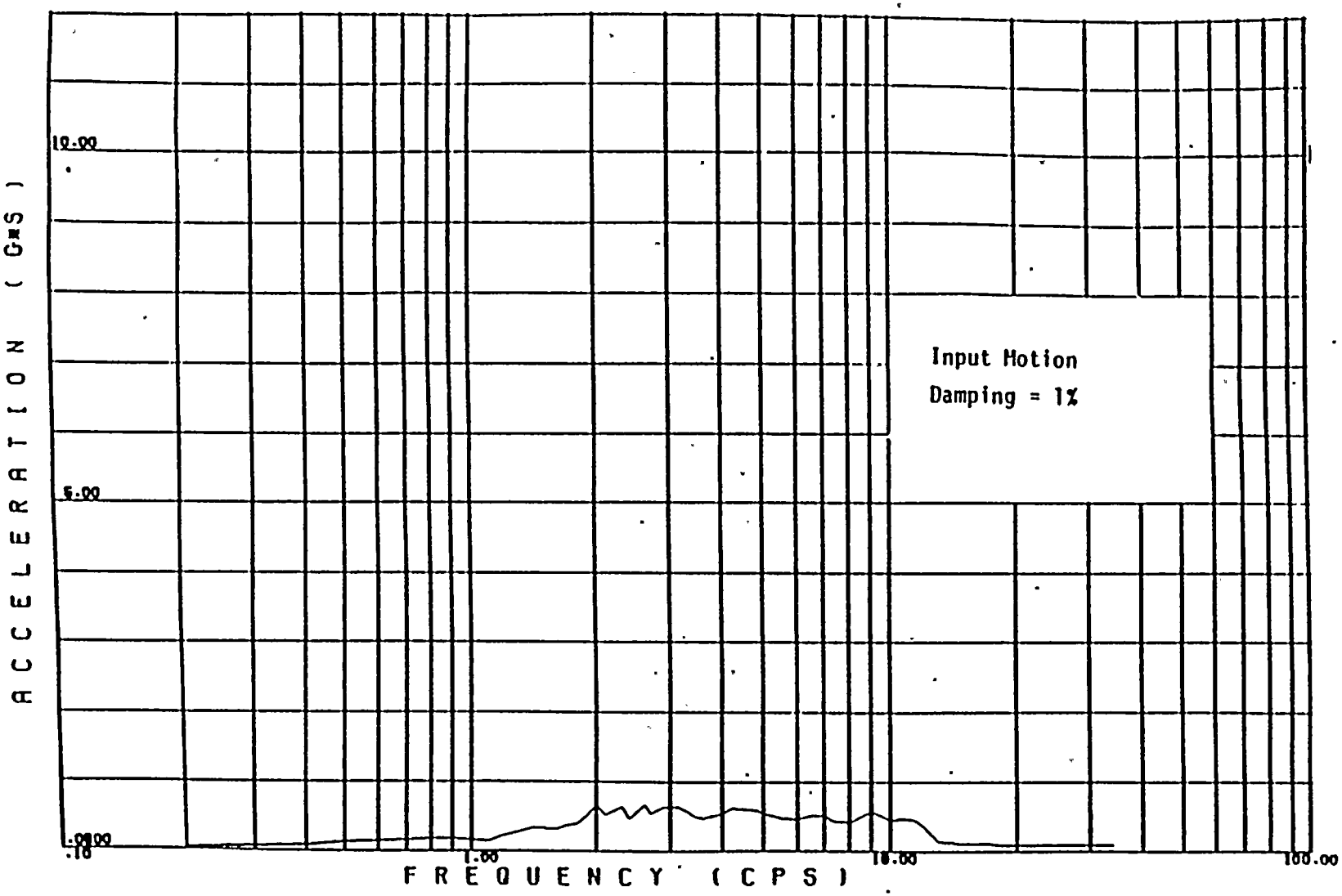

Figure 4.7-2. Absolute Acceleration Response Spectrum of Input Motion

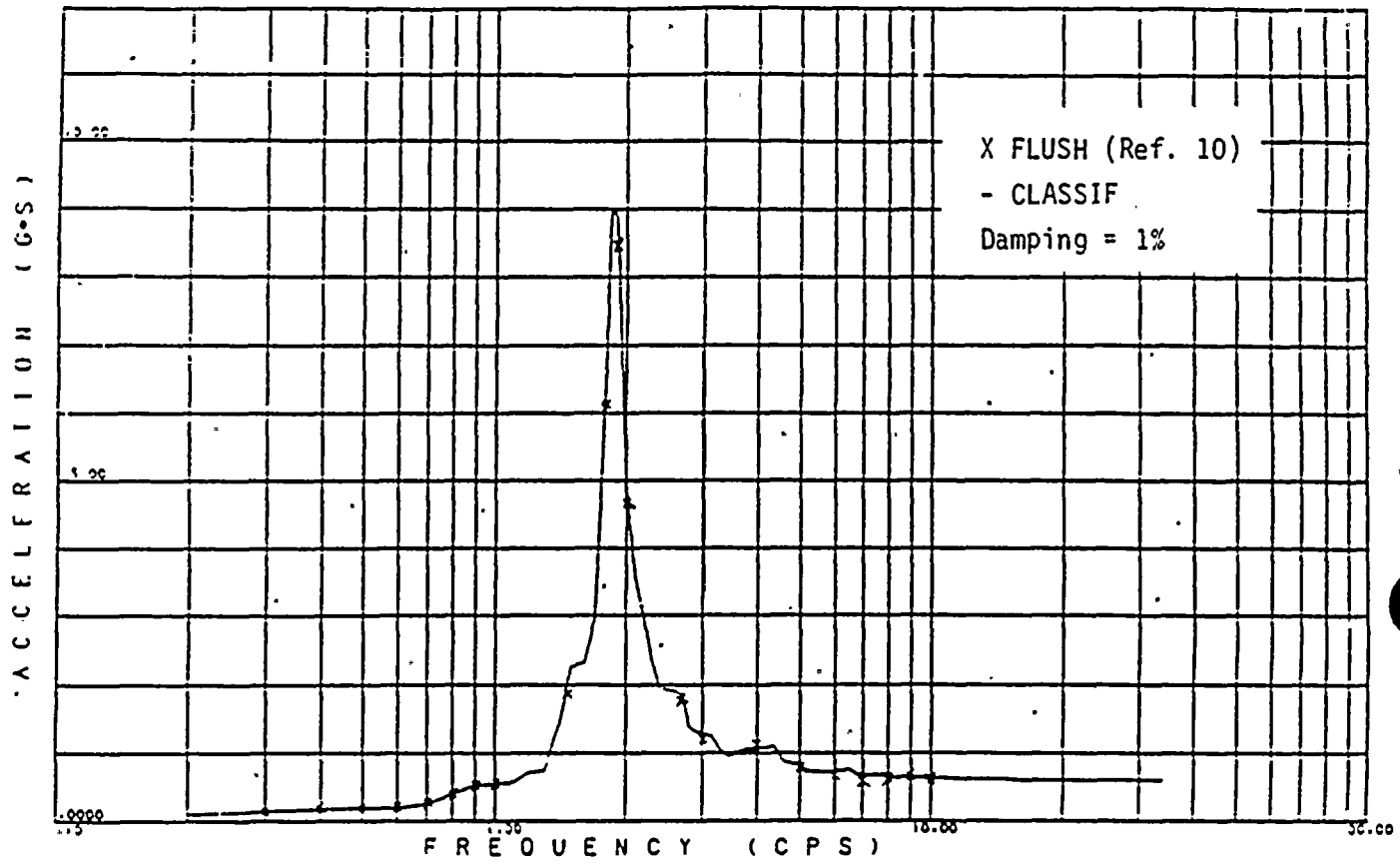

Figure 4.7-3. Comparison of Results Obtained from CLASSIF and FLUSH

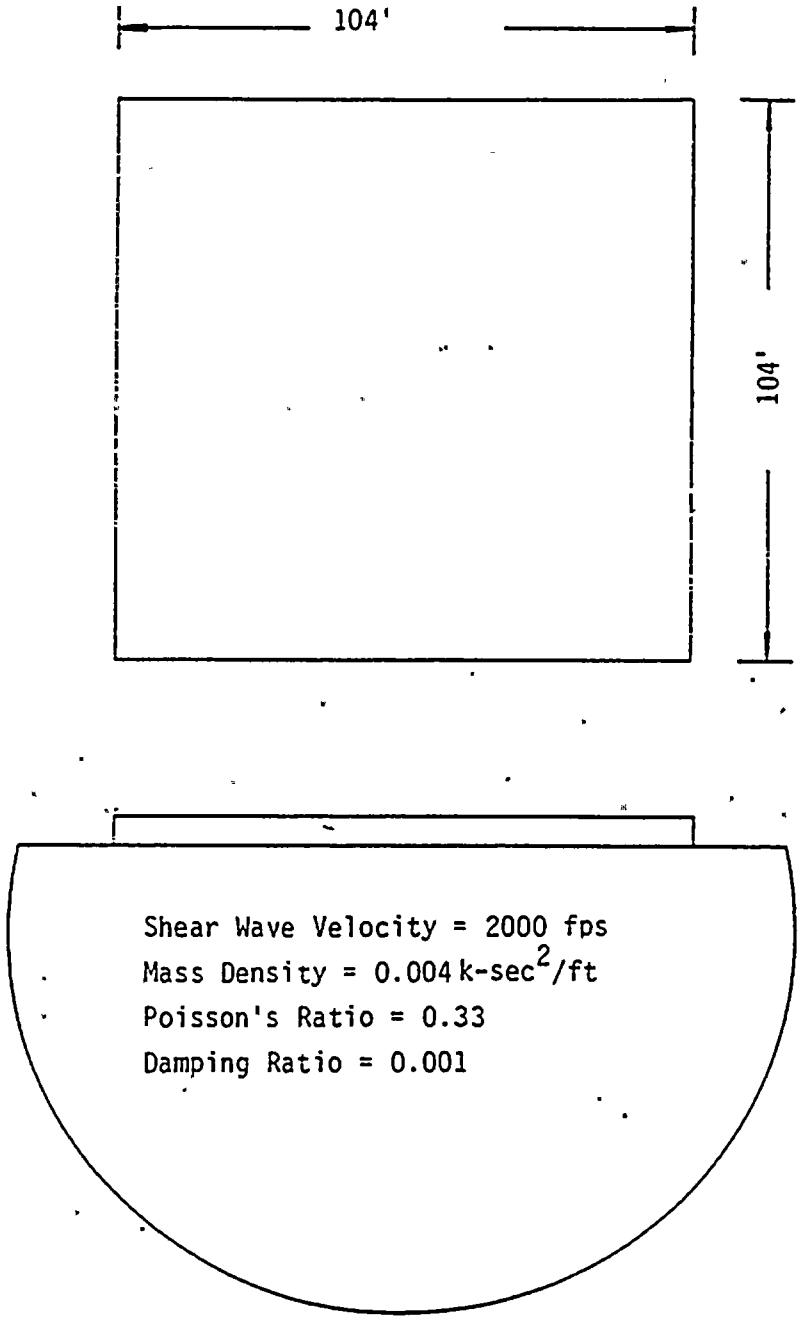

Figure 4.8-1. A Square Foundation Resting on Elastic Halfspace

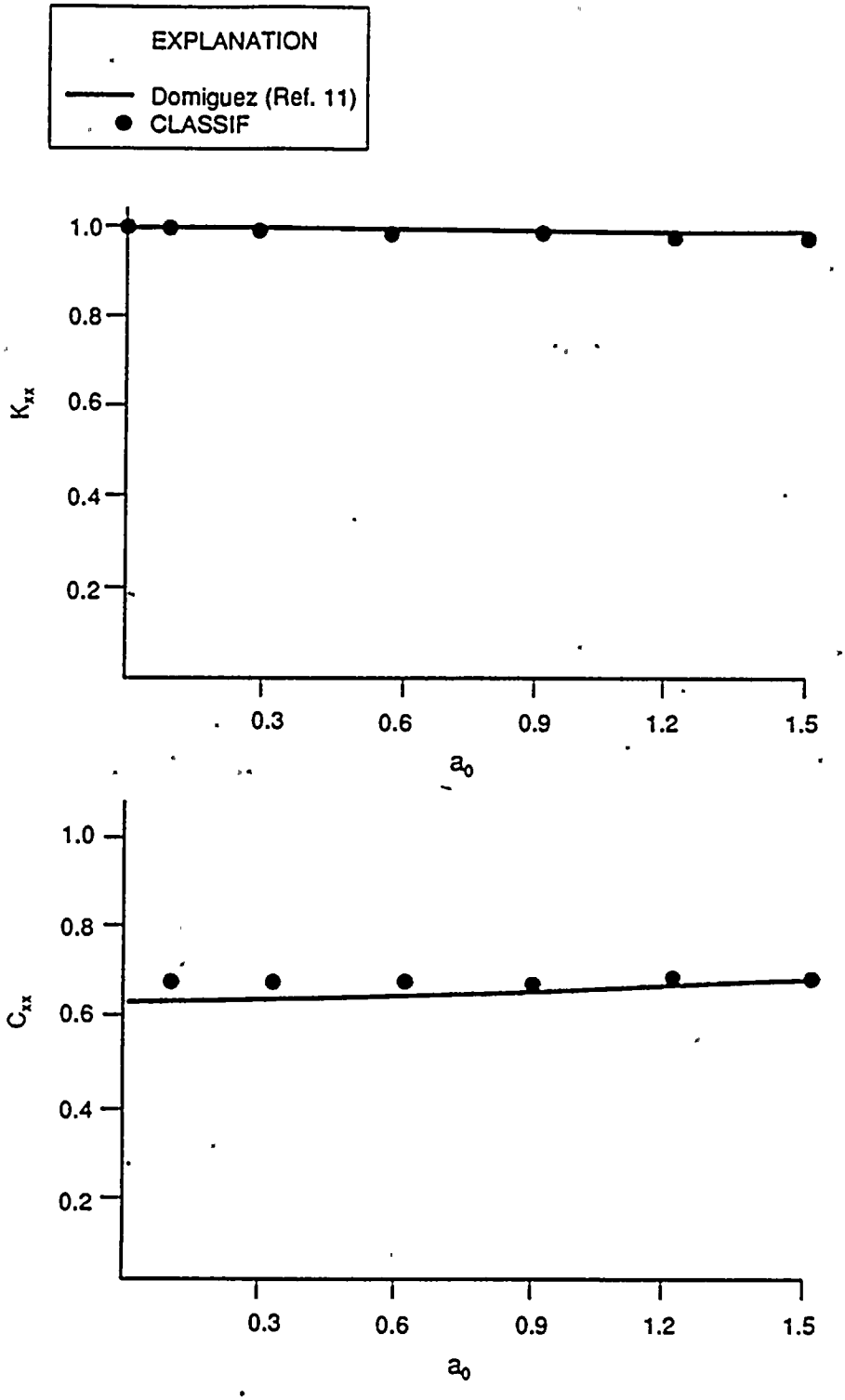

Figure 4.8-2. Horizontal Stiffness and Damping Coefficients for a Square Foundation

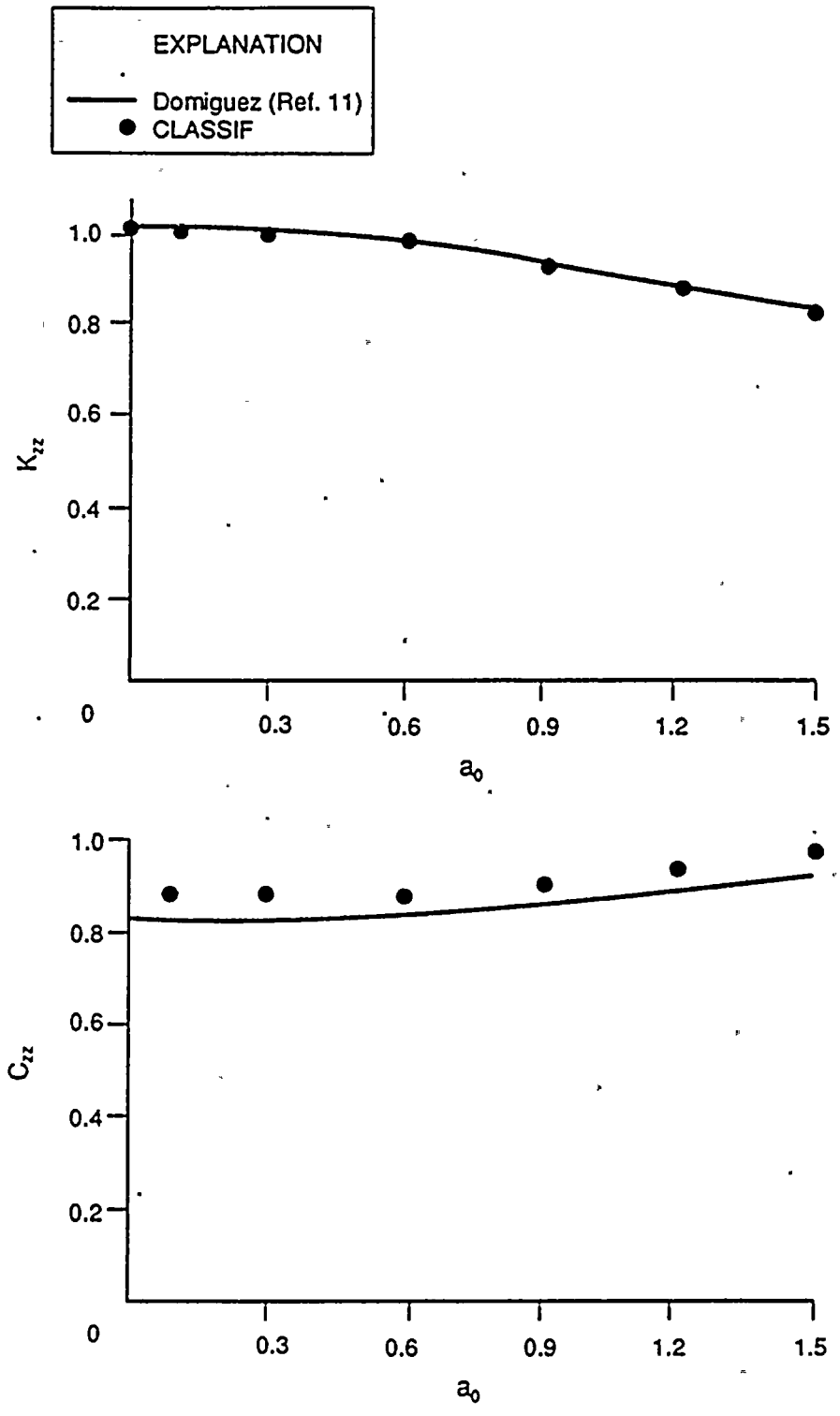

Figure 4.8-3. Vertical Stiffness and Damping Coefficients for a Square Foundation

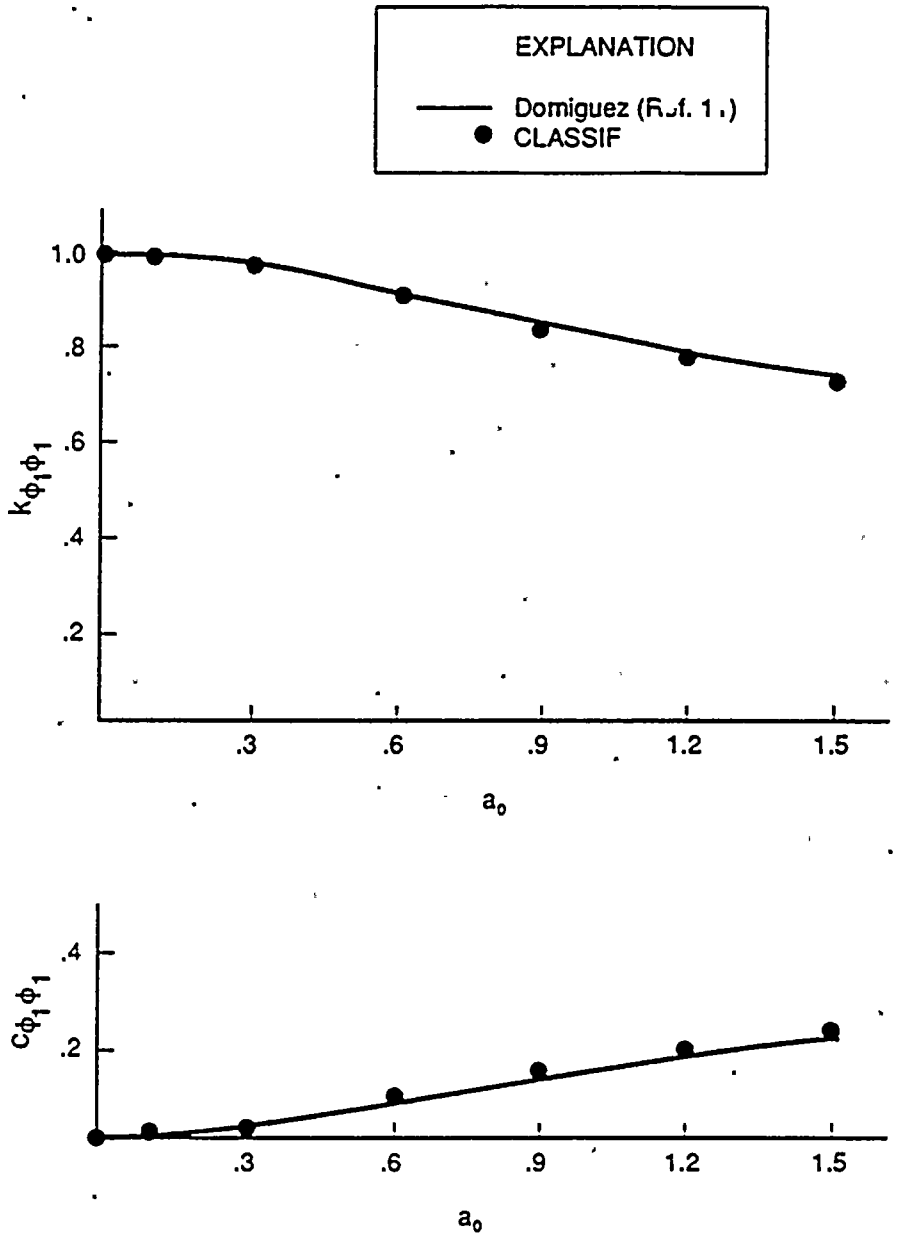

Figure 4.8-4. Rocking Stiffness and Damping Coefficients for a Square Foundation

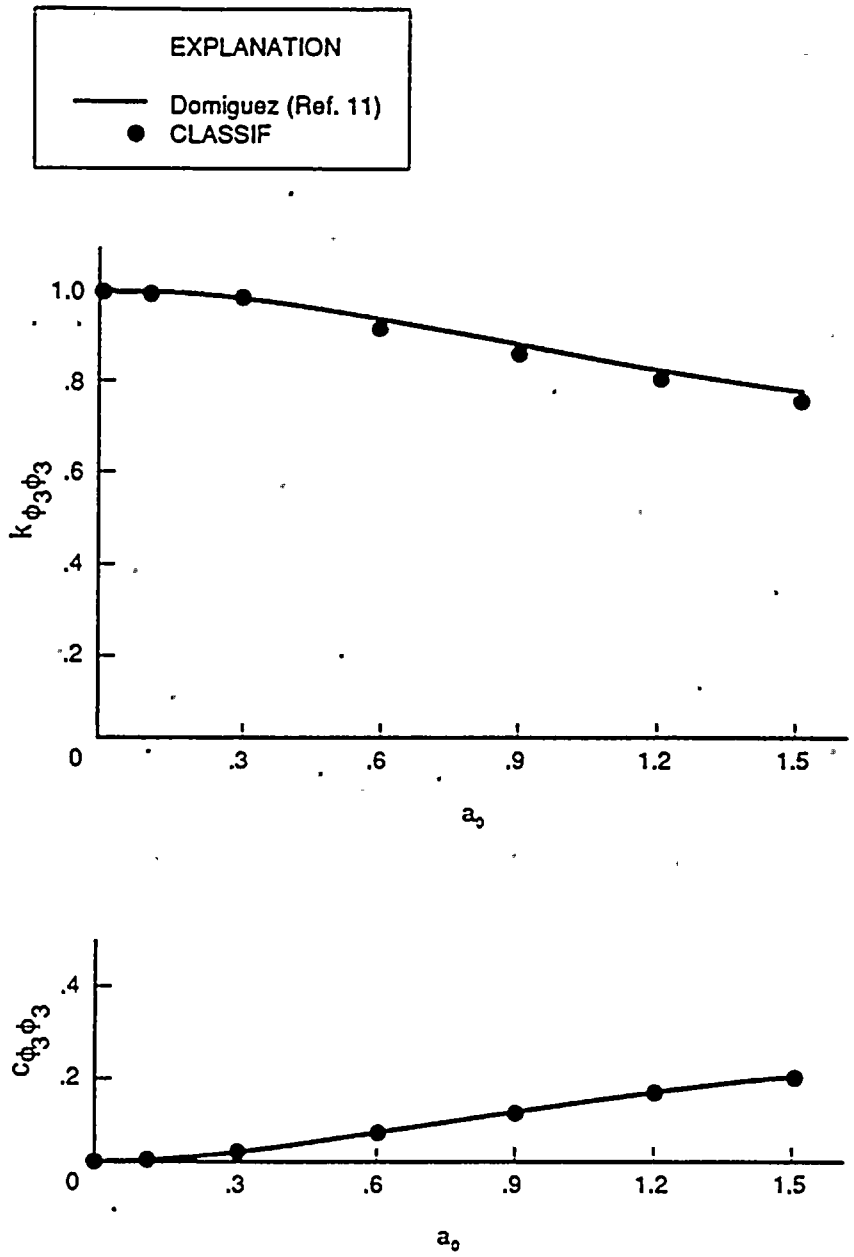

Figure 4.8-5. Torsional Stiffness and Damping Coefficients for a Square Foundation

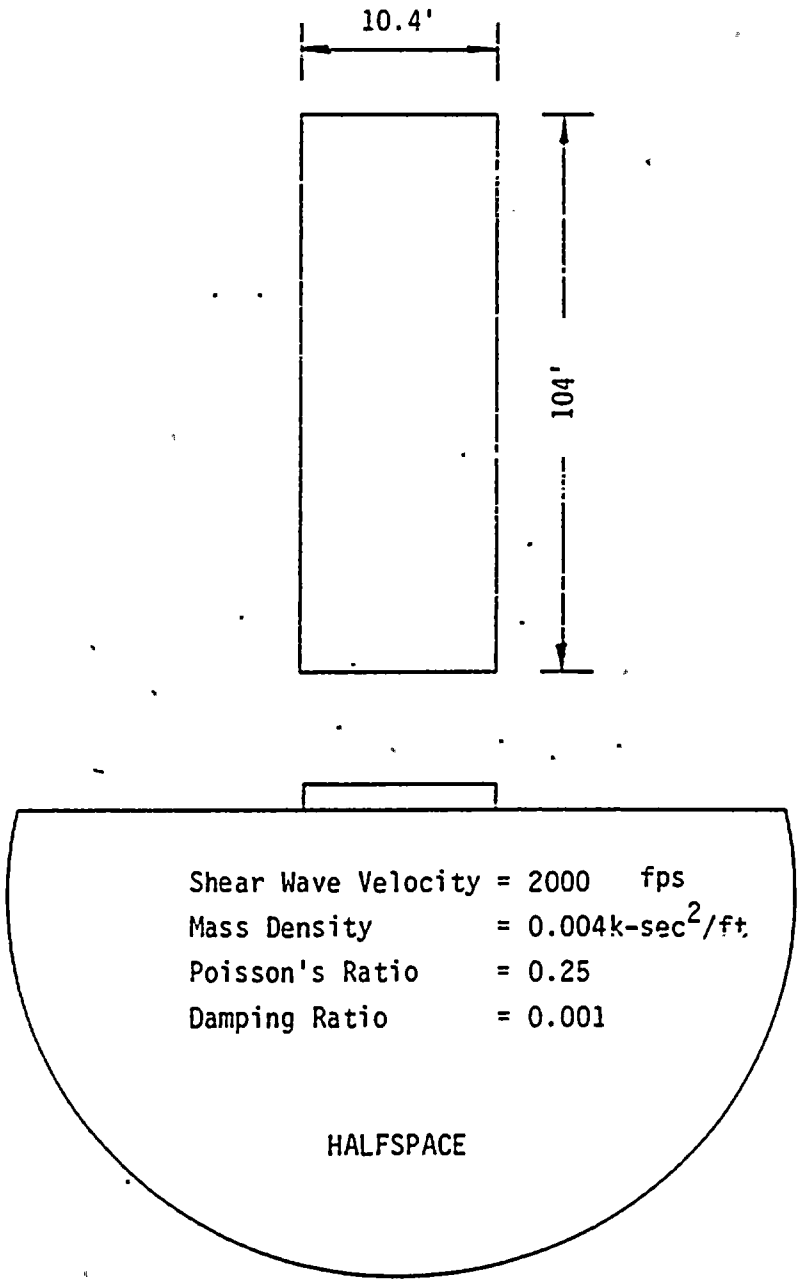

Figure 4.9-1. Rectangular Foundation on Elastic Halfspace

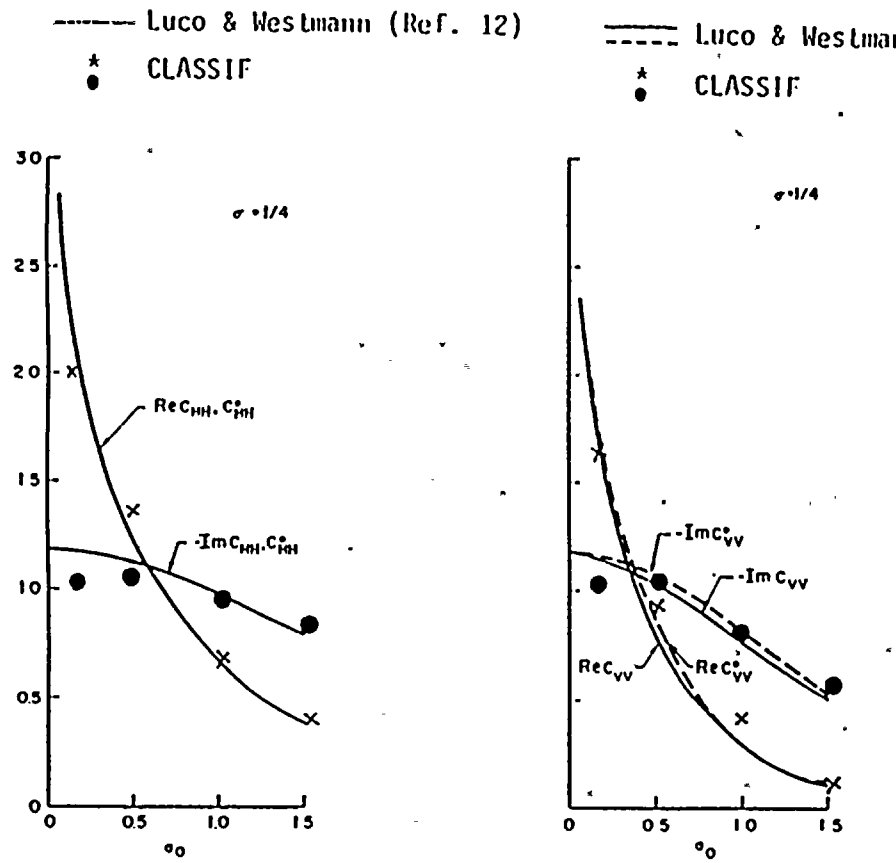

Figure 4.9-2. Horizontal Compliance

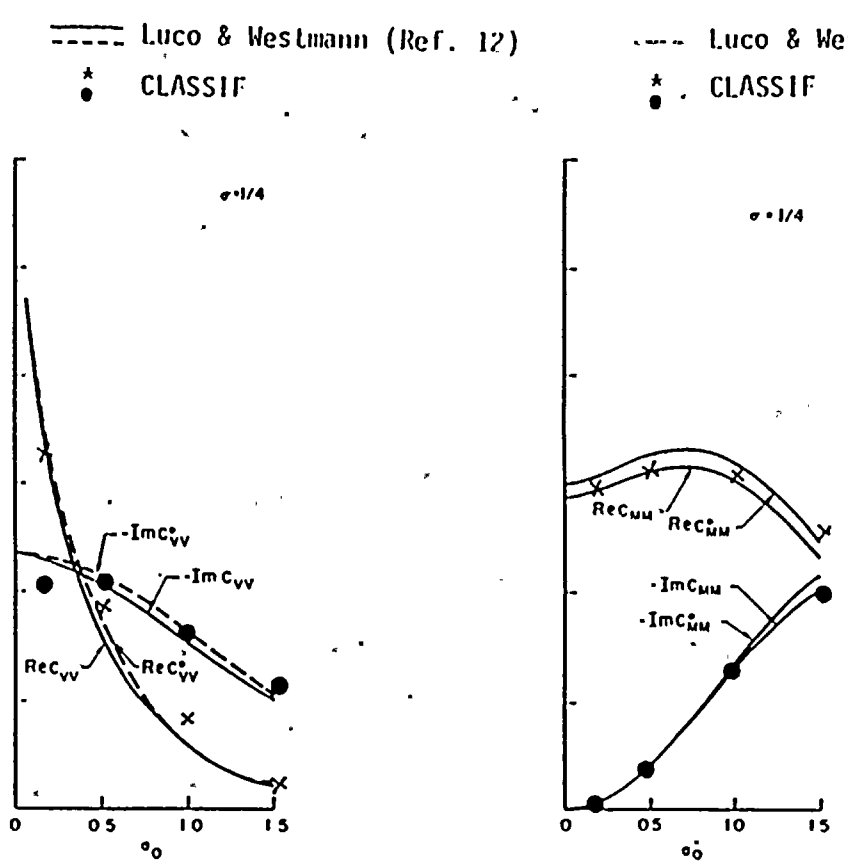

Figure 4.9-3. Vertical Compliance

Figure 4.9-4. Rocking Compliance

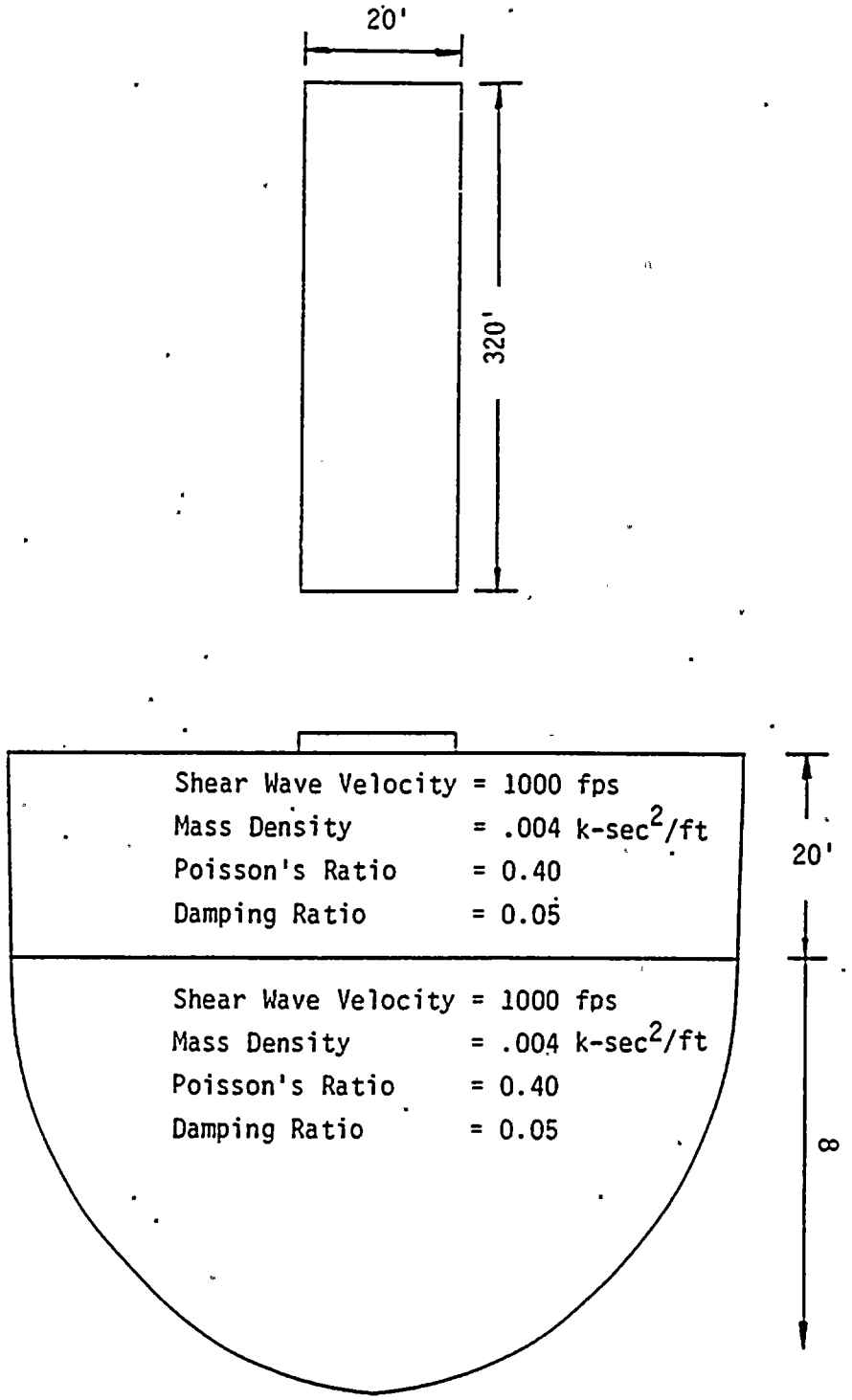

Figure 4.10-1. Soil-Foundation Model for Case 10 (a)

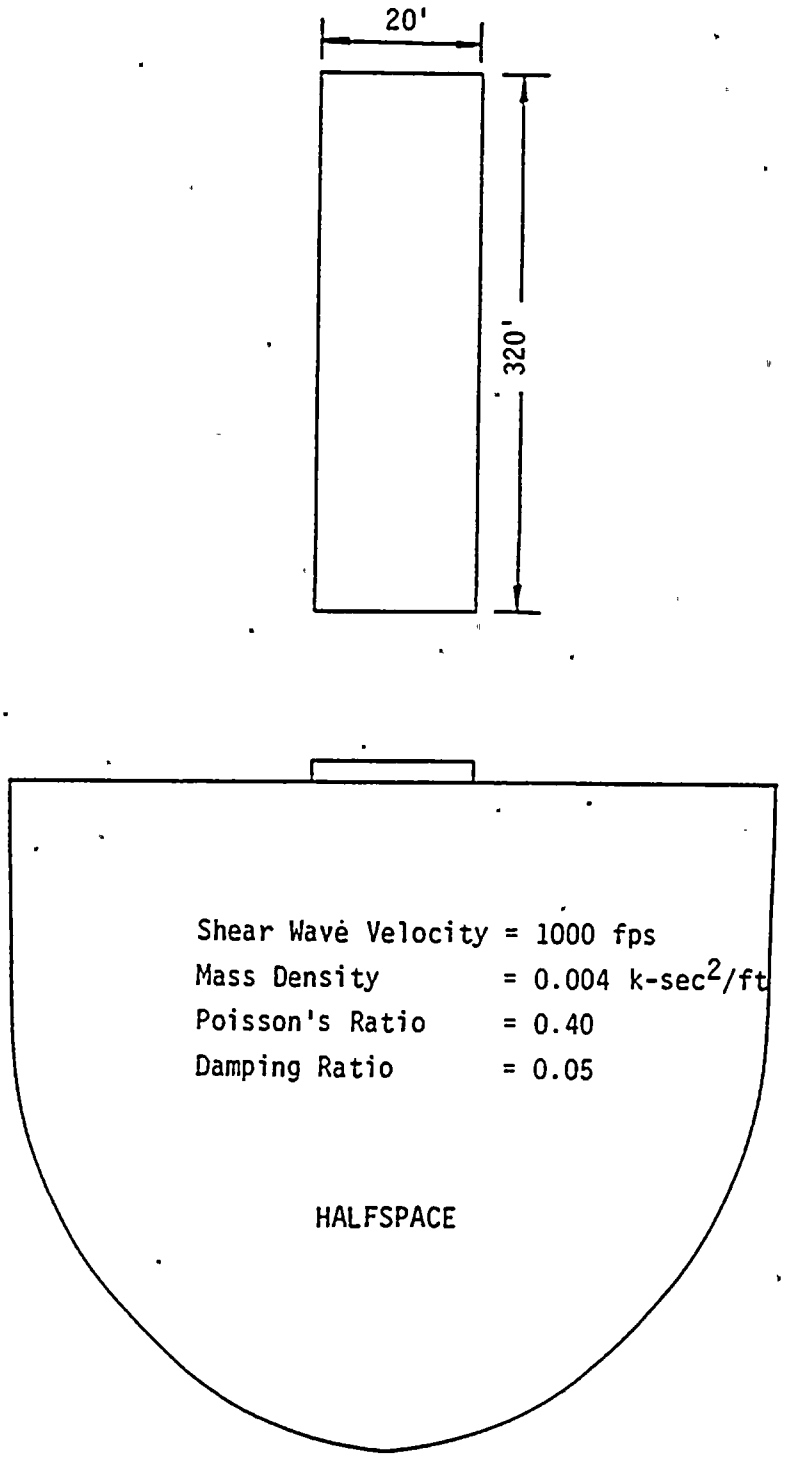

Figure 4.10-2. Soil-Foundation for Analysis Case 10 (b)

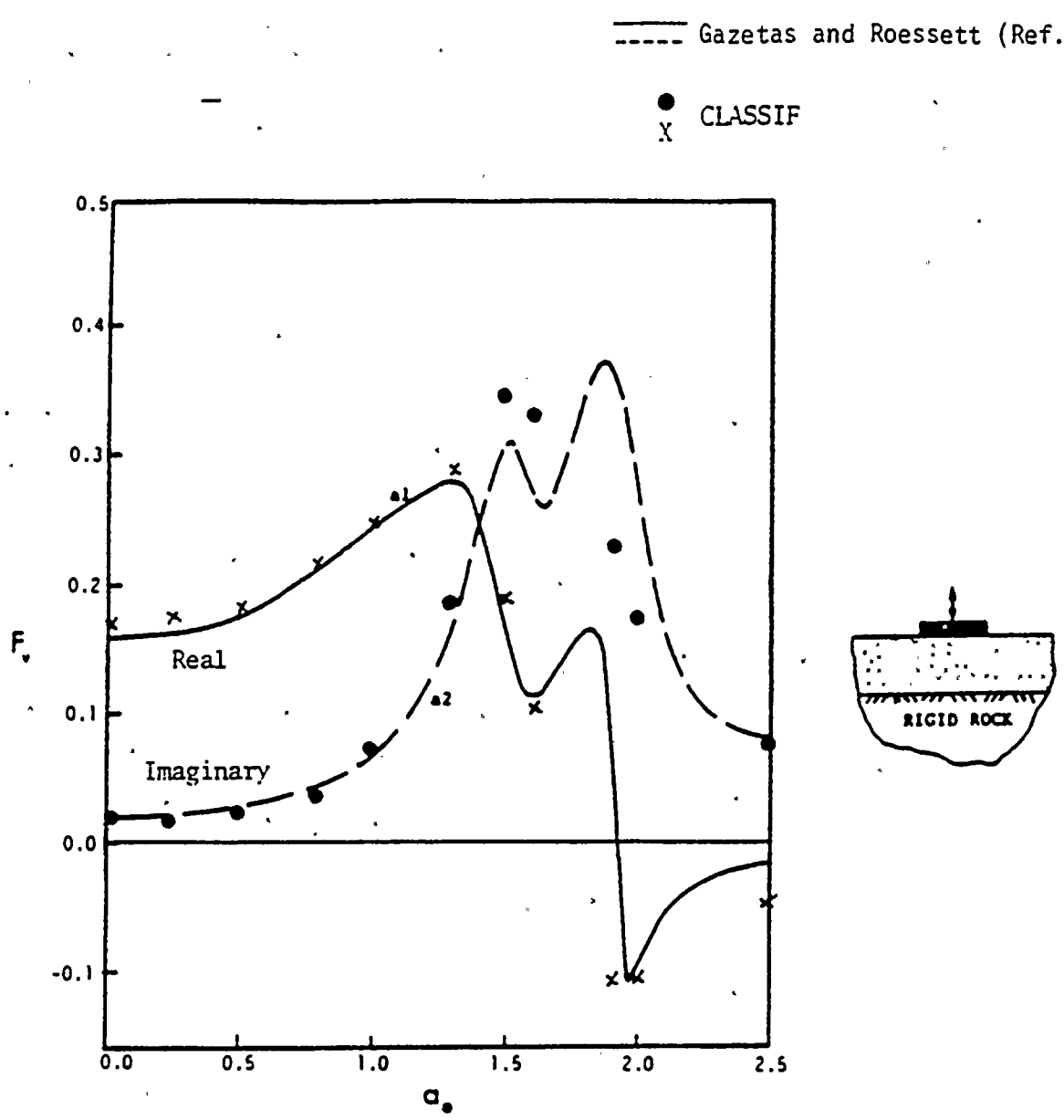

Figure 4.10-3. Vertical Compliance Function for Analysis Case 10(a)

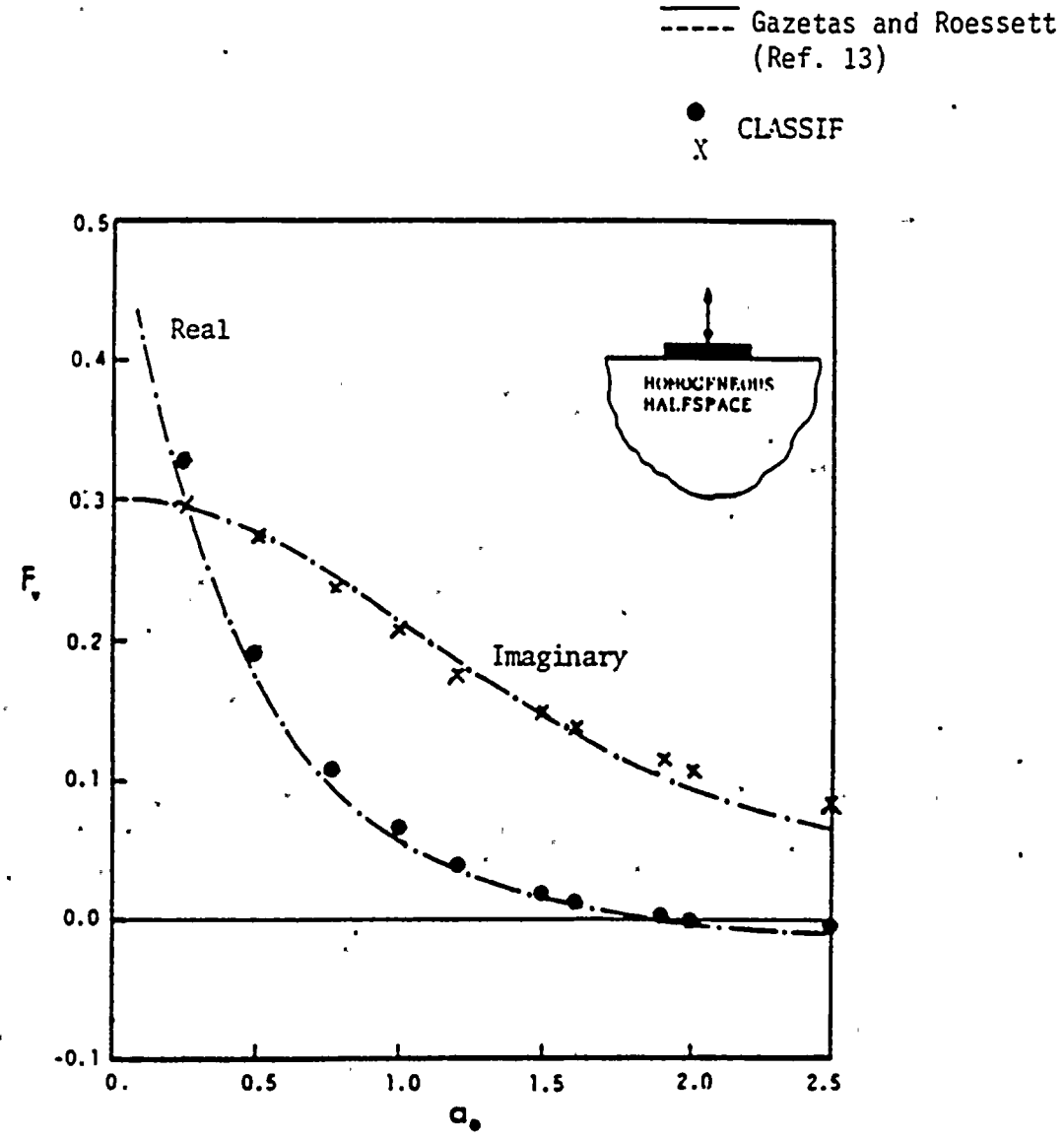

Figure 4.10-4. Vertical Compliance Function for Analysis Case 10 (b)

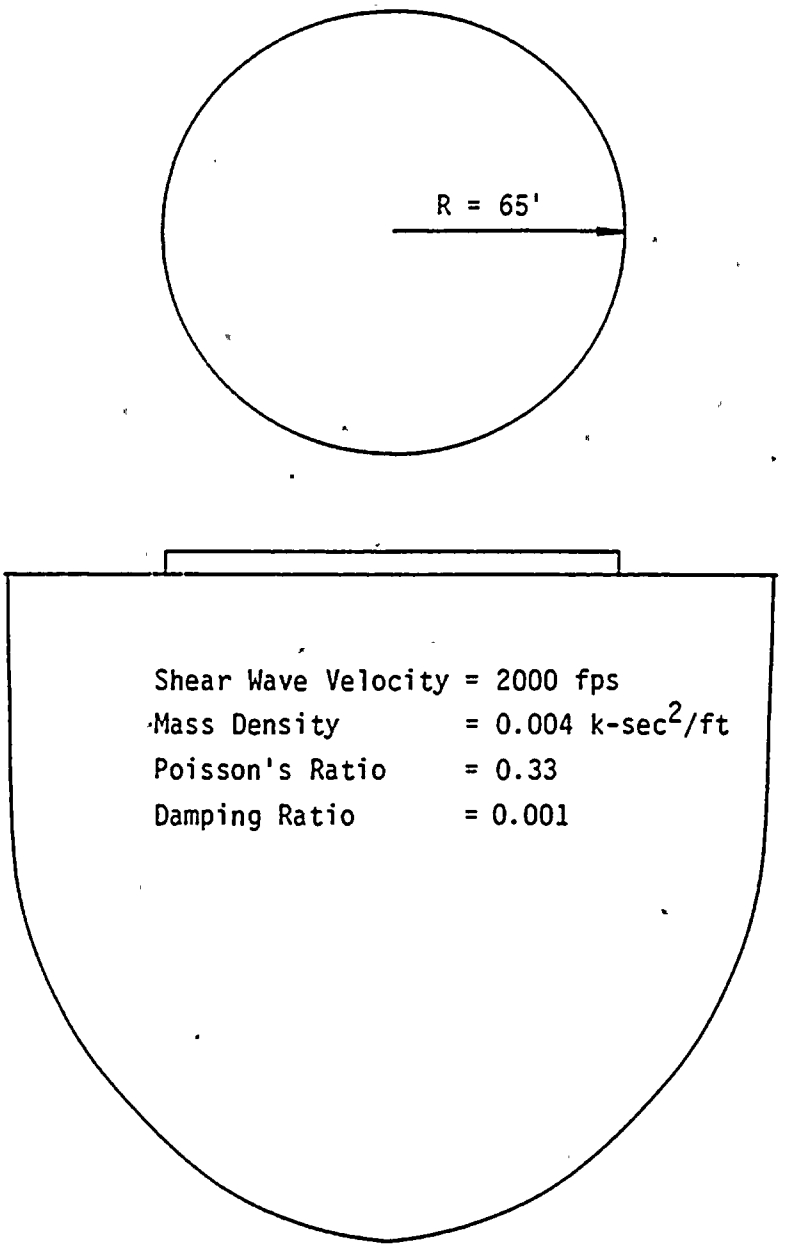

Figure 4.11-1. Circular Foundation on Elastic Halfspace

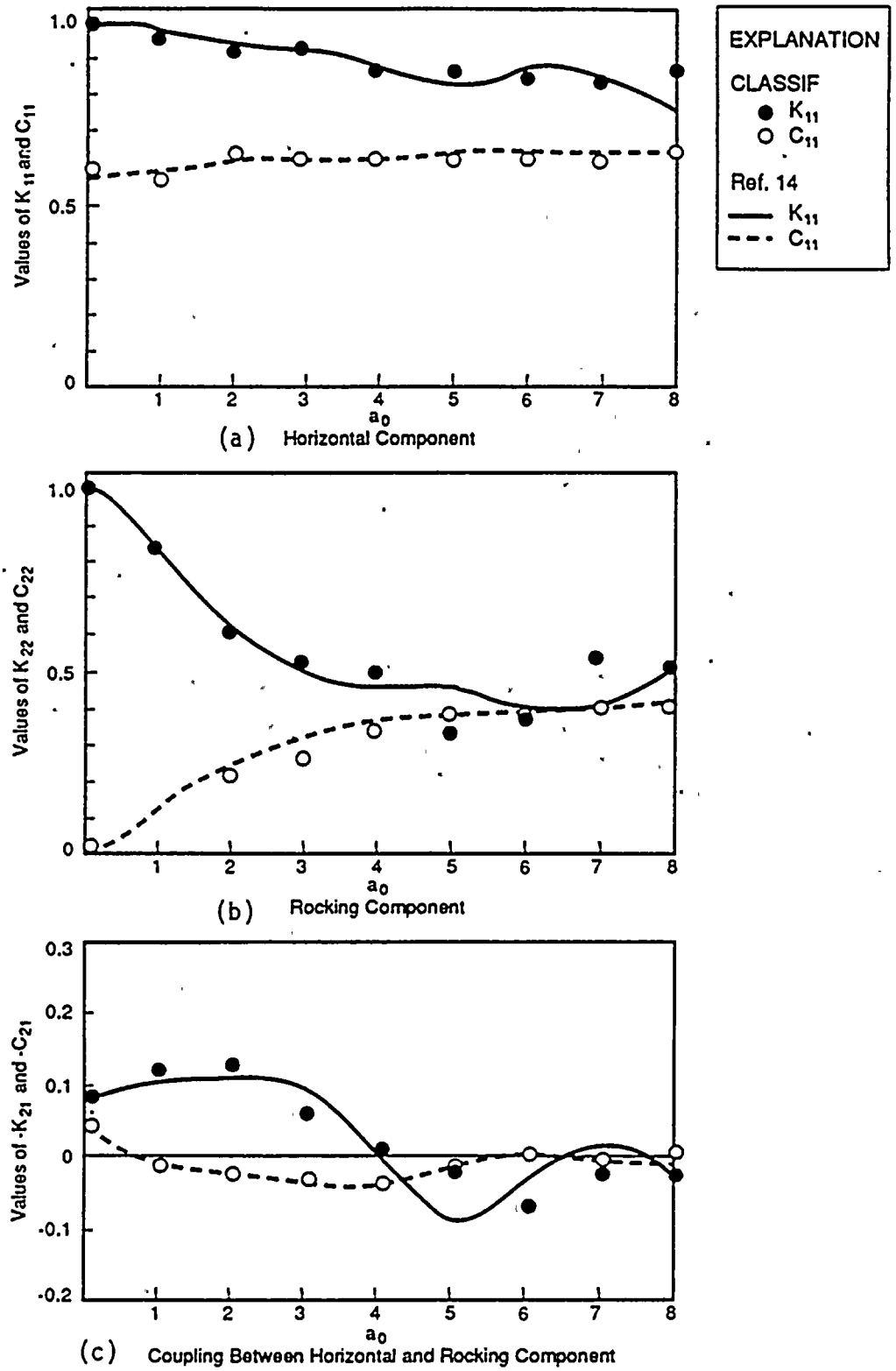

Figure 4.11-2. Stiffness and Damping Coefficients: (a) Horizontal Component; (b) Rocking Component; (c) Coupling Between Horizontal and Rocking Component

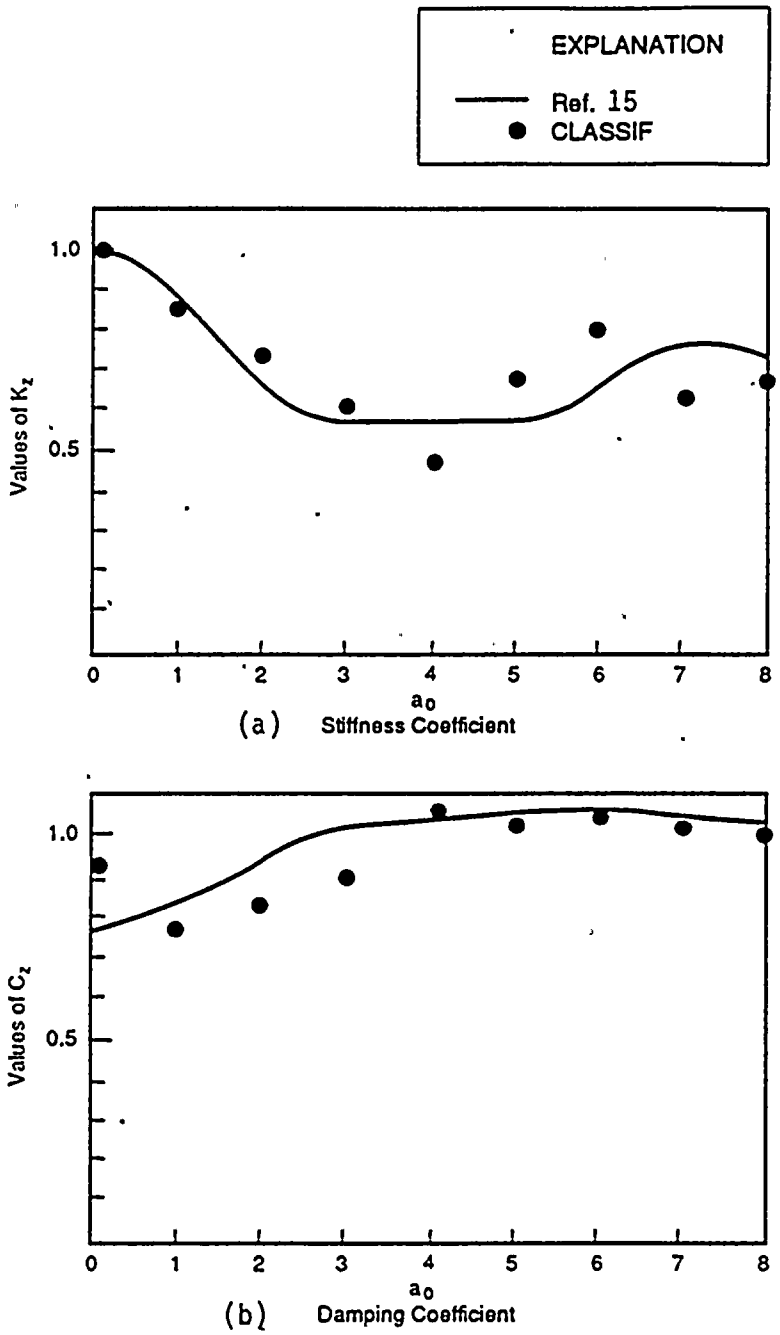

Figure 4.11-3. Vertical Impedance Function: (a) Stiffness Coefficient; (b) Damping Coefficient

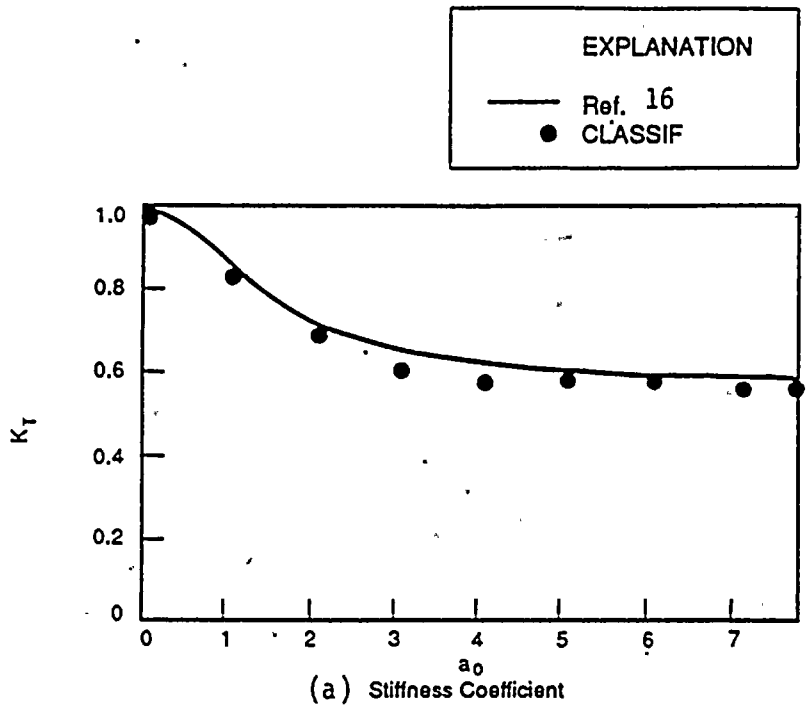

Figure 4.11-4. Torsion Impedance Functions: (a) Stiffness Coefficient; (b) Damping Coefficient

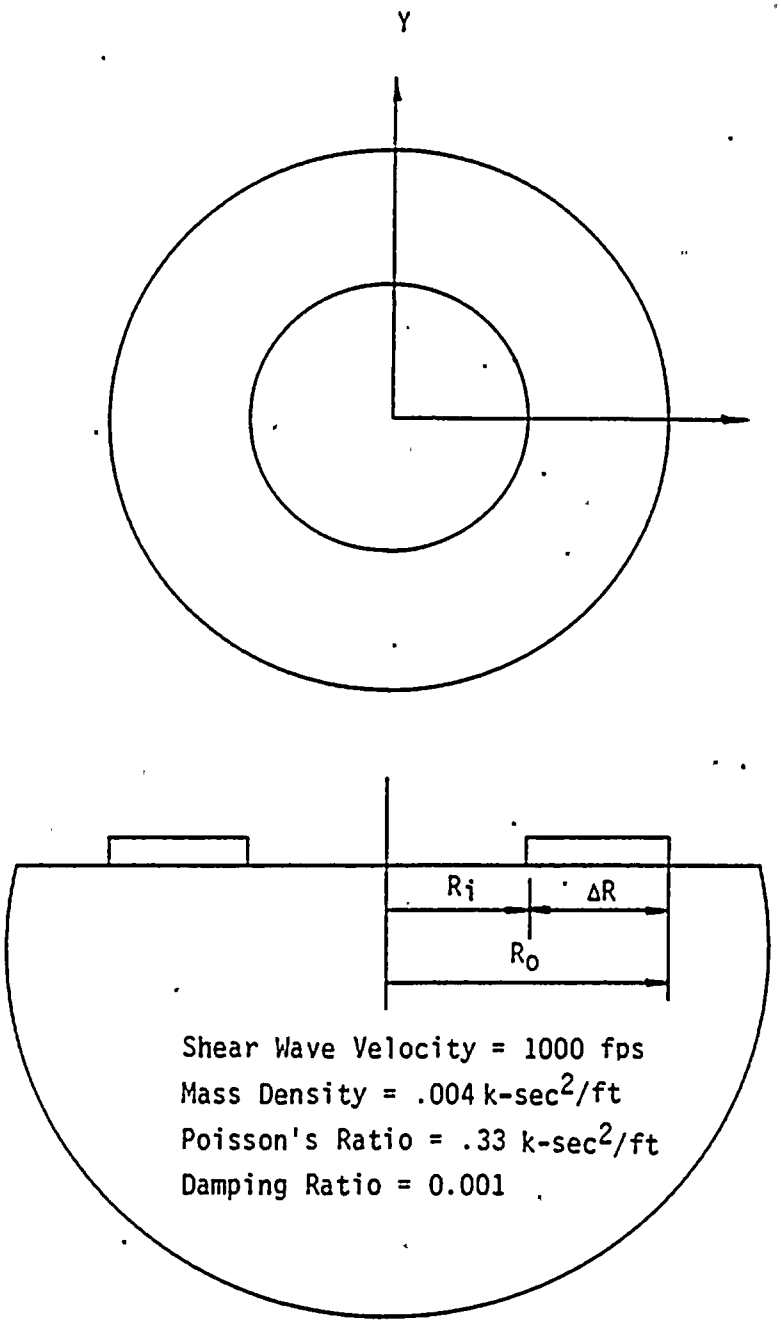

Figure 4.12-1 A Ring Foundation on Elastic Halfspace

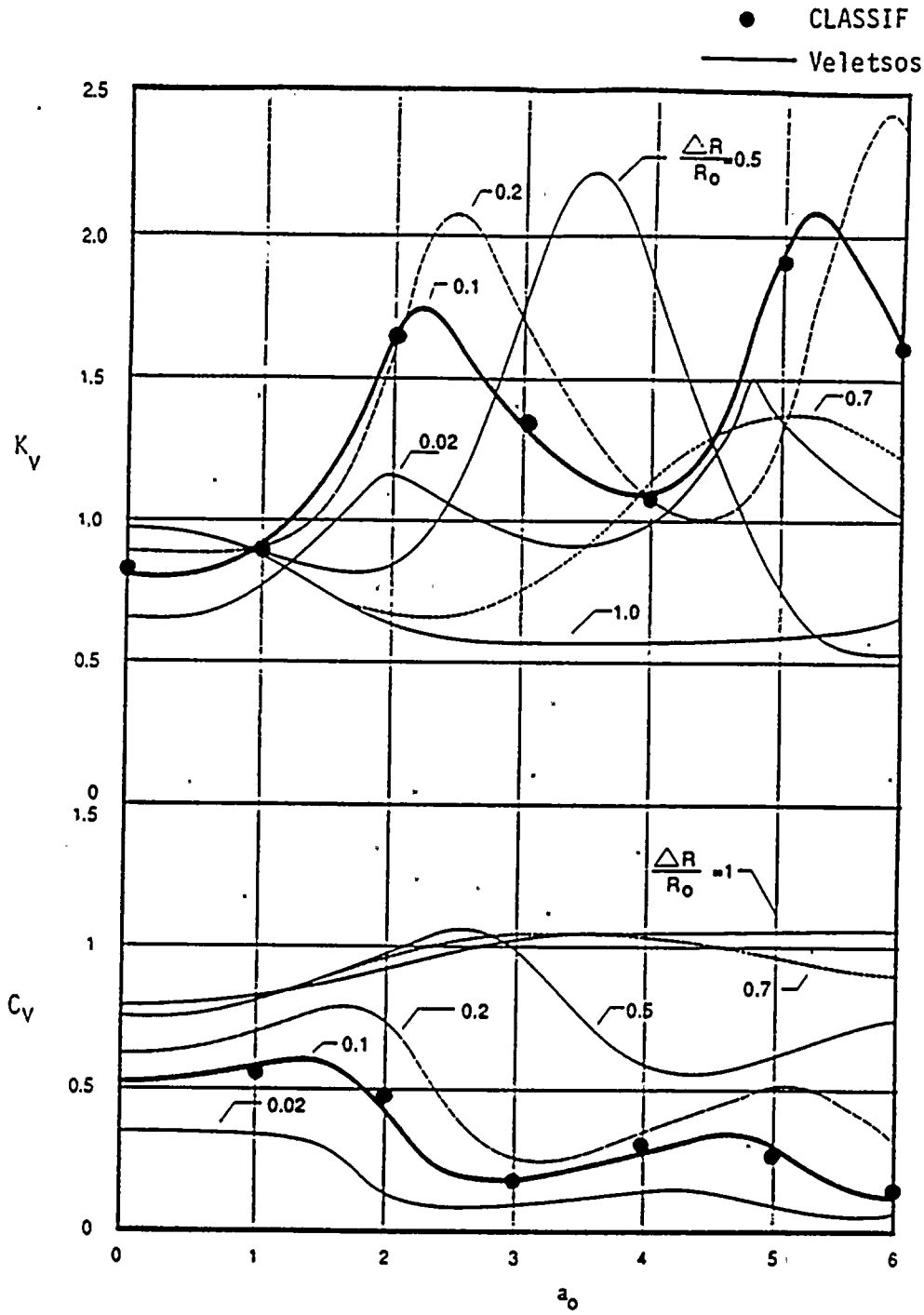

Figure 4.12-2. Stiffness and Damping Coefficients for a Ring Foundation

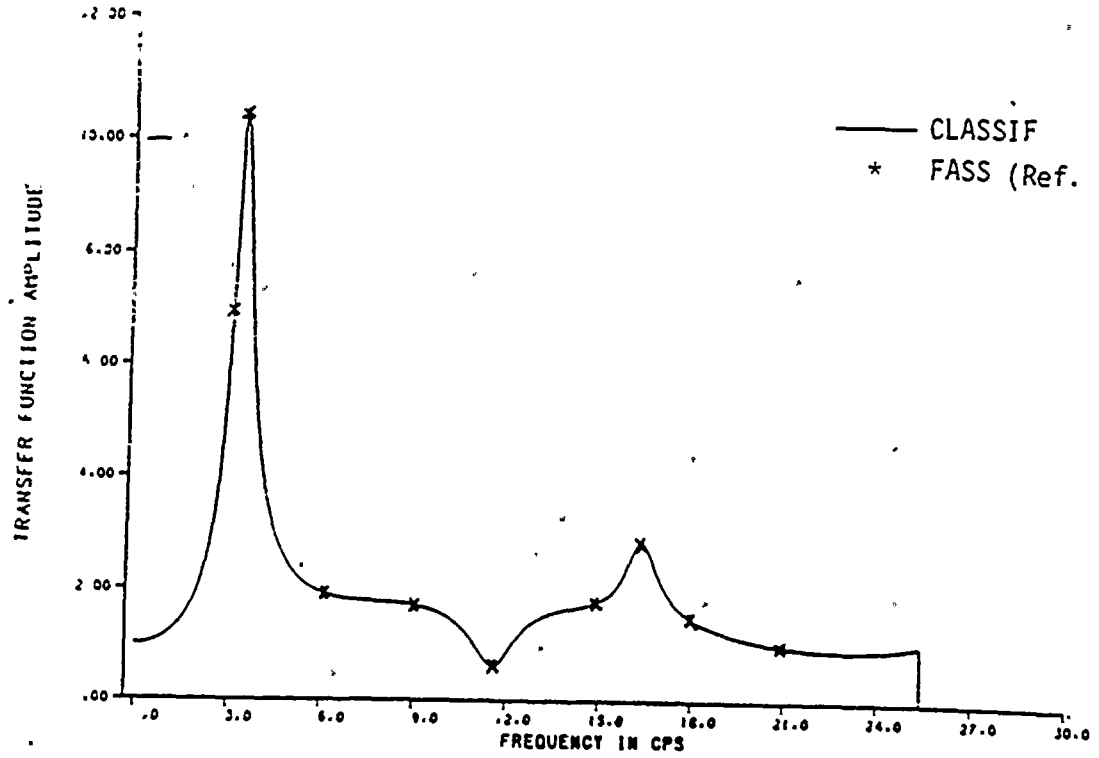

Figure 4.14-1. Transfer Function for Response at Top of Containments

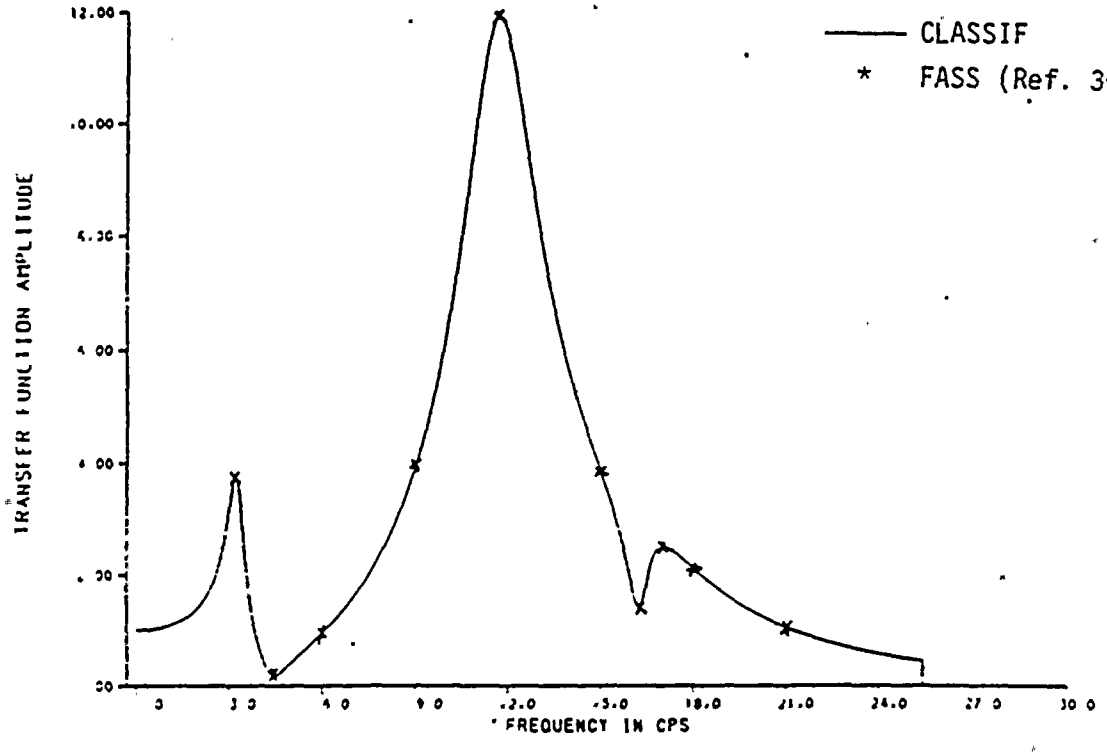

Figure 4.14-2. Transfer Function for Response at Top of Internal Structure

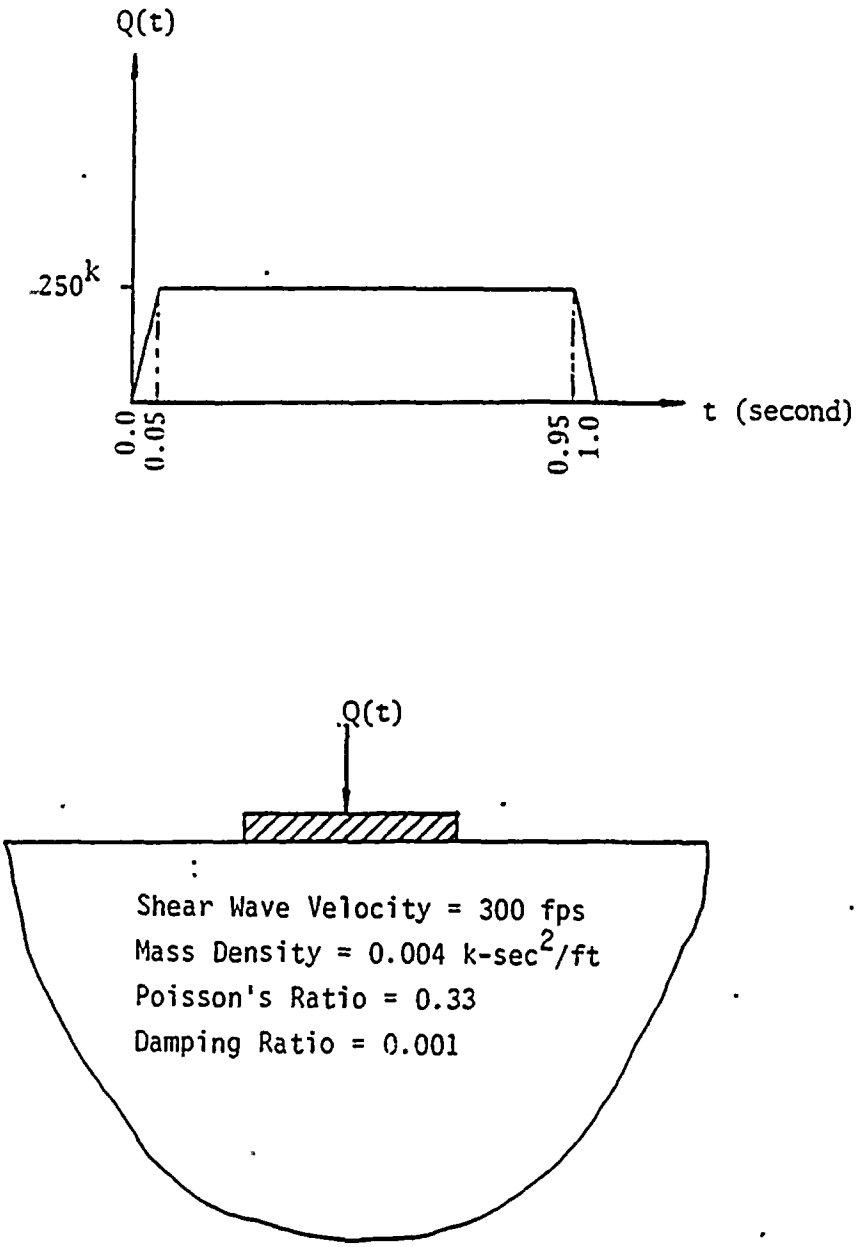

Figure 4.15-1. External Forced Vibration of a Disk Resting on an Elastic Halfspace

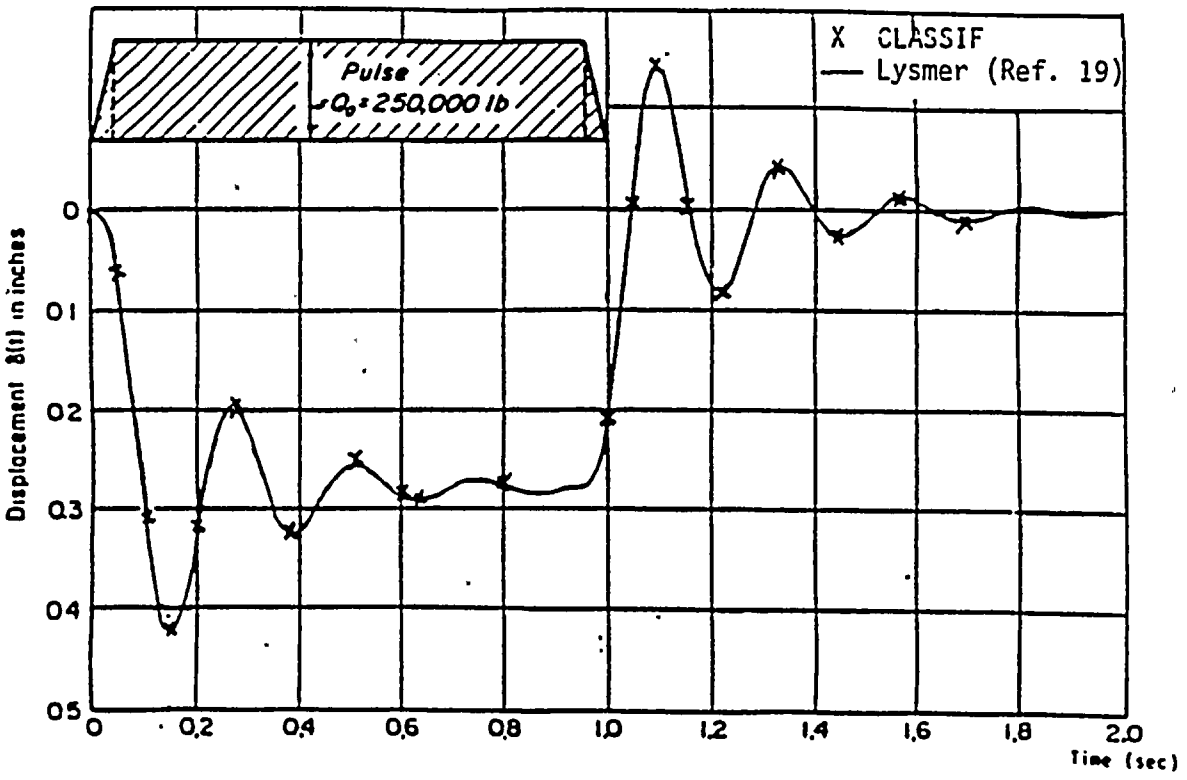

Figure 4.15-2. Response Displacement Time History Due to Trapezoidal Pulse Excitation

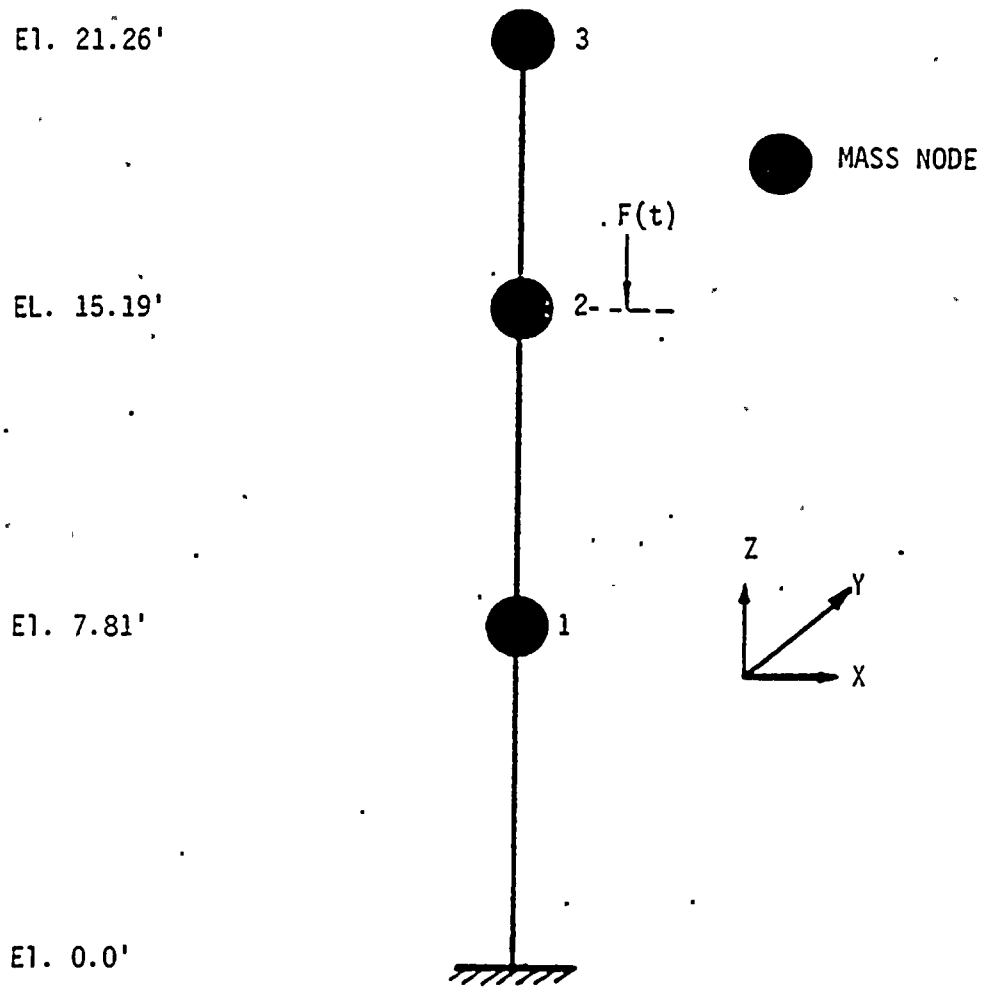

Figure 4.16-1. Lumped-Mass Stick Model of the Scaled Down Experimental Reactor Building Model

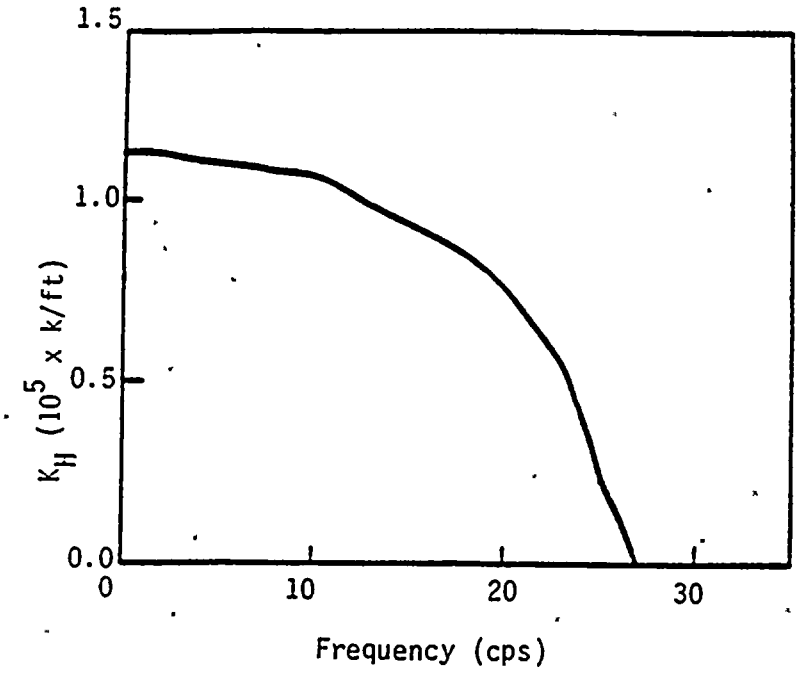

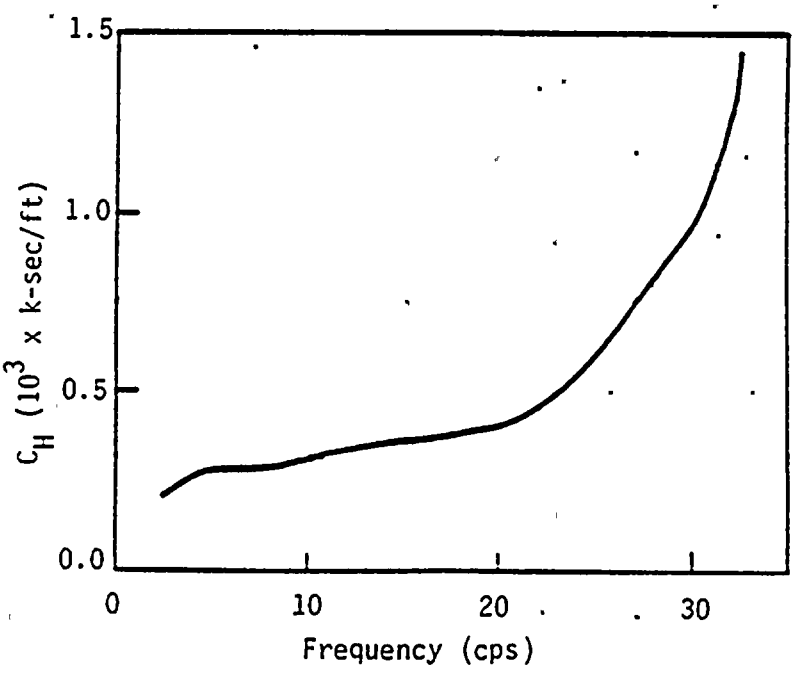

Figure 4.16-2. Horizontal Impedance Function from Experimental ...

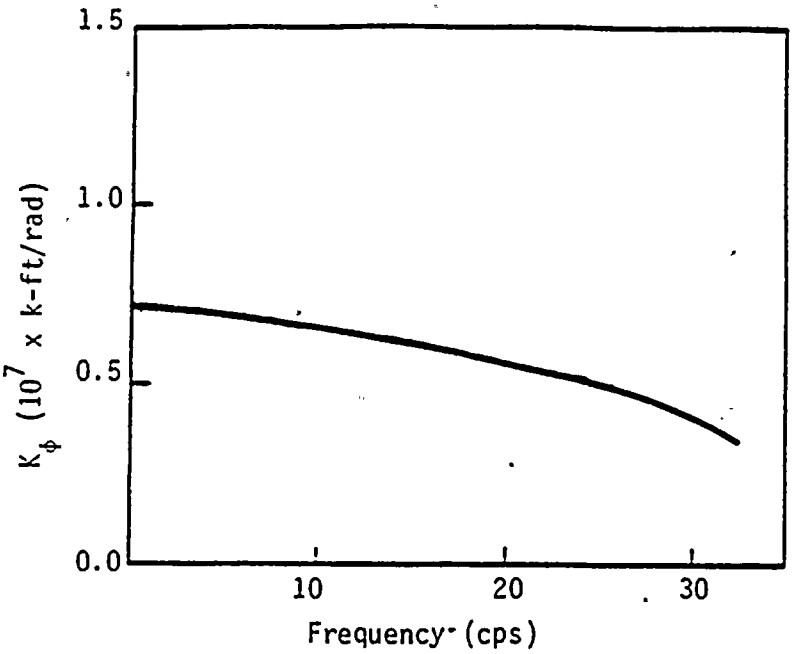

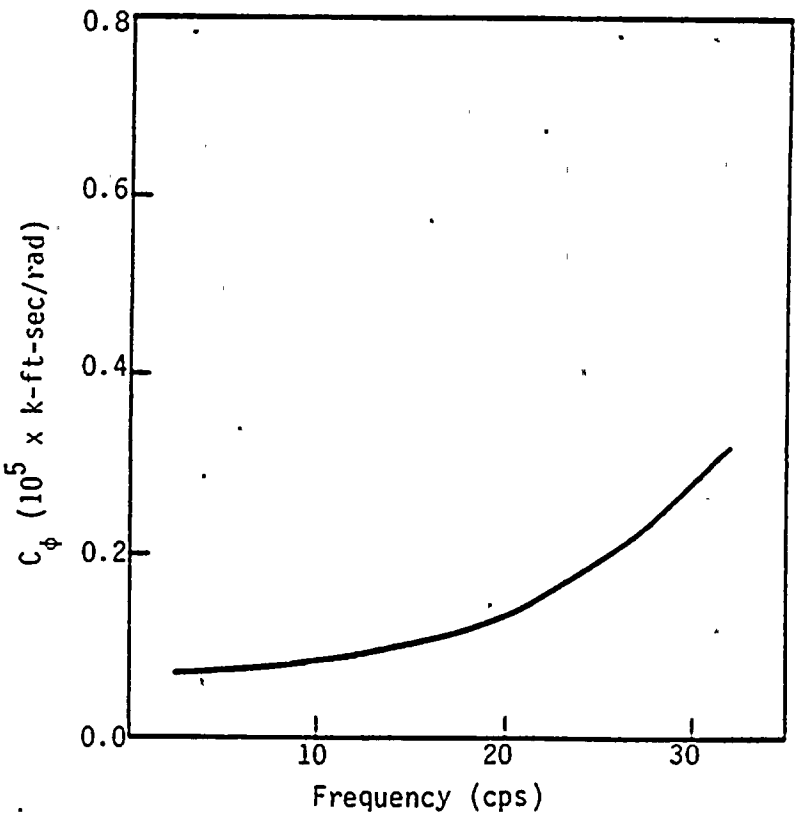

Figure 4.16-3. Rocking Impedance Function from Experimental Test

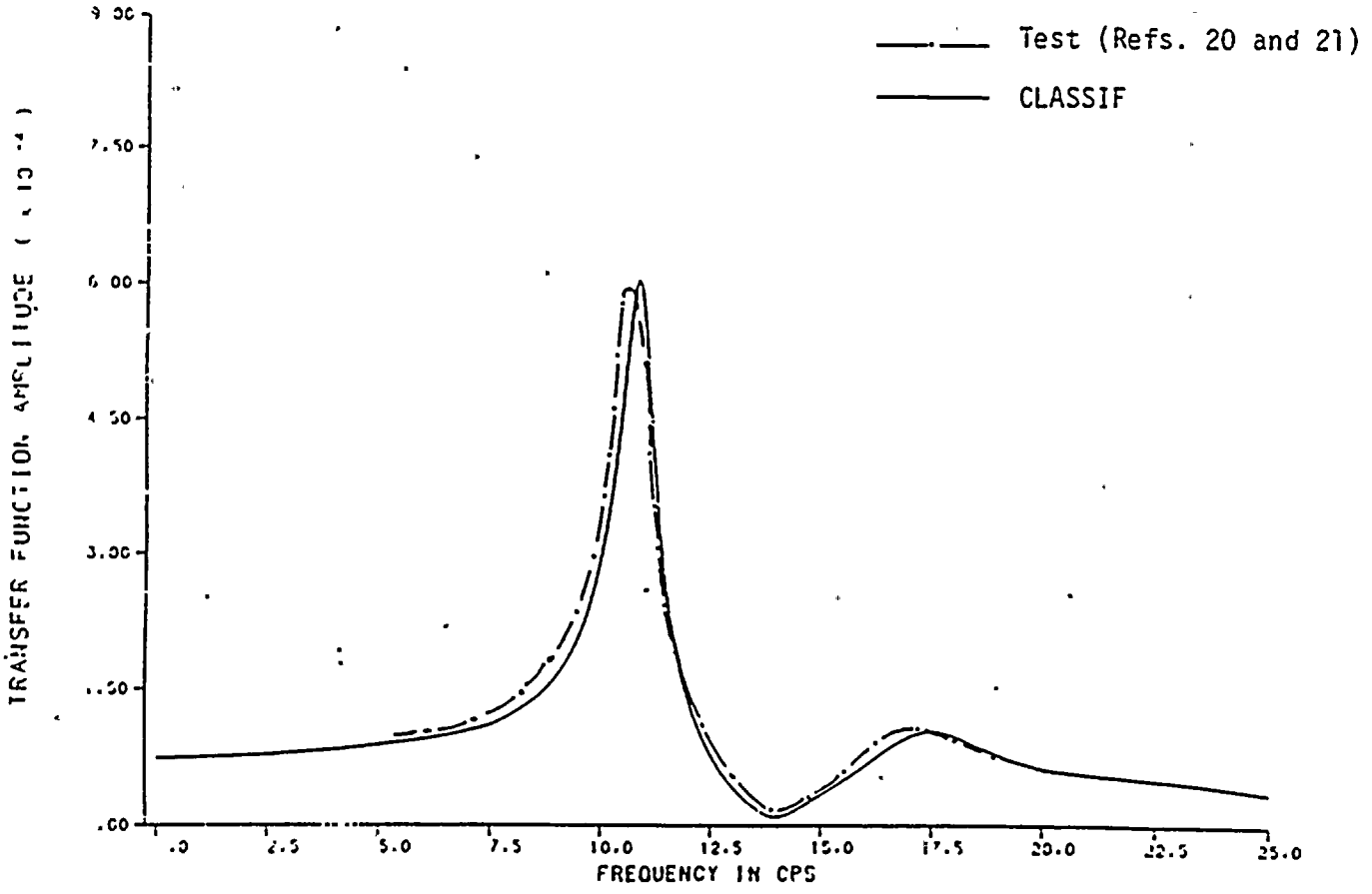

Figure 4.16-4. Comparison of Horizontal Displacement Response Transfer Functions for Node 2

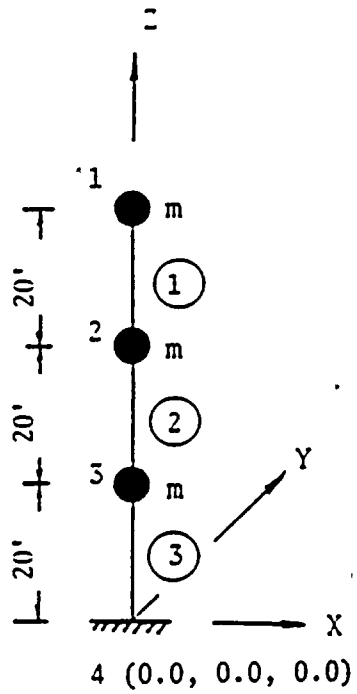

Figure 4.17-1 Fixed Base Structural Model for Problem 17 Case (a)

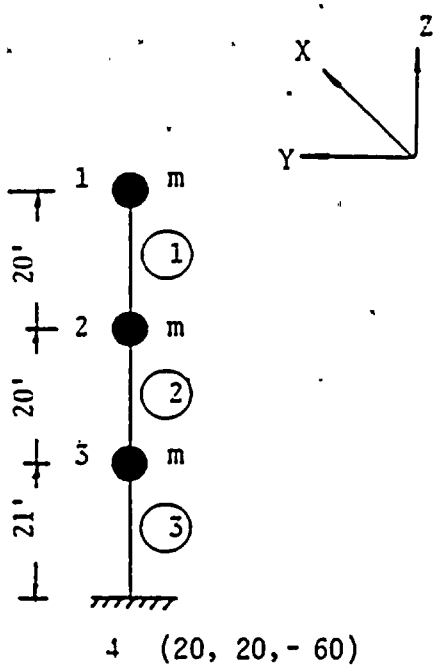

Figure 4.17-2. Fixed Base Structural Model for Problem 17 Case (b)

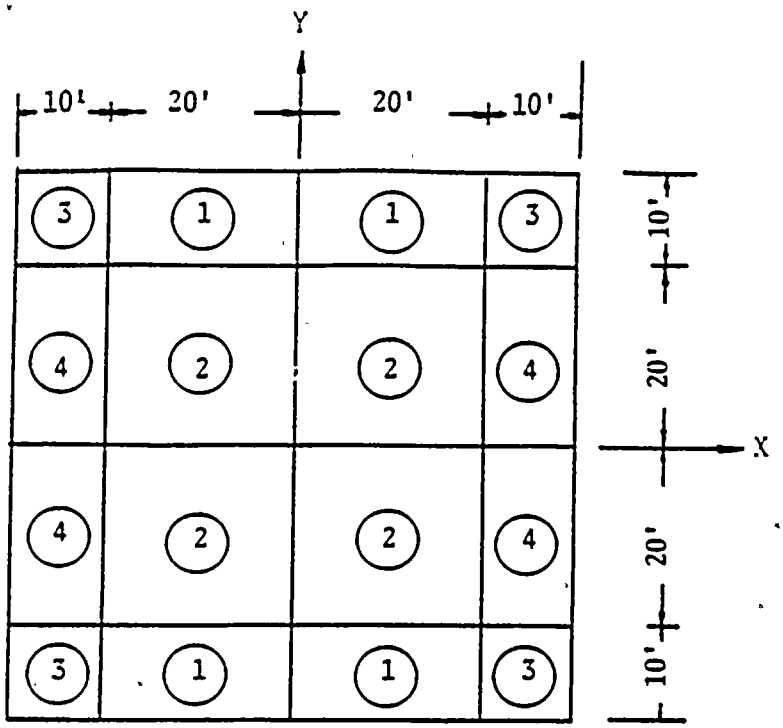

Subregion Type	X-Dimension	Y-Dimension
(1)	10'	20'
(2)	20'	20'
(3)	10'	10'
(4)	20'	10'

Figure 4.17-3. Foundation Model for Problem 17 Case (a)

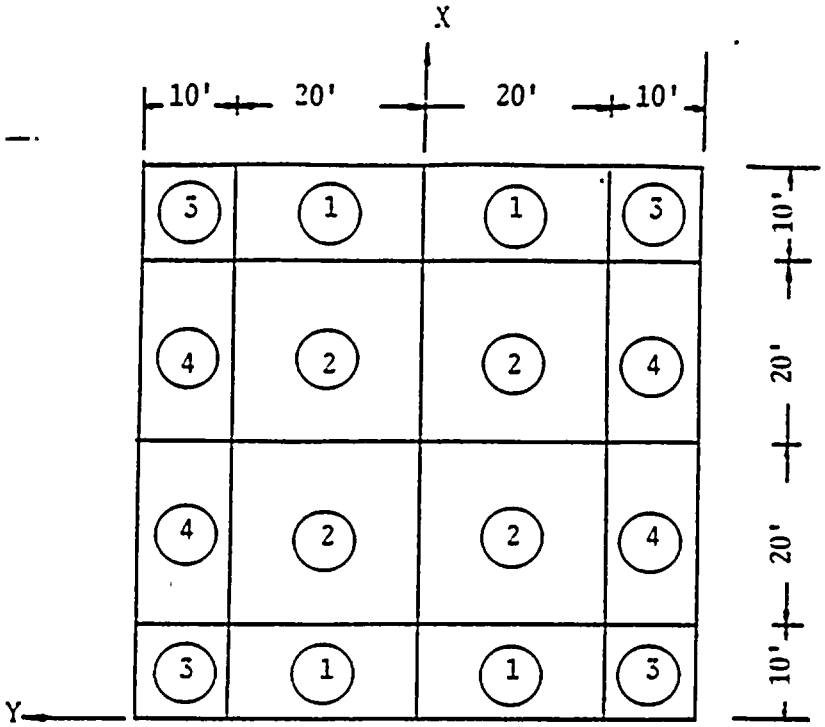

Subregion Type	X-Dimension	Y-Dimension
1	10'	20'
2	20'	20'
3	10'	10'
4	20'	10'

Figure 4.17-4. Foundation Model for Problem 17 Case (b)

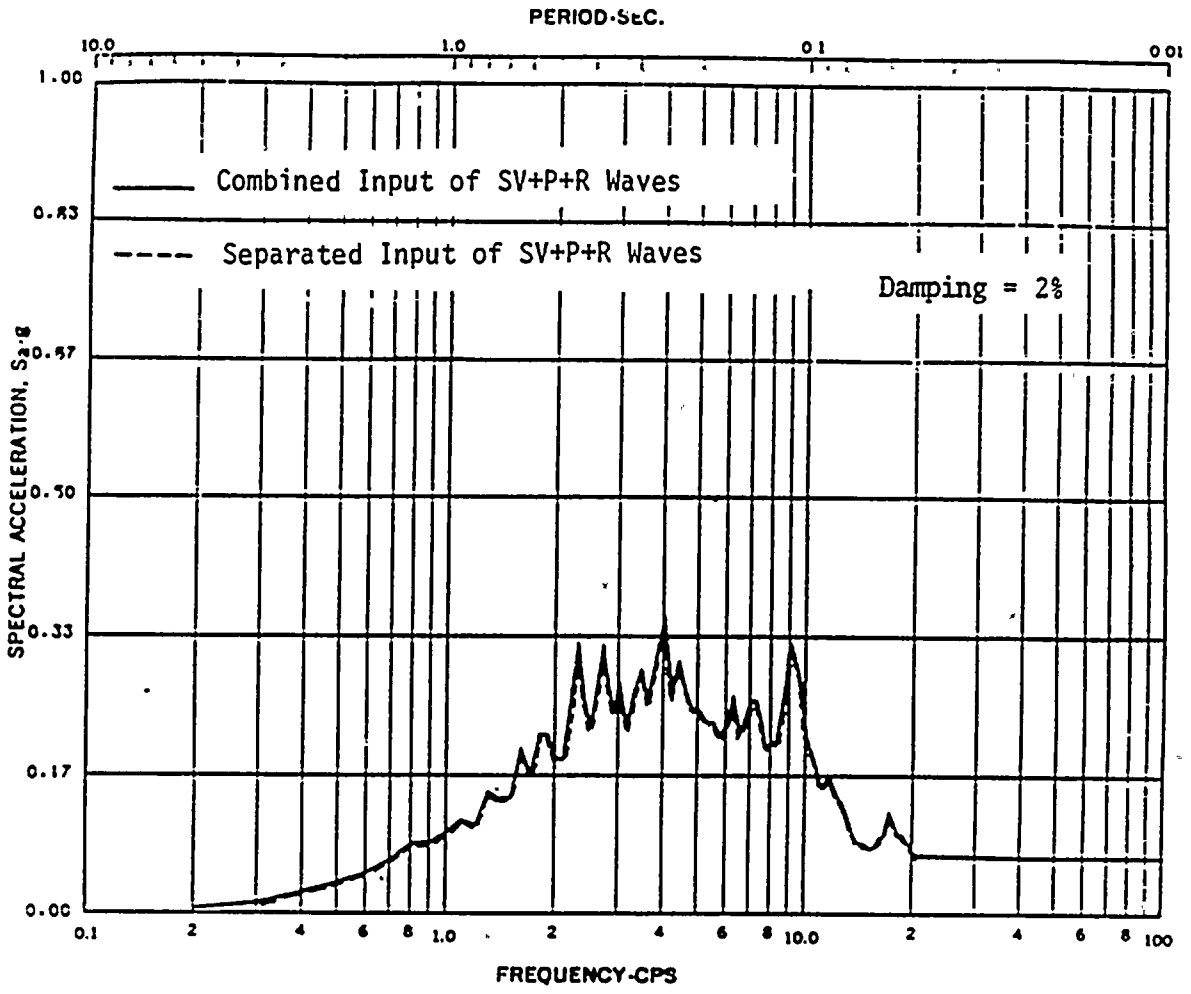

Figure 4.18-1. Horizontal Acceleration Response Spectrum at the Top of Foundation

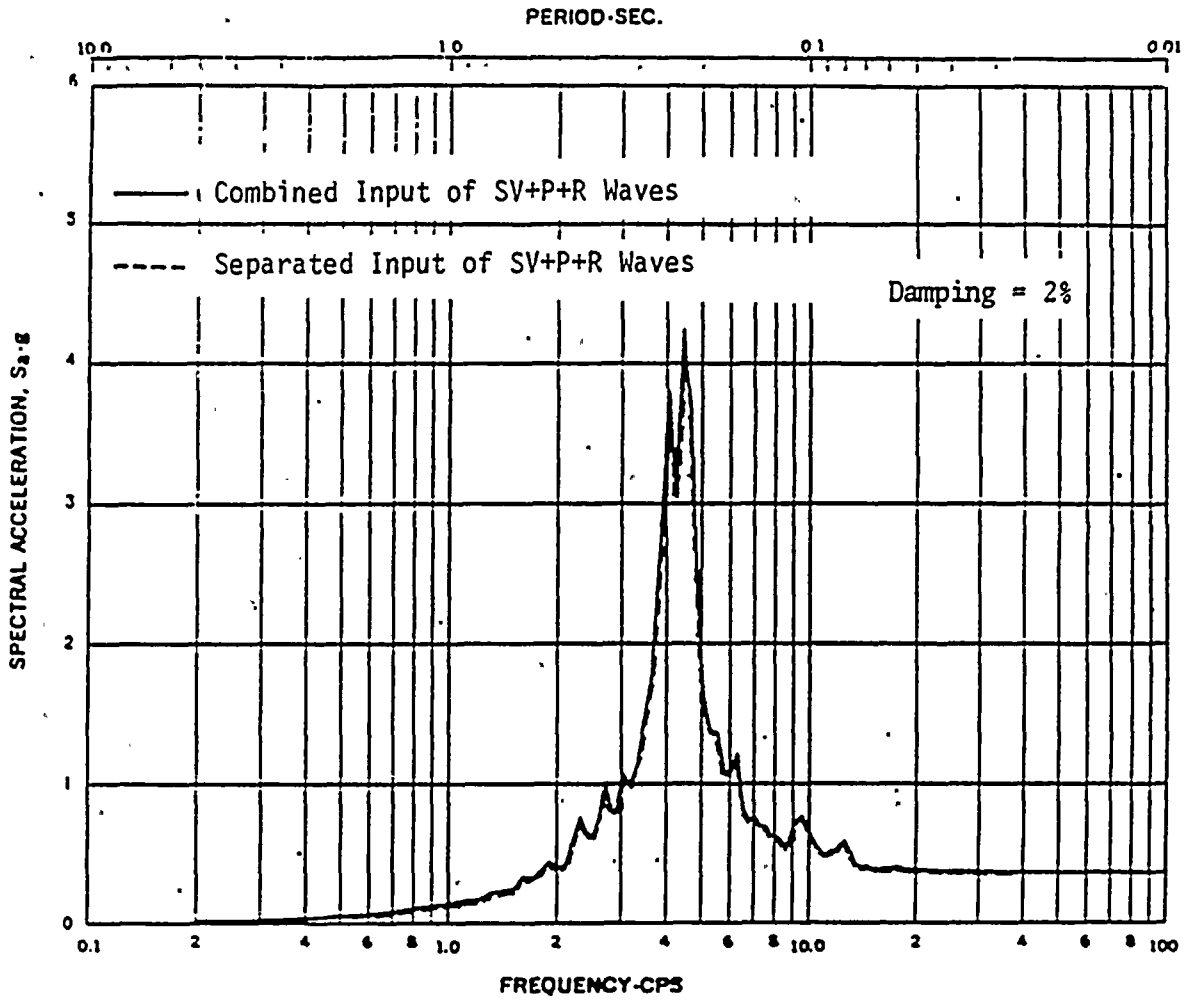

Figure 4.18-2. Horizontal Acceleration Response Spectrum at the Top of Containment Shell

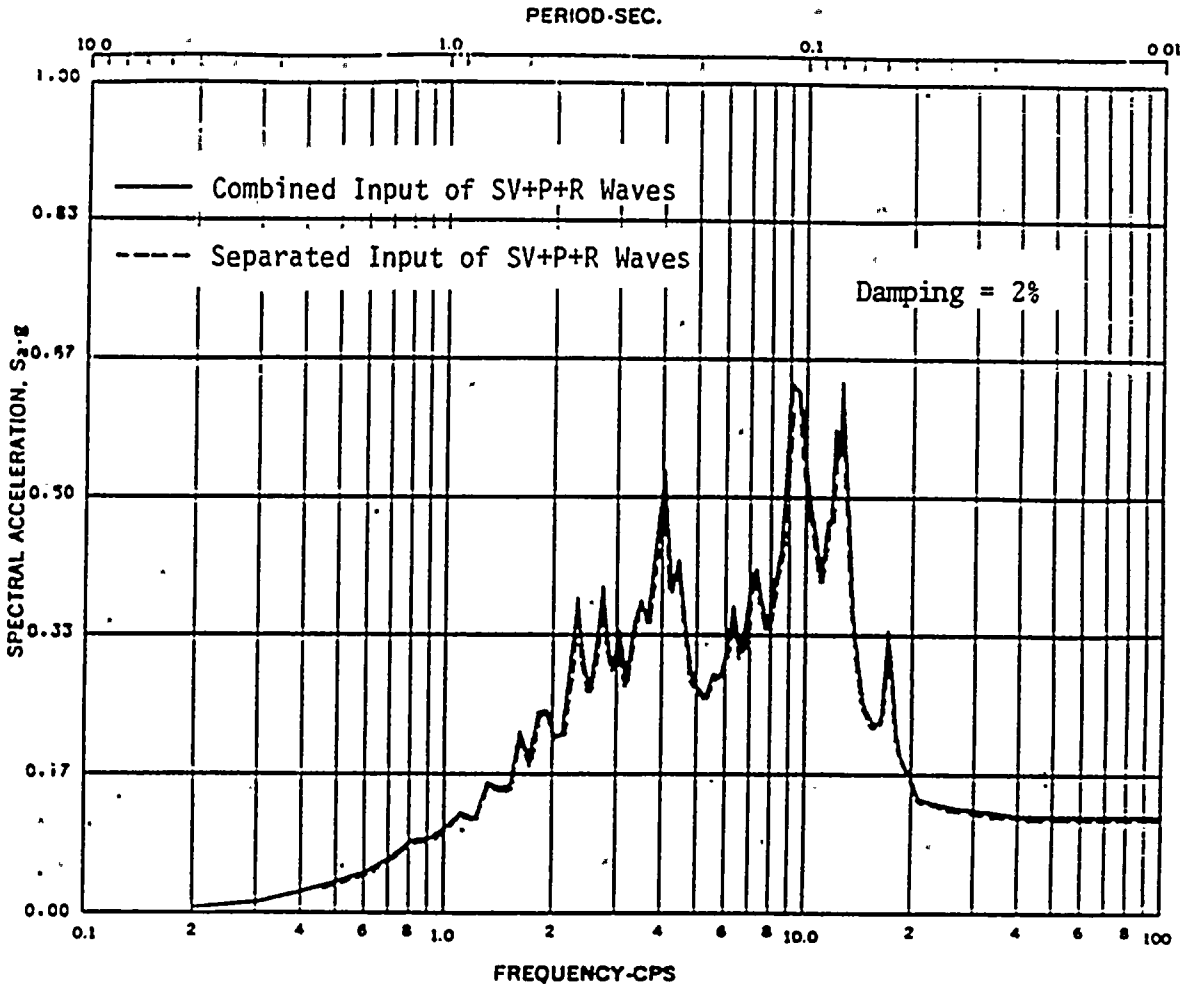

Figure 4.18-3. Horizontal Response Spectrum at the Top of Internal Structure

5. CONCLUSIONS

Based on the comparisons of CLASSIF analysis results with the benchmark solutions for each of the 18 validation test problems with test cases described in this report, it is concluded that the CLASSIF analysis capabilities as identified in Table 3-1 in Section 3.2 have been validated. Thus the program is considered valid for applications to SSI analysis involving those analysis capabilities tested in this validation report.

6. REFERENCES

1. BC-TOP-4A Report, Rev. 3, "Seismic Analyses of Structures and Equipment for Nuclear Power Plants," Bechtel Power Corporation, November 1974.

2. Luco, J. E., "Vibration of a Rigid Disc on a Layered Viscoelastic Medium," Nuclear Engineering and Design, 36, 1976.

3. Tseng, W. S., Computer Program FASS (CE933, Version B1), Bechtel Power Corporation, 1986.

4. Luco, J. E., "Impedance Functions for a Rigid Foundation on a Layered Medium," Nuclear Engineering and Design, 31, 1974.

5. Wong, H. L., and J. E. Luco, "Dynamic Response of Rectangular Foundations to Obliquely Incident Seismic Waves," Earthquake Engineering and Structural Dynamics, 6, 1978.

6. Seed, H. B., and J. Lysmer, "Analyses of Soil-Structure Interaction Effects During Earthquakes for the Diablo Canyon Nuclear Power Station," July 7, 1978.

7. "Computer Program SASSI: Validation Report," Report Prepared for PG&E by Bechtel Power Corporation, July 1988.

8. Wong, H. L., and J. E. Luco, "Dynamic Interaction Between Rigid Foundations in a Layered Halfspace," International Journal of Soil Dynamics and Earthquake Engineering, Vol. 5, No. 3, 1986.

9. Wong, H. L. and J. E. Luco, "Tables of Impedance Functions and Input Motions for Rectangular Foundations," Report No. CE 78-15, Dept. of Civil Engineering, University of Southern California, December 1978.

10. Lysmer, J., Udaka, T., Chan-Feng, T. and Seed, H. B., "FLUSH - A Computer Program for Approximate 3-D Analysis of Soil-Structure Interaction Problems," EERC Report No. 75-30, University of California, Berkeley, November 1975.

11. Dominguez, J., "Dynamic Stiffness of Rectangular Foundations," MIT Research Report R78-20, August 1978.

12. Luco, J. E., and R. A. Westmann, "Dynamic Response of a Rigid Footing Bonded to an Elastic Halfspace," ASME, Journal of Applied Mechanics, June 1972.

13. Gazetas, G. and Roesset, J. M., "Vertical Vibration of Machine Foundation," ASCE, Journal of the Geotechnical Engineering Division, Vol. 105, No. GT12, December 1979.

14. Veletsos, A. S., and Y. T. Wei, "Lateral and Rocking Vibration of Footings," ASCE, Journal of Soil Mechanics and Foundations Division, September, 1971.

15. Veletsos, A. S., and B. Verbic, "Basic Response Functions for Elastic Foundations," ASCE, Journal of the Engineering Mechanics Division, April, 1974.

16. Veletsos, A. S., and Damodaran Nair, V. V., "Torsional Vibration of Viscoelastic Foundations," ASCE Journal of the Engineering Mechanics Division, March, 1974.

17. Veletsos, A. S. and Tang, Y., "Vertical Vibration of Ring Foundations," Structural Report No. 32, Dept. of Civil Engineering, Rice University, Houston, Texas, July 1985.

18. Computer Program DATAN (CE928), Bechtel Power Corporation, 1986.

19. Lysmer, J., "Vertical Motion of Rigid Footings," U.S. Army Engineer Waterways Experiment Station, Corps of Engineers, Vicksburg, Mississippi, 1965.

20. Tanaka, H., Ohta, T., Uchiyama, S., "Experimental and Analytical Studies of a Deeply Embedded Reactor Building Model Considering Soil-Building Interaction (Part 1), SMiRT-5, 1979.

21. Tanaka, H., Ohta, T., Uchiyama, S., "Experimental and Analytical Studies of a Deeply Embedded Reactor Building Model Considering Soil-Building Interaction (Part 2), SMIRT-6, 1981.

22. The letter dated on September 29, 1982 from Hiroshi, Tanaka, Nuclear Power Construction Department of the Tokyo Electric Power Company, Inc. to Wen S. Tseng, San Francisco Power Division, Bechtel Power Corporation.

23. Bechtel Report No. SFPD-C/S-83-02, Rev. 1, "Test Correlation Study for Soil-Structure Interaction Analysis of Embedded Structures," May 1985.

RESPONSE TO QUESTION 2b
Volume 1 of 2

January 1989

This volume is part of a set that responds to 47 questions asked of PG&E by the Nuclear Regulatory Commission (NRC) on December 13, 1988. The responses provide data requested to augment or clarify the Final Report of the Long Term Seismic Program submitted by PG&E to the NRC on July 31, 1988.

RESPONSE TO QUESTION 2b

QUESTION 2b

Provide copies of the following reports referenced in the LTSP Final Report:

b. Bechtel Power Corporation, 1988, "SASSI" Computer Program: Theoretical Manual, User's Manual, and Validation Report.

The SASSI Computer Program Theoretical Manual (Attachment Q2b-1), User's Manual (Attachment Q2b-2) and Validation Manual (Attachment Q2b-3) follow. The "Description of Validation Test Problems and Results," Appendix A of the Validation Manual (Attachment Q2b-4) contains information proprietary to Bechtel Power Corporation. This attachment has been submitted to the NRC separately, with an Application for Withholding Proprietary Information from Public Disclosure, in accordance with 10 CFR 2.790 of the Commission's regulations.

ATTACHMENT Q2b-1

SYSTEM FOR
ANALYSIS OF
SOIL
STRUCTURE
INTERACTION

SASSI THEORETICAL MANUAL

JULY 1988

CE994

BECHTEL POWER CORPORATION

SASSI

A SYSTEM FOR ANALYSIS OF
SOIL-STRUCTURE INTERACTION

THEORETICAL MANUAL

Prepared
for

Diablo Canyon
Long Term Seismic Program
Pacific Gas and Electric Company
San Francisco, California

By

Bechtel Power Corporation
San Francisco, California 94119

July 30, 1988

PREFACE

The computer program SASSI was developed at the University of California, Berkeley, by a research team under the technical direction of Prof. John Lysmer. The CDC and IBM versions of the program were obtained from the University of California, Berkeley, under a license agreement with the University. During the course of installation, testing, and validation of the Bechtel version of the code on the CDC CRAY System, some modifications and enhancements were made to the code to improve the code performance. These include correcting the motion phases in Rayleigh wave calculation, replacing the plate element and providing the option for local end release condition in beam element. The original User's Manual issued by the University was revised to reflect the changes made to the code. A new chapter on application guide was also added to the User's Manual. The IBM version provided to PG&E contains the same modifications and enhancements made to the Bechtel CRAY version to date. The validation and theoretical manuals of the program were also prepared to complete the documentations of the program. The modifications and enhancements and preparation of the validation and theoretical manuals have been performed by the Civil/Structural Staff Group of Bechtel Power Corporation, San Francisco Office.

This manual has been prepared by Bechtel Power Corporation and has been reviewed following the Bechtel Standard Engineering Department Procedure for Nuclear Projects.

This manual was prepared under a contract agreement between PG&E and Bechtel and is intended for the exclusive use by PG&E only. Except for copies that may be required for the Nuclear Regulatory Commission (NRC) in satisfying a regulatory requirement, no copy should be distributed outside of PG&E without prior written consent from Bechtel.

DISCLAIMER

Every reasonable effort was made to provide a comprehensive and flexible computer program. However, the computer program itself and associated documentation are supplied without representation of warranty, expressed or implied, as to its content, accuracy, or freedom from defects or errors.

TABLE OF CONTENTS

TABLE OF CONTENTS (Cont'd)

1. INTRODUCTION

The computer program SASSI was developed in the University of California, Berkeley, by a research team consisting of 4 doctoral students under the direction of Prof. J. Lysmer. The theory and the analytical methods described in this manual are extracted from the 4 doctoral dissertations (Refs. 12, 22, 23, 25). A brief description of the theory and the program was first published in Ref. 11. This manual contains the basic description of the analytical methods and computational steps used in the program. Complete descriptions on various parts of the theory used by the program may be obtained from the 4 dissertations cited.

This manual is prepared in 8 sections. In Section 2, an overview of the substructuring methods of soil-structure interaction (SSI) analysis is presented. Following this background discussion, the flexible-volume substructuring method, the equations of motion, and the computational steps used by SASSI are then fully described.

Section 3 presents the theory and techniques used by SASSI to solve the site response problem. The models along with the equations of motion used to solve for the body and surface waves are described. Formulation of the transmitting boundary matrices for two dimensional and axisymmetric problems, the techniques for halfspace simulation and the methods for incorporating the dynamic soil properties are also presented.

In Section 4, the method used by SASSI to solve the impedance problem is presented. This includes descriptions of the analytical models used for computing the impedance matrix for two- and three-dimensional problems.

Section 5 describes the techniques for modelling the superstructure and basement in accordance with the flexible-volume substructuring technique. The analysis technique used by SASSI to obtain the steady state and transient dynamic response are described in Section 6, including the interpolation technique used in calculating the response transfer functions.

Finally, Section 7 presents the SASSI computer program layout and operational features. It also presents a brief summary of program validation and the example applications of the program to practical engineering problems.

2. THE FLEXIBLE-VOLUME SUBSTRUCTURING METHOD

2.1 Substructuring Methods of SSI Analysis

The soil-structure interaction problem is most conveniently analyzed using a substructuring approach. In this approach, the linear soil-structure interaction problem is subdivided into a series of simpler sub-problems. Each sub-problem is solved separately and the results are combined in the final step of the analysis to provide the complete solution, based on the principle of superposition.

For the case of structures with surface foundations for which the structure and the foundation interface boundary is on the surface of the foundation medium, the substructuring method is relatively simple and many solution techniques are available. For structures with embedded foundations, the substructuring method becomes considerably more complicated. Conceptually, these methods can be classified into three types depending on how the interaction at the soil and structure interface degrees-of-freedom is handled (Ref. 10). These three types are: 1) the rigid boundary method; 2) the flexible boundary methods, and 3) the flexible volume method. The seismic SSI sub-problems that these three types of substructuring methods are required to solve to obtain the final solution, are compared in Fig. 2.1-1. As shown in this figure, the solution for the site response problem is required by all three methods. This is, therefore, common to all methods. The analysis of the structural response problem is also required and involves essentially the same effort for all methods. The necessity and effort required for solving the scattering and impedance problems however, differ significantly among the different methods. For the rigid-boundary and the flexible-boundary methods, two explicit analyses are required separately for solving the scattering and impedance problems. On the other hand, the flexible-volume method, because of its unique substructuring technique as will be described in Section 2.2,

requires only one impedance analysis and the scattering analysis is eliminated. The SASSI computer program adopts this flexible-volume method of substructuring.

2.2 The Flexible Volume Substructuring Method

The flexible volume substructuring method is based on the concept of partitioning the total soil-structure system as shown in Fig. 2.2-1a into two substructure systems as shown in Fig. 2.2-1b and 2.2-1c. The substructure (b) consists of the original site, and the substructure (c) consists of the structure and basement minus the excavated soil which is replaced with the basement. The substructures (b) and (c) when combined together, form the original SSI system shown in Fig. 2.2-1a. The equations of motion for the total SSI system are formulated for substructure (c) in combination with the solution obtained from substructure (b). The theory and formulation that develop in the following are equally applicable to two- and three-dimensional SSI systems.

2.2.1 Equations of Motion

The equations of motion for the SSI system shown in Fig. 2.2-1c can be written in the following matrix form:

$$[M] \{\ddot{\hat{U}}\} + [K] \{\hat{U}\} = \{\hat{Q}\} \qquad (2.2\text{-}1)$$

where [M] and [K] are the total mass and stiffness matrices, respectively. $\{\hat{U}\}$ is the vector of total nodal point displacements and $\{\hat{Q}\}$ are the forces due to applied external dynamic forces or seismic excitations.

For the harmonic excitation at frequency ω, the load and the displacement vectors can be written as

$$\{\hat{Q}\} = \{Q\} \exp(i\omega t) \qquad (2.2\text{-}2)$$

and

$$\{\hat{U}\} = \{U\} \exp(i\omega t) \tag{2.2-3}$$

where $\{Q\}$ and $\{U\}$ are the complex force and displacement vectors at frequency ω. Hence, for each frequency, the equations of motion take the form

$$[C]\{U\} = \{Q\} \tag{2.2-4}$$

where $[C]$ is a complex frequency-dependent dynamic stiffness matrix:

$$[C] = [K] - \omega^2[M] \tag{2.2-5}$$

Using the following subscripts, which refer to degrees of freedom associated with different nodes (see Fig. 2.2-1):

Subscript	Nodes
s	superstructure excluding basement nodes
i	basement
f	excavated soil

equation (2.2-4) is partitioned as follows:

$$\begin{bmatrix} C_{ss} & C_{si} \\ C_{is} & (C_{ii} - C_{ff} + X_{ff}) \end{bmatrix} \cdot \begin{Bmatrix} U_s \\ U_f \end{Bmatrix} = \begin{Bmatrix} 0 \\ [X_{ff}] \cdot \{U_f\} \end{Bmatrix} \tag{2.2-6}$$

The term $(C_{ii} - C_{ff})$ simply indicates the stated partitioning according to which the stiffness and mass of the excavated soil are subtracted from the dynamic stiffness of the structure. For embedded structures number of interacting nodes in the basement of the structure (i) are smaller or equal to the number of interacting nodes in the excavated

volume of the soil (f). The frequency-dependent matrix $[X_{ff}]$ is called the impedance matrix which is obtained from the model in substructure b using the methods which will be described in Section 4. The vector $\{U'_f\}$ is computed from the free-field motion for the interacting nodes shown in substructure b. The motion is a function of prescribed wave field in the free-field. The methods for solving the site response problem for body and surface waves are described in Section 3.

If the source of excitation is applied dynamic loading within the model, as in the case of foundation vibrations impact loads, and wind loads, the free field motions $\{U_f\}$ vanish and Eq. (2.2-6) can be written as

$$\begin{bmatrix} C_{ss} & C_{si} \\ C_{is} & (C_{ii} - C_{ff} + X_{ff}) \end{bmatrix} \begin{Bmatrix} U_s \\ U_f \end{Bmatrix} = \begin{Bmatrix} P_s \\ P_f \end{Bmatrix} \qquad (2.2\text{-}7)$$

where the load vector has non-zero terms only where external loads are applied.

Seismic and external loads can, in principle, be considered together by simply adding the external loads $\{P\}$ to the load vector in Eq. (2.2-6). This method is not used in SASSI, since in practice, the seismic excitations and the external loads are seldom considered simultaneously.

2.2.2 Computational Steps

Based on the formulation presented previously, soil structure interaction problem subjected to the seismic or external force excitation can be solved in the frequency domain according to the following five main steps:

1. Solve the site response problem. For the seismic excitation, this step involves determining the free-field displacement amplitudes $\{U'_f\}$ only for the interacting nodes within the excavated volume using the model of substructure (b) shown in Fig. 2.2-1. For each frequency of analysis, the free-field displacement vector is a function of specified wave field (body or surface wave and incidence angle) and location of control point in the free-field soil system. Methods used for site response analysis are described in Section 3. The free-field displacement need not be computed for SSI problems subjected to external force excitation (see Eq.[2.2-7]).

2. Solve the impedance problem. This step involves determining the impedance matrix $[X_{ff}]$ which is a complex stiffness matrix corresponding to interacting nodes in free-field soil medium of substructure (b) in Fig. 2.2-1. Methods used for impedance analysis are described in Section 4.

3. Form the load vector. For the seismic excitation, the load vector in Eq. (2.2-6) can be obtained from the solutions of Steps 1 and 2 in accordance with Eq. (2.2-6). For the external force excitation, this step simply consists of forming the load vector in accordance with Eq. (2.2-7).

4. Form the complex stiffness matrix. This step, which is identical for the seismic or external force excitation involves forming the coefficient matrix in Eqs. (2.2-6) or (2.2-7). The method used for computing the mass and stiffness matrices used in the coefficient matrix are described in Section 5.

5. Solve the system of linear equations of motion of Eq. (2.2-6) or (2.2-7). The methods used to compute the steady state response and transient responses are described in Section 6.

   The flexible volume substructuring method described previously has recently been extended to handle the SSI problems involving pile foundations. Since the program modules for handling pile foundations have not been implemented in the version of SASSI described herein, the theory and the corresponding analysis steps are not presented in this manual but they may be obtained from Refs. 12 and 13.

Method	Rigid Boundary	Flexible Boundary	Flexible Volume
Site Response Problem	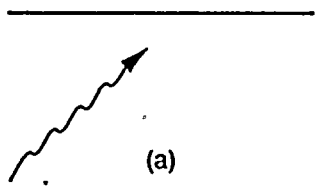	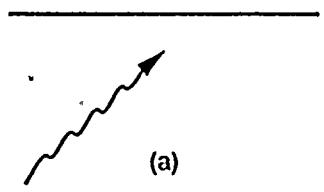	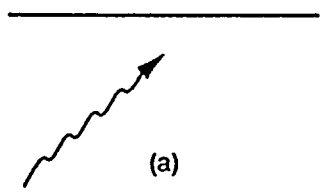
Scattering Problem	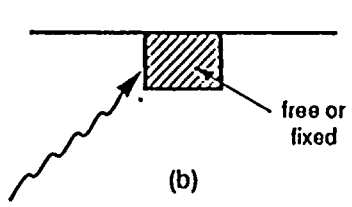	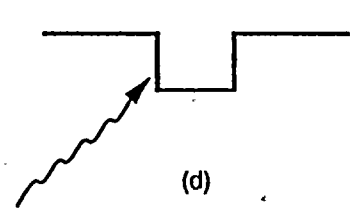	none
Impedance Problem (● Loaded Node)		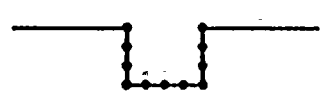	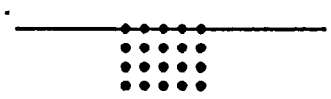
Structural Response Problem	Standard	Standard +	Standard +

Figure 2.1-1. Summary of Substructure Methods

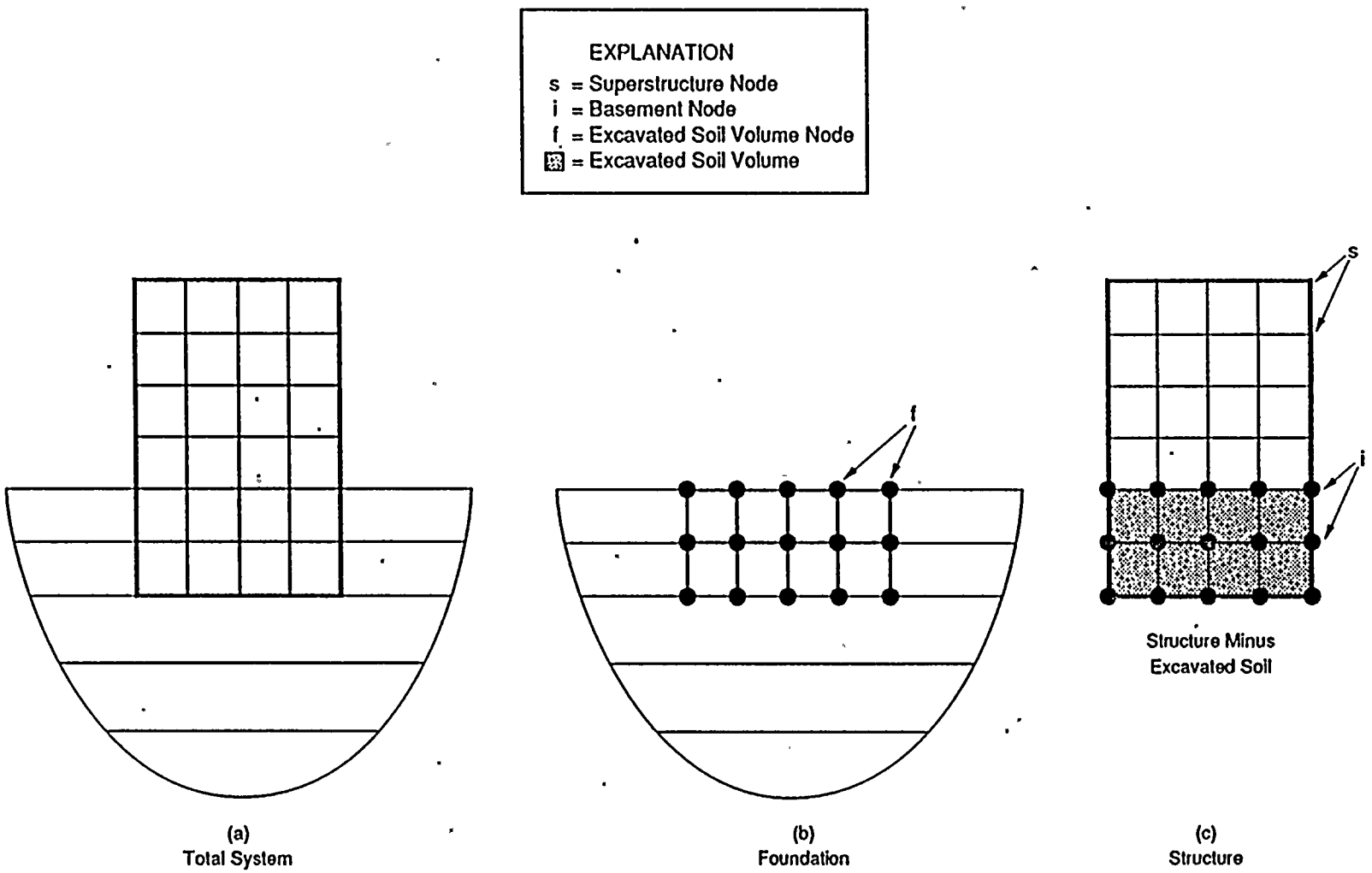

Fig. 2.2-1. Substructuring in the Flexible Volume Method

3. SITE RESPONSE ANALYSIS

For seismic excitation, as shown in the equation of motion in Eq. (2.2-6) the free-field motion at interacting nodes, U_f, must be computed. For this computation, substructure (b) in Fig. 2.2-1 is used and the free-field motion is assumed to result from a combination of coherent plane wave fields which may include P, SV and SH body waves or Rayleigh and Love surface waves. The following sections describe the analytical model and the analysis methods used to solve the site response problem. The techniques used to simulate the halfspace boundary condition at base and to characterize the dynamic soil properties in the formulation are also presented.

3.1. Site Response Analysis Model

The original site before the soil excavation to accommodate the structure is assumed to consist of horizontal soil layers overlaying either a rigid base or an elastic halfspace using the techniques to simulate the halfspace boundary condition at the base as described in Section 3.5. The soil material properties for the soil layer system are assumed to be viscoelastic with the complex modulus representation of the stiffness and damping properties of the soil layers. However, the stiffness and damping of each layer may be adjusted using the equivalent linear method to consider the strain-dependency of the properties, as will be described in Sections 3.6 and 3.7.

To solve the site response problem for surface waves, it is necessary to form and solve the eigenvalue problem for the site model. Furthermore, the submatrices computed from the properties of each layer to form the eigen equation are also used for body wave calculation. For these reasons, the eigen value problem for site model is discussed first.

3.2 Eigenvalue Problem for Site Model

Based on the horizontally layered site model described above and the assumption of linear variations of displacement within each layer, Waas (Ref. 26) has formulated the eigenvalue problem for the system. The eigenvalue problem can be subdivided into two uncoupled algebraic eigenvalue problems; one for generalized Rayleigh wave motion and another for generalized Love wave motions. A brief description of these two eigen equations which are in effect a reduced form of the equation of motion for the site model is presented as follows.

3.2.1 Eigenvalue Problem for Generalized Rayleigh Wave Motion

Using the discretized soil model shown in Fig. 3.2-1(a), the eigen equation for generalized Rayleigh wave motion may be written as

$$([A]k^2 + i[B]k + [G] - \omega^2 [M])\ \{V\} = 0 \qquad (3.2\text{-}1)$$

In this model there are 2 degrees-of-freedom associated with each layer interface with total of 2n degree-of-freedom for a n layer system. In the above equation ω is the circular frequency which is the frequency at which the model is excited, k is the eigenvalue known as the wave number and {V} is the associated eigen vector with 2n components the matrices [A], [B], [G], and [M] are of order 2n x 2n and they are assembled from submatrices for the soil layers according to the scheme shown in Figure 3.2-2. Each submatrix corresponds to a soil layer. Denoting the thickness of the j^{th} layer from the top by h_j, the mass density of ρ_j, the shear modulus by G_j, and the Lame's constant by λ_j, these layer submatrices are:

$$[A_j] = \frac{h_j}{6} \begin{bmatrix} 2(\lambda_j + 2G_j) & 0 & (\lambda_j + 2G_j) & 0 \\ 0 & 2G_j & 0 & G_j \\ (\lambda_j + 2G_j) & 0 & 2(\lambda_j + 2G_j) & 0 \\ 0 & G_j & 0 & 2G_j \end{bmatrix} \qquad (3.2\text{-}2)$$

$$[B_j] = 1/2 \begin{bmatrix} 0 & -(\lambda_j - G_j) & 0 & (\lambda_j + G_j) \\ (\lambda_j - G_j) & 0 & (\lambda_j + G_j) & 0 \\ 0 & -(\lambda_j + G_j) & 0 & (\lambda_j - G_j) \\ -(\lambda_j + G_j) & 0 & -(\lambda_j - G_j) & 0 \end{bmatrix} \quad (3.2\text{-}3)$$

$$[G_j] = \frac{1}{h_j} \begin{bmatrix} G_j & 0 & -G_j & 0 \\ 0 & (\lambda_j + 2G_j) & 0 & -(\lambda_j + 2G_j) \\ -G_j & 0 & G_j & 0 \\ 0 & -(\lambda_j + 2G_j) & 0 & (\lambda_j + 2G_j) \end{bmatrix} \quad (3.2\text{-}4)$$

$$[M_j]^{(c)} = \frac{\rho_j h_j}{6} \begin{bmatrix} 2 & 0 & 1 & 0 \\ 0 & 2 & 0 & 1 \\ 1 & 0 & 2 & 0 \\ 0 & 1 & 0 & 2 \end{bmatrix} \quad (3.2\text{-}5a)$$

$$[M_j]^{(\ell)} = \frac{\rho_j h_j}{2} \begin{bmatrix} 1 & 0 & 0 & 0 \\ 0 & 1 & 0 & 0 \\ 0 & 0 & 1 & 0 \\ 0 & 0 & 0 & 1 \end{bmatrix} \quad (3.2\text{-}5b)$$

The matrices $[M_j]^{(c)}$ and $[M_j]^{(\ell)}$ are the consistent and lump mass matrices, respectively. The mass matrix used in Eq. (3.1-1) is a combination of one-half lump mass matrix and one-half consistent mass matrix (see Section 5.4 for further description). Using the numerical techniques developed by Waas (Ref. 26), the eigenvalue in Eq. (3.2-1) can be solved. The solution yields to 2n Rayleigh modes and 2n wave numbers which will be used in computing the transmitting boundary condition for the wave motions moving in the plane of the site model.

3.2.2 Eigenvalue Problem for Generalized Love Wave Motion

Based on the n horizontally layered soil model shown in Fig. 3.2-1(b), the eigenvalue problem for generalized Love wave motion may be written in the form

$$([A]k^2 + [G] - \omega^2[M])\{V\} = 0 \qquad (3.2\text{-}6)$$

In this wave mode, only one degree-of-freedom associated with each layer interface is required. The matrices [A], [B], [G], and [M] in Eq. (3.2-6) are assembled in a similar manner from the 2 x 2 layer submatrices defined below.

$$[A_j] = h_j G_j \begin{bmatrix} 1/3 & 1/6 \\ 1/6 & 1/3 \end{bmatrix} \qquad (3.2\text{-}7)$$

$$[G_j] = \frac{G_j}{h_j} \begin{bmatrix} 1 & -1 \\ -1 & 1 \end{bmatrix} \qquad (3.2\text{-}8)$$

$$[M_j](c) = \frac{\rho_j h_j}{6} \begin{bmatrix} 2 & 1 \\ 1 & 2 \end{bmatrix} \qquad (3.2\text{-}9a)$$

$$[M_j]( ) = \frac{\rho_j h_j}{2} \begin{bmatrix} 1 & 0 \\ 0 & 1 \end{bmatrix} \qquad (3.2\text{-}9b)$$

The mass matrix used in Eq. (3.2-6) is similarly a combination of one-half lump mass matrix and one-half consistent mass matrix. The solution of eigen equation of Eq. (3.2-6) yields n Love wave mode shapes with the associated wave numbers which will be used in computing the transmitting boundary condition for the wave motions moving out of the plane of the site model.

3.3 Transmitting Boundary Matrices

Transmitting boundaries are formulated by using exact analytical solution in the horizontal direction and a displacement function

consistent with the finite element representation in the vertical direction. These boundaries accurately transmit energy in horizontal directions. Development of these boundaries are central to the development of impedance matrix which is presented in Section 4. Formulation of these boundary matrices for two-dimensional and axisymmetric problems are separately described in the following subsections.

3.3.1 Transmitting Boundary Matrix for Two-Dimensional Problems

Using the eigenvalues and eigen vectors obtained for the generalized Rayleigh wave motion, and using the stress-strain relationship in each layer, Waas (Ref. 26) has formulated the force-displacement relationship in the frequency domain for the layered system as follows:

$$\{P\} = [R]\ \{U\} \tag{3.3-1}$$

where $\{U\}$ is the vector of 2n displacement and $\{P\}$ are the associated forces and $[R]$ is the dynamic stiffness of the semi-infinite layered region that can be obtained from

$$[R] = i[A]\ [V]\ [K]\ [V]^{-1} + [D] \tag{3.3-2}$$

In the above equation all matrices are of order 2n X 2n, matrix $[A]$ is defined in Section 3.2.1, matrix $[V]$ is the matrix containing all 2n mode shapes and matrix $[K]$ is the diagonal matrix containing the wave numbers (eigenvalues) of the generalized Rayleigh wave motion. Matrix $[D]$ is assembled from the properties of each layer in the same manner as that described in Section 3.2-1. The matrix for the j^{th} layer can be written as:

$$[D_j] = \frac{1}{2} \begin{bmatrix} 0 & \lambda_j & 0 & -\lambda_j \\ G_j & 0 & -G_j & 0 \\ 0 & \lambda_j & 0 & -\lambda_j \\ G_j & 0 & -G_j & 0 \end{bmatrix} \qquad (3.3\text{-}3)$$

where G_j and λ_j are the shear modulus and Lam's constant as defined previously in Section 3.2. Matrix [R] is a symmetric full matrix and will be used in Section 4.1 for computation of the compliance matrix.

3.3.2 Transmitting Boundary Matrix for Axisymmetric Problems

Using the generalized Rayleigh and Love waves eigen solutions described in Sections 3.2.1 and 3.2.2 and the Fourier expansion techniques, the force-displacement relationship for the axisymmetric soil model shown in Fig. 3.3-1 may be written in the form:

$$\{P\}_m = [R]_m \{U\}_m \qquad (3.3\text{-}4)$$

where vectors $\{P\}_m$ and $\{U\}_m$ are the force and associated displacement shown in Fig. 3.3-1 of the order 3nX1 and matrix [R] is the 3nX3n axisymmetric dynamic stiffness of the layered system. The subscript m refers to the order of the Fourier expansion. The dynamic stiffness matrix [R] can be obtained using the relation

$$[R]_m = r_o \{[A] [\psi]_m [K^2] + ([D] - [E] + m [N]) [\varphi]_m [K] - m(\frac{m+1}{2} [L] + [Q]) [\psi]_m [W(r_o)]^{-1}\} \qquad (3.3\text{-}5)$$

where r_o is the radial distance from the central axis to the transmitting boundary. The matrices [K] and $[K^2]$ are simple diagonal matrices which contain the wave numbers k_s and k_s^2, respectively, on their diagonals in the same order as the

columns of $[W(r_o)]$. The wave numbers are obtained from the eigenvalues of the site model as shown in Eqs. (3.2-1) and (3.2-6). The $3_n x 3_n$ matrix $[W(r_o)]_m$ has the general elements

$$w_{is} = \begin{cases} H'_m(k_s r_o) v_{is} + \dfrac{m}{r_o} H_m(k_s r_o) v_{i+2,s} & \text{for } i=1,4,--,3_n-2 \\ H_m(k_s r_o) k_s v_{is} & \text{for } 1=2,5,---,3_n-1 \\ \dfrac{m}{r} H_m(k_s r_o) v_{i-2s} + H'_m(k_s r_o) v_{is} & \text{for } 1=3,6,---,3_n \end{cases} \tag{3.3-6}$$

where v_{is} is the i^{th} component of mode shape s, H_m is the Hankel function of order m of the second kind and H'_m is the derivative of this function.

The matrices [A], [D], [E], [N], [L], and [Q] are assembled from submatrices of the soil layers according to the scheme shown in Fig. 3.2-2. The submatrices for the j^{th} soil layer and defined as follows:

$$[A]_j = \frac{h_j}{6} \begin{bmatrix} 2(\lambda_j+2G_j) & 0 & 0 & (\lambda_j+2G_j) & 0 & 0 \\ 0 & 2G_j & 0 & 0 & G_j & 0 \\ 0 & 0 & 2G_j & 0 & 0 & G_j \\ 2(\lambda_j+2G_j) & 0 & 0 & (\lambda_j+2G_j) & 0 & 0 \\ 0 & G_j & 0 & 0 & 2G_j & 0 \\ 0 & 0 & G_j & 0 & 0 & 2Gj \end{bmatrix} \tag{3.3.-7}$$

which is related to the matrix defined by Eq. (3.2-2).

$$[D_j] = 1/2 \begin{bmatrix} 0 & \lambda_j & 0 & 0 & -\lambda_j & 0 \\ -G_j & 0 & 0 & G_j & 0 & 0 \\ 0 & 0 & 0 & 0 & 0 & 0 \\ 0 & \lambda_j & 0 & 0 & -\lambda_j & 0 \\ -G_j & 0 & 0 & G_j & 0 & 0 \\ 0 & 0 & 0 & 0 & 0 & 0 \end{bmatrix} \tag{3.3-8}$$

$$[E_j] = \frac{G_j h_j}{3r_o} \begin{bmatrix} 2 & 0 & 0 & 1 & 0 & 0 \\ 0 & 0 & 0 & 0 & 0 & 0 \\ 0 & 0 & 2 & 0 & 0 & 1 \\ 1 & 0 & 0 & 2 & 0 & 0 \\ 0 & 0 & 0 & 0 & 0 & 0 \\ 0 & 0 & 1 & 0 & 0 & 2 \end{bmatrix} \qquad (3.3\text{-}9)$$

$$[N_j] = \frac{G_j h_j}{6r_o} \begin{bmatrix} 0 & 0 & 4 & 0 & 0 & 2 \\ 0 & 2 & 0 & 0 & 1 & 0 \\ 4 & 0 & 0 & 2 & 0 & 0 \\ 0 & 0 & 2 & 0 & 0 & 4 \\ 0 & 1 & 0 & 0 & 2 & 0 \\ 2 & 0 & 0 & 4 & 0 & 2 \end{bmatrix} \qquad (3.3\text{-}10)$$

$$[L_j] = 2/3 \ \frac{G_j h_j}{r^2_o} \begin{bmatrix} 2 & 0 & -2 & 1 & 0 & 2 \\ 0 & 0 & 0 & 0 & 1 & 0 \\ -2 & 0 & 2 & -1 & 0 & 1 \\ 1 & 0 & -1 & 2 & 0 & -2 \\ 0 & 0 & 0 & 0 & 0 & 0 \\ -1 & 0 & 1 & -2 & 0 & 2 \end{bmatrix} \qquad (3.3\text{-}11)$$

$$[Q_j] = \frac{G_j}{2r_o} \begin{bmatrix} 0 & 0 & 0 & 0 & 0 & 0 \\ 1 & 0 & -1 & -1 & 0 & 1 \\ 0 & 0 & 0 & 0 & 0 & 0 \\ 0 & 0 & 0 & 0 & 0 & 0 \\ 1 & 0 & -1 & -1 & 0 & 1 \\ 0 & 0 & 0 & 0 & 0 & 0 \end{bmatrix} \qquad (3.3\text{-}12)$$

The $3n \times 3n$ matrices $[\Psi]_m$ and $[\Phi]_m$ are related to the mode shape vectors $\{V\}s$. They have the elements:

$$\psi_{is} = \begin{cases} H_m(k_s r_o)\cdot v_{is} , & \text{for } i = 1,4,\ldots,3n-2 \\ -H_{m-1}(k_s r_o)\cdot v_{is} , & \text{for } i = 2,5,\ldots,3n-1 \\ H_m(k_s r_o)\cdot v_{is} , & \text{for } i = 3,6,\ldots,3n \end{cases} \quad (3.3\text{-}13)$$

$$\phi_{is} = \begin{cases} -H_{m-1}(k_s r_o)\cdot v_{is} , & \text{for } i = 1,4,\ldots,3n-2 \\ H_m(k_s r_o)\cdot v_{is} , & \text{for } i = 2,5,\ldots,3n-1 \\ -H_{m-1}(k_s r_o)\cdot v_{is} , & \text{for } i = 3,6,\ldots,3n \end{cases} \quad (3.3\text{-}14)$$

The axisymmetric transmitting boundary matrix $[R]_m$, is used in Section 4.2 for computation of the compliance matrix for three-dimensional problems.

3.4 Free-Field Motion

Using the site response model, the techniques used for computing the site response for inclined body waves and surface waves are described.

3.4.1 Inclined SV- and P-Waves

Using the n layer soil system shown in Fig. 3.4-1, Chen (Ref. 4) has formulated the equation of motion for incident SV- and P-waves. Note that only the case of incident SV-wave is shown in this figure. The techniques, however, is applicable to both SV- and P-waves. The equation of motion to the soil system subjected to inclined P- and/or SV-wave can be written in the form:

$$([A]k^2 + [\bar{B}]k + [G] - \omega^2 [M]) \{U\} = \begin{Bmatrix} 0 \\ P_b \end{Bmatrix} \quad (3.4\text{-}1)$$

The matrices [A], [G] and [M] are assembled from the submatrices $[A_j]$, $G_j]$, and $[M_j]$ defined in Eqs. (3.2-2), (3.2-4), (3.2-5a), and (3.2-5b) following the scheme shown in Fig. 3.2-2. The matrix $[\bar{B}]$ is assembled from submatrices $[\bar{B}_j]$ defined by:

$$[\bar{B}_j] = 1/2 \begin{bmatrix} 0 & (3G_j-M_j) & 0 & -(G_j-M_j) \\ (3G_j-M_j) & 0 & (G_j-M_j) & 0 \\ 0 & (G_j-M_j) & 0 & (G_j-M_j) \\ -(G_j-M_j) & 0 & (3G_j-M_j) & 0 \end{bmatrix} \quad (3.4\text{-}2)$$

where M_j and G_j are the constrained and shear modulus of layer j. Note that the matrices in Eq. (3.4-1) are of order (2n+2n) x (2n+2) corresponding to degrees-of-freedom shown in Fig. 3.4-1. The vector P_b is a vector with 2 components and defines the load vector at the base. Depending on the angle of incidence of the wave and nature of the wave field (SV or P or combined SV + P) the load vector P_b and the wave number k are calculated (see Ref. 4).

Solution to Eq. (3.4-1) yields the displacement vector {U}. For vertically propagating waves Eq. (3.4-1) reduces to much simpler equation (Ref. 4). The free-field motion at any distance x can be obtained from the solution using the relation

$$\{U(X)\} = \delta\{U\} \exp(-ikx) \quad (3.4\text{-}3)$$

where δ is the mode participation factor which is obtained from the input control motion at control point at the frequency of analysis. Note that Eq. (3.4-3) defines the motion at any horizontal distance x and for all the points on layer interfaces within the soil model. Once the location of control point is selected, the horizontal distance x can be obtained for all the interaction nodes in Substructures (b) in Fig. 2.2-1. The free-field motion $\{U_f\}$ used in Eq. (2.2-6) can thus be obtained from Eq. (3.4-3) for all the interacting nodes for the case of SV and/or P incident waves.

3.4.2 Inclined SH-Wave

A similar technique has been developed for inclined SH-waves. The corresponding site model is shown in Fig. 3.4-2. For this model, the equation of motion for SH incident waves may be written in the form

$$([A]k^2 + [G] - \omega^2[M])\ \{U\} = \begin{Bmatrix} 0 \\ P_b \end{Bmatrix} \qquad (3.4\text{-}4)$$

The matrices [A], [G], and [M] are assembled from the submatrices $[A_j]$, $[G_j]$, and $[M_j]$ defined in Eqs. (3.2-7), (3.2-8), and (3.2-9a) and (3.2-9b), respectively, Note the assembled matrices are of the order (nx1) x (n+1). The wave number k and the load vector P_b (single component) are obtained from the angle of incidence and properties of the halfspace (see Ref. 4). Solution to Eq. (3.4-4) yields to the free-field motion of the site model subjected to inclined SH-wave. For vertically propagating SH-wave, Eq. (3.4-4) reduces to a much simpler equation (Ref. 4). Similarly, the free-field motion at any distance x from the control point can be computed using the relation of Eq. (3.4-3) to compute the free-field motion $\{U_f\}$ for inclined SH-waves.

3.4.3 Rayleigh Wave

The equation of motion for the site model subjected to Rayleigh wave is the same equation as defined by Eq. (3.2-1) and described in Section 3.2.1. From the solution to this equation 2n mode shape vectors {V} and 2n wave numbers k are selected for a n layer soil system. It should be noted, however, that in the engineering application, the input motion is defined in terms of the location of the control point and time history of the control motion which in effect defines the

time history of a particular component of the mode shapes. While this information is sufficient to define the wave field for the case of body waves consisting of single mode for each frequency, it is not adequate to define the wave field for the case of surface waves since multiple modes may exist for the same frequency. On the other hand since surface waves are highly dissipative it can be assumed that only fundamental mode travels with distance. As a result, the selection of fundamental mode for Rayleigh wave is based on the study of the characteristic of generalized Rayleigh wave modes to select the most appropriate mode from the set of 2n modes.

Depending on the soil profile model, one of the following two methods may be used. Once the fundamental mode is selected, computation of free-field motion at interacting nodes, $\{U_f\}$, follows the same procedures as described for body waves.

3.4.3.1 The Least-Decay Method

Consider a typical Rayleigh wave mode with wave number $k = k_r + ik_i$ where k_r and k_i are the real and imaginary components of the wave number. This mode has the wave length $2\pi/k_r$ and attenuates as exp $(k_i x)$ with distance X. Hence, the decay factor per wave length is exp $(2\pi k_i/k_r)$. The ratio $(-k_i/k_r)$ is thus a measure for how fast the wave mode decays. It is expected that the fundamental mode, which does not decay in the undamped case, will have a very small attenuation for damped cases. Therefore, for damped case, the mode with smallest $(-K_i/k_r)$ ratio is selected as the least-decay mode.

Study of the Rayleigh mode using the least-decay method for different soil profiles (see Ref. 4) shows

while the method produces reasonable mode shapes in many cases it does not yield to most realistic mode for sites with a soft highly damped surface layer overlaying a stiff halfspace with low damping. The method, in this case, tends to select a mode which corresponds to the classical Rayleigh mode in the halfspace without the surface layer (Ref. 4).

3.4.3.2 The Shortest Wave Length Method

In this method a mode with shortest wave length is selected. For undamped soil systems this mode is the one with the largest wavenumber k (hence shortest wave length and lowest phase velocity). This definition coincides with that used by seismologists.

However, actual sites cannot be modelled by undamped materials. It has been found (Ref. 4) that with the magnitude of the damping which are used in practical problems, the changes in the numerical values of wave numbers and mode shapes from the corresponding values obtained from undamped system are not very large. Based on this observation the following steps are taken to compute the fundamental mode.

1. Compute the undamped natural frequencies of the system by setting k=0 in Eq. (3.2-1).

2. Determine, m, the number of natural modes below the frequency of excitation

3. Sort the modes in order of magnitude of the imaginary part of the wave number

4. Select from the first m modes of step 3, the mode whose wave number k has the largest real part

It has been shown (Ref. 4) that this method leads to a mode shape with the usual characteristics of fundamental Rayleigh wave; i.e., decay with depth, simple mode shape and low phase and group velocities. Furthermore, for the undamped system, the definition coincides with that used by seismologists.

It should be noted, however, that in practical application only small percentage of Rayleigh wave, if any, is present in the control motion. Nevertheless, it is prudent to study the fundamental modes selected by both methods described above and select a mode which is appropriate for the site considered.

3.4.4 Love Wave Motion

Equation of motion for the site model subjected to Love wave motion is the same equation as defined by Eq. (3.2-6) and described in Section 3.2.2. For reasons similar to the case of Rayleigh wave, from the set of n mode shapes obtained from Eq. (3.2-6), one mode is selected as the fundamental mode. The method used is based on the shortest wave length method. Following the selection of the mode, the free-field motion at interacting nodes, $\{U_f\}$, can similarly be computed.

3.5 Modelling of Semi-Infinite Halfspace at Base

The approach described above was originally developed for layered sites resting on a rigid base. In many practical cases the site is a layered system which extends to such great depth that it becomes

necessary to introduce an artificial rigid boundary at some depth. This boundary will reflect some energy back into the system and will cause the site to have some erroneous natural frequencies which will affect the overall response. This becomes especially critical for sites with low material damping.

To remedy this problem, the two techniques as described in the following two subsections are used in the SASSI program to simulate the semi-infinite halfspace at the soil layer base.

3.5.1 The Variable Depth Method

In this method n extra layers which represent the halfspace are added to the base of the top soil layers (see Fig. 3.5-1). The total depth H of the added layers varies with frequency and is set to

$$H = 1.5 \frac{V_s}{f} \qquad (3.5\text{-}1)$$

where f is the frequency of analysis in Hz, and V_s in the shear wave velocity of halfspace. The choice of this depth is based on the observation that fundamental mode Rayleigh waves in a halfspace decay rapidly with depth and essentially vanish at a depth corresponding to one and a half wave length. Only a minimal error is therefore introduced by placing a rigid base at this depth.

Assuming the thickness of the last top layer to be h_0, and this layer has the same properties as the halfspace, the thickness of the j^{th} layer in the simulated halfspace is set to

$$h_j = \alpha^j h_0 \qquad (3.5\text{-}2)$$

where α is a constant coefficient. This coefficient is determined as follows:

The total thickness of the n layers is

$$H = h_0 + \alpha^2 h_0 + \text{---} + \alpha^n h_0 = \frac{(\alpha^n - 1)h_0}{\alpha - 1} \qquad (3.5\text{-}3)$$

Hence

$$\frac{(\alpha^n - 1)}{\alpha - 1} = \frac{H}{h_0} \qquad (3.5\text{-}4)$$

Equation (3.5-4), in which the right-hand side is known at each frequency, is solved by the Newton iteration method to determine α. The number, of layers n, used to represent the halfspace is usually chosen such that $\alpha > 1$ for the highest frequency of analysis.

Based on the above method of subdivision the layer thicknesses will increase with depth and decrease with frequency. This is the desired characteristic of the model since surface wave mode shapes decrease exponentially with depth and since their depth of penetration increases with decreasing frequency. The fact that the layer thickness becomes very large at low frequencies is acceptable since the thickness remains small as compared to the wave length. The choice of n=10 has been found to be adequate for all practical problems (Ref. 2).

3.5.2 Viscous Boundary at Base

The site model may be further improved by replacing the rigid boundary with a viscous boundary, as shown in Figure 3.5-1. This boundary which was developed by Lysmer and Kuhlemeyer

(Ref. 7) consists of two dashpots per unit area of the boundary. The dashpots have the damping coefficients

$$\text{Vertical dashpot:} \quad c_p = \rho V_p \tag{3.5-5a}$$

$$\text{Horizontal dashpot:} \quad c_s = \rho V_s \tag{3.5-5b}$$

where ρ is the mass density and V_p and V_s are the P- and S-wave velocities, respectively, of the halfspace below the boundary of the model. Thus the boundary condition is

$$\sigma(X, t) = V_p \dot{U}_Z (X, t) \tag{3.5-6a}$$

$$\tau(X, t) = V_s \dot{U}_X (N, t) \tag{3.5-6b}$$

where σ, τ, $\dot{u}_z$ and $\dot{u}_x$ are the normal stress, the shear stress, the normal velocity, and tangential velocity, respectively, at the boundary. The boundary condition in Eqs. (3.5-6) is the exact boundary condition for the (downward) vertically propagating P and S plane waves in a perfect elastic halfspace. Thus the dashpots exactly simulate the halfspace impedances below the base of the model for the special load cases shown in Fig. 3.5-2. In fact, all of the three models shown in Fig. 3.5-2(a) and 3.5-2(b) will result in the same surface response.

The inclusion of dashpots in the site model also greatly improves the accuracy of the impedance calculations to be discussed in Chapter 4. Thus, for the simulation of halfspace the site model as shown in Fig. 3.5-1 which combines both the variable depth method and the viscous boundary condition should be used when applying the SASSI program.

3.6 Dynamic Soil Properties and Equivalent Linear Method

The substructure methods used by SASSI is valid only for linear analyses. It is well known, however, that the response of soils to dynamic loading exhibits strain-dependent nonlinear behavior. The nonlinear behavior of the soil is considered approximately in SASSI using the equivalent linear method proposed by Seed and Idriss (Ref. 20). Using this method, the nonlinear properties of the soil are approximated by equivalent linear properties consisting of the equivalent linear shear modulus and damping ratio for the soil which are compatible with the induced strain amplitudes in the soil medium.

An extensive summary of data on strain compatible moduli and damping ratios for clays and sands has been presented by Seed and Idriss (Ref. 21). Additional data has been presented by Hardin and Drnevich (Ref. 6). The data are presented in the form of curves shown in Fig. 3.6-1. These curves show the effective dynamic shear moduli and damping ratios for clays and sands subjected to cyclic excitation at different strain amplitudes. The curves provide the essential data for the equivalent linear method which proceeds as follows: A linear analysis is performed with estimated soil properties. This analysis provides approximate values of the effective strain amplitude developed in each soil layer and these are used to estimate better soil properties from the curves for a second linear analysis. The process is continued until compatibility is obtained between soil properties and strain amplitudes and the results of the last linear analysis is assumed to represent the nonlinear response.

The effect of nonlinear soil behavior under seismic excitations can be considered in two parts: the primary nonlinearity attributed to the nonlinearity induced by the seismic excitation of the free field, and the secondary nonlinearity due to soil-structure interaction only. The primary nonlinearity is usually considered using Computer Program SHAKE (Ref. 19). The iterated soil properties obtained from SHAKE analysis are used for SASSI analysis.

The secondary nonlinearity, which occurs at soil elements adjacent to the structure, may also arise from separation or debonding between the soil and the structure and the subsequent closing of the gaps or sliding of the structure. The stress and strain in the soil elements near the structure can also be computed by SASSI. If need be, the properties of these elements are adjusted using the iterated equivalent linear soil properties and the analysis can be restarted with adjusted soil properties.

3.7 Complex Response Method

In SASSI, the soil material properties are represented by the complex shear, G*, and complex constrained moduli, M*, defined by the following equations:

$$G^* = G(1-2\beta_S^2 + 2i\beta_S\sqrt{1-2\beta_S^2}) \simeq G\,(1+2i\beta_S) \qquad (3.6\text{-}1a)$$

$$M^* = M(1-2\beta_P^2 + 2i\beta_P\sqrt{1-2\beta_P^2}) \simeq M\,(1+2i\beta_P) \qquad (3.6\text{-}1b)$$

where G and M are real numbers corresponding to the shear and constrained moduli, respectively and β_S and β_P are the critical damping ratios associated with S-wave and P-waves, respectively. Currently only limited data are available on the ratio between β_S and β_P and these quantities are therefore usually chosen to be equal, in which case the subscripts are dropped and the corresponding Poisson's ratio becomes real number.

Using the complex modulus described above, the spatial variation of damping can be included in the analysis. This is particularly important for SSI systems in which the material damping in the soil and structure are significantly different.

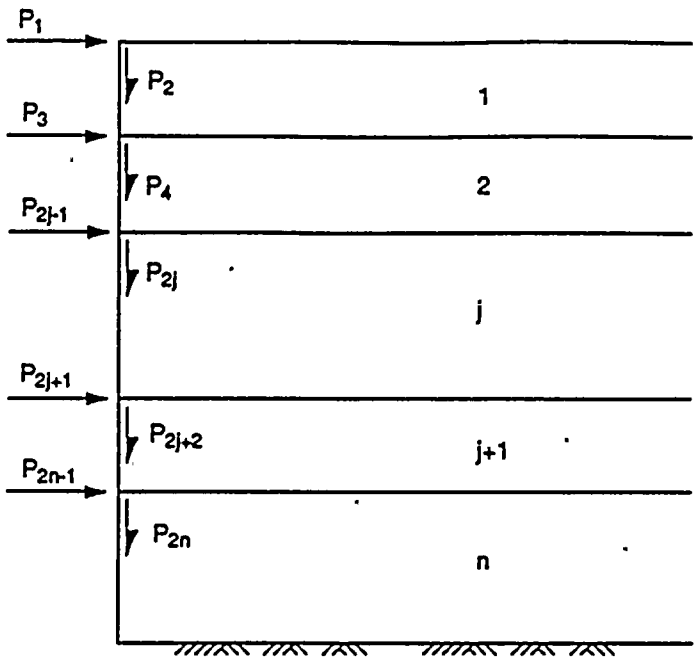

(a)

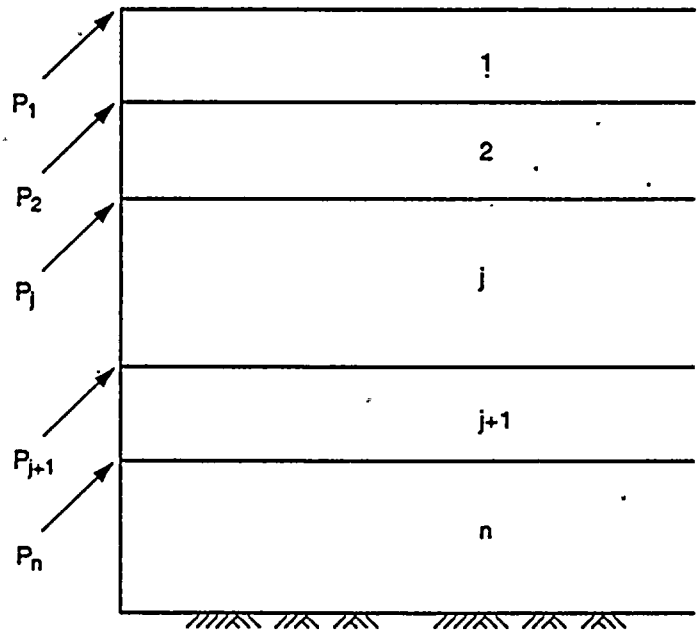

(b)

Figure 3.2-1. Degrees of Freedom: (a) Raleigh Wave, and (b) Love Wave

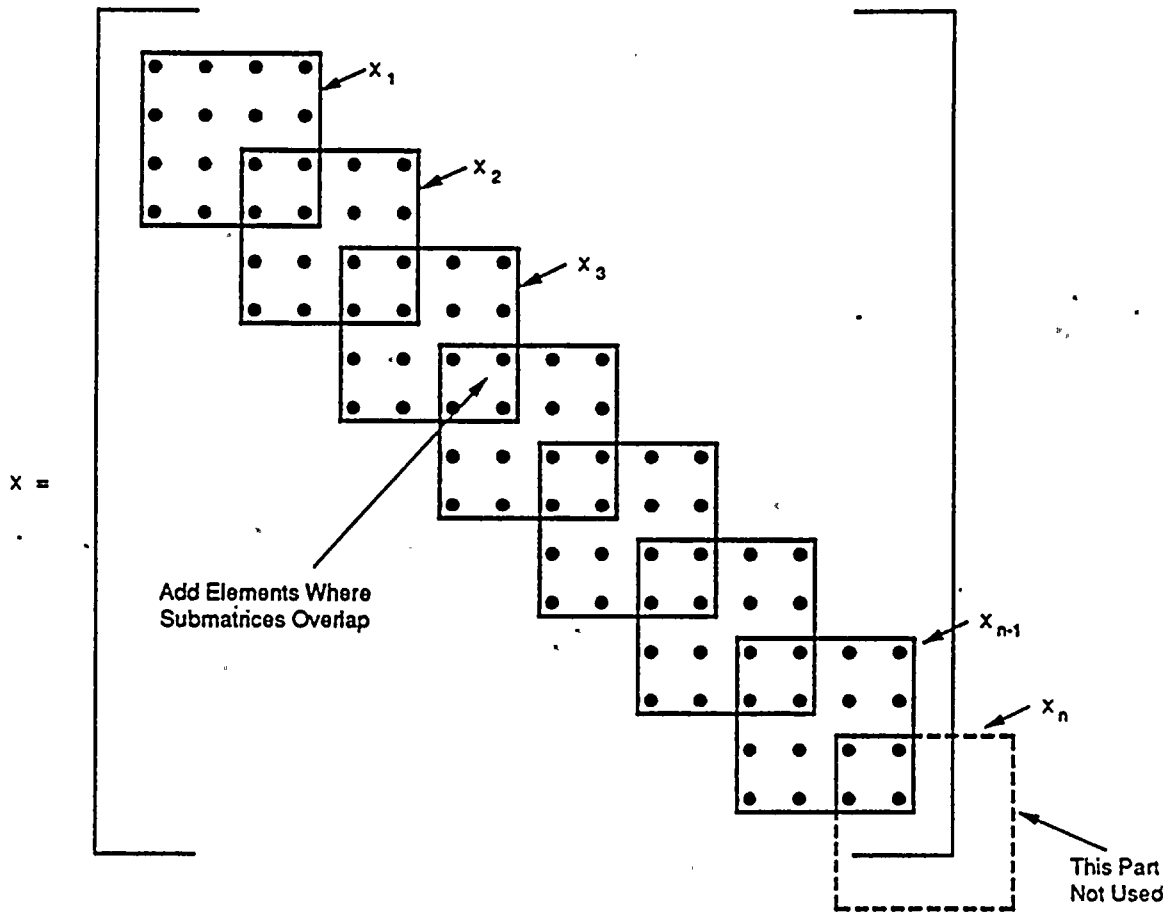

Figure 3.2-2. Assembling Submatrices of Each Layer

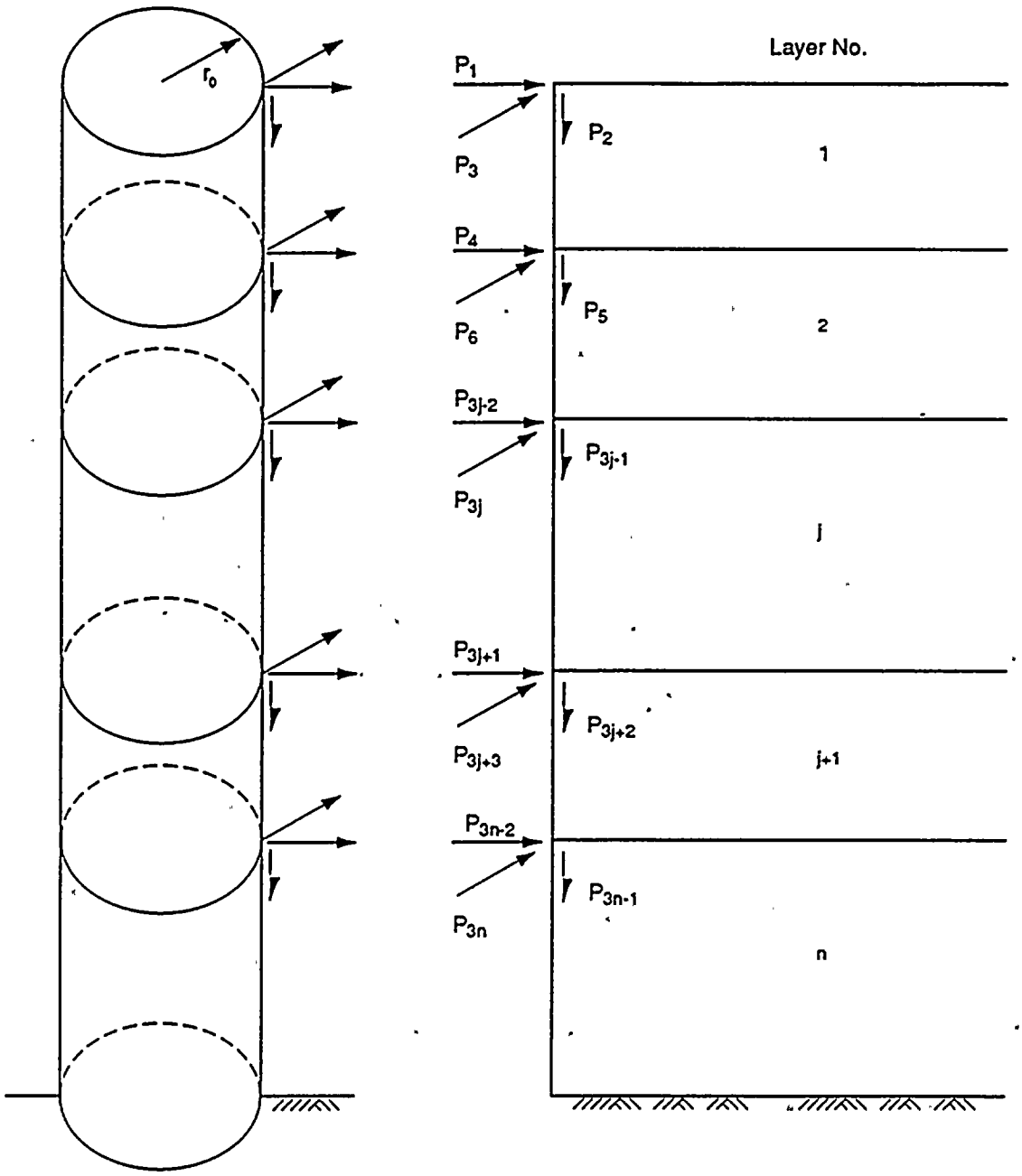

Figure 3.3-1. Degrees of Freedom on Axisymmetric Transmitting Boundary

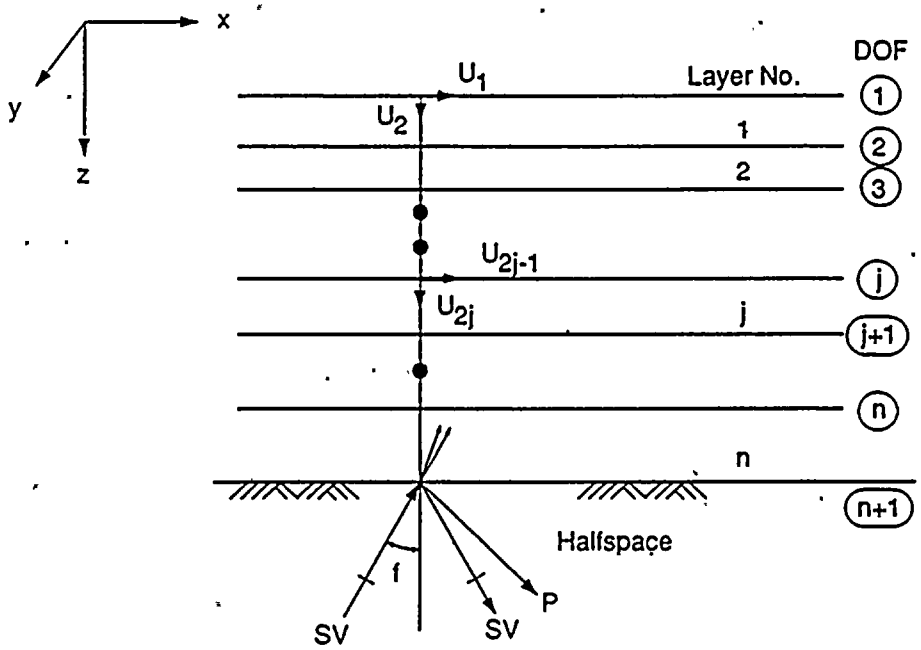

Figure 3.4-1. Model of Plane SV-Wave Incidence

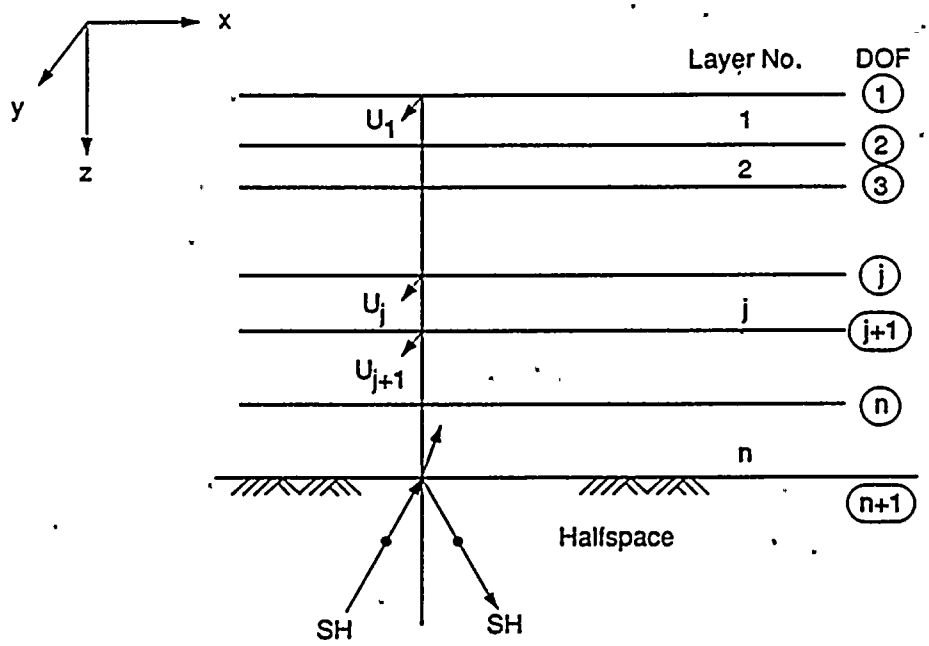

Figure 3.4-2. Model of Plane SH-Wave Incidence

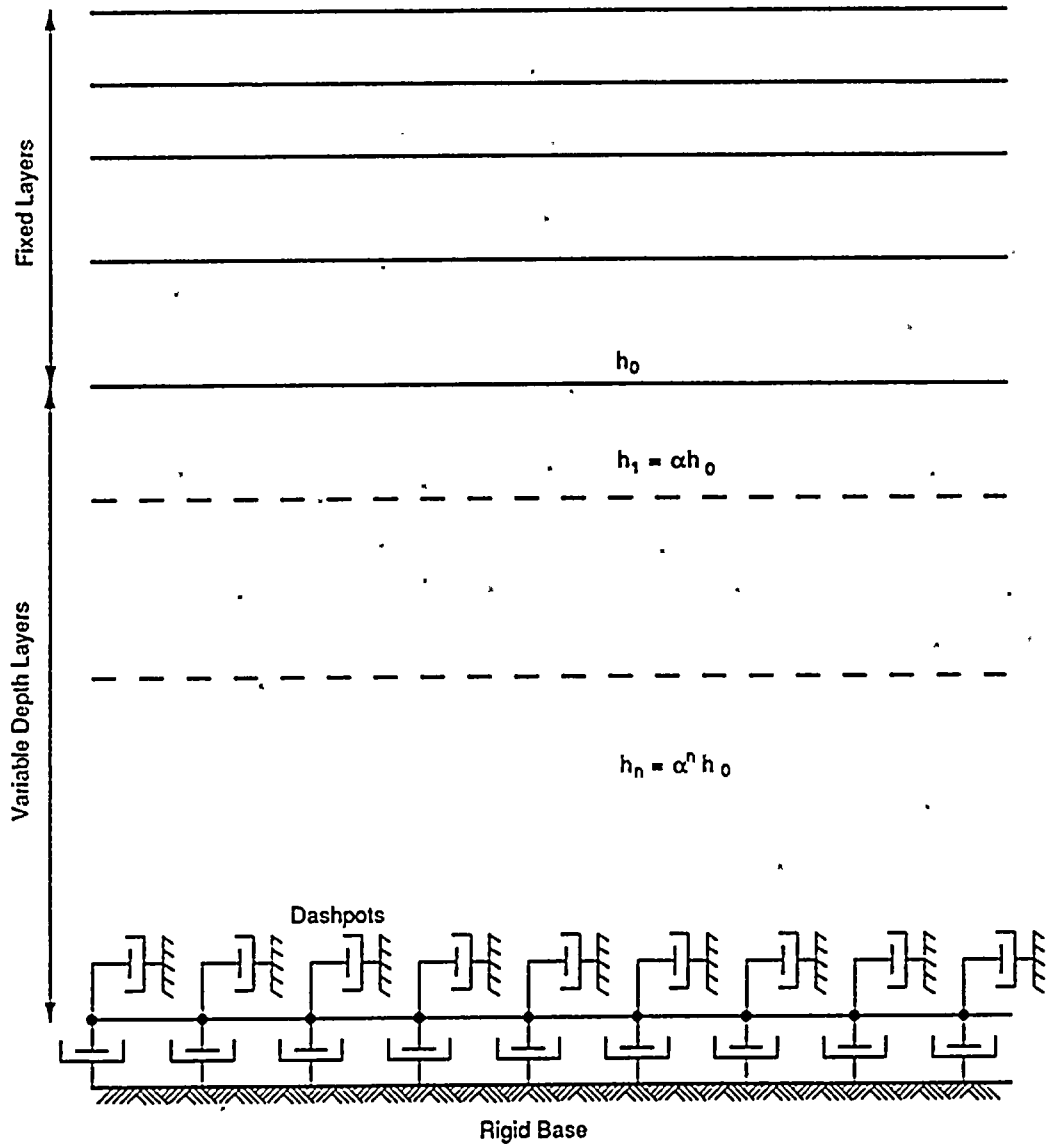

Figure 3.5-1. Simulation of Halfspace

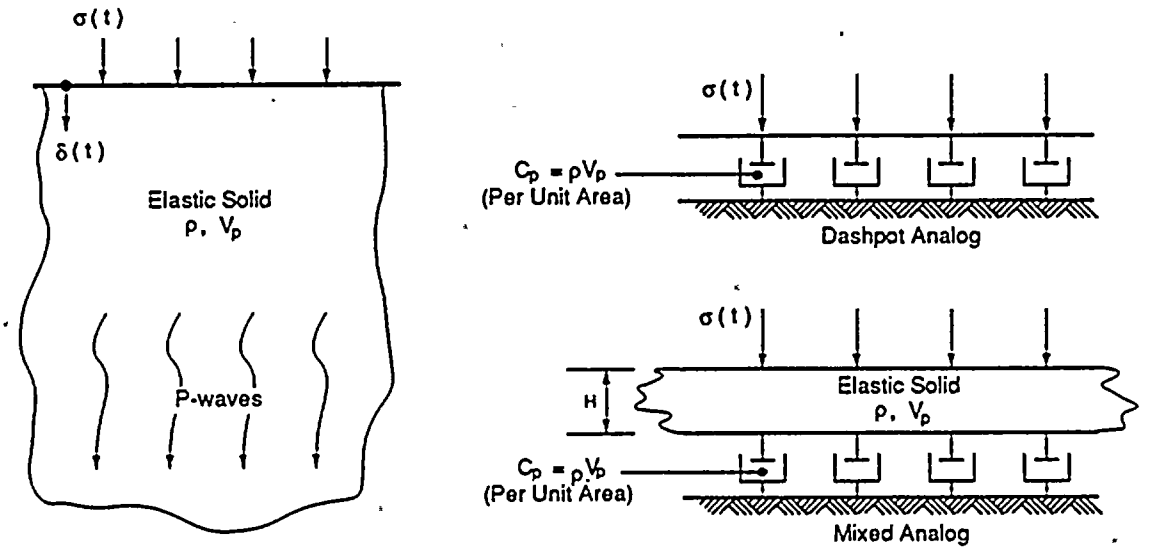

(a) Vertically Loaded Halfspace

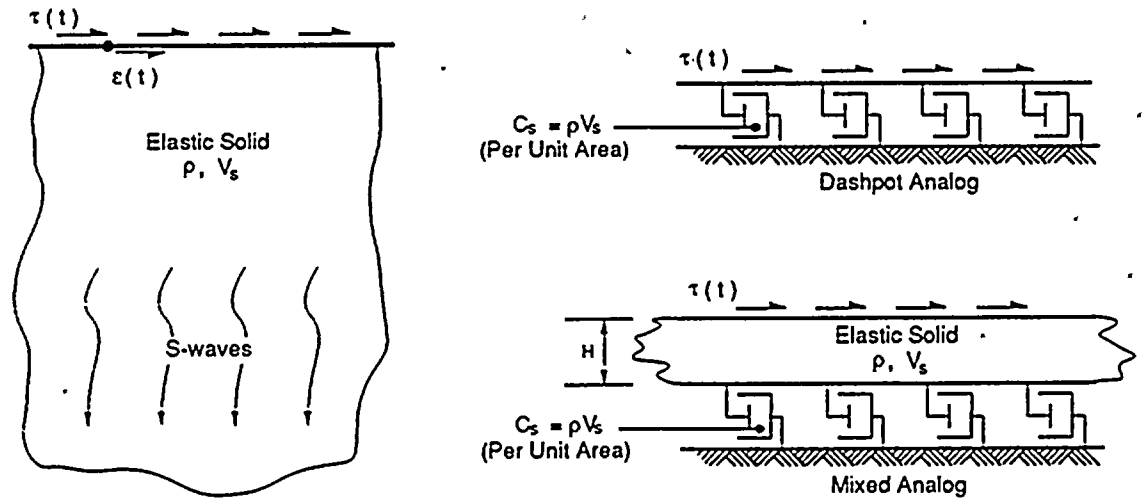

(b) Horizontally loaded Halfspace

Figure 3.5-2. Halfspace Simulation by Viscous Dashpots

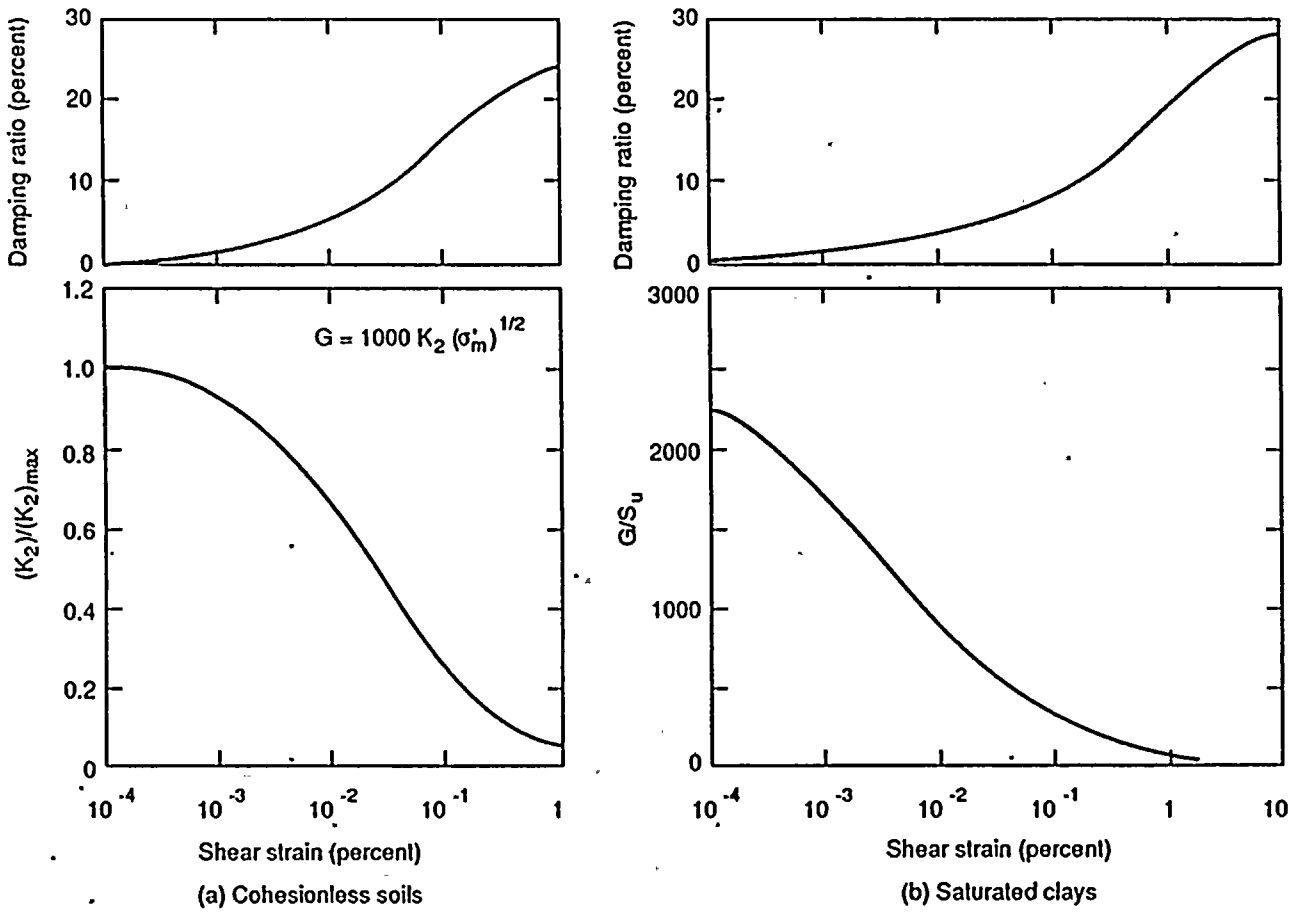

Figure 3.6-1. Average Shear Moduli and Damping Characteristics of Soils

4. IMPEDANCE ANALYSIS

The equations of motion of the SSI system based on the flexible volume substructuring method used by SASSI include the impedance matrix $[X_{ff}]$ as shown in Eqs. (2.2-6) and (2.2-7). The impedance matrix need be computed for all the interacting nodes in the flexible volume, i.e., the excavated soil volume. The calculation of the impedance matrix is achieved by inverting the dynamic flexibility (compliance) matrix for each frequency of analysis. The methods and analytical models used to compute the compliance matrix based on the model of substructure (b) shown in Figure 2.2-1 for two- and three-dimensional problems are described in Sections 4.1 and 4.2, respectively. Two methods, namely, the direct method and the skin method, are used in SASSI for the impedance analysis. Depending on which method is used, the compliance matrix is computed for all or part of the interacting nodes. The direct and skin methods of impedance analysis are described in Sections 4.3 and 4.4, respectively.

4.1 Compliance Matrix for Two-Dimensional Problems

By definition of the compliance matrix, the components of the i^{th} column of the matrix are the dynamic displacements of the interacting degrees-of-freedom caused by a harmonic force of unit amplitude acting at the i^{th} degree-of-freedom. Thus, the problem in determining the compliance matrix for two-dimensional problems is that of finding the harmonic response displacements of a layered halfspace to a harmonic line load. Figure 4.1-1 shows a layered system and the interaction nodes for which the matrix is to be determined. To obtain the compliance matrix, the basic problem is to determine the displacement responses of all the nodes subject to unit loads placed successively at one column of nodes shown as heavy dots in Fig. 4.1-1. Once this problem has been solved, solution corresponding to other nodes can be obtained simply by a shift of the horizontal coordinates.

The basic solution is obtained using a models which consists of a single column of plane-strain rectangular elements. This model, which takes advantage of symmetry, is shown in Figure 4.1-2 and is solved with different boundary conditions at the axis of symmetry depending on the direction of the applied forces at the loaded nodes. The existence of the semi-infinite layered region is simulated by applying the consistent transmitting boundary impedances as described in Section 3.3 on the nodes numbered n+1 to 2n, where n is the number of layers. The lower boundary may be fixed or a halfspace simulated using the variable depth method and the viscous boundary at base as discussed in Section 3.5.

The equations of motion for the model are

$$\begin{bmatrix} C_{cc} & C_{c\ell} \\ C_{\ell c} & C_{\ell\ell} + R \end{bmatrix} \begin{Bmatrix} U_c \\ U_\ell \end{Bmatrix} = \begin{Bmatrix} Q_c \\ 0 \end{Bmatrix} \qquad (4.1\text{-}1)$$

where C indicates a dynamic stiffness matrix of the form ($C = k - \omega^2 M$) and R is the transmitting boundary impedance matrix described in Section 3.3.1. The indices c and ℓ refer to degrees of freedom on the center line and the lateral boundary, respectively; and U_c and U_ℓ are the corresponding displacements. The load vector for each load case has only one non-zero element corresponding to a load of unit amplitude. Since the matrix in Eq. (4.1-1) is the same for all horizontal load cases (Figure 4.1-2a), only a single triangulation is required to find the solution vectors for these cases.

The unit horizontal harmonic loads are applied at the interacting nodes on the center line of the model (see Fig. 4.1-2a) successively. Solution to Eq. (4.1-1) yields to displacement responses on the center line and on the boundary of the model for each loading case. To compute the components of the flexibility matrix at interacting nodes outside the boundary of the model, the following relationship applicable to layered halfspace is used.

$$\{U\} = \sum_{s=1}^{2n} \alpha_s \{V\}_s \exp(-ik_s X) \qquad (4.1\text{-}2)$$

In this equation X is the horizontal distance, $\{V\}_s$, α_s and k_s are the mode shapes, mode participation factors and wave number associated with soil layered system. As discussed in Section 3.2, there are 2n modes for a n layer soil system. The mode shapes and the associated wave numbers are obtained from the solution of the eigenvalue problem of a layered system as discussed in Chapter 3. The mode participation factors are computed from Eq. (4.1-2) by letting X=0 and using the solution of Eq. (4.1-1) at the boundary nodes. Thus, by knowing the horizontal distance between the loaded nodes on the center line and the interacting nodes outside the boundary, the displacements at all other nodes are computed from Eq. (4.1-2).

A similar technique is used for the vertical loading case. In this case the model shown in Fig. 4.1-2b is used and the solution is obtained in the similar manner. Equation (4.1-2) is then used to compute the displacement at other interacting nodes.

It should be noted, however, that the analytical models shown in Figs 4.1-2a and 4.1-2b are analyzed only for one column of the interacting nodes as shown in Fig. 4.1-1. The same solution is successfully used for the remaining columns of interacting nodes and only the horizontal distance X in Eq. (4.1-2) needs to be computed to measure the horizontal distance between the new set of loaded nodes and the remaining interacting nodes.

Using the technique described above, a 2i x 2i compliance matrix associated with total of i interacting nodes is computed for each frequency of analysis.

4.2 Compliance Matrix for Three-Dimensional Problems

Similar to the 2-D Case, the problem of evaluating the dynamic flexibility matrix for a three-dimensional case reduces to the problem of finding the response of horizontally layered system to point loads at the layer interfaces. This problem, however, is an axisymmetric problem and can be solved using the axisymmetric model shown in Fig. 4.2-1. The model consists of a central zone with radius r_o of cylindrical elements enclosed by an axisymmetric transmitting boundary. As for the two-dimensional case, the lower boundary can either be fixed or halfspace simulated using the variable depth and viscous boundary methods. Taking advantage of symmetry and antisymmetry boundary conditions, the models shown in Figs. 4.2-2a and 4.2-2b are used for vertical and horizontal loading cases, respectively.

The mass and stiffness matrices of the elements in these models are computed in cylindrical coordinates system. Fourier harmonics are used to expand the displacement field within each element in tangential direction. In the model used for horizontal loading (Fig. 4.2-2b), up to 1st Fourier expansion terms are used. In the model used for vertical loading (Fig. 4.2-2a) only zero harmonic terms are needed since the model and the loading are symmetric. Following the computation of element mass and stiffness matrices, the equation of motion is assembled in the following form:

$$\begin{bmatrix} C_{cc} & C_{cp} \\ C_{pc} & C_{pp} + R \end{bmatrix} \begin{Bmatrix} U_c \\ U_p \end{Bmatrix} = \begin{Bmatrix} Q_c \\ 0 \end{Bmatrix} \qquad (4.2\text{-}1)$$

where C indicates the dynamic stiffness matrix ($C = k - \omega^2 M$) and R is the axisymmetric transmitting boundary impedance matrix described in Section 3.3.2. The indices C and P refer to degrees of freedom on the center line and perimeter of the model, respectively, and U_c and U_p are the corresponding displacement amplitudes. The displacements of the nodes outside the model ($r>r_o$)may be obtained from

$$\{U(r)\}_m = [W(r)]_m \{\Delta\}_m \qquad (4.2\text{-}2)$$

where the subscript m refer to Fourier harmonic order (zero or one) and

$$\{\Delta\}_m^T = \langle \alpha 1, \alpha 2, \text{---}, \alpha 3n \rangle \qquad (4.2\text{-}2)$$

is the modal participation factors associated with 3n modes of the n layer soil system. The 3n x3n matrix $[W(r)]_m$ has the general elements defined in Eq. (3.3-6).

The displacement of the nodes on the perimeter of the model ($r=r_o$) obtained from Eq. (4.2-1) are used in Eq. (4.2-2) to compute the mode participation vector $\{\Delta\}_m$. Knowing the mode participation vector, Eq. (4.2-2) can be used to compute the displacement at any point with radius of r from the axis of the model. These displacements are in cylindrical coordinates. The displacement components at each node are transformed into Cartesian coordinate and used to construct the comnpliance matrix.

Using the technique described above, a 3i x 3i flexibility matrix is computed for a system with i interacting nodes in the free-field soil medium for each frequency of analysis.

4.3 Direct Method of Impedance Analysis

In this method, the compliance matrix $[F_{ff}]$ need be computed for all the interacting nodes using the methods described above. The impedance matrix $[X_{ff}]$ is obtained by inverting the compliance matrix, i.e.,

$$[X_{ff}] = [F_{ff}]^{-1} \qquad (4.3\text{-}1)$$

The impedance matrix as obtained is subsequently used in the assemblage of the equations of motion as described in Section 2.2. The inversion of the matrix is computer cpu intensive and needs to be performed for every frequency of analysis. An efficient in-place inversion routine is used to invert the flexibility matrix which is a full matrix in the direct method of analysis. For total number of i interacting nodes, the resultant impedance matrix is of the order of 2i x 2i or 3i x 3i for two- and three-dimensional problems, respectively.

4.4 Skin Method of Impedance Analysis

According to this method the interacting nodes are grouped into three groups defined as skin, intermediate and internal nodes. These groups are shown in Fig. 4.4-1. By definition, skin nodes are those located along the physical boundary between the structure basement and the soil region (labeled by digit 1 in Fig. 4.4-1). Intermediate nodes are defined as those interaction nodes within the flexible volume which are directly connected to the skin nodes (labeled by digit 2 in Figure 4.4-1). The remaining interaction nodes, which are not connected to skin nodes, are internal nodes (labeled by digit 3 in Figure 4.4-1).

According to the above definition, the impedance and compliance matrices are partitioned as follows:

$$\begin{bmatrix} X_{11} & X_{12} & X_{13} \\ X_{21} & X_{22} & X_{23} \\ X_{31} & X_{32} & X_{33} \end{bmatrix} = \begin{bmatrix} F_{11} & F_{12} & F_{13} \\ F_{21} & F_{22} & F_{23} \\ F_{31} & F_{32} & F_{33} \end{bmatrix}^{-1} \qquad (4.4\text{-}1)$$

Consider the embedment region separated from the surrounding environment as shown in Figure 4.4-1b. The dynamic stiffness matrix of this region is identical to the matrix C_{ff} in Eq. (2.2-6) and has the form

$$[C_{ff}] = \begin{bmatrix} C_{11} & C_{12} & 0 \\ C_{21} & C_{22} & C_{23} \\ 0 & C_{32} & C_{33} \end{bmatrix} \qquad (4.4\text{-}2)$$

where $C = K - \omega^2 M$ are formed from the mass and stiffness properties of the "excavated" soil.

By the definition of a stiffness matrix, the elements of X and C are the forces at all degrees of freedom when a particular degree of freedom is given a unit displacement while all other nodes remain fixed. By this definition the following relations are obtained:

$$x_{12} = C_{12} \qquad (4.4\text{-}3)$$
$$x_{22} = C_{22} \qquad (4.4\text{-}3b)$$
$$x_{32} = C_{32} \qquad (4.4\text{-}3c)$$
$$x_{13} = 0 \qquad (4.4\text{-}3d)$$
$$x_{23} = C_{23} \qquad (4.4\text{-}3e)$$
$$x_{33} = C_{33} \qquad (4.4\text{-}3f)$$

These relations are exact if the same displacement fields are used in the layered site and in modeling the excavated soil. In actual analysis, plane strain or brick elements with linear displacement fields are used to model the excavated soil while continum formulation (see Eqs. [4.1-2] and [4.2-2]) are used to compute the displacements in layered site with respect to horizontal distance. Therefore, the above equations are only approximately satisfied. However, the errors introduced by assuming Eqs. (4.4-3) are acceptable for practical purposes.

Multiplication of the impedance matrix, X, with flexibility matrix, F, yields the identity matrix. Hence, substituting for elements of X from the above equations,

$$\begin{bmatrix} F_{11} & F_{12} & F_{13} \\ F_{21} & F_{22} & F_{23} \\ F_{31} & F_{32} & F_{33} \end{bmatrix} \begin{bmatrix} X_{11} & C_{12} & 0 \\ C_{21} & C_{22} & C_{23} \\ 0 & C_{32} & C_{33} \end{bmatrix} = \begin{bmatrix} I & 0 & 0 \\ 0 & I & 0 \\ 0 & 0 & I \end{bmatrix} \qquad (4.4\text{-}4)$$

x_{11} is obtained from the first set of equations and is

$$X_{11} = F_{11}^{-1} \cdot (I - F_{12} \cdot C_{12}^T) \quad . \tag{4.4-5}$$

The entire impedance matrix is now of the form

$$[X_{ff}] = \begin{bmatrix} F_{11}^{-1}(I - F_{12} \cdot C_{12}^T) & C_{12} & 0 \\ C_{21} & C_{22} & C_{23} \\ 0 & C_{32} & C_{33} \end{bmatrix} \tag{4.4-6}$$

As is evident from Eq. (4.4-6), only F_{11} and F_{12} of the total flexibility matrix needs to be formed and only F_{11} needs to be inverted. The efficiency of the skin method is clearly highest when the number of skin nodes is small compared to the total number of interaction nodes. This will usually be the case for deep foundations.

Following the computation of the impedance matrix, this matrix is used in the equation of motion as described in Section 2.2

4.5 Impedance Matrices for Symmetric and Antisymmetric Systems

For SSI systems with symmetric properties and symmetric or antisymmetric loading, the model size and cost of analysis can be reduced by using one-half or one-fourth of the model. This requires calculation of the impedance matrix for the symmetric systems. Using the direct method as described in Section 4.3, the symmetric impedance matrix X_{ff} can be determined as the inverse of the corresponding symmetric dynamic flexibility matrix F_{ff} using

$$[X_{ff}] = [F_{ff}]^{-1} \tag{4.5-1}$$

The elements of the symmetric flexibility matrix f_{ij}^s represent the displacement at degree-of-freedom i due to unit harmonic loads acting at degree-of-freedom j and degree-of-freedom j' which is the mirror

image of j relative to the axis of symmetry. The displacements are computed using the methods described in Sections 4.1 and 4.2.

Similarly for SSI systems with antisymmetric loading, the antisymmetric compliance matrix can be computed with the exception that the unit harmonic load at degree-of-freedom j'' takes the opposite direction.

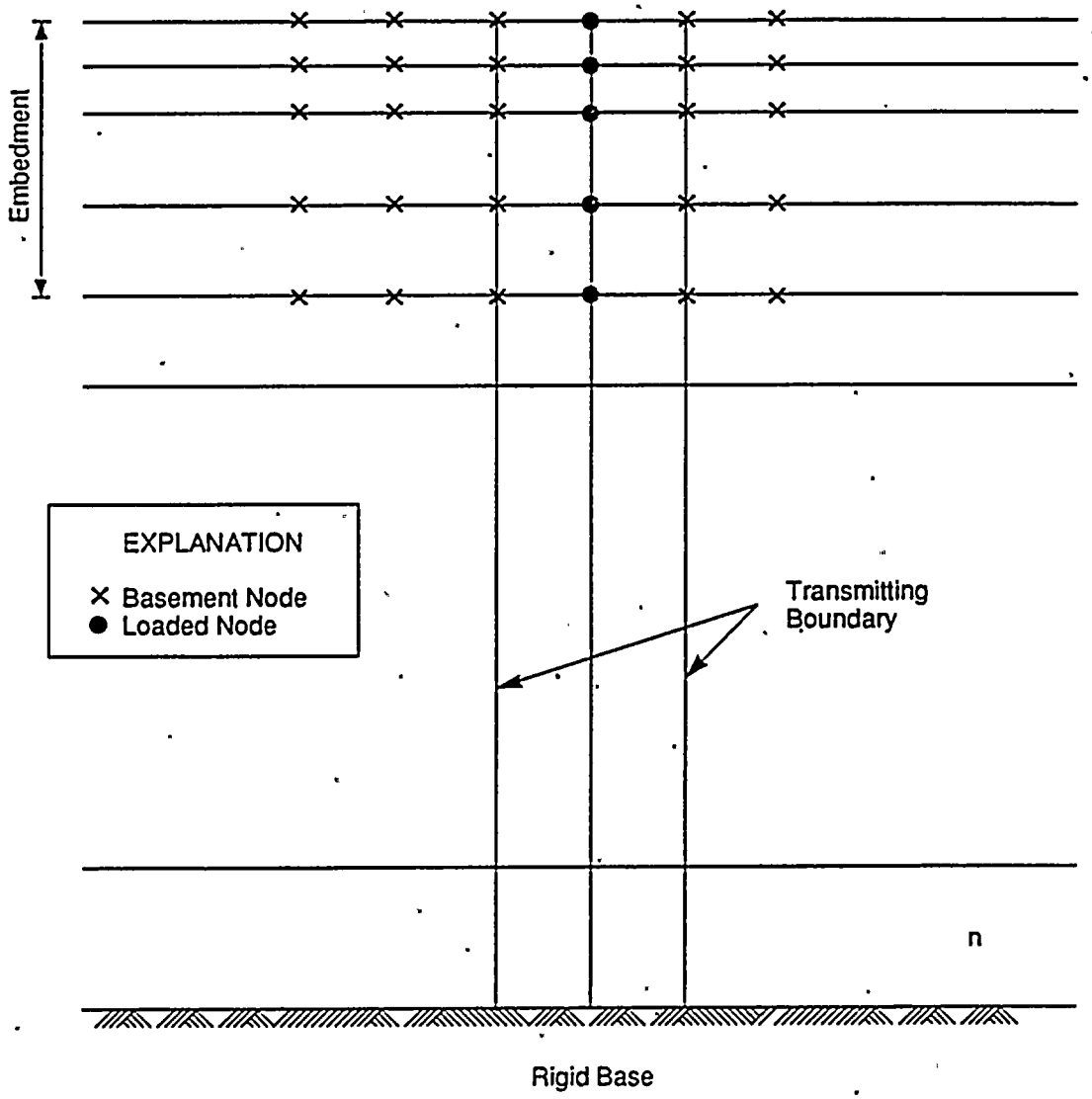

Fig. 4.1-1 Plane-Strain Model for Impedance Analysis

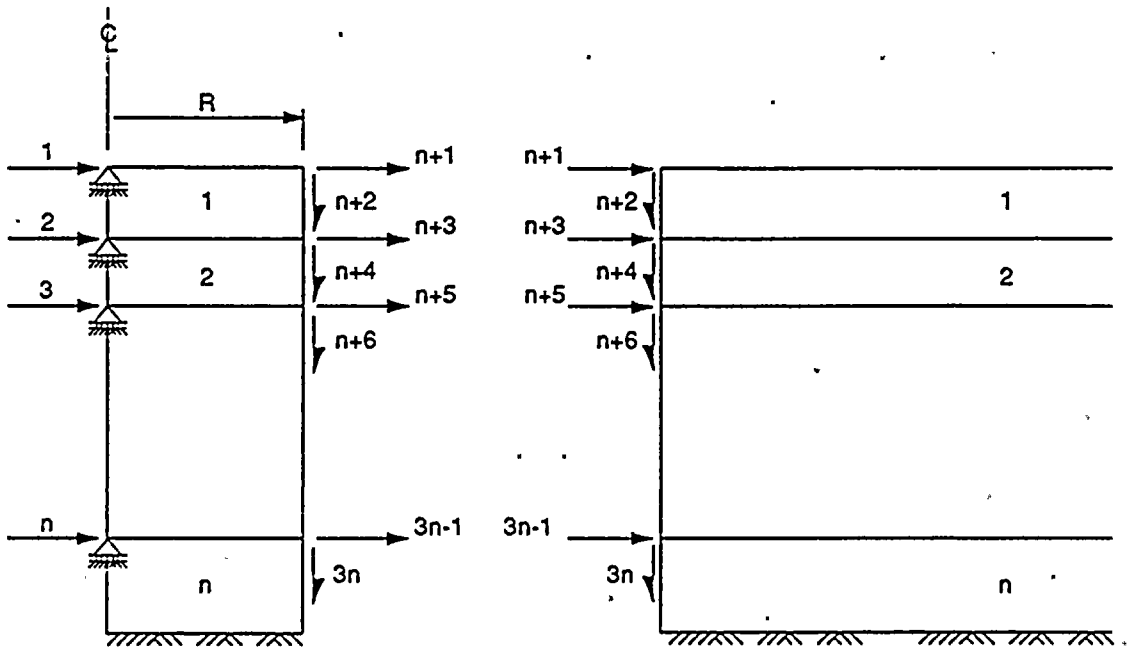

Figure 4.1-2(a). Boundary Conditions for Horizontal Loading

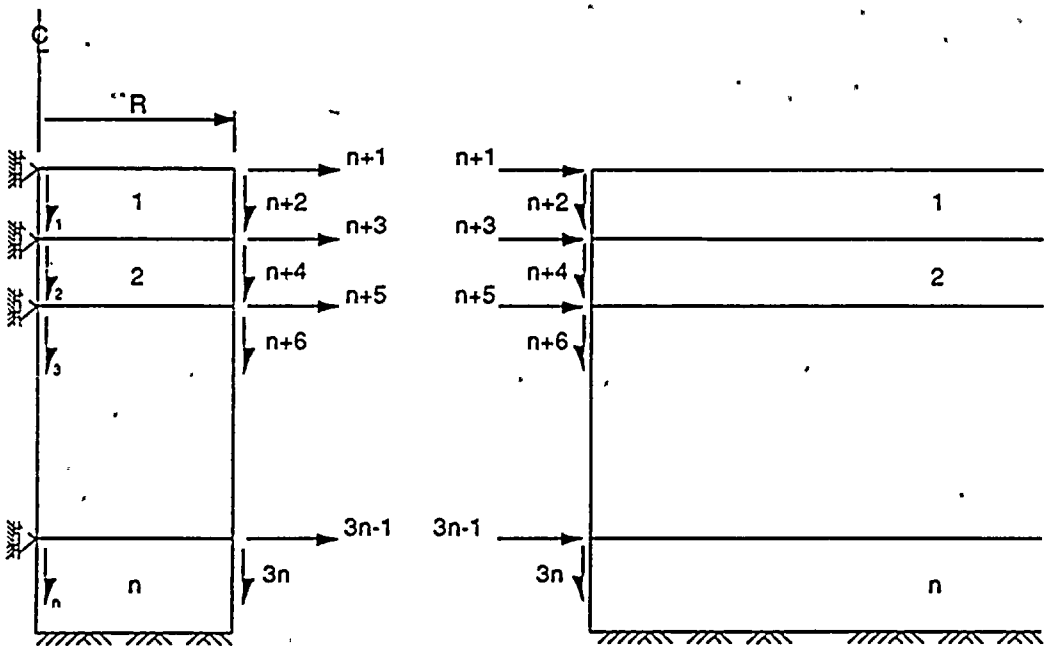

Figure 4.1-2(b). Boundary Conditions for Vertical Loading

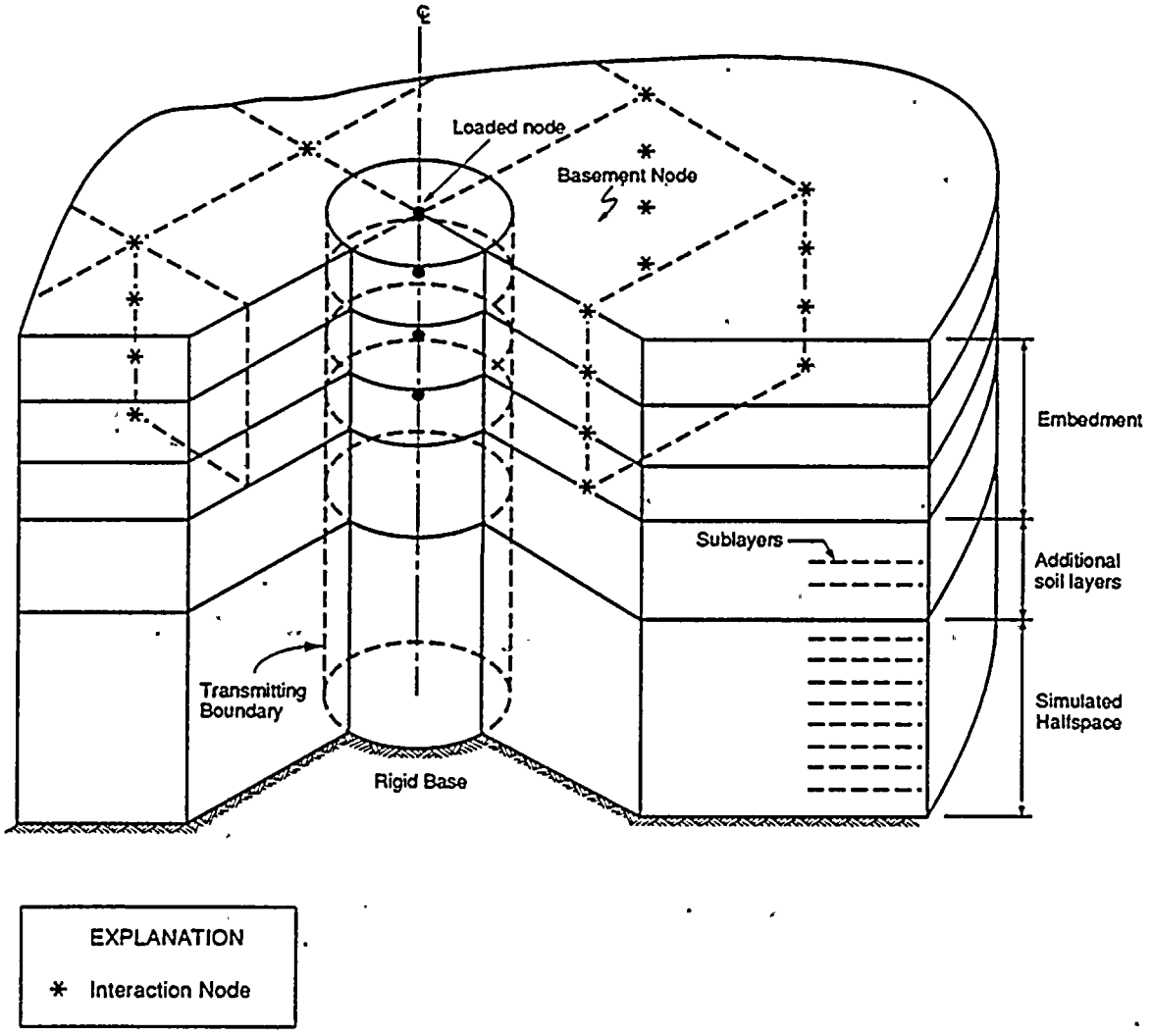

Figure 4.2-1. Axisymmetric Model for Impedance Analysis

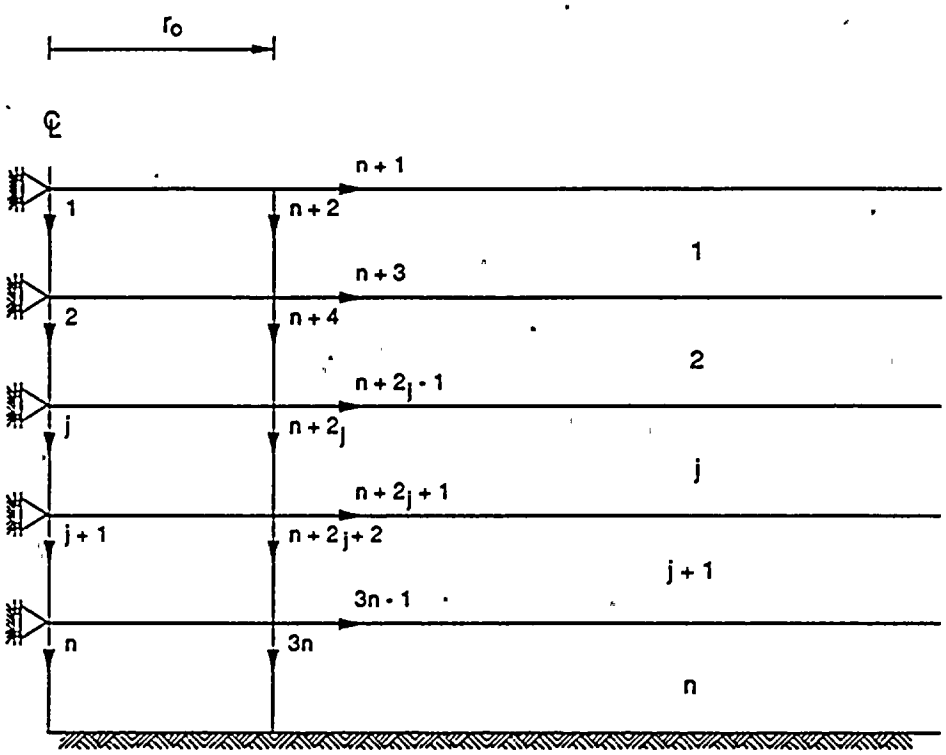

Figure 4.2-2 (a). Boundary Conditions for Vertical Loading

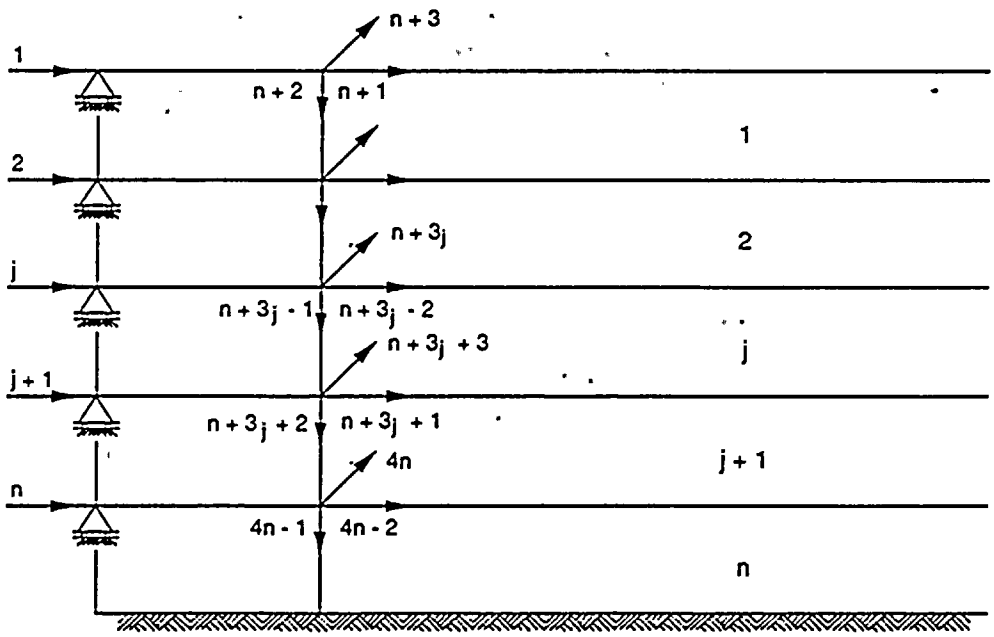

Figure 4.2-2 (b). Boundary Conditions for Horizontal Loading

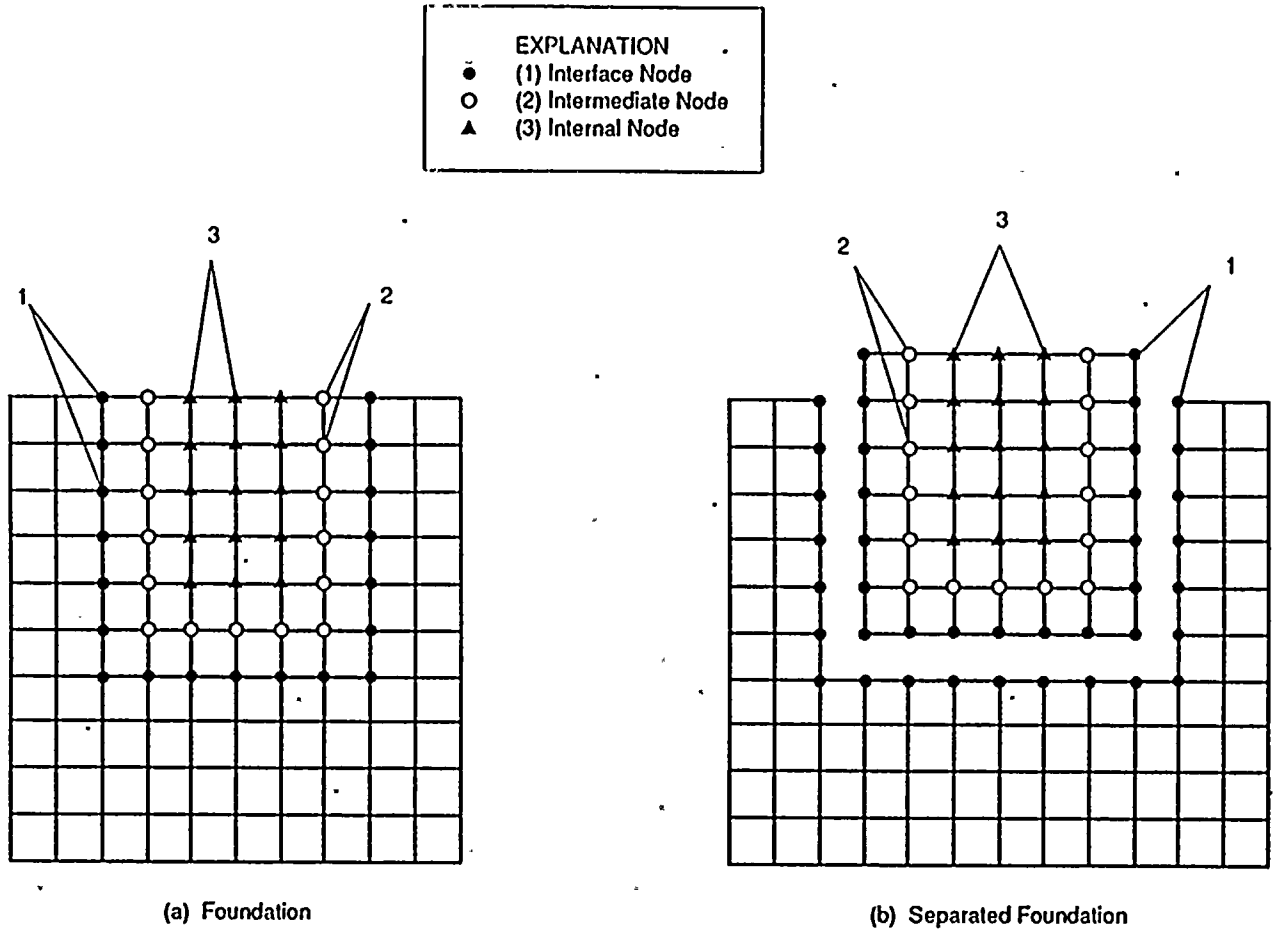

(a) Foundation

(b) Separated Foundation

Figure 4.4-1. Foundation System for Skin Method

5. STRUCTURAL ANALYSIS

In this section, computation of the structural and excavated soil properties used in the coefficient matrix of the equations of motion, namely the components C_{ss}, C_{si}, C_{ii}, and C_{ff} in Eq. (2.2.-6) are described.

5.1 Modelling of Structure

The structure which consists of the superstructure and the basement is modelled by finite elements. Several types of elements are included in the finite element library of SASSI. These elements include 3- to 4-node plane-strain elements (Ref. 1), 4- to 8-node three-dimensional solid elements (Ref. 1), straight beam elements (Ref. 1), spring elements (Ref. 1), LSST9 plate/shell elements (Ref. 1), and special matrix elements to assign stiffness or inertia relating any two nodes in the model. Formulation of mass and stiffness matrices for the above element types are not described but may be obtained from the reference cited. Basic theory for formulation of finite elements may be obtained from general finite element text books (e.g., Ref. 28).

The material damping is incorporated in the stiffness matrix using the complex modulus representation as described in Section 3.6. With this representation the material damping ratio defined at element level will be used to compute the complex stiffness of the element, thus allowing for variation of damping from element to element in the model. The mass matrices are either computed by the program by specifying the density for each element or is assembled from the nodal lump mass input at the nodal points. When mass matrix is computed by the program, the matrix consists of half lump mass half consistent mass (see Section 5.4) except for the plate and beam elements for which only lump mass and consistent mass matrices are computed, respectively.

Special inter-pile elements have also been developed to model the pile foundations. Since the routines for these elements have not yet been upgraded for implementation in the current enhanced version of SASSI, the formulation of these elements are not presented, but may be obtained from Refs. 12 and 14.

Once the mass and stiffness elements are formed, they are assembled into global matrices. These matrices are frequency independent and need to be formed only once. Furthermore, they are symmetric and sparse and therefore can be stored in blocks using active column method (Ref. 27) to minimize computer storage.

5.2 Modelling of Excavated Soil

The excavated soil is modelled using either plane-strain or three-dimensional solid elements for two- and three-dimensional problems, respectively. These elements are assigned two or three translational degrees of freedom per node. Thus, the moments from beam or plate elements need be transferred to the soil through several common connecting nodes.

5.3 Extended Near Field Zone

In some cases it may become necessary to include an additional volume of the soil in the immediate vicinity of the basement in the SSI model. This may be the case where the soil properties around the basement are different from those of the otherwise horizontal layered site (e.g., due to backfilling) or when magnitude of the stress and strain in the soil around the basement are needed to measure the secondary nonlinear effects. For these cases, an additional soil volume is modelled with plane strain or brick elements and these elements are treated as structural elements. Subsequently, the excavated soil elements must cover the additional soil volume already modelled as structural elements.

5.4 Finite Element Size

The accuracy of a finite element analysis depends on the type of interpolation function used to represent the displacement field in the element and element sizes. The interpolation functions which are used for solid and plane strain elements in SASSI vary linearly within the element.

It has been shown (Ref. 8) that for such elements the accuracy of the solution is a function of the method used to compute the mass matrix and an accuracy better than 10 percent on wave amplitude is obtained if the element size h follows the relations shown below:

$$h \leq \begin{cases} 1/8\ \lambda_s \text{ for lumped mass matrix} \\ 1/8\ \lambda_s \text{ for consistent mass matrix} \\ 1/5\ \lambda_s \text{ for mixed mass matrix} \end{cases} \qquad (5.4\text{-}1)$$

In the above relation λ_s is the shortest wave length which occurs in the volume represented by the elements. The wave length is obtained from

$$\lambda_s = \frac{V_s}{f_{max}} \qquad (5.4\text{-}2)$$

where V_s is the shear wave velocity and f_{max} is the maximum frequency of analysis which must be transmitted through the finite elements. Thus, larger element size can be used in the zones with higher shear wave velocity.

In calculating the mass matrices for brick and plain strain elements, combination of half consistent mass matrix with half lump mass matrix is used. Thus, the criteria of $h<1/5\lambda$ need to be followed in selecting the finite element sizes.

This criteria along with the appropriate choice of f_{max} for the problem control the size of the model in terms of the degrees of freedom and subsequently the cost of analysis.

6. SOLUTION OF THE EQUATION OF MOTION

Following the computations of free-field motion, $\{U_f\}$, as described in Section 3, impedance matrix $[X_{ff}]$ as presented in Section 4, and the coefficient matrix of the structures and excavated soil volume as described in Section 5, the equations of motion can be formed and solved. Depedending on the types of excitations, the following solution techniques are used.

6.1 Steady State Response Analysis

For steady state response analysis such as force vibration or seismic excitation of the SSI system at discrete harmonic frequencies, Eqs. (2.2-6) and (2.2-7) are formed for each selected frequency of analysis and solved. The results of analysis (U_s and U_f) are the harmonic complex displacements for the case of external loading with units consistent with the selected system of units for the analysis. For the case of harmonic seismic excitation, the results (U_s and U_f) are the harmonic complex response functions representing the total response with respect to the harmonic input motion at control point.

6.2 Transient Response Analysis

The complex response method described in Section 3.6 is formulated for steady state vibrations. However, transient motions such as earthquake motions or impulse loads can be analyzed using discrete Fourier transform techniques. These techniques are described for the case of transient external loading. However, they are equally applicable to transient earthquake motions.

Using these techniques the basic input is specified at N discrete points uniformly distributed over the period T. The given function values are

$$P_j(t) = P(j.\Delta t) \; ; \; j = 0, 1, \ldots, N-1 \qquad (6.2\text{-}1)$$

where Δt is the time interval T/N. The input can then be extended using trigonometric functions

$$P_j(t) = R_e \sum_{j=0}^{N/2} P_j \exp(i\omega_j t) \qquad (6.2\text{-}2)$$

where ω_j are the frequencies,

$$\omega_j = \frac{2\pi j}{N\Delta t} \qquad (6.2\text{-}3)$$

and P_j are complex amplitudes

$$P_j = \frac{2}{N} \sum_{j=0}^{N-1} P_j \exp(-i\omega_j j\Delta t) \qquad (6.2\text{-}4)$$

which can be computed by the very efficient Fast Fourier Transform (FFT) algorithm, developed by Cooley and Tukey (Ref. 5), which requires that N be a power of two. A further requirement is that since Eq. (6.2-2) is a truncated Fourier series, the function $P_j(t)$ has to be periodic over the period T. Actual earthquakes or impact loads are not periodic. However, by the addition of a "quiet zone" consisting of a limited number of trailing zeroes to the input, both the above requirements can be met. The quiet zone should be chosen sufficiently long such that the response occurring at the beginning of the next cycle is very small due to the system damping. In this case, the response within each cycle is not influenced by the previous cycle.

The solution for a single harmonic can be obtained by solving the equations of motion in Eq. (2.2-7). Since superposition of solutions is valid for linear systems, solution of Eq. (2.2-7) are obtained independently at each frequency, and the results are superimposed to obtain the complete response, using the following equation:

$$\begin{Bmatrix} U_s(t) \\ U_f(t) \end{Bmatrix} = R_e \sum_{j=0}^{N/2} \begin{Bmatrix} U_{sj} \\ U_{fj} \end{Bmatrix} \exp(i\omega_j t) \qquad (6.2\text{-}5)$$

Discrete values of $\{u(t)\}$ at time intervals Δt can be computed by using the inverse Fourier transform on $\{U_j\}$ which is the solution for a single harmonic input.

To obtain a complete solution, the system of linear equations in Eq. (2.2-7) must, in principle, be formed and solved for all of the following FFT frequencies.

$$f_j = \frac{\omega_j}{2\pi} = \frac{j}{T}, \; j = 1,\ldots,N/2 \qquad (6.2\text{-}6)$$

This is a formidable computational task. To minimize the cost, a cutoff frequency is introduced whereby the response for frequencies above a given f_{max} are set to zero. The choice of f_{max} depends on the SSI problem and type of the loading. This feature will considerably cut the number of frequencies to be solved. To further reduce the number of frequencies to be solved, the SASSI program uses an efficient interpolation scheme, whereby the complex response amplitudes U_s and U_f are computed for a certain number of selected frequencies, and the values for the rest of the FFT frequencies are obtained by interpolation. One interpolation technique that has been used previously is the interpolation based on the single-degree-of-freedom complex response function (Lysmer et al., Ref. 9).

For the program SASSI, a new technique based on the two-degrees-of-freedom compleX response function is developed and used. This technique is more general and it is possible to choose the computed frequencies at wider intervals to further reduce the cost of analysis. This interpolation technique is described below.

6.3 SASSI Interpolation Technique

The interpolation technique used in SASSI to interpolate the response for frequencies in between the calculated frequencies and to obtain the response for all FFT frequencies is based on the frequency response function of a two-degree-of-freedom system. The total response of a two-degree-of-freedom system subjected to harmonic base excitation for each degree-of-freedom has the following general form

$$r(\omega) = \frac{a_1 \omega^4 + a_2 \omega^2 + a_3}{\omega^4 + a_4 \omega^2 + a_5} \qquad (6.3\text{-}1)$$

where $r(\omega)$ is the response at frequency ω and a_1, a_2, a_3, a_4, and a_5 are the constants. Thus, if the response of the system is known at 5 frequencies i.e., r_1, r_2, r_3, r_4, and r_5 are known at frequencies 1, 2, 3, 4,and 5, the constants in Eq. (6.3-1) can be obtained from

$$\begin{bmatrix} \omega_1^4 & \omega_1^2 & 1-\omega_1^2 r_1 & -r_1 \\ \omega_2^4 & \omega_2^2 & 1-\omega_2^2 r_2 & -r_2 \\ \omega_3^4 & \omega_3^2 & 1-\omega_3^2 r_3 & -r_3 \\ \omega_4^4 & \omega_4^2 & 1-\omega_4^2 r_4 & -r_4 \\ \omega_5^4 & \omega_5^2 & 1-\omega_5^2 r_5 & -r_5 \end{bmatrix} \begin{Bmatrix} a_1 \\ a_2 \\ a_3 \\ a_4 \\ a_5 \end{Bmatrix} = \begin{Bmatrix} \omega_1^4 r_1 \\ \omega_2^4 r_2 \\ \omega_3^4 r_3 \\ \omega_4^4 r_4 \\ \omega_5^4 r_5 \end{Bmatrix} \qquad (6.3\text{-}2)$$

Following the computation of the 5 constants from the above equation, Eq. (6.3-1) can be used to compute the response (the interpolated response) for all the frequencies in between the range from ω_1 to ω_5.

The interpolation technique described above can be used for interpolating transfer functions for multi-degree-of-freedom when, the transfer functions behave like those of the two-degree-of-freedom system within small frequency regions. Following this technique, the frequency range for which Eqs. (2.2-6) and (2.2-7) are solved are subdivided into smaller regions each of which contains the transfer function solution for 5 frequencies of the analysis. For the last region, the solution from the previous region can be augmented,

if necessary, to form the solution of 5 frequencies needed for the interpolation. Using the above technique, the transfer function in each region is interpolated so that by covering all the regions, the transfer function values are computed for all FFT frequencies shown in Eq. (6.2-6).

6.4 Criteria for Choosing Frequencies of Analysis

The frequencies to be selected for the analysis depend on the number of peaks in the transfer function at the specific response location and how close these peaks are located relative to each other. This information can be obtained from the fixed-base modal analysis of the structure. The modal properties show the significance of different frequencies in the response of the structure depending on the modal participation factors. The frequencies of analysis can be selected by recognizing that the SSI effects usually shift the frequencies to the lower frequency range and tend to flatten the sharp peaks or sometimes even eliminate the fixed-base response peaks. For most of the practical problems it is sufficient to solve the system for 10 to 20 frequencies. In the event that the fixed-base modal properties are not available, it is necessary to select adequate number of frequencies with uniform increment throughout the frequency range of interest.

In SASSI, it is, possible to first calculate the transfer functions based on an initial set of selected frequencies and by examining this initial transfer function, if additional frequencies need be added, the program SASSI has the capability to obtain and combine the solutions from several sets of frequencies and subsequently interpolates the transfer function of the response based on the combined solution set.

7. COMPUTER PROGRAM ORGANIZATION

The program SASSI (Ref. 11) is written in the Fortran IV language. The program is organized in modules and the analysis steps as described in Section 2.2 are handled by separate modules. The program layout, operational features, its capabilities and limitations, and a summary description of its validation and application, are presented in this section.

7.1 Program Layout

Figure 7.1-1 shows the layout of the SASSI program. A brief description of the function of each module and its interaction with other modules are presented in the following:

a. HOUSE

In this program the mass and stiffness matrices of all the elements used in the model are determined and stored on Tape 4. These properties are frequency independent and the program is executed only once.

b. MOTOR

This program forms the load vector in Eq. (2.2-7). The loads may correspond to impact forces, rotating machinery, or simple unit forces to be used to determine the impedance of a foundation. It is possible to allow for loads acting out of phase. The results are stored on Tape 9.

c. SITE

This program solves the site response problem. The control point and wave composition of the control motion are defined. The

information needed to compute vector U_f used in Eq. (2.2-6) is computed at this stage and is saved on Tape 1. The program also stores information required for the transmitting boundary calculation on Tape 2. The actual time history of the control motion is not required in this program.

d. POINT

This program consists of two subprograms, namely POINT2 and POINT3 for two- and three-dimensional cases, respectively. The modules described in Sections 4.1 and 4.2 are solved and the results, which provide the information required to form the flexibility matrix, are saved on Tape 3. Tape 2 created by program SITE is used as input.

e. MATRIX

In this program, Tapes 3 and 4 are used as input to form the impedance matrix $[X_{ff}]$, for each frequency. The impedance matrix is saved on Tape 5. The coefficient matrix in Eqs. (2.2-6) or (2.2-7) is also formed, triangularized and stored on Tape 6.

f. LOADS

Using the data of Tapes 1 and 9, this program computes the load vectors in Eqs. (2.2-6) or (2.2-7) for each frequency and stores them on Tape 7.

g. SOLVE

In this program the reduced stiffness matrices are read from Tape 6. The program then performs the back-substitution using the load vectors on Tape 7. If Eq. (2.2-6) is being solved, the

solution is the transfer functions from the control motion to the final motions. If Eq. (2.2-7) is being solved, the solution is a set of transfer functions from external loads to total displacements. In either case, the results are stored on Tape 8.

The subprograms MATRIX, LOAD, and SOLVE are combined into a controlling program called ANALYS.

Interpolation of the transfer functions in the frequency domain and further output requirements are handled by the following subprograms.

h. MOTION

This program is a post-processor. It reads the transfer functions from Tape 8, performs the interpolations described in Section 6.3, and computes the final response at a specified node selected by the user. Acceleration, velocity, or displacement of the response in terms of time history, peak value, or the response spectrum may be requested.

i. STRESS

This program reads Tapes 8 and 4 and computes requested stress, strain, and forces time histories and peak values in structural members.

j. COMBINE

If after interpolation it is found that some additional frequencies need to be included, this program combines the corresponding Tapes 8 and produces a new Tape 8.

7.2 Operational Features

If some changes occur in the design parameters, only part of SASSI system would need to be re-executed. This feature makes it possible to perform parametric studies in a very effective manner. The following examples illustrate the possible uses of the restart capabilities:

a. Change in seismic environment

The seismic environment is defined in terms of (1) the time history of the control motion, (2) the location of the control point, and (3) the composition as to type and direction of the waves assumed to cause the control motion. A re-analysis with a different time history requires only a simple re-execution of the program MOTION. If the control point and/or the wave composition are changed, only the programs SITE, LOAD, SOLVE, and MOTION need to be re-executed. This costs only a small fraction of a complete re-analysis since the expensive impedance matrix calculation does not have to be repeated.

b. Change in structure

If part of the structure is changes by changing material properties or by adding or subtracting elements, only HOUSE, part of MATRIX, SOLVE, and MOTION would have to be re-executed; as long as no new interaction nodes are added.

7.3 Capabilities and Limitations

The current version of computer program SASSI has the following capabilities and limitations:

- The site consists of semi-infinite horizontal layers resting on a rigid base or a semi-infinite halfspace.

- The seismic environment consists of an arbitrary three-dimensional superposition of inclined body waves and surface waves. It is also possible to introduce external forces such as impact loads, wave forces, or loads from rotating machinery acting directly on the structure.

- The structure(s) are represented by standard two- or three-dimensional finite element models.

- The method is restricted to linear analysis. However, approximate nonlinear analysis can be performed by an interative scheme called "The Equivalent Linear Method".

- Primary nonlinear effects in the free field and secondary nonlinear effects in a limited region near the structure can be considered.

Within the above limitations and that of available computer capacity the system can handle:

- Two- and three-dimensional SSI problems involving single or multiple structures

- Structure with rigid or flexible embedded foundation of arbitrary shape

- Machine foundation vibration problems

- Impact problems or problems involving wave and ice loadings

- Seismic loadings involving body waves and surface waves

- Effects of torsional ground motions

For the future versions, the program is planned to be upgraded to include capabilities for handling pile foundations.

7.4 Program Validation and Application

During the development of the theory and the corresponding analytical models, many example problems were analyzed to test the modules. These example problems and comparisons of the results with reference solutions are reported in Refs. 12, 22, 23, and 25. A comprehensive program validation has also been carried out to benchmark the SASSI solutions against the published solutions of 20 validation problems with a total of 60 validation cases. The results of this validation is documented in the program validation report (Ref. 2). The benchmark solutions consist of simple hand solutions, analytical or closed form solutions reported in the literature, and solutions obtained from other validated computer programs. The validation covers many capabilities of the program ranging from calculation of finite element mass and stiffness properties, impedance analysis of surface and embedded single and multiple foundations with rigid and flexible properties, scattering analysis of surface and embedded foundation subjected to vertical and inclined P, SV, and SH waves, and surface Rayleigh and Love waves; and SSI analysis of surface and embedded structures. The favorable agreements between the SASSI results and the benchmark solutions obtained for all problem cases validate many capabilities of computer program SASSI. In addition to the above validation report, SASSI capabilities have also been recently tested through the course of application of the program to a research project sponsored by EPRI. The objective of this research project was to evaluate the validities of the current industry SSI methodologies by using the forced-vibration test data and the recorded actual earthquake response data obtained for the scale containment structure constructed and instrumented in Lotung, Taiwan. The results of the SASSI analyses and correlation with the test results and the results of other SSI methods used are reported in Ref. 3. Results of this study provide a validation of the SASSI analysis capability for embedded structures against test results.

SASSI has been applied to many engineering projects. The first application of the program for analyses of an embedded power plant structure, an offshore structure, and an underground structure is reported in Ref. 11. The recent applications of the program are reported in Refs. 15, 16, 17, 18 and 24.

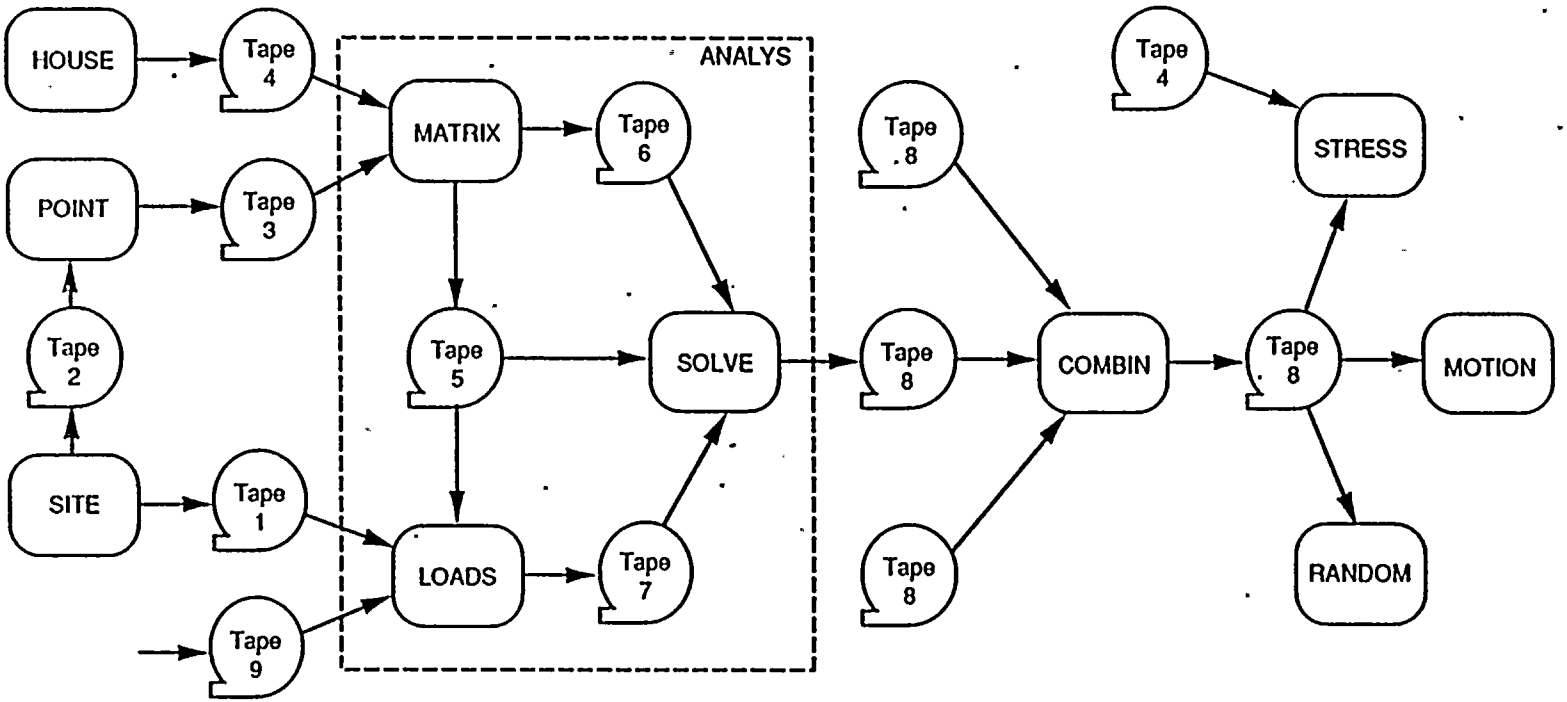

Figure 7.1-1. Layout of Computer Program SASSI

8. REFERENCES

1. Bathe, K. L., Wilson, E. L., Peterson, F. E. (1974) "SAP IV - A Structural Analysis Program for Static and Dynamic Response of Linear Systems," Report No. EERC 73-11, Earthquake Engineering Center, UCB, April.

2. Bechtel Power Corporation (1988): "SASSI Validation Report," Prepared for PG&E for Diablo Canyon Power Plant, Long Term Seismic Program, July.

3. Bechtel Western Power Corporation (1987): "Soil-Structure Interaction analyses of Quarter-Scale Containment Model Experiment in Lotung, Taiwan," Prepared for Electric Power Research Institute, Palo Alto, CA, December.

4. Chen, J-C. (1980): "Analysis of Local Variation in Free Field Seismic Ground Motions," Ph.D. Dissertation, University of California, Berkeley, November.

5. Cooley, J. W. and Tukey, J. W. (1965): "An algorithm for the machine calculation of complex Fourier series," Mathematics of Computation, Vol. 19, No. 19, 297-301.

6. Hardin, B. O. and Drnevich, V. P. (1972): "Shear modulus and damping in soils: design equations and curves," Journal of the Soil Mechanics and Foundations Division, ASCE, Vol. 98, No., SM7, 667-692.

7. Lysmer, J. and Kuhlemeyer, R. L. (1969): "Finite dynamic model for infinite media," Journal of Engineering Mechanics Division, ASCE, Vol. 95, No. EM4, 859-877.

8. Lysmer, J., Udaka, T., Seed, H. B. and Hwang, R. (1974): "LUSH - A computer program for complex response analysis of soil-structure systems," Report No. EERC 74-4, Earthquake Engineering Research Center, UCB, April.

9. Lysmer, J., Udaka, T., Tsai, C-F. and Seed, H. B. (1975): "FLUSH - A computer program for approximate 3-D analysis of soil structure interaction problems," Report No. ERC 75-30, Earthquake Engineering Research Center, UCB, November.

10. Lysmer, J. (1978): "Analytical procedures in soil dynamics," Report No. EERC 78/29, Earthquake Engineering Research Center, University of California, Berkeley, December.

11. Lysmer, J., Tabatabaie-Raissi, M., Tajirian, F., Vahdani, S., and Ostadan, F. (1981): "SASSI - A system for analysis of soil-structure interaction," Report No. UCB/GT/81-02, Geotechnical Engineering, University of California, Berkeley, April.

12. Ostadan, F. (1983): "Dynamic Analysis of Soil-Pile-Structure Systems," Ph.D. Dissertation, University of California, Berkeley.

13. Ostadan, F., Lysmer, J. (1985): "Dynamic Analysis of Directly Loaded Structures on Pile Foundations," 8th SMiRT Conference, Brussels, Belgium.

14. Ostadan, F., Lysmer, J. (1986): "Simplified Dynamic Analysis of Soil-Pile-Structure Systems," 5th International Symposium & Exhibition on Offshore Mechanics and Arctic Engineering, Tokyo, Japan.

15. Ostadan, F., Tseng, Wen S., Lilhanand, K. (1987): "Application of Flexible Volume Method to Soil- Structure Interaction Analysis of Flexible and Embedded Foundation," 9th SMiRT Conference, Lausanne, Switzerland.

16. Ostadan, F., Tseng, Wens S. (1988): "Effect of Foundation Flexibility and Embedment on the Soil-Structure Interaction Response," 9th World Conference on Earthquake Engineering, Tokyo, Japan, August.

17. Ostadan, F., Tseng, Wen S. (1989): "Effect of Site Soil Properties on Seismic SSI Response of Embedded Structures," submitted for possible publication in ASCE Foundation Engineering Congress, Evanston, Illinois.

18. Ostadan, F., Tseng, Wen S., Sawhney, P. S., Liu, A., Goll, P. F., (1989): "Seismic Load Reduction with Increasing Embedment Depth for Advanced Boiling Water Reactor Building and Equipment Design," submitted for possible publication in 10th SMiRT Conference, Los Angeles, California, U.S.A.

19. Schnabel, P. B., Lysmer, J. and Seed, H. B. (1972): "SHAKE - A computer program for earthquake response analysis of horizontally layered sites," Report No. EERC 72-12, Earthquake Engineering Research Center, UCB, December.

20. Seed, H. B. and Idriss, I. M. (1969): "The influence of soil conditions on ground motion during earthquake," Journal of SOil Mechanics and Foundations Division, ASCE, VOl. 94, No., SMl., 99-137, December.

21. Seed, H. B. and Idriss, I. M. (1970): "Soil moduli and damping factors for dynamic response analysis," Report EERC 70-10, Earthquake Engineering Research Center, UCB, December.

22. Tabatabaie-Raissi, M. (1982): "The Flexible Volume Method for Dynamic Soil-Structure Interaction Analysis," Ph.D. Dissertation, University of California, Berkeley.

23. Tajirian, F. (1981): "Impendance Matrices and Interpolation Techniques for 3-D Interaction Analysis by the Flexible Volume Method," PhD. Dissertation, University of California, Berkeley.

24. Tseng, Wen S., Ostadan, F. (1989): Structure-Soil-Structure Interaction in Different Seismic Environments," submitted for possible publication in the 10th SMiRT Conference, Los Angeles, California.

25. Vahdani, S. (1984): "Impedance Matrices for Soil-Structure Interaction Analysis by the Flexible Volume Method," Ph.D. Dissertation, University of California, Berkeley.

26. Waas, G. (1972): "Earth vibration effects and abatement for military facilities - analysis method for footing vibrations through layered media," Technical Report S-71-14, U.S. Army Engineer Waterways Experimental Station, Vicksburg, Mississippi, September. (Also a Ph.D. Dissertation entitled, "Linear Two-Dimensional Analysis of Soil Dynamics Problems in Semi-Infinite Layered Media,". University of California, Berkeley.)

27. Wilson, E. L. and Dovey, H. H. (1978): "Solution or reduction of equilibrium equations for large complex structural systems," Advances in Engineering Software, Vol. 1, No. 1, 19-25.

28. Zienkiewicz, O. C., (1977): The Finite Element Method, 3rd edition. (McGraw Hill).

ATTACHMENT Q2b-2

SYSTEM FOR
ANALYSIS OF
SOIL
STRUCTURE
INTERACTION

SASSI USER'S MANUAL

JULY 1988

CE994

BECHTEL POWER CORPORATION

A SYSTEM FOR ANALYSIS OF
SOIL-STRUCTURE INTERACTION

USER'S MANUAL
(CDC CRAY-XMP AND PG&E IBM VERSIONS)

Prepared for Diablo Canyon
Long Term Seismic Program
Pacific Gas and Electric Company

MANUAL

by

THE SASSI DEVELOPMENT TEAM:

John Lysmer
Farhang Ostadan
Mansour Tabatabaie - Fredrick Tajirian - Shahriar Vahdani

Geotechnical Engineering Division
Civil Engineering Department
University of California, Berkeley, CA 94720

Revised by

Bechtel Power Corporation
San Francisco, California

July 30, 1988

PREFACE

The computer program SASSI was developed at the University of California, Berkeley, by a research team under the technical direction of Prof. John Lysmer. The CDC and IBM versions of the program were obtained from the University of California, Berkeley, under a license agreement with the University. During the course of installation, testing, and validation of the Bechtel version of the code on the CDC CRAY System, some modifications and enhancements were made to the code to improve the code performance. These include correcting the motion phases in Rayleigh wave calculation, replacing the plate element and providing the option for local end release condition in beam element. The original User's Manual issued by the University was revised to reflect the changes made to the code. A new chapter on application guide was also added to the User's Manual. The IBM version provided to PG&E contains the same modifications and enhancements made to the Bechtel CRAY version to date. The validation and theoretical manuals of the program were also prepared to complete the documentations of the program. The modifications and enhancements and preparation of the validation and theoretical manuals have been performed by the Civil/Structural Staff Group of Bechtel Power Corporation, San Francisco Office.

This manual has been prepared by Bechtel Power Corporation and has been reviewed following the Bechtel Standard Engineering Department Procedure for Nuclear Projects.

This manual was prepared under a contract agreement between PG&E and Bechtel and is intended for the exclusive use by PG&E only. Except for copies that may be required for the Nuclear Regulatory Commission (NRC) in satisfying a regulatory requirement, no copy should be distributed outside of PG&E without prior written consent from Bechtel.

DISCLAIMER

Every reasonable effort was made to provide a comprehensive and flexible computer program. However, the computer program itself and associated documentation are supplied without representation of warranty, expressed or implied, as to its content, accuracy, or freedom from defects or errors.

CONTENTS

SECTION PAGE

CHAPTER 1

INTRODUCTION

1.1 Program Description

SASSI - a System for Analysis of Soil Structure Interaction - consists of a number of interrelated computer program modules which can be used to solve a wide range of dynamic soil-structure interaction problems in two or three dimensions.

1.2 Capabilities and Limitations

The computer program SASSI has the following capabilities and limitations:

1.2.1 Soil and structure idealization

1. The site consists of semi-infinite elastic or viscoelastic horizontal layers on a rigid base or a semi-infinite elastic or viscoelastic halfspace.

2. The structure(s) are idealized by standard two- or three-dimensional finite elements connected at nodal points.

3. Each nodal point on the structure may have up to six displacement degrees of freedom. The user has the option to delete one or more of the degrees of freedom thereby reducing the size of the problem accordingly.

4. The excavated soil zone(s) are idealized by standard plane strain or three-dimensional solid elements connected at the nodal points also common to the structure.

5. Interaction between the foundation and the structure occurs at all basement nodes, including those in the basement volume.

6. All the interaction nodes lie on the soil layer interfaces with translational degree-of-froodom. Rotations from the structure are transferred by translation by connecting at several interacting nodes.

7. The mass matrix is assumed to be 50% lumped and 50% consistent except for the structural beam elements and plate elements where consistent mass matrix and lump mass matrix are used, respectively.

8. Material damping is introduced by the use of complex moduli, which leads to effective damping ratios which are frequency independent and may vary from element to element.

1.2.2 Dynamic loadings

1. The seismic environment may consist of an arbitrary three-dimensional superposition of inclined body waves and surface waves.

2. Earthquake excitation is defined by a time history of acceleration called control motion. The control motion is assigned to one of the three global directions at the control point which lies on a soil layer interface.

3. In addition to seismic loads, it is possible to introduce external forces or moments such as impact loads, wave forces, or loads from rotating machinery acting directly on the structure. The external forces are applied at the nodal points and are assumed to have similar time histories.

However, it is possible to assign different maximum amplitudes and arrival times to each dynamic load applied at a nodal point. This feature enables the program user to define moving dynamic loads on the structure.

4. Transient input time histories such as earthquake record or impact loads are handled by the Fast Fourier Transform technique. Therefore, the time histories must be specified at equal time intervals. Besides, the total number of points in the time histories must be a power of 2.

1.2.3 Finite element library

The current library of SASSI elements consists of the following element types:

1. Three-dimensional solid element (eight-node brick) with three translational degrees of freedom per node. It is also possible to include nine incompatible displacement modes in this element when it is used to model the structure.

2. Three-dimensional beam element with three translational and three rational degrees of freedom per node.

3. Four-node quadrilateral plate/shell element with three translational and three rational degrees of freedom per node.

4. Two-dimensional four-node plane strain finite element with two translational degrees of freedom per node.

5. Three-dimensional spring element with three translational and three rational degrees of freedom per node.

6. Three-dimensional stiffness/mass matrix element with three translational and three rational degrees of freedom per node.

In addition to the above elements, a two-dimensional pile element with two transitional and one rotational degrees of freedom per node and a three-dimensional pile element with three translational and three rotational degrees of freedom per node are under development and will be implemented in the next version of the program. Also, other element types which are under consideration to be added later to the element library include fluid type elements and higher order solid elements.

1.2.5 Nonlinear Analysis

1. The analytical method used in the SASSI program is restricted to linear analysis. However, approximate nonlinear analysis can be performed by an iterative scheme called "Equivalent Linear Method."

2. Primary nonlinear effects in the free field and secondary nonlinear effects in a limited region near the structure can be considered.

1.2.5 Interpolation Scheme

An efficient interpolation scheme on complex response functions has been developed for the SASSI program. By the use of the new interpolation scheme it is sufficient to compute the response at, say, 15 to 20 frequencies, from which the intermediate solutions can be obtained by interpolation.

1.2.6 System of Units

Any system of units may be chosen to be used in the SASSI program as long as the units of the input data are consistent in all the program modules.

1.3 ORGANIZATION OF THE MANUAL

An introduction to the SASSI computer program was given in Chapter 1. This chapter also lists the capabilities and limitations of the SASSI program modules.

In Chapter 2, a brief description of the theoretical background is given to describe the analytical procedure used in the SASSI program.

In Chapter 3, the organization and operational features of the SASSI program are presented.

In Chapter 4, the application guide to SASSI analysis is presented. This chapter explains the logical approach to SASSI analysis of SSI problems and how to run a SASSI job. A sample problem to illustrate these steps has also been included in this chapter.

In Chapter 5, the SASSI program modules are individually described. The general description of each program module begins with an introduction to the program operation, followed by the input guide. The input guide also contains numerous comments which are helpful to the user in the day-to-day use of the program.

Appendix A contains the input data files used for example problem in Chapter 4. Appendix B includes the comment forms and error report forms.

CHAPTER 2

THEORETICAL BACKGROUND

2.1 The Flexible Volume Method

The basic method of analysis adopted by the computer program SASSI is called the flexible volume substructuring method (Refs. 1 and 3). The method is formulated in the frequency domain using the complex response method and the finite element technique.

In the flexible volume method, the complete soil-structure system, shown in Fig. 2.1-1(a), is partitioned into two substructures, namely, the foundation and the structure, as shown in Figs. 2.1-1(b) and 2.1-1(c), respectively. In this partitioning, the structure consists of the superstructure plus the basement minus the excavated soil; i.e., the soil to be excavated is retained with the foundation. Interaction between the structure and the foundation occurs at all basement nodes.

The equations of motion for the flexible volume method are developed by combining the equation of motion for the structure with those of the soil in the frequency domain using the concepts of substructuring, thus leading to:

$$\begin{bmatrix} C_{ss} & C_{si} \\ C_{is} & (C_{ii} - C_{ff} + X_{ff}) \end{bmatrix} \begin{Bmatrix} u_s \\ u_f \end{Bmatrix} = \begin{Bmatrix} 0 \\ X_{ff} \cdot u'_f \end{Bmatrix} \qquad (2.1\text{-}1)$$

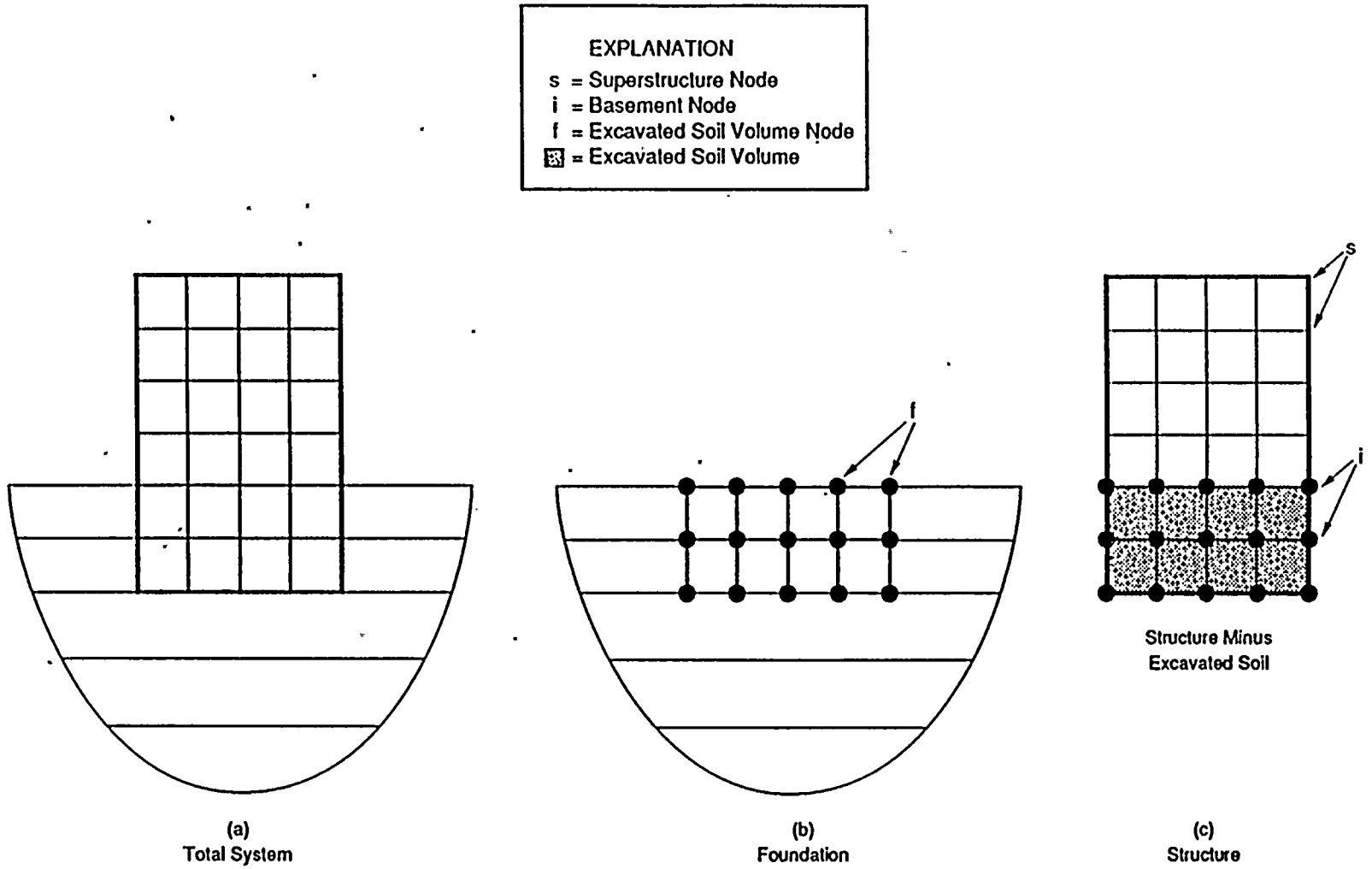

Figure 2.1-1. Substructuring in the Flexible Volume Method

from which the final total motions of the structure can be determined. In these equations, the subscripts s, i, and f refer to degrees of freedom associated with the nodes on superstructure, basement, and excavated soil, respectively. C is the complex frequency-dependent stiffness matrix:

$$C(\omega) = K - \omega^2 M \qquad (2.1\text{-}2)$$

where M and K are the total mass and complex stiffness matrices, respectively, assembled as described in Volume II (Ref. 1), and 3 is the frequency of vibration; u is the vector of complex nodal point displacements; X_{ff} is a frequency-dependent matrix which represents the dynamic stiffness of the foundation at the interaction nodes. X_{ff} will be referred to as the impedance matrix.

Equation (2.1-1) considers only seismic forces. External loads at the superstructure and basement nodes can be considered simply by adding the amplitudes of these forces to the load vector (right-hand side of Eq. (2.1-1) at each frequency. Thus the final motions of the structure can be determined from the following equations:

$$\begin{bmatrix} C_{ss} & C_{si} \\ C_{is} & (C_{ii} - C_{ff} + X_{ff}) \end{bmatrix} \begin{Bmatrix} u_s \\ u_f \end{Bmatrix} = \begin{Bmatrix} P_s \\ P_f \end{Bmatrix} \qquad (2.1\text{-}3)$$

where P_s and P_f are the amplitudes of external forces at the superstructure and basement nodes, respectively.

According to this formulation, the solution of the soil-structure interaction problem reduces to three main steps (for each frequency):

1. Solve the site response problem to determine the free field motions u_f' within the embedded part of the structure.

2. Solve the impedance problem to determine the matrix X_f.

3. Solve the structural problem. This involves forming the complex stiffness matrices and load vectors shown in Eqs. (2.1-1) and (2.1-3) and solving these equations for the final displacements.

2.2 Site Response Analysis

The original site is assumed to consist of horizontal soil layers overlying a uniform halfspace. All material properties are assumed to be viscoelastic. However, the stiffness and damping of each layer are adjusted by the equivalent linear method as described in Volume II (Ref. 1).

Methods for solving the site response problem corresponding to inclined body waves and surface waves have been described in Volume II (Ref. 1).

In this formulation only the free-field displacements of the layer interfaces where the structure is connected are of interest. Accordingly, and this is possible for all of the above-mentioned wave types, displacement amplitudes will be expressed in the form:

$$u_f'(x) = U_f e^{i(\omega t - kx)} \qquad (2.2\text{-}1)$$

where U_f is a vector (mode shapes) which contains the interface amplitudes at and below the control point (x=0) and k is a complex wave number which expresses how fast the wave propagates and decays in the horizontal x-direction. Effective discrete methods have been developed (Volume II) for determining appropriate mode shapes and wave numbers corresponding to control motions at any layer interface for inclined P-, SV-, and SH-waves, Rayleigh waves, and Love waves. Any combination of such waves can be applied.

2.3 Impedance Analysis

As previously stated, the impedance matrix represents the dynamic stiffness of the foundation at the interaction nodes. Thus it can be determined as the inverse of the dynamic flexibility matrix F_f for these nodes:

$$X_{ff} = F_{ff}^{-1} \tag{2.3-1}$$

F_{ff} is a full symmetric complex matrix, and an efficient in-place inversion subroutine is currently used for such operation. This method is called "the direct method" for computing the impedance matrix.

Another method which is less rigorous then the direct method but is more cost effective has also been developed. This method is called "The skin method." In this method the interaction nodes are grouped into three different categories, namely, interface, intermediate, and internal nodes. By definition, interface nodes are nodes which lie along the physical boundaries between the structure and the soil region (labeled by digit 1 in Fig. 2.3-1). Intermediate nodes are defined as those interaction nodes which are directly connected to interface nodes (labeled by digit 2 in Fig. 2.3-1). The remaining interaction nodes are internal nodes (labeled by digit 3 in Fig. 2.3-1).

With the above definitions Eq. (2.3-1) can be partitioned, and when combined with the submatrices of the direct stiffness matrix of the excavated soil region the entire impedance matrix for the interaction nodes is obtained as follows:

$$X_{ff} = \begin{bmatrix} F_{11}\,(I - F_{12} \cdot C_{12}) & C_{12} & 0 \\ C_{21} & C_{22} & C_{23} \\ 0 & C_{32} & C_{33} \end{bmatrix} \tag{2.3-2}$$

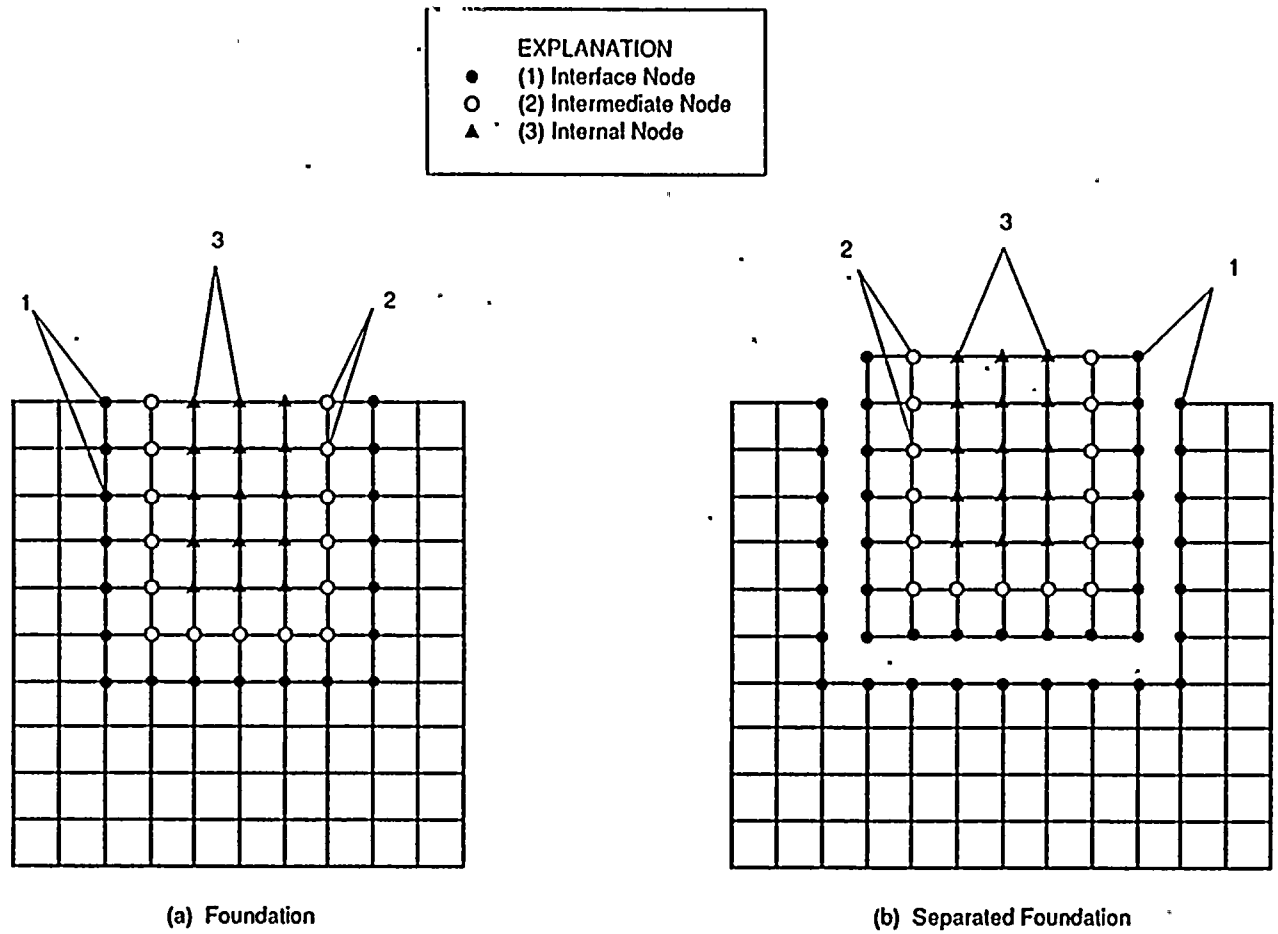

(a) Foundation

(b) Separated Foundation

Figure 2.3-1. Foundation System for Skin Method

Also, the size of a soil-structure system with symmetric properties and loading can be drastically reduced if only one-half or one-fourth of the model is analyzed. This will require the derivation of special impedance matrices, which has been discussed in Volume II.

2.4 Structural Analysis

The superstructure plus the basement minus the excavated soil (Fig. 2.1-1[c]), will be collectively called the near-field zone. This entire zone may be modeled in two or three dimensions using the finite element method described in Volume II.

Effective methods of modeling this zone and solving the resulting equations of motion, Eq. (2.1-1) or Eq. (2.1-3), are described in detail in Volume II.

2.5 Summary of Computational Steps

The steady-state equations of motion for the near-field zone are stated in Eq. (2.1-1) for earthquake loading and in Eq. (2.1-3) for direct forces. As indicated by these equations, for each frequency, ω, the impedance matrix, the load vector, and the dynamic stiffness matrices ($C = K - \omega^2 M$) for the structure (including the basement and any irregular zone) and the excavated soil are formed. After forming the equations of motion, they must be solved. The matrices involved are often very large, especially for three-dimensional problems, and must be stored in blocks on low-speed storage devices even when large electronic computers are used. An efficient scheme for performing the necessary operations of SASSI analysis are described in the next chapter.

Below are given some details of the operations which must be performed for each frequency of the analysis:

1. Form dynamic stiffness of structure: The total frequency-dependent complex stiffness of the structure is computed from Eq. (2.1-2) using the total stiffness and mass matrices. This matrix is stored in blocks as shown below in preparation for solution by the active column method.

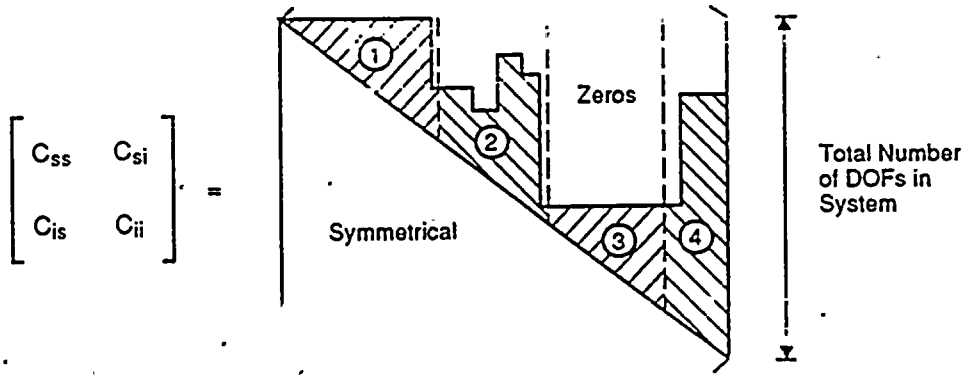

2. Form dynamic stiffness of excavated soil: The total frequency-dependent complex stiffness of the excavated soil is computed from Eq. (2.1-2) using the total stiffness and mass matrices. This matrix is also stored in blocks as shown below.

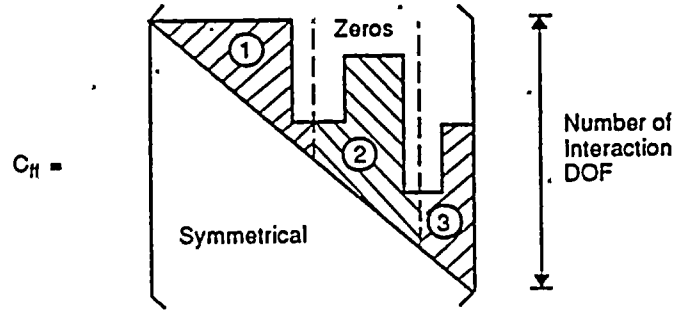

3. Form impedance matrix: If the direct method is used, then the entire flexibility matrix for the interaction nodes is constructed using the method described in Volume II. It is stored in blocks as follows:

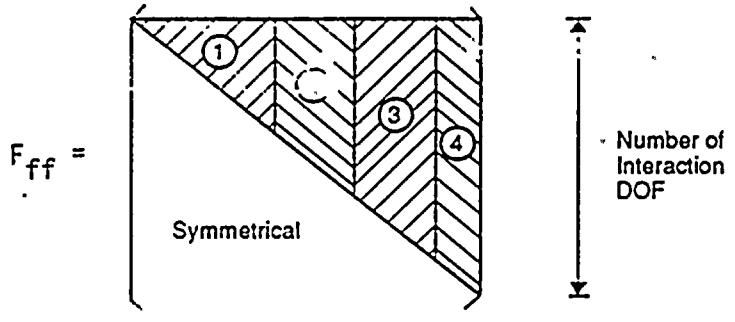

The matrix is then inverted in place, using a special subroutine for symmetric matrices, to obtain the impedance matrix, which is stored in the same form:

X_{ff} =

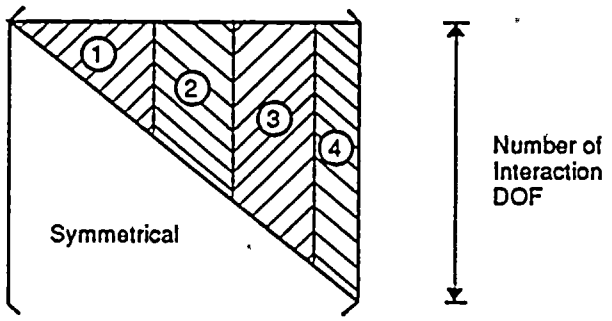

Alternately, if the skin method is used, the flexibility matrix is constructed only for interface and intermediate nodes. It is then stored in blocks as follows:

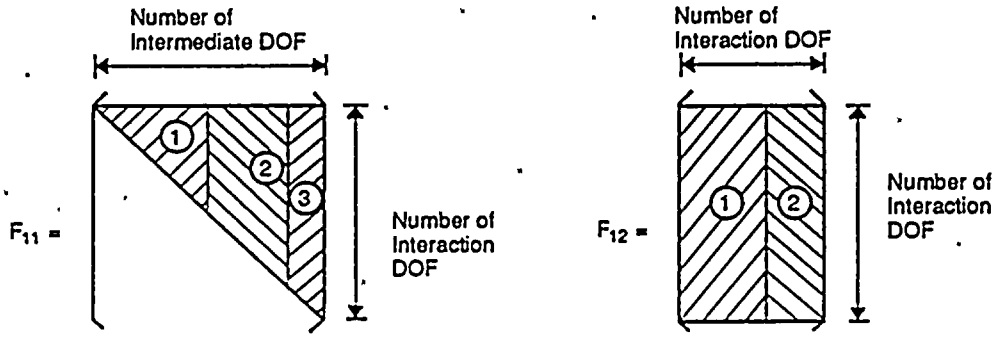

Finally, using the direct stiffness matrix of the excavated soil obtained in Step 2, the entire impedance matrix is computed from Eq. (2.3-2) and stored as for the direct method.

4. Form the total stiffness of the system: The total stiffness of the system can now be obtained by adding X_f to and subtracting C_{ff} from the total stiffness of the structure:

$$\text{coefficient matrix} = \begin{bmatrix} C_{ss} & C_{si} \\ C_{is} & C_{ii} - C_{ff} + X_{ff} \end{bmatrix}$$

5. Triangularization: The coefficient matrix obtained above is then triangularized and stored again in the same form as for the stiffness of the structure.

6. Form load vector: For seismic analysis the load vector is computed by multiplying the impedance matrix, X_{ff}, by a vector which contains the free-field motions at all the interaction degrees of freedom, $\ddot{u}_f$,

$$\text{load vector} = \begin{Bmatrix} 0 \\ X_{ff} \cdot \ddot{u}_f \end{Bmatrix}$$

and for foundation vibration analysis, the load vector is formed from the given external forces,

$$\text{load vector} = \begin{Bmatrix} P_s \\ P_f \end{Bmatrix}$$

7. Solution of the equations: Finally, the acceleration (or displacement) amplitudes are obtained by forward reduction and back-substitution of the load vector using the reduced coefficient matrix obtained in Step 5.

CHAPTER 3

THE COMPUTER CODE SASSI

A modular computer code, SASSI (Ref. 3), has been developed to perform the operations described in Chapter 2. The code has been arranged specifically for practical applications and has the following characteristics:

a. The site response analysis, the impedance analysis, and the formation of the basic stiffness and mass matrices for the structure can be performed separately and the results stored on magnetic tapes or disks.

b. Thus, if the seismic environment, the external loads, the soil properties, or the arrangement of the superstructure are changed, only part of the computations have to be repeated.

c. The final solution is stored (in the form of transfer functions) on a magnetic tape from which specific information can be extracted when required without recomputation of the entire solution.

d. Both deterministic (time history) and probabilistic results can be obtained from the above tape.

3.1 Layout

The general layout of the system is shown in Fig. 3.1-1.

a. HOUSE

The basic frequency-indepedent stiffness matrices M and K for the structure and excavated soil are formed by the program module HOUSE and stored on Tape 4.

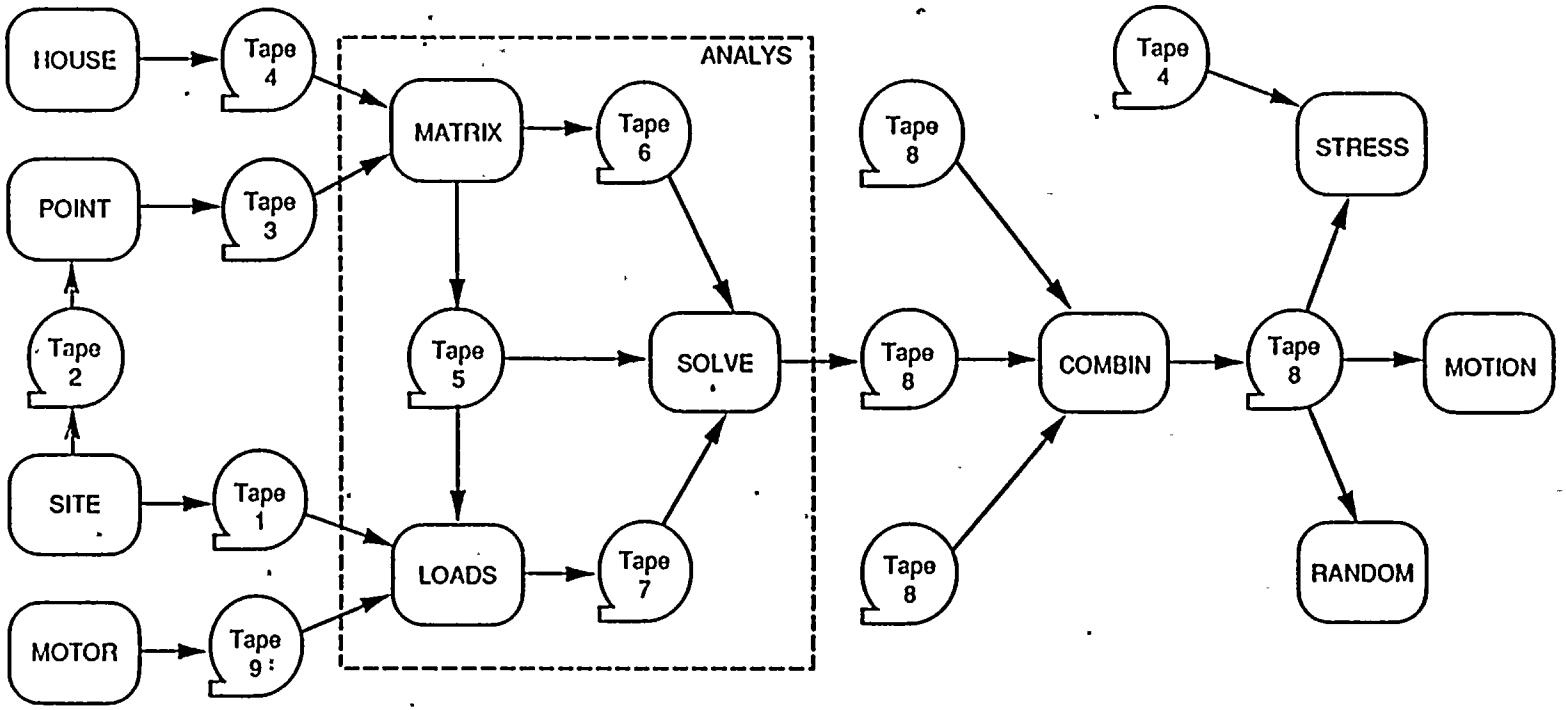

Figure 3.1-1. Layout of Computer Program SASSI

b. MOTOR

This program module forms elements of the load vector in Eq. (2.1-3) which correspond to external forces such as impact forces acting on the structure or forces from rotating machinery within the structure. The generated information is stored on Tape 9.

c. SITE

The site response problem is solved by the program module SITE. Based on site soil properties and the nature of the control motion free-field mode shapes are computed and written on Tape 1, which is later used for earthquake analysis. Thus this tape will not be generated for foundation vibration problems. The actual time history of the control motion is not required at this time. Only the composition of wave types causing the motion are required to be specified. The program also provides, on Tape 2, the information required to compute the transmitting boundaries used in solving the impedance problem.

d. POINT

The point load solution needed for computing the flexibility matrix, F_f, for the interaction nodes is obtained by the program module POINT for each frequency of analysis, and the matrices are stored on Tape 3. This program requires Tape 2 as input. Thus the program SITE must be executed before the program module POINT.

e. MATRIX

Using input from Tapes 3 and 4, the subprogram MATRIX forms, for each frequency, the impedance matrices $X(\omega)$. These are written on Tape 5. It also forms the modified complex stiffness matrices in Eq. (2.1-1) or Eq. (2.1-3), triangularizes them, and stores the triangularized form on Tape 6.

f. LOADS

This program computes the load vector in Eq. (2.1-1) or Eq. (2.1-3) for each frequency and stores them on Tape 7.

g. SOLVE

Subprogram SOLVE reads the reduced stiffness matrices from Tape 6 and the load vectors from Tape 7. It then performs the back-substitution to obtain the total displacement amplitudes from Eq. (2.1-1) or Eq. (2.1-3). These amplitudes are actually transfer functions from the control motion to the final motions. The results are stored on Tape 8, which now contains the complete solution in terms of transfer functions.

For a typical problem, the above operations need to be performed at only 10 to 20 frequencies. The remaining values of the transfer functions are determined by interpolation in the frequency domain. The actual interpolation are performed in the postprocessors, MOTION, STRESS, or RANDOM.

h. ANALYS

The program module ANALYS is the heart of program SASSI. It drives the three subprograms, MATRIX, LOAD, and SOLVE and thereby controls the restart modes of the program.

i. COMBIN

This program module makes it possible to add to the frequencies of analysis by combining the results of 2 frequency sets. Basically what this program does is to take two Tape 8s and combine them into a new Tape 8 which includes the solution of the 2 frequency sets.

j. MOTION

The main purpose of this (deterministic) postprocessor is to produce time histories of output acceleration, velocities, and displacements. It may also output transfer functions and response spectra.

In its basic mode, the program reads the acceleration time history of the control motion from input file and transforms it to the frequency domain using Fast Fourier Transform techniques. It then reads the uninterpolated transfer functions from Tape 8 for selected output motions, performs the interpolation and the convolution with the control motion, and returns to the time domain using the inverse Fast Fourier Transform algorithm. The resulting time histories of acceleration may be output directly or converted to output response spectra. Other output functions can be included for the program module MOTION as the need develops.

k. RANDOM

This (probabilistic) postprocessor is in many respects similar to the program module MOTION. However, instead of accepting the time history of the control motion it accepts a power or response spectrum of this motion. It then evaluates the probabilistic response of the structure.

The output consists of mean values and confidence limits on selected design parameters such as maximum accelerations and bending moments. The program can also produce mean values and confidence limits of acceleration response spectra.

Previous experience indicates that probabilistic output through the program module RANDOM can be produced at a small fraction of the cost required to produce deterministic output through the program module MOTION. Furthermore, the probabilistic procedure eliminates the need to develop time histories of motion which fit given design response spectra. The postprocessor is not available yet.

1. STRESS

The program module STRESS is a postprocessor which can be used to evaluate maximum stresses and strains in structural elements and/or to approximate values of maximum shear strain in soil through evaluation of maximum octahedral strain in the center of each soil element.

Secondary nonlinearity of soil can be taken into account by modification of soil properties according to calculated values of shear strain in each soil element.

Tapes 4 and 8 and the time history of control motion should be part of the input to this program.

3.2 Operational Features

The system shown in Fig. 3.1-1 has been specifically designed to provide maximum flexibility and economy for practical applications.

Clearly, on any given project most of the programs have to be executed. However, if changes occur in the design parameters, only parts of the system have to be re-executed. Consider the following changes:

a. Change in control motion

Suppose results are required for a different time history (or response spectrum) of the control motion. Then, as long as the nature of the seismic environment (i.e., the type of wave field) is not changed, only the program module MOTION (or RANDOM) has to be re-executed.

b. Change in seismic environment

Suppose the structure was originally analyzed for the effects of vertically propagated body waves and that results are required for the case of incident Rayleigh waves causing the same motion at the control point as in the free field. In this case only part of the program module SITE and all of the program modules, LOAD, SOLVE, and MOTION (RANDOM) have to be re-executed. This is so because the information on Tapes 2, 5, and 6 remains unchanged.

c. Change in dynamic loading

If changes are made in dynamic loads applied directly on the structure, only the program modules MOTOR, LOAD, SOLVE, and MOTION have to be re-executed. However, if only the time history of dynamic loads is changed while the loading pattern is not changed, only the program module MOTION has to be re-executed.

d. Changes is superstructure

If changes are made in the superstructure, only HOUSE and part of MATRIX, SOLVE, and MOTION (or RANDOM) have to be re-executed.

e. Postprocessors

Since the data on Tape 8 are independent of the manner in which the frequency content of the control motion is specified, the user has at any time the choice of deterministic or probabilistic analysis.

Also, since the postprocessors can be restarted from Tape 8, the user has at any time the option of outputting only the data which he actually needs. This is especially important for three-dimensional analysis for which the printing cost and volume of the complete solution output easily become unmanageable.

CHAPTER 4

APPLICATION GUIDE

4.1 Introduction

Performing a three-dimensional soil-structure interaction (SSI) analysis by the computer program SASSI may become expensive especially when the number of interaction nodes exceeds several hundred nodes. Thus, it is important that the program users understand on how to effectively utilize the capabilities of the program in order to efficiently perform the SASSI analysis. This requires knowledge of the analytical procedures used in this computer program. A set of guidelines with some examples describing step-by-step on how to proceed with SASSI analysis is considered to be very helpful for the users to utilize the program capabilities. It is therefore the purpose of this chapter to provide such guidelines with examples.

Section 4.2 describe the steps which are usually taken during a SASSI analysis. In the second part of this section, these steps are further elaborated and the important parameters of the analysis are discussed in more detail.

Section 4.3 describes the SASSI program modules which are executed to perform the initiation, post-processing and re-starting analyses.

Section 4.4 describes the means of organizing and saving the output tapes generated by the program.

Finally, an example problems is presented in Section 4.5 to show the applications of the program to seismic soil-structure interaction problems.

4.2 SASSI SSI Analysis Procedure

4.2.1 Steps Involved in SASSI Analysis

The seismic soil-structure interaction analysis by the SASSI program usually involves the following steps:

Step 1 Select the time history of control motion and compute its response spectra to highlight the dominant frequencies contained in the input motion.

Step 2 Determine the possible important frequency ranges of the soil-structure interaction response by examining the dominant frequencies of the structure(s) of the fixed-base condition. These frequencies can be obtained either by SASSI or another standard finite element program such as SAP, STARDYNE, etc.

Step 3 Based on the results of Steps 1 and 2, determine the cut-off frequency of the analysis (see item 7 of Section 4.2.2.

Step 4 Based on the assumption of vertically propagating shear wave and specified location of the control motion, compute the strain-compatible free-field soil properties by using, e.g., the computer program SHAKE (see item 14 of Section 4.2.2).

Step 5 Based on the cut-off frequency and the iterated soil properties obtained from the SHAKE analysis performed in Step 4, select the soil profile for the SASSI analysis (see item 8 of Section 4.2.2).

Step 6 Select the discrete structural model as explained in item 9 of Section 4.2.2.

Step 7 Select the discrete excavated soil model as described in item 10 of Section 4.2.2.

Step 8 Select the method of computing the impedance matrix as described in item 11 of Section 4.2.2.

Step 9 Select the frequencies for which the site response and point load problems are to be solved. It is recommended to choose at least 15 to 20 frequencies, possibly at equal intervals. Note, however, that the impedance problem and the final response of the system are usually solved at fewer frequencies than those specified above. These frequencies are selected according to the information obtained from Steps 1 and 2 and later on, can be increased, if necessary, to improve the accuracy of the interpolated transfer functions.

Step 10 Perform SASSI initiation analysis to compute the uninterpolated transfer functions at all the nodes of the system. This analysis, as outlined in Section 4.4.1, requires five computer runs:

a. Execute program module SITE in Mode 1 based on the information of Steps 5 and 9 and the specified location of the control motion. This analysis yields the information needed to form the transmitting boundary in the program module POINT and to solve for the site response problem in the program module SITE in Mode 2. This information is saved on Tape 2 (item A of Section 4.4.1).

b. Execute the program module POINT by using Tape 2 as inputand specifying the maximum embedment of the structure and also the radius of the point load as given by the formula in POINT User's Manual.

This radius ensures the compatibility of the point load solution and discretized geometry of the basement of the structure. This analysis yields the information on point load solution, saved on Tape 3, to be used to form the flexibility matrix of the basement of the structure (item B of Section 4.4.1).

c. Execute the program module HOUSE based on the information of Steps 6, 7, and 8. This analysis yields the complex stiffness and mass matrices of the structure and excavated soil, saved on Tape 4 (item C of Section 4.4.1).

d. Execute the program module SITE in Mode 2 to perform the site response analysis by using Tape 2 as input and specifying the nature of the seismic wave field. This analysis yields a set of free-field motions which are saved on Tape 1 (item D of Section 4.4.1).

e. Execute the program module ANALYS by using Tapes 1, 3 and 4 as input. This analysis yields the impedance matrices on Tape 5, the triangularized stiffness of the total system on Tape 6 ad the final uninterpolated transfer functions at all the nodal points on Tape 8 (item E of Section 4.4.1). The frequencies selected at this stage for interaction analysis are based on the information obtained from Steps 1 and 2. However, in order to expedite the execution of the program module ANALYS as well as reduce the size of the files generated by this program, it is recommended to break the frequency array into several sub-arrays whereby the analysis for each sub-array is performed separately, as discussed in item 12 of Section 4.2.2.

Step 11 Based on the results of Step 10, perform SASSI post-processing analyses to compute the response of the system. This analysis, as outlined in Section 4.4.2, usually consists of the following computer runs:

a. Execute the program module COMBIN, if necessary, to combine the transfer functions (on Tape 8's) obtained for different frequency arrays in Step 10 (item A of Section 4.4.2).

b. Execute the program modules MOTION and STRESS, based on the results of Step 10 and item 1 of this step, to compute the response of the system (item B of Section 4.4.2). MOTION uses Tape 8, while STRESS uses Tapes 4 and 8 as input.

Step 12 It is also possible at this stage to add new frequencies to the response based on the results obtained in Step 11. The procedure involved is described in item 12 of Section 4.2.2.

Step 13 Perform SASSI re-starting analysis if changes occur in either the superstructure, or the seismic environment of the problem analyzed above. The procedures involved are described in Sections 4.4.3.1 and 4.4.3.2, accordingly.

In the case of foundation vibration analysis by the SASSI program, the above steps described for the seismic analysis are still applicable except that:

1. The time history of control motion in Step 1 is replaced by the reference time history of the external dynamic forces.

2. Step 4 is unnecessary.

3. The iterated soil properties in Step 5 are replaced by the initial soil properties

4. The site response problem is eliminated from Step 9 and second part of item a of Step 10.

5. Item d of Step 10 is replaced by a different analysis performed by the program module MOTOR to obtain the load vector on Tape 9 which replaces Tape 1 in item e of Step 10.

6. The dynamic environment in Step 13 is replaced by the external dynamic forces.

4.2.2 Considerations Prior to SASSI Analysis

In order to make effective use of the program SASSI, the user should consider the following items:

1. Rigid vs Flexible Basement

Currently, the program does not take advantage of the rigid basement assumption since a flexible basement is always assumed in the program. As a result, no saving is obtained by the rigid basement assumption. It is, therefore, recommended to carry out the analysis for actual properties of the basement. If it is necessary to evaluate the effect of rigid basement assumption, a restart analysis can be performed by selecting an elastic modulus for basement to be 10^4 to 10^5 times the elastic modulus of the soil. The restart analysis can be performed at a fraction of the initial cost.

2. Surface vs. Embedded Structure (ZSRFCE)

It is possible to treat the embedded structures as surface structures if the embedment effect is negligible. By doing so, a big saving can be achieved in the SASSI analysis since the number of interaction nodes is largely reduced.

The parameter ZSRFCE in the program HOUSE controls the embedment condition of the structure. For surface structures, this parameter is equal to the Z-coordinate of the base of the structure.

3. Symmetry of the System (NSYMPL)

SASSI has the capability to take advantage of the geometrical symmetry of structures subjected to symmetric or anti-symmetric loading. Therefore, the cost of the analysis can be drastically reduced by utilizing this capability of the program.

The parameter NSYMPL is used to specify the number of symmetric planes of the system.

4. Rigid Base Rock vs Halfspace Condition (LSUB)

SASSI has the capability to simulate the existence of a uniformly damped, or undamped, halfspace below the top soil layers. Therefore, it can avoid using very deep soil models with many sublayers and leads to additional savings when the soft soil extends to relatively large depth or when the rock boundary can not be established.

In case of halfspace simulation, the program automatically adds an additional soil layer below the top layers with the thickness of $(1.5*V_s)/f$, where, V_s is the shear wave velocity of the halfspace and f is the frequency of analysis. This added soil layer is further subdivided into LSUB sublayers specified by the user in program module SITE. In addition to this, the viscous dashpots are added to the base of the new soil model.

The input parameter LSUB is recommended to be set at 10. If LSUB=0, there is no halfspace simulation.

5. Cut-off Frequency (f_{NF})

The cut-off frequency is an important parameter since it not only sets an upper limit on the number of frequencies to be analyzed but also controls the maximum allowable element sizes, and thus, the dimension of the stiffness and mass matrix of the problem. The input form of the cut-off frequency f_{NF} to SASSI is described in Item (7). The factors governing the choice of the cut-off frequency are:

a. The frequency content of the input motion.

b. The dominant frequencies of the entire system.

c. The time increment of the input time history.

6. Selection of frequency points (f_i)

The frequencies to be selected for the SASSI analysis depend on the number of peaks in the transfer function and how close these peaks are located relative to each other. This information can be obtained from the fixed-base analysis of

the structure. The fixed-base natural frequencies will show the approximate location of the peaks in the structure and the importance of each peak can be seen from either the mode participation factors or the fixed-base transfer functions. Since an efficient interpolation scheme on complex response functions has been incorporated into SASSI, and since the effect of the soil-structure interaction is to flatten the sharp peaks and sometimes eliminate some of the structural peaks, it is usually sufficient to solve for 10 to 20 frequencies and the intermediate solutions can then be obtained by interpolation.

Also, SASSI has the capability which enables the user to add new solved frequency responses to the old solved frequency set. Therefore, it is possible to start the analysis with few frequencies, and then examine the transfer functions and add new frequencies as needed.

7. Input of Frequency Points ($NFREQ_i$)

In the SASSI program, the transfer functions are computed at discrete frequency points which are integer multiples of the frequency step, DF. For general deterministic analysis, the frequency step is calculated from

$$DF = 1/(DT * NFFT)$$

where the input parameters DT and NFFT are the time step and number of points to be used in the Fourier transform of the time history, respectively. For probabilistic analysis of single harmonic forced vibration analysis, the time history input is not required, therefore, the user can directly specify DF.

Once the frequency step is defined, the frequency points f_i are input through the use of integer frequency numbers, $NFREQ_i$, defined as follows:

$$NFREQ_i = f_i/DF \qquad i = 1, 2, ...NF$$

where NF is the total number of frequency points selected for the analysis according to item 6 of this section.

The maximum frequency number to be specified in the SASSI program is controlled by the cut-off frequency and can be obtained as follows:

$$NFREQ_{NF} = f_{NF}/DF$$

where f_{NF} is the cutoff frequency.

8. Modelling of Soil Profile

The soil supporting the structure must consist of semi-infinite elastic or viscoelastic horizontal layers resting on a rigid base rock or semi-infinite elastic or viscoelastic halfspace.

The allowable layer thickness for the SASSI analysis is determined using the simple rule that the layer thickness must not exceed one fifth of the wave length at the highest frequency of analysis. Based on this, the soil profile is selected by subdividing the soil layers into several sublayers.

9. Modelling of Structure

The structure is modelled by the two- or three-dimensional finite elements available in the SASSI program. The selection of elements and nodal points follows the same procedure as in the other standard finite element programs. The only limitations are:

a. The structure must contain the interaction nodes inside the basement volume(s) even if there is no structural element to connect such nodes.

b. All the interaction nodes of the structure(s), which are below the ground surface, must lie on the soil layer interfaces.

c. The maximum horizontal distance between two adjacent interaction nodes in an excavated volume must be smaller than $V_S/(5*f_{NF})$, where V_S is the smaller shear wave velocity of the top and bottom soil layers connected to the two interaction nodes and f_{NF} is the highest frequency of analysis.

10. Modelling of Excavated Soil

In the SASSI analysis of the embedded structures, the excavated soil zone(s) must be modeled by the two dimensional plane strain or three-dimensional solid elements connecting the interaction nodes of the structure. The element sizes for the excavated soil elements are controlled by the distance between the interaction nodes obtained in item 9 in this section.

11. Direct vs Skin Method (NIMP)

Currently, there are two methods available for calculation of the impedance matrix in SASSI. Namely, the direct (NIMP=1) and the skin (NIMP=2) methods. In the direct method, the impedance matrix of the interaction nodes is computed by the direct inversion of the corresponding dynamic flexibility matrix. A less rigorous but more cost-effective solution can be obtained by using, the skin method where the impedance matrix is computed through a special formulation by combining submatrices of the dynamic flexibility matrix and the direct stiffness matrix of the excavated soil.

The skin method is more cost effective for deep foundations. However, its accuracy in reproducing the impedance matrix for 3-D problems deteriorates significantly if the embedment region consists of distorted soil elements. Such error can be greatly reduced by using brick type soil elements in the basement. Furthermore, for basements which consists only of brick elements, the skin method can predict 3-D compliance functions with reasonable accuracy. It should be noted that in the validation of the program (Ref. 2) only direct method of analysis has been validated. The skin method should be used following the validation of the method for at least one case pertaining to the actual problem to be analyzed or following obtaining favorable comparison of the direct method and skin method solutions of the problem at least for few frequencies.

12. Addition of new frequencies to the transfer function on Tape 8

The program SASSI has an additional provision which enables the user to solve for the transfer function at any additional frequencies by the program module ANALYS. The results are later combined by the program module COMBIN, as long as the specified frequencies reside on the input tapes. For example, suppose the program modules SITE and POINT were executed for 10 frequencies (0.98, 2.93, 4.88, 6.84, 8.79, 10.74, 12.70, 14.65, 15.6662 and 17.58 Hz) and Tapes 9 and 3 were created. Furthermore, it is assumed that the program module ANALYS was executed only for 5 frequencies which reside on the above Tapes 9 and 3. Let us now assume that the analysis is to be repeated for two new frequencies (2.93 and 15.66 Hz) and the results are to be combined with those of the old frequencies. Since the new frequencies reside on the above Tapes 9, 3, and Tape 4 is frequency independent, program module ANALYS is executed to solve for the new 2 frequencies. Subsequently, program module COMBIN can be used to add new frequency responses to the old ones on Tape 8.

13. Impedance Matrices of a Rigid Foundation

The impedance matrices, $\underline{K}$ and $\underline{C}$, of a rigid foundation are computed from the foundation compliance matrices, f and g, using formula

$$K + i\omega D = (f + ig)^{-1} \qquad (4.2\text{-}1)$$

where ω is the frequency of analysis and $i = \sqrt{-1}$.

In the program SASSI, the columns of the foundation compliance matrices can be obtained by applying a unit amplitude force or moment in the desired direction at a specified point on the foundation, and computing the resulting real and imaginary parts of displacements or rotations of that point (i.e., f and g). By inverting the compliance matrices using the above formula, the corresponding impedance matrices (i.e., K and D) are computed.

14. Nonlinear Soil Behavior

SASSI is a frequency domain analysis program which uses the principle of superposition, and therefore, is restricted to linear analysis. However, approximate nonlinear analyses can be performed using an iterative scheme called "Equivalent Linear Method." In applying this method to seismic soil-structure interaction problems, it is useful to consider the nonlinear effect in two parts. The effect due to free field motion is called the primary effect, and the effect due to interaction is called the secondary effect. The latter one is confined to a limited region near the structure (irregular zone) and have only a minor influence on the motions of deeply embedded structures, such as nuclear power plants. Thus, in many cases, it is sufficient to consider only the primary effect, i.e., the iteration on soil properties involved in the equivalent linear method needs to be performed only for the free field analysis.

In view of the above assumption, an efficient way of performing a seismic soil-structure interaction analysis is to separate it into two stages. The first stage is a site response analysis with iteration on soil properties, say, by the computer program SHAKE. This analysis takes care of all primary nonlinear effects and yields a horizontally layered site profile with properties which are compatible with the levels of strain in the free field. The second stage is an interaction analysis by SASSI. In this stage, the above strain compatible soil profile is used for the site profile and no interation are performed on the soil properties, i.e., the secondary nonlinear effect is neglected.

The secondary effect in a limited region encompassing the basement of the structure can be considered by including in the model an extended near field zone. The soil strains within the irregular part of this zone can be computed by the program and the properties of the irregular zone can be changed iteratively according to the equivalent linear method. The procedure for the secondary effect iterations has not yet been implemented in the computer program SASSI. If need be, the iterations can be performed by hand calculations of the new soil properties and input to SASSI for re-analysis.

The secondary nonlinear effect may be important for surface structures subjected to high intensity earthquakes. They may also have some influence on the distribution of dynamic earth pressures for embedded structures.

4.3 Additional Numerical and Modelling Criteria

4.3.1 Finite Element Discretization

In order to accurately transmit the waves, the finite element model should be discretized so that the largest side of each element does not exceed $\lambda/8$; where λ is the shortest wave length of interest in the analysis. The wave length criteria can be relaxed to $\lambda/5$ if the mass matrix used in the analysis is constructed from the combination of consistent and lump mass matrices (usually 50% each). Since the mass matrix computation in SASSI is automated to consist of 50% lump mass and 50% consistent mass, the $\lambda/5$ criteria can be used in constructing the models.

4.3.2 Halfspace Simulation

In order to simulate the halfspace condition at the bottom boundary, two techniques of variable depth method and viscous boundary at the base are used (Ref. 1). In the variable depth method, n extra layers with total thickness of 1.5λ and with the properties of halfspace are added to the soil profile. The wave length, λ, is the shear wave length in halfspace and is a function of frequency. Thus, the added soil layer thickness varies with frequency. The choice of $1.5\ \lambda$ arose from the observation that fundamental modes Rayleigh wave in halfspace decay with depth and essentially vanish at a depth corresponding to 1.5λ. Furthermore, the 1.5λ layer thickness is subdivided into n layers with increasing thickness with depth. The choice of n=10 is sufficient for many practical cases. With this technique, the layer thickness will increase with depth and decreasing frequency. This is the desired characteristic of the model since surface wave mode shapes decrease exponentially with depth and since their depth of penetration increase with decreasing frequency.

The soil model with added extra layers is further improved by replacing the rigid boundary at the base of the extended layer system with viscous boundary by placing dashpots in horizontal and vertical directions. The halfspace simulation is specified in program module SITE.

The effectiveness and adequacy of this halfspace simulation technique has been demonstrated in benchmark problems which were used as validation test problems for SASSI (Ref. 2).

4.3.3 Computation of Impedance Matrix

As described in Ref. 1, computation of flexibility matrix follows the point load solution of a soil column. The soil column is modelled by finite elements (plane strain of axisymmetric elements). The impedance matrix used in the formulation of SASSI is obtained by inverting the flexibility matrix. In a layered system with large contrast of properties between adjacent layers, the solution to impedance problem may include some numerical inaccuracy due to weak form of the flexibility matrix. Systematic parametric study has not been performed to establish numerical criteria in terms of the property contrast in layered system. However, for all the practical problems analyzed with SASSI such inaccuracies have not been observed. In addition, in the validation problem set (Ref. 2), a layered system with shear wave velocity ratio of 2.5 for which a reference solution is available is successfully analyzed. Thus, it is expected that for most of the practical problems additional criteria need not be established for modelling layered system. However, in view of the absence of systematic study for layered systems with very large property contrast, the solution to the impedance problem need to be checked more closely.

4.4 How To Run A SASSI JOB

The first step in running a SASSI job is to determine to which of the following three groups the job belongs:

1. Initiation (or Basic Runs)

2. Post-processing

3. Re-starting

Each of the above groups require one or several interrelated SASSI program modules, shown in Fig. 4.4-1 to be executed in a specified order. Therefore, the next step would be to perform the operations of the corresponding group described in the following sections.

4.4.1 Initiation

The initiation of SASSI for interaction analysis basically consists of 5 major computer runs:

A. RUN 1 - SITE RUN (Mode 1)

B. RUN 2 - POINT RUN

C. RUN 3 - HOUSE RUN

D. RUN 4 - SITE RUN (Mode 2) or MOTOR RUN

E. RUN 5 - ANALYS RUN (Mode 1)

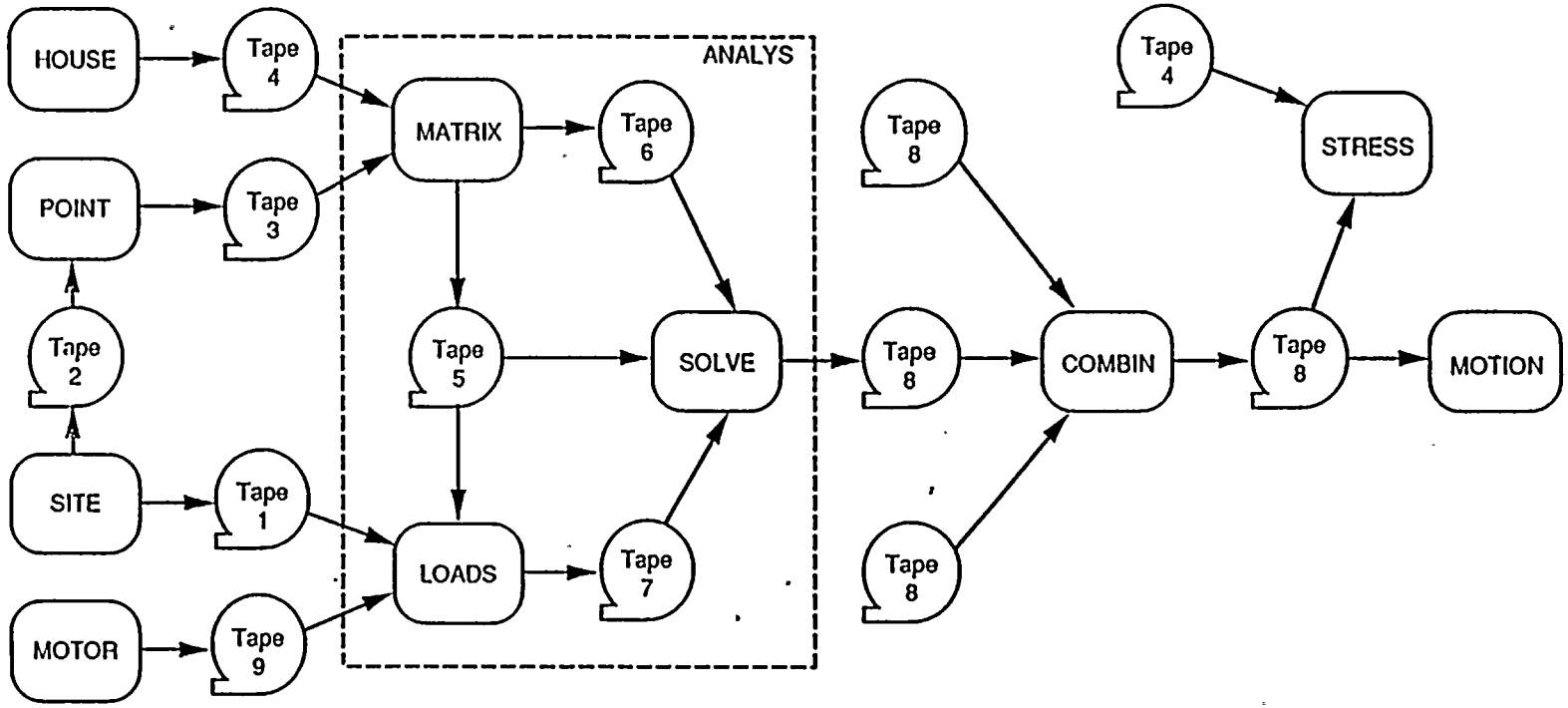

Figure 4.4-1. SASSI Program Modules

These runs generate the output Tapes 1 through 9 (Tape 7 is not currently used) which are then saved on either the disk or the magnetic tapes. Tape 8 contains the uninterpolated transfer functions computed for the specified frequencies at all the nodal points of the system and is used in the post-processors to compute the final response of the system. The remaining tapes contain the information which may be used later to re-start the program module ANALYS to analyze a new problem.

The 5 basic runs listed above are illustrated in Figs. 4.4-2 and 4.4-3 for seismic and forced vibrations problem, respectively. For seismic poblems RUN 1 and RUN 4 can be combined into one run at user's option. It is also possible to change the order of the runs such that RUN 3 is performed before RUN 1 is executed. However, since the foundation of the structure (in HOUSE) must be compatible with the soil layer system (in SITE) and the point load solution (in POINT), it is recommended that the first runs are performed after the models for the structure and the site have been established.

4.4.2 Post-Processing

Once Tape 8 is obtained, it is used to compute the required response(s) of the system through one or more of the following runs:

A. RUN 1 - COMBIN RUN

B. RUN $(2)_1$ - MOTION RUN

C. RUN $(2)_2$ - STRESS RUN

It should be noted that RUN 1 is necessary only if new frequencies are to be added to the old Tape 8. These runs are illustrated in Figure 4.4-4.

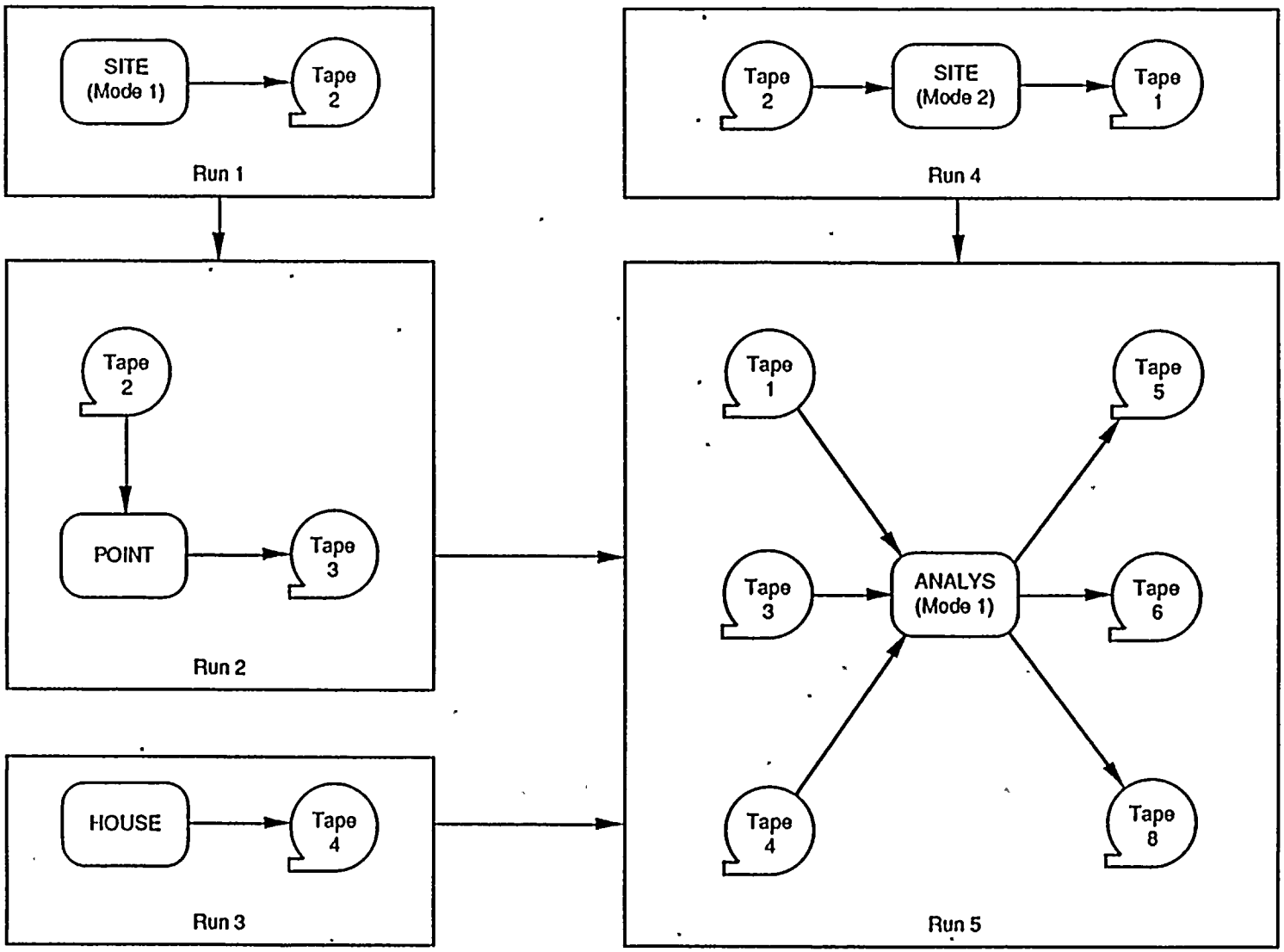

Fig. 4.4-2. SASSI Initiation Runs for Seismic Interaction Analysis

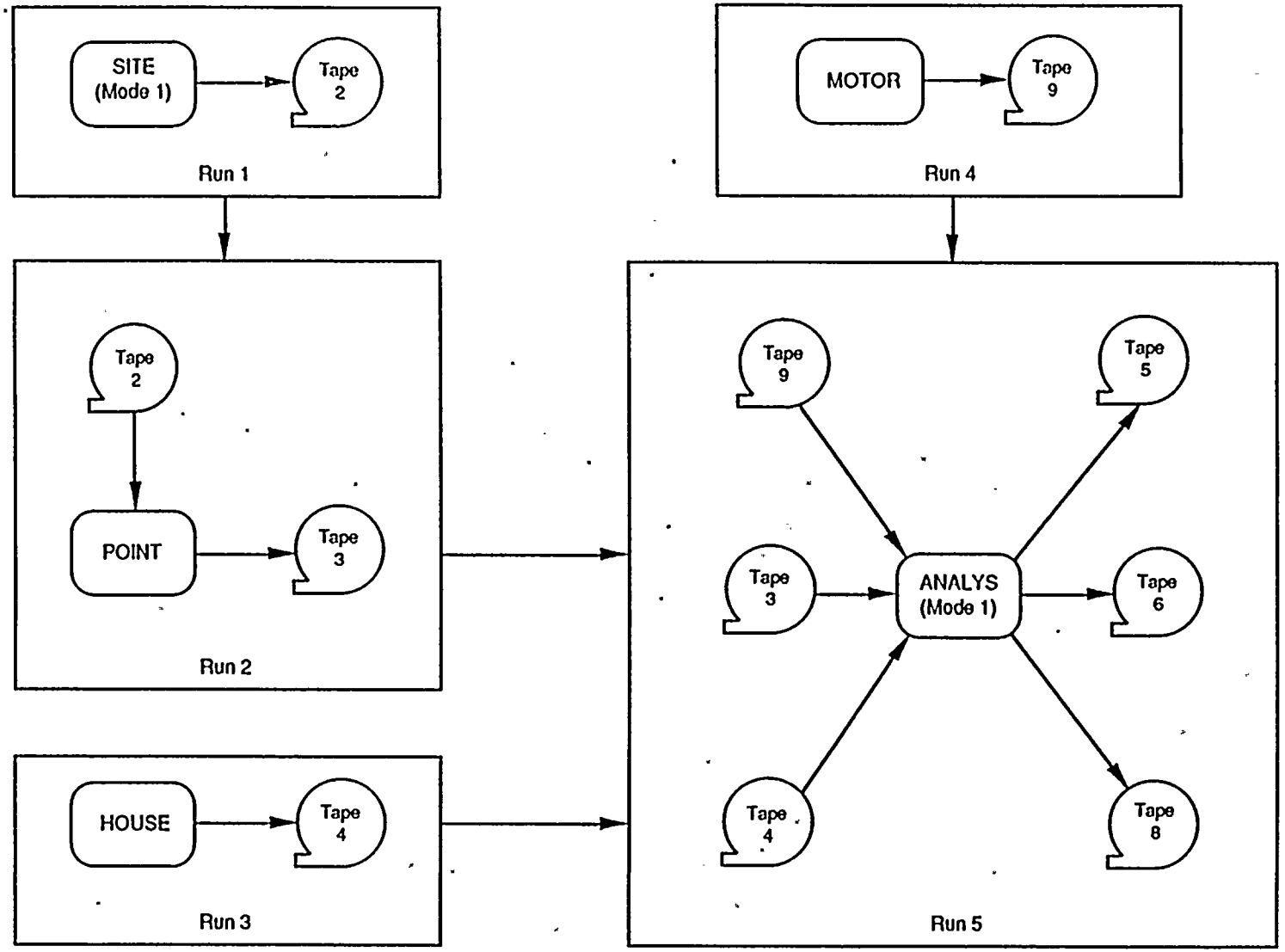

Fig. 4.4-3. SASSI Initiation Runs for Force Vibration Interaction Analysis

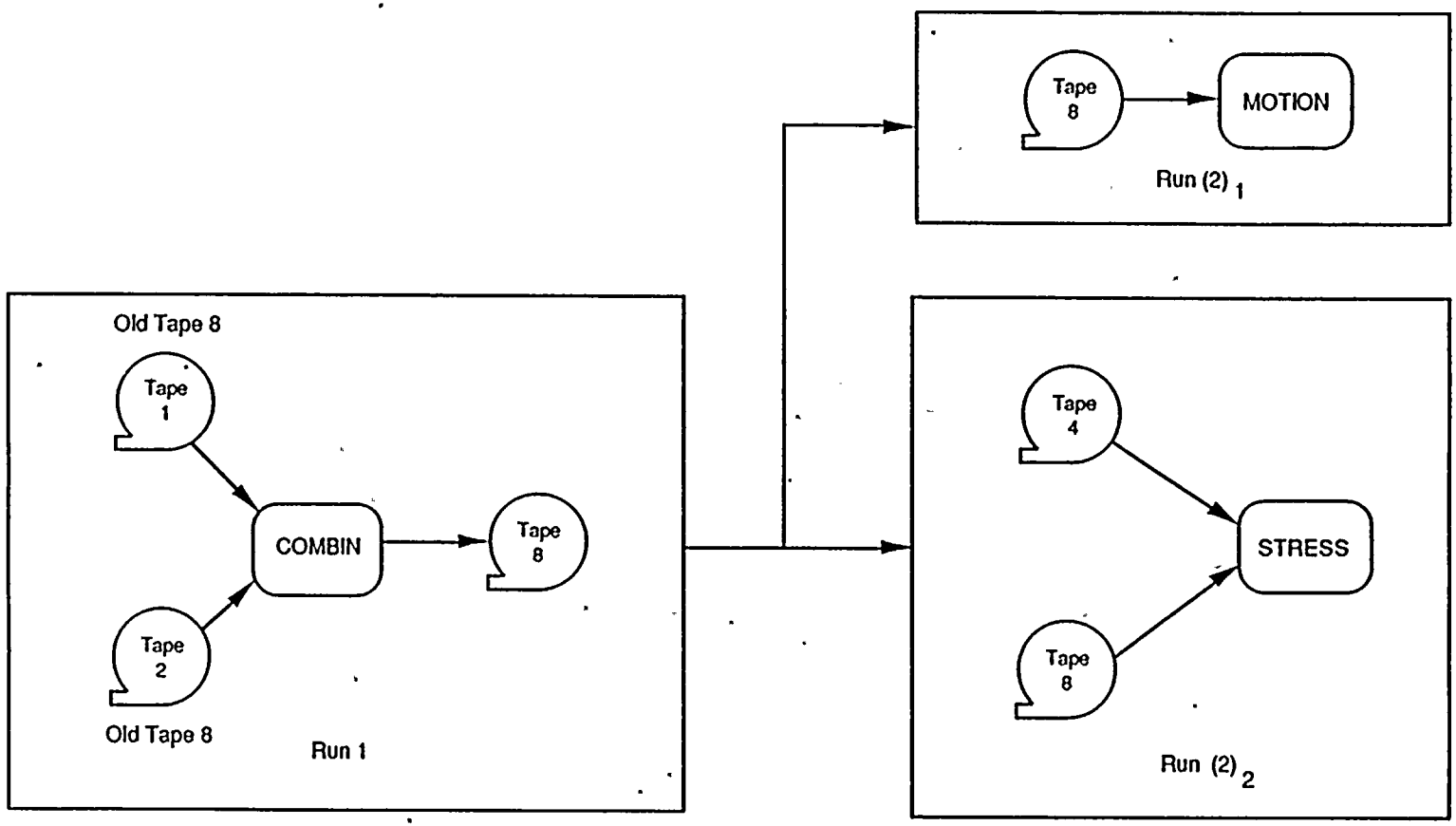

Fig. 4.4-4. SASSI Postprocessing Runs

4.4.3 Re-Starting

The basic re-start modes of SASSI include:

1. Restart with new superstructure

2. Restart with new seismic environment

3. Restart with new dynamic loading

Each of the above modes involves only two computer runs as described below.

4.4.3.1 Re-start with new Superstructure

This mode which can be performed for both the seismic and foundation vibration problems consists of the following two runs:

A. RUN 1 - HOUSE RUN

B. RUN 2 - ANALYS RUN (Mode 2)

The new Tape 4 obtained from RUN 1 is used with the old Tape 5 and Tape 1 (or Tape 9) as input to RUN 2. RUN 2 will then create Tape 6 and Tape 8. Figures 4.4-5(a) and 4.4-5(b) illustrate these runs for the seismic and foundation vibration analyses, respectively.

4.4.3.2 Re-Start with New Seismic Environment

This mode which can be performed only for seismic problems consists of the following two runs:

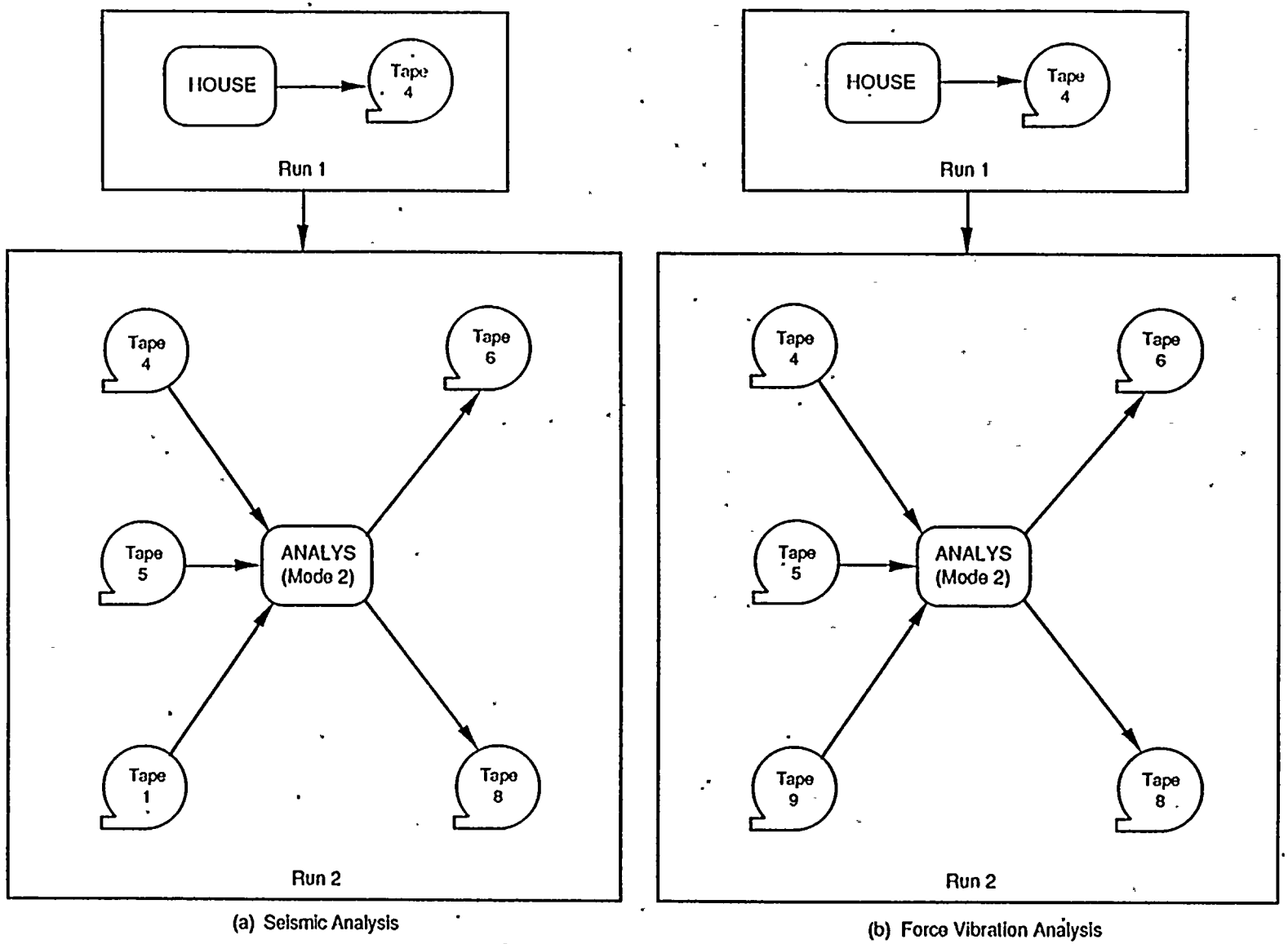

Fig. 4.4-5. SASSI Restart Runs for New Superstructure Case

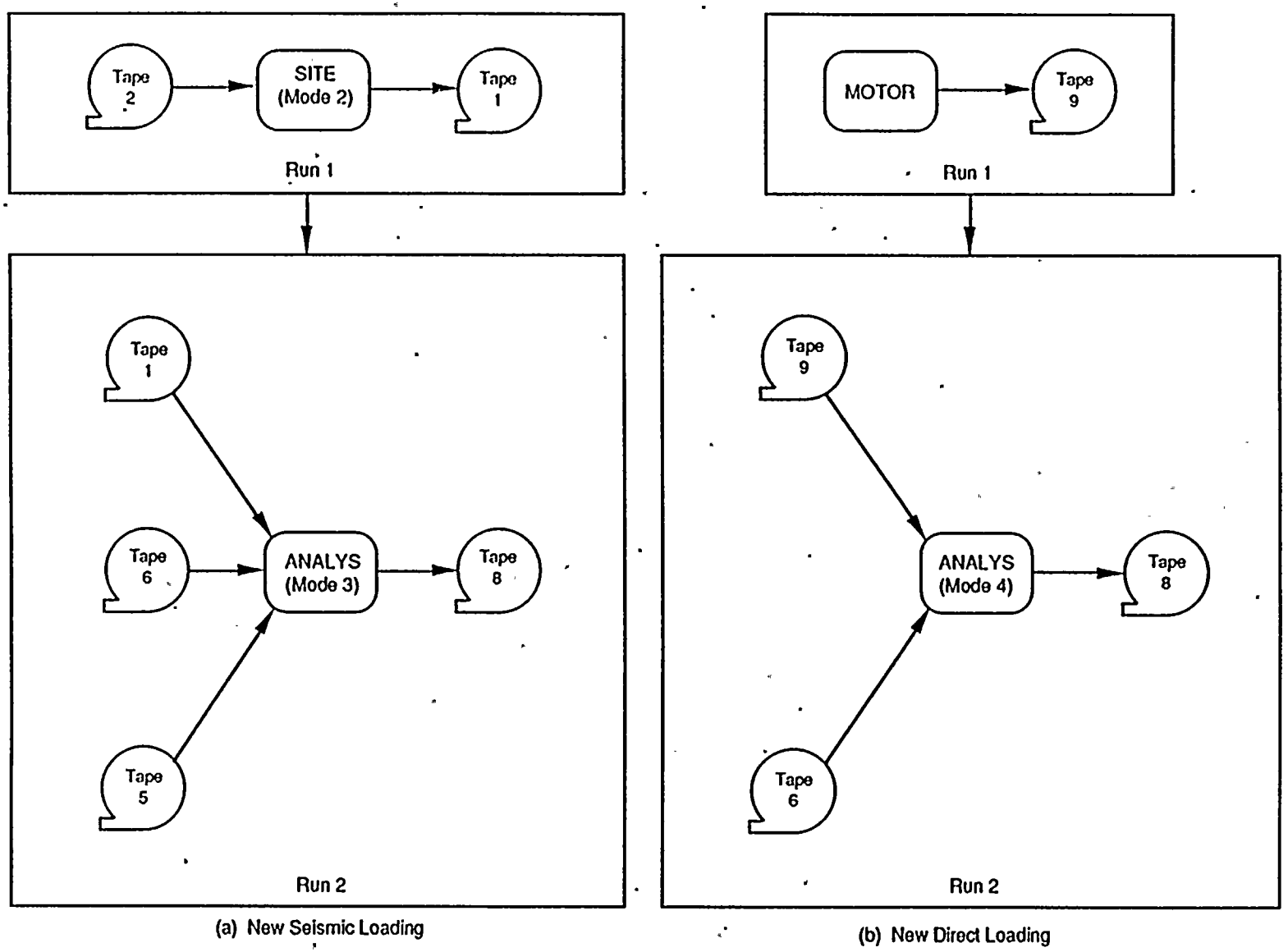

(a) New Seismic Loading

(b) New Direct Loading

Fig. 4.4-6. SASSI Restart Runs for New Loading Case

A. RUN 1 - SITE RUN (Mode 2)

B. RUN 2 - ANALYS RUN (Mode 3)

The new Tape 1 obtained from RUN 1 is used with the old Tape 5 and Tape 6 as input to RUN 2. RUN 2 will then create a new Tape 8. This runs are illustrated in Figure 4.4-6(a).

4.4.3.3 Re-Start with New Dynamic Loading

This mode which can be performed only for the foundation vibration problems consists of the following two runs:

A. RUN 1 - MOTOR RUN

B. RUN 2 - ANALYS RUN (Mode 4)

The new Tape 9 obtained from RUN 1 is used with the old Tape 6 as input to RUN 2. RUN 2 will then create a new Tape 8. The runs are illustrated in Figure 4.4-6(b).

4.5 Saving SASSI Output Files

The basic SASSI runs create 8 files as shown in Figures 4.4-2 and 4.4-3. However, the number of files created in a SASSI analysis usually exceed 8 because of:

a. Repeating the entire analysis for new frequencies;

b. Re-starting the program with new superstructures;

c. Re-starting the program with new seismic environment (or dynamic loading)

Therefore, it becomes very important to organize these files in such a way that the later access to the files can be done easily.

There are basically two types of device which can be used on any computer system to save the data in the output files:

1. Disk

2. Magnetic tapes

4.5.1 Disk Storage

Even though it is more convenient and faster to save or access the data on disk, the permanent disk storage is not recommended due to its high cost, especially, for the case in which the amount of data generated on some of the output files are very large. However, if disk was selected as the primary storing device, then the user can choose an arbitrary name for each output file, thus making organization and access very easy.

4.5.2 Magnetic Tape Storage

There are two types of magnetic tape storage:

4.4.2.1 Mass Storage on Magnetic Tapes (also called File Manager)

In this type of storage, first the output files are saved on disk and then a later stage, they are copied from disk onto magnetic tapes by running a separate job. On some computer systems these two tasks are performed simultaneously. Therefore, there is no need to submit the second job.

If the files on the mass storage are assigned names and accessed randomly like the permanent files on disk, this type of storage is probably the most effective way of saving and accessing SASSI output files.

In case this type of storage is not available on a computer system, the standard storage described in the next section can be used.

4.5.2.2 Standard/Sequential Storage on Magnetic Tapes

In this type of storage, the output files are saved sequentially on a magnetic tape separated by a file mark. Since the system can not identify each individual file by the name, the user has to keep track of the order in which the files are saved on the magnetic tapes. This will make it possible to add new files to the existing files on a tape or to skip certain number of files before reading the target file.

4.6 Example Problem

An example problem is presented to illustrate the application of SASSI to impedance and soil-structure interaction (SSI) analysis. This problem also describes how to select the finite element model for the soil profile, the structure, and the number of frequencies to be used for the analysis. The input data of the example problem is provided in Appendix A.

4.6.1 Problem Considered

4.6.1.1 Description

The problem considered is a pressurized water reactor (PWR) building supporting on a uniform damped halfspace (see BC-TOP-4A, Ref. 5) subjected to vertically propagating shear waves with the control motion specified at the ground surface. The total soil-structure system is shown in Fig. 4.6-1. The building consisting of a containment structure and internal walls are modeled by stick models.

The problem is analyzed for two cases. In the first case, the horizontal and rocking impedance functions of the rigid massless foundation are computed and the results are compared with reference solution of the problem. In the second case, the SSI response of the containment is computed.

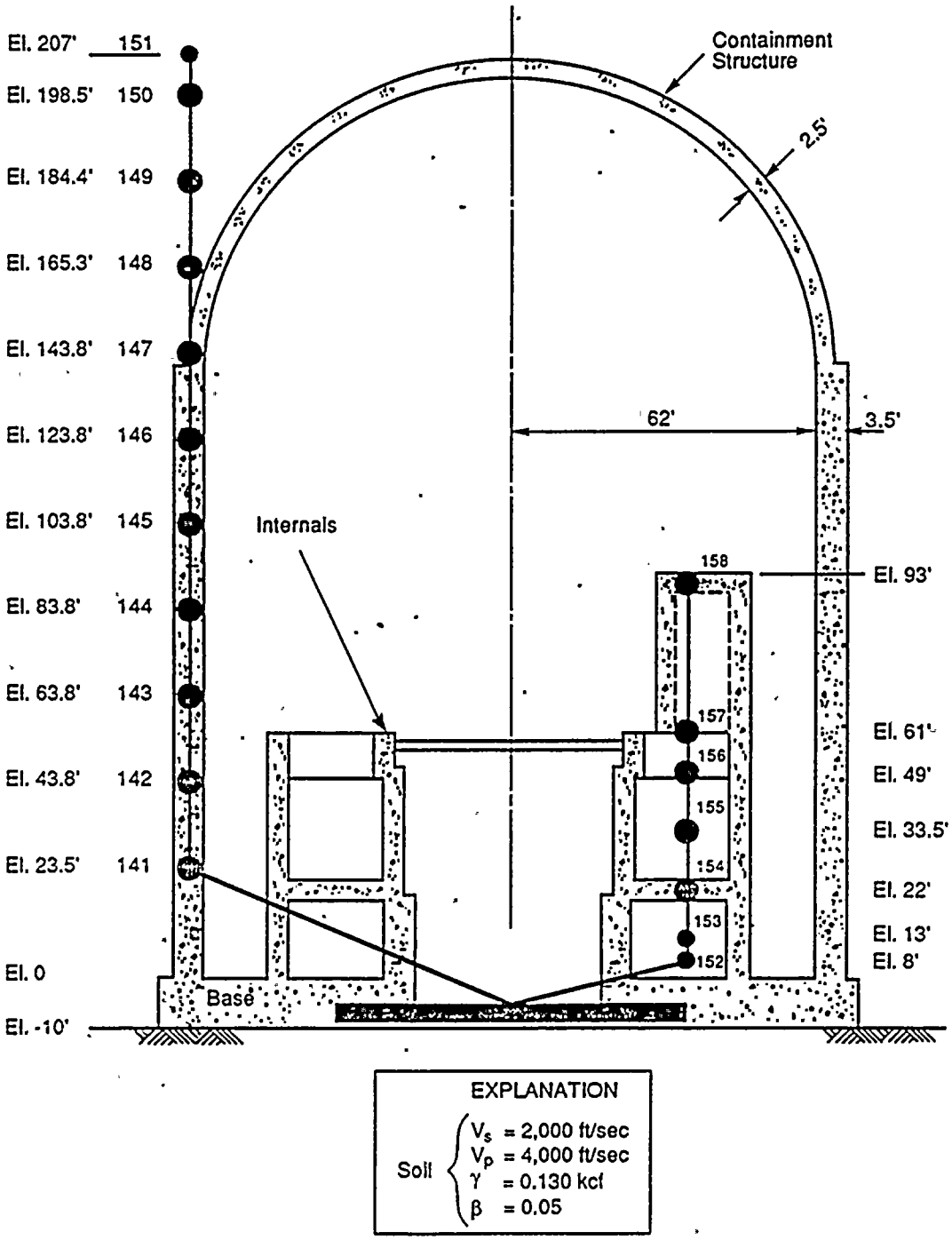

Figure 4.6-1. Lumped-Mass Stick Models of the Containment and Internal Structures

The material properties of the soil and geometry of the structure are given in Fig. 4.6-1. The sectional properties of the structure are given in Table 4.6-1. A uniform critical damping of 2% was used for the superstructure and basemat. The control motion selected for the analysis is a scaled version of the El Centro 1940 NS Component. The acceleration time history of the motion is shown in Figure 4.6-2. The motion is scaled to maximum acceleration of 0.1g with duration of 10.24 seconds digitized at time interval of 0.005 second. The corresponding acceleration response spectra at 2% damping is shown in Fig. 4.6-3. The cut-off frequency used for the analysis is specified at 25 Hz.

4.6.1.2 Modelling

4.6.1.2.1 Soil Model

The maximum allowable layer thickness were computed according to the criteria described in item 8 of Section 4.2.2:

Max.allowable thickness = 2000/(5x25) = 16 ft

Based on this value, the soil profile for the SASSI analysis was selected as shown in Figure 4.6-4. This profile consists of 4 top layers and 10 extra layers with variable thickness plus viscous dashpots. The extra 10 layers and viscous dashpots are added by the program at the user's request to simulate the halfspace condition.

Table 4.6-1 - PROPERTIES OF THE STRUCTURAL MODELS OF THE CONTAINMENT BUILDING AND INTERNALS

(Concrete Modulus E = 6.9 x 10^5 ksf, G = 2.7 x 10^5 ksf)

Joint Properties			Member Properties			
Mass No.	m_{ig} (kips)		Location between Joint No.	Area (ft^2)	Shear Area (ft^2)	Moment of Inertia x 10^{-6} (ft^4)
base	20000	C				
1	46000	O	base to 1	1400	700	2.8
3	4200	N	1 to 2	1400	700	2.8
4	4200	T	3 to 4	1400	700	2.8
5	4200	A	4 to 5	1400	700	2.8
6	4200	I	5 to 6	1400	700	2.8
7	4610	N	6 to 7	1400	700	2.8
8	3020	M	7 to 8	990	500	1.9
9	2470	E	8 to 9	990	500	1.5
10	2120	N	9 to 10	990	500	0.8
11	190	T	10 to 11	990	500	0.2
12	2800	I	base to 12	2000	1320	1.1
13	2510	N	12 to 13	2560	1560	1.2
14	6290	T	13 to 14	2210	1460	1.2
15	3760	E	14 to 15	1960	730	1.3
16	8540	R	15 to 16	1740	600	0.9
17	1220	N	16 to 17	780	360	0.2
18	820	A	17 to 18	190	70	0.004
		L				

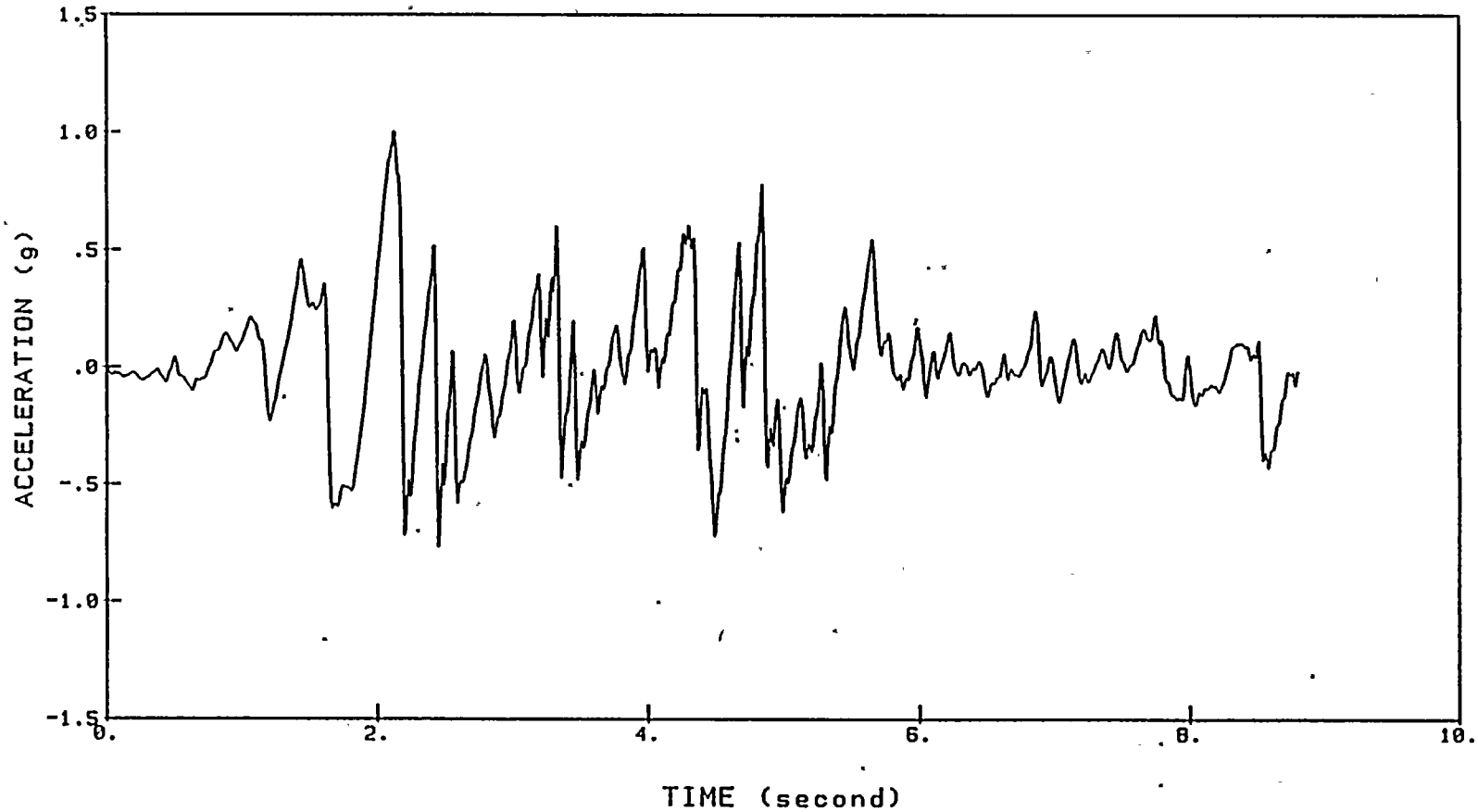

Figure 4.6-2. Acc. Time History of El Centro 1940 (N-S)

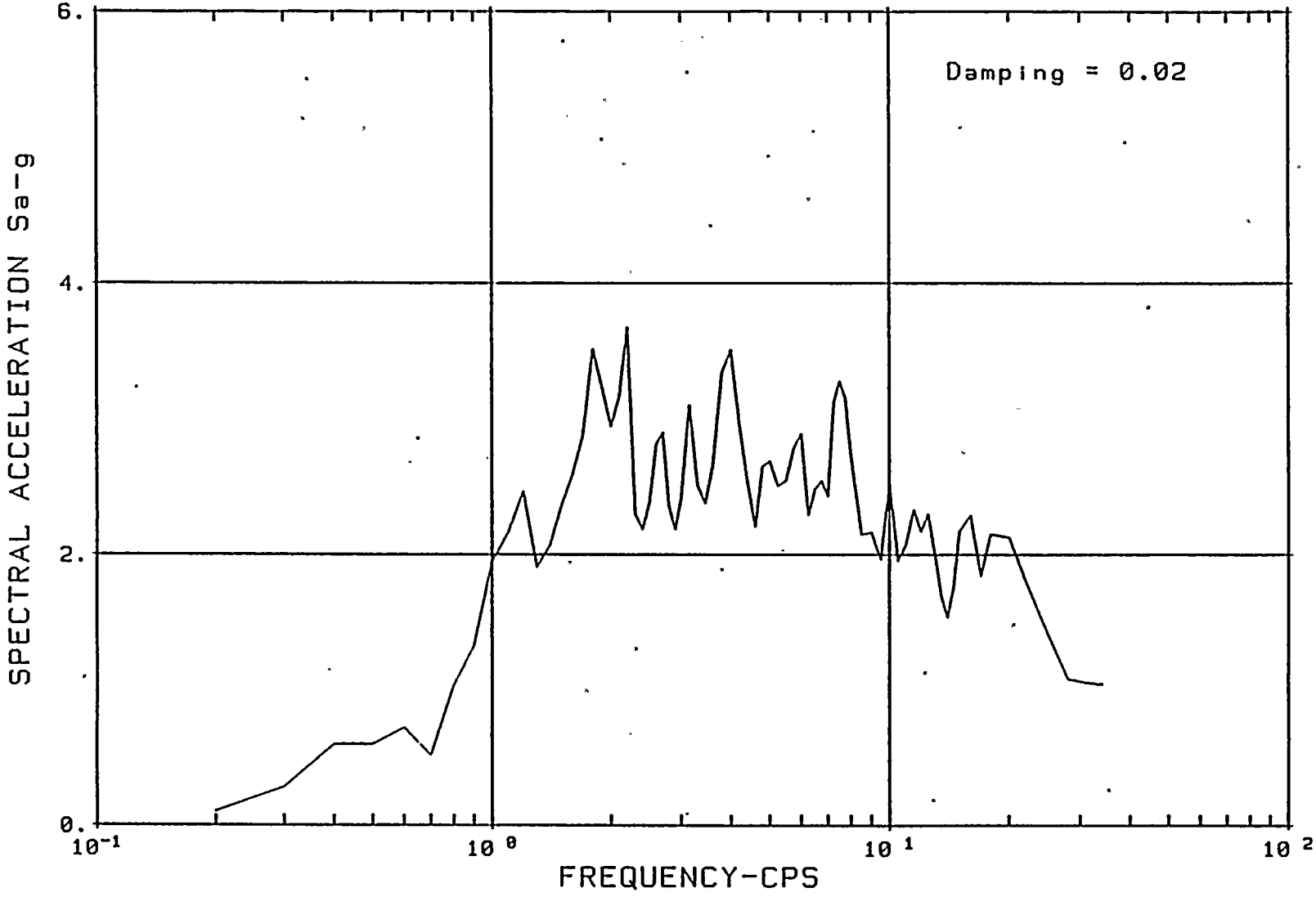

Figure 4.6-3. Acc. Response Spectrum of El Centro 1940 (N-S)

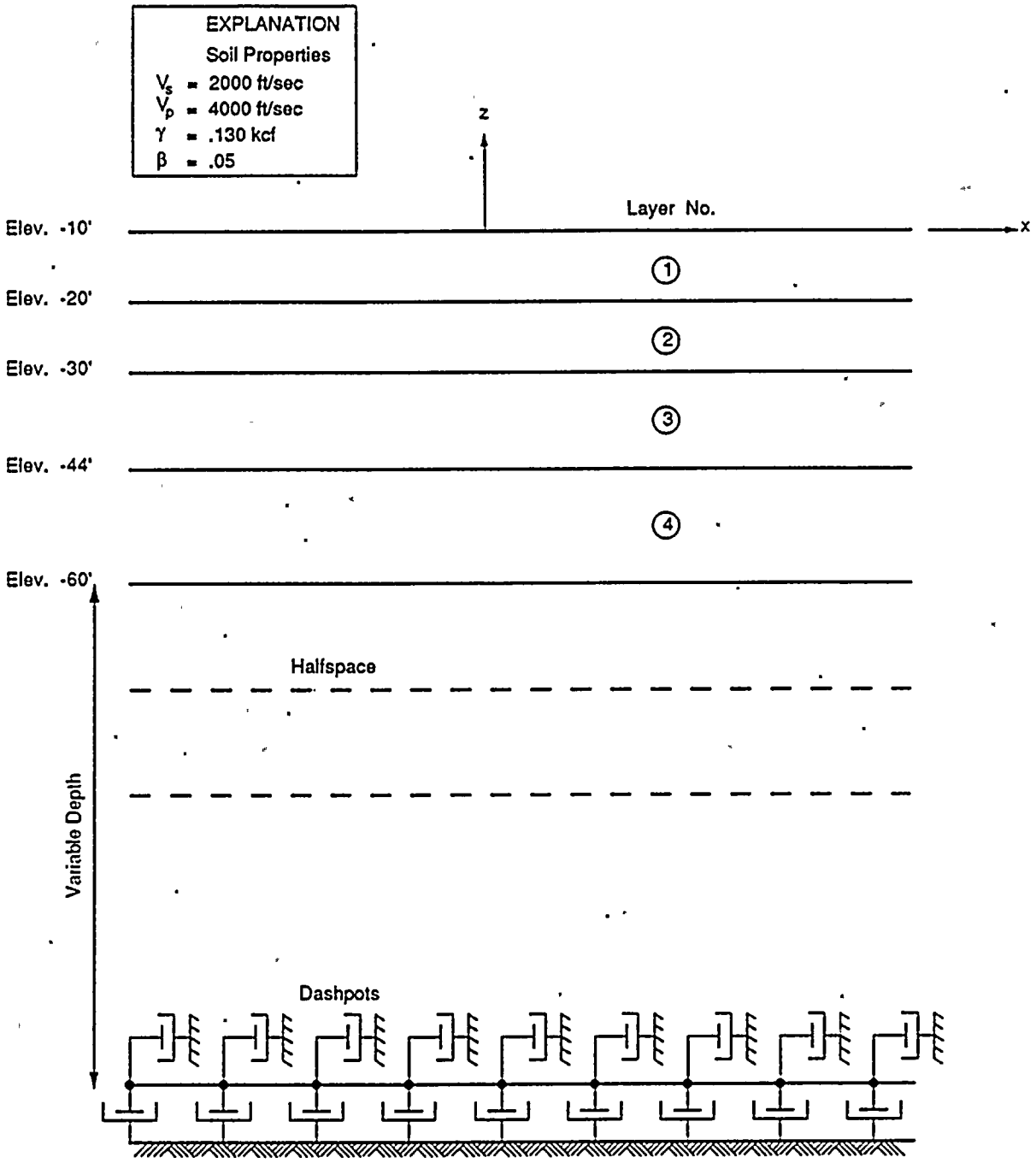

Figure 4.6-4. Soil Profile and Properties

4.6.1.2.2 Structural Model

The structural finite element model used in the interaction analysis is shown in Figure 4.6-5. It includes the superstructure and the basemat. The superstructure (the containment and internals) are modeled by 18 beam elements as shown in Figure 4.6-6 and the basemat is modeled by 88 solid elements connected to the underlying soil at 69 nodes as shown in Figs. 4.6-7, 4.6-8 and 4.6-9. Rigid links represented by beams of large flexural and axial rigidities are used to connect the stick models to the basemat. Figure 4.6-10 shows the rigid link model for the containment structure and internal walls, respectively.

The wave length criteria described in item 9 of Section 4.2.2 was used to select the element sizes of the basemat in the horizontal direction.

$$\text{Max. allowable element size} = \frac{2000}{5 \times 25} = 16 \text{ ft}$$

The selected element sizes for the basemat slightly violates the 16 feet length limit obtained above, but its effect is considered to be negligible.

Rotational mass of the superstructures was ignored during these analyses.

4.6.1.2.3 Excavated Soil Model

Since this is a surface structure, there is no excavated soil model.

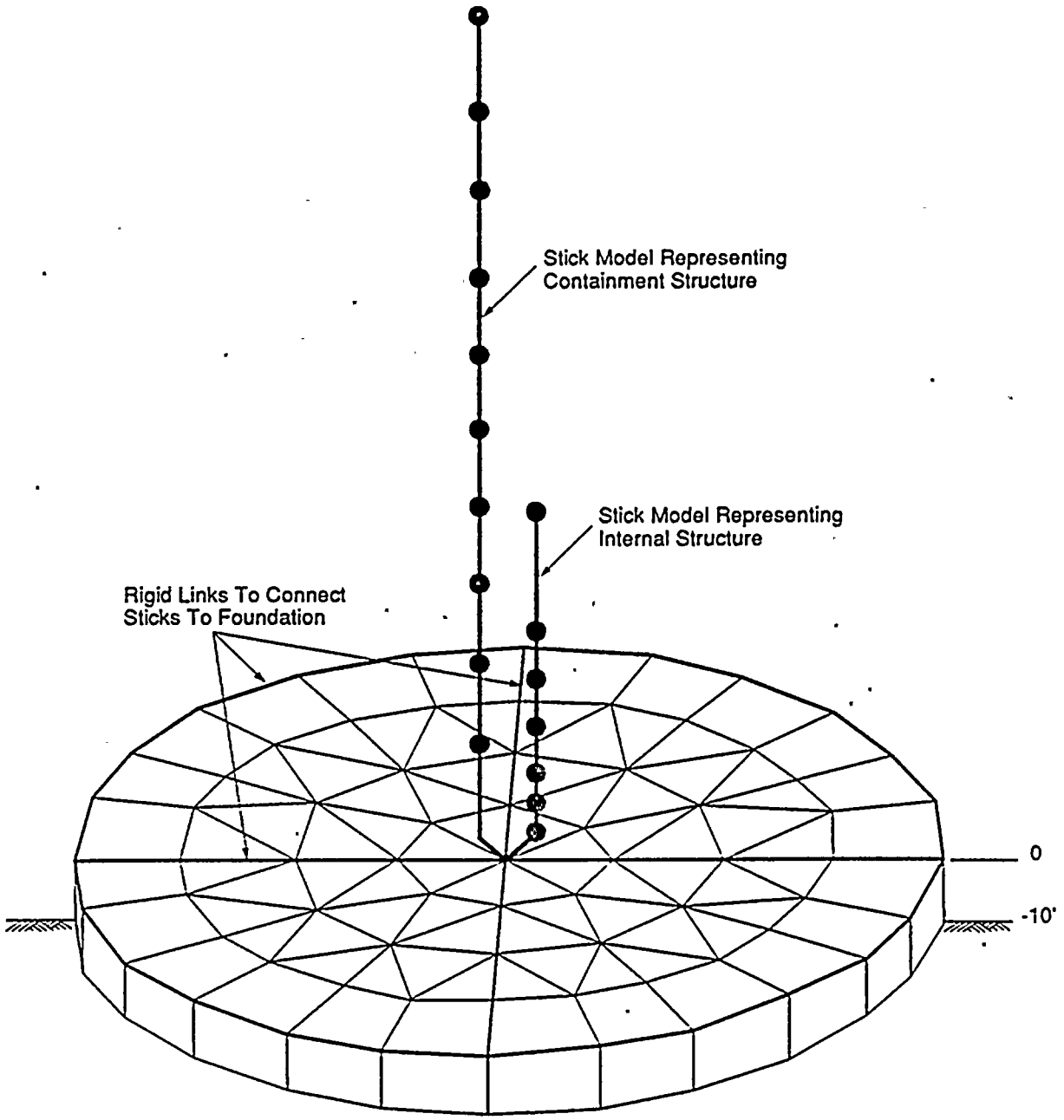

Figure 4.6-5. Finite Element Model

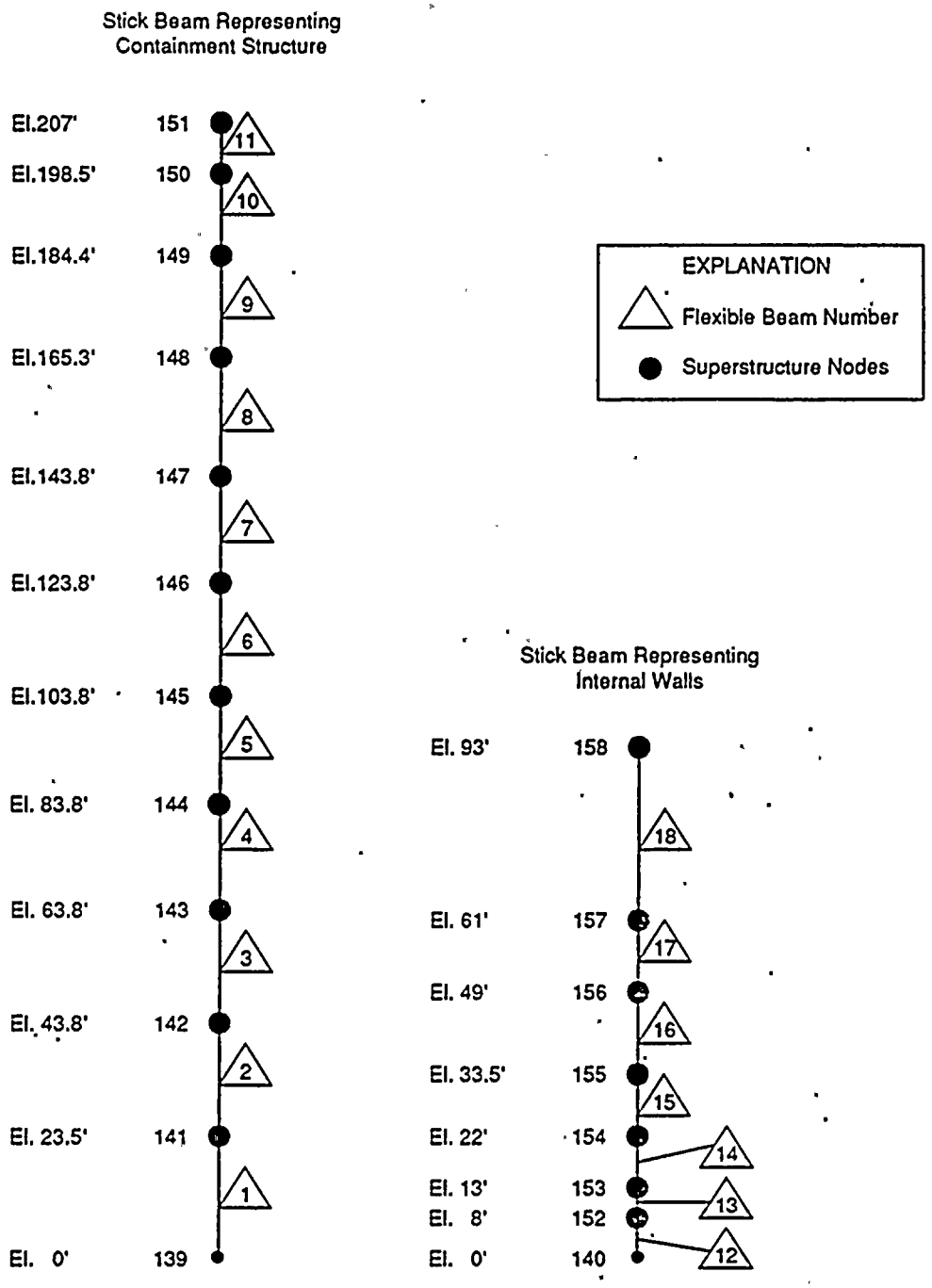

Figure 4.6-6. Finite Element Stick Models Representing Containment and Internal Structures

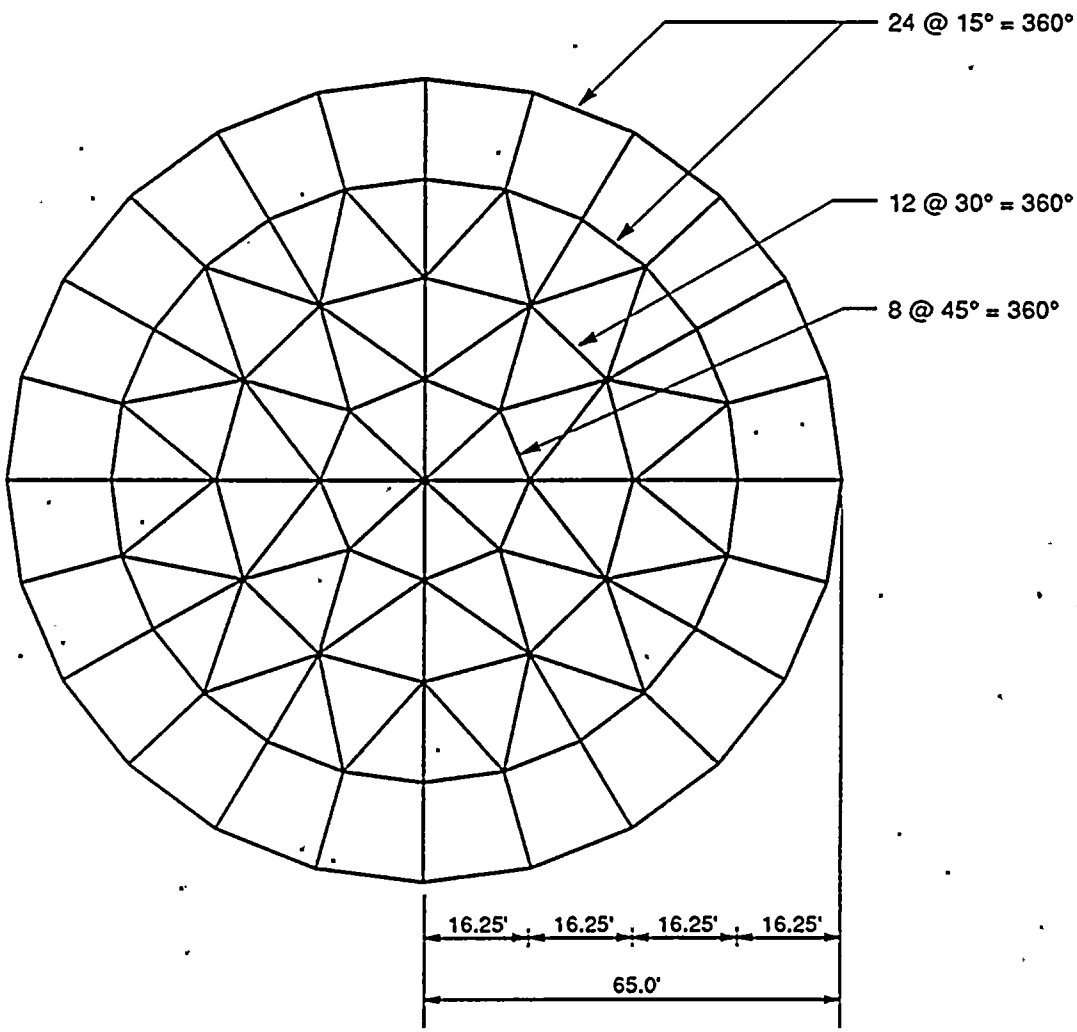

Figure 4.6-7. Geometry of Basemat Discretization

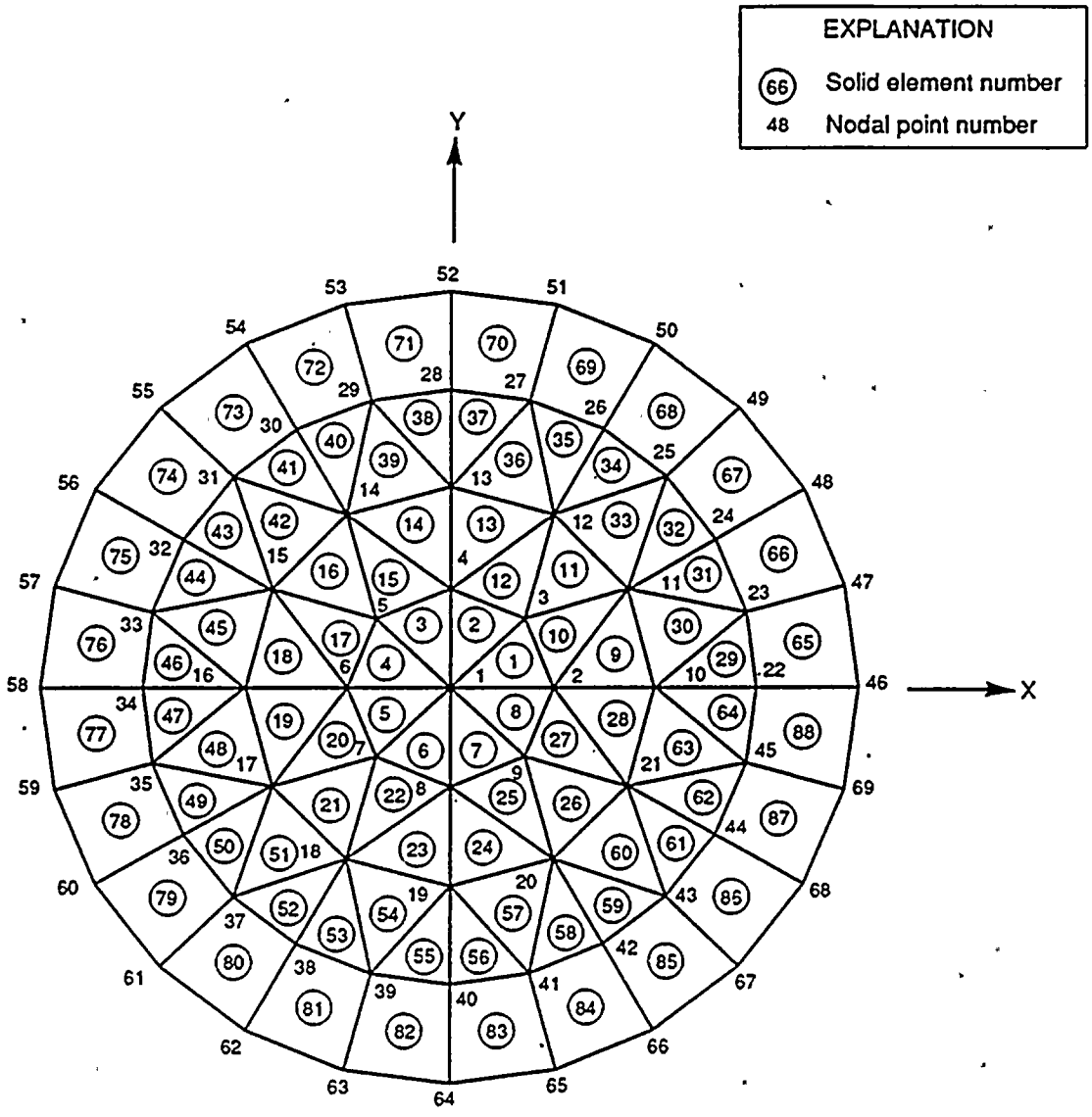

Figure 4.6-8. Nodal Point and Element Numbers for Basemat (Elevation -10 ft)

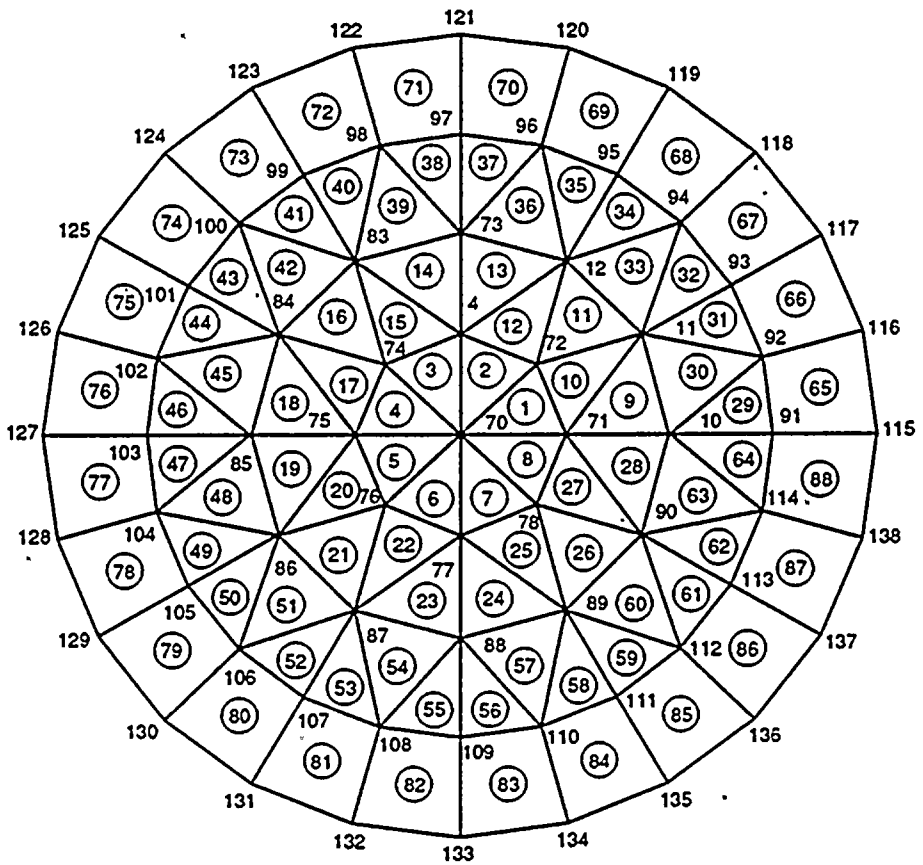

Figure 4.6-9. Nodal Point and Element Numbers for Basemat (Elevation 0 ft)

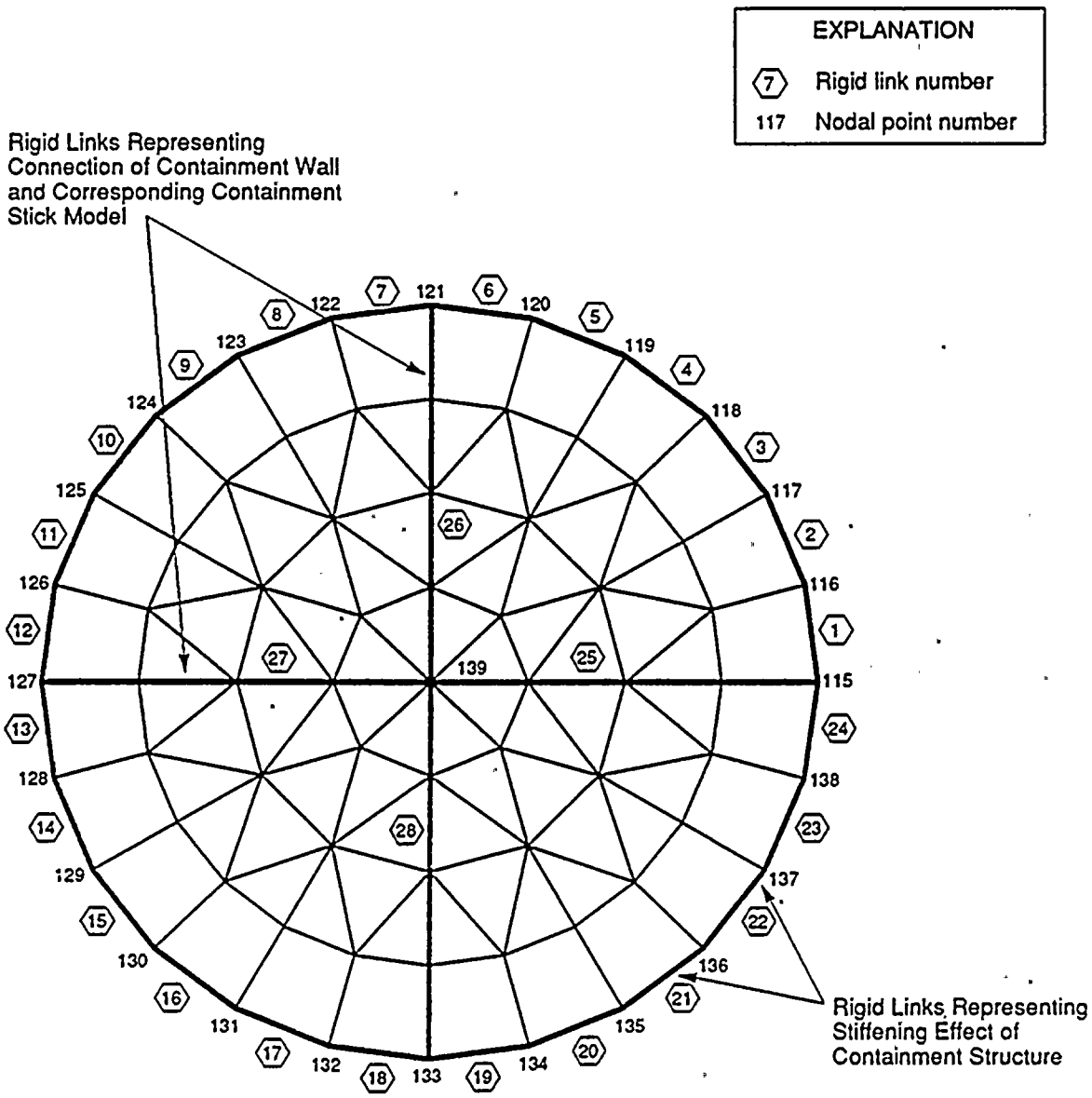

Figure 4.6-10. Rigid Link Model for Containment Structure (Elevation 0 ft)

4.6.1.3 Description of Analyses

The analyses performed are described below:

4.6.1.3.1 Foundation Impedance Analysis

The foundation impedance matrices are computed and saved by the computer program SASSI. These matrices are later used in the interaction analysis. In order to illustrate the accuracy of these matrices, the impedance coeffficients of the rigid massless basemat are calculated and compared with available solutions.

4.6.1.3.2 Interaction Analysis

The foundation impedance matrices obtained above are used to perform the complete interaction analysis by the computer program SASSI.

4.6.1.4 Analysis Cases Performed

4.6.1.4.1 Foundation Impedance Analysis

The frequency step and the highest frequency number used in the SASSI analysis are calculated according to item 5 of Section 4.2.2 as follows:

$$DF = 1/(2048 \times 0.005) = .0976 \text{ Hz}$$

$$NFREQ_{max} = 25/.0976 = 256$$

Highest frequency number selected is 260. The frequencies used in the analysis are listed in Table 4.6-2.

The horizontal and rocking foundation impedance coefficients at the base of the rigid massless basemat were then computed at the above frequencies following the procedures described in item 13 of Section 4.2.2. This required the following SASSI program modules to be executed in order to compute the horizontal/rocking compliance coefficients:

d. SITE (Mode 1)

e. POINT

f. HOUSE

g. MOTOR

h. ANALYS (Mode 1)

and the following restart runs as described in Section 4.4.3.3 to compute the rocking/coupling compliance coefficients:

j. MOTOR

k. ANALYS (Mode 4)

Table 4.6-2 - FREQUENCIES SELECTED FOR IMPEDANCE AND INTERACTION ANALYSIS BY SASSI

Frequency Number	Frequency (Hz)	Circular Frequency (Rad/sec)
10	.9766E + 00	.6136E + 01
30	.2940E + 01	.1841E + 02
50	.4883E + 01	.3068E + 02
60	.5859E + 01	.3682E + 02
80	.7813E + 01	.4909E + 02
100	.9766e + 01	.6136E + 02
120	.1172E + 02	.7363E + 02
140	.1367E + 02	.8590E + 02
160	.1563E + 02	.9817E + 02
180	.1758E + 02	.1104E + 03
210	.2051E + 02	.1289E + 03
230	.2246E + 02	.1411E + 03
260	.2539E + 02	.1595E + 03

The structural model used in this analysis consists of only the basemat with the nodal point numbering shown in Figs. 4.6-8 and 4.6-9. The basemat is modeled by massless elements with very large elastic modulus so that it behaves like a rigid massless circular footing.

The triangularized stiffness of the total system (on Tape 6) obtained from the ANALYS run in item (h) above is saved to restart the program ANALYS in item (k) above. The impedance matrix (on Tape 5) is also saved to be used in the interaction analysis described in the next section. The analysis results are discussed in Section 4.6.1.5.2

4.6.1.4.2 Interaction Analysis

The interaction analysis was performed by running the following SASSI program modules, as described in Section 4.4.3.1 and by computing the transfer function at the frequencies listed in Table 4.6-2.

n. House

o. SITE (Mode 2)

p. ANALYS (Mode 2)

q. MOTION

Since the impedance matrices on Tape 5 can be recovered from the analysis performed in Section 4.6.1.4.1, only part of the program module ANALYS in item (p) above was re-executed.

4.6.1.5 Analysis Results

4.6.1.5.1 Input/Output Files

The input/output files corresponding to the impedance and SSI analysis are listed in Table 4.6-3. This table also includes the names that are assigned to the tapes for conveniences of tapein/tapeout activity.

4.6.1.5.2 Foundation Impedance Analysis

The SASSI analysis yields the horizontal and rocking stiffness and damping coefficients of the foundation as shown in Figure 4.6-11 through 4.6-14. The impedance is computed by inverting the resultant displacements obtained from SASSI analysis. The horizontal impedance coefficients are obtained using Eq. (4.2-1) (see Section 4.2.2) by using the horizontal displacement of Node 1 (see Figure 4.6-8) from output E2C1HA0 (see Table 4.6-3). Similarly, the rocking impedance are computed from the rocking compliance coefficients obtained from vertical displacement of Node 46 from output E2C1RA0 (see Table 4.6-3) divided by the radius of the footing.

Table 4.6-3 Input/Output Files of Example Problem

MODULE USED	HORIZONTAL IMPEDANCE				ROCKING IMPEDANCE				SSI			
	INPUT FILE	OUTPUT FILE	TAPE IN	TAPE OUT	INPUT FILE	OUTPUT FILE	TAPE IN	TAPE OUT	INPUT FILE	OUTPUT FILE	TAPE IN	TAPE OUT
SITE	E2C1SD*	E2C1SO	-	E2C1T2**	-	-	-	-	-	-	-	-
POINT3	E2PD	E2PO	E2C1T2	E2C1T3	-	-	-	-	-	-	-	-
HOUSE	E2C1HD	E2C1HO	-	E2C1T4	-	-	-	-	E2C2HD	E2C2HO	-	E2C2T4
MOTOR	E2C1HMD	E2C1HMO	-	E2C1HT9	E2C1RMD	E2C1RMO	-	E2C1RT9	-	-	-	-
ANALYS	E2C1HAD	E2C1HAO	E2C1T3 E2C1T4 E2C1HT9	E2C1T5 E2C1T6 E2C1HT8	E2C1RAD	E2C1RAO	E2C1RT9 E2C1T6	E2C1RT8	E2C2AD	E2C2AO	E2C1T1 E2C1T5 E2C2T4	E2C2T6 E2C2T8
MOTION	-	-	-	-		-	-	-	E2C2OD	E2C2OO	E2C2T8	E2C2T12

* E2C1SD - Stands for Example 2, Case 1, Site Data
** E2C1T2 -- Stands for Example 2, Case 1, Tape 2

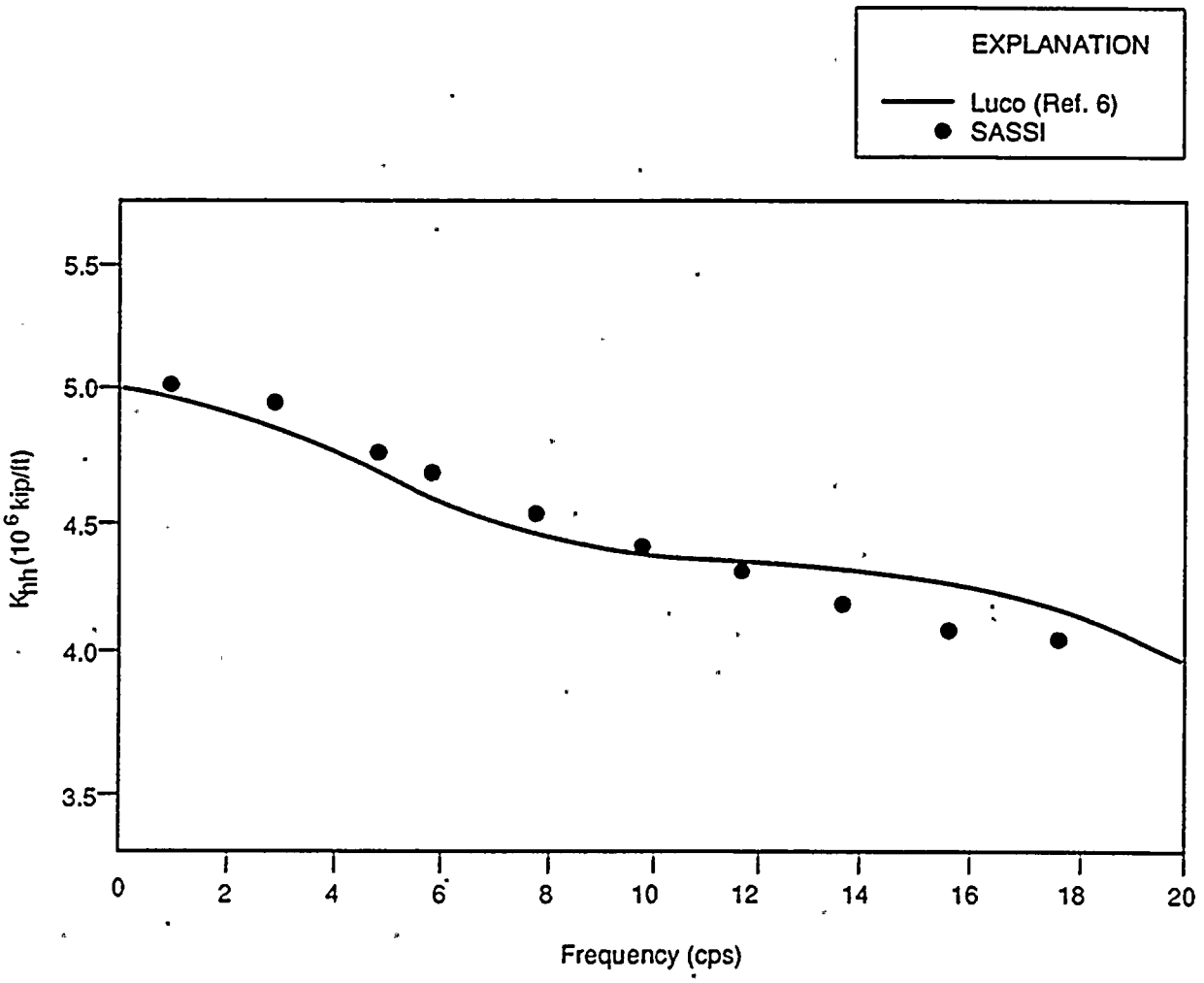

Figure 4.6-11. Horizontal Stiffness Coefficients

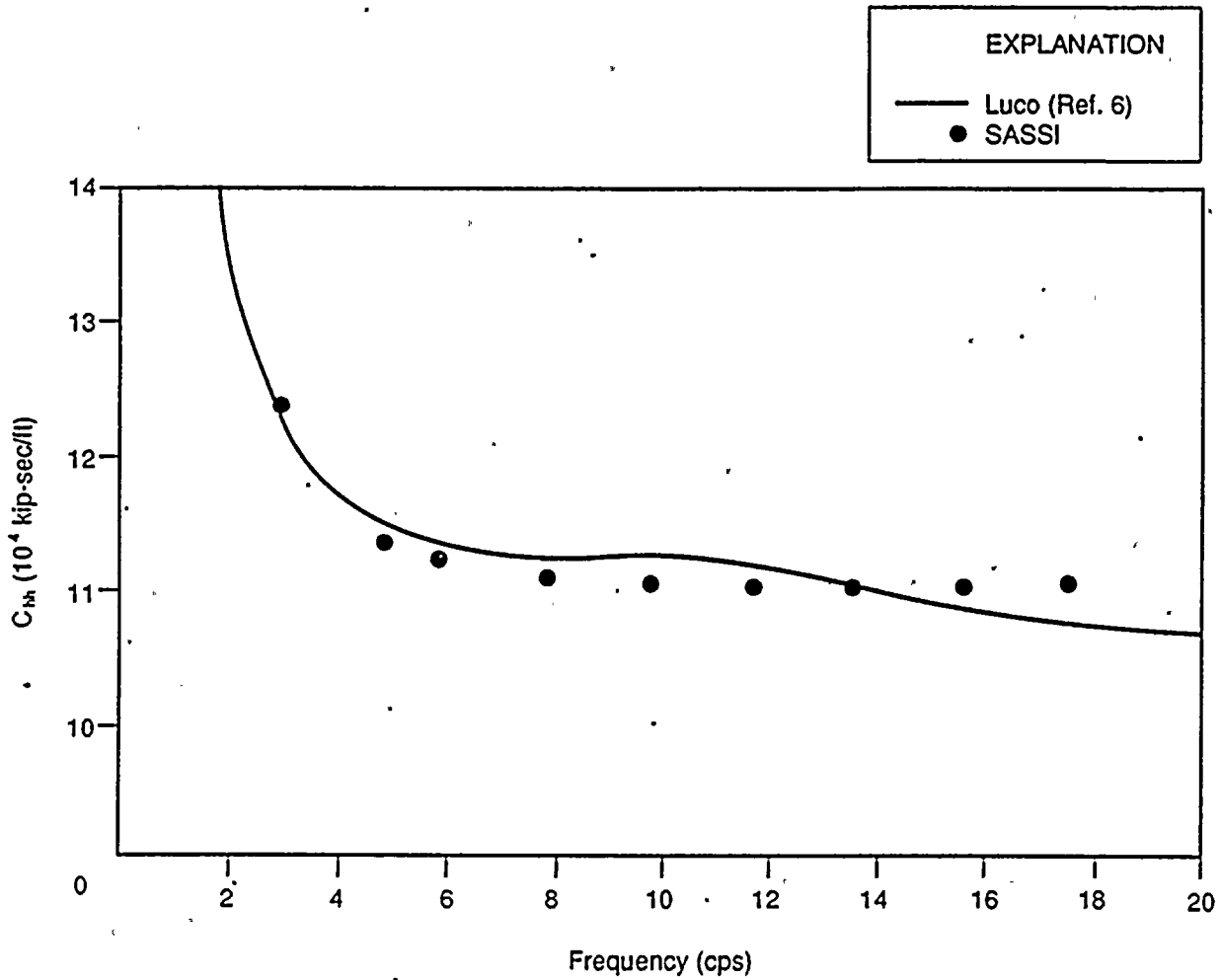

Figure 4.6-12. Horizontal Damping Coefficients

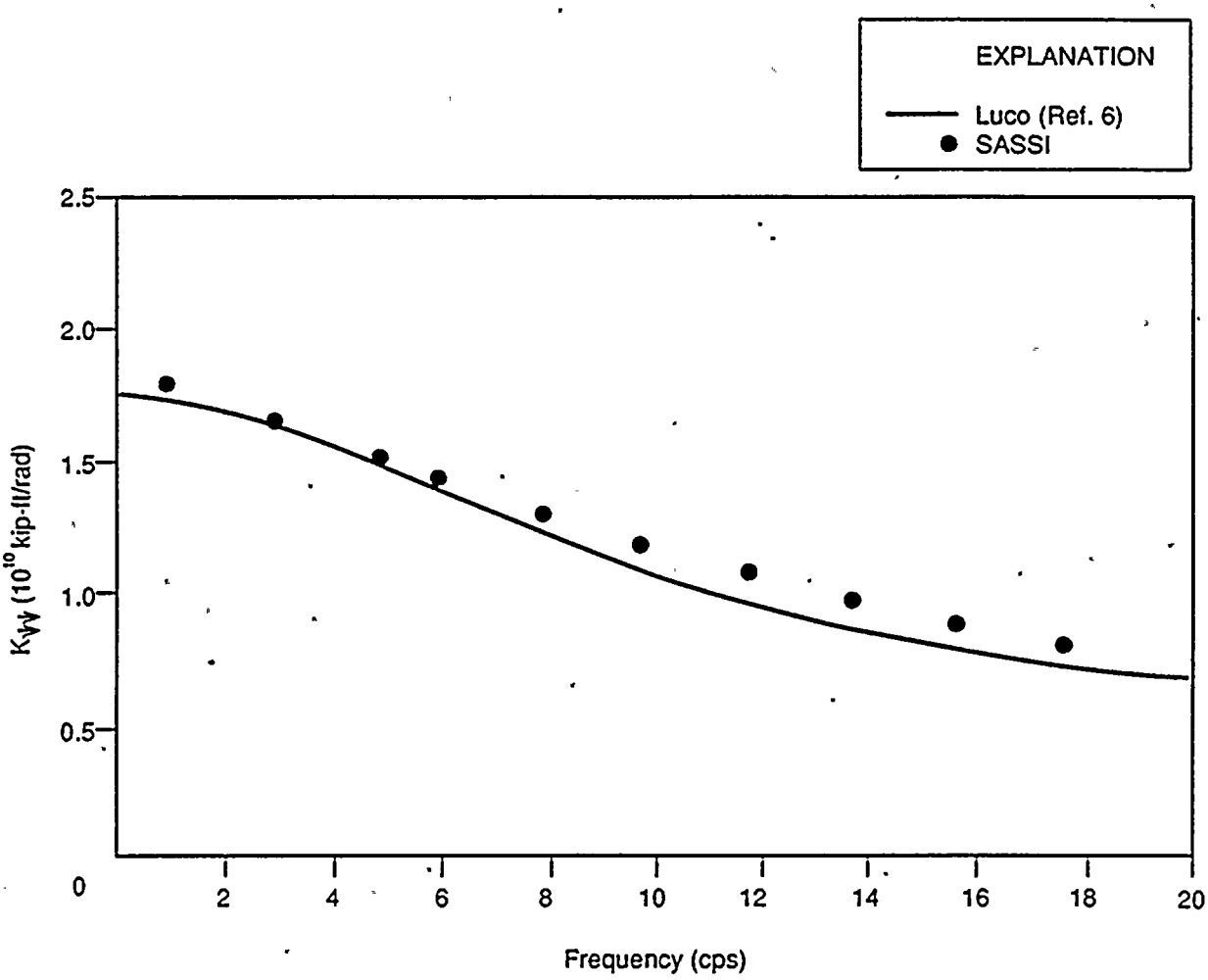

Figure 4.6-13. Rocking Stiffness Coefficients

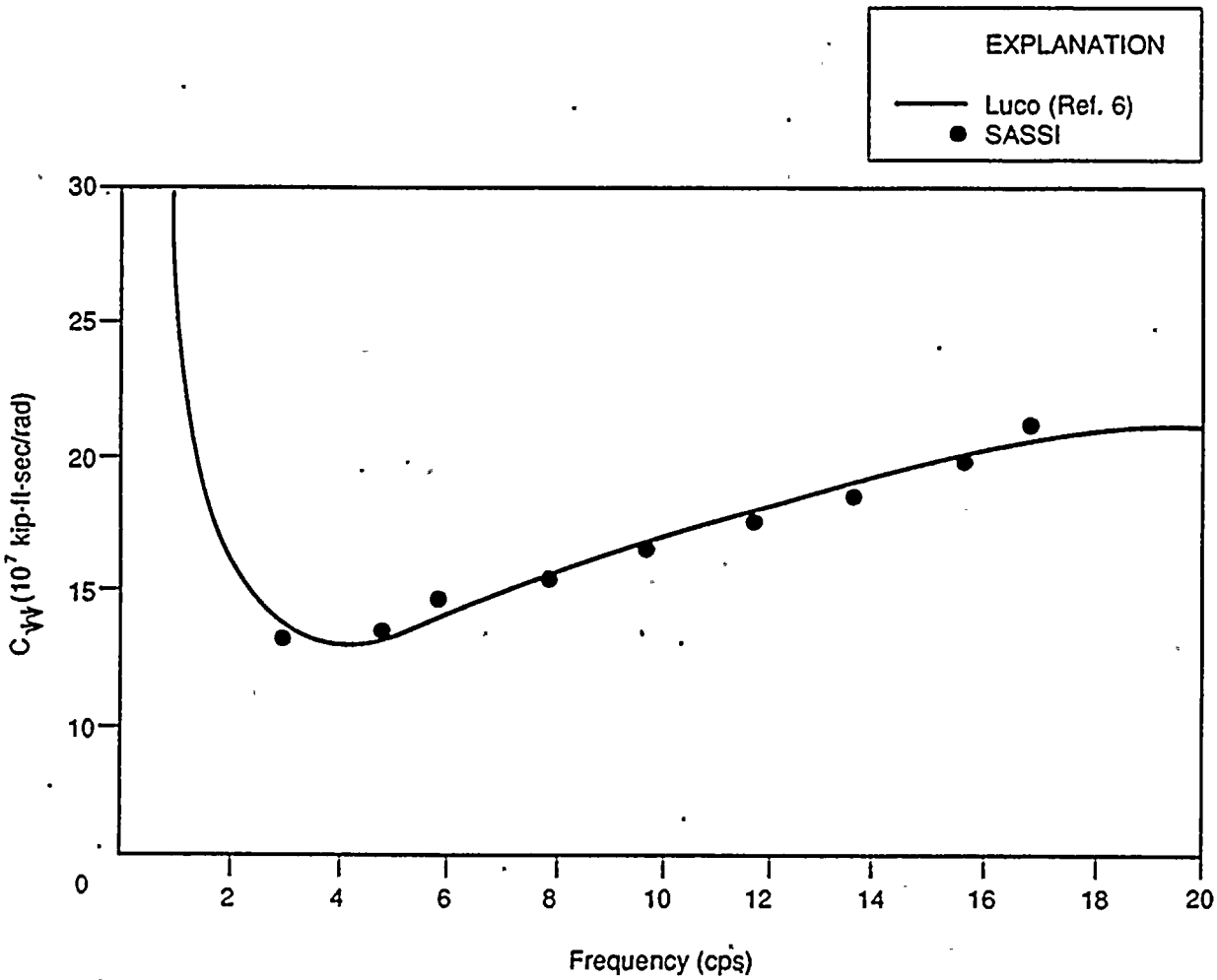

Figure 4.6-14. Rocking Damping Coefficients

The figures also show the corresponding foundation impedances reported by Luco (Ref. 6). The comparison of these results shows good agreement over the frequency range of analysis.

4.6.1.5.3 Interaction Analysis

Table 4.6-4 shows the maximum absolute acceleration of the containment building and internal walls obtained from the interaction analysis by SASSI.

Additional results include the 2% acceleration spectra computed for the horizontal motions at the top of the internal and shown in Figure 4.6-15. The results are compared with the results obtained from computer program FASS (Ref. 7) using the impedance functions obtained from SASSI. The comparison of the results shows good agreement between the two solutions.

Table 4.6-4 - MAXIMIM ABSOLUTE ACCELERATIONS (g's)
OBTAINED FROM SASSI ANALYSIS

Node No.	Interaction
141	0.090
142	0.089
143	0.083
144	0.073
145	0.053
146	0.027
147	0.010
148	0.046
149	0.080
150	0.101
151	0.111
152	0.084
153	0.073
154	0.052
155	0.027
156	0.013
157	0.036
158	0.174

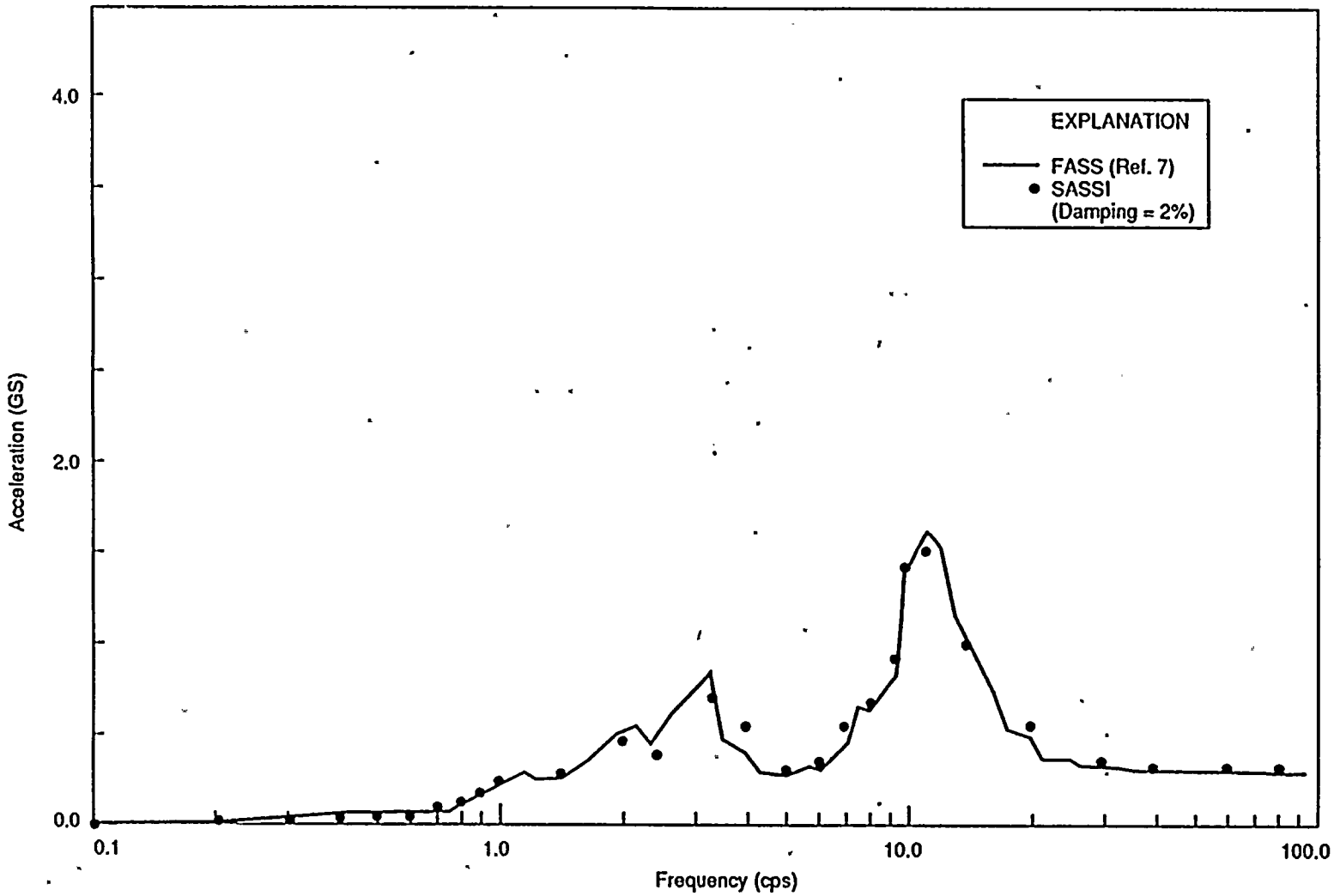

Fig. 4.6-15. Absolute Acceleration Response at Top of Internal Structure

CHAPTER 5

INPUT GUIDE TO SASSI PROGRAM MODULES

5.1 Computer Program for SASSI Modules

The current version of the SASSI program consists of the following computer programs:

A. SITE
B. POINT2 and POINT3
C. HOUSE
D. MOTOR
E. ANALYS
F. COMBIN
G. MOTION
H. STRESS

5.2.1 SITE

The program module SITE has two basic functions:

1. Form and solve transmitting boundary eigenvalue problem - Mode 1

The program reads the soil layer properties and for each specified frequency forms the transmitting boundary submatrices for Rayleigh and Love wave cases. Then it solves the two eigenvalue problems:

$$k^2A_2 + kA_1 + A_0 - \omega^2 M = 0 \qquad (5.2\text{-}1)$$

$$k^2A_2 + A_0 - \omega^2 = 0 \quad , \qquad (5.2\text{-}2)$$

from which the eigenvalues (k) and eigenvectors are obtained. The results are then written on Tape 2.

The halfspace condition is also simulated at this stage. The program automatically generates a specified number of sublayers whose thicknesses vary with frequency attached to viscous dashpots at the base. The generated sublayers and dashpots are then added to the fixed top layers. Such provision requires some modifications in the above equations which are carried out in this program.

Tape 2 provides the information needed to run Mode 2 in the program module SITE as well as to compute for the transmitting boundary in the program module POINT. Thus, this tape always has to be generated.

Since the eigenvalue problems to be solved for an arbitrary three-dimensional horizontally layered site are the same as those to be solved for a plane strain model, the information on Tape 2 can be used for both two- and three-dimensional cases as well.

In order to run this mode, all the input cards from A.1 to A.6 of this section must be supplied. If the execution is to be stopped after Mode 1, the card A.6 must be entered as a blank card.

2. Solve the site response problem - Mode 2

The program recovers the soil layer properties and the eigensolutions for Rayleigh and Love wave cases from Tape 2. Then, according to the existence of each wave type, the program computes the mode shapes and wave numbers for each wave type in the coordinate system defined in the program module SITE. Then, once the composition of the wave types causing the seismic environment and the nature of the control motion is known, the program will scale and superimpose the results of all the wave types. These results are then stored on Tape 1, which is used later for seismic analysis. Thus, this tape will not be generated for foundation vibration analysis.

If the seismic environment is the same for a two- and three-dimensional case, the information on Tape 1 can be used for both problems.

In order to run Mode 1 and Mode 2 together, all the input cards from A.1 to A.10 of this section must be supplied. However, to restart the program in Mode 2 alone, only the input cards from A.6 to A.10 of this section are needed.

A.1 OPERATION MODE CARD AND TITLE (I5, 3X, 12A6)

Columns	Variable	Notes	Entry
1-5	NOPT		Operation mode
		(1)	= 1, complete solution for MODE 1
		(2)	= -1, data check only
6-8			Blank
9-80	HED		Contain information to be printed with output

Notes:

(1) If the program is to be restarted in Mode 2 using Tape 2 as input, then skip all the input cards A.1 through A.5 and start from Section A.6.

(2) If NOPT < 0, most of the calculation required during execution of Mode 1 will be bypassed.

A.2 MASTER CONTROL CARD (315)

Columns	Variable	Notes	Entry
1-5	NTL	(1)	Number of soil layers (maximum = 100)
6-10	NF		Total number of frequencies of analysis (maximum = 100)
15	LSUB	(2)	=0, no simulation of halfspace
			> 3. number of layers generated to simulate halfspace (maximum = 20)

Notes:

(1) All the soil layers must be labeled with integer numbers starting from 1 at the surface to NTL. It does not include halfspace or layers generated to simulate halfspace.

(2) If LSUB = 0, the soil profile will be assumed on rigid base. Otherwise, LSUB sublayers whose thicknesses vary with frequency are generated to simulate halfspace. Also, the program will add viscous boundary to account for radiation damping in the halfspace through the lower boundary. Using LSUB = 10 is recommended for the case of halfspace.

A.3 SYSTEM OF UNITS CARD (F10.0)

Columns	Variable	Notes	Entry
1-10	GRAV	(1)	Acceleration of gravity

Notes:

(1) To be used for computation of mass matrix.

A.4 SOIL LAYER DATA CARDS

A.4.1 TOP LAYERS (I5, 6F10.)

Columns	Variable	Notes	Entry
1-5	N	(1)	Layer number
5-15	H		Layer thickness
16-25	W		Unit weight
26-35	VS		S-wave velocity
36-45	VP		P-wave velocity
46-55	DS		S-wave associated damping ratio
56-65	DP		P-wave associated damping ratio

A.4.2 HALFSPACE (15X, 5F10.0)

Columns	Variable	Notes	Entry
1-15			Blank
16-25	WH	(2)	Unit weight of halfspace
26-35	VSH		S-wave velocity
36-45	VPH		P-wave velocity
46-55	DSH		S-wave associated damping ratio
56-65	DPH		P-wave associated damping ratio

Notes:

(1) Total of NTL cards must be given and all soil layer data must be defined in soil layer number sequence.

(2) One card must be given to define properties of halfspace. For example, if a hard layer exists at depth or LSUB=0, then properties of competent rock should be supplied; otherwise, properties of existing materials at depth must be provided.

A.5 FREQUENCY DATA CARDS

A.5.1 FREQUENCY CONTROL CARD (2F10.0, I15)

Columns	Variable	Notes	Entry
1-10	DF	(1)	Frequency step (HZ)
11-20	DT	(1)	Time step of control motion (sec)
21-25	NFFT	(1)	Number of values to be used in Fourier transform of control motion. Must be power of 2.

A.5.2 FREQUENCY NUMBER CARDS (16I5)

Columns	Variable	Notes	Entry
1-5	NFR(1)	(2)	Frequency no. 1
6-10	NFR(2)		Frequency no. 2
11-15	NFR(3)		Frequency no. 3
.	.		.
.	.		.
.	.		.

Notes:

(1) Case A - Deterministic Analysis

DT and NFFT for the selected time history of the control motion must be given, and the frequency step may be left blank. The program will compute the frequency step as follows:

DF = 1/(NFFT*DT)

This frequency step may then be used to set up frequency numbers in Section A.5.2.

Case B - Probabilistic (or Single Harmonic) Analysis

DF must be given and may be directly used to set up frequency numbers in Section A.5.2. In this case, DT and NFFT are never used and therefore may be left blank.

(2) The total of NF frequency numbers must be given. All the frequency numbers must be positive nonzero integer numbers. The program will automatically reorder the input frequency numbers in ascending order and will stop if two or more equal-frequency numbers are detected. Frequencies f_i, for which solutions are obtained, are defined as follows:

$$f_i = NFR(i)*DF$$

The highest frequency of analysis is then equal to the highest frequency number multiplied by the frequency step.

A.6 OPERATION MODE CARD AND TITLE (I5, 3X, 12A6)

Columns	Variable	Notes	Entry
1-5	NOPT		Operation mode
		(1)	= 0, stop, no more data
		(2)	= 2, complete solution for MODE 2
		(3)	= -1, data check only
6-8			Blank
9-80	HED		Contain information to be printed with output

Notes:

(1) NOPT = 0 terminates the execution of the program at the end of Mode 1, and no data are required after this card.

(2) If NOPT = 2, continue providing the remaining data cards. However, if this is the restart of Mode 2 with Tape 2 as input, then the input cards A.1 to A.5 are not required.

(3) If NOPT < 0, most of the calculations required during normal execution of Mode 2 are bypassed. Mode 1 must be executed before the data check can be done in Mode 2.

A.7 WAVE FIELD DATA CARDS

A.7.1 WAVE FIELD TYPE CARD (2I5)

Columns	Variable	Notes	Entry
5	IWTYP		= 1, combination OF P-, SV-, and R-waves (use for 1-D or 3-D analyses)
			= 2, combination of SH- and L-waves (use for 1-D or 3-D analyses)

A.7.2 WAVE FIELD TYPE 1 CARD (3I5, 2F10.0)

Skip this section if IWTYP = 2

Columns	Variable	Notes	Entry
5	IRWAVE	(1)	= 0, no R-wave field
			= 1, R-wave field (shortest wavelength method)
			= 2, R-wave field (least decay method)
10	IVWAVE	(1)	= 0, no SV-wave field
			= 1, SV-wave field
15	IPWAVE	(1)	= 0, no P-wave field
			= 1, P-wave field
16-25	ANGS	(2)	Incident angle of SV-wave (degree)
25-35	ANGP	(2)	Incident angle of P-wave (degree)

A.7.2 WAVE FIELD TYPE 1 CARD (3I5, 2F10.0)

Skip this section if IWTYP = 1

Columns	Variable	Notes	Entry
5	ILWAVE	(1)	= 0, no L-wave field
			= 1, L-wave field
10	IHWAVE	(1)	= 0, no SH-wave field
			= 1, SH-wave field
11-20	ANGH	(2)	Incident angle of SH-wave (degree)

Notes:

(1) The seismic environment may be assumed to consist of one single wave type or several wave types. The basic wave types are P-waves and S-waves, which are also called body waves. When these waves impinge on the ground surface or layer interfaces, surface waves may be generated which include R-waves and L-waves.

P-waves involve motions in the direction of wave propagation. S-waves involve motions perpendicular to the direction of wave propagation. S-wave motions in the vertical plane are called SV-waves. Horizontal S-waves are called SH-waves. R-waves involve horizontally propagating elliptical motions in the vertical plane and L-waves consist of horizontal motions perpendicular to the horizontal direction of wave propagation.

With the above definitions, a coordinate system in program SITE has been set up such that P-waves, SV-waves, and R-waves involve particle displacements in $x'z'$-plane while SH-waves and L-waves particle displacements along y'-axis. Therefore z' is always vertical up, x' is in the vertical plane of wave propagation, and y' is perpendicular to x' and z' and following the right-hand rule.

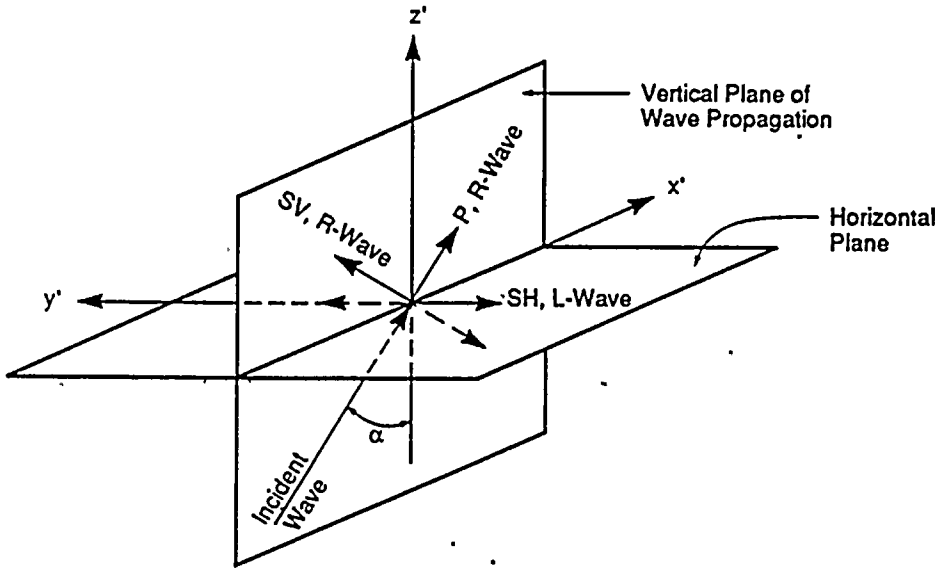

(2) Incident angle is defined as the angle between direction of propagation z' axis shown as α in the figure. For vertically propagating body waves, this angle is zero.

A.8 CONTROL MOTION CARD (4X, A1, 2I5)

Columns	Variable	Notes	Entry
5	KCOMP	(1)	= X, control motion in X' direction
			= Y, control motion in Y' direction
			= Z, control motion in Z' direction
6-10	NLCP	(2)	Layer number of control point
11-15	NFCP	(3)	Number of frequencies used to define ration curve of wave participations in control motion ($\leq$2)

Notes:

(1) Transformation of x' y' z' coordinate to final xyz coordinate of soil structure system will be done in the program module ANALYS.

(2) Control point is defined as the point where the control motion is specified. It will be located at the top of the given layer number, e.g., NLXZ = 1 for control point at the surface.

(3) In the case of seismic environment composed of two or more wave types, the ratio of participation of each wave type must be given. This ratio in general may be frequency dependent and is defined at a number of selected discrete frequencies for each wave type. These frequencies must cover the frequency range of analysis. The ratio values for intermediate frequencies will be obtained by simple interpolation and therefore need not be given at exact frequencies for which complete solution is required.

In the case of seismic environments consisting of one simple wave type, two frequencies (one in the beginning and the other at the end of the frequency range of analysis) with assigned ratio value of 1 are enough to define the ratio curve.

Also note that all the ratio values are positive decimal numbers less than or equal to 1, and summation of the ratio values of all the participating wave types at any frequency must be 1.

A.9 WAVE COMPOSITION OF CONTROL MOTION ON X'Z'-PLANE

Skip this section if IWTYP = 2.

A.9.1 FREQUENCY CARDS (16I5)

Columns	Variable	Notes	Entry
1-5	NFXZ(1)	(1)	Frequency no. 1 to define ratio curve
6-10	NFXZ(2)		Frequency no. 2 to define ratio curve
.	.		.
.	.		.
.	.		.

A.9.2 R-WAVE RATIO CARDS (8F10.0)

Skip if no R-wave field (IRWAVE = 0).

Columns	Variable	Notes	Entry
1-10	XZR(1)	(1)	R-wave ratio at frequency no. 1
11-20	XZR(2)		R-wave ratio at frequency no. 2
.	.		.
.	.		.
.	.		.

A.9.3 SV-WAVE RATIO CARDS (8F10.0)

Skip if no SV-wave field (IVWAVE = 0).

Columns	Variable	Notes	Entry
1-10	XZS(1)	(1)	SV-wave ratio at frequency no. 1
11-20	XZS(2)		SV-wave ratio at frequency no. 2
.	.		.
.	.		.
.	.		.

A.9.4 P-WAVE RATIO CARDS (8F10.0)

Skip if no P-wave field (IVWAVE = 0).

Columns	Variable	Notes	Entry
1-10	XZP(1)	(1)	P-wave ratio at frequency no. 1
11-20	XZP(2)		P-wave ratio at frequency no. 2
.	.		.
.	.		.
.	.		.

Notes:

(1) Refer to note 3 in Section A.8.

A.10 WAVE COMPOSITION OF CONTROL MOTION ALONG Y -AXIS

Skip this section if IWTYP = 1.

Columns	Variable	Notes	Entry
1-5	NFY(1)	(1)	Frequency no. 1 to define ratio curve
6-10	NFY(2)		Frequency no. 2 to define ratio curve
.	.		.
.	.		.
.	.		.

A.10.2 L-WAVE RATIO CARDS (8F10.0)

Skip if no L-wave field (ILWAVE = 0).

Columns	Variable	Notes	Entry
1-10	YL(1)	(1)	L-wave ratio at frequency no. 1
11-20	YL(2)		L-wave ratio at frequency no. 2
.	.		.
.	.		.
.	.		.

A.10.3 SH-WAVE RATIO CARDS (8F10.0)

Skip if no SH-wave field (IHWAVE = 0).

Columns	Variable	Notes	Entry
1-10	YS(1)	(1)	SH-wave ratio at frequency no. 1
11-20	YS(2)		SH-wave ratio at frequency no. 2
.	.		.
.	.		.
.	.		.

Notes:

(1) Refer to note 3 in Section A.8.

A.11 OPERATION MODE CARD (I5)

Columns	Variable	Notes	Entry
5	NOPT	(1)	Operation mode = 0, stop, no more data

Notes:

(1) Must be the last data card

5.2.2 POINT

The program module POINT recovers the soil layer properties and the eigensolutions for the Rayleigh and Love wave cases from Tape 2. Then, for each frequency specified in the program module SITE and for given radius of the central zone, the program solves for the point loads applied at the surface of the layered system and on the layer interfaces below the ground surface. The maximum number of layers that the structure is embedded into the ground determines how deep the point loads are applied below the ground surface.

The results which are obtained in the local coordinate system of the program module POINT are saved on Tape 3 and are later used to compute the flexibility matrix of the interaction nodes in the program module ANALYS.

For two-dimensional problems the program module POINT2 and for three-dimensional problems the program module POINT3 must be executed.

B.1 OPERATION MODE CARD AND TITLE (I5, 3X, 12A6)

Columns	Variable	Notes	Entry
1-5	NOPT		Operation mode
			= 1, complete solution
		(1)	< 0, data check only
5-8			Blank
9-80	HED		Contain information to be printed with output

Notes:

(1) If NOPT < 0, most of the calculations required during normal execution are bypassed.

B.2 GENERAL INFORMATION CARD (I5, F10.0)

Columns	Variable	Notes	Entry
1-5	LSTFCE	(1)	Last layer number in the near field zone
6-15	RADIUS	(2)	Radius of the central zone in the point load solution. Must be positive and nonzero.

Notes:

(1) This parameter is the maximum number of layers in the ground that the structure (including the irregular soil zone) is embedded into. The smaller this number, the less information need be passed on to Tape 3 and therefore less computation and storage will be needed to form the flexibility matrix in the program module ANALYS. However, this number must be large enough to ensure that the excavated soil region will not extend deeper than the specified layer number. For surface structures with no assumed irregular soil zone, let LSTFCE = 0.

(2) The value of this parameter depends on the geometry of foundation discretization by finite element method. For two relatively uniform meshes, this value is given below.

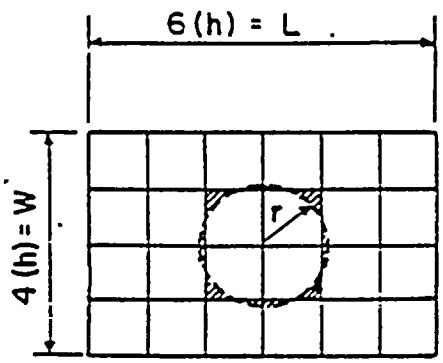

Radius = r = 0.90 h

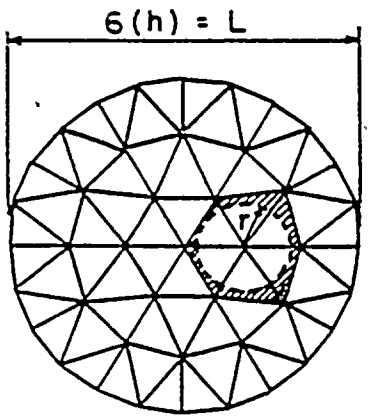

Radius = r = 0.85 h

An average value can be obtained for uniform meshes, but using uniform meshes as much as possible is recommended. For 2-D cases, the radius of the central zone shall be selected as follows:

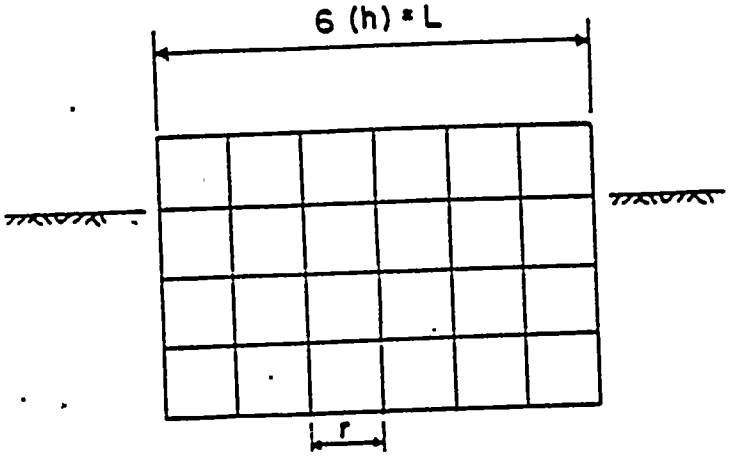

Radius = r = h

For 2-D cases, the results are not sensitive to changes in the assumed radius for the central zone as long as this radius is of the same order as the dimension of the finite elements in the interaction volume (refer to verification manual).

B.3 OPERATION MODE CARD (I5)

Columns	Variable	Notes	Entry
5	NOPT	(1)	Operation layer = 0, stop, no more data.

Notes:

(1) Must be the last data card.

5.2.3 HOUSE

The program module HOUSE is a standard finite element program which computes the basic frequency independent global mass and stiffness matrices, M and K, for the structure and excavated soil.

Two separate finite element models are constructed, one for the structure and the other for the excavated soil. The models share the same nodal points at/below the ground surface which are called the interaction nodes.

Each nodal point on the structure may have up to six displacement degrees of freedom. The program has the capability to delete any number of the degrees of freedom specified by the user. Therefore, the user can control and optimize the size of the equations to be solved.

The several element types available to model the structure include:

1. 3-D eight-node solid element (with option for inclusion of nine incompatible displacement modes)
2. 3-D beam element
3. Four-node quadrilateral plate/shell element
4. 2-D four-node plane strain finite element
5. 3-D spring element
6. 3-D stiffness/mass element

Other element types to be added to the program in the future to model the structure are:

1. 2-D pile element
2. 3-D pile element

3. 2-D fluid element
4. 3-D fluid element
5. 2-D four- to eight-node quadrilateral element
6. 3-D high order solid element
7. 1-D plane love wave element

The excavated soil zones are modeled by the following element types:

1. 3-D eight-node solid elements (without incompatible modes)
2. 2-D four-node plane strain finite element.

The finite element models of the structure and the excavated soil must be selected in such a way that every interaction node below the ground should lie on a soil layer interface.

The program reads the nodal point input data, nodal types, soil layer properties, and element data for the structural and excavated soil elements, then forms the element mass and stiffness matrices for these elements which are later assembled into the corresponding global mass and stiffness matrices. These matrices are stored in compacted blocks in preparation for solution by the active column method later in the program module ANALYS. The results are written on Tape 4.

If the skin method is to be used for computation of the impedance matrix, the excavated soil elements are once again assembled but this time in a different format to form the global matrices M_{12} and K_{12}. The columns of these matrices follow the same order as the degrees of freedom to be used later to form the flexibility matrix F_{12}, thus making it possible to carryout the matrix operation in Eq. (2.3-2) efficiently. The matrices M_{12} and K_{12} are full matrices which are stored in blocks and are then written on Tape 4.

C.1 OPERATION MODE CARD AND TITLE (I4, 3X, 12A6)

Columns	Variable	Notes	Entry
1-5	NOPT		Operation mode
			= 1, complete solution
		(1)	< 0, data check only
6-8			Blank
9-80	HED		Contain information to be printed with output

Notes:

(1) If NOPT < 0, most of the calculations required during normal execution are bypassed.

C.2 CORE AND BLOCK STORAGE CONTROL CARD (3110)

Columns	Variable	Notes	Entry
1-10	MAXC	(1)	Maximum number of columns to be assigned to each block (can be ignored if initiation run)
11-20	MAXT	(1)	Maximum number of terms to be assigned to each block (can be ignored if initiation run)
21-30	MUSE	(2)	Maximum decimal field length to be used for blank common (modified by program so that it will be integer multiple of 512); leave blank if program does not use dynamic core storage allocation

Notes:

(1) MAXC and MAXT are used to set block sizes for out-of-core operations. If either one is left blank during initiation runs, both are automatically set by the program. Enter MAXC and MAXT values which were used in the initiation runs to set the block sizes of stiffness matrices during restart runs with new superstructure. This will enable the program to recover the impedance matrices with compatible block storage. MAXC and MAXT are printed in the table labeled "BLOCK STORAGE INFORMATION" in the output.

(2) This parameter is used to set the blank common size in the program. If left blank, maximum available field length is used.

C.3 MASTER CONTROL CARD (815)

Columns	Variable	Notes	Entry
1-5	NUMNP	(1)	Total number of nodes in the system
6-10	NUMGP	(2)	Total number of nodes at/below ground surface which act as interaction nodes
11-15	NUMEG	(3)	Total number of different element groups
16-20	NUML	(4)	Total number of soil layers
21-25	NUMLM		Total number of nodes with lumped mass or inertia
30	NSYMPL	(5)	Total number of planes/line of symmetry or anti-symmetry (maximum of 2)
35	NIMP	(6)	Method of computing impedance matrix
			= 1, direct flexible volume method
			= 2, skin flexible volume method
40	NDIM		Dimension of analysis
			= 1, 1-D plane love wave (not available)
			= 2, 2-D plane strain
			= 3, general 3-D

Notes:

(1) All the nodes in the structure must be labeled with integer numbers starting from 1 to NUMNP. The numbering is arbitrary. However, in order to minimize storage, computation, and block operations as well as to provide flexibility to restart the program with a new superstructure, it is recommended to number the nodes at or below the ground surface first, preferably layer by layer starting from the bottom. The figures shown below are examples of good and bad numbering systems.

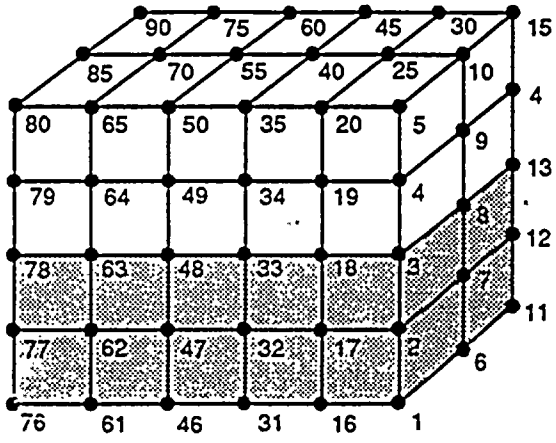

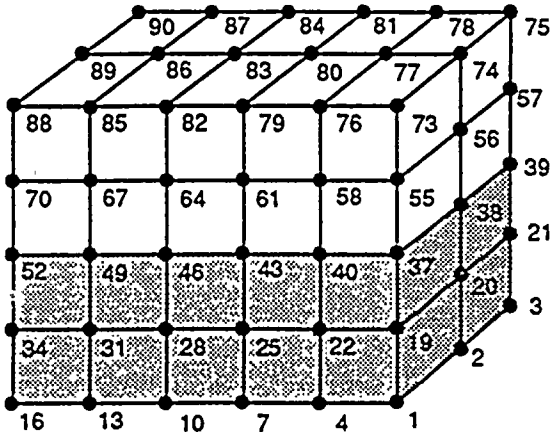

(2) Count the total number of nodal points which reside below the ground elevation, including ground surfaces (e.g., NUMGP = 54 in the previous example).

(3) All the elements in the system must be grouped separately according to their type, e.g., beam, pile, etc. The elements in each group must be labeled sequentially from 1 to total number of elements in that group.

It is also possible to use more than one group for an element type. For example, all structural brick elements may be considered as one group and all excavated soil elements as another group.

(4) Only soil layers which reside in the basement of the structure need be specified. They will be used to compute properties of excavated soil elements. All the soil layers must be labeled sequentially from 1 at the top to NUML at the bottom. For surface structures with no irregular soil zone, let NUML = 0.

(5) Any combination of a maximum of two structural planes/line of symmetry which are symmetric or anti-symmetric relative to the loading can be considered in the program. In case of 3-D analysis, the planes of symmetry or anti-symmetry must be parallel to the xz or yz planes. In case of 1-D or 2-D analysis, the line of symmetry/anti-symmetry must be parallel to the z-axis. Also note that the name symmetry or anti-symmetry is used in relation to the loading. Leave blank if no advantage is to be taken of symmetry or anti-symmetry.

(6) Currently two methods are used for the computation of the impedance matrix, namely, the direct and skin methods. If the direct method is to be used (NIMP = 1), all the nodes common to both the structure and the soil are interaction nodes. These nodes are entered in Section C.8.1.2. The direct method involves inversion of a full complex symmetric matrix as big as 3* (total number of interaction nodes).

If the skin method is to be used (NIMP = 2), all the interaction nodes are divided into three different types, namely, interface (nodes by boundary), intermediate (nodes connected directly to interface nodes), and internal (remaining nodes). These nodes are entered in Sections C.8.2.2 through C.8.2.4. This method involves inversion of a full complex symmetric matrix only as big as 3* (total number of interface nodes) and therefore is more economical.

It should also be noted that all the nodes in the superstructure (or above the ground surface) are not connected to the soil are therefore not interaction nodes.

C.4 SYSTEM OF UNITS CARD (F10.0)

Columns	Variable	Notes	Entry
1-10	GRAV	(1)	Acceleration of gravity

Notes:

(1) To be used for computation of mass matrix.

C.5 GROUND ELEVATION CARD (F10.0)

Columns	Variable	Notes	Entry
1-10	ZSRFCE	(1)	Z-coordinate of ground level

Notes:

(1) All the nodes below this elevation are assumed to be connected to the ground unless interaction nodes are specified (see Section C.8).

C.6 PLANE(S)/LINE OF SYMMETRY/ANTI-SYMMETRY CONTROL CARD (515)

Skip this section if NSYMPL = 0; otherwise provide NSYMPL cards.

Columns	Variable	Notes	Entry
1-5	N	(1)	Plane/line of symmetry/anti-symmetry number
5-10	NPLTYP (N)		Type of plane/line = 1 for symmetry = -1 for anti-symmetry
11-15	NPT(1,N)	(2)	First reference nodal point number on this plane/line
16-20	NPT(2,N)	(2)	Second reference nodal point number on this plane/line
21-25	NPT(3,N)	(2)	Third reference nodal point number on this plane (ignore for 1-D or 2-D analysis)

Notes:

(1) Plane(s)/line of symmetry or anti-symmetry can be labeled in any order starting from 1 to NSYMPL (NSYMPL $\leq$ 2).

(2) Each plane (or line) of symmetry/anti-symmetry is defined by three (or two) reference nodal points. The three nodes which define a plane must not lie on a straight line.

C.7 NODAL POINT CARDS (A1, I4, 6I5, 3F10.0, 215)

Columns	Variable	Notes	Entry
1	NC	(1),	Symbol describing coordinate system for this node = (blank), Cartesian (x,y,z) = C, cylindrical (R,θ,Z) = S, spherical (R,θ,ϕ)
4-5	N	(2)	Nodal point number
10	ID(N,1)	(3)	x-translation B.C. code
15	ID(N,2)		y-translation B.C. code
20	ID(N,3)		z-translation B.C. code
25	ID(N,4)		xx-rotation B.C. code
30	ID(N,5)		yy-rotation B.C. code
35	ID(N,6)		zz-rotation B.C. code
36-45	XORD(N)		x-ordinate (R if cylindrical or spherical)
46-55	YORD(N)	(4)	y-ordinate (θ-degree if cylindrical or spherical); leave blank or 2-D analysis
56-65	ZORD(N)		z-translation (Z if cylindrical,ϕ -degree if spherical); Z-axis must always point upward
66-70	KN	(5)	Node number increment

Notes:

(1) A special cylindrical or spherical coordinate system is allowed for the global description of nodal point locations. If a "c" or "s" is entered in column 1, then the entries given in columns 36 through 65 are taken to be referenced to a global (R,θ,Z) or (R,θ,ϕ) system rather than to be the standard (X,Y,Z) system (see Figure in page 5-39). The program converts the cylindrical or spherical coordinate system to cartesian coordinates using the formulas:

$$X = R\cos\theta \qquad X = R\cos\theta\sin\phi$$
$$Y = R\sin\theta \qquad Y = R\sin\theta\sin\phi$$
$$Z = Z \qquad Z = R\cos\phi$$

Cylindrical or spherical coordinate input is merely a user convenience for locating nodes in the standard (X,Y,Z) system, and no other references to the cylindrical or spherical system is implied; i.e., boundary condition specifications, output displacement components, etc., are referenced to the (X,Y,Z) system. Cylindrical or spherical coordinates are echoed in the printout labeled "NODAL INPUT DATA" (indicated by a "c" or "s" preceding the node number). The corresponding cartesian coordinates are printed in the GENERATED NODAL POINT DATA.

(2) Nodal data must be defined for all NUMNP nodes. Nodal cards need not be in sequence but the last one must be the last node number in the system. If nodal cards are defined more than once, the last definition will be used. All the nodal points at or below the ground surface must reside on the soil layer interfaces.

(3) Six boundary conditions codes must be assigned to each nodal point number. They can have only the following numbers:

ID(N,M) = 0, free translation (or rotation)
= 1, fixed translation (or rotation)

In general, any nodal point can have six degrees of freedom (three translation and three rotation). Therefore, the maximum number of degrees of freedom in a system is six times the total number of nodal points. A free degree of freedom will allow the node to translate (or rotate) in that direction as the solution dictates. Concentrated masses (or forces) then may be applied at this degree of freedom. One system equilibrium equation is required for each free degree of freedom.

A fixed degree of freedom will not allow the node to translate or rotate in that direction. Therefore, it will be removed from the final set of equilibrium equations. Any concentrated masses (or forces) assigned to this degree of freedom will be ignored by the program.

Nodes that are used for geometric references only (i.e., nodes not assigned to any elements) must have all six degrees of freedom fixed. These nodes are sometimes needed to define the geometry of beam sections. Also, nodal degrees of freedom having undefined stiffness (such as rotations in all brick elements, out-of-plane components in a two-dimensional plane strain model) should be deleted. Removing unwanted degrees of freedom has the advantage of reducing the size of the set of equations that must be solved. The following table lists the degrees of freedom that are defined by each different element type.

ELEMENT TYPE	DOF WITH DEFINED STIFFNESS/MASS					
	X	Y	Z	XX	YY	ZZ
1. 3-D/Brick	X	X	X			
2. 3-D/Beam	X	X	X	X	X	X
3. 3-D/Plate/Shell	X	X	X	X	X	X
4. 2-D/Plane Strain	X		X			
5. 3-D/Pile	X	X	X	X	X	X
6. 2-D/Pile	X		X		X	
7. 3-D/Spring	X	X	X	X	X	X
8. 1-D/Plane Love Wave		X				

Note, for example, that for all-3-D/brick model, only the X,Y,Z, translations are defined at the nodes and the number of equations can be cut in half by deleting the three rotational components at every node. If a node is common to two or more element types, then the non-trivial degrees of freedom are found by combination. For example, all six components are possible at a node common to both beam and solid elements; i.e., beam governs. Symmetric structures (with symmetric loading only) may also be analyzed by modeling only one-half or one quarter of the structure and constraining appropriate degrees of freedom on the planes of symmetry.

(4) The Z-coordinate must always be chosen vertical upward and the right-hand rule must be used to set X and Y coordinates. For 1-D or 2-D analysis, the program will ignore the Y-coordinate of the nodal points (see the following figure).

(5) The nodal data for a series of nodal points which are sequentially numbered between the beginning and end of any straight line, and which are equally spaced along that line, may be generated from information given on the first and last nodal card in the series. If $(N_1,\ldots,KN_1)$ and $(N_2,\ldots KN_2)$ are the information on the first and last nodal cards in a series, the first generated node

will be $N_1 + KN_2$ and the second generated node will be $N_1 + 2*KN_2$, etc. Generation will continue until node number $N_2 - KN_2$ is established. Therefore $N_2 - N_1$ must be evenly divisible by KN_2. The boundary condition codes and nodal point type code for the generated nodal points are set equal to the values given on the first card.

Coordinate generation is done in cartesian, cylindrical, or spherical coordinates if the first card in the series is in cartesian, cylindrical, or spherical coordinates, respectively.

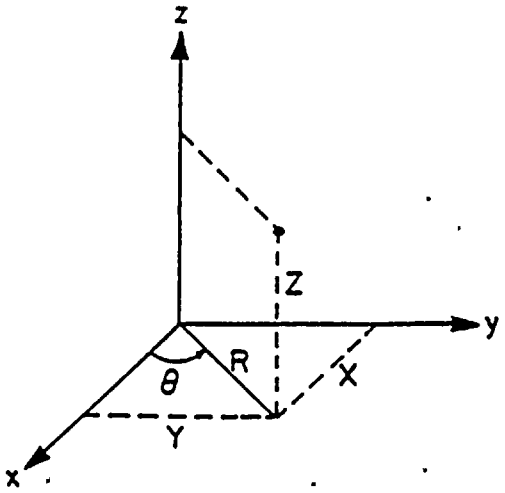

3-D Cartesian/Cylindrical

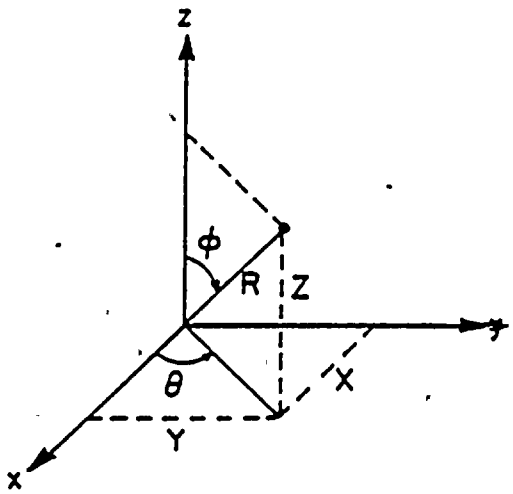

3-D Cartesian/Spherical

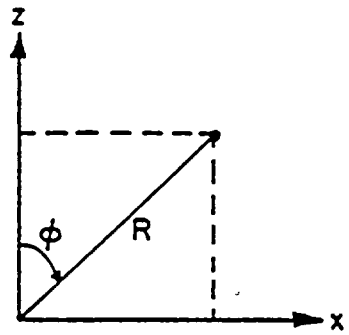

Plane Cartesian/Spherical

C.8 INTERACTION NODES CARDS

Provide the required data cards only for the section which corresponds to the method to be used for computing impedance matrix (NIMP = 1 or 2).

C.8.1 METHOD 1 (complete only if NIMP = 1)

C.8.1.1 INTERACTION NODES CONTROL CARD (I5)

Columns	Variable	Notes	Entry
1-5	INTACT	(1)	Total number of interaction nodes to be entered

C.8.1.2 INTERACTION NODES DATA CARDS (16I5)

Skip this section if INTACT = 0; otherwise provide INTACT node numbers.

Columns	Variable	Notes	Entry
1-5	N(1)	(2)	First interaction node number
6-10	N(2)		Second interaction node number
.	.		.
.	.		.
.	.		.

Terminate by a zero node number.

C.8.2 METHOD 2 (complete only if NIMP = 2)

C.8.2.1 INTERACTION NODES CONTROL CARD (3I5)

Columns	Variable	Notes	Entry
1-5	INTFCE		Total number of interaction nodes
6-10	INTMED		Total number of intermediate nodes
11-15	INTRNL		Total number of internal nodes

C.8.2.2 INTERFACE NODES DATA CARDS (16I5)

Provide INTFCE node numbers.

Columns	Variable	Notes	Entry
1-5	NE(1)	(2)	First interface node number
6-10	NE(2)		Second interface node number
.	.		.
.	.		.
.	.		.

Terminate by a zero node number.

C.8.2.3 INTERMEDIATE NODES DATA CARDS (16I5)

Provide INTMED node numbers.

Columns	Variable	Notes	Entry
1-5	ND(1)	(2)	First intermediate node number
6-10	ND(2)		Second intermediate node number
.	.		.
.	.		.
.	.		.

Terminate by a zero node number.

C.8.2.4 INTERNAL NODES DATA CARDS (16I5)

Skip this section if INTRNL = 0; otherwise provide INTRNL node numbers.

Columns	Variable	Notes	Entry
1-5	NL(1)	(2)	First internal node number
6-10	NL(2)		Second internal node number
.	.		.
.	.		.
.	.		.

Terminate by a zero node number.

Notes:

(1) if this parameter is zero, the program automatically assumes that every node at or below the ground surface is an interaction node.

(2) A series of nodes can be generated by entering the first node in the series, the last node in the series, and the generation code as a negative number; e.g.:

(5 11 -2 4 15 19 17 -1 0) is equivalent to
(5 7 9 11 4 15 19 18 17 0).

C.9 SOIL LAYER DATA (I5, 6F10.0)

This section must be skipped if NUML = 0 (e.g., in the case of surface structures).

Columns	Variable	Notes	Entry
1-5	N	(1)	Layer number
6-15	H		Thickness
16-25	W		Unit weight
26-35	VS		S-wave velocity
36-45	VP		P-wave velocity
46-55	DS		S-wave associated damping ratio
56-65	DP		P-wave associated damping ratio

Notes:

(1) Layer data cards need not be input in layer-order sequence; eventually, however, all layers in the set (1, NUML) must be defined.

C.10 ELEMENT LIBRARY

This element library consists of the following nine element types:

C.10.1 Three-dimensional solid element (eight-node brick) with three translational degrees of freedom per node. This element is identified with number 1 in the element library.

C.10.2 Three-dimensional beam element with three translational and three rotational degrees of freedom per node. This element is identified with number 2 in the element library.

C.10.3 Four-dimensional quadrilateral plate/shell element with three translational and three rotational degrees of freedom per node. This element is identified with number 3 in the element library.

C.10.4 Two-dimensional four-node plane strain finite element with two translational degrees of freedom per node. This element is identified with number 4 in the element library.

C.10.5 Three-dimensional pile element with three translational and three rotational degrees of freedom per node. This element is identified with number 5 in the element library (not available).

C.10.6 Two-dimensional pile element with two translational and one rotational degrees of freedom per node. This element is identified with number 6 in the element library (not available).

C.10.7 Three-dimensional spring element with three translational and three rotational degrees of freedom per node. This element is identified with number 7 in the element library.

C.10.8 One-dimensional plane love wave element with one out-of-plane translational degree of freedom per node. This element is identified with number 8 in the element library.

C.10.9 Three-dimensional stiffness/mass matrix element with three translational and three rotational degrees of freedom per node. This element is identified with number 9 in the element library.

C.10.1 THREE-DIMENSIONAL SOLID ELEMENTS

Groups of solid elements are described by the following sequence of cards.

C.10.1.1 CONTROL INFORMATION (5I5)

Columns	Variable	Notes	Entry
5	NPAR(1)		The number 1
6-10	NPAR(2)		Total number of 8-node solid elements
11-15	NPAR(3)	(1)	Number of material types
19-20	NPAR(4)	(2)	Material property code
			= -1, input elastic modulus and Poisson's ratio
			= 0, input constrained and shear modulus
			= 1, input P- and S-wave velocities
25	NPAR(5)	(3)	Incompatible mode code
			= 0, include incompatible modes
			≠ 0, suppress incompatible modes

C.10.1.2 MATERIAL PROPERTY CARDS (I5, 5F10.0)

Skip this section if NPAR(3) = 0.

Columns	Variable	Notes	Entry
1-5	N		Material-type number
6-15	M(N)	(2)	Elastic modulus/constrained modulus/P-wave velocity
16-25	G(N)	(2)	Poisson's ratio/shear modulus/S-wave velocity
26-35	W(N)		Unit weight of material
36-45	DP(N)		P-wave-associated damping ratio
46-55	DN(N)		S-wave-associated damping ratio

C.10.1.3 EIGHT-NODE SOLID ELEMENT CARDS (13I5)

Columns	Variable	Notes	Entry
1-5	INEL	(4)	Element number
6-10	INP(1)	(5)	Nodal point 1
11-15	INP(2)		Nodal point 2
16-20	INP(3)		Nodal point 3
21-25	INP(4)		Nodal point 4
26-30	INP(5)		Nodal point 5
31-35	INP(6)		Nodal point 6
36-40	INP(7)		Nodal point 7
41-45	INP(8)		Nodal point 8
50	ININT	(6)	Integration order

Columns	Variable	Notes	Entry
54-55	INTYP	(7)	Element type = 1, structural element = -1, excavated soil element
56-60	IMAT	(8)	Material-type number for structural elements/soil layer number for soil elements
61-65	IINC	(9)	Element generator code

Notes:

(1) The value of this parameter is selected as zero if all the elements in this group are excavated soil elements.

(2) The following table shows how M and G are defined on material property cards of an element group by choosing a material property code:

MATERIAL PROPERTY CODE	M	G
-1	Elastic modulus	Poisson's ratio
0	Constrained modulus	Shear modulus
1	P-wave velocity	S-wave velocity

(3) Nine incompatible displacement modes are included in the formation of the stiffness matrix and can be suppressed at user's option by assigning a nonzero integer number to NPAR(5). The program will automatically suppress all incompatible modes for excavated soil elements. Also, incompatible modes must not be used for solid elements with fewer than eight nodes.

(4) Element cards must be in ascending order.

(5) Element numbering for a general eight-node solid element and some other configurations is shown below.

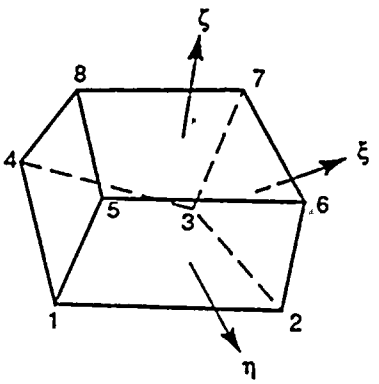

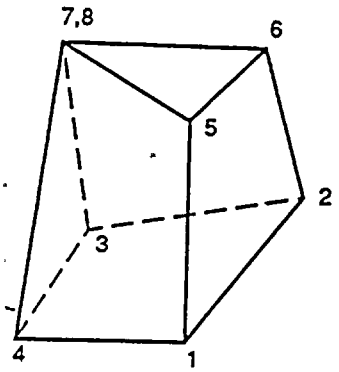

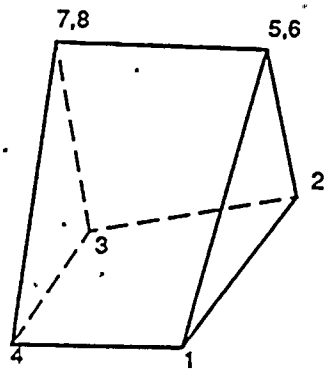

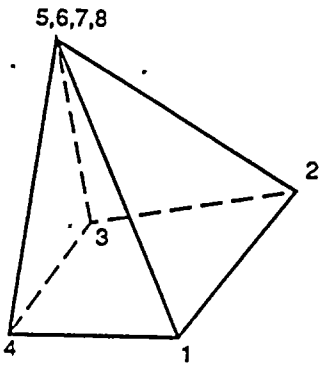

(6) The following integration orders are recommended for solid elements.

ININT	ELEMENT
2	Rectangular
3	Skewed
4	Extremely distorted in shape

However, using very distorted elements should be avoided as much as possible.

(7) INTYP = 1 (or -1) will cause the element mass and stiffness to be eventually added or subtracted from total mass and stiffness of the system.

(8) The material properties of structural elements (INTYP = 1) are obtained from Section C.10.1.2, where IMAT refers to the material type number. For excavated soil elements (INTYP = -1), these properties are obtained from Section C.9, where IMAT refers to the layer number in the free field from which the excavated soil element is obtained.

(9) If a series of cards is omitted, then generation will be possible as follows:

(a) Element cards must be in ascending order.

(b) Nodal point numbers are generated by adding IINC to those of the preceding element. (If omitted, IINC is set to 1.)

(c) The same material properties, integration order, and element type are used as for the preceding element.

(d) An element card for the last element must be supplied.

Element Stiffness Generation

If ININT = 0: A new element stiffness is not formed. Element stiffness is assumed to be identical to that of the preceding element.

C.10.2 THREE-DIMENSIONAL BEAM ELEMENTS

Groups of beam elements are described by the following sequence of cards.

C.10.2.1 CONTROL INFORMATION (5I5)

Columns	Variable	Notes	Entry
5	NPAR(1)		The number 2
6-10	NPAR(2)		Total number of beam elements
11-15	NPAR(3)		Number of material types
16-20	NPAR(4)		Number of geometric property types
24-25	NPAR(5)	(1)	Material property code
			= -1, input elastic modulus and Poisson's ratio
			= 0, input constrained and shear moduli
			= 1, input P- and S-wave velocities

C.10.2.2 MATERIAL PROPERTY CARDS (I5, 5F10.0)

Columns	Variable	Notes	Entry
1-5	N		Material identification number
6-15	M(N)	(1)	Elastic modulus/constrained modulus/P-wave velocity
16-25	G(N)	(1)	Poisson's ratio/shear modulus/S-wave velocity
26-35	W(N)		Unit weight of material
36-45	DP(N)		P-wave-associated damping ratio
46-55	DS(N)		S-wave-associated damping ratio

C.10.2.3 ELEMENT GEOMETRIC PROPERTY CARDS (I5, 6F10.0)

Columns	Variable	Notes	Entry
1-5	N		Geometric property identification number
6-15	ELP(1,N)	(2)	Axial area
16-25	ELP(2,N)	(2)	Shear area associated with shear forces in local 2-direction
26-35	ELP(3,N)	(2)	Shear area associated with shear forces in local 3-direction
36-45	ELP(4,N)	(2)	Torsional inertia
46-55	ELP(5,N)	(2)	Flextural inertia about local 2-axis
56-65	ELP(6,N)	(2)	Flextural inertia about local 3-axis

C.10.2.4 BEAM ELEMENT CARDS (7I5)

Columns	Variable	Notes	Entry
1-5	INEL	(3)	Element number
6-10	INI		Node number I
11-15	INJ		Node number J
16-20	INK	(4)	Node number K
21-25	IMAT		Material property number
26-30	IMEL		Element geometric property number
31-35	IINC	(5)	Element generator code
40-45	IB1	(6)	End release code at node number I
50-55	IB2	(6)	End release code at node number J

Notes:

(1) Refer to note 2 of Section C.10.1.

(2) Section properties of some mostly used cross sections are given below. One card is required for each unit set of properties. If shear deformations are not going to be included in the analysis, let ELP(2,N) and ELP(2,N) be zero.

(3) Element cards must be in ascending order.

(4) Node K is a geometric reference point which is used to define local 1, 2, and 3 axes of the beam element. Node K, which can also be any other nodal point in the system, must not lie on the local 1 axis. See figure below.

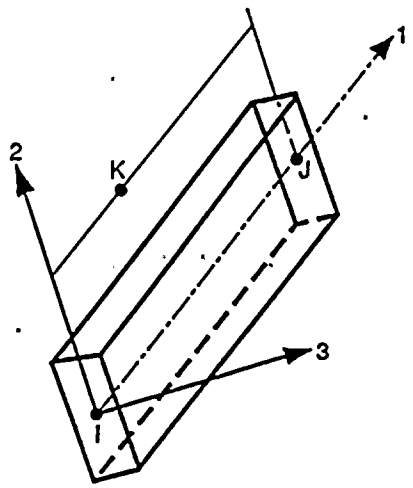

(5) If a series of cards is omitted, then generation will be possible as follows:

(a) Element cards must be in ascending order.

(b) Nodal points I and J are generated by adding IINC to those of the preceding element. (If omitted, IINC is set to 1.)

(c) Nodal point K is duplicated from the preceding element.

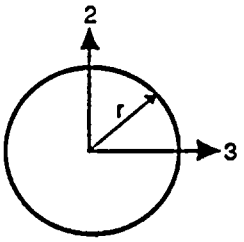

$I_2 = \pi r^4/4$
$I_3 = \pi r^4/4$
$J = \pi r^4/2$

$f_2 = f_3 = 10/9$
$A = \pi r^2$

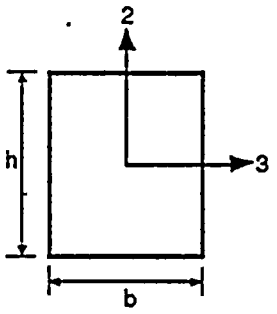

$I_2 = hb^3/12$
$I_3 = hb^3/12$
$J \equiv [1/3 - 0.21(b/h)(1-b^4/12h^4)]hb^3$

$f_2 = f_3 = 6/5$
$A = bh$

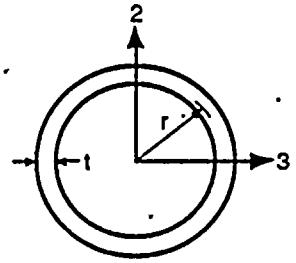

$I_2 \equiv \pi r^3 t$
$I_3 \equiv \pi r^3 t$
$J \equiv 2\pi r^3 t$

$f_2 = f_3 = 2$
$A = 2\pi rt$

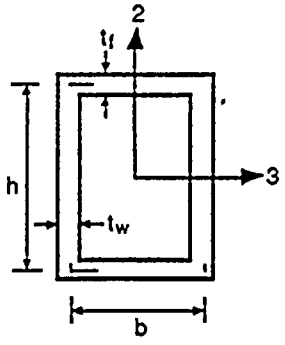

$I_2 \equiv (h^2/6)\,(ht_w + 3bt_f)$
$I_3 \equiv (b^2/6)\,(bt_f + 3ht_w)$
$J \equiv 2\,b^2h^2(t_f\,t_w)/(bt_w + ht_f)$

$f_2 = A/(2ht_w)$
$f_3 = A/[2(b + 2t_w)t_f]$
$A = 2(bt_f + ht_w)$

Note: Ratio of Shear Area / Axial Area = 1/f

(d) The same material properties, and section properties are used as for the preceding element.

(e) An element card for the last element must be supplied.

(6) The end release code at each node is a six digit number to be zero and/or one. The 1st, 2nd, ------ 6th digits, respectively correspond to the force components P1, P2, P3, M1, M2, M3 at each node. If one of the element end forces is known to be zero (hinge or roller), the digit corresponding to that component is one.

C.10.3 PLATE/SHELL ELEMENTS

Groups of plate/shell elements are described by the following sequence of cards.

C.10.3.1 CONTROL INFORMATION (4I5)

Columns	Variable	Notes	Entry
5	NPAR(1)		The number 3
6-10	NPAR(2)		Total number of plate/shell elements
11-15	NPAR(3)		Number of material types
19-20	NPAR(4)	(1)	Material property code
			= -1, input elastic modulus and Poisson's ratio
			= 0, input constrained and shear moduli
			= 1, input P- and S-wave velocities

C.10.3.2 MATERIAL PROPERTY CARDS (I5, 5F10.0)

Columns	Variable	Notes	Entry
1-5	N		Material-type number
6-15	M(N)	(1)	Elastic modulus/constrained modulus/P-wave velocity
16-25	G(N)	(1)	Poisson's ratio/shear modulus/S-wave velocity
26-35	W(N)	(2)	Unit weight
36-45	DP(N)	(3)	P-wave-associated damping ratio
46-55	DS(N)	(3)	S-wave-associated damping ratio

C.10.3.3 PLATE/SHELL ELEMENT CARDS (8I5, F10.0)

Columns	Variable	Notes	Entry
1-5	INEL	(4)	Element number
6-10	INP(1)	(5)	Nodal point I
11-15	INP(2)		Nodal point J
16-20	INP(3)		Nodal point K
21-25	INP(4)	(6)	Nodal point L
26-30	INP(5)	(7)	Nodal point O
31-35	IMAT		Material-type number
36-40	IINC	(8)	Element generator code
41-50	TH		Element thickness

Notes:

(1) Refer to note 2 of Section C.10.1.

(2) Mass matrix is lumped mass matrix for plate elements.

(3) P-wave and S-wave damping ratios must be equal.

(4) Element cards must be in ascending order.

(5) The nodal point numbers I, J, K, and L must be in sequence in a counterclockwise direction around the element. Local coordinates in a four-node shell element are shown below.

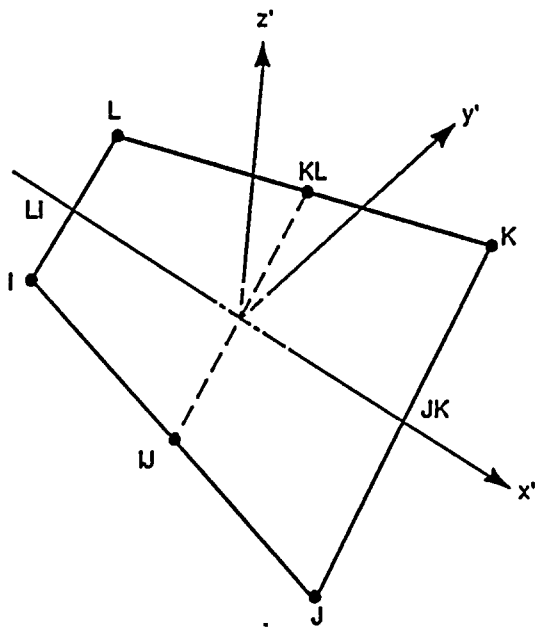

X' specified by LI-JK, where LI and JK are midpoints of sides L-I and J-K.

Z' normal to X' and to the line adjoining midpoints IJ and KL.

Y' normal to X' and Z' to complete the right handed systems the local system is used to compute the resultant forces.

(6) Leave blank for triangular elements.

(7) When left blank, mid-node properties are computed by averaging the four modes.

(8) If a series of cards is omitted, then generation will be possible as follows:

(a) Element cards must be in ascending order.

(b) Nodal points I, J, K, and L are generated by adding IINC to those of the preceding element. (If omitted, IINC is set to 1.)

(c) The same material properties and element thickness are used as for the preceding element.

(d) An element card for the last element must be supplied.

C.10.4 TWO-DIMENSIONAL FINITE ELEMENTS

Groups of 2-D finite elements are described by the following sequence of cards.

C.10.4.1 CONTROL INFORMATION (4I5)

Columns	Variable	Notes	Entry
5	NPAR(1)		The number 4
6-10	NPAR(2)		Total number of 2-D finite elements
11-15	NPAR(3)	(1)	Number of material types
19-20	NPAR(4)	(2)	Material property code = -1, input elastic modulus and Poisson's ratio = 0, input constrained and shear moduli = 1, input P- and S-wave velocities

C.10.4.2 MATERIAL PROPERTY CARDS (I5, 5F10.0)

Skip this section if NPAR(3) = 0.

Columns	Variable	Notes	Entry
1-5	N		Material-type number
6-15	M(N)	(2)	Elastic modulus/constrained modulus/P-wave velocity
16-25	G(N)	(2)	Poisson's ratio/shear modulus/S-wave velocity
26-35	W(N)		Unit weight
36-45	DP(N)		P-wave-associated damping ratio
46-55	DS(N)		S-wave-associated damping ratio

C.10.4.3 2-D FINITE ELEMENT CARDS (8I5)

Columns	Variable	Notes	Entry
1-5	INEL	(3)	Element number
6-10	INP(1)	(4)	Nodal point 1
11-15	INP(2)		Nodal point 2
16-20	INP(3)		Nodal point 3
21-25	INP(4)		Nodal point 4
26-30	INTYP	(5)	Element type = 1, structural element = -1, soil element
31-35	IMAT	(6)	Material-type number for structural element/soil layer number for soil elements
36-40	IINC	(7)	Element generator code

Notes:

(1) Refer to note 1 of Section C.10.1.

(2) Refer to note 2 of Section C.10.1.

(3) Element cards must be in ascending order.

(4) The nodal point numbers 1, 2, 3, and 4 must be in sequence in a counterclockwise direction around the element.

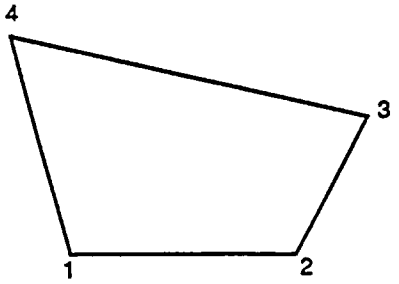

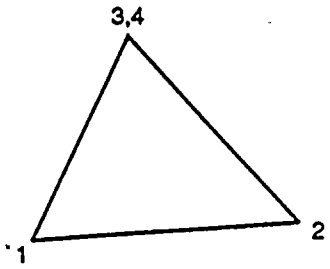

For triangular elements, the number of nodal point 3 must be equal to that of nodal point 4.

(5) Refer to note 7 of Section C.10.1.

(6) Refer to note 8 of Section C.10.1.

(7) If a series of cards is omitted, then generation will be possible as follows:

(a) Element cards must be in ascending order.

(b) Nodal point numbers are generated by adding IINC to those of the preceding element. (If omitted, IINC is set to 1.)

(c) The same material properties and element type are used as for the preceding element.

(d) An element card for the last element must be supplied.

C.10.5 THREE-DIMENSIONAL PILE ELEMENTS (not available)

This element is capable of considering compatibility between soil and pile by taking into account the effect of pile diameter. The compatibility is considered at the edges where the piles are connected, and therefore, if there is no pile, the common linear displacement variation along the boundary is assumed. The existence of pile at each corner is recognized by the program if one assigns area to the pile at that corner (see Section C.10.5.3.2). The individual piles must be modeled by standard beam elements when considering soil-pile interaction.

Groups of 3-D pile elements are described by the following sequence of cards.

C.10.5.1 CONTROL INFORMATION (4I5)

Columns	Variable	Notes	Entry
1-5	NPAR(1)		The number 5
6-10	NPAR(2)		Total number of 3-D pile elements
11-15	NPAR(3)		Number of soil material types
19-20	NPAR(4)	(1)	Material property code
			= -1, input elastic modulus and Poisson's ratio
			= 0, input constrained and shear moduli
			= 1, input P- and S-wave velocities

C.10.5.2 MATERIAL PROPERTY CARDS (I5, 5F10.0)

Columns	Variable	Notes	Entry
1-5	N		Material-type number
6-15	M(N)	(1)	Elastic modulus/constrained modulus/P-wave velocity
16-25	G(N)	(1)	Poisson's ratio/shear modulus/S-wave velocity
26-35	W(N)		Unit weight
36-45	DP(N)		P-wave-associated damping ratio
46-55	DS(N)		S-wave-associated damping ratio

C.10.5.3 3-D PILE ELEMENT CARDS

C.10.5.3.1 NODAL CARDS (16I5)

Columns	Variable	Notes	Entry
1-5	INEL	(2)	Element number
6-10	INP(1)	(3)	Nodal point 1
11-15	INP(2)		Nodal point 2
16-20	INP(3)		Nodal point 3
21-25	INP(4)		Nodal point 4
26-30	INP(5)		Nodal point 5
31-35	INP(6)		Nodal point 6
36-40	INP(7)		Nodal point 7
41-45	INP(8)		Nodal point 8
46-50	ININT	(4)	Integration order
51-55	IMAT		Material number for soil element
56-60	IINC	(5)	Element generator code

C.10.5.3.2 AREAS OF THE PILE SECTIONS INCLUDED IN THE ELEMENT (4F10.0)

Columns	Variable	Notes	Entry
1-10	AX(1)	(6)	Part of area of pile 1 inside the element
11-20	AX(2)		Part of area of pile 2 inside the element
21-30	AX(3)		Part of area of pile 3 inside the element
31-40	AX(4)		Part of area of pile 4 inside the element

Notes:

(1) Refer to note 2 of Section C.10.1.

(2) Element cards must be in ascending order.

(3) See the following figure for numbering of element connectivities.

(4) The value of ININT is of no significance; however, the following are possible:

ININT=0 A new element stiffness is not formed; element stiffness is assumed to be identical to that of the preceding element.

ININT>0 Stiffness of the element is formed.

ININT<0 A new element stiffness is formed only for the first element in the series and the same element stiffness is used for succeeding elements that are to be generated.

(5) If a series of cards is omitted, then generation is possible as follows:

(a) Element cards must be in ascending order.

(b) Nodal point numbers are generated by adding IINC to those of the preceding element (if omitted, IINC is set to 1).

(c) Same material properties are used as for the preceding element.

(d) Element card for the last element must be supplied.

(6) See the following figure for areas of the pile.

N_1	N_2	N_3	N_4	N_5	N_6	N_7	N_8	AX_1	AX_2	AX_3	AX_4
10	16	20	4	2	9	11	14	a_1	a_2	a_3	a_4

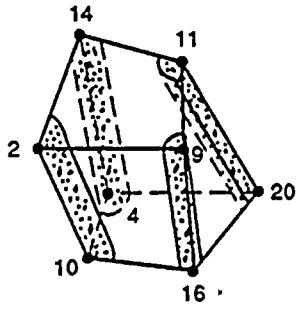

21	29	33	11	17	2	9	7	a_1	a_2	0	0

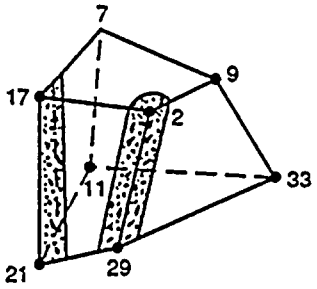

10	20	30	10	40	50	60	40	a_1	a_2	a_3	a_1

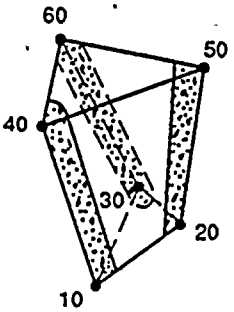

10	20	30	10	40	50	60	40	a_1	0	0	a_1

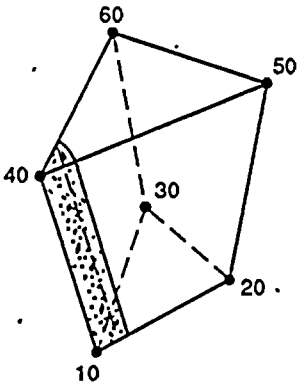

C.10.6 TWO-DIMENSIONAL PILE ELEMENTS (not available)

This element is capable of considering compatibility between soil and pile by taking into account the effect of pile diameter. The compatibility is considered at the edges where the piles are connected, and therefore, if there is no pile, the common linear displacement variation along the boundary is assumed. The existence of pile at each corner is recognized by the program if one assigns area to the pile at that corner (see Section C.10.6.3.2). The individual piles must be modeled by standard beam elements when considering soil-pile interaction.

Groups of 2-D pile elements are described by the following sequence of cards.

C.10.6.1 CONTROL INFORMATION (4I5)

Columns	Variable	Notes	Entry
1-5	NPAR(1)		The number 6
6-10	NPAR(2)		Total number of 2-D pile elements
11-15	NPAR(3)		Number of soil material types
19-20	NPAR(4)	(1)	Material property code
			= -1, input elastic modulus and Poisson's ratio
			= 0, input constrained and shear moduli
			= 1, input P- and S-wave velocities

C.10.6.2 MATERIAL PROPERTY CARDS (I5, 5F10.0)

Columns	Variable	Notes	Entry
1-5	N		Material-type number
6-15	M(N)	(1)	Elastic modulus/constrained modulus/P-wave velocity
16-25	G(N)	(1)	Poisson's ratio/shear modulus/S-wave velocity
26-35	W(N)		Unit weight
36-45	DP(N)		P-wave-associated damping ratio
46-55	DS(N)		S-wave-associated damping ratio

C.10.6.3 2-D PILE ELEMENT CARDS

C.10.6.3.1 NODAL CARDS (16I5)

Columns	Variable	Notes	Entry
1-5	INEL	(2)	Element number
6-10	INP(1)	(3)	Nodal point 1
11-15	INP(2)		Nodal point 2
16-20	INP(3)		Nodal point 3
21-25	INP(4)		Nodal point 4
26-30	ININT	(4)	Integration order
31-35	IMAT		Material number for soil element
36-40	IINC	(5)	Element generator code

C.10.6.3.2 AREAS OF THE PILE SECTIONS INCLUDED IN THE ELEMENT (2F10.0)

Columns	Variable	Notes	Entry
1-10	AX(1)	(6)	Part of area of pile 1 inside the element
11-20	AX(2)		Part of area of pile 2 inside the element

Notes:

(1) Refer to note 2 of Section C.10.1.

(2) Element cards must be in ascending order.

(3) See the following figure for numbering of element connectivities.

(4) The value of ININT is of no significance; however, the following are possible:

ININT=0	A new element stiffness is not formed; element stiffness is assumed to be identical to that of the preceding element.
ININT>0	Stiffness of the element is formed.
ININT<0	A new element stiffness is formed only for the first element in the series and the same element stiffness is used for succeeding elements that are to be generated.

(5) If a series of cards is omitted, then generation is possible as follows:

(a) Element cards must be in ascending order.

(b) Nodal point numbers are generated by adding IINC to those of the preceding element (if omitted, IINC is set to 1).

(c) Same material properties are used as for the preceding element.

(d) Element card for the last element must be supplied.

(6) See the following figure for areas of the pile.

N_1	N_2	N_3	N_4	AX_1	AX_2
10	30	40	70	a_1	a_2

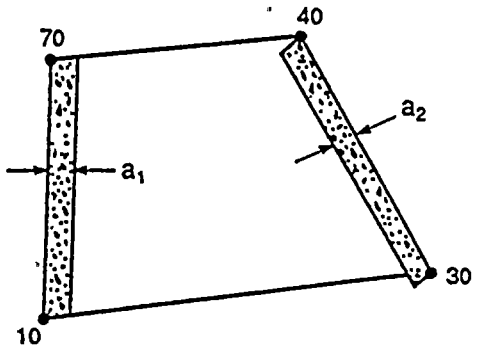

20	40	50	70	0	a_1

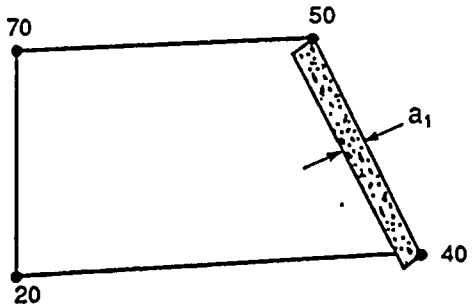

10	20	30	40	a_1	0

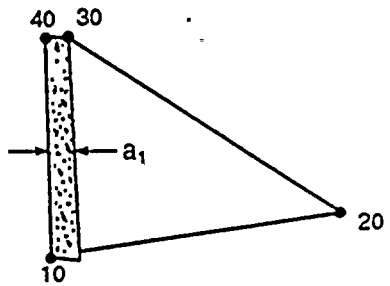

70	90	20	30	0	a_1

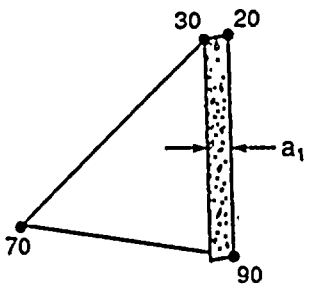

C.10.7 THREE-DIMENSIONAL SPRING ELEMENTS

Group of spring elements are described by the following sequence of cards.

C.10.7.1 CONTROL INFORMATION (3I5)

Columns	Variable	Notes	Entry
5	NPAR(1)		The number 7
6-10	NPAR(2)		Total number of 3-D spring elements
11-15	NPAR(3)		Total number of different element types

C.10.7.2 ELEMENT TYPE CARDS (I5, 6F10.0)

Columns	Variable	Notes	Entry
1-5	N		Element-type number
6-15	SPR(1,N)	(1)	Translational spring constant in global x-direction
16-25	SPR(2,N)		Translational spring constant in global y-direction
26-35	SPR(3,N)		Translational spring constant in global z-direction
36-45	SPR(4,N)		Rotational spring constant in global xx-direction
46-55	SPR(5,N)		Rotational spring constant in global yy-direction
56-65	SPR(6,N)		Rotational spring constant in global zz-direction

C.10.7.3 3-D SPRING ELEMENT CARDS (5I5)

Columns	Variable	Notes	Entry
1-5	INEL		Element number
6-10	INI	(2)	Node number I
11-15	INJ		Node number J
16-20	IMAT		Element type number
21-25	IINC	(3)	Generation code

Notes:

(1) Spring constants are directly added to the global stiffness matrix and thus these constants must be given in global xyz directions. Note that the spring constants in the six global directions are uncoupled.

(2) I is the node number at one end of the spring element and J is the node number at the other end.

(3) If a series of cards is omitted, then generation will be possible as follows:

(a) Element cards must be in ascending order.

(b) Nodal points I and J are are generated by adding IINC to those of the preceding element. (If omitted, IINC is set to 1).

(c) The same spring constants are used as for the preceding element.

(d) An element card for the last element must be supplied.

C.10.8 ONE-DIMENSIONAL PLANE LOVE-WAVE ELEMENTS (not available)

Group of love-wave elements are described by the following sequence of cards.

C.10.8.1 CONTROL INFORMATION (4I5)

Columns	Variable	Notes	Entry
5	NPAR(1)		The number 8
6-10	NPAR(2)		Total number of love-wave elements
11-15	NPAR(3)	(1)	Number of material types
16-20	NPAR(4)	(2)	Material property code
			= -1, input elastic modulus and Poisson's ratio
			= 0, input constrained and shear moduli
			= 1, input P- and S-wave velocities

C.10.8.2 MATERIAL PROPERTY CARDS (I5, F10.0)

Columns	Variable	Notes	Entry
1-5	N		Material-type number
6-15	M(N)	(2)	Elastic modulus/constrained modulus/P-wave velocity
16-25	G(N)	(2)	Poisson's ratio/shear modulus/S-wave velocity
26-35	W(N)		Unit weight
36-45	DP(N)		P-wave-associated damping ratio
46-55	DS(N)		S-wave-associated damping ratio

C.10.8.3 LOVE-WAVE ELEMENT CARDS (8I5)

Columns	Variable	Notes	Entry
1-5	INEL	(3)	Element number
6-10	INP(1)	(4)	Nodal point 1
11-15	INP(2)		Nodal point 2
16-20	INP(3)		Nodal point 3
21-25	INP(4)		Nodal point 4
26-30	INTYP	(5)	Element type = 1, structural element = -1, soil element
31-35	IMAT	(6)	Material type number for structural elements/soil layer number for soil elements
36-40	IINC	(7)	Element generator code

Notes:

(1) Refer to note 1 of Section C.10.1.

(2) Refer to note 2 of Section C.10.1.

(3) Element cards must be in ascending order.

(4) Refer to note 4 of Section C.10.4.

(5) Refer to note 7 of Section C.10.1.

(6) Refer to note 8 of Section C.10.1.

(7) Refer to note 7 of Section C.10.4.

C.10.9 STIFFNESS/MASS MATRIX ELEMENTS

Groups of stiffness/mass matrix elements are described by the following sequence of cards.

C.10.9.1 CONTROL INFORMATION (4I5)

Columns	Variable	Notes	Entry
5	NPAR(1)		The number 9
6-10	NPAR(2)		Total number of matrix elements
15	NPAR(3)	(1)	Mass type code
			= 0 (or blank), enter mass
			≠ 0, enter weight

C.10.9.2.1 MASS MATRIX ELEMENT CARDS

Columns	Variable	Notes	Entry
1-5	NEL		Element number
6-10	NI		Node number I
11-15	NJ		Node number J
16-20	NK	(2)	Node number K

C.10.9.2.2 ELEMENT STIFFNESS/MASS MATRIX CARDS

Columns	Variable	Notes	Entry
1-5	NR(I)	(3)	Row number
6-10	NC(I)	(3)	Column number
11-20	ZSR(I)	(4)	Real part of stiffness term
21-30	ZSI(I)	(4)	Imaginary part of stiffness term
31-40	ZM(I)		Mass/weight value

Notes:

(1) If this parameter is non-zero, the values entered in columns 31-40 in Section C.10.9.2.2 are considered in weight unit and therefore are divided by the acceleration of gravity to be converted to mass unit.

(2) This node is used to set up the element local coordinate system in which the element stiffness/mass matrix is defined. Item 4 of Section C.10.2 describes how this local coordinate system is set up. If this node is left blank, the stiffness/mass entries for this element are considered in the global coordinate system.

(3) The parameters NR and NC refer to the rows and columns of the element stiffness/mass matrix, respectively, as shown in figure. Because of the symmetry, only the upper triangular matrix needs to be input.

(4) The elements of the complex stiffness matrix are computed in the program from the following formula:

$$K(I) = ZSR(I) + i*ZSI(I)$$

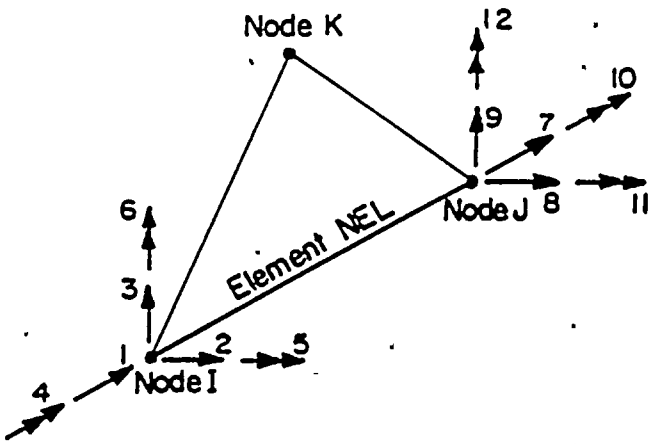
Node K
12
10
9
7
6
Node J
8
11
Element NEL
3
1
2
5
Node I
4

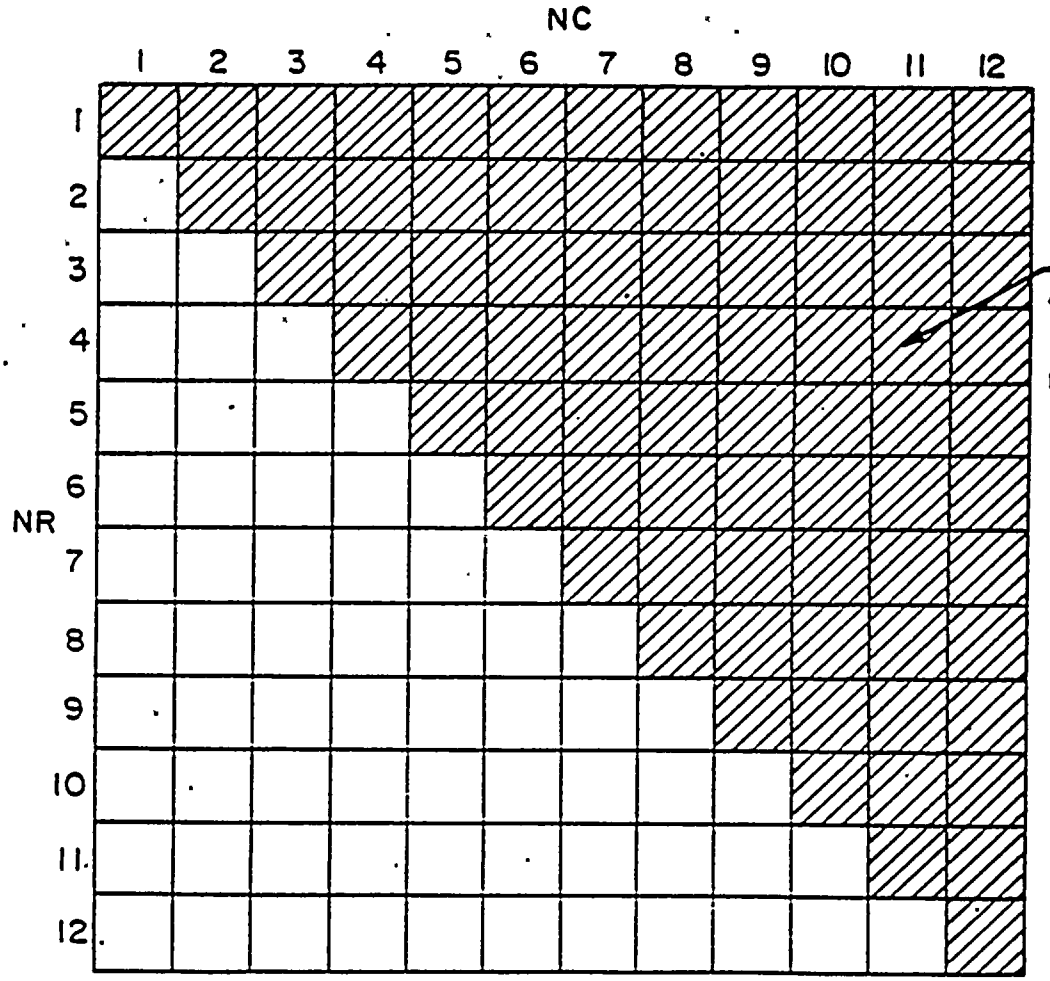
NC
1 2 3 4 5 6 7 8 9 10 11 12
NR
1
2
3
4
5
6
7
8
9
10
11
12
Only upper
triangular sti
mass matrix
needs to be inpu

C.11 CONCENTRATED MASS CARDS

If no concentrated mass (NUMLM = 0), skip this section.

C.11.1 FIRST AND CONSECUTIVE CARDS (2I5, 6F10.0)

Columns	Variable	Notes	Entry
1-5	N	(1)	Nodal point number
6-10	MTYP	(2)	Type of mass entry = 0, entry in mass units 0, entry in weight units
11-20	XMASS (N,1)		Translational mass acting in x-direction
21-30	XMASS (N,2)		Translational mass acting in y-direction
31-40	XMASS (N,3)		Translational mass acting in z-direction
41-50	XMASS (N,4)		Rotational mass acting in xx-direction
51-60	XMASS (N,5)		Rotational mass acting in yy-direction
61-70	XMASS (N,6)		Rotational mass acting in zz-direction

Notes:

(1) Total of NUMLM cards must be provided for this section.

(2) If a non-zero value is assigned by MTYP, then the entries given in columns 11 through 70 are taken to be in weight units rather than mass units. Thus, in order to convert these values to mass units, the program divides these values by the acceleration of gravity given in Section C.4.

C.12 OPERATION MODE CARD (I5)

Columns	Variable	Notes	Entry
5	NOPT	(1)	Operation mode = 0, stop no more data

Notes:

(1) Must be the last data card.

5.2.4 MOTOR

For each specified frequency, the program module MOTOR forms the elements of the load vector in Eq. (2.1-3) which corresponds to external forces such as impact loads and rotating machinery acting directly on the structure. The results are stored on Tape 9.

D.1 OPERATION MODE CARD AND TITLE (I5, 3X, 12A6)

Columns	Variable	Notes	Entry
1-5	NOPT		Operation mode
			= 1, complete solution
		(1)	< 0, data check only
6-8			Blank
9-80	HED		Contain information to be printed with output

Notes:

(1) If NOPT < 0, most of the calculations required during normal execution are bypassed.

D.2 MASTER CONTROL CARD (2I5)

Columns	Variable	Notes	Entry
1-5	NLP		Total number of loaded points
6-10	NF		Total number of frequencies of analysis

D.3 SYSTEM OF UNITS CARD (F10.0)

Columns	Variable	Notes	Entry
1-10	GRAV		Acceleration of gravity

D.4 FREQUENCY DATA CARDS

D.4.1 FREQUENCY CONTROL CARD (2F10.0, I5)

Columns	Variable	Notes	Entry
1-10	DF	(1)	Frequency step (HZ)
11-20	DT	(1)	Time step of control motion (sec)
21-25	NFFT	(1)	Number of values to be used in Fourier Transform of control motion; must be a power of 2

D.4.2 FREQUENCY CONTROL CARDS (16I5)

Columns	Variable	Notes	Entry
1-5	NFR(1)	(2)	Frequency no. 1
6-10	NFR(2)		Frequency no. 2
11-15	NFR(3)		Frequency no. 3
.	.		.
.	.		.
.	.		.

Notes:

(1) Case A - Deterministic Analysis

DT and NFFT for the dynamic input motion must be given, and the frequency step may be left blank. The program will compute the frequency step as follows:

$$DF = 1/(NFFT * DT)$$

Then this frequency step may be used to set up frequency numbers in Section D.4.2.

DF must be given and may be directly used to set up frequency numbers in Section D.4.2 in which case DT and NFFT are never used and may be left blank.

(2) The total of NF frequency numbers must be given. All the frequency numbers must be positive nonzero integer numbers. The program will automatically reorder the input frequency numbers in ascending order and will stop if two or more equal frequency numbers are detected. Frequencies f_i, for which solutions are obtained, are defined as follows:

$$f_i = NFR(i) * DF \quad .$$

The highest frequency of analysis is then equal to the highest frequency number multiplied by the frequency step.

D.5 CONCENTRATED DYNAMIC LOAD DATA CARDS

D.5.1 FIRST CARD - LOAD FACTORS (I5, 5X, 6F10.0, 2I5)

Columns	Variable	Notes	Entry
1-5	NODE	(1)	Nodal point number
11-20	AMPL(1)	(2)	Force factor in x-direction
21-30	AMPL(2)		Force factor in y-direction
31-40	AMPL(3)		Force factor in z-direction
41-50	AMPL(4)		Moment factor in x-direction
51-60	AMPL(5)		Moment factor in y-direction
61-70	AMPL(6)		Moment factor in z-direction
71-75	KN	(3)	Node number increment
80	KT	(2)	Arrival time code
			= 0, zero arrival time
			=-1, nonzero arrival time

D.5.2 SECOND CARD - LOAD ARRIVAL TIMES (6F10.0)

Skip this card if no arrival time at this node (KT = 0).

Columns	Variable	Notes	Entry
1-10	DTX	(2)	Force arrival time in x-direction (sec)
11-20	DTY		Force arrival time in y-direction (sec)
21-30	DTZ		Force arrival time in z-direction (sec)
31-40	DTXX		Moment arrival time in x-direction (sec)
41-50	DTYY		Moment arrival time in y-direction (sec)
51-60	DDTZZ		Moment arrival time in z-direction (sec)

Notes:

(1) One card must be given for every nodal point with nonzero applied dynamic force or moment. Nodal cards need not be in node order sequence. If nodal cards are defined more than once, the new force or moment will be added up to current values at that node.

(2) Dynamic loads with similar time history but different maximum amplitude and arrival time may be applied at nodal points. Reference time history is defined as having maximum reference amplitude and zero arrival time, which means the load starts acting on the nodal point at time zero. All otner time histories must be given relative to reference time history by defining load factor and arrival time. Load factor is defined as the ratio between maximum amplitude of applied load to maximum reference amplitude. See figure below.

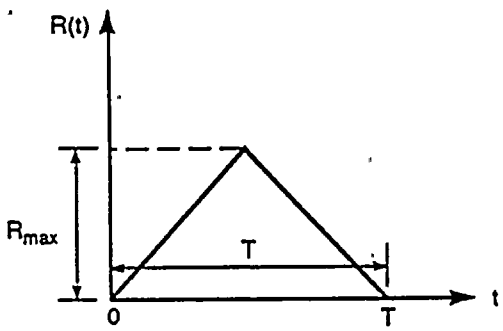

Reference Time History

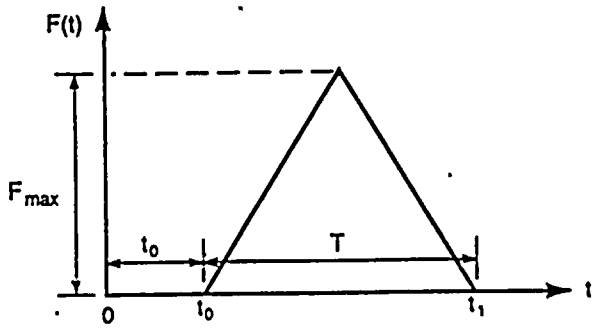

Arbitrary Time History

where

$$\text{Load factor} = \frac{F_{max}}{R_{max}}$$

$$\text{Arrival time} = t_0$$

(3) Generation is possible for a number of nodal points omitted in a series. If ($NODE_1$,..., KN_1, KT_2 are the information on the first and last cards in a series, the first generated node will be $NODE_1$ + KN_2 and second generated node will be $NODE_1$ + 2 * KN_2, etc. Generation will continue until node number $NODE_2$ - KN_2 is established. Therefore, $NODE_2$ - $NODE_1$ must be evenly divisible by KN_2. Load factors and arrival times of forces and moments applied at generated nodes are set equal to the values given on the first card in the series. If no generation is required, leave KN blank for all nodal point cards.

D.6 OPERATION MODE CARD(I5)

Columns	Variable	Notes	Entry
5	NOPT	(1)	Operation mode = 0, stop no more data

Notes:

(1) Must be the last data card.

5.2.5 ANALYS

The program module ANALYS is the heart of the program SASSI. It drives the three subprograms MATRIX, LOAD, and SOLVE and therefore controls the restart modes of the program.

The program basically functions in four different modes. The first mode is the initiation mode and the other three are the restart modes of the program.

5.2.5.1 Mode 1 - initiation

This is the first mode to be executed for a new problem. In this mode the program basically reads the three input tapes-Tape 1 (or Tape 9), Tape 3, and Tape 4-and generates the output tapes-Tape 5, Tape 6, and Tape 8. Tape 5, Tape 6, and Tape 8 contain the impedance matrices of the interaction nodes, the reduced modified stiffnesses of the total system, and the acceleration (or displacement) transfer functions relative to the control motion (input dynamic force), respectively, computed for the specified frequencies which must reside on the input tapes. This mode involves performing all the operations given in Step 1 through Step 7 in Section 2.5. In addition to the three output tapes, it is also possible to request the printout of the uninterpolated transfer functions.

It should be noted that the control motion defined by the user (on Tape 1) for seismic problems is in the SITE coordinate system x'y'z' and must be transformed to the global structural coordinate system xyz in ANALYS. Therefore, the user must enter the angle between two coordinate systems in program module ANALYS. In addition to this, the user also enters the location of the control point on the horizontal plane at this stage.

5.2.5.2 Mode 2 - new superstructure

If the physical properties of the structure(s) are changed or the geometry of the structure is altered, then, as long as other data remain intact, program module ANALYS can be restarted using Mode 2. This mode requires only part of program ANALYS to be re-executed.

In order to use this mode, a new Tape 4 has to be generated by re-executing program module HOUSE. Since the geometry and numbering of the nodal points below the ground have not changed, the impedance matrices can be recovered from Tape 5. The information on the two input tapes is then used to compute the new reduced modified stiffness of the structure to be saved on a new Tape 6. Tape 7 (or Tape 9) is also input so that the new transfer functions of the response can be computed and then saved on a new Tape 8.

This mode involves the same operations as Mode 1 except that Step 3 is skipped in Section 2.5.

5.2.4.3 Mode 3 - new seismic environment

If the seismic environment is changed, the information on Tape 1 will change while Tapes 5 and 6 remain intact. Therefore, if Tape 5 and Tape 6 had been created and saved from some previous analysis, program ANALYS could be restarted in Mode 3 by inputting a new Tape 1 and recovering the information on Tapes 5 and 6. The results are saved on a new Tape 8.

This mode involves only the operations given in Steps 6 and 7 of Section 2.5.

5.2.4.4 Mode 4 - new dynamic loading

If the problem is to be analyzed for a new set of external forces; then the program module ANALYS can be restarted by using Mode 4. This mode is very similar to Mode 3 except that it is for foundation vibration rather than seismic problems. Therefore, Tape 5 is not required as input. Only Tape 6 and a new Tape 9 are required. The results are also stored on a new Tape 8.

The mode involves operations similar to those in Mode 3.

E.1 OPERATION MODE CARD AND TITLE (I5, 3X, 12A6)

Columns	Variable	Notes	Entry
1-5	NOPT		Operation mode
			= 1, complete solution
		(1)	< 0, data check only
6-8			
9-80	HED		Contain information to be printed with output

Notes:

(1) If NOPT < 0, most of the calculations required during normal execution are bypassed.

E.2 MASTER CONTROL CARD

Columns	Variable	Notes	Entry
5	MEOF		Type of analysis = 1, seismic analysis = 2, foundation vibration analysis
10	MODE	(1)	Mode of analysis = 1, Mode 1 = 2, Mode 2 = 3, Mode 3 = 4, Mode 4
15	MSAVE	(2)	Tape save option = 0, do not save Tape 6 = 1, save Tape 6
16-20	NUMFR	(3)	> 0, total number of frequencies of analysis = 0; NUMFR and frequency numbers are taken from tape 1 (or Tape 9)
25	NPRINT	(4)	Print option = 0, don't print transfer functions ≠ 0, print transfer functions

Notes:

(1) The program may be run in one of the following modes shown in the following table.

Mode of Analysis	Case	Tapes to Be Mounted	Tapes to be Created
1	Initiation	1 (or 9), 3, 4	5, 6, 8
2	Restart - new superstructure (new Tape 4)	1 (or 9), 4, 5	6, 8
3	Restart - new seismic environment (new Tape 1)	1, 5, 6	8
4	Restart - new dynamic loading (new Tape 9)	9, 6	8

As seen from the preceding table, Mode 3 will run only for the case of seismic analysis (MEOF = 1) while Mode 4 will run only for the case of foundation vibration analysis (MEOF = 2).

(2) This option will allow the user to save Tape 6 (reduced complex stiffness of the system) in order to be able to restart Mode 3 and Mode 4 at a later time.

(3) Frequencies for which a complete solution is desired must be specified at this stage. The program will automatically survey these frequencies to make sure that they reside on the tapes that are mounted before starting the execution. If one or more frequencies are not found on the mounted tapes, the program will stop.

It is also possible to break the complete frequency array into smaller groups and then run each group separately. Later results of these separate runs can be combined into the complete solution. This has the advantage that the runs will be smaller and the created files will occupy smaller space in the computer during the program execution.

This option also makes it possible to solve the problem for new frequencies and combine the results with those of old frequencies if the analysis so demands at a later time.

Since more than 90% of the cost of the complete analysis goes to this program, assessment of the final cost of the job can be made in advance by estimating the cost of doing one single frequency and multiplying it by the number of frequencies for which a solution is desired.

If NUMFR = 0, then Section E.3 must be skipped and the program will take NUMFR and frequency numbers of analysis from Tape 1 (or Tape 9).

(4) If NPRINT $\neq$ 0, the program will print out the response of all the nodal points to all frequencies for which the solution has been obtained. The print option in ANALYS may be used for machine vibration problems in which the exciting load is harmonic. In most other cases, the print option in ANALYS should not be used to avoid a large print output which is not needed.

E.3 FREQUENCY NUMBER CARDS (16I5)

Skip this section if NUMFR = 0.

Columns	Variable	Notes	Entry
1-5	NFR(1)	(1)	Frequency no. 1
6-10	NFR(2)		Frequency no. 2
11-15	NFR(3)		Frequency no. 3
.	.		.
.	.		.
.	.		.

Notes:

(1) Total of NUMFR frequency numbers must be given. All the frequency numbers must be positive nonzero integer numbers. The program will automatically reorder the input frequency numbers in ascending order and will stop if two or more equal frequency numbers are detected.

If NUMFR = 0, skip this section and the program will obtain NUMFR and frequency numbers from Tape 1 (or 9).

Frequency step, time step, and number of FFT points are obtained from Tape 1 (or 9) and are checked against other input tapes for consistency. This information, along with frequency numbers at this section, will pass on to every tape created.

E.4 CONTROL MOTION CARD FOR SEISMIC ANALYSIS (3F10.0)

Skip this section if foundation vibration analysis (MEOF = 2).

Columns	Variable	Notes	Entry
1-10	XCNTROL		x-coordinate of control point
11-20	YCNTROL		y-coordinate of control point
21-30	ANG	(1)	Coordinate transformation angle (degrees)

Note:

(1) This is the angle between x' component of the control motion (as defined in program SITE) and x coordinate of the system.

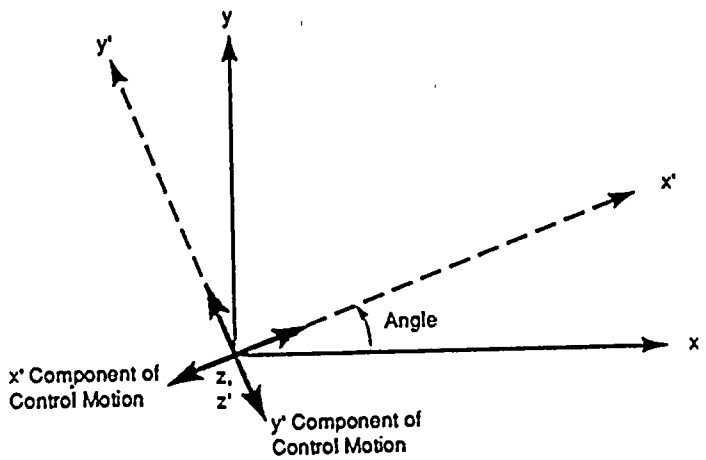

Coordinate System	Program
x y z x' y' z'	HOUSE SITE

5.2.6 COMBIN

The program module COMBIN combines the frequencies on two Tape 8's created in the program ANALYS and creates a new Tape 8 which now contains the frequencies from both tapes.

The old Tape 8's must be mounted as Tape 1 and Tape 2 and the results will be written on Tape 8. No other input data are required by this program.

If two equal frequencies are encountered on the mounted tapes, the program will select the one which resides on Tape 1 and discard the other one.

F.1 OPERATION MODE CARD (I5)

Columns	Variable	Notes	Entry
5	NOPT	(1)	Operation mode = 0, stop no more data

Notes:

(1) Must be the last data card.

5.2.7 MOTION

The main function of the program module MOTION is to compute acceleration, velocity, and displacement (only for foundation vibration) time histories of the response. It may also output transfer functions and response spectra. The program also provides punched output or printer plots of the response at user's option.

In case of seismic problems, the program reads the acceleration time history of the control motion from cards and transforms it to the frequency domain using Fast Fourier Transform techniques. It then reads the uninterpolated transfer functions from Tape 8 for selected output points, performs the interpolation and the convolution with the control motion, and returns to the time domain using the inverse Fast Fourier Transformer algorithm. The resulting time histories of acceleration or computed velocity may be output directly or converted to output response spectra.

G.1 OPERATION MODE CARD AND TITLE (I5, 3X, 12A6)

Columns	Variable	Notes	Entry
1-5	NOPT		Operation mode
			= 1, complete solution
		(1)	< 0, data check only
2-8			Blank
9-80	HED		Contain information to be printed with output

Notes:

(1) If NOPT < 0, most of the calculations required during normal execution are bypassed.

G.2 OUTPUT CONTROL CARD (4I5, F10.0)

Columns	Variable	Notes	Entry
5	NTIME	(1)	Analysis type code
			= 0, only transfer functions to be output
			= 1, otherwise
6-10	NOUT		Total number of nodal points where output is required
11-15	ND		Number of damping values for response spectrum analysis; skip if NTIME = 0
16-20	NSKIP		Output code for all time histories; skip if NTIME = 0
			= 0, only table to be printed
			> 1, plot every NSKIP-th point
21-30	DUR		Total duration of time histories to be plotted; skip if NTIME = 0

Notes:

(1) If NTIME = 0, only transfer function plots may be requested at nodal points and time history of input motion need not be supplied.

G.3 OUTPUT REQUEST CARDS

G.3.1 OUTPUT CONTROL CARD (I5)

Skip this card if seismic analysis (MEOF = 1).

Columns	Variable	Notes	Entry
1-5	NTYPE	(1)	Type of response = 1, output only displacements = 2, output only velocities = 3, output only accelerations

G.3.2 NODAL OUTPUT CONTROL CARDS (I5, 4X, 6I1, 4X, 6I1, 4X, 6I1)

Columns	Variable	Notes	Entry
1-5	NODE(I)	(2)	Nodal point number where output is required
10-15	KEY(I,J)	(3)	Output control key for response in x-direction
20-25	KEY(I,J)		Output control key for response in y-direction
30-35	KEY(I,J)		Output control key for response in z-direction
40-45	KEY(I,J)		Output control key for response in xx-direction
50-55	KEY(I,J)		Output control key for response in yy-direction
60-65	KEY(I,J)		Output control key for response in zz-direction

Notes:

(1) Only accelerations can be requested for seismic problems. NTYPE controls the type of response to be output for the foundation vibration problem.

(2) Total of NOUT cards must be given in this section. Nodal point cards where output is requested need not be in node order sequence; the program will reorder them automatically. Also, output control keys in directions which are constrained will be ignored.

(3) Output control keys are six-digit integer numbers (ijklmn) which are defined as follows:

i = 1--plot transfer function*
  = 0--otherwise

j = 1--save time history of requested response on Tape 12**
  = 0--otherwise.

k = 1--plot time history of requested response**
  = 0--otherwise

l = 1--plot acceleration and velocity response spectra***
  = 0--otherwise

m = 1--save acceleration and velocity response spectra on Tape 12***
  = 0--otherwise

n = 1--print maximum requested response**
  = 0--otherwise

If J = 1, time histories of the requested response are computed and stored on Tape 12. This tape can later be used to recover time histories for plotting purposes. The following example shows how the time histories are obtained from Tape 12:

```
DIMENSION A(NFFT)
DO 1000 N=1,NN
```

```
      READ (12,100) DIR, NODE, NFFT, (A(I),I=1,NFFT)
100   FORMAT (////29X,A2,29X,I4/17X,I5//(8F9.6))
      .
      .
      .
1000  CONTINUE
```

where

NN = total number of time histories

DIR = direction of motion

NODE = nodal point number to which the time history belongs

NFFT = total number of points in the time history

A = vector containing the time history of the response

---

* Transfer function for seismic problems is defined for total acceleration response while for foundation vibration problems it is defined for total displacement response.

** Requested response for seismic problems is acceleration; for foundation vibration problems it is determined by NTYPE.

*** Response spectra is computed independent of the value of NTYPE. Therefore, displacement response spectra cannot be requested.

G.4 RESPONSE SPECTRA DATA CARDS

Skip this section if ND = 0.

G.4.1 FIRST CARD (2F10.4, I5)

Columns	Variable	Notes	Entry
1-10	FSTRT	(1)	First frequency used in response spectrum analysis--HZ
11-20	FLAST		Last frequency used in response spectrum analysis--HZ
21-25	NINT		Total number of frequency steps for response spectra. NINT + 1 spectral values are computed

G.4.2 SECOND CARD (8F10.4)

Columns	Variable	Notes	Entry
1-10	DAMP(1)	(2)	Damping ratio used in response spectra
.	.		.
.	.		.
.	.		.

Notes:

(1) If first card is left blank, standard values (FSTRT = 0.4, FLAST = 40, NINT = 40) are assumed. This will lead to a plot which fills one page.

(2) Total of ND damping ratios must be given.

G.5 INPUT MOTION DATA CARDS

Skip this section if NTIME = 0.

G.5.1 CONTROL CARD (2I5, 3F10.0)

Columns	Variable	Notes	Entry
1-5	NFFT	(1)	Number of values to be used in Fourier Transform
6-10	NEQZ		Number of acceleration (or force) values to be read from cards
11-20	DT	(2)	Time step -- sec
21-30	EQMUL		Multiplication factor for scaling time history. Use only if UGMAX = 0; leave blank otherwise
31-40	UGMAX		Maximum value of time history to be used. The values of time history will be scaled to give maximum value = UGMAX. Use only if EQMUL = 0; leave blank otherwise

G.5.2 CONTROL TIME HISTORY ID CARD (12A6)

Columns	Variable	Notes	Entry
1-72	ID(I)		Identification for control time history

G.5.3 CONTROL TIME HISTORY VALUES (8F9.6/8E10.3)

Total of (NEQZ + 7)/8 cards.

Columns	Variable	Notes	Entry
1-72	A(I)	(3)	8 values

Notes:

(1) NFFT must be a power of 2 and includes the trailing zeroes. If this number does not agree with the NFFT value in SITE (or MOTOR), the program will stop.

(2) The program will compute the frequency step from the following formula:

$$DF = 1/(NFFT * DT) .$$

If DF and DT do not agree with those in SITE (or MOTOR), the program will stop.

(3) All time history values must be given at time steps DT. For seismic problems, provide acceleration values in (G) in (8F9.6) format; for foundation vibration problems, provide force values in (8E10.3) format.

G.6 OPERATION MODE CARD (I5)

Columns	Variable	Notes	Entry
5	NOPT	(1)	Operation mode = 0, stop no more data

Notes:

(1) Must be the last data card.

5.2.8 STRESS

The main function of the program module STRESS is to compute and output maximum stress, forces, or moments in the elements. The user may also request time histories of these components to be printed out and also saved on a magnetic tape.

The program reads acceleration (displacement) transfer functions from Tape 8 and information about elements from Tape 4. Then, for each requested element, the program calculates the stress, force, or moment components at each frequency, performs interpolation and convolution with the control motion, and finds the corresponding time histories by returning to the time domain using the inverse Fast Fourier Transform algorithm.

Time history of octahedral shear stress (strain), which is a measure of maximum shear stress (strain), is calculated in time domain for each time interval DT. From this, the effective shear strain (0.65 * maximum shear strain) for the soil elements can be estimated and used to find new strain-compatible soil properties.

H.1 OPERATION MODE CARD AND TITLE (I5, 3X, 12A6)

Columns	Variable	Notes	Entry
1-5	NOPT		Operation mode
			= 1, complete solution
		(1)	< 0, data check only
6-8			Blank
9-80	HED		Contain information to be printed with output

Notes:

(1) If NOPT < 0, most of the calculations required during normal execution are bypassed.

H.2 MASTER CONTROL CARD (I5, 4X, I1)

Columns	Variable	Notes	Entry
1-5	NGOUT	(1)	Total number of element groups
10	ITER	(2)	Iteration control key
			= 1, automatic computation of strains in all soil elements (not available)
			= 0, otherwise
15	IFPU		Output control key
			= 1, save stress time histories on Tape 12
			= 0, otherwise

Notes:

(1) This is the total number of element groups for which output is requested.

(2) If secondary nonlinear effects are going to be considered, then let ITER = 1; otherwise, leave blank.

H.3 ELEMENT GROUP CARDS

One set of cards for each element group requested in Section H.2 must be provided as follows:

H.3.1 THREE-DIMENSIONAL SOLID ELEMENTS

Skip this section if no request for stresses or strains in 3-D solid elements.

H.3.1.1 CONTROL INFORMATION (4X, I1, 2I5)

Columns	Variable	Notes	Entry
5	ICODE(1)		The number 1
6-10	ICODE(2)	(1)	The order number
11-15	ICODE(3)	(2)	Total number of elements in this group for which output is requested

H.3.1.2 OUTPUT REQUEST CARDS (I5, 4X, 7I1, 13X, I1)

Columns	Variable	Notes	Entry
1-5	N		Element number
10	Key(1)	(3)	Output control key for stress (strain in xx-direction
11	Key(2)		Output control key for stress (strain in yy-direction
12	Key(3)		Output control key for stress (strain in zz-direction
13	Key(4)		Output control key for stress (strain in xy-direction
14	Key(5)		Output control key for stress (strain in xz-direction
15	Key(6)		Output control key for stress (strain in yz-direction
16	Key(7)		Output control key for octahedral shear stress (strain)
30	KN	(4)	Generation control key
			= 0, no generation
			= 1, otherwise

Notes:

(1) If there is more than one group of 3-D solid elements, specify the order of the requested group, e.g., ICODE(2) = 2 will request the second set of 3-D solid elements. If left blank, the program will select the first group of solid elements it encounters.

(2) This number must be less than or equal to the total number of elements in this group. Otherwise the program will stop.

(3) KEY = 0, no request for this component
= 1, print only maximum response
= 2, print maximum response and save response time history on Tape 12

The stresses in 3-D solid elements are computed at the centroid of the element and are referred to in global axes. These stresses are shown in the following figure.

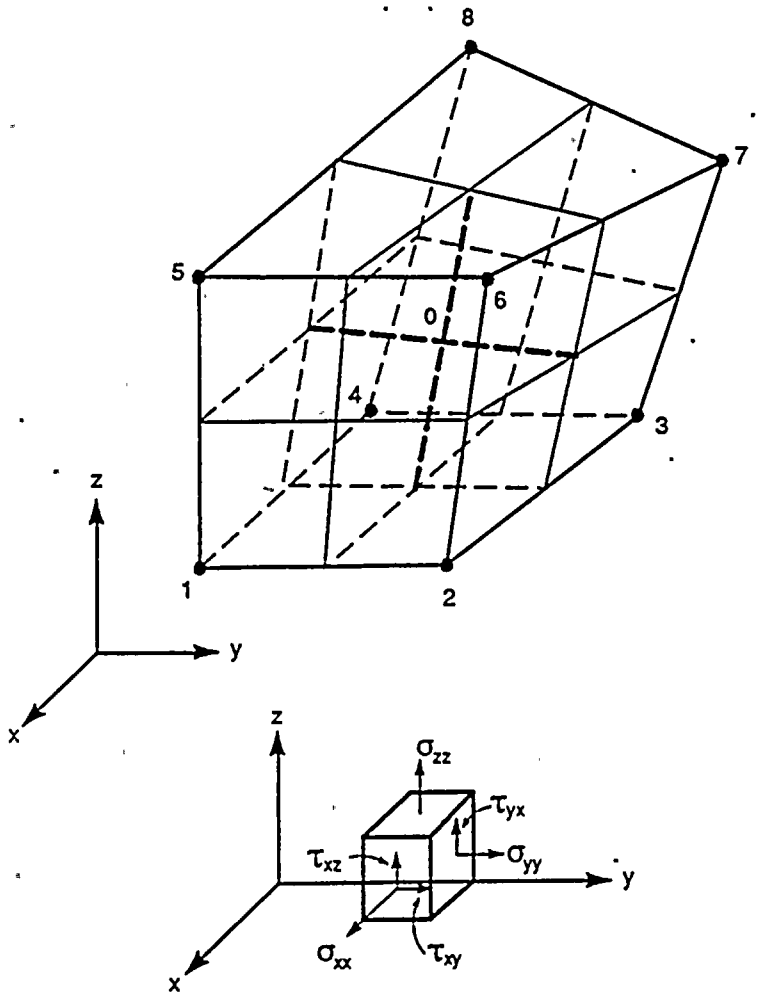

If KEY=2, time histories of the requested response are computed and stored on Tape 12. This tape can later be used to recover the time histories for plotting purposes. The following example shows how the time histories are obtained from Tape 12:

```
      DIMENSION A(NFFT)
      DO 1000 N=1,NN
      READ (12,100) N1,N2,DIR, (A(I),I=1,NFFT)
100   FORMAT (2I10,A4/(8E10.3))
         .
         .
         .
1000  CONTINUE
```

where

NN = total number of requested time histories
N1 = element number
N2 = element group number
NFFT = total number of points in the time history
A = array containing the time history of the response

In addition to the user-requested response, the program may also output other components of the response if calculation of these components is necessary in order to determine the requested response. For example, in order to output maximum octahedral shear stress for 3-D solid elements, all six components of stress (σ_{xx}, σ_{yy}, σ_{zz}, τ_{xy}, τ_{xz}, τ_{zx}) must be calculated. Therefore, the program will also output the maximum response of these components. However, the corresponding time histories will not be saved on Tape 12 unless they are specifically requested by the user.

(4) Generation is possible for a number of elements omitted in a series. Suppose (N_1,...,KN_1) and (N_2,...,KN_2) are the information on two consecutive cards--if KN_1 is equal to 1, all the elements between N_1 and N_2 will be generated and the output control keys for the generated elements will be set equal to the values given on the first card. On the other hand, if KN_1 is equal to 0, no generation between N_1 and N_2 will take place.

H.3.2 THREE-DIMENSIONAL BEAM ELEMENTS

Skip this section if no request for forces or moments in 3-D beam elements.

H.3.2.1 CONTROL INFORMATION (4X, I1, 2I5)

Columns	Variable	Notes	Entry
5	ICODE(1)		The number 2
6-10	ICODE(2)	(1)	The order number
11-15	ICODE(3)	(2)	Total number of elements in this group for which output is requested

H.3.2.2 OUTPUT REQUEST CARDS (I5, 4X, 12I1, 8X, I1)

Columns	Variable	Notes	Entry
1-5	N		Element number
10	KEY(1)	(3)	Output control key for force in 1-direction (node I)
11	KEY(2)		Output control key for force in 2-direction (node I)
12	KEY(3)		Output control key for force in 3-direction (node I)
13	KEY(4)		Output control key for moment in 1-direction (node I)
14	KEY(5)		Output control key for moment in 2-direction (node I)
15	KEY(6)		Output control key for moment in 3-direction (node I)
16	KEY(7)		Output control key for force in 1-direction (node J)
17	KEY(8)		Output control key for force in 2-direction (node J)
18	KEY(9)		Output control key for force in 3-direction (node J)
19	KEY(10)		Output control key for moment in 1-direction (node J)
20	KEY(11)		Output control key for moment in 2-direction (node J)
21	KEY(12)		Output control key for moment in 3-direction (node J)
30	KN	(4)	Generation control key = 0, no generation = 1, otherwise

Notes:

(1) See note 1 of Section H.3.1

(2) See note 2 of Section H.3.1

(3) See note 3 of Section H.3.1. The forces and moments in beam elements are computed at the end and are referenced in local beam axes, in the following figure.

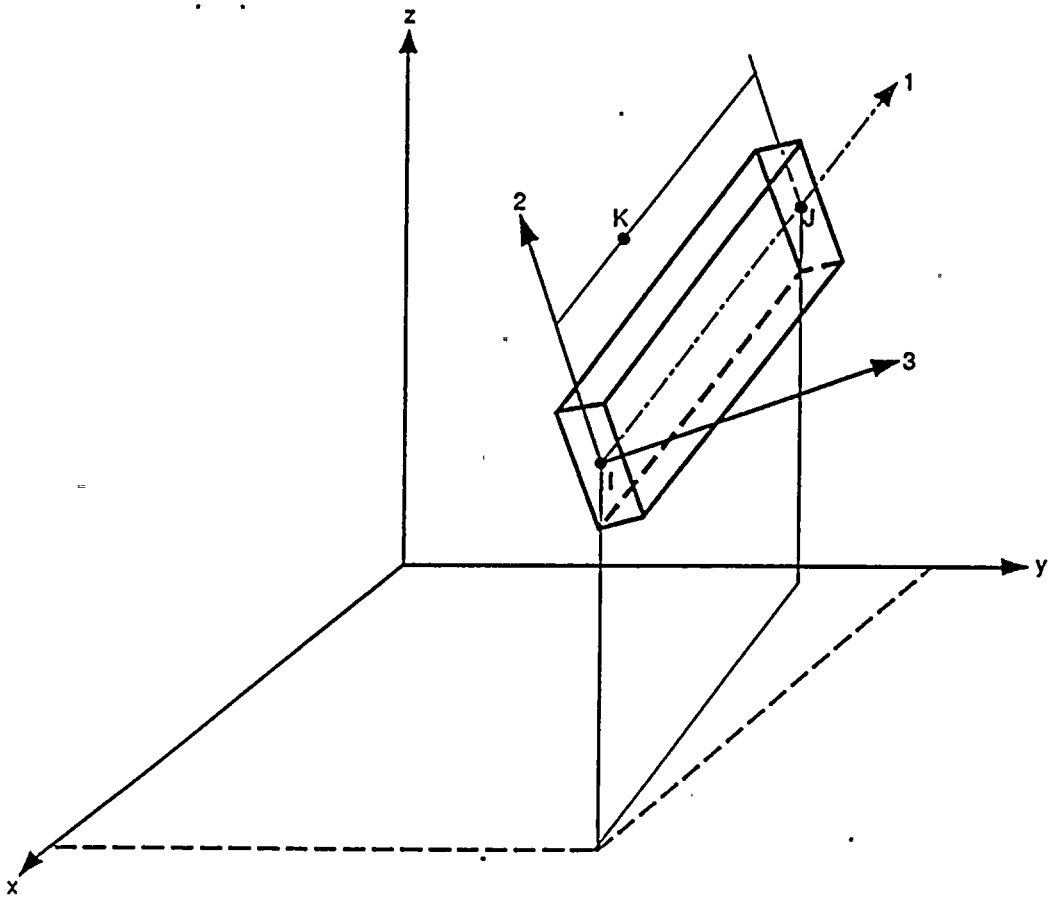

(4) See note 4 of Section H.3.1.

H.3.3 PLATE/SHELL ELEMENTS

Skip this section if no request for forces or moments in plate elements.

H.3.3.1 CONTROL INFORMATION (4X, I1, 2I5)

Columns	Variable	Notes	Entry
5	ICODE(1)		The number 3
6-10	ICODE(2)	(1)	The order number
11-15	ICODE(3)	(2)	Total number of elements in this group for which output is requested

H.3.3.2 OUTPUT REQUEST CARDS (I5, 4X, 6I1, 14X, I1)

Columns	Variable	Notes	Entry
1-5	N		Element number
10	KEY(1)	(3)	Output control key for force component resultant S''_{xx}
11	KEY(2)	(3)	Output control key for force component S''_{yy}
12	KEY(3)	(3)	Output control key for force component S''_{xy}
13	KEY(4)	(3)	Output control key for moment component M''_{xx} (not available)
14	KEY(5)	(3)	Output control key for moment component M''_{yy} (not available)
15	KEY(6)	(3)	Output control key for moment component M''_{xy} (not available).
30	KN	(4)	Generation control key = 0, no generation = 1, otherwise

Notes:

(1) See note 1 of Section H.3.1.

(2) See note 2 of Section H.3.1

(3) The membrane force and bending moments are computed with respect to local element coordinates. The forces are in units of force/length (F/L) and the moments are in moment/length (F.L/L). The location of the infinitesimal elements where the forces and moments are computed and the positive definitions of each component are shown in the figure.

POSITIVE PLATE ELEMENT OUTPUT FORCES

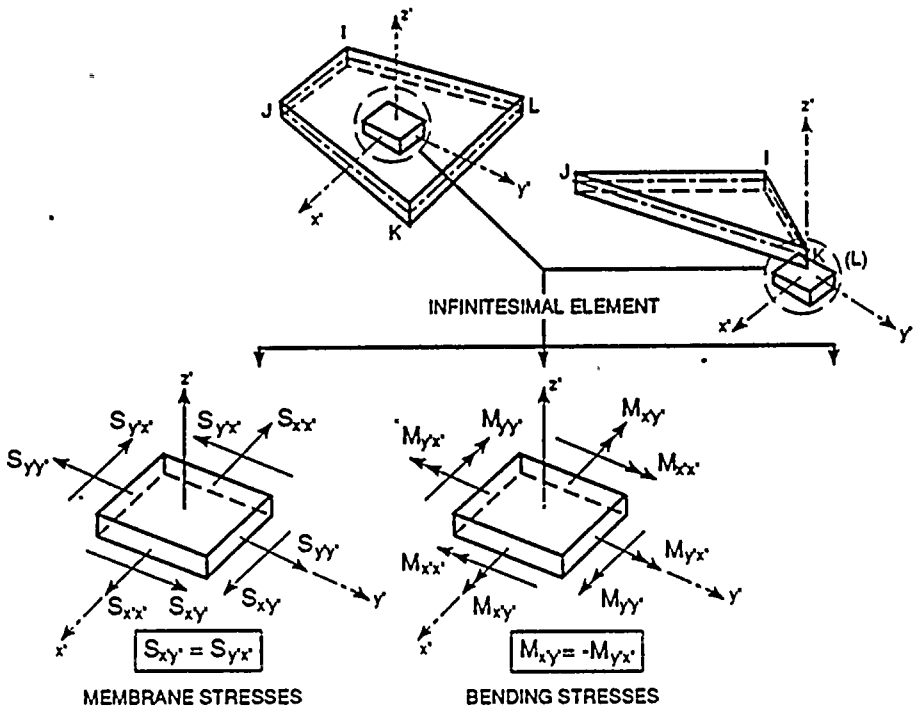

(4) See note 4 of Section H.3.1.

H.3.4 TWO-DIMENSIONAL FINITE ELEMENTS

Skip this section if no request for stresses or strains in 2-D finite elements.

H.3.4.1 CONTROL INFORMATION (4X, I1, 2I5)

Columns	Variable	Notes	Entry
5	ICODE(1)		The number 4
6-10	ICODE(2)	(1)	The order number
11-15	ICODE(3)	(2)	Total number of elements in this group for which output is requested

H.3.4.2 OUTPUT REQUEST CARDS (I5, 4X, 6I1, 14X, I1)

Columns	Variable	Notes	Entry
1-5	N		Element number
10	KEY(1)	(3)	Output control key for stress (strain) in yy-direction
11	KEY(2)		Output control key for stress (strain) in zz-direction
12	KEY(3)		Output control key for stress (strain) in yz-direction
30	KN	(4)	Generation control key = 0, no generation = 1, otherwise

Notes:

(1) See note 1 of Section H.3.1.

(2) See note 2 of Section H.3.1.

(3) See note 3 of Section H.3.1. The stresses in 2-D finite elements are computed at the center of the element and are referred to in global axes. These stresses are shown in the next figure.

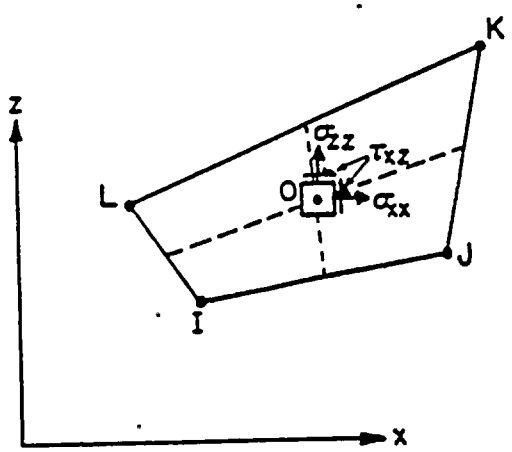

(4) See note 4 of Section H.3.1.

H.3.5 THREE-DIMENSIONAL PILE ELEMENTS

Not available.

H.3.6 TWO-DIMENSIONAL PILE ELEMENTS

Not available.

H.3.7 THREE-DIMENSIONAL SPRING ELEMENTS

Skip this section if no request for forces or moments in spring elements.

H.3.7.1 CONTROL INFORMATION (4X, I1, 2I5)

Columns	Variable	Notes	Entry
5	ICODE(1)		The number 7
6-10	ICODE(2)	(1)	The order number
11-15	ICODE(3)	(2)	Total number of elements in this group for which output is requested

H.3.7.2 OUTPUT REQUEST CARDS (I5, 4X, 6I1, 14X, I1)

Columns	Variable	Notes	Entry
1-5	N		Element number
10	KEY(1)	(3)	Output control key for force in x-direction
11	KEY(2)		Output control key for force in y-direction
12	KEY(3)		Output control key for force in z-direction
13	KEY(4)		Output control key for moment in xx-direction
14	KEY(5)		Output control key for moment in yy-direction
15	KEY(6)		Output control key for moment in zz-direction
30	KN	(4)	Generation control key = 0, no generation = 1, otherwise

Notes:

(1) See note 1 of Section H.3.1.

(2) See note 2 of Section H.3.1.

(3) See note 3 of Section H.3.1.

(4) See note 4 of Section H.3.1.

H.3.8 ONE-DIMENSIONAL PLANE LOVE-WAVE ELEMENTS

Not available.

H.3.9 STIFFNESS/MASS MATRIX ELEMENTS

No component can be requested.

H.4 INPUT MOTION DATA CARDS (2I5, 3F10.0)

Columns	Variable	Notes	Entry
1-5	NFFT	(1)	Number of values to be used in Fourier Transform
6-10	NEQZ		Number of acceleration (or force) values to be read from cards
11-20	DT	(2)	Time step -- sec.
21-30	EQMUL		Multiplication factor for scaling time history. Use only if UGMAX = 0; leave blank otherwise
31-40	UGMAX		Maximum value of time history to be used. The values of time history will be scaled to give maximum value = UGMAX. Use only if EQMUL = 0 ; leave blank otherwise

H.4.1 CONTROL TIME HISTORY ID CARD (12A6)

Columns	Variable	Notes	Entry
1-72	ID(I)		Identification for control time history

H.4.2 CONTROL TIME HISTORY VALUES (8F9.6/8E10.3)

Total of (NEQZ + 7)/8 cards.

Columns	Variable	Notes	Entry
1-72	A(I)	(3)	8 values

Notes:

(1) NFFT must be a power of 2 and includes the trailing zeroes. If this number does not agree with the NFFT value in SITE (or MOTOR), the program will stop.

(2) The program will compute the frequency step from the following formula:

$$DF = 1/(NFFT * DT) .$$

If DF and DT do not agree with those in SITE (or MOTOR), the program will stop.

(3) All time history values must be given at time steps DT. For seismic problems, provide acceleration values in (G) in (8F9.6) format; for foundation vibration problems, provide force values in (8E10.3) format.

H.5 OPERATION MODE CARD

Columns	Variable	Notes	Entry
5	NOPT	(1)	Operation mode = 0, stop no more data

Notes:

(1) Must be the last data card.

CHAPTER 6

REFERENCES

1. Computer Program SASSI - Theoretical Manual, prepared for PG&E, Diablo Canyon Long Term Seismic Program, Bechtel Power Corporation, San Francisco, CA, July 1988.

2. Computer Program SASSI - Validation Report, prepared for PG&E, Diablo Canyon Power Plant, Long Term Seismic Program, Bechtel Power Corporation, San Francisco, CA, July 1988.

3. Lysmer, J., Tabatabaie-Raissi, M. Tajirian, F. Vahdani, S., and Ostadan, F., "SASSI - A System for Analysis of Soil-Structure Interaction," Report No. UCB/GT/81-02, Geotechnical Engineering, University of California, Berkeley, CA April 1981.

4. Schnabel, P. B., Lysmer, J. and Seed, H. B., "SHAKE - A Computer Program for Earthquake Response Analysis of Horizontally Layered Sites," Report No. EERC 72-12, Earthquake Engineering Research Center, University of California, Berkeley, CA, 1972.

5. BC-TOP-4A, "Seismic Analysis of Structures and Equipment for Nuclear Power Plants," Rev. 3, November 1974, Bechtel Power Corporation, San Francisco, CA.

6. Luco, J. E., "Impedance Functions for a Rigid Foundation on a Layered Medium," Nuclear Engineering and Design 31, 204-217, 1974.

7. Computer Program CE933 (FASS), (Version A1-1), Fourier Analysis of Soil-Structure System, Bechtel Power Corporation, San Francisco, CA.

APPENDIX A

INPUT DATA FILES

OF

EXAMPLE PROBLEM

```
    1    E2C1SD - FREE FIELD OF EXAMPLE 2 (BC-TOP-4)
    4   13   10
 32.2
    1  10.        .130      2000.     4000.     .05       .05
    2  10.        .130      2000.     4000.     .05       .05
    3  14.        .130      2000.     4000.     .05       .05
    4  16.        .130      2000.     4000.     .05       .05
                  .130      2000.     4000.     .05       .05
          .005       2048
   10   30   50   60   80  100  120  140  160  180  210  230  260
    2    E2C2SD - VERTICALLY PROPAGATING SV WAVE (BC-TOP-4)
    1
    0    1    0
    X    1    2
    1 1000
 1.0        1.0
    0
```

(E2PD)

```
1    E2PD - POINT LOAD SOLUTION FOR EXAMPLE 2 (BC-TOP-4)
1  13.8
0
```

```
1    E2C1HD - FINITE ELEMENT MODEL OF EXAMPLE 2 (BC-TOP-4)

  138   69    1    0    0    0    1    3
 32.2
-10.0
C   1    0    0    0    1    1    1   .0        .0        -10.0        0
C   2    0    0    0    1    1    1   16.25     .0        -10.0        0
C   9    0    0    0    1    1    1   16.25     315.      -10.0        1
C  10    0    0    0    1    1    1   32.5      .0        -10.0        0
C  21    0    0    0    1    1    1   32.5      330.      -10.0        1
C  22    0    0    0    1    1    1   48.75     .0        -10.0        0
C  45    0    0    0    1    1    1   48.75     345.      -10.0        1
C  46    0    0    0    1    1    1   65.00     .0        -10.0        0
C  69    0    0    0    1    1    1   65.00     345.      -10.0        1
C  70    0    0    0    1    1    1   .0        .0        0.000        0
C  71    0    0    0    1    1    1   16.25     .0        0.000        0
C  78    0    0    0    1    1    1   16.25     315.      0.000        1
C  79    0    0    0    1    1    1   32.5      .0        0.000        0
C  90    0    0    0    1    1    1   32.5      330.      0.000        1
C  91    0    0    0    1    1    1   48.75     .0        0.000        0
C 114    0    0    0    1    1    1   48.75     345.      0.000        1
C 115    0    0    0    1    1    1   65.00     .0        0.000        0
C 138    0    0    0    1    1    1   65.00     345.      0.000        1

  1   88    1   -1    1
  1     .1E10  .3333      .0          .0          .0
  1    2    3    1    1   71   72   70   70    3    1    1
  2    3    4    1    1   72   73   70   70    3    1    1
  3    4    5    1    1   73   74   70   70    3    1    1
  4    5    6    1    1   74   75   70   70    3    1    1
  5    6    7    1    1   75   76   70   70    3    1    1
  6    7    8    1    1   76   77   70   70    3    1    1
  7    8    9    1    1   77   78   70   70    3    1    1
  8    9    2    1    1   78   71   70   70    3    1    1
  9   10   11    2    2   79   80   71   71    3    1    1
 10    2   11    3    3   71   80   72   72    3    1    1
 11   11   12    3    3   80   81   72   72    3    1    1
 12    3   12    4    4   72   81   73   73    3    1    1
 13   12   13    4    4   81   82   73   73    3    1    1
 14    4   13   14   14   73   82   83   83    3    1    1
 15    4   14    5    5   73   83   74   74    3    1    1
 16    5   14   15   15   74   83   84   84    3    1    1
 17    5   15    6    6   74   84   75   75    3    1    1
 18    6   15   16   16   75   84   85   85    3    1    1
 19   16   17    6    6   85   86   75   75    3    1    1
 20    6   17    7    7   75   86   76   76    3    1    1
 21   17   18    7    7   86   87   76   76    3    1    1
 22    7   18    8    8   76   87   77   77    3    1    1
 23    8   18   19   19   77   87   88   88    3    1    1
 24    8   19   20   20   77   88   89   89    3    1    1
 25    8   20    9    9   77   89   78   78    3    1    1
 26    9   20   21   21   78   89   90   90    3    1    1
 27   21    2    9    9   90   71   78   78    3    1    1
 28    2   21   10   10   71   90   79   79    3    1    1
 29   22   23   10   10   91   92   79   79    3    1    1
 30   10   23   11   11   79   92   80   80    3    1    1
 31   11   23   24   24   80   92   93   93    3    1    1
 32   24   25   11   11   93   94   80   80    3    1    1
 33   11   25   12   12   80   94   81   81    3    1    1
 34   12   25   26   26   81   94   95   95    3    1    1
```

(E2C1HD----)

35	26	27	12	12	95	96	81	81	3	1	1
36	12	27	13	13	81	96	82	82	3	1	1
37	13	27	28	28	82	96	97	97	3	1	1
38	28	29	13	13	97	98	82	82	3	1	1
39	13	29	14	14	82	98	83	83	3	1	1
40	14	29	30	30	83	98	99	99	3	1	1
41	30	31	14	14	99	100	83	83	3	1	1
42	14	31	15	15	83	100	84	84	3	1	1
43	15	31	32	32	84	100	101	101	3	1	1
44	32	33	15	15	101	102	84	84	3	1	1
45	15	33	16	16	84	102	85	85	3	1	1
46	16	33	34	34	85	102	103	103	3	1	1
47	34	35	16	16	103	104	85	85	3	1	1
48	16	35	17	17	85	104	86	86	3	1	1
49	17	35	36	36	86	104	105	105	3	1	1
50	36	37	17	17	105	106	86	86	3	1	1
51	17	37	18	18	86	106	87	87	3	1	1
52	18	37	38	38	87	106	107	107	3	1	1
53	38	39	18	18	107	108	87	87	3	1	1
54	18	39	19	19	87	108	88	88	3	1	1
55	19	39	40	40	88	108	109	109	3	1	1
56	40	41	19	19	109	110	88	88	3	1	1
57	19	41	20	20	88	110	89	89	3	1	1
58	20	41	42	42	89	110	111	111	3	1	1
59	42	43	20	20	111	112	89	89	3	1	1
60	20	43	21	21	89	112	90	90	3	1	1
61	21	43	44	44	90	112	113	113	3	1	1
62	44	45	21	21	113	114	90	90	3	1	1
63	21	45	10	10	90	114	79	79	3	1	1
64	10	45	22	22	79	114	91	91	3	1	1
65	22	46	47	23	91	115	116	92	3	1	1
66	23	47	48	24	92	116	117	93	3	1	1
67	24	48	49	25	93	117	118	94	3	1	1
68	25	49	50	26	94	118	119	95	3	1	1
69	26	50	51	27	95	119	120	96	3	1	1
70	27	51	52	28	96	120	121	97	3	1	1
71	28	52	53	29	97	121	122	98	3	1	1
72	29	53	54	30	98	122	123	99	3	1	1
73	30	54	55	31	99	123	124	100	3	1	1
74	31	55	56	32	100	124	125	101	3	1	1
75	32	56	57	33	101	125	126	102	3	1	1
76	33	57	58	34	102	126	127	103	3	1	1
77	34	58	59	35	103	127	128	104	3	1	1
78	35	59	60	36	104	128	129	105	3	1	1
79	36	60	61	37	105	129	130	106	3	1	1
80	37	61	62	38	106	130	131	107	3	1	1
81	38	62	63	39	107	131	132	108	3	1	1
82	39	63	64	40	108	132	133	109	3	1	1
83	40	64	65	41	109	133	134	110	3	1	1
84	41	65	66	42	110	134	135	111	3	1	1
85	42	66	67	43	111	135	136	112	3	1	1
86	43	67	68	44	112	136	137	113	3	1	1
87	44	68	69	45	113	137	138	114	3	1	1
88	45	69	46	22	114	138	115	91	3	1	1

C

(E2C1HMD)

```
  1     E2C1HMD - SLIDING UNIT LOAD EXAMPLE 2
  2    13
32.2
           .005        2048
 10    30    50    60    80   100   120   140   160   180   210   230   260
 46         .50
 58         .50
  0
```

(E2C1HAD)

```
1    E2C1HAD - ANALYS FOR SLIDING - EXAMPLE 2 - RIGID M=0 FOUND.
2    1    1    0    7
0
```

```
  1    E2C1RMD - ROCKING UNIT MOMENT EXAMPLE 2
  2   13
32.2
          .005       2048
 10   30   50   60   80  100  120  140  160  180  210  230  260
 46                          -.0076923
 58                           .0076923
  0
```

```
1     E2C1RAD - ANALYS FOR ROCKING - EXAMPLE 2 - RIGID M=0 FOUND.
2     4     0     0     7
0
```

```
    1    E2C2HD - FINITE ELEMENT MODEL OF EXAMPLE 2 (BC-TOP-4)
         414       75852
  158    69     3     0    18     0     1     3
 32.2
-10.0
C   1     0     0     0     1     1     1   .0          .0          -10.0          0
C   2     0     0     0     1     1     1   16.25       .0          -10.0          0
C   9     0     0     0     1     1     1   16.25       315.        -10.0          1
C  10     0     0     0     1     1     1   32.5        .0          -10.0          0
C  21     0     0     0     1     1     1   32.5        330.        -10.0          1
C  22     0     0     0     1     1     1   48.75       .0          -10.0          0
C  45     0     0     0     1     1     1   48.75       345.        -10.0          1
C  46     0     0     0     1     1     1   65.00       .0          -10.0          0
C  69     0     0     0     1     1     1   65.00       345.        -10.0          1
C  70     0     0     0     1     1     1   .0          .0          0.000          0
C  71     0     0     0     1     1     1   16.25       .0          0.000          0
C  78     0     0     0     1     1     1   16.25       315.        0.000          1
C  79     0     0     0     0     0     0   32.50       .000        0.000          0
C  90     0     0     0     0     0     0   32.50       330.        0.000          1
C  91     0     0     0     1     1     1   48.75       .0          0.000          0
C 114     0     0     0     1     1     1   48.75       345.        0.000          1
C 115     0     0     0     0     0     0   65.00       .000        0.000          0
C 138     0     0     0     0     0     0   65.00       345.0       0.000          1
  139     0     0     0     0     0     0   0.0         0.0         0.0
  140     0     0     0     0     0     0   0.0         0.0         0.0
  141     0     0     0     0     0     0   0.0         0.0         23.5
  142     0     0     0     0     0     0   0.0         0.0         43.8
  143     0     0     0     0     0     0   0.0         0.0         63.8
  144     0     0     0     0     0     0   0.0         0.0         83.8
  145     0     0     0     0     0     0   0.0         0.0         103.8
  146     0     0     0     0     0     0   0.0         0.0         123.8
  147     0     0     0     0     0     0   0.0         0.0         143.8
  148     0     0     0     0     0     0   0.0         0.0         165.3
  149     0     0     0     0     0     0   0.0         0.0         184.4
  150     0     0     0     0     0     0   0.0         0.0         198.5
  151     0     0     0     0     0     0   0.0         0.0         207.0
  152     0     0     0     0     0     0   0.0         0.0         8.00
  153     0     0     0     0     0     0   0.0         0.0         13.00
  154     0     0     0     0     0     0   0.0         0.0         22.00
  155     0     0     0     0     0     0   0.0         0.0         33.5
  156     0     0     0     0     0     0   0.0         0.0         49.00
  157     0     0     0     0     0     0   0.0         0.0         61.00
  158     0     0     0     0     0     0   0.0         0.0         93.00

    1    88     1    -1     1
    1     .10E13  .2780        .150          .00          .00
    1     2     3     1     1    71    72    70    70     3     1     1
    2     3     4     1     1    72    73    70    70     3     1     1
    3     4     5     1     1    73    74    70    70     3     1     1
    4     5     6     1     1    74    75    70    70     3     1     1
    5     6     7     1     1    75    76    70    70     3     1     1
    6     7     8     1     1    76    77    70    70     3     1     1
    7     8     9     1     1    77    78    70    70     3     1     1
    8     9     2     1     1    78    71    70    70     3     1     1
    9    10    11     2     2    79    80    71    71     3     1     1
   10     2    11     3     3    71    80    72    72     3     1     1
   11    11    12     3     3    80    81    72    72     3     1     1
   12     3    12     4     4    72    81    73    73     3     1     1
   13    12    13     4     4    81    82    73    73     3     1     1
   14     4    13    14    14    73    82    83    83     3     1     1
```

(E2C2HD----)

15	4	14	5	5	73	83	74	74	3	1	1
16	5	14	15	15	74	83	84	84	3	1	1
17	5	15	6	6	74	84	75	75	3	1	1
18	6	15	16	16	75	84	85	85	3	1	1
19	16	17	6	6	85	86	75	75	3	1	1
20	6	17	7	7	75	86	76	76	3	1	1
21	17	18	7	7	86	87	76	76	3	1	1
22	7	18	8	8	76	87	77	77	3	1	1
23	8	18	19	19	77	87	88	88	3	1	1
24	8	19	20	20	77	88	89	89	3	1	1
25	8	20	9	9	77	89	78	78	3	1	1
26	9	20	21	21	78	89	90	90	3	1	1
27	21	2	9	9	90	71	78	78	3	1	1
28	2	21	10	10	71	90	79	79	3	1	1
29	22	23	10	10	91	92	79	79	3	1	1
30	10	23	11	11	79	92	80	80	3	1	1
31	11	23	24	24	80	92	93	93	3	1	1
32	24	25	11	11	93	94	80	80	3	1	1
33	11	25	12	12	80	94	81	81	3	1	1
34	12	25	26	26	81	94	95	95	3	1	1
35	26	27	12	12	95	96	81	81	3	1	1
36	12	27	13	13	81	96	82	82	3	1	1
37	13	27	28	28	82	96	97	97	3	1	1
38	28	29	13	13	97	98	82	82	3	1	1
39	13	29	14	14	82	98	83	83	3	1	1
40	14	29	30	30	83	98	99	99	3	1	1
41	30	31	14	14	99	100	83	83	3	1	1
42	14	31	15	15	83	100	84	84	3	1	1
43	15	31	32	32	84	100	101	101	3	1	1
44	32	33	15	15	101	102	84	84	3	1	1
45	15	33	16	16	84	102	85	85	3	1	1
46	16	33	34	34	85	102	103	103	3	1	1
47	34	35	16	16	103	104	85	85	3	1	1
48	16	35	17	17	85	104	86	86	3	1	1
49	17	35	36	36	86	104	105	105	3	1	1
50	36	37	17	17	105	106	86	86	3	1	1
51	17	37	18	18	86	106	87	87	3	1	1
52	18	37	38	38	87	106	107	107	3	1	1
53	38	39	18	18	107	108	87	87	3	1	1
54	18	39	19	19	87	108	88	88	3	1	1
55	19	39	40	40	88	108	109	109	3	1	1
56	40	41	19	19	109	110	88	88	3	1	1
57	19	41	20	20	88	110	89	89	3	1	1
58	20	41	42	42	89	110	111	111	3	1	1
59	42	43	20	20	111	112	89	89	3	1	1
60	20	43	21	21	89	112	90	90	3	1	1
61	21	43	44	44	90	112	113	113	3	1	1
62	44	45	21	21	113	114	90	90	3	1	1
63	21	45	10	10	90	114	79	79	3	1	1
64	10	45	22	22	79	114	91	91	3	1	1
65	22	46	47	23	91	115	116	92	3	1	1
66	23	47	48	24	92	116	117	93	3	1	1
67	24	48	49	25	93	117	118	94	3	1	1
68	25	49	50	26	94	118	119	95	3	1	1
69	26	50	51	27	95	119	120	96	3	1	1
70	27	51	52	28	96	120	121	97	3	1	1
71	28	52	53	29	97	121	122	98	3	1	1
72	29	53	54	30	98	122	123	99	3	1	1
73	30	54	55	31	99	123	124	100	3	1	1
74	31	55	56	32	100	124	125	101	3	1	1

(E2C2HD----)

```
 75   32   56   57   33  101  125  126  102    3    1    1
 76   33   57   58   34  102  126  127  103    3    1    1
 77   34   58   59   35  103  127  128  104    3    1    1
 78   35   59   60   36  104  128  129  105    3    1    1
 79   36   60   61   37  105  129  130  106    3    1    1
 80   37   61   62   38  106  130  131  107    3    1    1
 81   38   62   63   39  107  131  132  108    3    1    1
 82   39   63   64   40  108  132  133  109    3    1    1
 83   40   64   65   41  109  133  134  110    3    1    1
 84   41   65   66   42  110  134  135  111    3    1    1
 85   42   66   67   43  111  135  136  112    3    1    1
 86   43   67   68   44  112  136  137  113    3    1    1
 87   44   68   69   45  113  137  138  114    3    1    1
 88   45   69   46   22  114  138  115   91    3    1    1
  2   18    1   12   -1
  1    .69E06  .278      .0       .02       .02
  1    .14E04   .70E03    .70E03    .10E10    .28E07    .28E07
  2    .99E03   .50E03    .50E03    .10E10    .19E07    .19E07
  3    .99E03   .50E03    .50E03    .10E10    .15E07    .15E07
  4    .99E03   .50E03    .50E03    .10E10    .80E06    .80E06
  5    .99E03   .50E03    .50E03    .10E10    .20E06    .20E06
  6    .20E04   .132E04   .132E04   .10E10    .11E07    .11E07
  7   .256E04   .156E04   .156E04   .10E10    .12E07    .12E07
  8   .221E04   .146E04   .146E04   .10E10    .12E07    .12E07
  9   .196E04   .73E03    .73E03    .10E10    .13E07    .13E07
 10   .174E04   .60E03    .60E03    .10E10    .90E06    .90E06
 11    .78E03   .36E03    .36E03    .10E10    .20E06    .20E06
 12    .19E03   .70E02    .70E02    .10E10    .40E04    .40E04
  1  139  141   46    1    1
  2  141  142   46    1    1
  3  142  143   46    1    1
  4  143  144   46    1    1
  5  144  145   46    1    1
  6  145  146   46    1    1
  7  146  147   46    1    1
  8  147  148   46    1    2
  9  148  149   46    1    3
 10  149  150   46    1    4
 11  150  151   46    1    5
 12  140  152   46    1    6
 13  152  153   46    1    7
 14  153  154   46    1    8
 15  154  155   46    1    9
 16  155  156   46    1   10
 17  156  157   46    1   11
 18  157  158   46    1   12
  2   32    1    1   -1
  1     .1E13  .300
  1     .1E06   .50E06    .50E06    .10E13    .20E10    .20E10
  1  115  116  139    1    1
 23  137  138  139    1    1    1
 24  138  115  139    1    1
 25  139  115  118    1    1
 26  139  121  118    1    1
 27  139  127  118    1    1
 28  139  133  118    1    1
 29  140  115  118    1    1
 30  140  121  118    1    1
 31  140  127  118    1    1
 32  140  133  118    1    1
```

(E2C2HD----)

141	1	.46E04	.46E04	.46E04
142	1	.42E04	.42E04	.42E04
143	1	.42E04	.42E04	.42E04
144	1	.42E04	.42E04	.42E04
145	1	.42E04	.42E04	.42E04
146	1	.42E04	.42E04	.42E04
147	1	.461E04	.461E04	.461E04
148	1	.302E04	.302E04	.302E04
149	1	.247E04	.247E04	.247E04
150	1	.212E04	.212E04	.212E04
151	1	.190E03	.190E03	.190E03
152	1	.280E04	.280E04	.280E04
153	1	.251E04	.251E04	.251E04
154	1	.629E04	.629E04	.629E04
155	1	.376E04	.376E04	.376E04
156	1	.854E04	.854E04	.854E04
157	1	.122E04	.122E04	.122E04
158	1	.820E03	.820E03	.820E03
0				

(E2C2AD)

```
 1     E2C2AD - ANALYS FOR EXAMPLE 2 (BC-TOP-4)
 1     2    1    0    7
.0       .0
 0
```

(E2C20D)

```
    1    E2C20D - MOTION FOR EXAMPLE 2 (BC-TOP-4)
    1   20    1    1   10.0
  139    100111    000001    000001
  140    100111    000001    000001
  141    100000    000001    000001
  142    100000    000001    000001
  143    100000    000001    000001
  144    100000    000001    000001
  145    100000    000001    000001
  146    100000    000001    000001
  147    100000    000001    000001
  148    100000    000001    000001
  149    100000    000001    000001
  150    100000    000001    000001
  151    100111    000001    000001
  152    100000    000001    000001
  153    100000    000001    000001
  154    100000    000001    000001
  155    100000    000001    000001
  156    100000    000001    000001
  157    100000    000001    000001
  158    100111    000001    000001
  .10      100.0       100
  .02
 2048 1759  .005                .100
EL CENTRO N-S, DT=.05 SEC, DUR=10.0 SEC, MAX. ACC.=.10G
 -.002048 -.004097 -.010768 -.017438 -.024522 -.031605 -.033579 -.035554      1
 -.032556 -.029557 -.026996 -.024434 -.025095 -.025755 -.026994 -.028232      2
 -.028018 -.027804 -.028373 -.028941 -.032029 -.035117 -.038147 -.041176      3
 -.041366 -.041556 -.040171 -.038785 -.038122 -.037459 -.036852 -.036244      4
 -.034218 -.032191 -.029754 -.027316 -.026096 -.024877 -.024575 -.024273      5
 -.024575 -.024877 -.027135 -.029393 -.033865 -.038337 -.042582 -.046826      6
 -.049166 -.051507 -.053032 -.054558 -.055666 -.056775 -.055579 -.054383      7
 -.050897 -.047410 -.044982 -.042553 -.042348 -.042142 -.040840 -.039538      8
 -.035572 -.031605 -.028403 -.025200 -.024600 -.023999 -.022390 -.020781      9
 -.016537 -.012292 -.010761 -.009230 -.014273 -.019316 -.026000 -.032685     10
 -.035511 -.038337 -.040617 -.042896 -.049250 -.055604 -.060771 -.065937     11
 -.061649 -.057360 -.046414 -.035468 -.027392 -.019316 -.014496 -.009677     12
 -.000449  .008780  .021368  .033956  .037610  .041264  .030015  .018767     13
  .002213 -.014341 -.024053 -.033765 -.035612 -.037459 -.037678 -.037898     14
 -.040020 -.042142 -.045946 -.049749 -.054579 -.059409 -.064151 -.068894     15
 -.072492 -.076091 -.080009 -.083928 -.089520 -.095112 -.098093 -.101074     16
 -.095313 -.089551 -.077626 -.065700 -.058018 -.050336 -.051281 -.052227     17
 -.054940 -.057653 -.055856 -.054058 -.050880 -.047702 -.047736 -.047771     18
 -.047883 -.047995 -.042793 -.037591 -.028600 -.019609 -.012050 -.004490     19
  .001413  .007317  .015306  .023294  .033596  .043898  .052413  .060929     20
  .064998  .069067  .070126  .071186  .072468  .073750  .077957  .082165     21
  .090248  .098331  .108434  .118537  .127019  .135500  .139878  .144255     22
  .144120  .143985  .139801  .135617  .129120  .122623  .117139  .111654     23
  .108359  .105063  .100457  .095851  .087581  .079311  .072499  .065687     24
  .067230  .068774  .076925  .085076  .092142  .099209  .103486  .107764     25
  .114169  .120574  .129970  .139365  .147235  .155106  .161460  .167814     26
  .177411  .187007  .197759  .208512  .211367  .214223  .208059  .201895     27
  .196354  .190812  .189437  .188062  .181681  .175300  .159605  .143909     28
  .130485  .117062  .115881  .114700  .115881  .117062  .102359  .087657     29
  .053047  .018438 -.025171 -.068780 -.109748 -.150716 -.180405 -.210094     30
 -.220206 -.230319 -.220322 -.210324 -.193398 -.176471 -.165928 -.155384     31
 -.148514 -.141643 -.127772 -.113901 -.093533 -.073165 -.056289 -.039413     32
 -.028340 -.017267 -.004936  .007395  .023305  .039215  .053492  .067768     33
  .078952  .090136  .102778  .115421  .130727  .146033  .161046  .176060     34
```

(E2C20D----)

.191922	.207784	.228037	.248290	.269741	.291192	.308039	.324886	35
.340817	.356747	.379334	.401922	.424695	.447469	.452759	.458049	36
.441052	.424055	.399706	.375357	.356686	.338016	.322366	.306716	37
.290174	.273632	.263912	.254191	.257619	.261047	.268211	.275375	38
.273187	.270998	.261889	.252779	.249159	.245538	.250057	.254576	39
.259128	.263681	.266558	.269436	.280021	.290606	.311457	.332308	40
.343064	.353820	.320480	.287140	.191565	.095990	-.041045	-.178080	41
-.304872	-.431665	-.503676	-.575688	-.590156	-.604624	-.595297	-.585969	42
-.584030	-.582091	-.589005	-.595919	-.595588	-.595258	-.581326	-.567394	43
-.549428	-.531462	-.520401	-.509339	-.507084	-.504829	-.506975	-.509121	44
-.510926	-.512731	-.512507	-.512283	-.512653	-.513024	-.517011	-.520998	45
-.524620	-.528243	-.521863	-.515484	-.496256	-.477028	-.453995	-.430962	46
-.412584	-.394206	-.377471	-.360737	-.339426	-.318115	-.294516	-.270916	47
-.249886	-.228856	-.206663	-.184470	-.155010	-.125549	-.092889	-.060228	48
-.032601	-.004975	.019893	.044760	.075058	.105355	.139111	.172867	49
.201300	.229734	.254513	.279292	.309971	.340650	.375681	.410713	50
.439188	.467663	.490645	.513626	.543615	.573604	.610380	.647156	51
.676520	.705884	.726492	.747100	.772877	.798655	.828346	.858038	52
.873268	.888499	.892472	.896446	.916470	.936494	.969115	1.001735	53
1.000868	1.000000	.952465	.904929	.865254	.825578	.817877	.810175	54
.745152	.680129	.462852	.245574	-.052513	-.350601	-.534947	-.719292	55
-.706881	-.694470	-.606618	-.518766	-.499361	-.479955	-.516864	-.553773	56
-.549787	-.545800	-.485417	-.425033	-.372745	-.320456	-.299023	-.277590	57
-.248980	-.220369	-.172197	-.124024	-.087327	-.050629	-.033215	-.015800	58
.008634	.033069	.068656	.104243	.130113	.155984	.175982	.195980	59
.228953	.261925	.293336	.324747	.335918	.347089	.371460	.395831	60
.455013	.514194	.515923	.517652	.343111	.168569	-.121050	-.410669	61
-.590321	-.769973	-.729488	-.689004	-.570870	-.452737	-.431860	-.410983	62
-.458492	-.506000	-.488600	-.471200	-.383684	-.296167	-.240995	-.185822	63
-.177634	-.169447	-.126593	-.083738	-.007189	.069360	.065558	.061755	64
-.067162	-.196080	-.340546	-.485013	-.532235	-.579457	-.550729	-.522002	65
-.501124	-.480245	-.486717	-.493190	-.493156	-.493122	-.477623	-.462124	66
-.447773	-.433421	-.419560	-.405700	-.382980	-.360259	-.338121	-.315982	67
-.304465	-.292948	-.280230	-.267513	-.243648	-.219783	-.197551	-.175319	68
-.164189	-.153058	-.139895	-.126732	-.103022	-.079311	-.058190	-.037068	69
-.024973	-.012877	.003030	.018938	.036978	.055019	.049152	.043286	70
.007741	-.027804	-.061916	-.096028	-.111374	-.126720	-.146850	-.166980	71
-.206113	-.245246	-.272745	-.300245	-.289280	-.278314	-.252140	-.225967	72
-.217753	-.209540	-.209571	-.209602	-.192451	-.175300	-.149341	-.123381	73
-.110563	-.097746	-.089256	-.080767	-.056186	-.031605	-.001654	.028297	74
.041219	.054141	.061152	.068163	.095539	.122915	.158709	.194504	75
.195731	.196958	.148814	.100670	.036142	-.028386	-.067972	-.107558	76
-.108212	-.108867	-.084319	-.059771	-.035739	-.011707	-.004661	.002385	77
.002802	.003219	.019926	.036633	.068653	.100673	.123850	.147027	78
.156188	.165350	.182134	.198919	.228666	.258413	.280790	.303168	79
.316933	.330699	.354292	.377885	.388386	.398888	.340792	.282696	80
.173394	.064092	.011575	-.040943	.014793	.070530	.142518	.214506	81
.207194	.199882	.164243	.128603	.165120	.201638	.279755	.357872	82
.371795	.385718	.352561	.319403	.357683	.395962	.498884	.601807	83
.599411	.597014	.403328	.209642	-.031410	-.272461	-.373181	-.473902	84
-.428347	-.382792	-.315456	-.248119	-.225318	-.202516	-.197228	-.191940	85
-.175865	-.159789	-.128337	-.096884	-.037906	.021072	.094868	.168665	86
.183104	.197543	.096653	-.004238	-.158249	-.312261	-.395901	-.479542	87
-.457506	-.435469	-.384760	-.334051	-.323742	-.313432	-.329288	-.345144	88
-.342604	-.340065	-.312082	-.284099	-.253551	-.223003	-.204513	-.186022	89
-.174808	-.163594	-.145235	-.126875	-.094898	-.062921	-.037135	-.011350	90
-.024112	-.036873	-.084592	-.132312	-.164781	-.197251	-.180942	-.164633	91
-.129726	-.094819	-.086324	-.077830	-.088227	-.098624	-.091127	-.083631	92
-.057764	-.031898	-.016468	-.001038	.001969	.004975	.019246	.033517	93
.060510	.087502	.106438	.125373	.134093	.142814	.154462	.166111	94

(E2C20D----)

.172022	.177934	.157878	.137821	.101396	.064970	.040179	.015388	95
.003012	-.009365	-.026913	-.044461	-.058081	-.071701	-.057123	-.042545	96
-.010005	.022536	.039751	.056967	.059358	.061750	.079250	.096749	97
.131489	.166228	.191308	.216388	.229061	.241734	.264780	.287826	98
.320384	.352942	.374576	.396211	.414377	.432543	.463358	.494173	99
.501257	.508341	.436948	.365554	.244381	.123208	.051464	-.020281	100
-.005897	.008487	.042569	.076651	.076225	.075799	.068406	.061013	101
.073379	.085746	.080849	.075952	.029928	-.016097	-.051328	-.086559	102
-.064790	-.043020	-.003511	.035998	.038923	.041849	.030256	.018663	103
.039475	.060287	.095721	.131154	.138594	.146033	.142174	.138315	104
.163539	.188763	.225863	.262964	.271517	.280070	.277557	.275045	105
.302579	.330114	.369245	.408376	.415925	.423473	.419215	.414956	106
.445846	.476736	.521038	.565340	.567277	.569213	.545634	.522054	107
.532610	.543166	.573768	.604370	.592499	.580628	.542960	.505291	108
.511498	.517706	.534691	.551677	.458749	.365820	.160235	-.045350	109
-.199292	-.353235	-.343810	-.334386	-.246502	-.158618	-.122457	-.086296	110
-.099337	-.112379	-.108390	-.104401	-.097707	-.091014	-.135329	-.179645	111
-.253416	-.327187	-.373909	-.420632	-.453365	-.486098	-.546715	-.607332	112
-.664216	-.721100	-.711965	-.702830	-.647729	-.592627	-.563477	-.534327	113
-.535673	-.537020	-.514167	-.491314	-.438370	-.385426	-.348698	-.311969	114
-.296459	-.280948	-.245804	-.210661	-.152887	-.095112	-.052044	-.008976	115
.018046	.045068	.088024	.130981	.184894	.238807	.275766	.312725	116
.349368	.386011	.443485	.500958	.516502	.532047	.426319	.320591	117
.151808	-.016975	-.092387	-.167799	-.108629	-.049458	.021732	.092922	118
.088165	.083408	.065187	.046965	.088892	.130818	.191010	.251202	119
.269441	.287680	.299110	.310540	.363640	.416741	.470564	.524388	120
.533338	.542288	.559012	.575737	.647248	.718759	.748532	.778305	121
.635714	.493122	.229592	-.033939	-.218902	-.403864	-.413629	-.423394	122
-.357878	-.292362	-.275639	-.258915	-.288808	-.318700	-.326449	-.334197	123
-.299817	-.265437	-.221081	-.176725	-.156991	-.137256	-.167287	-.197318	124
-.281569	-.365820	-.458576	-.551332	-.584563	-.617794	-.583696	-.549597	125
-.511411	-.473224	-.474018	-.474813	-.484992	-.495171	-.475133	-.455095	126
-.418651	-.382206	-.362012	-.341818	-.333479	-.325139	-.305345	-.285551	127
-.255886	-.226222	-.203059	-.179896	-.164575	-.149253	-.140385	-.131516	128
-.145360	-.159204	-.204965	-.250726	-.300956	-.351186	-.368245	-.385305	129
-.369562	-.353820	-.339546	-.325272	-.332083	-.338894	-.349248	-.359603	130
-.347346	-.335089	-.301414	-.267739	-.238786	-.209833	-.199273	-.188713	131
-.174251	-.159789	-.116016	-.072244	-.026756	.018731	-.002773	-.024277	132
-.129786	-.235295	-.342009	-.448722	-.463461	-.478199	-.414280	-.350360	133
-.300876	-.251392	-.257062	-.262731	-.271986	-.281241	-.247923	-.214605	134
-.165248	-.115891	-.091128	-.066365	-.054693	-.043020	-.014245	.014530	135
.053943	.093356	.121163	.148969	.169305	.189641	.213143	.236645	136
.246505	.256364	.234226	.212088	.175111	.138134	.113580	.089026	137
.073486	.057946	.037322	.016699	.004399	-.007902	.008213	.024327	138
.054890	.085454	.102021	.118589	.124411	.130232	.148980	.167728	139
.198731	.229734	.252512	.275291	.288802	.302313	.322550	.342788	140
.369228	.395669	.415509	.435350	.452677	.470004	.494250	.518497	141
.531563	.544629	.518186	.491743	.433316	.374890	.319761	.264632	142
.225966	.187300	.152294	.117289	.088496	.059702	.056904	.054105	143
.072999	.091892	.103428	.114965	.112063	.109160	.113336	.117513	144
.131334	.145155	.140434	.135713	.102243	.068774	.034769	.000763	145
-.011911	-.024584	-.028524	-.032463	-.040814	-.049166	-.050911	-.052656	146
-.042863	-.033069	-.032162	-.031254	-.049136	-.067018	-.080013	-.093009	147
-.082794	-.072579	-.057847	-.043115	-.044530	-.045946	-.048985	-.052023	148
-.036109	-.020194	.002353	.024901	.033961	.043020	.050587	.058155	149
.084536	.110916	.140133	.169350	.169398	.169447	.143871	.118296	150
.096462	.074628	.060008	.045389	.016695	-.011999	-.051346	-.090693	151
-.107975	-.125257	-.108460	-.091662	-.065292	-.038922	-.021785	-.004649	152
.011578	.027804	.046349	.064894	.066103	.067311	.042093	.016874	153
-.010438	-.037751	-.041109	-.044467	-.029550	-.014633	-.001970	.010692	154

(E2C20D----)

.017053	.023414	.031589	.039765	.050611	.061458	.072196	.082935	155
.097072	.111209	.127402	.143596	.146424	.149253	.128441	.107629	156
.076788	.045946	.025886	.005826	-.001769	-.009365	-.015603	-.021841	157
-.027162	-.032483	-.028110	-.023737	-.011137	.001463	.010618	.019774	158
.021008	.022243	.020353	.018462	.014352	.010243	.000861	-.008521	159
-.018163	-.027804	-.027717	-.027630	-.019083	-.010536	-.005450	-.000363	160
-.002523	-.004683	-.004659	-.004634	.003244	.011121	.019037	.026953	161
.025915	.024877	.016128	.007379	-.004505	-.016389	-.032341	-.048292	162
-.068629	-.088966	-.104997	-.121028	-.122118	-.123208	-.110598	-.097988	163
-.084698	-.071408	-.067596	-.063783	-.066425	-.069067	-.068101	-.067134	164
-.059467	-.051800	-.044988	-.038175	-.037963	-.037751	-.036333	-.034916	165
-.020092	-.005268	.018082	.041432	.050420	.059409	.041375	.023341	166
-.004132	-.031605	-.040932	-.050259	-.038446	-.026633	-.015255	-.003876	167
-.006914	-.009951	-.018495	-.027038	-.029029	-.031020	-.029425	-.027829	168
-.030156	-.032483	-.035194	-.037905	-.033438	-.028971	-.020082	-.011192	169
-.005889	-.000585	.002272	.005130	.013247	.021365	.034636	.047908	170
.058341	.068774	.074990	.081207	.092550	.103892	.127018	.150144	171
.178232	.206321	.223792	.241263	.234621	.227978	.193233	.158487	172
.106167	.053848	.007620	-.038607	-.057788	-.076969	-.070006	-.063043	173
-.049666	-.036288	-.029936	-.023584	-.017938	-.012292	.001916	.016124	174
.031328	.046532	.046839	.047146	.030597	.014048	-.006940	-.027927	175
-.046010	-.064092	-.082593	-.101094	-.118882	-.136671	-.142463	-.148255	176
-.136756	-.125257	-.107151	-.089044	-.076129	-.063214	-.053029	-.042844	177
-.027714	-.012585	.004797	.022178	.034355	.046532	.055985	.065438	178
.079543	.093648	.107866	.122084	.122353	.122623	.104785	.086946	179
.061471	.035995	.012907	-.010182	-.028503	-.046824	-.056926	-.067028	180
-.063365	-.059702	-.047273	-.034844	-.029421	-.023999	-.032213	-.040428	181
-.050358	-.060287	-.059191	-.058095	-.049094	-.040093	-.032906	-.025719	182
-.020908	-.016097	-.008831	-.001564	.006974	.015511	.021482	.027452	183
.033333	.039215	.048977	.058740	.068293	.077847	.079582	.081316	184
.074606	.067896	.057378	.046860	.034991	.023121	.012505	.001888	185
-.000227	-.002341	.008876	.020094	.039313	.058531	.077212	.095894	186
.111599	.127305	.138108	.148912	.146449	.143985	.124302	.104618	187
.080257	.055897	.043318	.030740	.028833	.026926	.021723	.016520	188
.005041	-.006439	-.012268	-.018096	-.012121	-.006146	.002411	.010968	189
.013094	.015219	.015097	.014974	.021096	.027218	.039337	.051456	190
.063042	.074628	.082962	.091296	.099496	.107697	.118793	.129889	191
.141766	.153643	.159796	.165949	.162138	.158326	.148649	.138972	192
.131676	.124379	.121571	.118762	.117620	.116477	.121171	.125866	193
.144730	.163594	.188266	.212938	.217092	.221247	.194650	.168053	194
.137436	.106819	.102298	.097776	.109028	.120281	.111403	.102524	195
.065601	.028679	-.005900	-.040478	-.050090	-.059702	-.057911	-.056120	196
-.064496	-.072872	-.088401	-.103930	-.111228	-.118525	-.117510	-.116494	197
-.118680	-.120867	-.127491	-.134115	-.135978	-.137842	-.133515	-.129187	198
-.127954	-.126720	-.131615	-.136510	-.135273	-.134037	-.112786	-.091535	199
-.054109	-.016682	.014316	.045313	.048702	.052092	.028154	.004216	200
-.028328	-.060872	-.086205	-.111538	-.127761	-.143985	-.152533	-.161082	201
-.158094	-.155106	-.141543	-.127980	-.116960	-.105941	-.107213	-.108486	202
-.113506	-.118525	-.114241	-.109956	-.100046	-.090136	-.087392	-.084648	203
-.088563	-.092478	-.091705	-.090932	-.084244	-.077555	-.074617	-.071679	204
-.074617	-.077555	-.079005	-.080456	-.079591	-.078725	-.082440	-.086155	205
-.093560	-.100965	-.102469	-.103973	-.097201	-.090429	-.082720	-.075010	206
-.069258	-.063506	-.055127	-.046749	-.034789	-.022828	-.011016	.000795	207
.013128	.025462	.040755	.056048	.069142	.082237	.086620	.091003	208
.090863	.090722	.093814	.096906	.100838	.104770	.103913	.103055	209
.101425	.099795	.102197	.104600	.104685	.104770	.098072	.091373	210
.087683	.083993	.088472	.092951	.091104	.089258	.072829	.056401	211
.044589	.032776	.040318	.047861	.055245	.062628	.052967	.043306	212
.041553	.039800	.066313	.092827	.102603	.112379	.045925	-.020528	213
-.136253	-.251977	-.324962	-.397947	-.396369	-.394791	-.378617	-.362443	214

(E2C20D----)

```
-.377593 -.392742 -.409525 -.426308 -.411281 -.396254 -.373627 -.351000      215
-.350069 -.349137 -.349780 -.350423 -.327685 -.304947 -.278877 -.252806      216
-.247709 -.242612 -.239880 -.237147 -.213833 -.190519 -.165114 -.139710      217
-.134825 -.129940 -.126951 -.123962 -.099734 -.075506 -.048979 -.022452      218
-.020006 -.017560 -.025693 -.033826 -.030230 -.026633 -.024341 -.022049      219
-.037656 -.053263 -.064876 -.076489 -.059755 -.043020 -.016985               220
   0
```

APPENDIX B

ERROR REPORTS

AND

COMMENT FORMS

S A S S I

READER'S COMMENT FORM

Manual Title: _____ Version No.: _____ Revision No. _____

Please complete this form and return to:

Bechtel Power Corp.
Attn: Dr. Farhang Ostadan
Fifty Beale St., P. O. Box 3965
San Francisco, CA 94119, U.S.A.

Your comments and suggestions about this manual may help to improve its usefulness. Your possible comments may include clarity, accuracy, completeness, organization, index, etc.

COMMENTS: (Please give specific page and line reference where appropriate.)

_____

_____

_____

_____

_____

_____

_____

_____

_____

_____

_____

_____

FROM Name or Title: _____

Company Name: _____

Company Address: _____

City: _____ State: _____ Zip Code: _____

Country: _____

S A S S I

SUSPECTED ERROR REPORT

Please complete this form and return to:

Bechtel Power Corp.
Attn: Dr. Farhang Ostadan
Fifty Beale St., P. O. Box 3965
San Francisco, CA 94119, U.S.A.

only if you wish to report a suspected error in the computer code SASSI.

Program Module Name: _____ Version No. _____

Machine: _____ System: _____

REPORTED BY: Name or Title: _____

Company Name: _____

Company Address: _____

City: _____ State: _____ Zip Code: _____

Country: _____

DESCRIPTION (Please be complete. Append relevant decks, listings, core dumps, etc.) _____

ATTACHMENT Q2b-3

SASSI
SYSTEM FOR
ANALYSIS OF
SOIL
STRUCTURE
INTERACTION

SASSI VALIDATION MANUAL

JULY 1988

CE994

BECHTEL POWER CORPORATION

SASSI

A SYSTEM FOR ANALYSIS OF
SOIL-STRUCTURE INTERACTION

VALIDATION REPORT
(CDC CRAY-XMP AND PG&E IBM VERSIONS)

Prepared for

Diablo Canyon
Long Term Seismic Program
Pacific Gas and Electric Company
San Francisco, California

by

Bechtel Power Corporation
San Francisco, California 94119

July 30, 1988

PREFACE

The computer program SASSI was developed at the University of California, Berkeley, by a research team under the technical direction of Prof. John Lysmer. The CDC and IBM versions of the program were obtained from the University of California, Berkeley, under a license agreement with the University. During the course of installation, testing, and validation of the Bechtel version of the code on the CDC CRAY System, some modifications and enhancements were made to the code to improve the code performance. These include correcting the motion phases in Rayleigh wave calculation, replacing the plate element and providing the option for local end release conc tion in beam element. The original User's Manual issued by the University was revised to reflect the changes made to the code. A new chapter on application guide was also added to the User's Manual. The IBM version provided to PG&E contains the same modifications and enhancements made to the Bechtel CRAY version to date. The validation and theoretical manuals of the program were also prepared to complete the documentations of the program. The modifications and enhancements and preparation of the validation and theoretical manuals have been performed by the Civil/Structural Staff Group of Bechtel Power Corporation, San Francisco Office.

This manual has been prepared by Bechtel Power Corporation and has been reviewed following the Bechtel Standard Engineering Department Procedure for Nuclear Projects.

This report was prepared under a contract agreement between PG&E and Bechtel and is intended for the exclusive use by PG&E only. Appendix A of this report contains technical information proprietary to Bechtel Power Corporation. Except for copies that may be required for the Nuclear Regulatory Commission (NRC) in satisfying a regulatory requirement, no copy should be distributed outside of PG&E without prior written consent from Bechtel.

DISCLAIMER

Every reasonable effort was made to provide a comprehensive and flexible computer program. However, the computer program itself and associated documentation are supplied without representation of warranty, expressed or implied, as to its content, accuracy, or freedom from defects or errors.

TABLE OF CONTENTS

TABLE OF CONTENTS (Cont'd)

1. INTRODUCTION

The computer program SASSI (System for Analysis of Soil-Structure Interaction) is a modular program for linear two- and three-dimensional (2- and 3-D) soil-structure-interaction (SSI) analysis using standard finite element method and the flexible volume substructuring method. The foundation medium that can be modelled using SASSI is the horizontally layered viscoelastic soil system overlaying a uniform viscoelastic halfspace. The structure and its foundation can be represented by 3-D beam, spring, solid brick, plate, and 2-D plane strain elements. The materials of the soil and structure system are represented by their complex moduli to include the material damping using complex response method.

The program can analyze SSI responses due to applied dynamic loads on the structure or seismic ground motion input consisting of an arbitrary 3-D superposition of inclined plane body waves (P- and S-waves) and surface waves (Rayleigh and Love waves).

The program is for a linear SSI analysis. The equivalent linear method of SSI analysis can be performed using SASSI through multiple iteration runs.

The SSI system that can be analyzed using SASSI may consist of single or multiple structures with or without embedment and with rigid or flexible foundations interacting with the foundation medium.

The program is coded in FORTRAN IV and uses dynamic storage allocation so that the size of SSI problem that can be accommodated by SASSI is limited only by the computer storage available.

The program has undergone extensive validation testing and benchmarking against published solutions of SSI problems. A total of 20 validation test problems consisting of 56 test cases have been performed. The objective of this report is to present the results of SASSI program validation tests. Detailed descriptions are given to the SASSI analysis capabilities tested, the validation methods, the validation test problems used, and summaries of the validation results.

Section 2 of this report presents SASSI program description, including a brief description of theory and program layout and operations. Section 3 presents the validation methods and the scope of the validation. Section 4 describes the validation test problems analyzed and summaries of the results obtained. Finally, Section 5 presents the conclusions. Detailed descriptions of each of the 20 validation test problems analyzed and the results obtained for each are presented in Appendix A.

2. PROGRAM DESCRIPTION

2.1 Theory

In this section, a brief summary of SASSI theoretical background is presented. The detailed descriptions on the theory may be obtained from Refs. 1 and 33.

The flexible volume substructuring method used in SASSI considers the structure(s) and the foundation(s) to be partitioned as shown in Fig. 2.1-1. In this partitioning, the structure (Fig. 2.1-1C) consists of the superstructure plus the basement minus the excavated soil. The foundation (Fig. 2.1-1b), consists of the original site i.e., the site without soil excavation for the structure basement. Interaction between the structure and the foundation occurs at all basement nodes. For seismic analysis, the equation of motion for substructure C in Fig. 2.1-1 can be written in the frequency domain as follows:

$$\begin{bmatrix} C_{ss} & C_{si} \\ C_{is} & C_{ii}-C_{ff}+X_{ff} \end{bmatrix} \begin{Bmatrix} U_s \\ U_f \end{Bmatrix} = \begin{Bmatrix} 0 \\ [X_{ff}]\ U_f \end{Bmatrix} \qquad (2.1\text{-}1)$$

where the sub-matrices C are defined by the following relation:

$$[C] = [K] - \omega^2 [M] \qquad (2.1\text{-}2)$$

[K] is the complex stiffness and [M] is the mass-matrix. The subscripts used in Eq. (2.1-1) are defined in Fig. 2.1-1. The matrix $[X_{ff}]$ is the impedance computed for all the interacting nodes, U_f is the free-field motion at the interacting nodes and U_s and U_f are the complex total displacements of the superstructure and foundation nodes.

In modeling the embedded foundations it should be noted that while the nodes used for the excavated soil elements are all interacting

nodes, the nodes used for the basement of the structure may be selected entirely from the set of interacting nodes or use a different set of nodes (non-interacting nodes) with the nodes on the boundary of the basement being selected from the set of interacting nodes.

The complex response method is used to compute the complex stiffness of the elements allowing for variation of material damping in each element. If the source of excitation is not seismic excitation, but is the applied dynamic loading, the equation of motion becomes

$$\begin{bmatrix} C_{ss} & C_{si} \\ C_{is} & C_{ii}-C_{ff}+X_{ff} \end{bmatrix} \begin{Bmatrix} U_s \\ U_f \end{Bmatrix} = \begin{Bmatrix} P_s \\ P_f \end{Bmatrix} \qquad (2.1\text{-}3)$$

where P_s and P_f are the complex harmonic amplitude of the load acting on the superstructure and/or foundation nodes. Based on the above equations of motions, the solution to the harmonic soil-structure interaction problem can be achieved in the following five steps:

1. Solve the site response problem. This step involves determining the free-field displacement amplitudes U_f within the excavated volume. This step does not have to be performed for the case of applied dynamic loading.

2. Solve the impedance problem. This step involves determining the matrix $[X_f]$ which can be obtained efficiently from a series of plane strain or axisymmetric solution of substructure (b) in Fig. 2.1-1 (see Ref. 33).

3. Form the load vector. In the seismic case, excitation load vector in Eq. (2.1-1) can be computed from the product of the solutions in Steps 1 and 2. In the applied external load case, this step consists of setting the vector P in Eq. (2.1-3).

4. From the complex dynamic stiffness matrix. This step which is identical to the seismic and external load cases, involves forming the coefficient matrices in the left-hand sides of Eqs. (2.1-1) and (2.1-3).

5. Solve the structural problem. This step involves solving the linear equations, Eqs. (2.1-1) or (2.1-3), for each frequency.

   For seismic excitations and transient loadings, the above steps are performed at several selected frequencies. An effective interpolation scheme (see Ref. 33) is used to compute the responses at all frequencies required by the Fourier transform techniques.

2.2 Program Layout and Operations

The SASSI program is written in FORTRAN IV language. The basic version of the program consists of 9 sub-programs (modules). The program layout and the interaction between the modules are shown in Fig. 2.2-1. The individual modules and their functions are described as follows:

a. SITE

   This module solves the site response problem. The control point and wave composition of the control motion are defined. The information needed to form vector U_f' used in Eq. (2.1-1) is computed at this stage and saved on Tape 1. It also stores information required for the transmitting boundary on Tape 2.

b. POINT2 & POINT3

   These two modules, POINT2 and POINT3, are used to solve the point load solution for two- and three-dimensional analysis, respectively. The results are saved on Tape 3 to be used to construct the flexibility matrix for interacting nodes.

c. HOUSE

This module computes the mass and complex stiffness matrices of all finite elements used in the SSI model and stores the results on Tape 4.

d. MOTOR

This module forms the load vector in Eq. (2.1-3). The loads may correspond to impact forces, rotating machinery or simple harmonic forces to be used to determine the impedance functions. It also allows the specification of loads to act out of phase. The results are saved on Tape 9.

e. MATRIX

In this module, Tapes 3 and 4 are used as input to form the impedance matrix X_{ff} in Eq. (2.1-1). The matrix X_{ff} is saved on Tape 5. The modified complex stiffness matrices in Eqs. (2.1-1) or (2.1-3) are also formed, triangularized and stored on Tape 6.

f. LOADS

Using the data from Tapes 1 and 9, this module computes the load vectors in Eqs. (2.1-1) or (2.1-3) and stores them on Tape 7.

g. SOLVE

This module reads the reduced dynamic stiffness matrices from Tape 6, then performs the back-substitution using the vectors on Tape 7. The transfer function results are saved on Tape 8.

The modules MATRIX, LOAD, and SOLVE are combined into a controlling module called ANALYS.

h. MOTION

This module is a response output post-processor. It reads the transfer functions from Tape 8 and computes the final response at a specific node selected by the user. The response in terms of the transfer functions, the time history of the response and response spectrum and maximum response may be requested.

i. STRESS

This module reads Tapes 8 and 4 and computes requested stress, strain and force time histories on structural members.

j. COMBIN

If after interpolation it is found that solutions for additional frequencies are needed, this module combines the corresponding Tapes 8 created by SOLVE and produces a new Tape 8.

2.3 Restart Capabilities

SASSI provides several restart capabilities to perform the analysis efficiently if changes occur in the input parameters. The followings are the major restart capabilities of SASSI.

a. Change in Seismic Input

If the control motion and/or the wave composition are changed, only the modules SITE and ANALYS have to be re-executed, without having to re-perform the impedance calculation.

b. Change in the Structure Model

If the structure model is changed by changing the material properties or by adding or subtracting elements, only HOUSE and part of ANALYS need to be re-executed.

c. Change in Loading Input

If the external load applied to the structure changes only program MOTOR and part of ANALYS need to be re-executed.

d. Add Additional Frequencies for Solution

If additional frequencies need to be added to the solution, the problem is analyzed for the added frequencies and the results are combined using the module COMBIN.

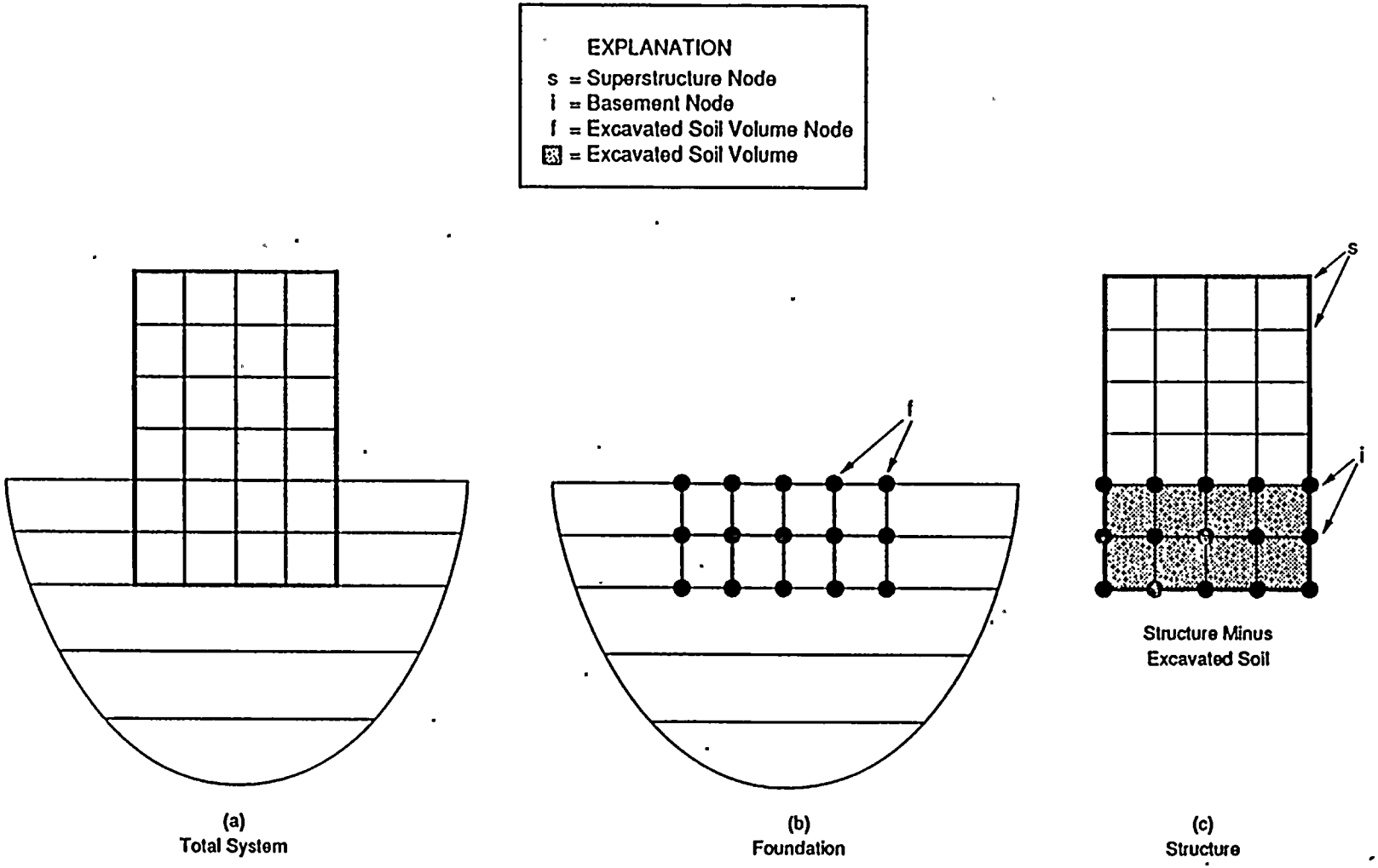

Figure 2.1-1. Substructuring in the Flexible Volume Method

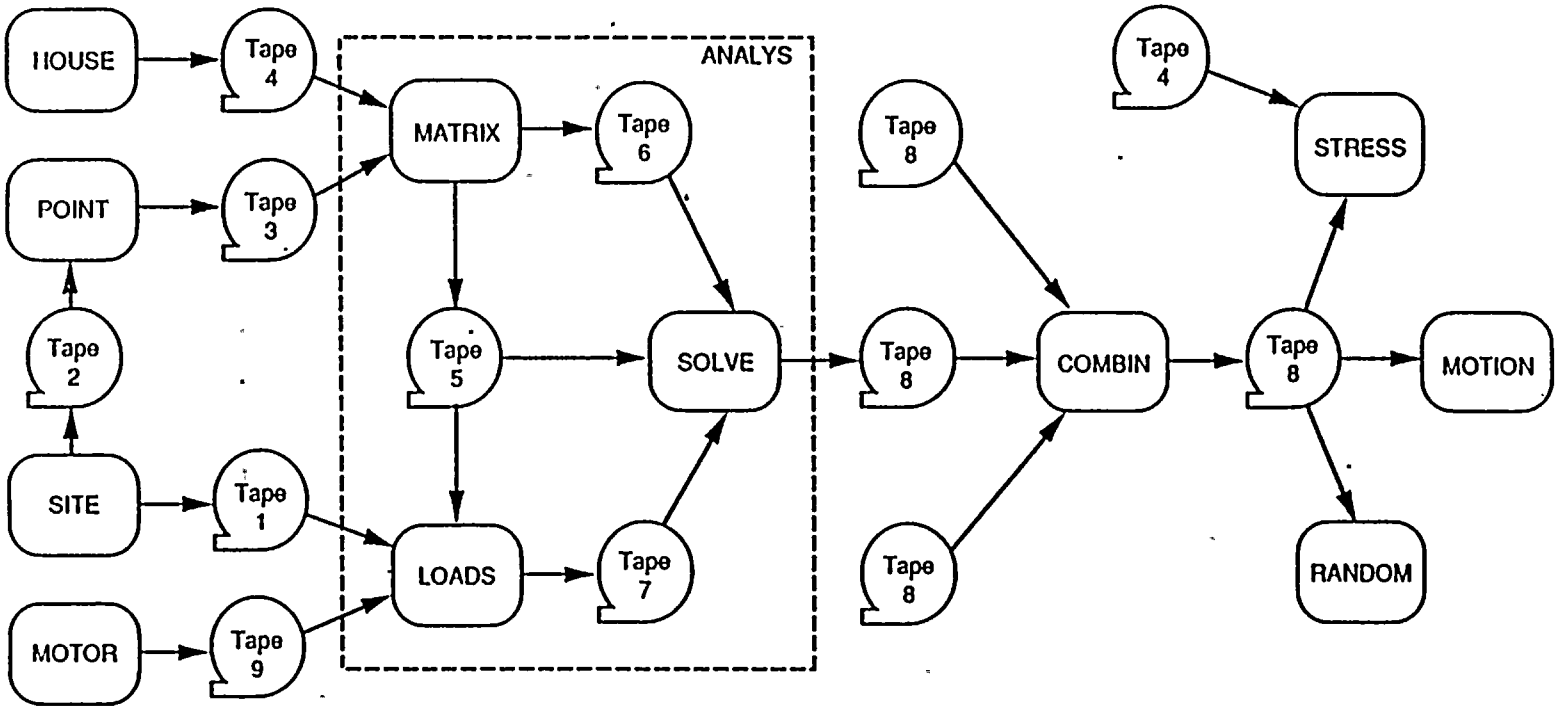

Figure 2.2-1. Layout of Computer Program SASSI

3 VALIDATION METHODS AND SCOPE

3.1 Validation Methods

The methods used to validate the capabilities of SASSI are in accordance with the methods used in the nuclear industry. Typically, for any validation test problem selected, the problem is modelled and analyzed using SASSI. The SASSI solution is then compared with the benchmark solution (basis of comparison) to assess the validity and accuracy of SASSI results. The basis of comparison is provided by one or more of the following methods:

a. Hand calculations are used for simple problems to provide the solution for cross-checking the results. The calculations when used are fully described.

b. Bechtel standard computer programs or comparable validated public domain programs are used to provide the solution for comparison. If Bechtel in-house program is used, the reference in made accordingly and the results are transferred from the in-house validation report. If an already validated public domain program is used, the analysis model is described and the results are transferred from the applicable validation report.

c. The analytical solutions obtained from the technical literature are used as the basis of comparison. This validation method is most extensively used for SASSI validations. An extensive effort is made to locate and select reference solutions from the literature for SASSI validations.

3.2 Capabilities Validated

SASSI as a general soil-structure interaction code, can handle a wide variety of SSI problems in two- and three-dimensions. It is applicable to the seismic excitation or forced vibration SSI analysis of above and under ground structures.

The capabilities of SASSI that have been validated in this report are described as follows:

A. Finite Element Calculations

Calculation of the dynamic properties such as mass, stiffness, and damping matrices of finite elements commonly used from the finite element library of SASSI are validated. Several simple models are constructed and the resultant displacement response (amplitude, phase angle, natural frequency) are computed and validated. In addition, the same problems are used to validate the element stress, strain, force and/or moment calculations. The problem numbers and reference solutions correponding to this catagory of validation test problems are shown in Table 3.2-1.

B. Impedance Analysis

The problems included in the impedance analysis cover a variety of soil model configurations (halfspace or layered system) with foundation rigidity ranging from totally rigid to partly rigid and to totally flexible properties. Two-dimensional and three-dimensional impedance analyses have both been considered. The validation test problems corresponding to this catagory are shown in Table 3.2-2.

C. Scattering Analysis

The validation test problems of scattering analysis are shown in Table 3.2-3. These problems cover a variety of surface and embedded foundations subjected to vertical and inclined body waves and surface waves.

D. SSI Analysis

Finally, to validate the accuracy of SASSI SSI analysis capability, a set of test problems are designed to compute the SSI response of single and multiple structures. These set of problems are identified in Table 3.2-4.

Table 3.2-1 Validated Capabilities of SASSI
(Finite Element Calculation)

Capability Validated	Validation Test Problem Number	Solution Reference Number
1. Force vibration displacement-response analysis (spring, beam, brick, plate elements)	11	3, 32
2. Force vibration force-response analysis (spring, beam, brick, plate elements)	10	2, 3

Table 3.2-1 Validated Capabilities of SASSI
(Impedance Analysis)

Tested Capability	Validation Test Problem Number	Solution Reference Number
1. Rigid Surface Foundation on Uniform Halfspace		
1.1 Circular Foundation	2, 19	20, 21, 29, 30, 34.
1.2 Strip Foundation	17	7
1.3 Ring Foundation	18	9
2. Rigid Surface Foundation on Layered System		
2.1 Circular Foundation	5	6
2.2 Strip Foundation	17	7
3. Flexible Surface Foundation on Uniform Halfspace		
3.1 Rigid-Flexible Foundation	7	8
3.2 Totally Flexible Foundation	12	10
4. Rigid Multiple Surface Foundations	8	11

Table 3.2-3 Validated Capabilities of SASSI
(Scattering Analysis)

Tested Capability	Validation Test Problem Number	Solution Reference Number
1. Vertically propagating Body Waves		
1.1 Free-Field	1	4
1.2 Embedded Foundations		
1.2.1 Halfspace System	6	14
1.2.2 Layered System	15	15
2. Inclined Body Waves		
2.1 Surface Foundation	4	12
2.2 Embedded Foundation		
2.2.1 Rigid Cylinder	6	14
2.2.2 Rigid Cube	13	16
3. Surface Waves		
3.1 Free-Field	20	5
3.2 Surface Foundation	4	13
3.3 Embedded Foundation	16	17

Table 3.2-4 Validated Capabilities of SASSI
(SSI Analysis)

Tested Capability	Validation Test Problem Number	Solution Reference Number
1. Seismic Response		
1.1 Surface Foundation	2	20-24, 31
1.2 Embedded Foundation	9	24-25
1.3 Multiple Surface Foundation		
1.3-1 3-D Analysis	14	26
1.3-2 2-D Analysis	14	26
2. Forced Excitation Response	3	18

4. SUMMARY OF VALIDATION TEST PROBLEMS AND RESULTS

In this section a brief summary of validation test problems and their results as compared to benchmark solutions are presented. The detailed descriptions on the validation test problems and comparison of results are presented in Appendix A.

4.1 Validation Test Problem No. 1

Description

The free-field analyses of an halfspace subjected to vertically propagating SV- and P-Wave are considered. The halfspace model shown in Fig. 4.1-1 is used. The results at surface and at various points at depth are compared with the closed form solution obtained from the general solution in Ref. 4.

Results

The results of analysis at 3 frequencies (1, 5 and 15 Hz) are compared with the corresponding closed form solutions in Table 4.1-1. The good agreement between the SASSI results and the closed form solutions validates the free-field analysis capability of SASSI for vertical SV- and P-waves.

4.2 Validation Test Problem No. 2

Description

SSI response of a containment building subjected to vertically propagating SV is computed. The containment model obtained from Ref. 20 is shown in Fig. 4.2-1. The acceleration response spectrum of input motion is shown in Fig. 4.2-2. In performing the analysis, first the impedance functions of foundation are computed and the results are compared with the solution provided in Refs. 20 and 21.

Results

The horizontal and rocking stiffness and damping coefficients are compared with the reference solution in Figs. 4.2-3 thru 4.2-6. As shown the results are in good agreement. The SSI response, in terms of 2% acceleration response spectrum at the top of the internal structure are compared in Fig. 4.2-7. The reference solution has been obtained using the Bechtel in-house computer program FASS (Ref. 23) using the frequency dependent impedance functions from SASSI. As shown both results are in good agreement. The good agreement between the results of this problem and the reference solution validates the impedance and SSI calculation capabilities of SASSI for structures on surface foundations.

4.3 Validation Test Problem No. 3

Description

Displacement response of rigid disk on the surface of an elastic halfspace subjected to vertical trapezoidal pulse is computed. The model and the pulse load time history are shown in Figure 4.3-1. The results are compared with the solution provided by Lysmer in Ref. 18.

Results

The result of analysis in terms of vertical displacement time history of the response is compared with the reference solution in Figure 4.3-2. The good agreement between the results and the reference solution validates the SSI calculation capability of SASSI for structures subjected to external dynamic loading.

4.4 Validation Test Problem No. 4

Description

The scattering response of a rigid massless square foundation on the surface of an elastic halfspace subjected to inclined SH-, SV-, and P-Waves and Rayleigh wave is computed. The model is shown in Fig. 4.4-1. The results are compared with the solution provided by Wong and Luco in Refs. 12 and 13.

Results

The results of the analysis for the case of SH-Wave are compared with the reference solution in terms of the scattering matrix coefficients in Fig. 4.4-2. The normalized horizontal and vertical foundation displacements for SV- and P-Wave cases are compared with reference solution in Fig. 4.4-3 and 4.4-4. The response for the case of Rayleigh wave is compared in Fig. 4.4-5. As shown, the results of all cases are in good agreeement with the reference solutions. The good agreement shown validates the scattering calculation capability of SASSI for surface foundations subjected to inclined SH-, SV- and P-waves and surface Rayleigh wave.

4.5 Validation Test Problem No. 5

Description

The impedance functions of a circular foundation on a layered system (Fig. 4.5-1) in horizontal, vertical, and rocking modes of vibration are computed. The results are compared with the solution provided by Luco (Ref. 6).

Results

The stiffness and damping coefficients corresponding to vertical, horizontal, and rocking modes of vibration are compared with the reference solution in Figs. 4.5-2, 4.5-3, and 4.5-4, respectively. The comparison shows good agreement within the frequency limit of the mesh size. Beyond this frequency limit, the agreement is not as good as expected. This shows the importance of the model mesh size

frequency limit. The good agreement between the two solutions validates the impedance calculation capability of SASSI for surface foundations on layered systems.

4.6 Validation Test Problem No. 6

Description

The scattering response of a rigid massless cylinder fully embedded in elastic halfspace and subjected to: 1) Vertically propagating SV-wave; 2) horizontally propagating SH-wave is computed. The foundation model is shown in Figure 4.6-1. The results are compared with the solution reported by Day (Ref. 14).

Results

Normalized rocking and horizontal translation of the foundation subjected to vertically propagating SV-Wave are compared with the reference solution in Fig. 4.6-2. Normalized horizontal translation and torsional response of foundation subjected to horizontally propagating SH-Wave are compared with the reference solution in Fig. 4.6-3. As shown, the results are in good agreement with the reference solution. The good agreement shown validates the scattering analysis capability of SASSI for embedded foundations subjected to SV- and SH-waves.

4.7 Validation Test Problem No. 7

Description

The stiffness and damping coefficients of a rigid-flexible surface foundation shown in Fig. 4.7-1 in vertical and rocking modes of vibration are computed. The results are compared with the solution reported by Iguchi et al, (Ref. 8).

Results

The impedance coefficients in vertical and rocking modes of vibration are compared with the reference solutions in Fig. 4.7-2 and 4.7-3, respectively. As shown, both results are in good agreement. The good agreement shown validates the impedance calculation capability of SASSI for flexible foundations.

4.8 Validation Test Problem No. 8

Description

The impedance functions of 2 rigid square foundations resting side-by-side on the surface of a viscoelastic halfspace are computed. The model is shown in Fig. 4.8-1. The results of analysis are compared with the solution provided Wong et al in Ref. 11.

Results

The impedance functions in terms of the degrees of freedom defined in Fig. 4.8-1 are compared in Figs. 4.8-2 through 4.8-5. The results are computed in terms of impedance functions of one the foundations (foundation 1) and the coupling impedance functions between the 2 foundations. In general, SASSI results and the reference solution are in good agreement especially for larger on-diagonal components of impedance functions. The discrepancies occur for relatively small off-diagonal components of the impedance functions. These differences, however, have insignificant effect in the final SSI response due to their small numerical values. The good agreement between the two results in general, validates the impedance calculation capability of SASSI for multiple surface foundations.

4.9 Validation Test Problem No. 9

Description

The SSI responses of an embedded containment building subjected to: 1) Rayleigh; 2) vertically propagating SV- and P-waves are computed. The containment model and site soil profile are shown in Figs. 4.9-1 and 4.9-2, respectively. The acceleroation time history of input motion and its corresponding 2% response spectrum are shown in Figs. 4.9-3 and 4.9-4, respectively. The model properties and the input motions are similar to those used in Ref. 24.

Results

The results of SASSI analysis are compared with the results obtained from CLASSIF (Ref. 25) analysis. In CLASSIF analysis, the foundation is assumed to rest on the surface of the soil layer system since CLASSIF program capability is limited to analysis of structures with surface foundation configuration. The results of analysis for the case of Rayleigh wave analysis in terms of horizontal acceleration response spectrum at the top of the foundation, top of the containment and top of internal structure are compared in Figs. 4.9-5, 4.9-6 and 4.9-7, respectively. The corresponding vertical response are compared in Figs. 4.9-8 through 4.9-10. Similarly, the results for the use of SV+P wave analysis are compared in Figs. 4.9-11 through 4.9-16. As shown, the SASSI and CLASSIF results are in-good agreement. Small discrepancy in the results is due to the fact that in CLASSI analysis, foundation embedded cannot be considered and surface foundation configuration is assumed. The consistency shown contributes confidence to both results.

4.10 Validation Test Problem No. 10

Description

A series of simple problems using the spring, beam, brick and plate elements are analyzed. The models are shown in Fig. 4.10-1 through

4.10-5. The results in terms of the amplitude of the force are obtained and compared with the solutions in Refs. 2 and 32.

Results

The results of analysis for spring, beam, and brick elements are compared with the closed form solutions in Table 4.10-1. The results for the plate element are compared in Fig. 4.10-6. As shown the results are in good agreement. The good agreement shown validates the accuracy of the stress, force and moment calculations in the elements considered from the finite element library of SASSI.

4.11 Validation Test Problem No. 11

Description

A series of simple problems similar to those used in validation test problem No. 10 are analyzed to compute the amplitude and phase angle of the response at various frequencies. The results are compared with the closed form solution in Refs. 2 and 3.

Results

The comparison of the results for one typical test case is shown in Fig. 4.11-1. The comparison of the results for other test cases is described in Appendix A, Section A.11. The comparison of the results for all cases shows good agreement between the SASSI solutions and the closed from solutions.

4.12 Validation Test Problem No. 12

Description

The displacement response of flexible plate resting on the surface of an elastic halfspace subjected to: 1) Uniformly distributed vertical harmonic load; 2) vertical point load at the center are

computed. The model is shown in Fig. 4.12-1. The results are compared with the solution provided by Whittaker, et al (Ref. 10).

Results

The response of the foundation at different locations of the mat for uniform and point loading are compared with the reference solution in Figs. 4.12-2 and 4.12-3, respectively. As shown, both results are in good agreement. The good agreement shown validates the impedance calculation capability of SASSI for flexible foundations.

4.13 Validation Test Problem No. 13

Description

The scattering response of an embedded massless rigid cube subjected to inclined SH-Wave with angles of incidence of 90 degree and 45 degree from vertical are computed. The model is shown in Fig. 4.13-1. The results are compared with the solution provided by Dominguez, et al (Ref. 16).

Results

The results of analysis in terms of the normalized translation, rocking, and torsion of the foundation are compared with the reference solution in Figs. 4.13-2, 4.13-3 and 4.13-4, respectively. As shown, both results are in good agreement. The good agreement shown validates the scattering analysis capability of SASSI for embedded foundations subjected to SH-waves.

4.14 Validation Test Problem No. 14

Description

The SSI response of 2 structures resting side-by-side on the surface of a layered soil system is computed. The analysis is performed

using the two- and three-dimensional capability of SASSI. The SSI models are shown in Figs. 4.14-1 and 4.14-2. The results of analysis are compared with the FLUSH (Ref. 26) results. The model used in FLUSH analysis is shown in Fig. 4.14-3. The input motion consits of vertically propagating SV-Wave with control point defined at the grade level. The response spectrum of input motion is shown in Fig. 4.14-4.

Results

The results of analysis from the SASSI 2-D, 3-D, and FLUSH analysis are compared in Fig. 4.14-5. FLUSH and SASSI 3-D analysis are in good agreement. The SASSI 2-D analysis results compare reasonably well with the FLUSH results. As expected, the SASSI 2-D responses are larger because the 2-D analysis is a plane strain analysis and does not simulate the 3-D effect as does the FLUSH analysis.

4.15 Validation Test Problem No. 15

Description

The scattering response of a rigid massless cylinder fully embedded in a layered system and subjected to vertically propagating SV-wave is computed. The model is shown in Fig. 4.15-1. The results of analysis are compared with the solution provided by Kausel, et al (Ref. 15).

Results

The results of analysis in terms of the normalized translation and rocking of the foundation are compared with the reference solution in Figs. 4.15-2 and 4.15-3, respectively. The good agreement between the results shown validates the scattering analysis capability of SASSI for embedded foundations in layered systems.

4.16 Validation Test Problem No. 16

Description

The scattering response of rigid massless cylinder fully embedded in an elastic halfspace and subjected to surface Rayleigh wave is computed. The model is shown in Fig. 4.16-1. The results of analysis is compared with the solution provided by Iguchi (Ref. 17).

Results

The results of analysis in terms of horizontal and vertical translation and rocking rotation of the foundation are compared with the reference solution in Fig. 4.16-2. The good agreement shown between the results validates the scattering analysis capability of SASSI for embedded foundations subjected to Rayleigh waves.

4.17 Validation Test Problem No. 17

Description

The compliance functions of a strip footing on the surface of a viscoelastic halfspace and a soil layered system in vertical mode of vibration are computed. The analysis models are shown in Figs. 4.17-1 and 4.17-2 for the case of halfspace and soil layered system, respectively. The results are compared with the solution provided by Gazetas, et al (Ref. 7).

Results

The results of analysis in terms of the real and imaginary parts of the compliance functions are compared with the reference solution in Figs. 4.17-3 and 4.17-4 for halfspace and soil layered system, respectively. Small discrepancies occurs at frequency ratio of 1.9 in the case of the layered soil system. These are considered to be due to the sensitivity of solutions at the soil layer frequencies

caused by the differences in the analytical solution techniques used in the two solutions. These discrepancies are not expected to affect the final SSI results. As shown in Figs. 4.17-3 and 4.17-4, the results are in good agreement, except the discrepancies noted. The favorable agreement between the SASSI analysis results and the reference solution validates the impedance analysis capability of SASSI for impedance analysis of strip foundations on uniform halfspace and layered systems.

4.18 Validation Test Problem No. 18

Description

The compliance and impedance functions of a ring foundation on the surface of an elastic halfspace in vertical mode of vibration are computed. The model is shown in Fig. 4.18-1. The results are compared with the solution provided by Veletsos, et al (Ref. 9).

Results

The results of analysis in terms of real and imaginary parts of the compliance functions are compared in Fig. 4.18-2. The corresponding stiffness and damping coefficients are compared in Fig. 4.18-3. As shown in Figs. 4.18-2 and 4.18-3, the results are in good agreement. The good agreement shown validates the impedance analysis capability of SASSI for ring foundations.

4.19 Validation Test Problem No. 19

Description

The compliance functions of a rigid circular foundation on the surface of an elastic halfspace in horizontal, vertical, rocking and torsional modes of vibration are computed. The model is shown in Fig. 4.19-1. The results of analysis are compared with the solution provided by Veletsos, et al (Refs. 29, 30, 34).

Results

The results of analyses in terms of horizontal, vertical and rocking compliance functions are compared in Fig. 4.19-2. Torsional compliance functions are compared in Fig. 4.19-3. The good agreement between the results shown above validates the impedance calculation capability of SASSI for surface foundations.

4.20 Validation Test Problem No. 20

Description

The free-field response of a layered soil system subjected to surface Love wave is computed. The free-field soil system is shown in Fig. 4.20-1. The results of analysis is compared with the solution provided by Wolf, et al (Ref. 5).

Results

The results of analysis in terms of the amplification of the top soil layer and variation of motion with depth at several frequencies are compared with the reference solution in Fig. 4.20-2. The good agreement shown validates the free-field response analysis capability of SASSI for surface Love waves.

Table 4.1-1 Comparison of SASSI Results and Closed Form Solutions (Validation Test Problem No. 1)

(f = 1.0 Hz)

Depth (ft)	CLOSED FORM SV-Wave	CLOSED FORM P-Wave	SASSI RESULTS SV-Wave	SASSI RESULTS P-Wave
.01	1.000	1.000	1.000	1.000
10	.998	1.000	.998	.999
20	.992	.998	.992	.998
30	.982	.996	.982	.996
40	.969	.992	.969	.992
50	.951	.988	.951	.988
60	.930	.982	.930	.982

(f = 5.0 Hz)

Depth (ft)	CLOSED FORM SV-Wave	CLOSED FORM P-Wave	SASSI RESULTS SV-Wave	SASSI RESULTS P-Wave
.0	1.000	1.000	1.000	1.000
10	.951	.988	.951	.988
20	.809	.951	.809	.951
30	.588	.891	.588	.891
40	.309	.809	.309	.809
50	.000	.707	.000	.707
60	.309	.588	.309	.588

(f = 15.0 Hz)

Depth (ft)	CLOSED FORM SV-Wave	CLOSED FORM P-Wave	SASSI RESULTS SV-Wave	SASSI RESULTS P-Wave
.0	1.000	1.000	1.000	1.000
10	.588	.891	.586	.891
20	-.309	.588	-.312	.588
30	-.951	.156	-.952	.156
40	-.809	-.309	-.805	-.309
50	.000	-.707	-.008	-.707
60	.809	-.951	.815	-.951

Table 4.10-1 Comparison of SASSI Results and Closed Form Solutions

	CLOSED FORM	SASSI
Spring Element (axial force)	1.00	1.001
Beam Element (base moment)	.549	.548
Beam Element-End Release (base shear)	.549	.548
Brick Element (normal stress)	25.04	25.05

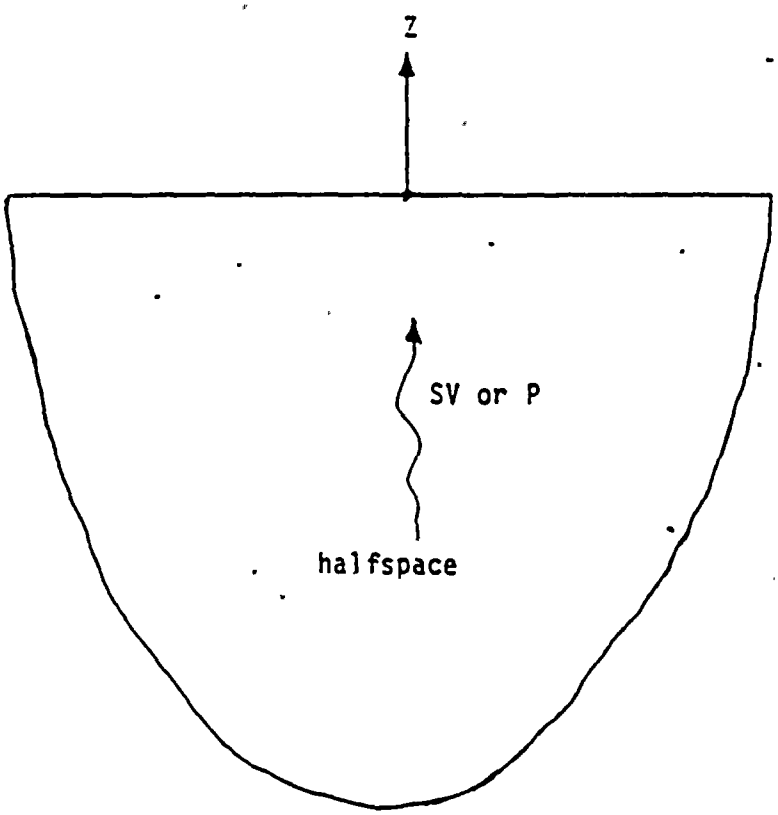

Figure 4.1-1. Halfspace Model for Closed Form Solution

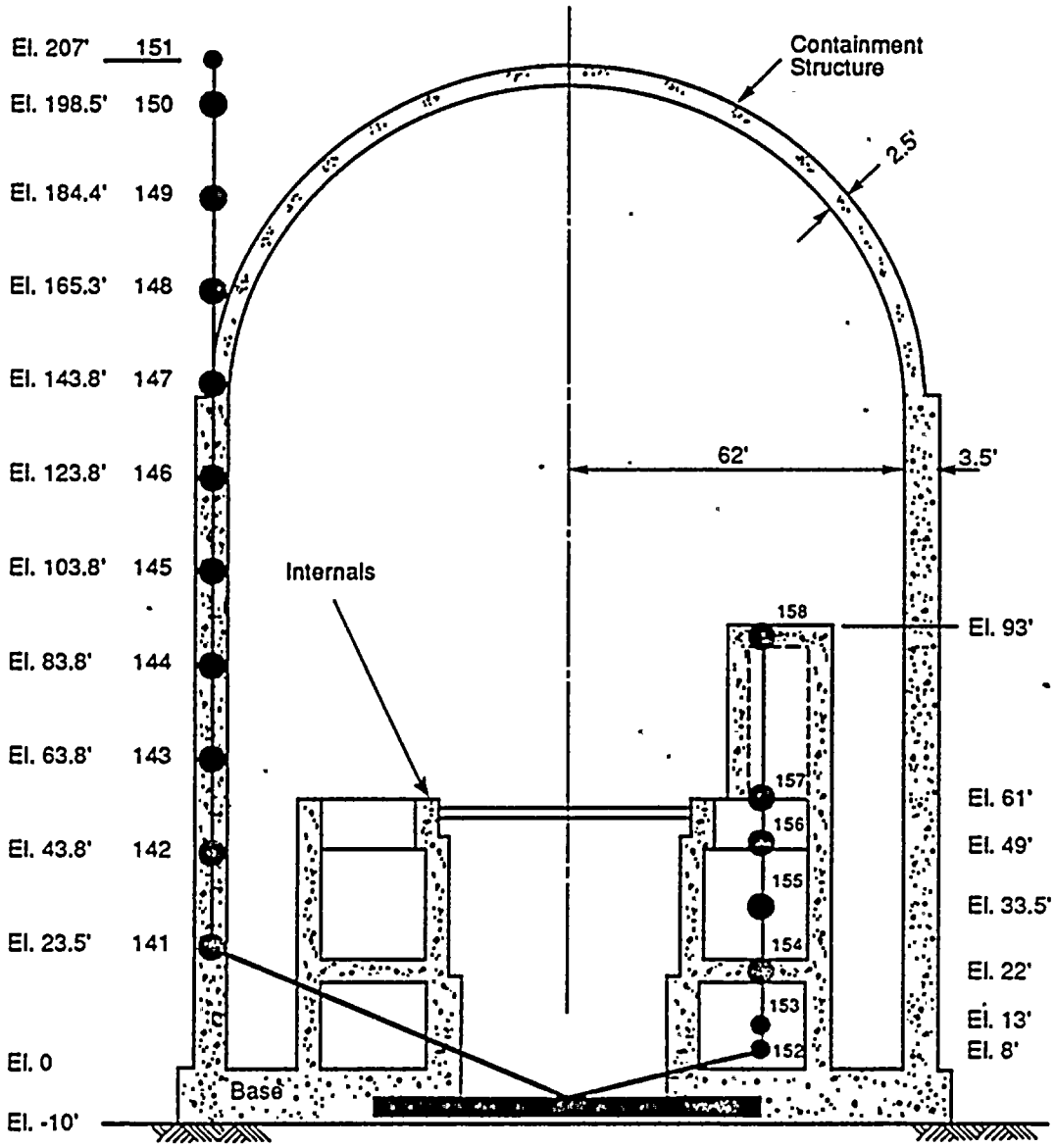

Figure 4.2-1. Lumped-Mass Stick Models of the Containment and Internal Structures

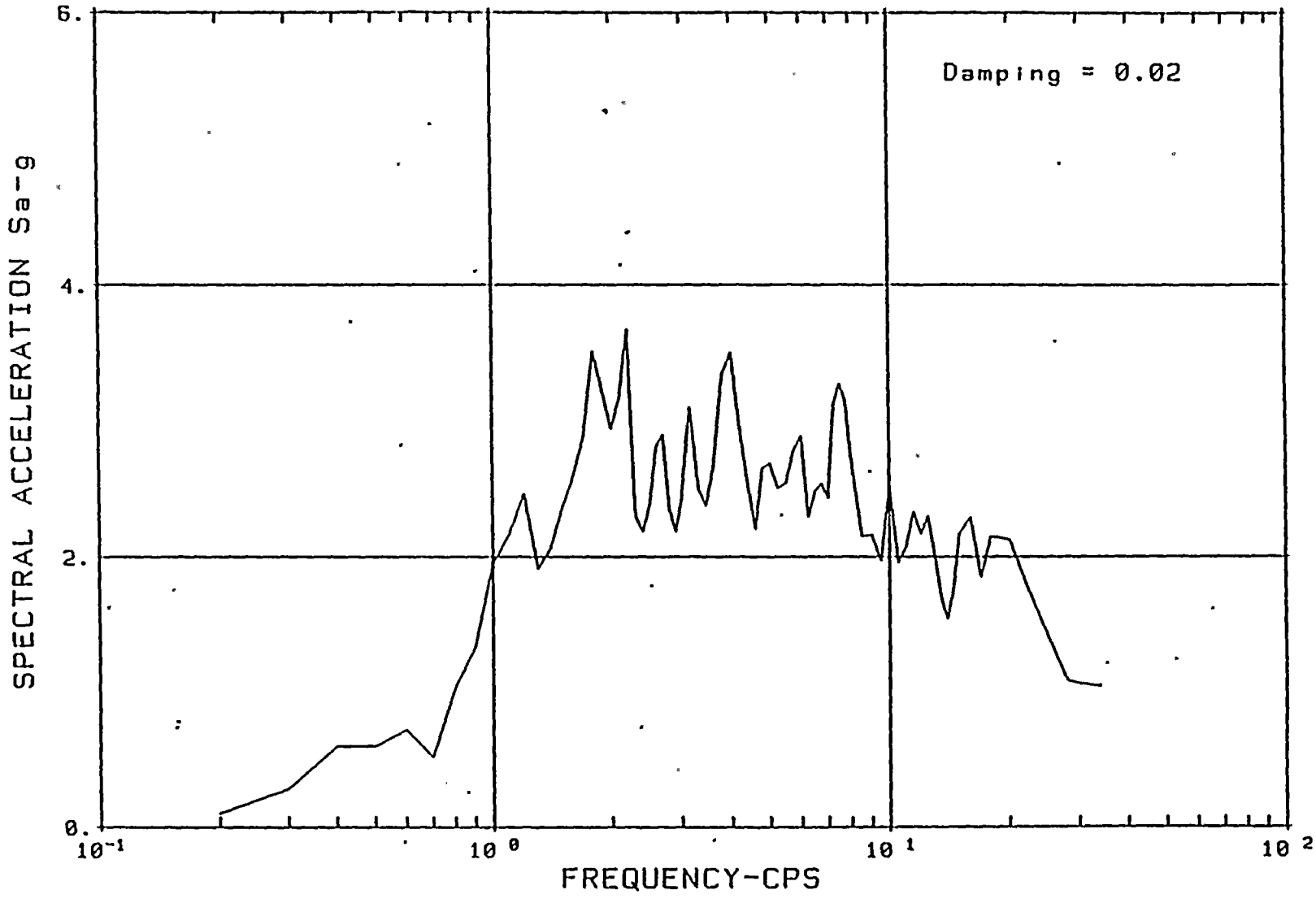

Figure 4.2-2. Acceleration Response Spectra of El. Centro 1940 - NS Component

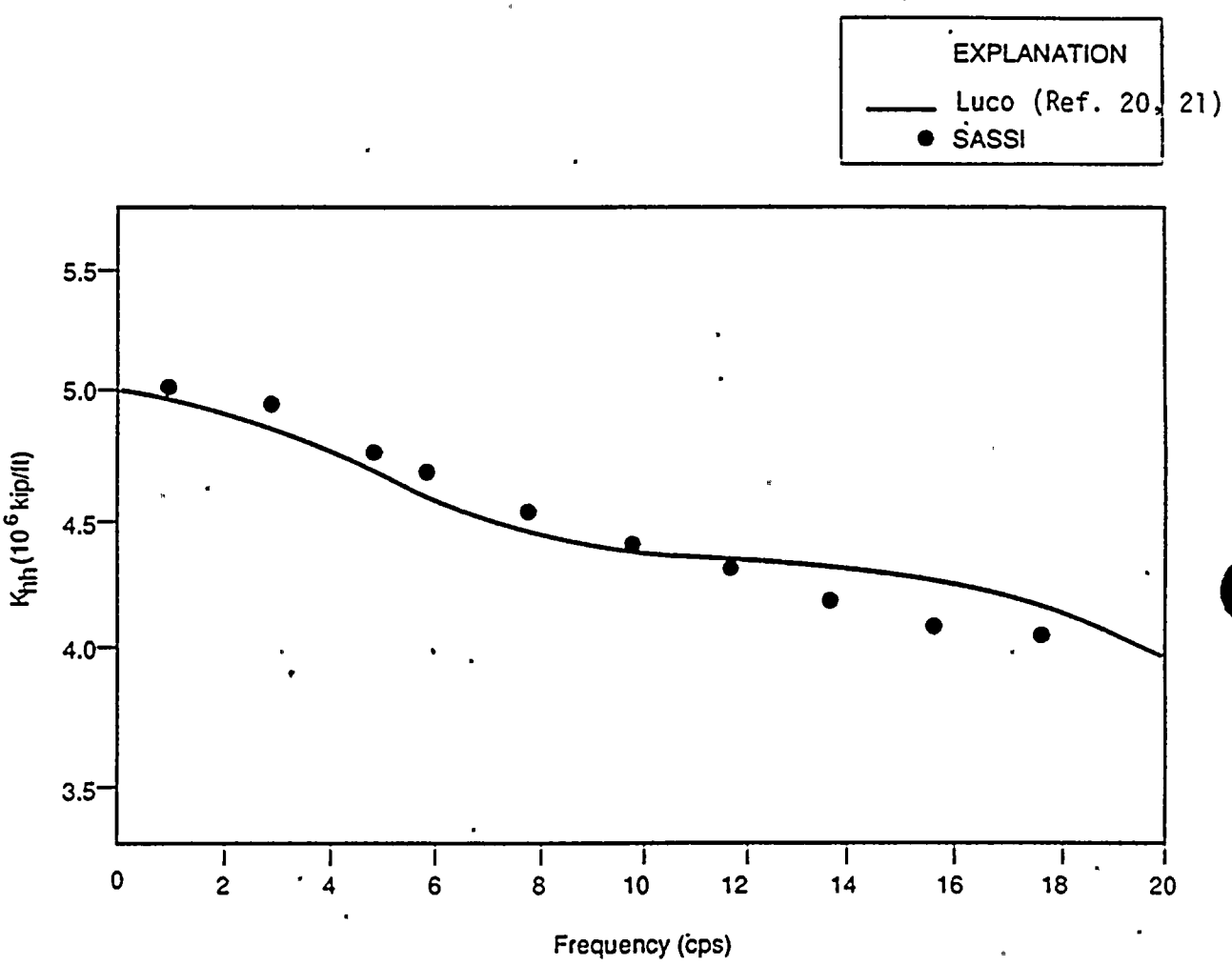

Figure 4.2-3. Horizontal Stiffness Coefficients

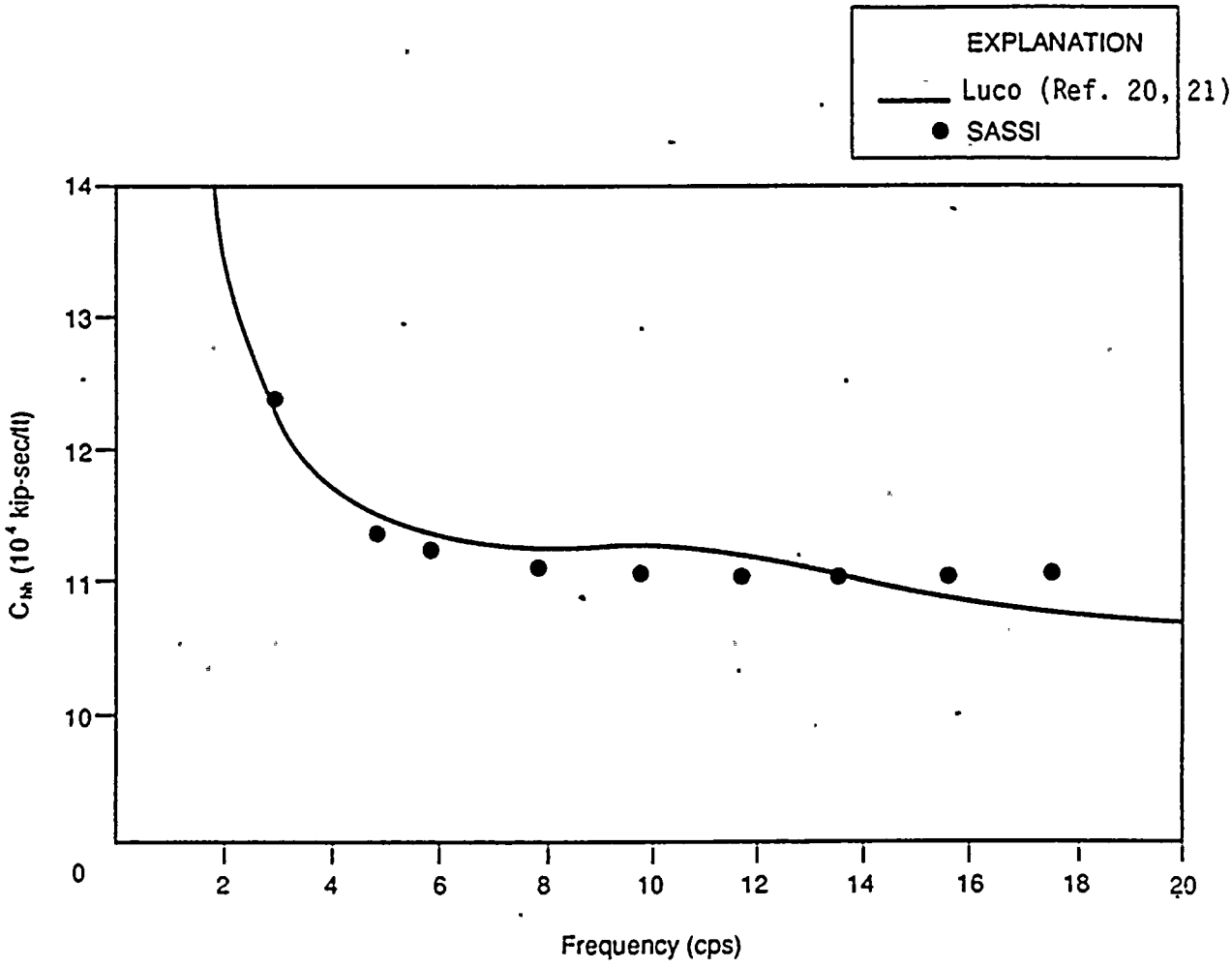

Figure 4.2-4. Horizontal Damping Coefficients

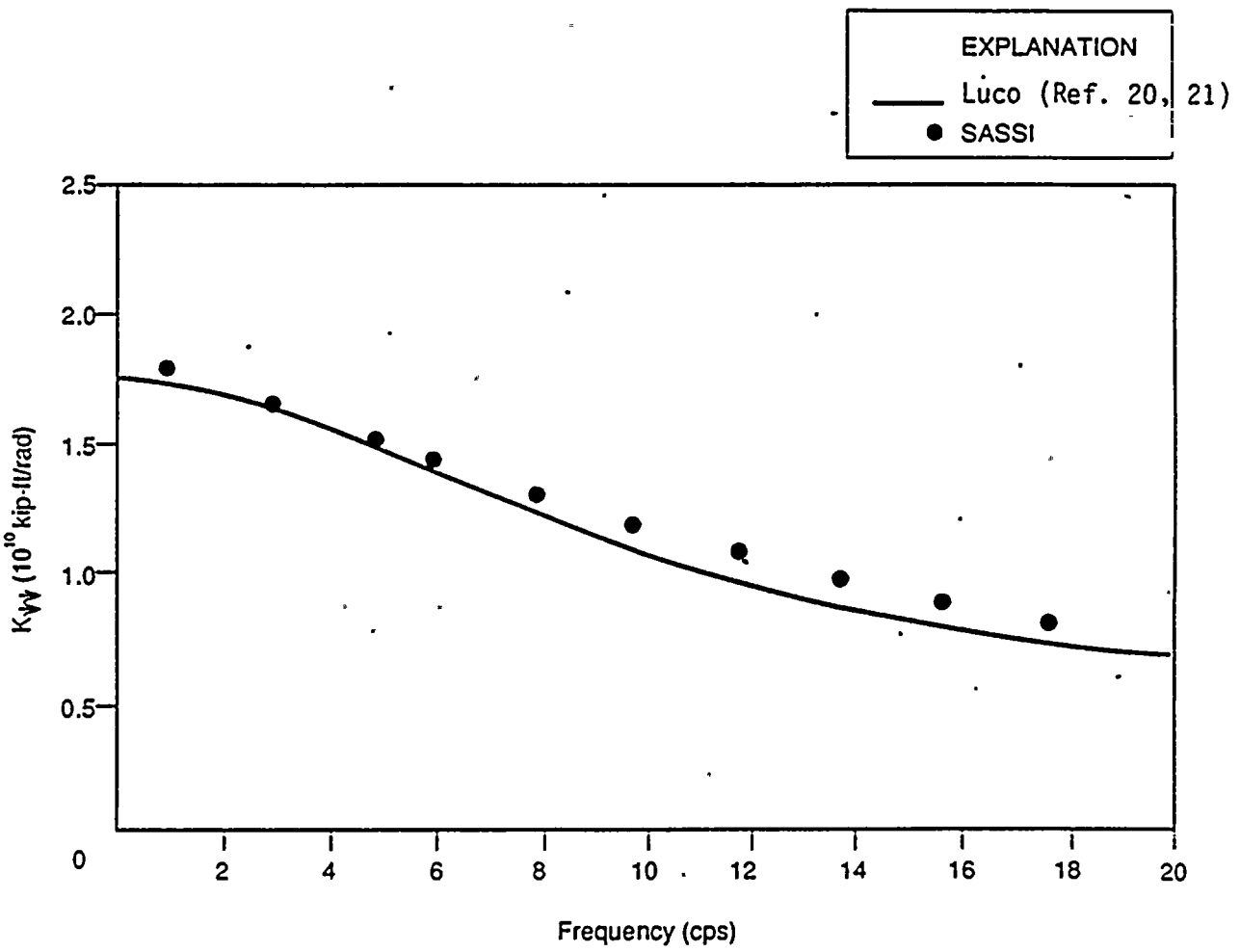

Figure 4.2-5. Rocking Stiffness Coefficients

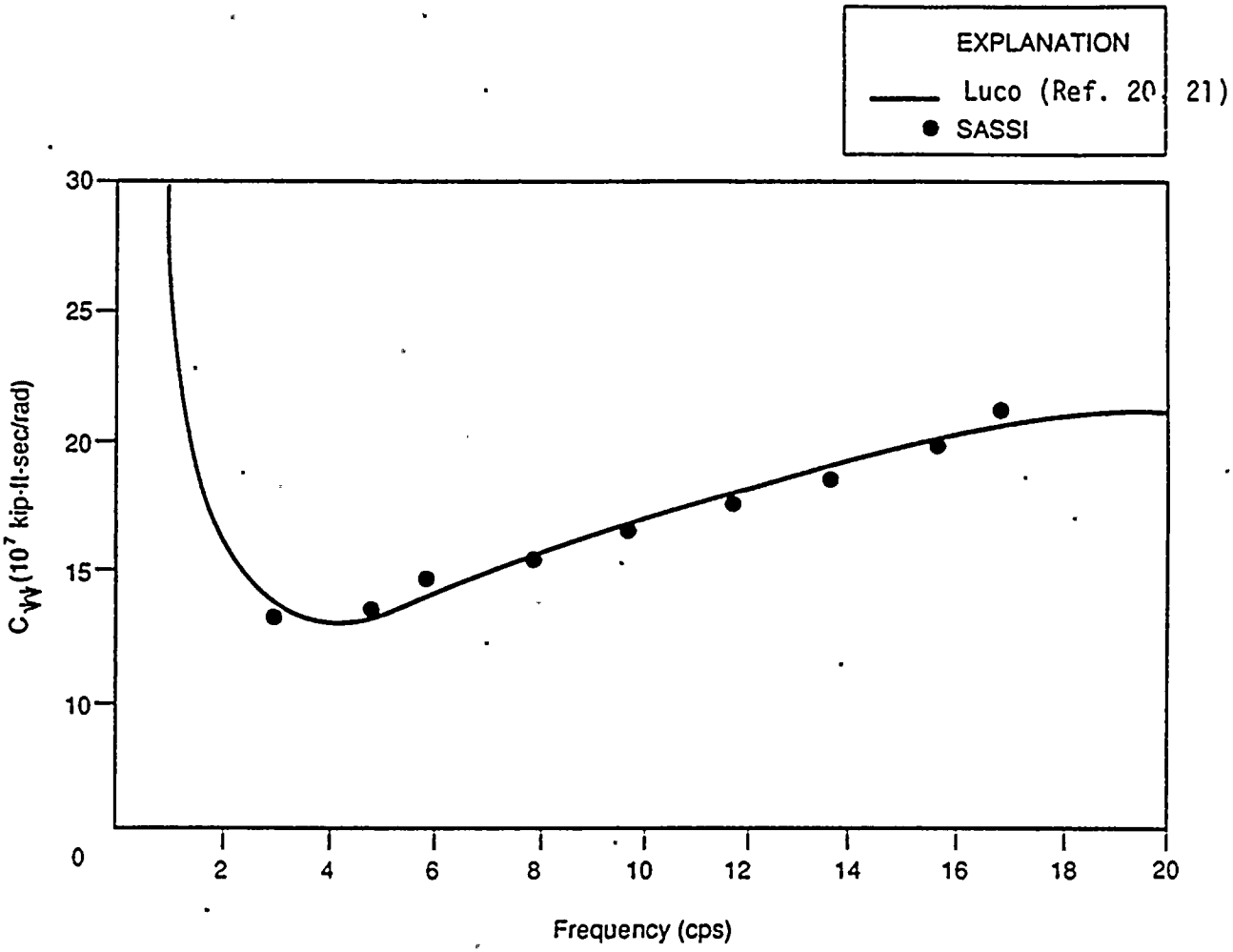

Figure 4.2-6. Rocking Damping Coefficients

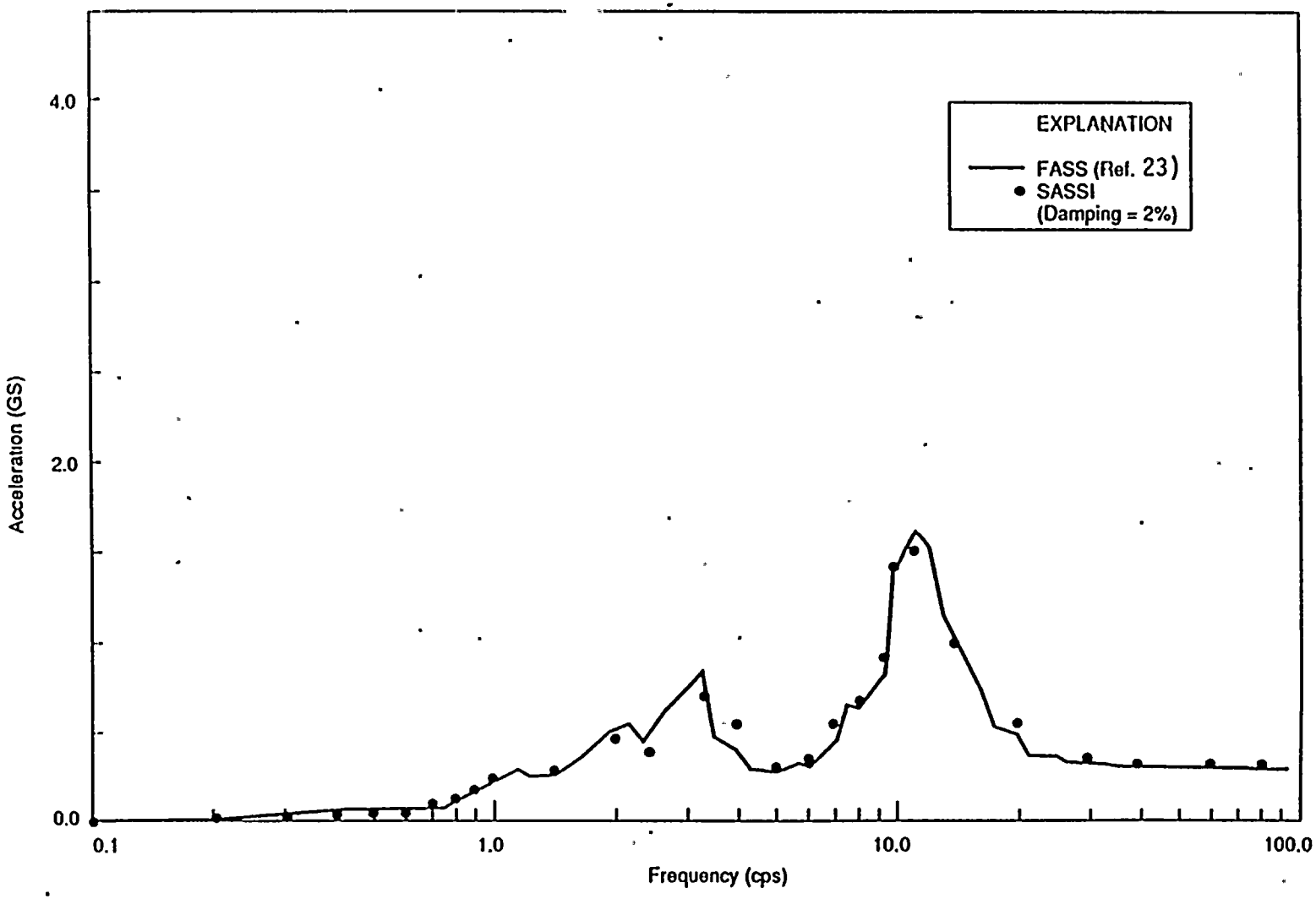

Figure 4.2-7. Absolute Acceleration Response at Top of Internal Structure

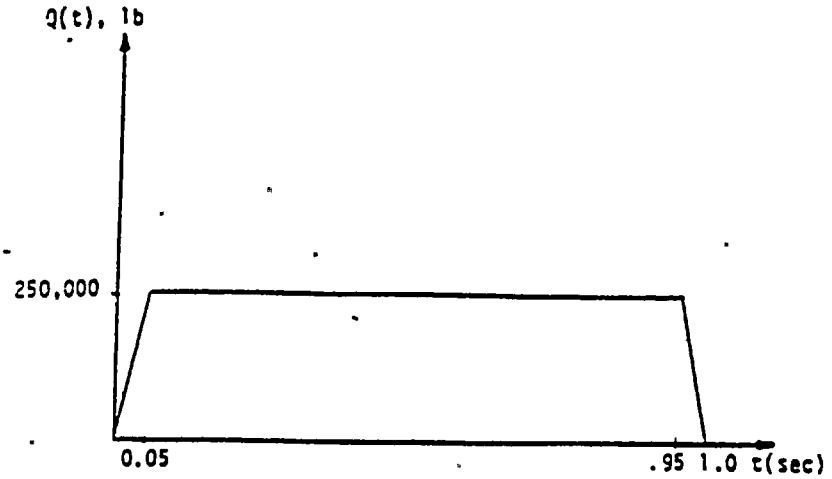

Pulse Load Time History

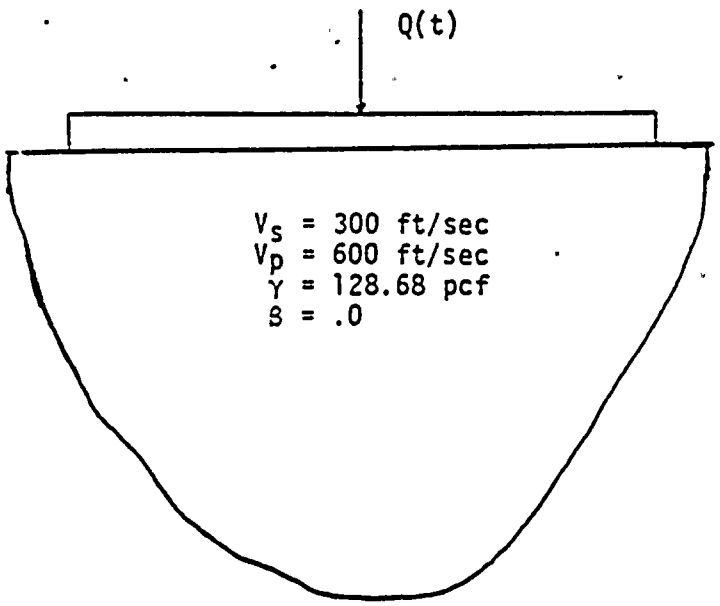

Figure 4.3-1. Foundation Model

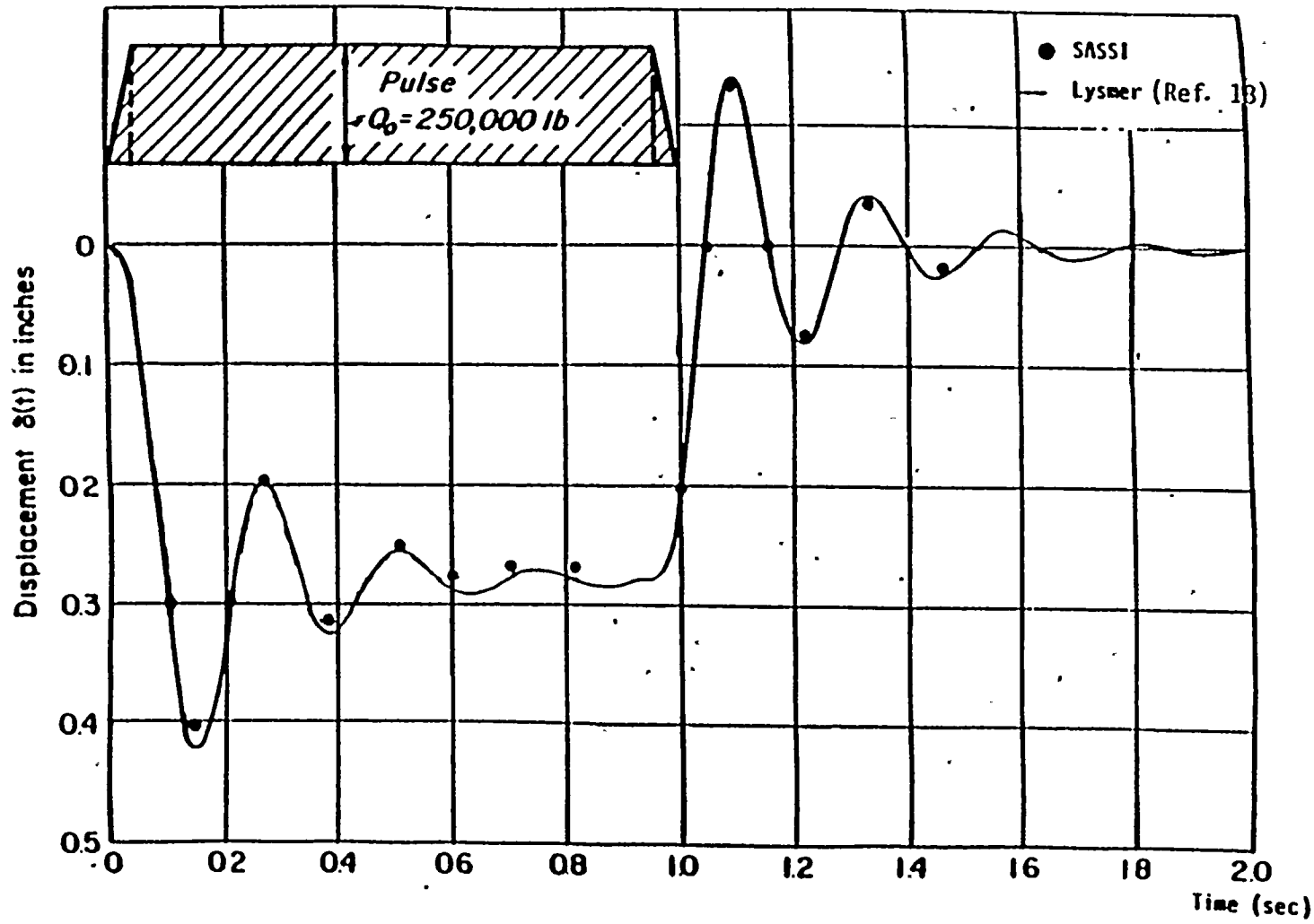

Figure 4.3-2. Response Curve for Trapezoidal Pulse

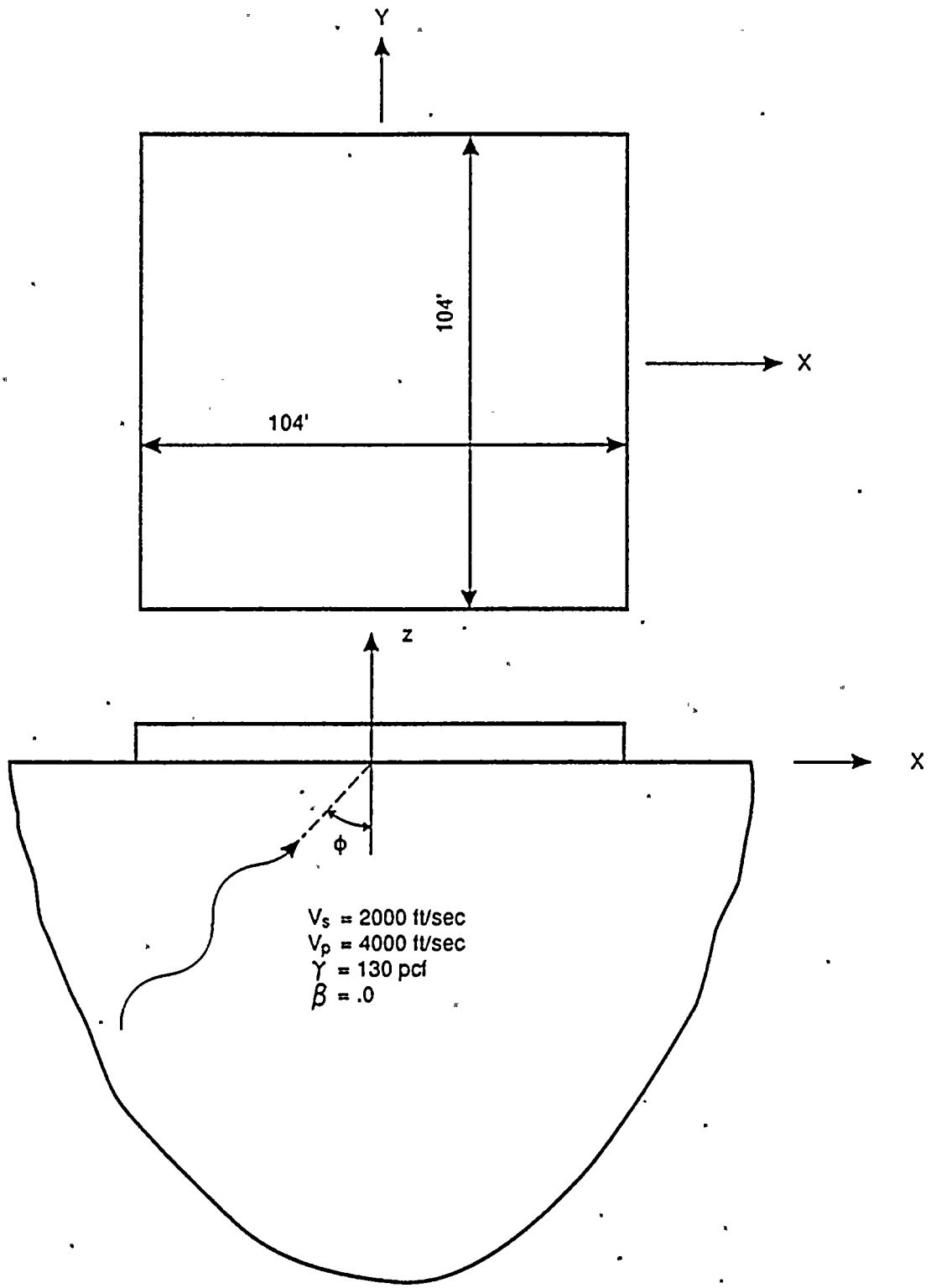

Figure 4.4-1 Foundation Model

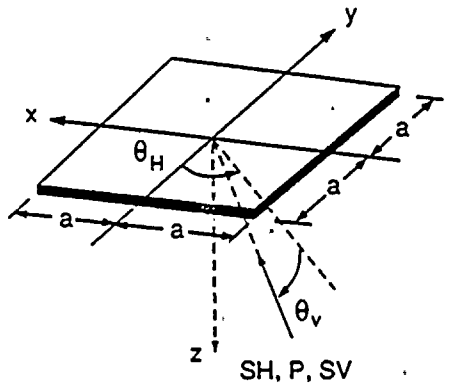

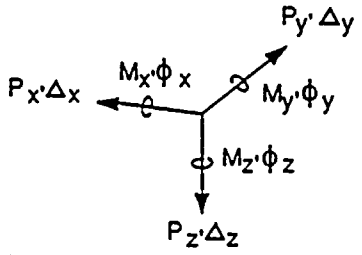

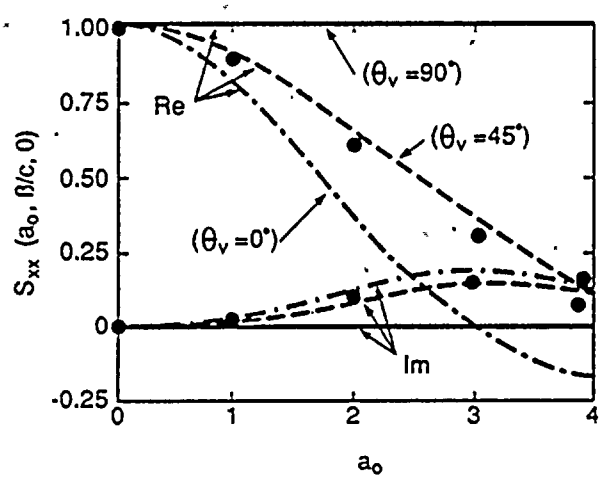

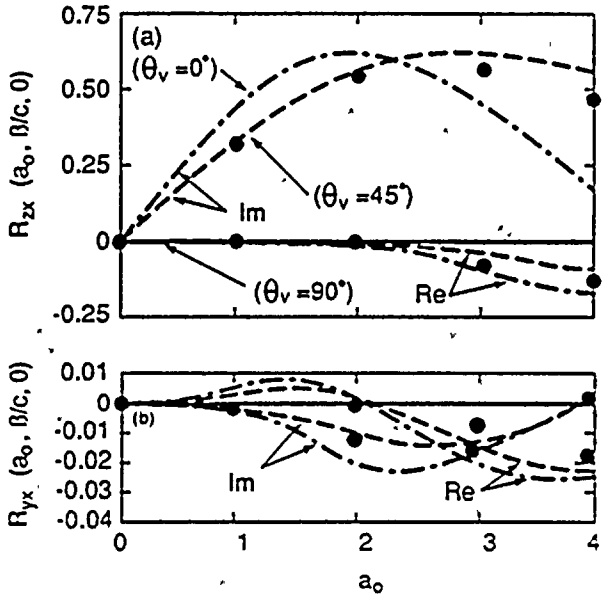

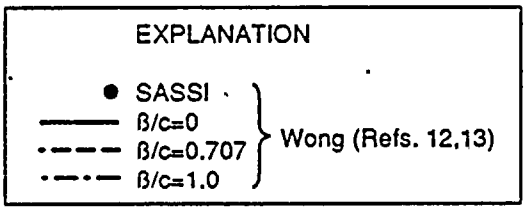

Figure 4.4-2. Response to Inclined SH-Wave

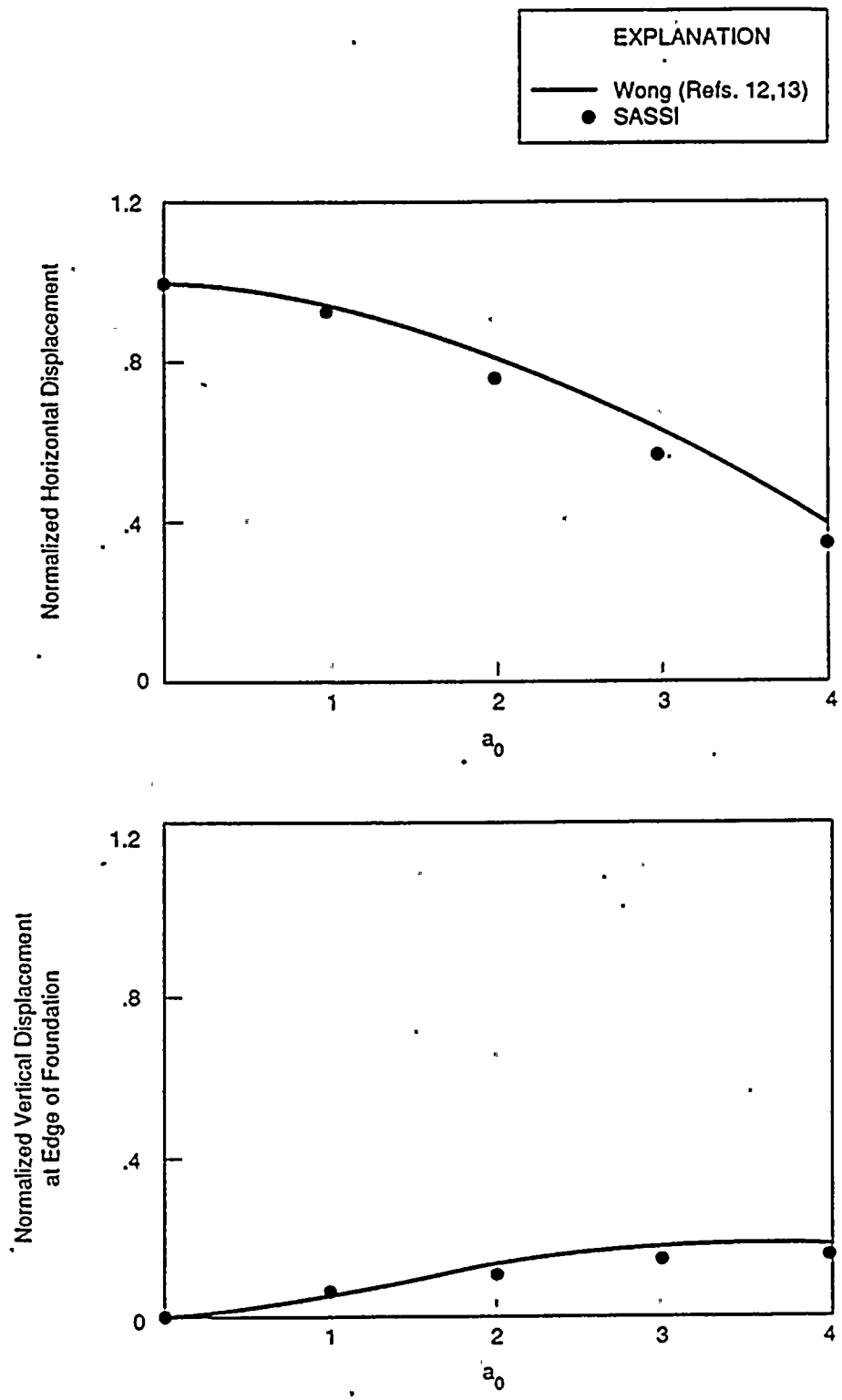

Figure 4.4-3. Response to Inclined SH-Wave

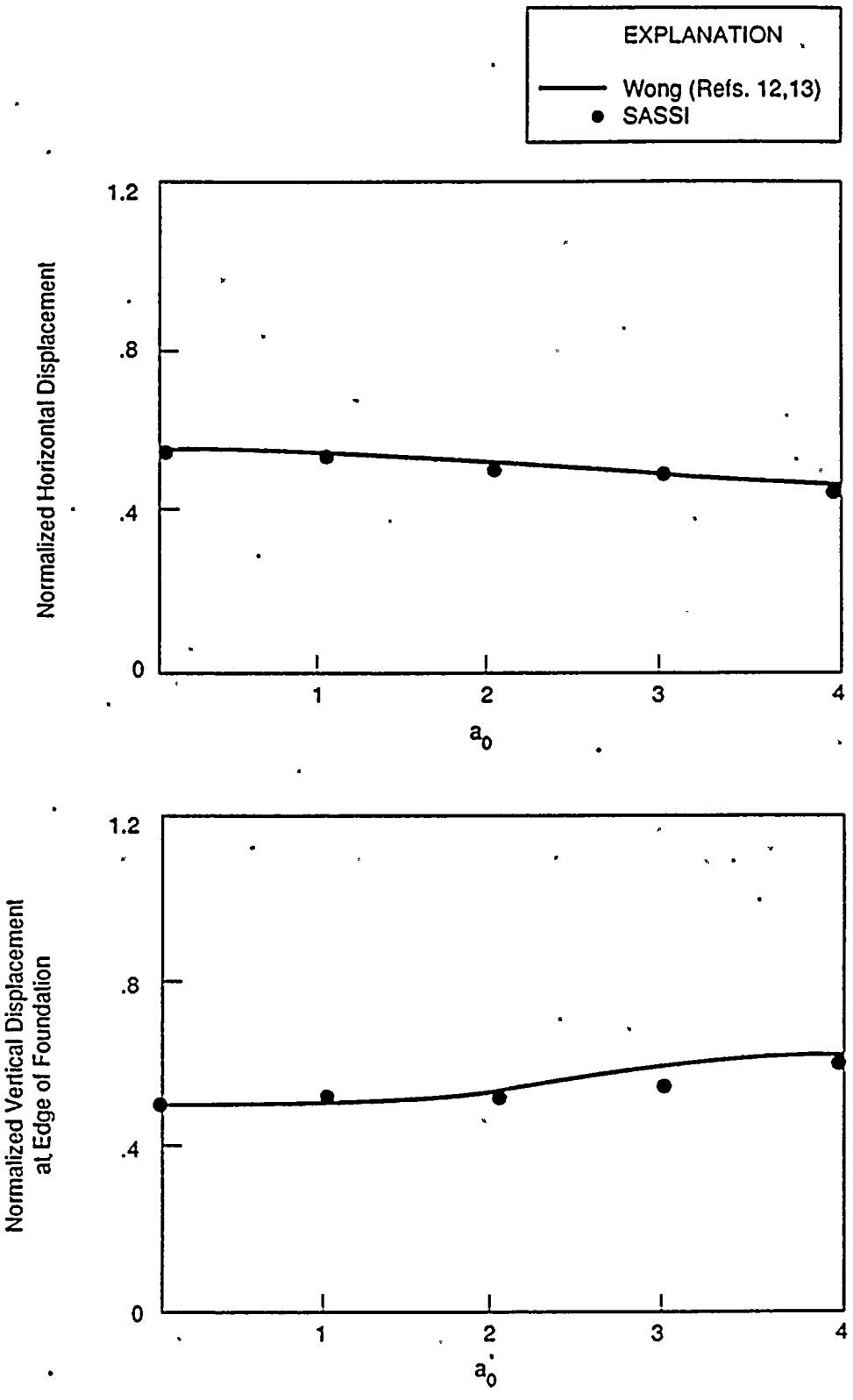

Figure 4.4-4. Response to Inclined P-Wave

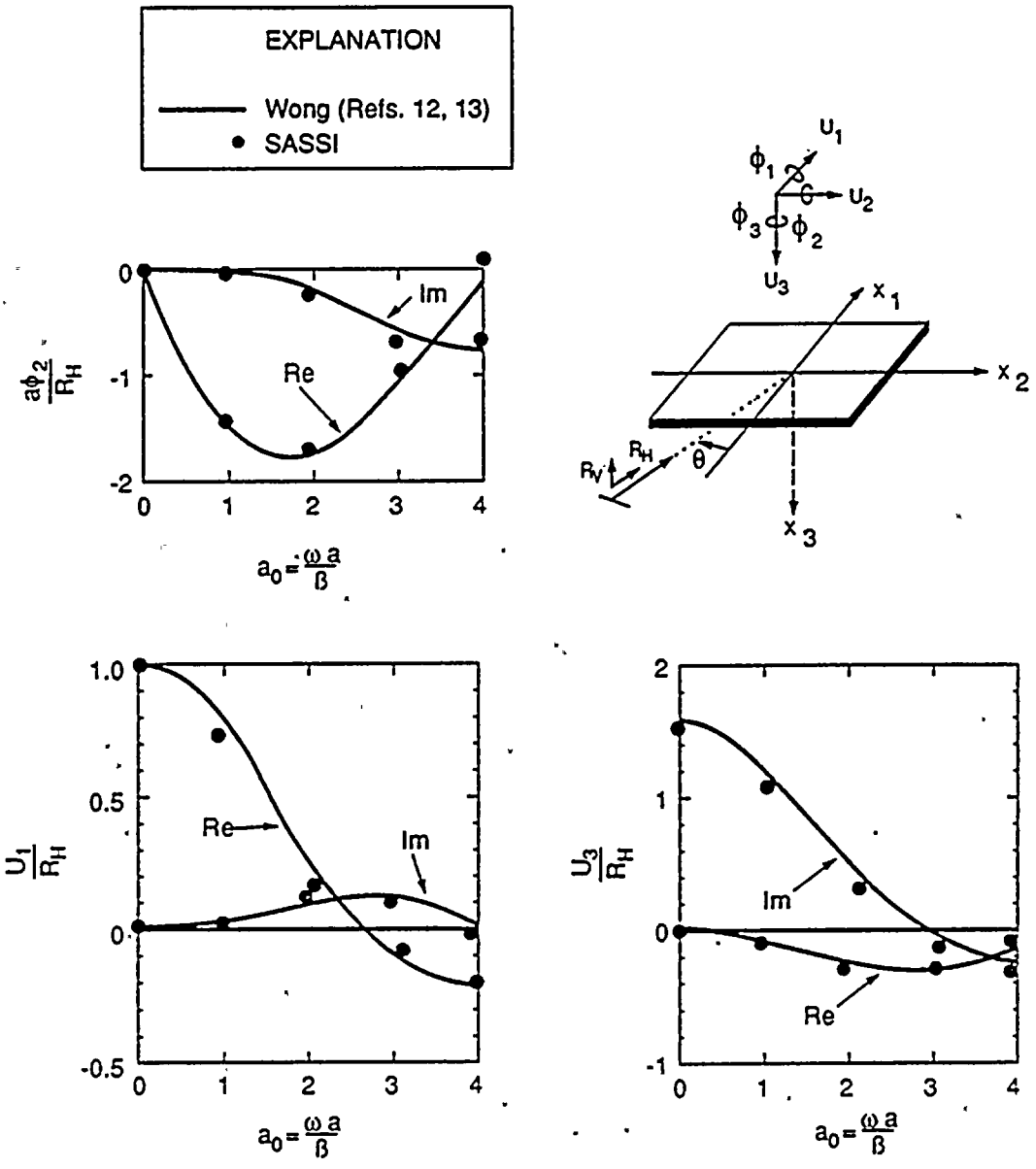

Figure 4.4-5. Response to Rayleigh Wave

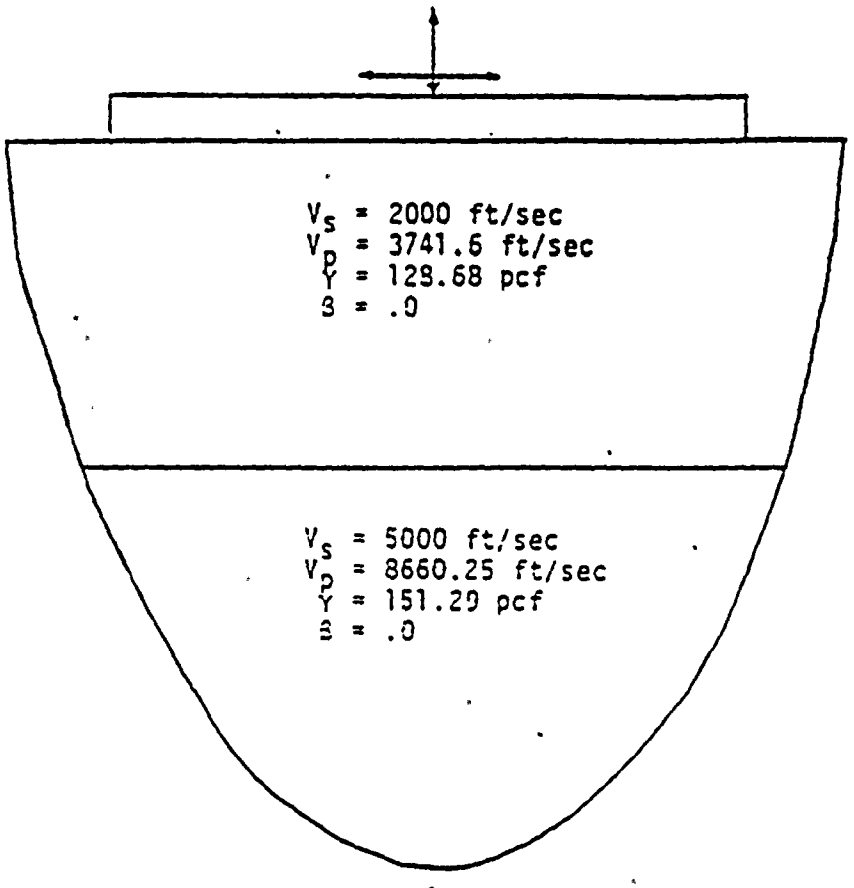

Figure 4.5-1. Foundation Model

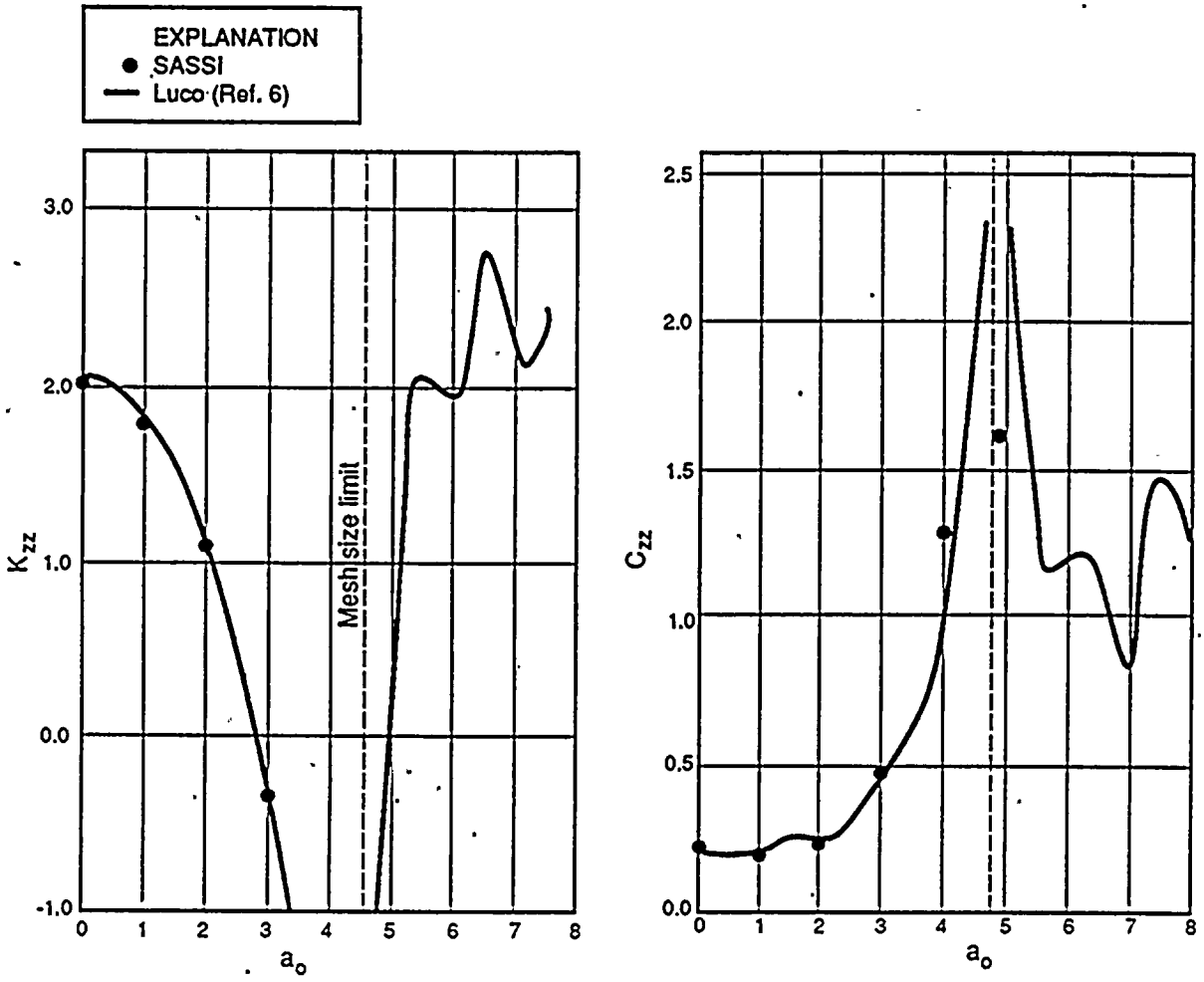

Figure 4.5-2. Vertical Stiffness and Damping Coefficients

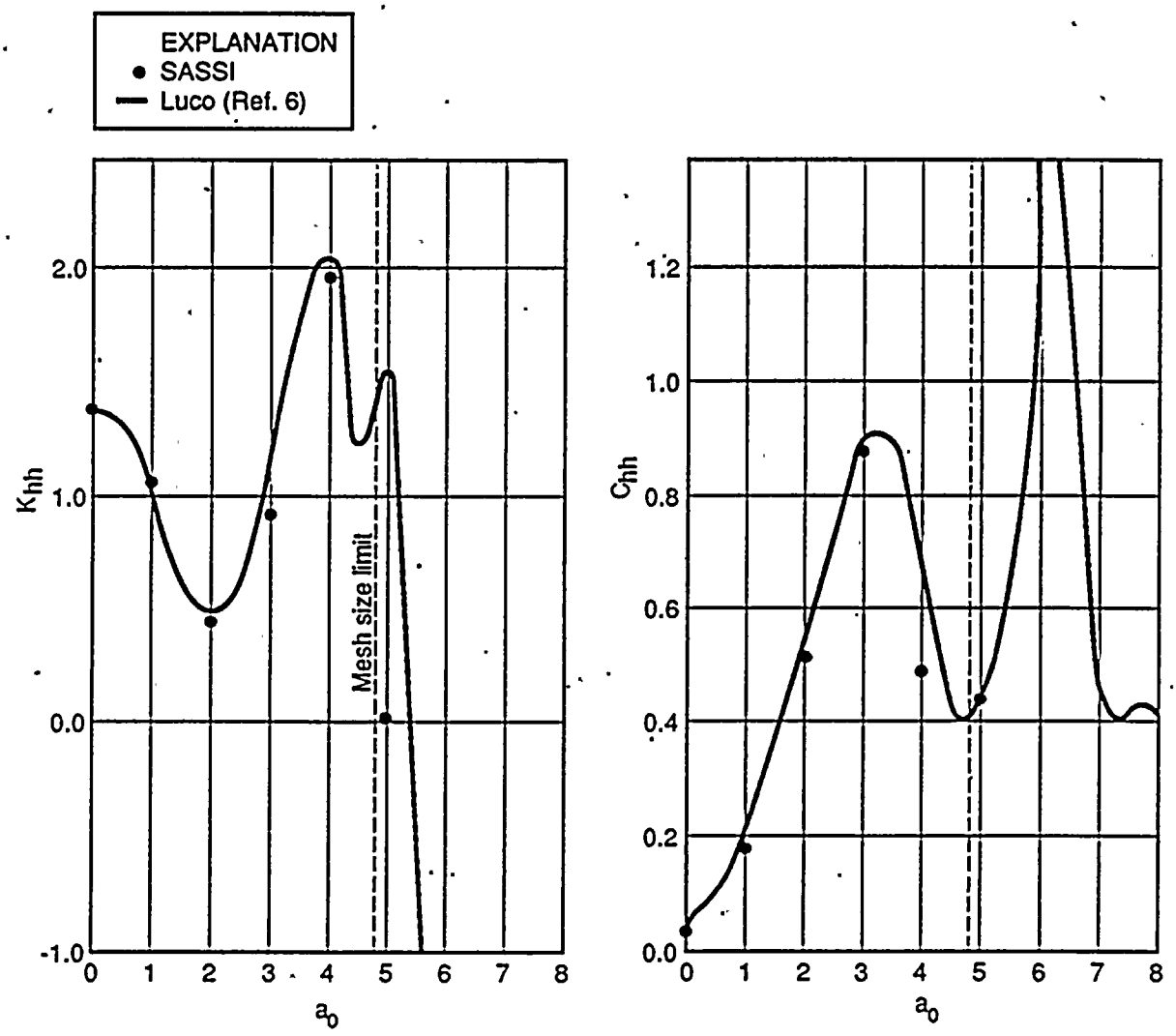

Figure 4.5-3. Horizontal Stiffness and Damping Coefficients

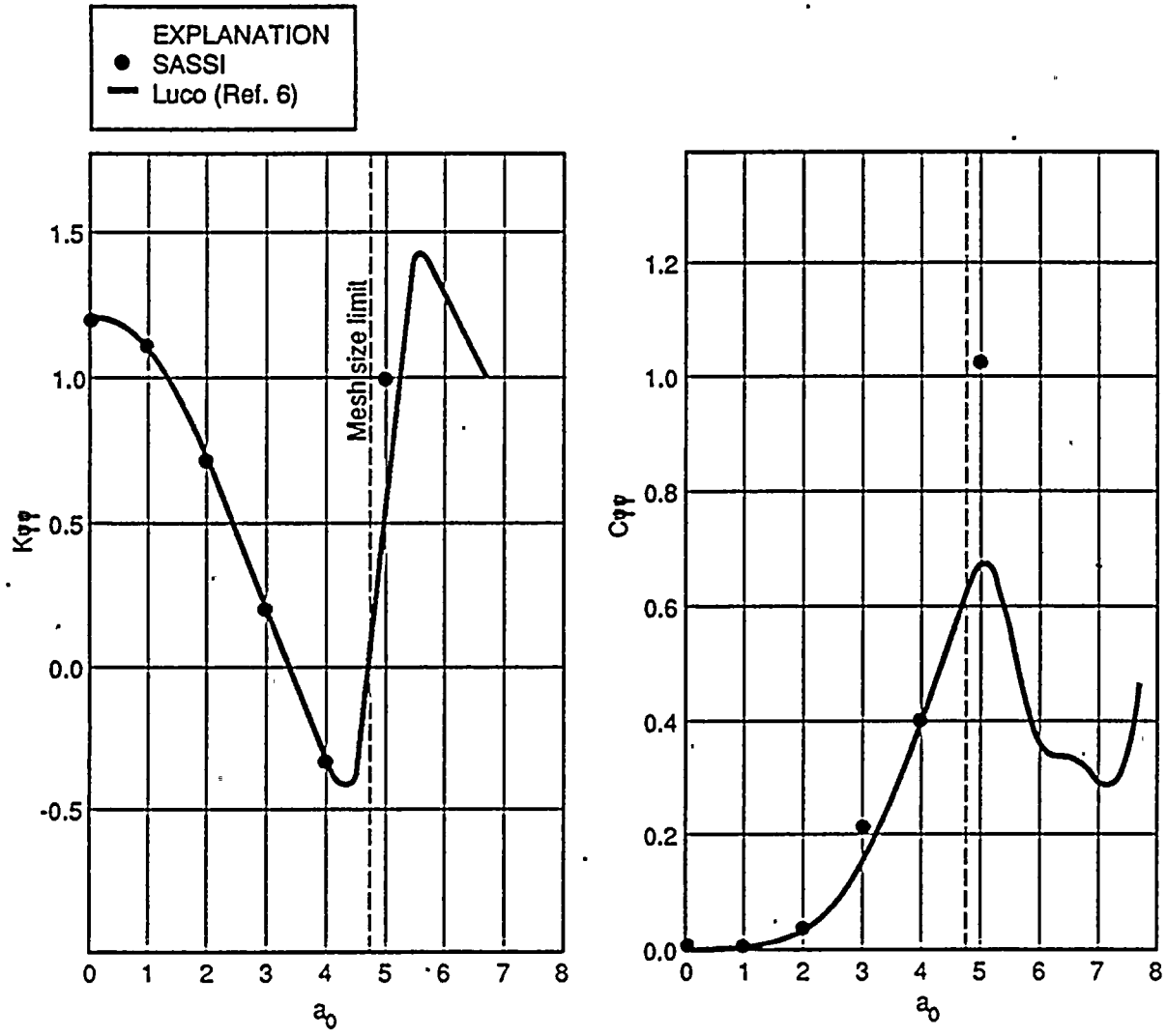

Figure 4.5-4. Rocking Stiffness and Damping Coefficients

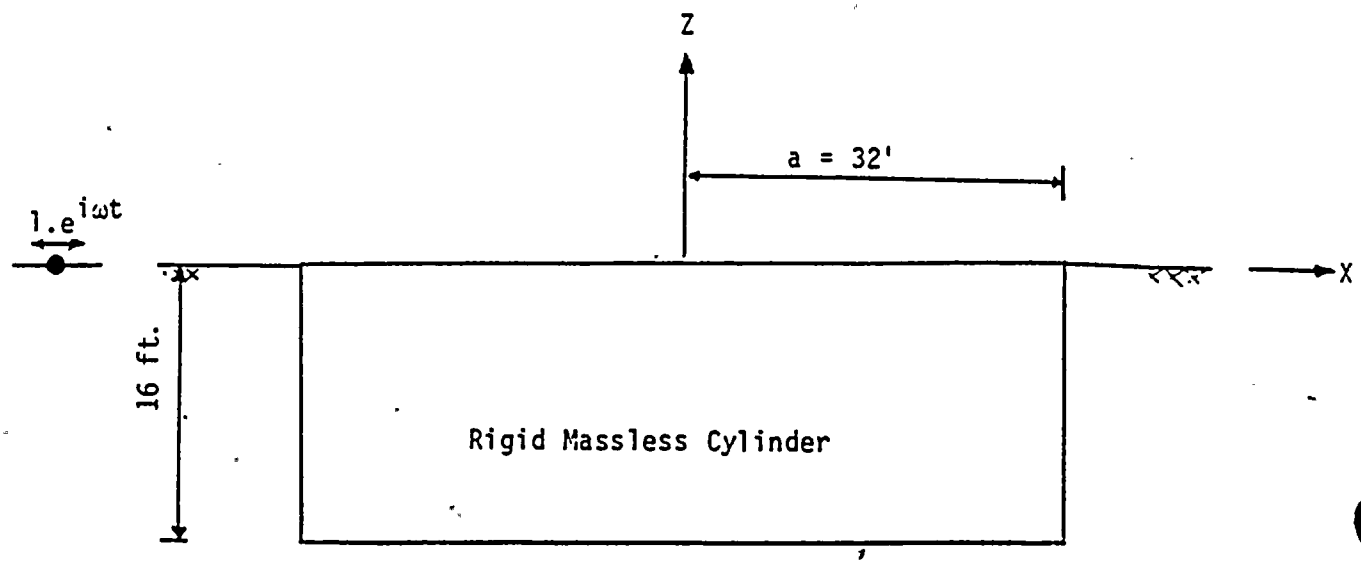

Figure 4.6-1. Geometry of Foundation Cross Section

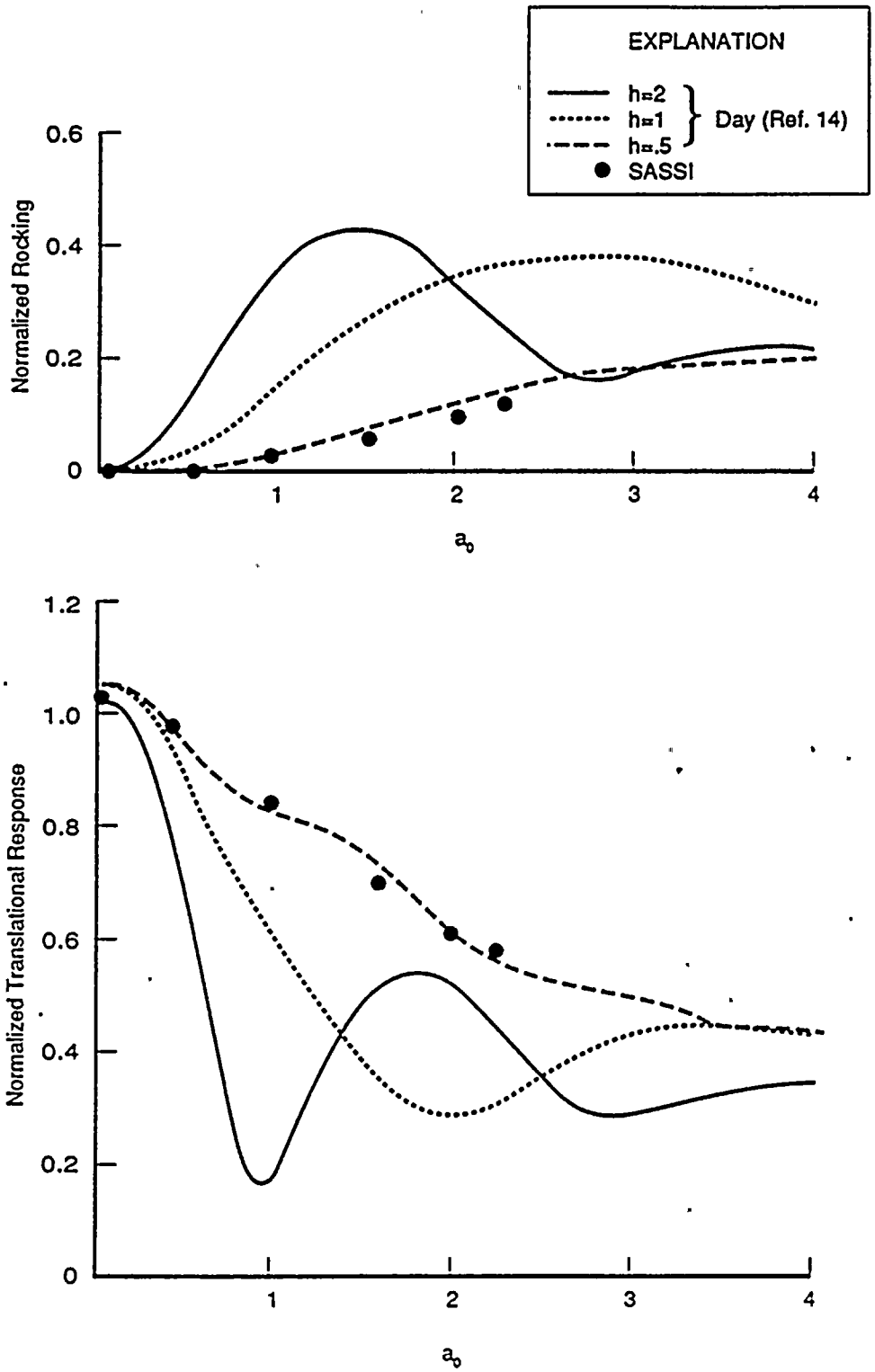

Figure 4.6-2. Response of Foundation due to Vertically Propagating SV-Wave

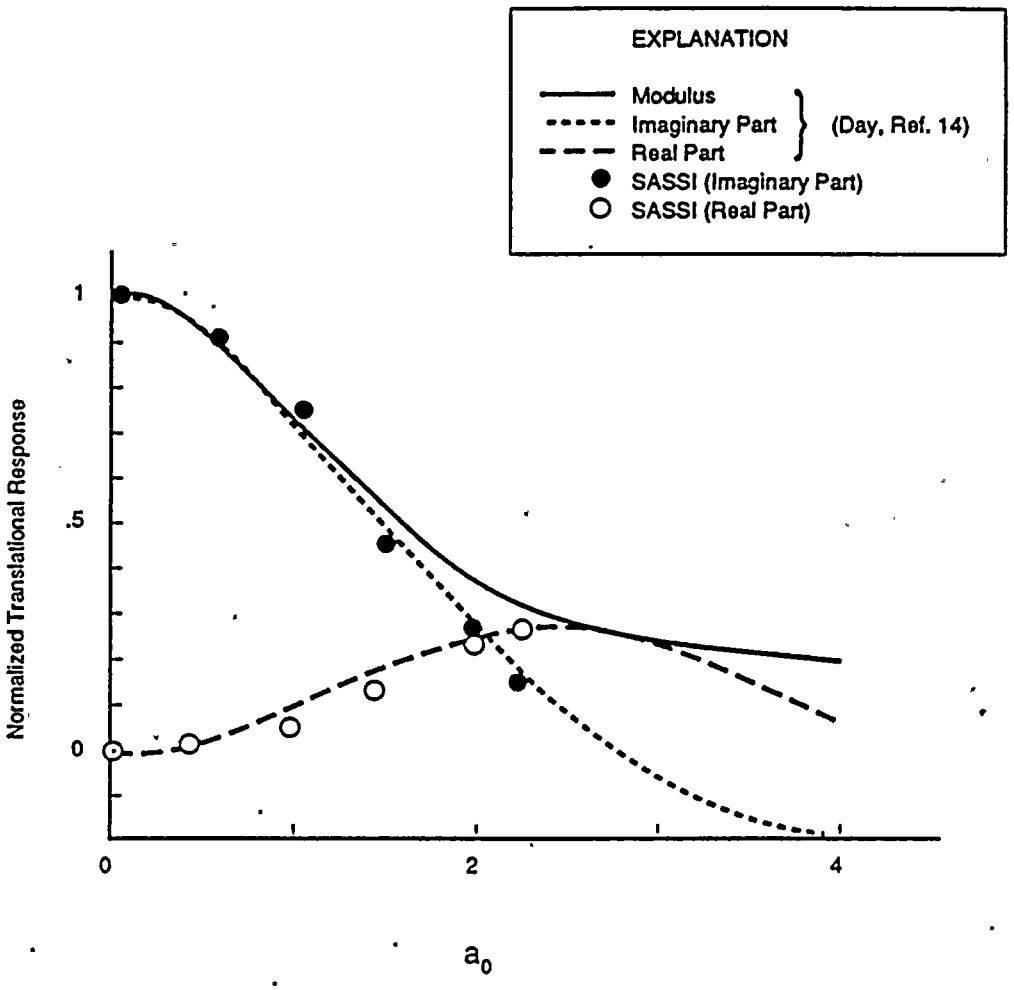

Figure 4.6-3(a). Translational Response of Foundation due to Horizontally Propagating SH-Wave

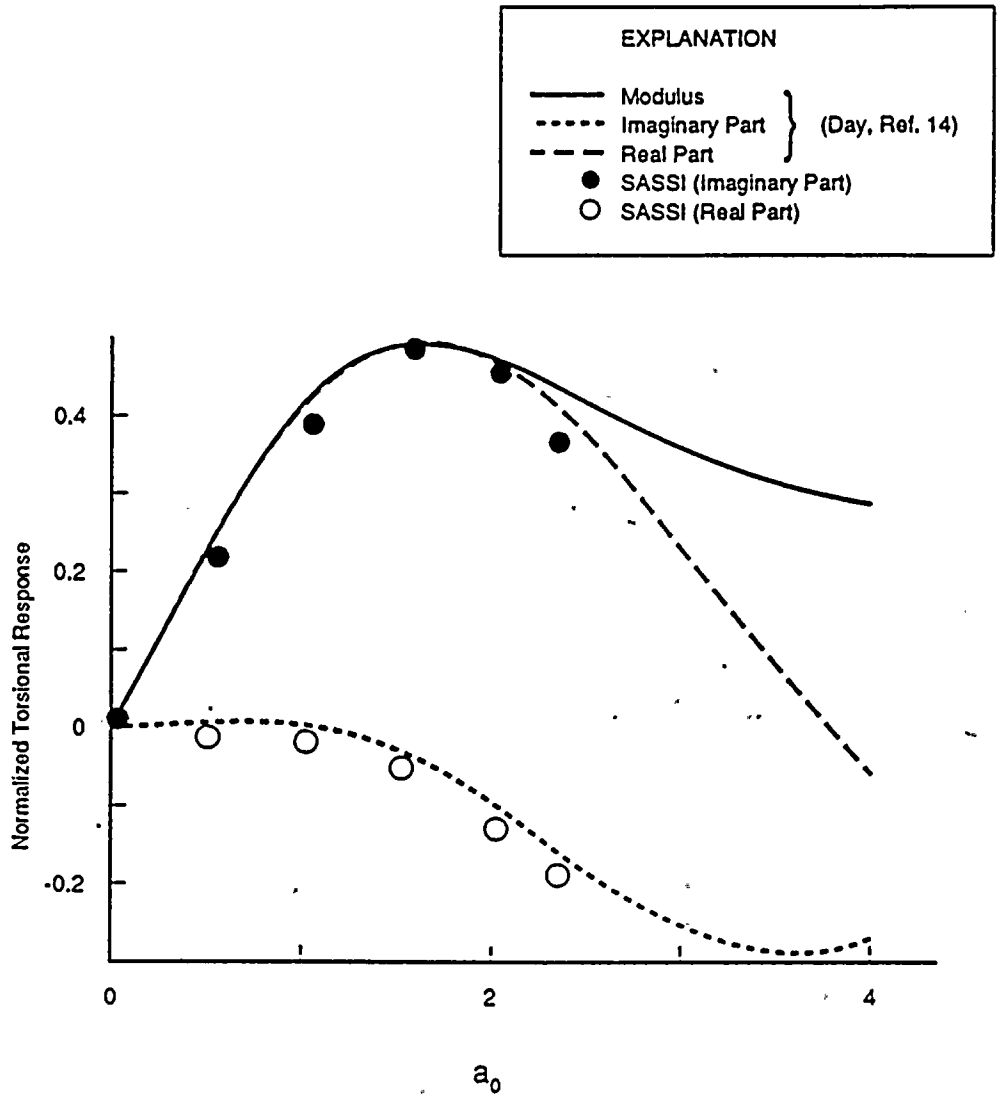

Figure 4.6-3(b). Torsional Response of Foundation due to Horizontally Propagating SH-Wave

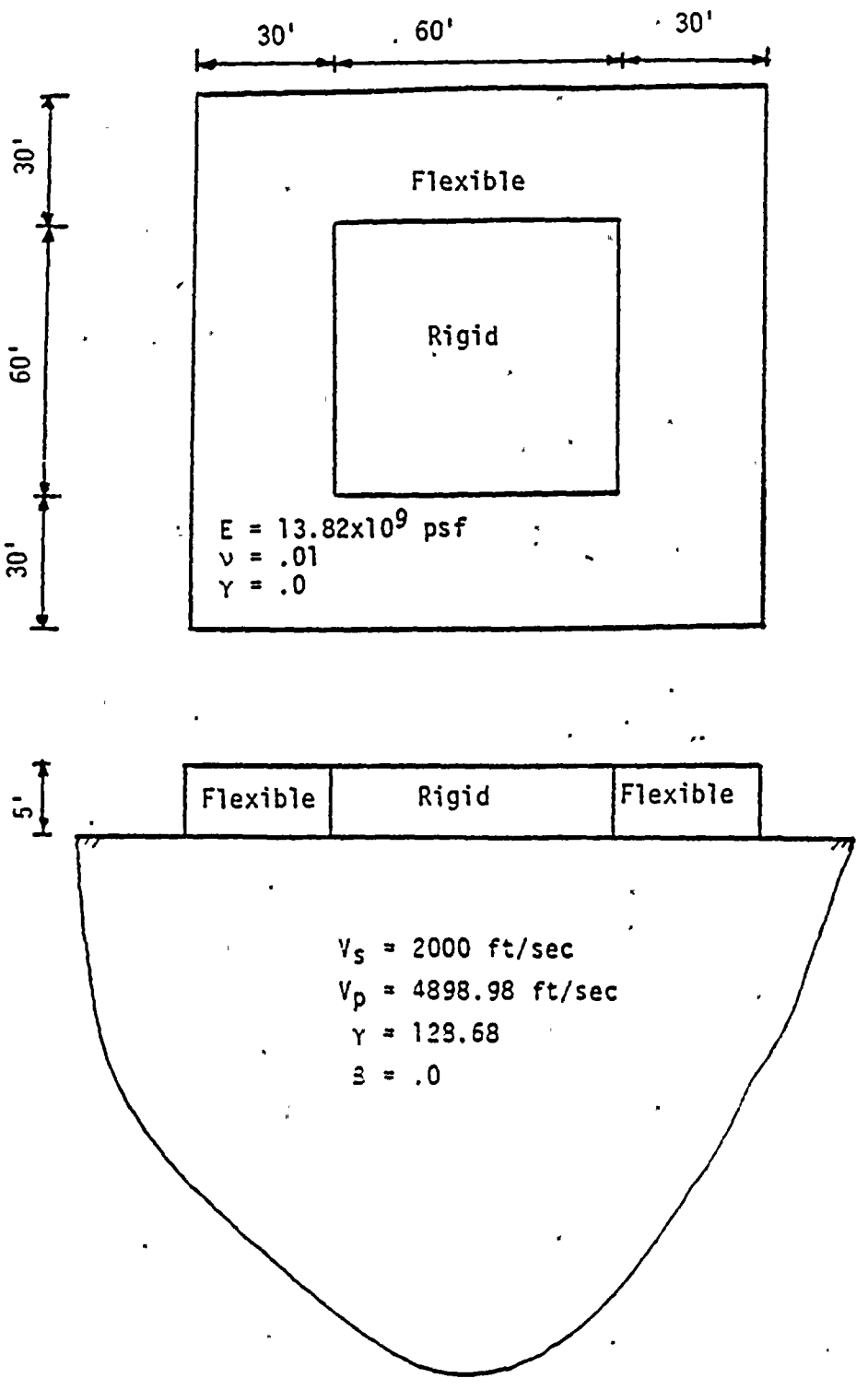

Figure 4.7-1. Foundation Model

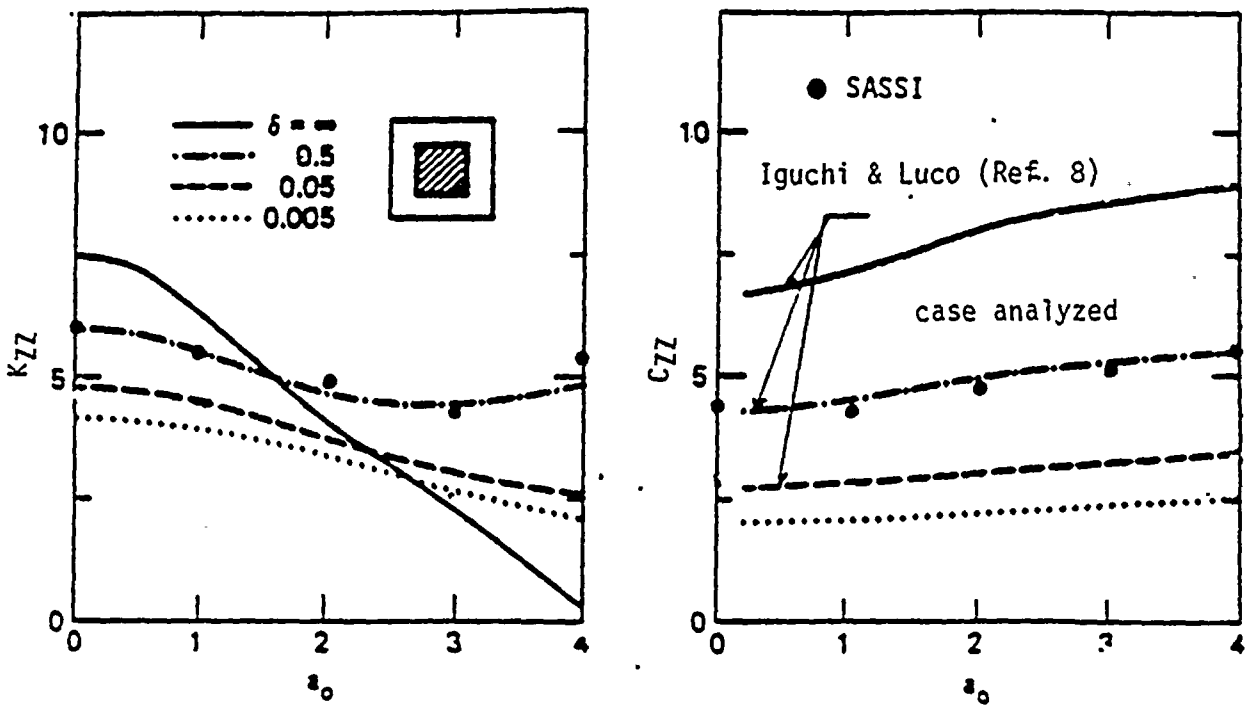

Figure 4.7-2. Vertical Stiffness and Dynamic Coefficients

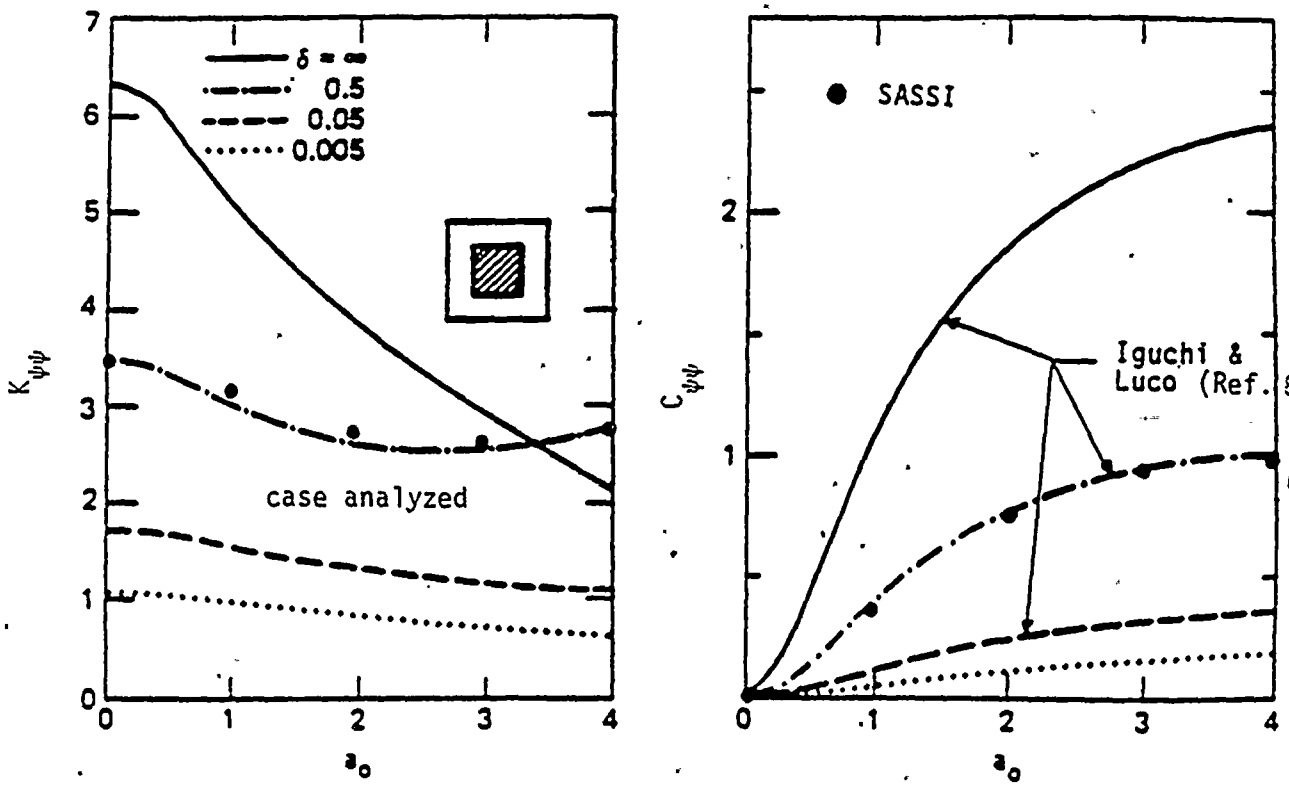

Figure 4.7-3. Rocking Stiffness and Damping Coefficients

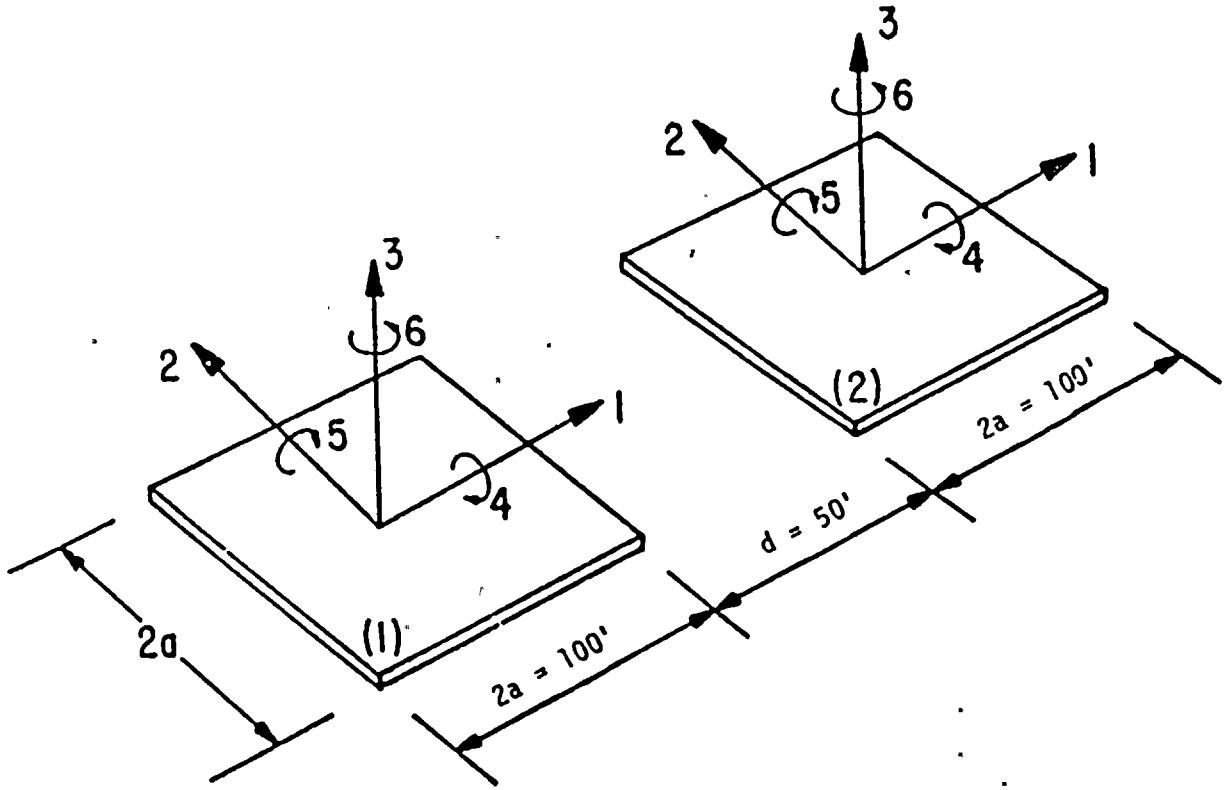

Figure 4.8-1. Geometry and Degrees of Freedom of 2 Foundation Systems

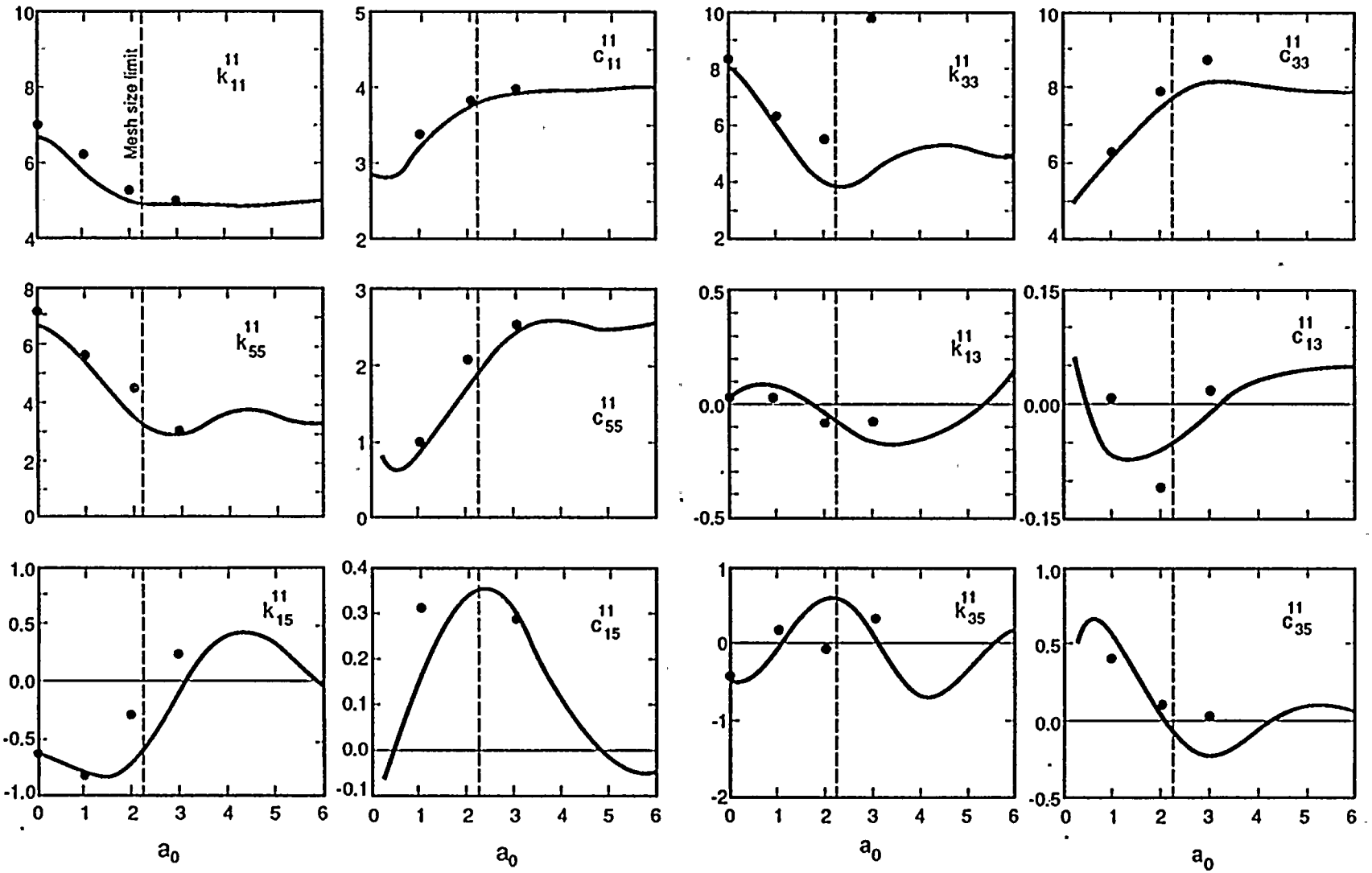

Figure 4.8-2. Impedance Functions for Foundation No. 1 Associated with DOFs in Coordinate Directions 1, 3, and 5

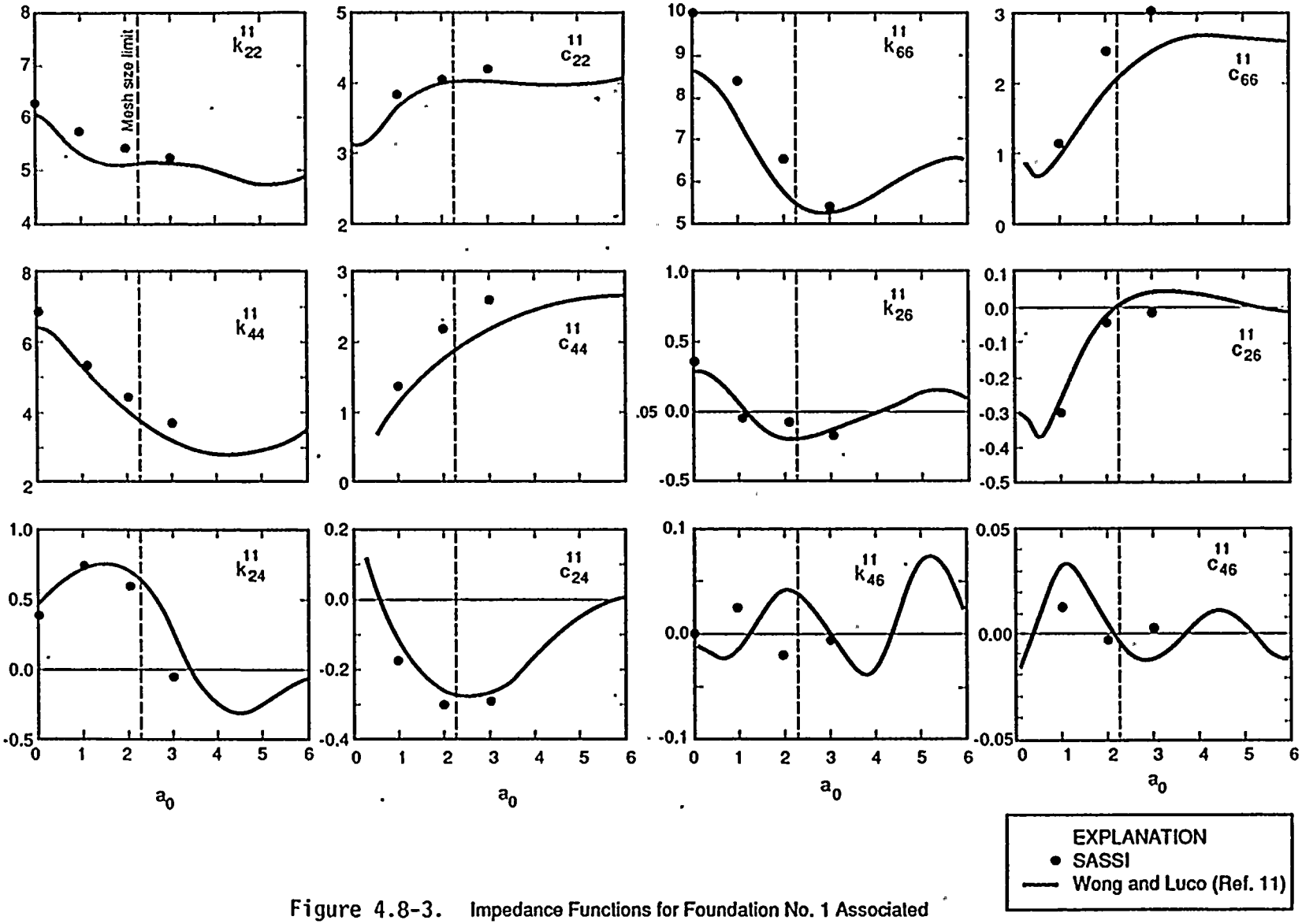

Figure 4.8-3. Impedance Functions for Foundation No. 1 Associated with DOFs in Coordinate Directions 1, 3, and 5

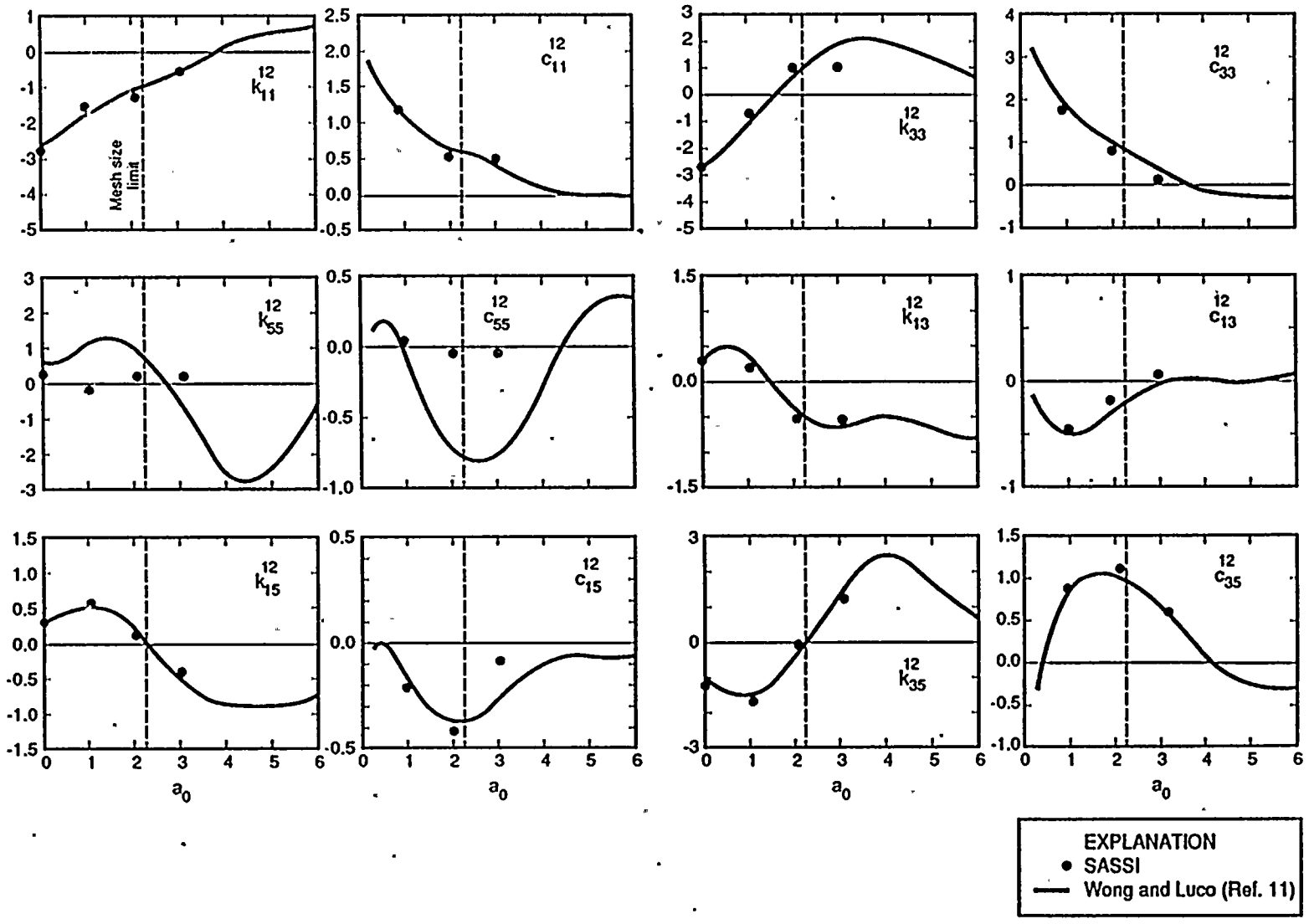

Figure 4.8-4. Impedance Functions for Foundation No. 1 due to Coupling from Foundation No. 2 for DOFs in Coordinate Directions 1, 3, and 5

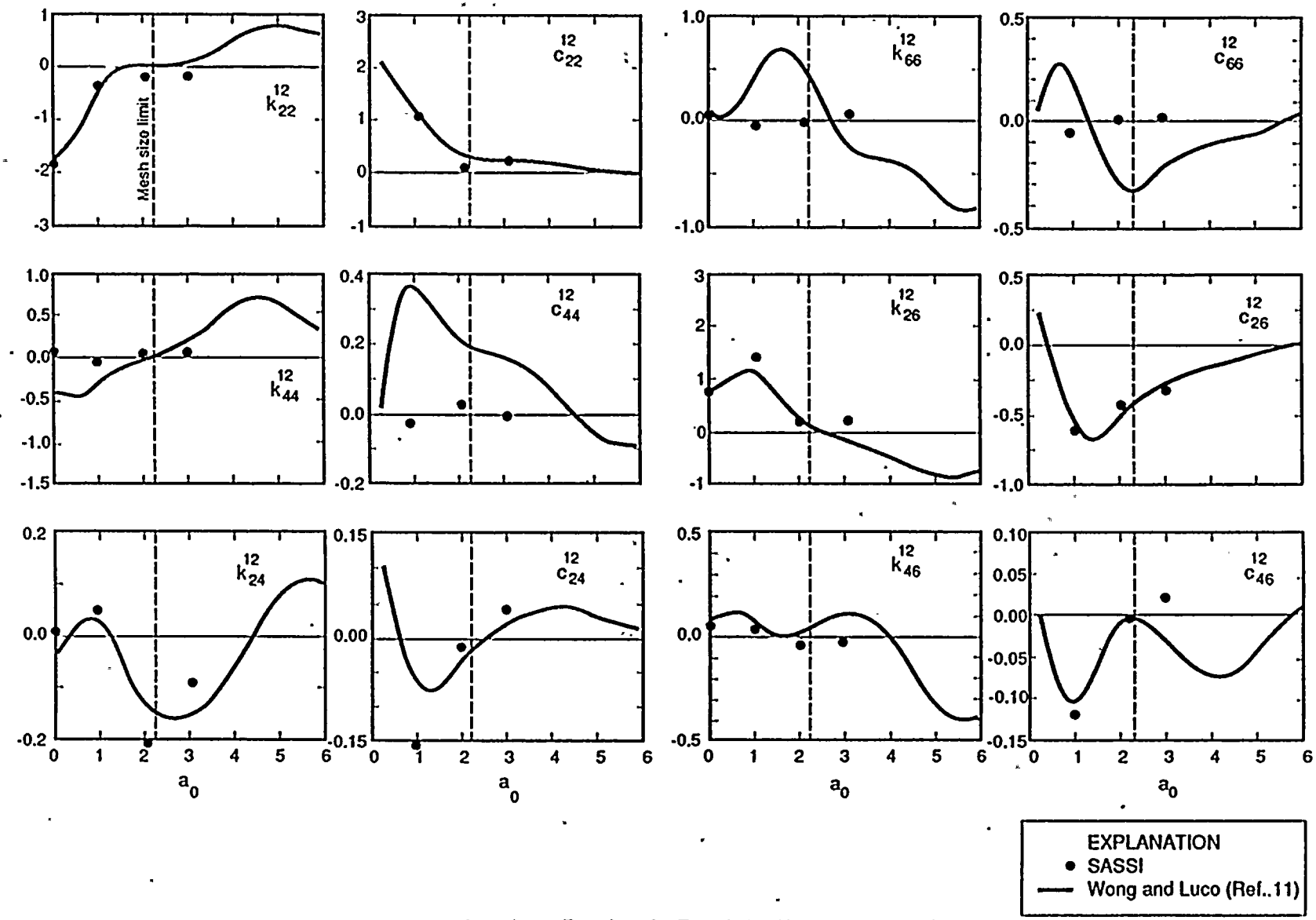

Figure 4.8-5. Impedance Functions for Foundation No. 1 due to Coupling from Foundation No. 2 for DOFs in Coordinate Directions 1, 3, and 5

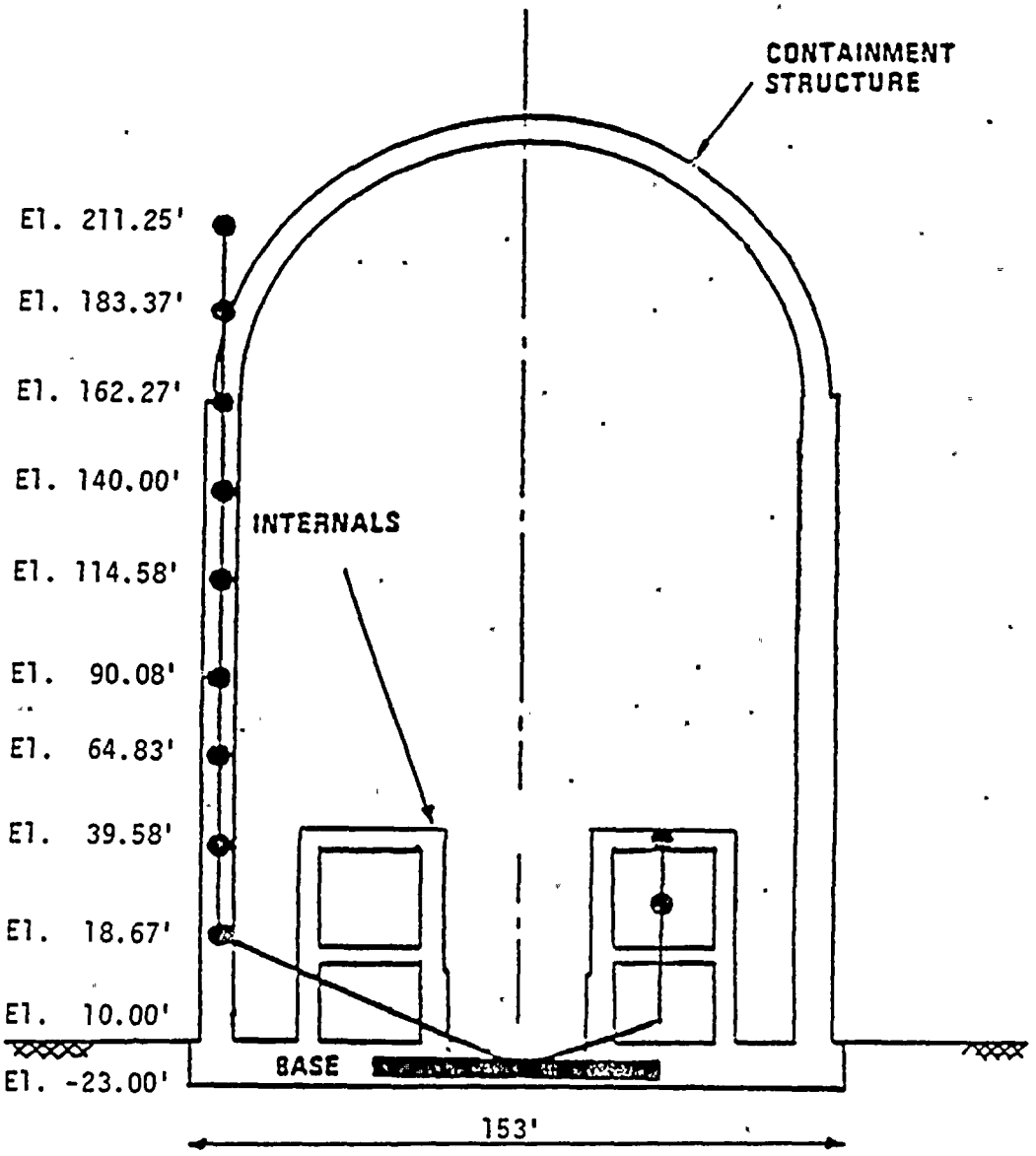

Figure 4.9-1. SSI Model with Embedded Foundation

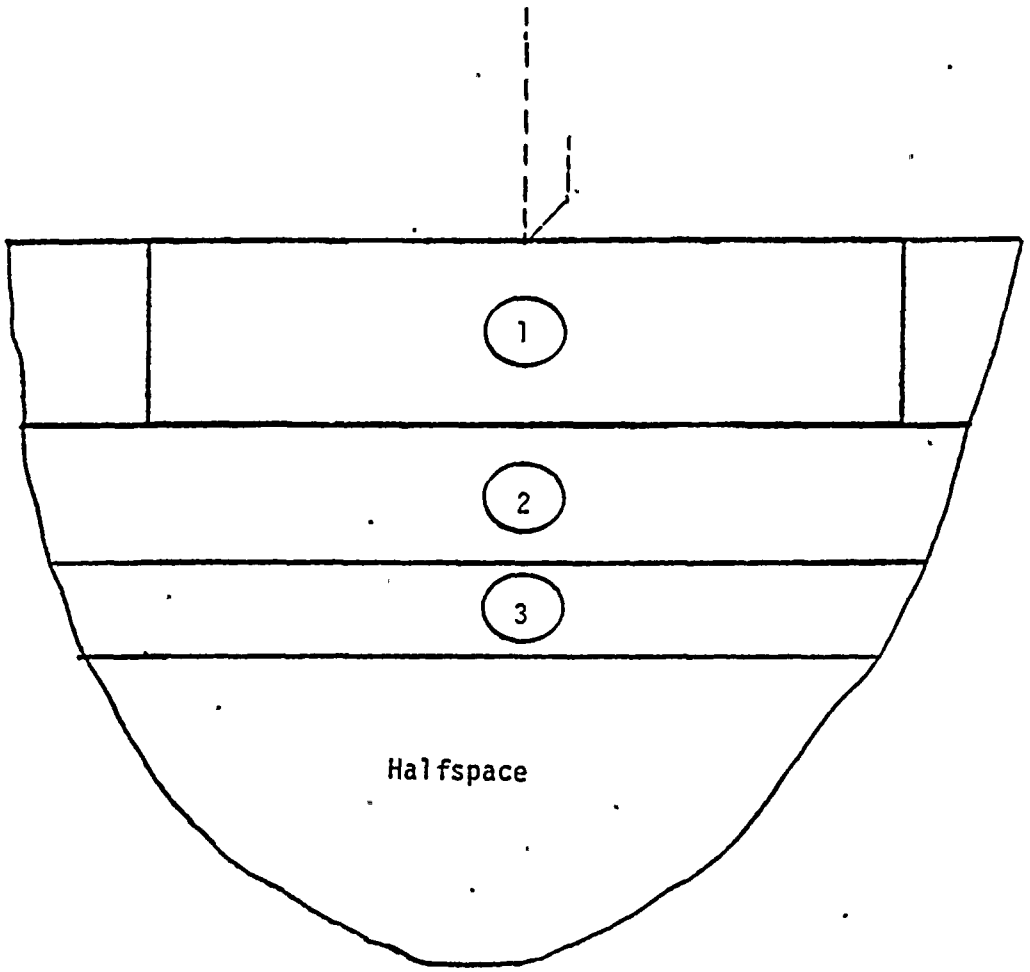

Layer No.	Thickness (ft)	V_s (ft/sec)	V_p (ft/sec)	γ (pcf)	β (%)
1	23	3600	6100	150	2
2	17	3600	6100	150	2
3	10	3900	6600	150	2
halfspace	-	5600	8700	150	2

Figure 4.9-2. SASSI Site Model

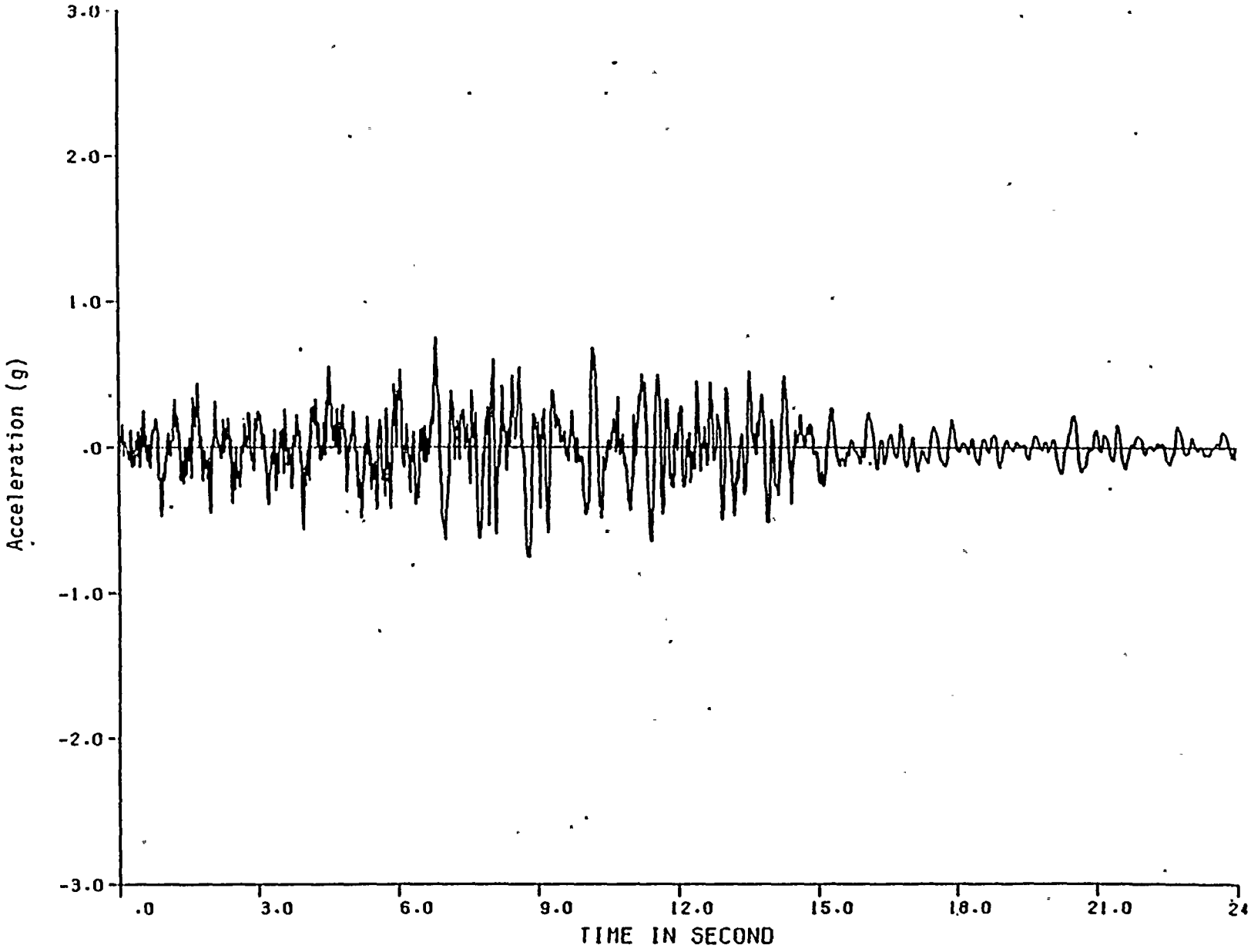

Figure 4.9-3. Acceleration Time History of Input Motion

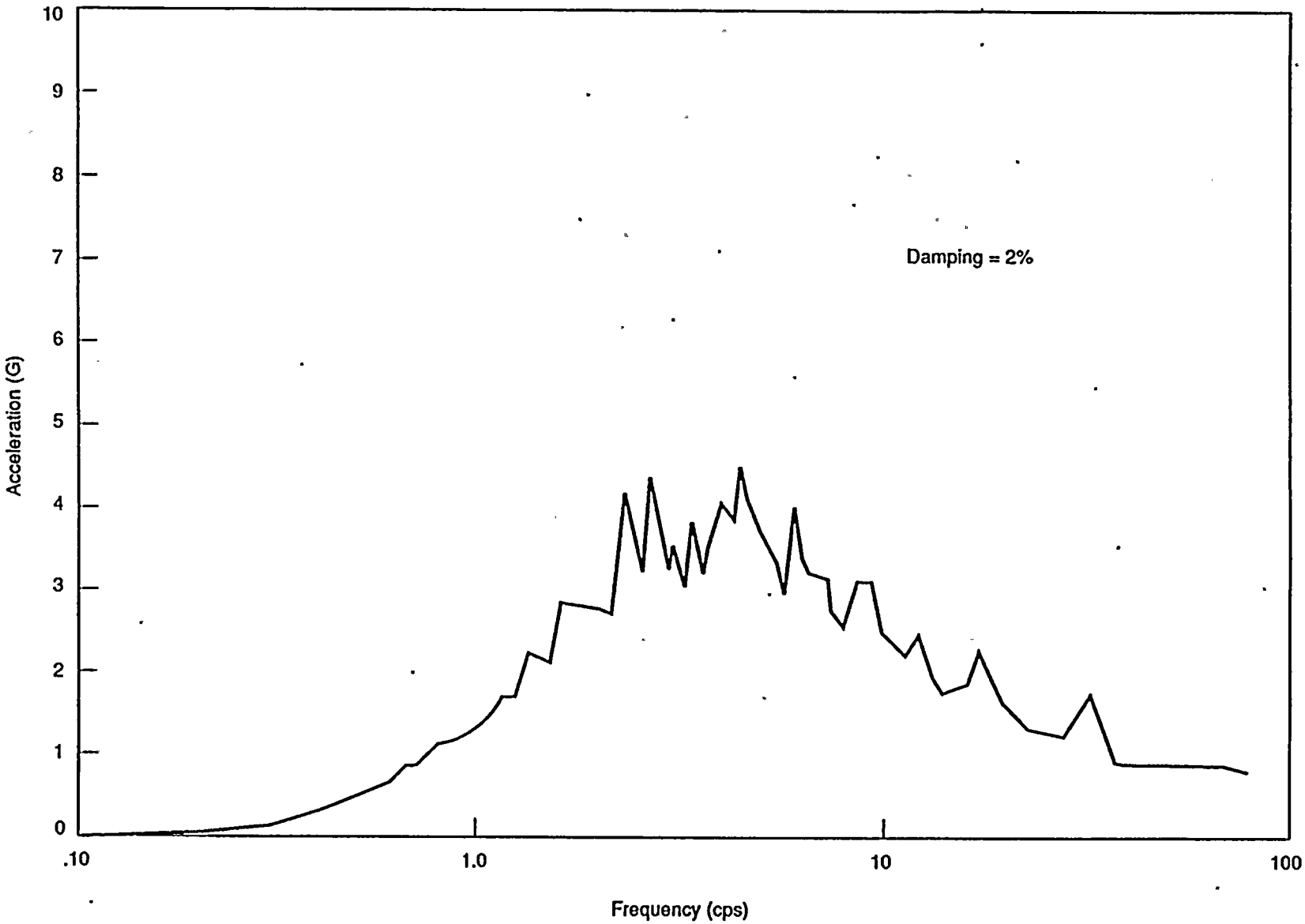

Figure 4.9-4. Acceleration Response Spectrum of Input Motion

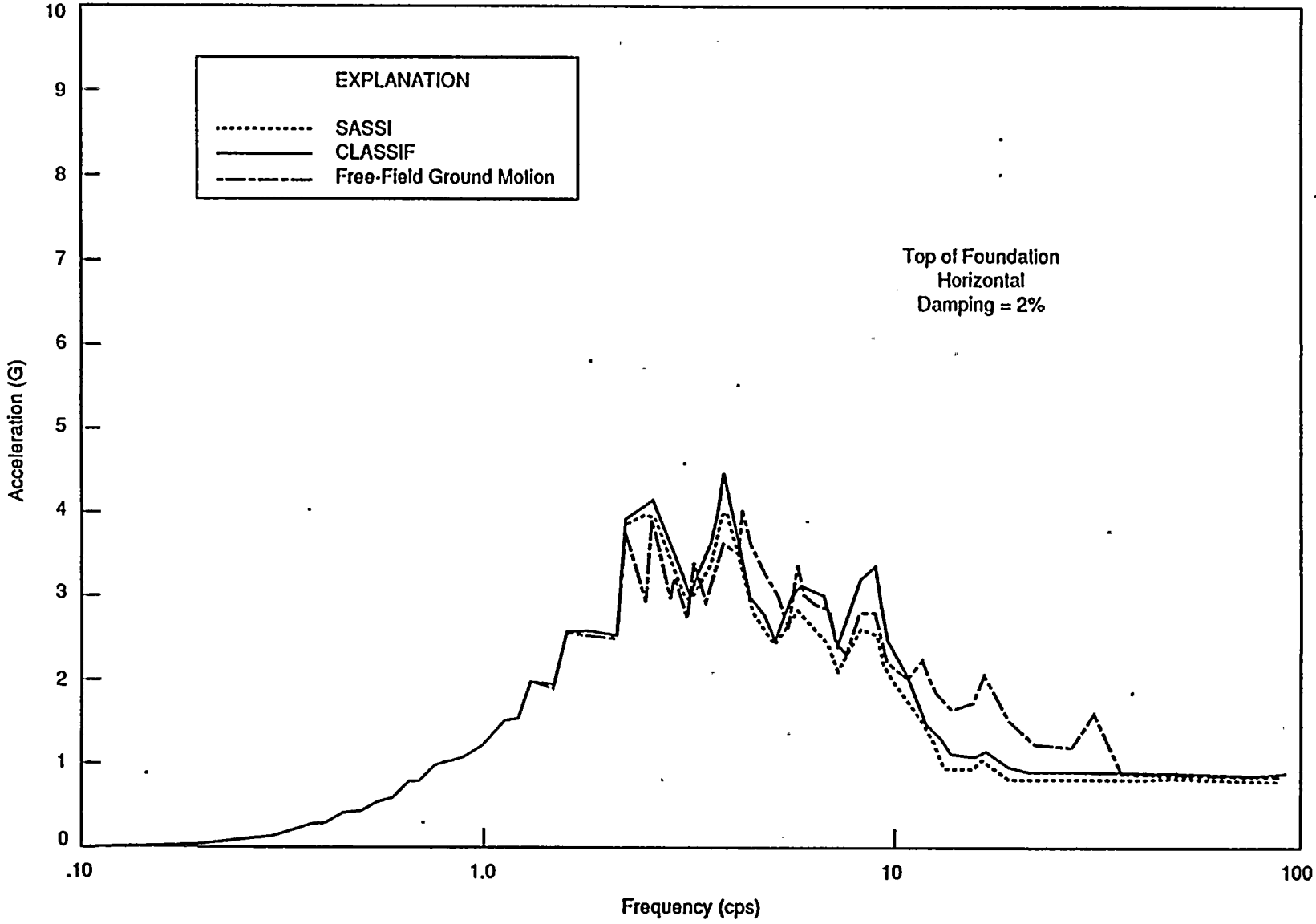

Figure 4.9-5. Acceleration Response Spectrum at the Top of the Foundation (Rayleigh Wave Case)

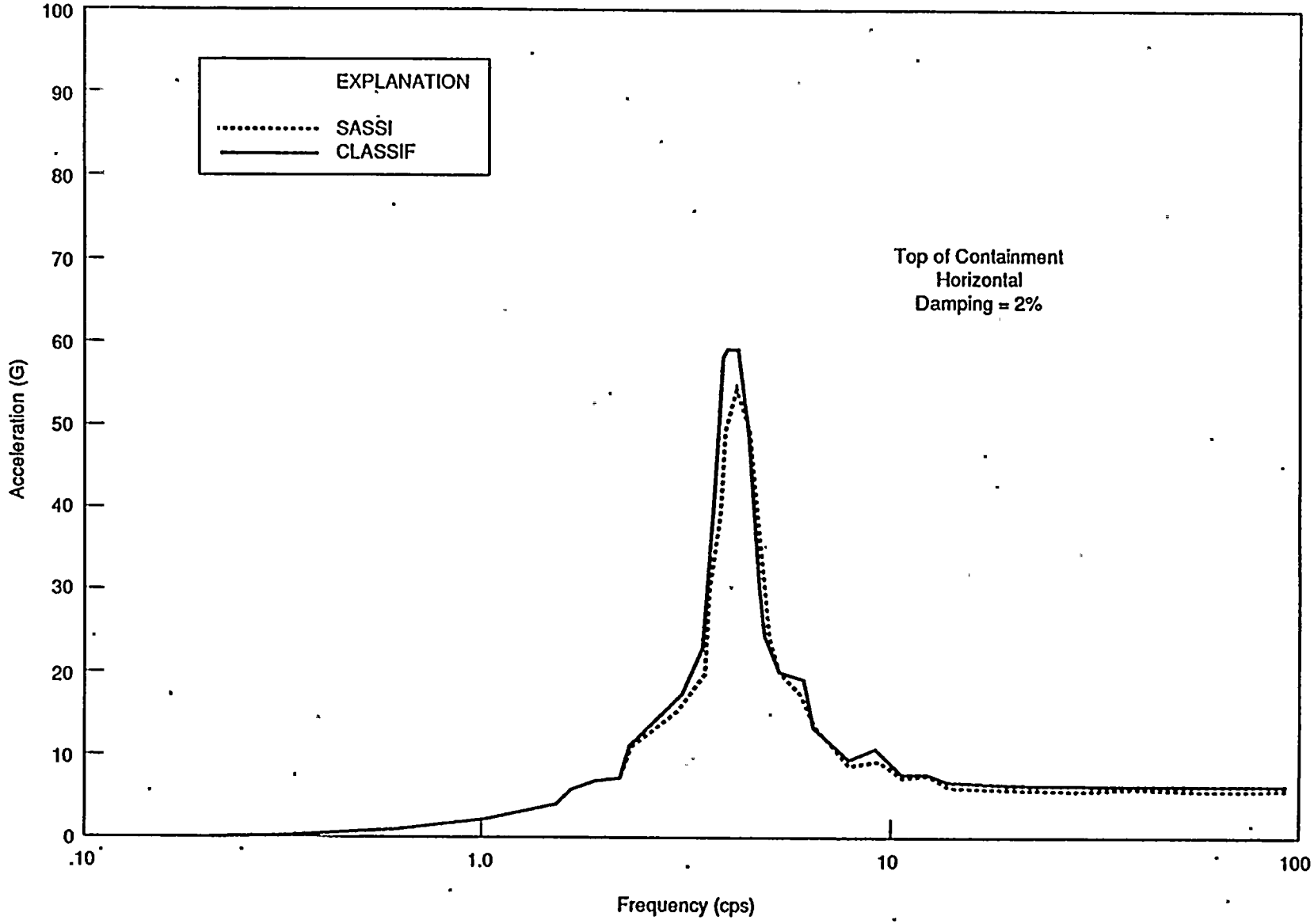

Figure 4.9-6. Horizontal Acceleration Response Spectrum at the Top of Containment (Rayleigh Wave Case)

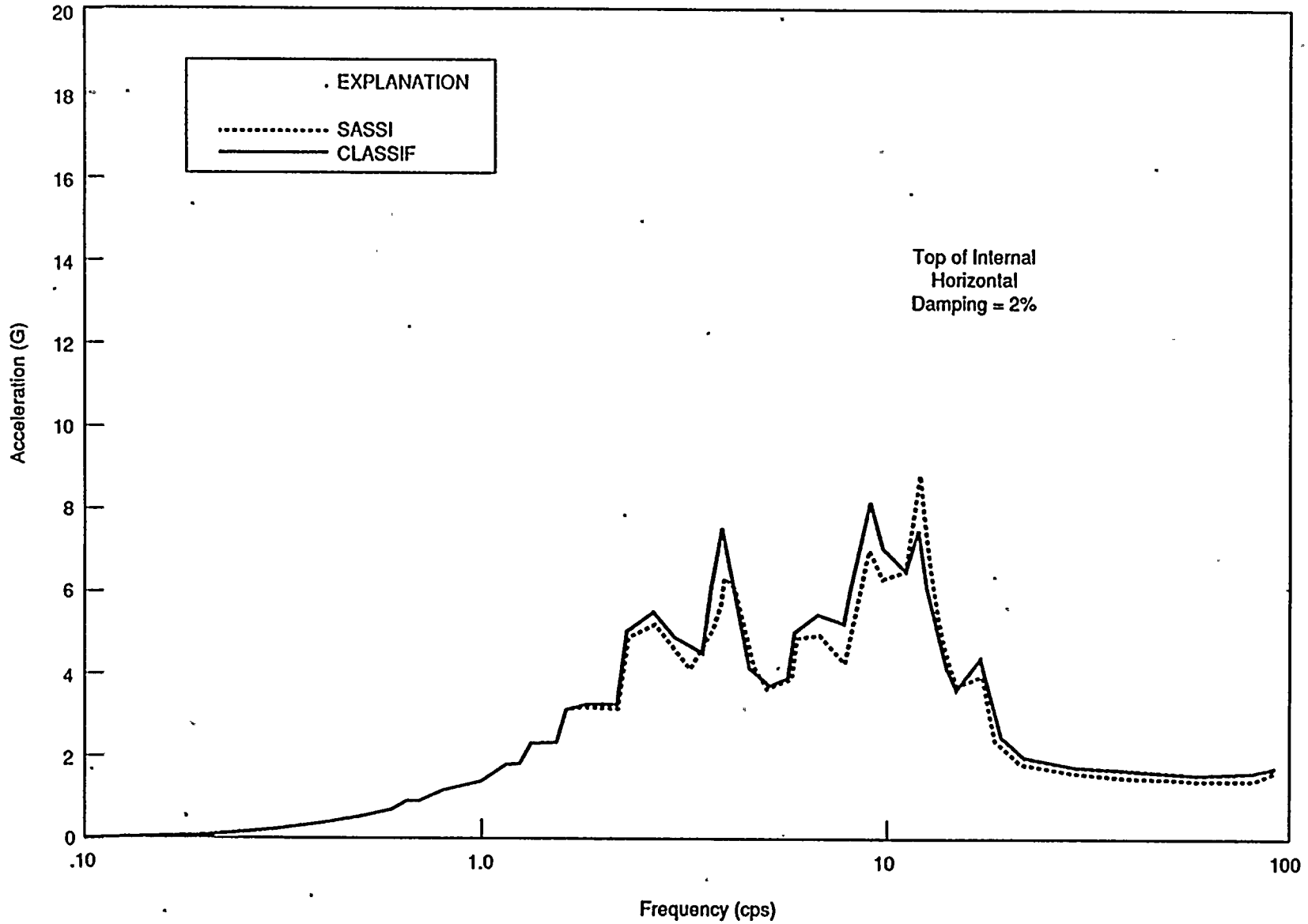

Figure 4.9-7. Horizontal Acceleration Response Spectrum at the Top of Internal (Rayleigh Wave Case)

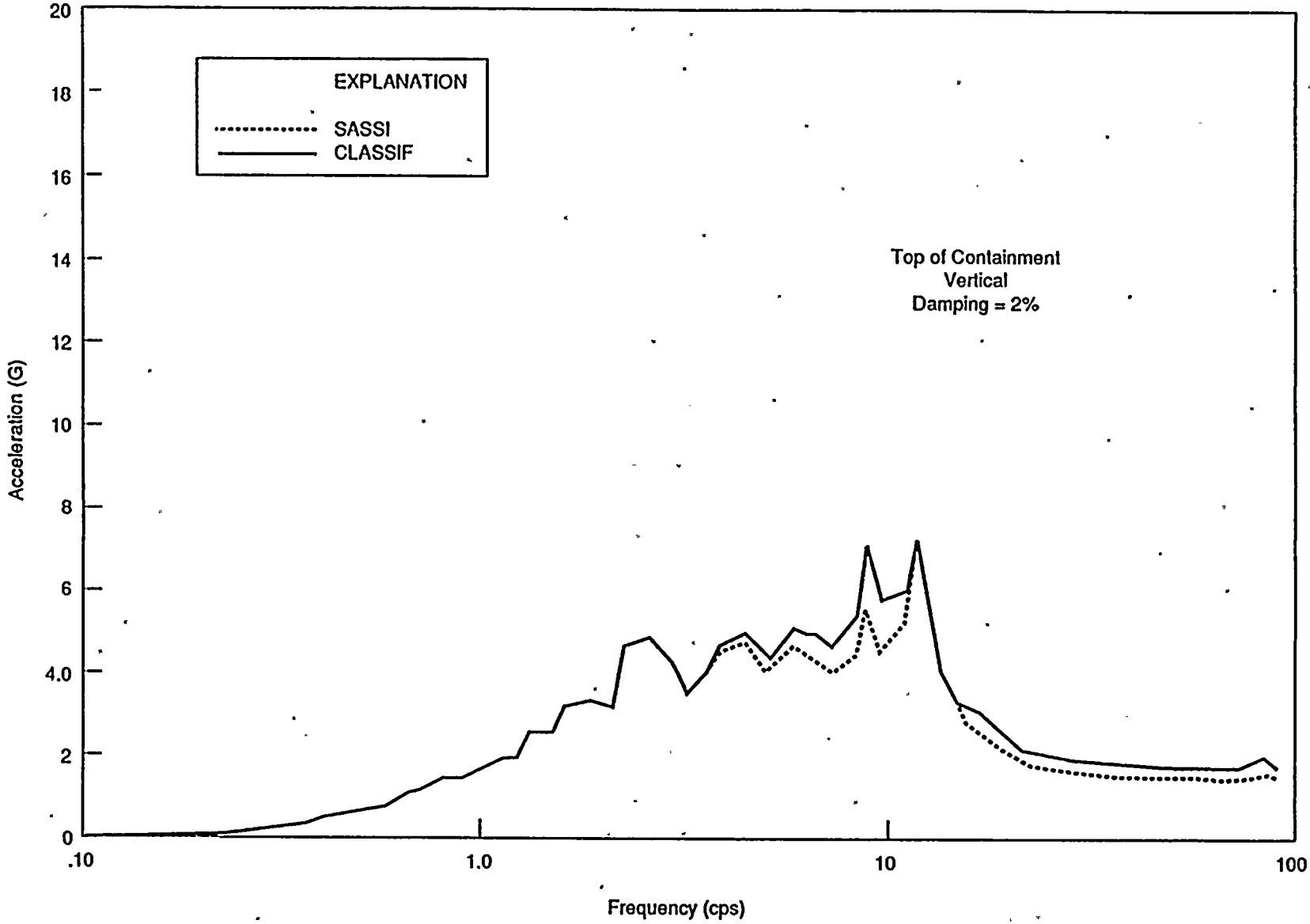

Figure 4.9-9. Vertical Acceleration Response Spectrum at the Top of Containment (Rayleigh Wave Case)

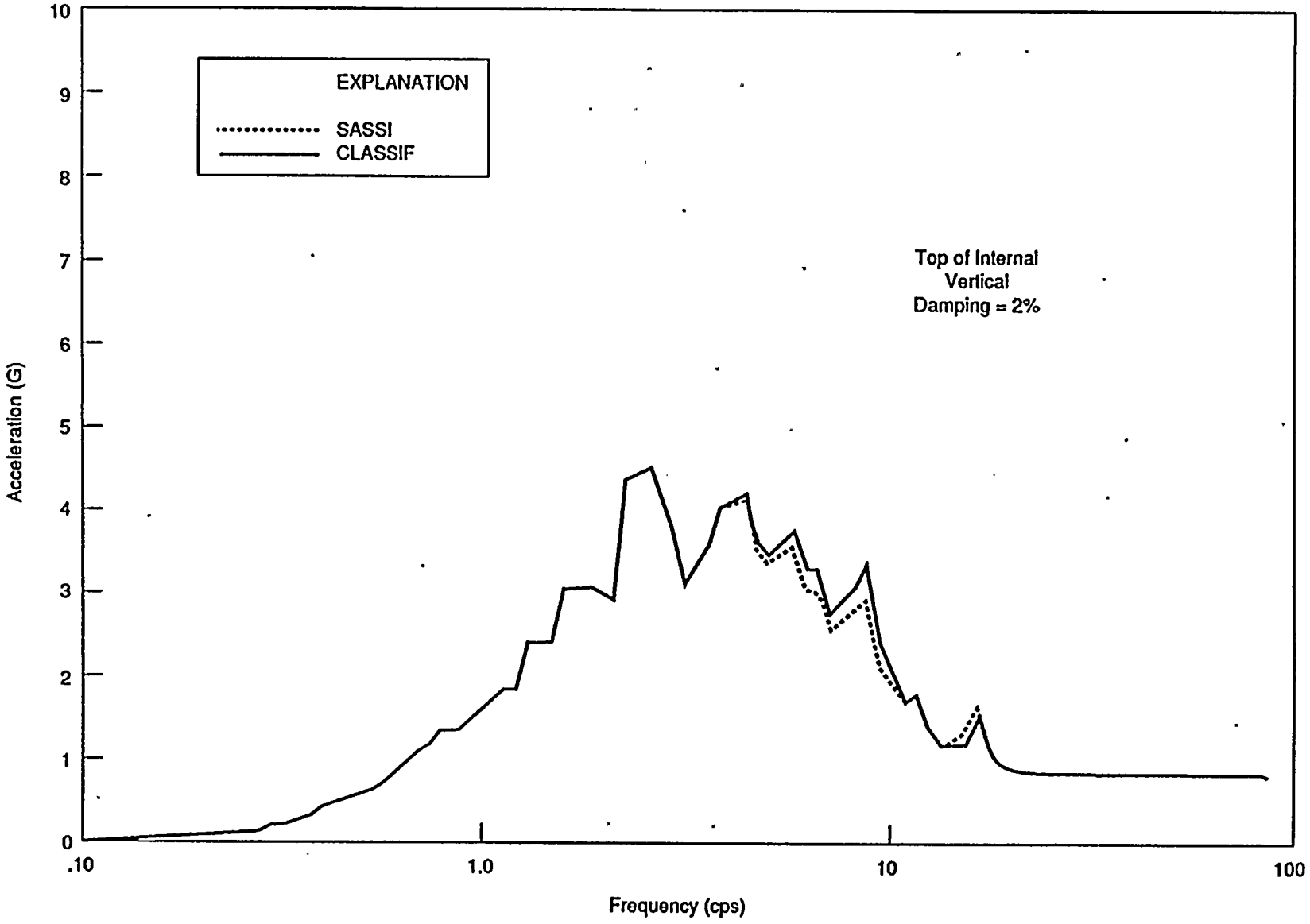

Figure 4.9-10. Vertical Acceleration Response Spectrum at the Top of Internal (Rayleigh Wave Case)

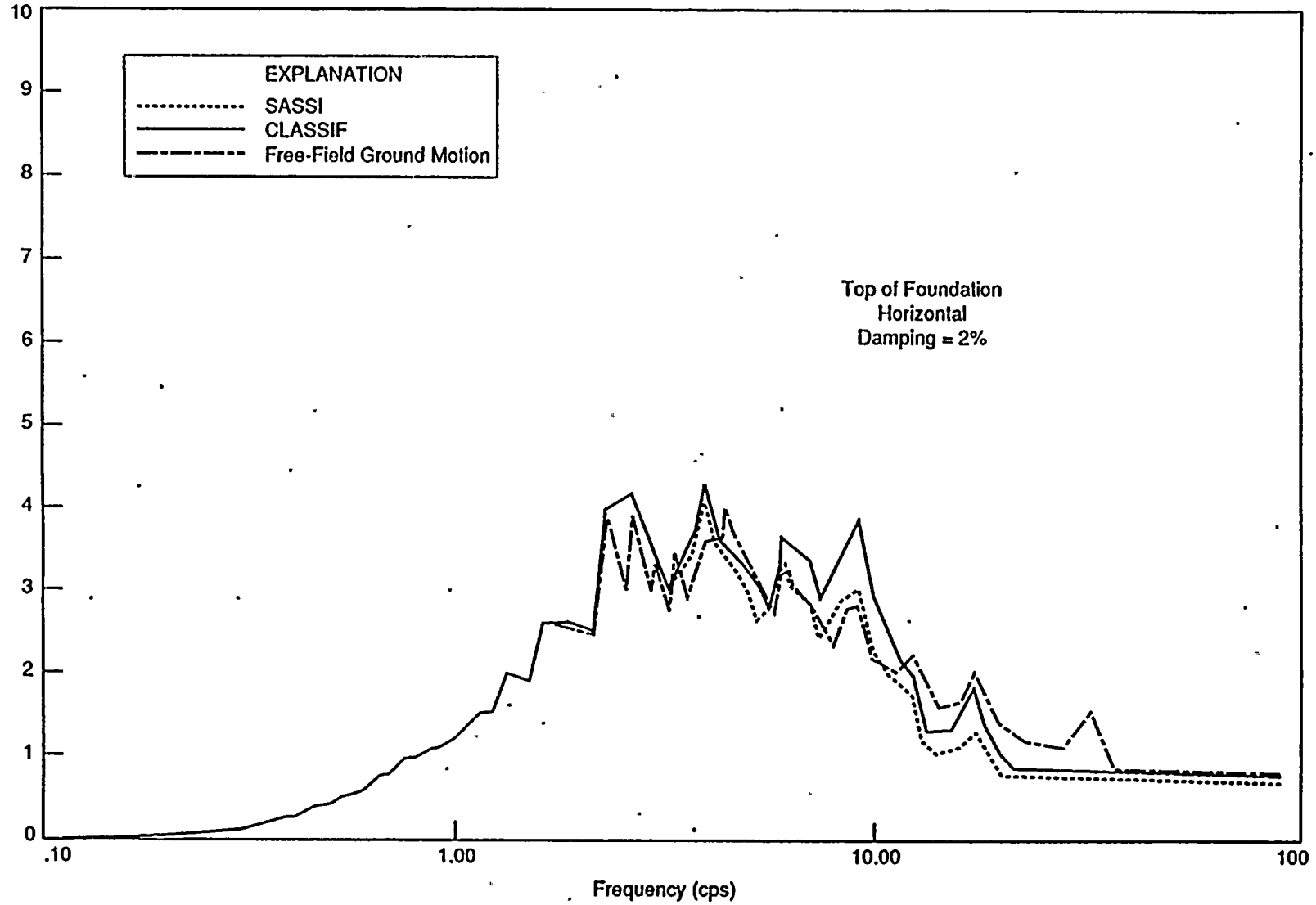

Figure 4.9-11. Horizontal Acceleration Response Spectrum at the Top of Foundation (SV+P Wave Case)

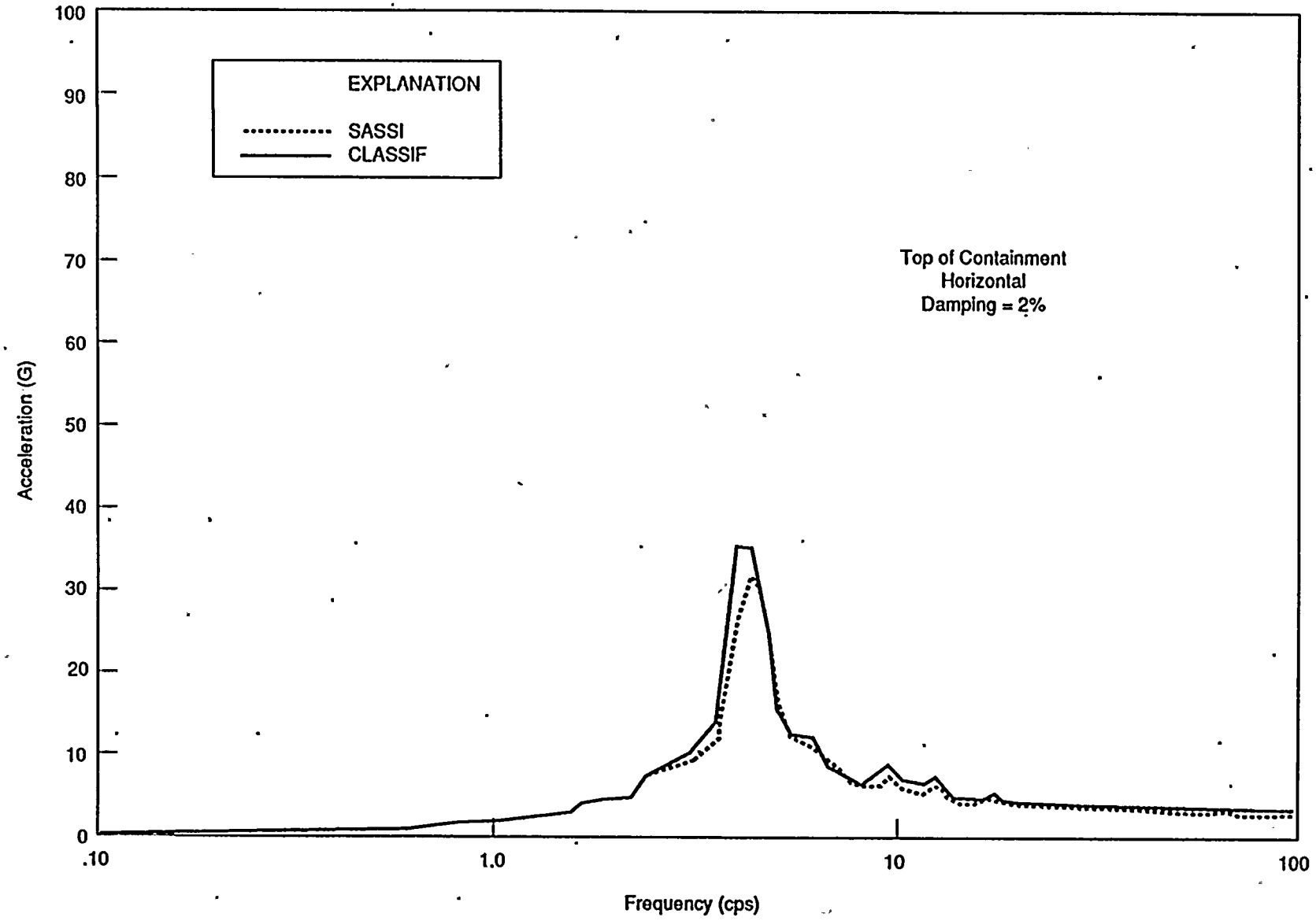

Figure 4.9-12. Horizontal Acceleration Response Spectrum at the Top of Containment (SV+P Wave Case)

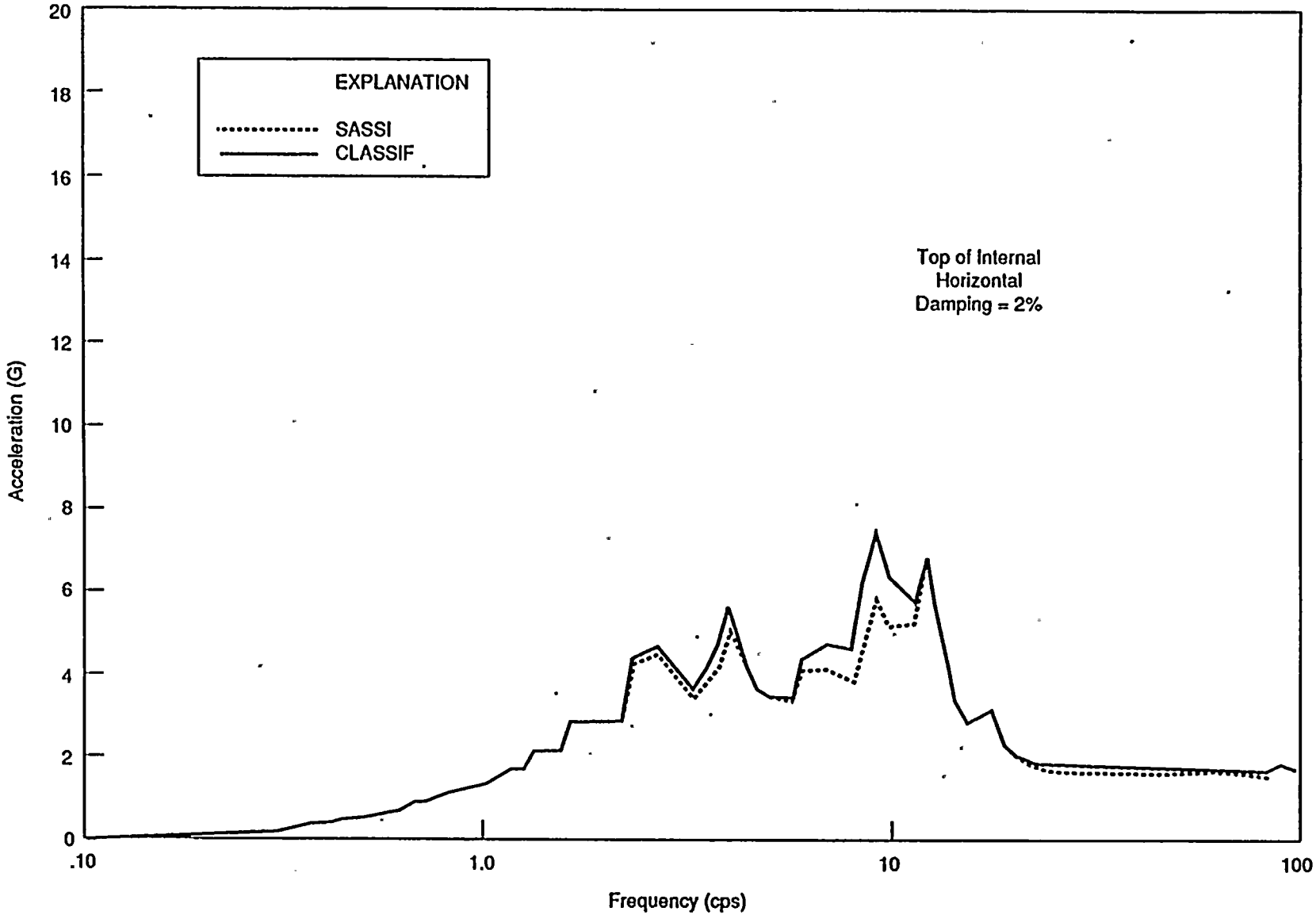

Figure 4.9-13. Horizontal Acceleration Response Spectrum at the Top of Internal (SV+P Wave Case)

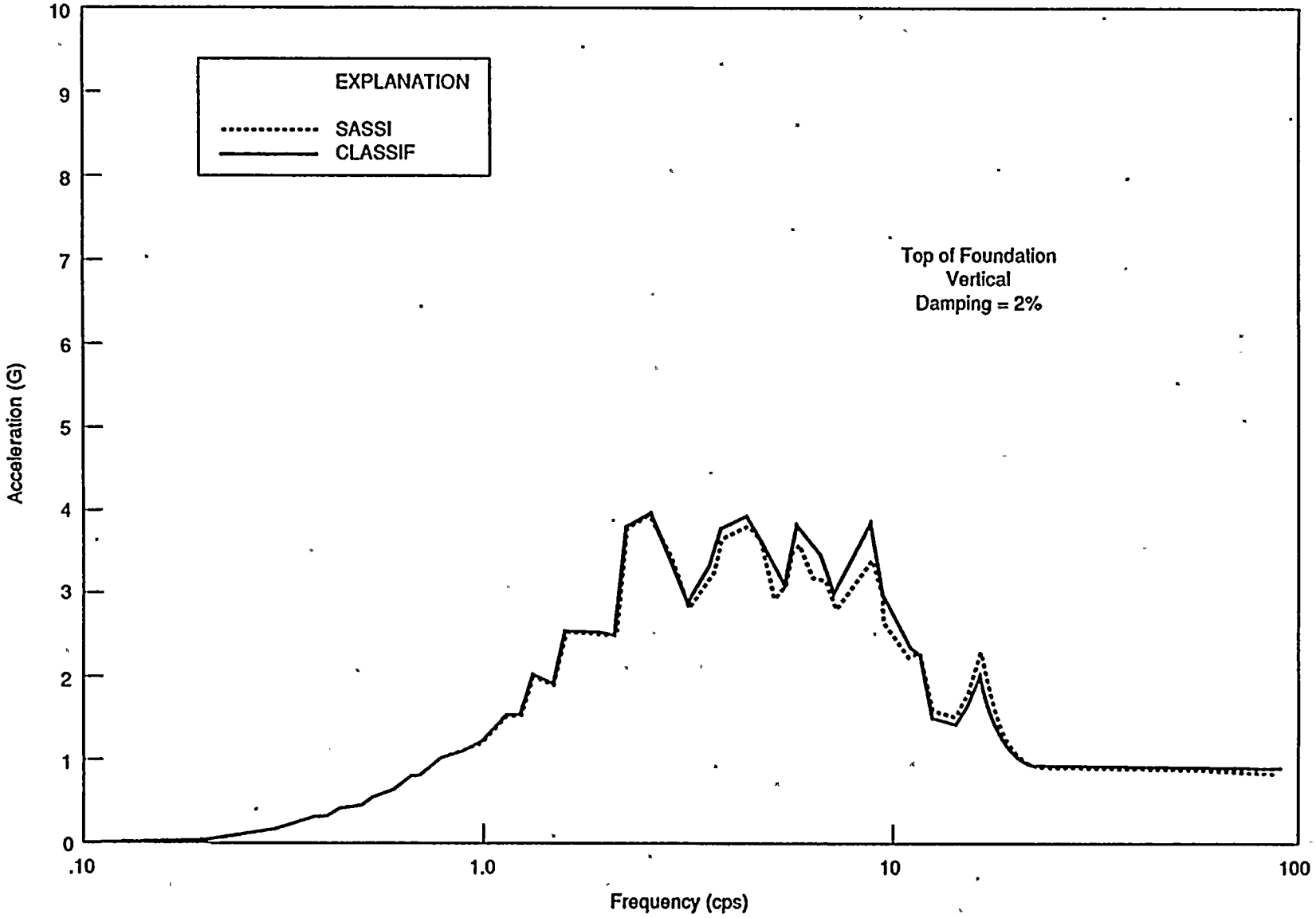

Figure 4.9-14. Vertical Acceleration Response Spectrum at the Top of Foundation (SV+P Wave Case)

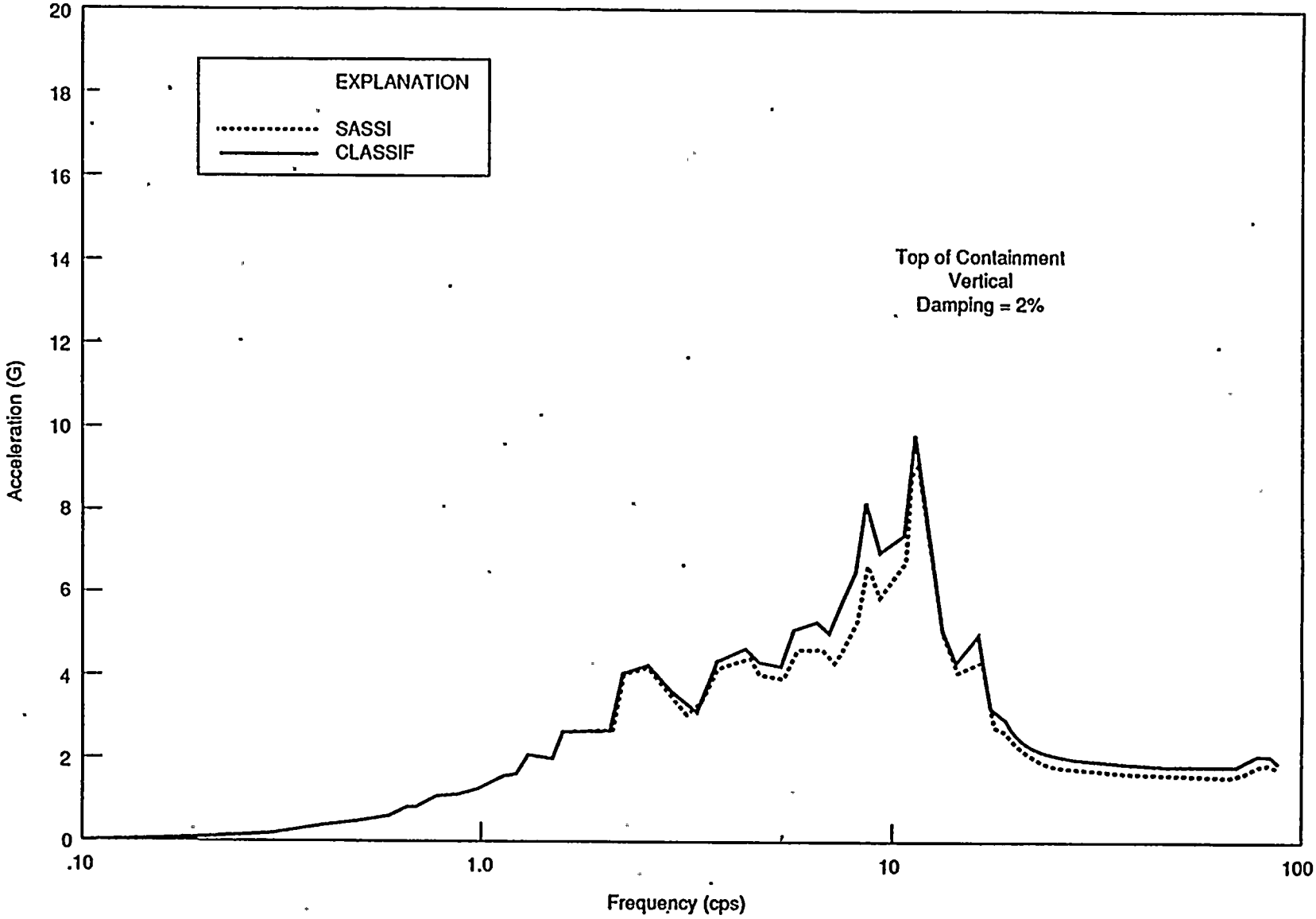

Figure 4.9-15. Vertical Acceleration Response Spectrum at the Top of Containment (SV+P Wave Case)

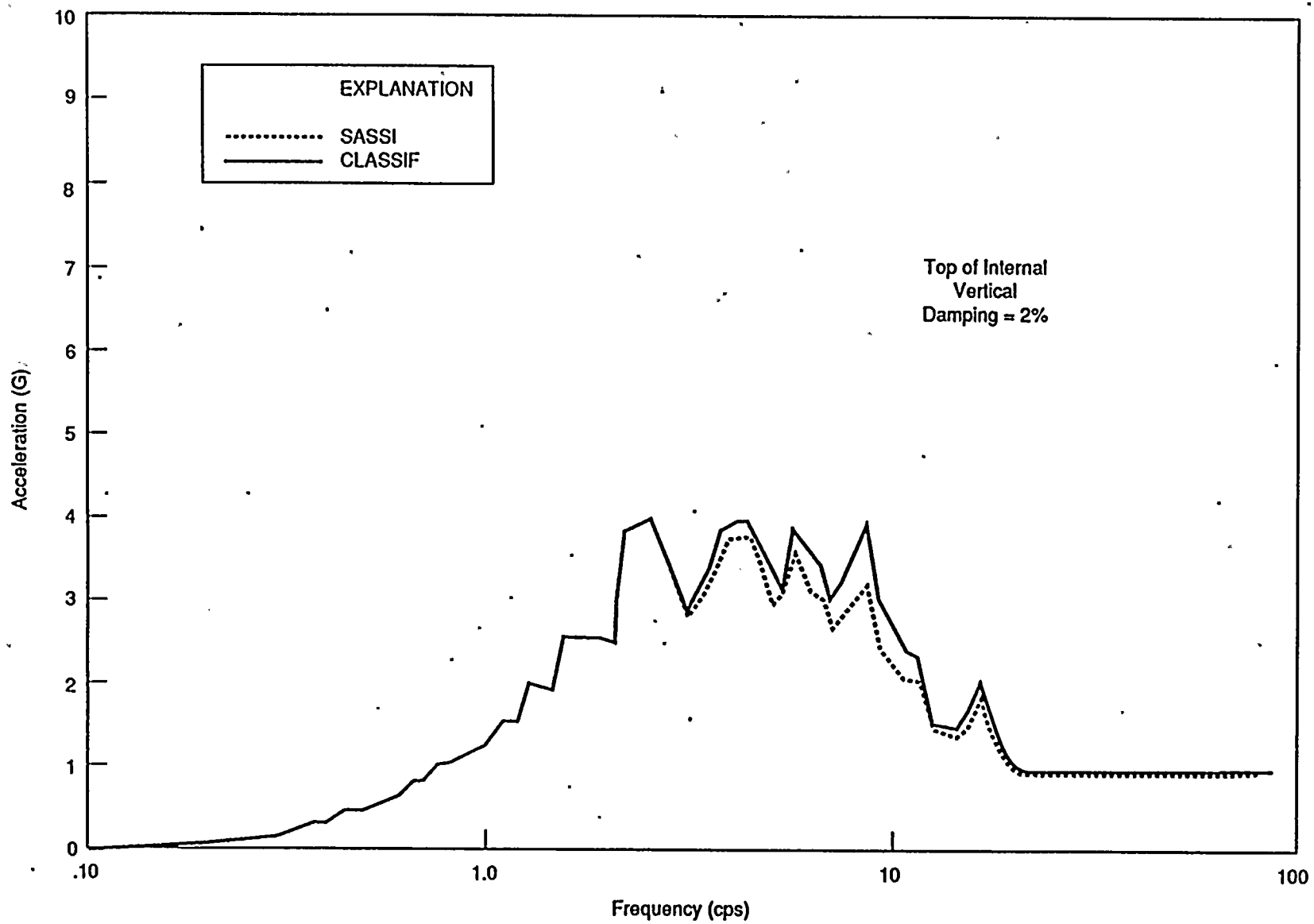

Figure 4.9-16. Vertical Acceleration Response Spectrum at the Top of Internal (SV+P Wave Case)

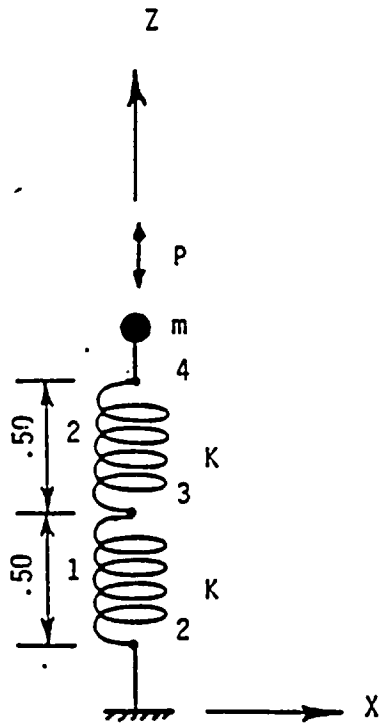

$k = .2\ m \simeq .0$, $P = 1.0 \exp(i\omega t)$

Material Damping = 10%

Figure 4.10-1. Spring Element Model (Case 1)

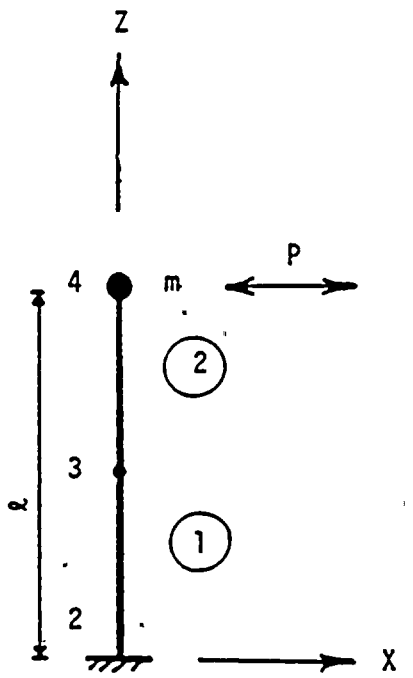

ℓ = 1.0, m = 1.0, axial area = 1.0, I = 1/3
Young's Modulus E = .25, Material Damping = 10%
P = 1.0 exp (iωt)

Figure 4.10-2. Beam Element Model (Case 2)

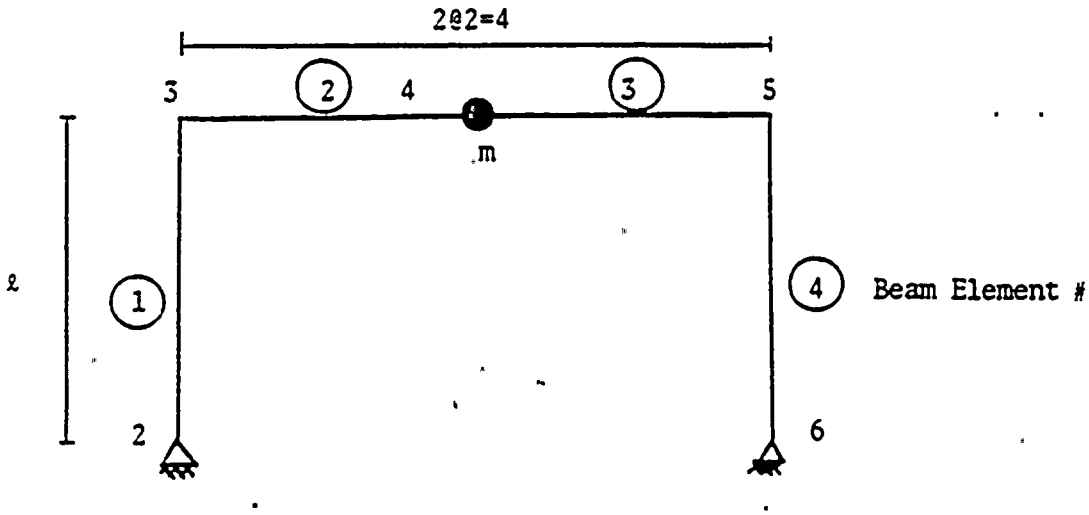

ℓ = 1, m = 1
beam elements 2 and 3 are rigid beams
beam elements 1 and 4 are flexible in bending
using the following properties
E=.25, I=1/3, ℓ=1, material damping = 10%

Figure 4.10-3. Beam Element with End Release (Case 23)

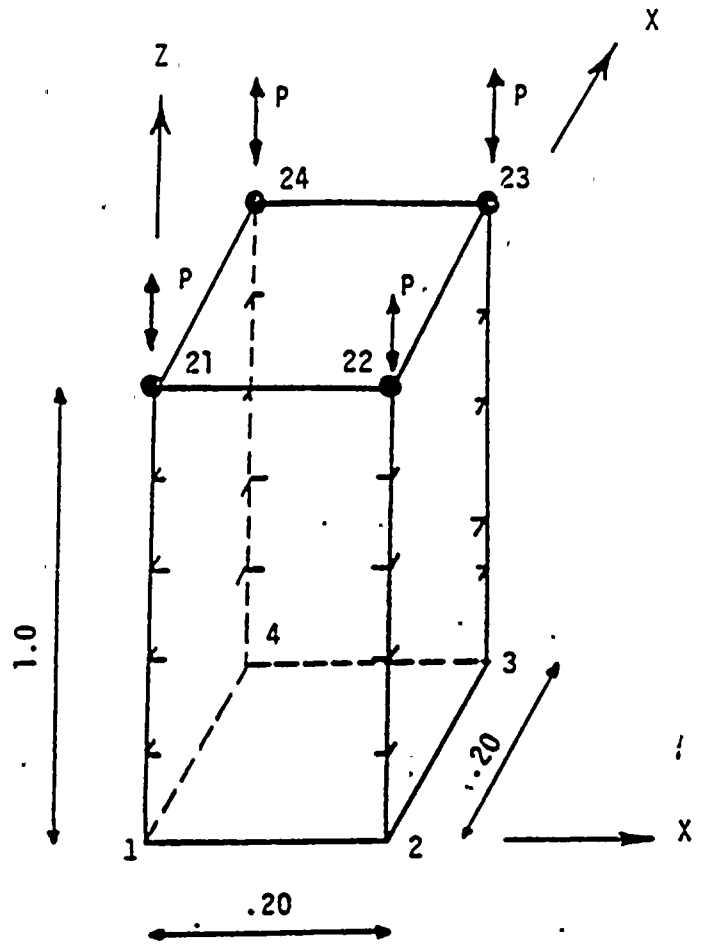

m = .25, Young's Modulus E = 25.0, γ = 32.17
Poisson's ratio = .25, Material Damping = 10%
P = .25 exp (iωt)

Figure 4.10-4. Brick Element Model (Case 3)

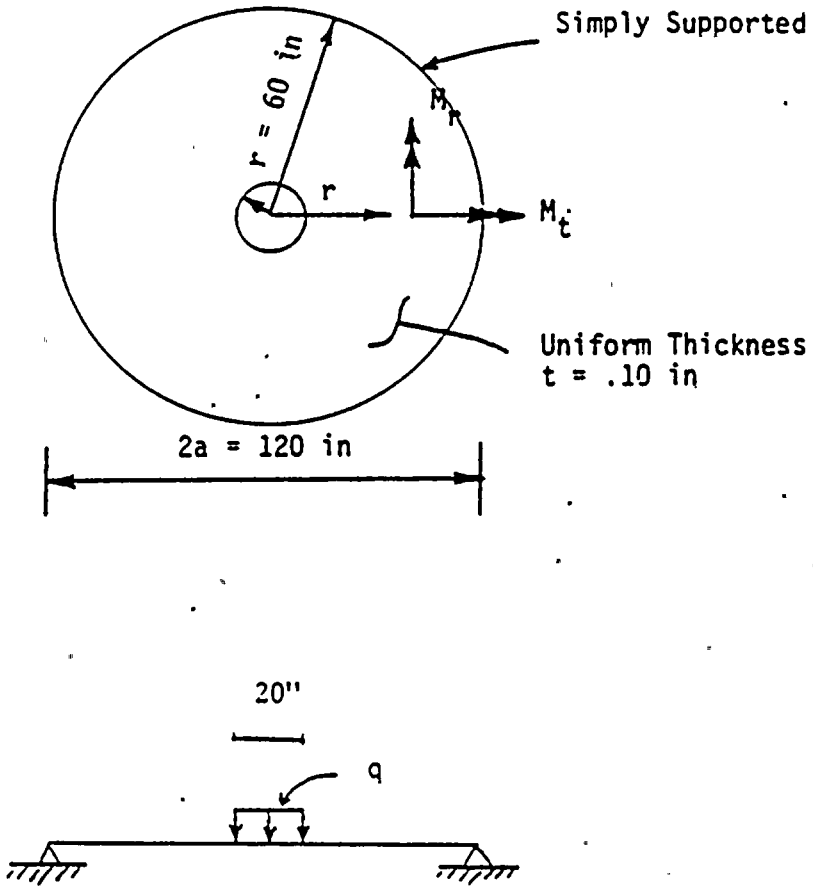

Figure 4.10-5. Simply Supported Plate (Case 4)

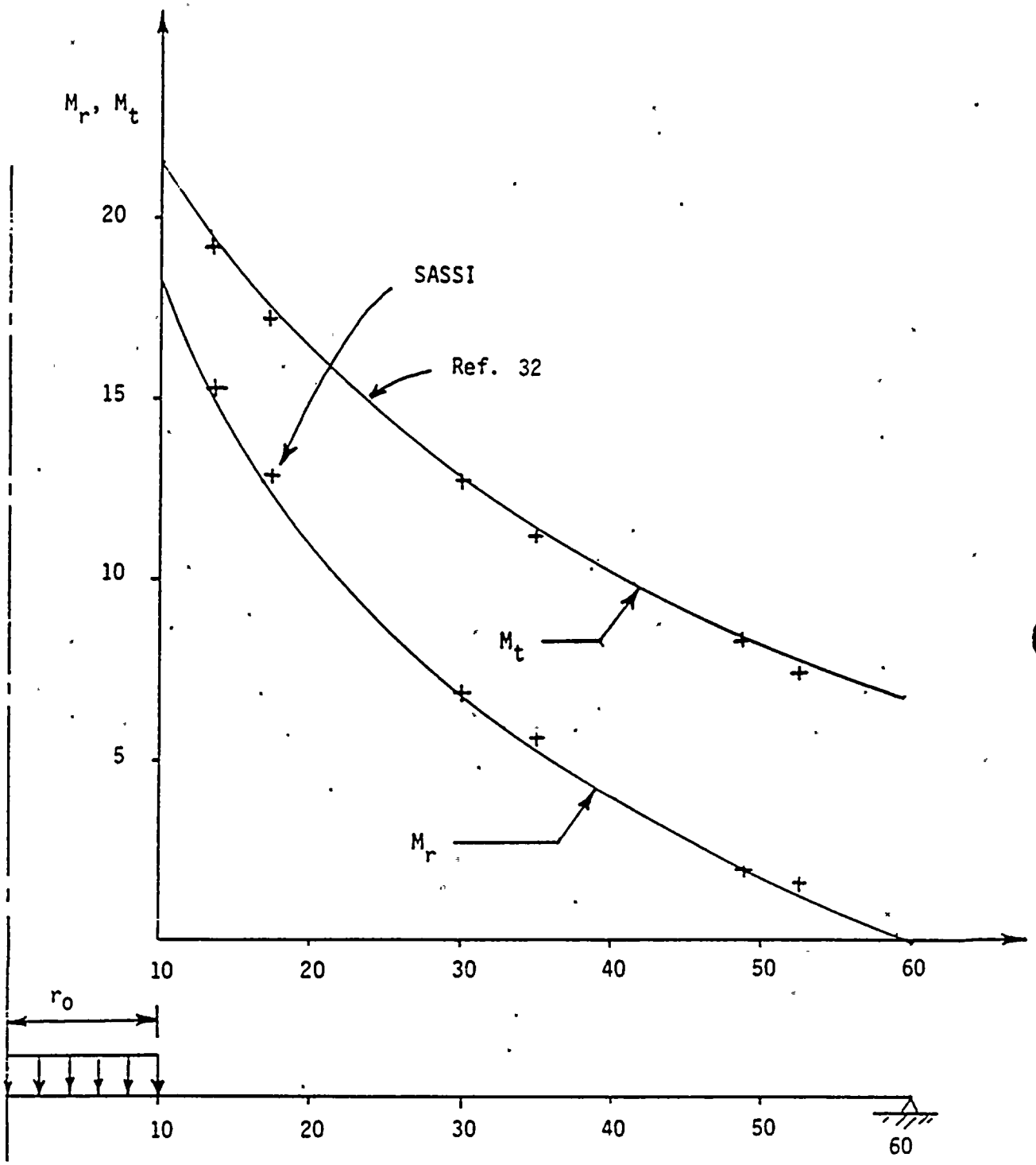

Figure 4.10-6. Comparison of Tangential and Radial Moments (Case 4)

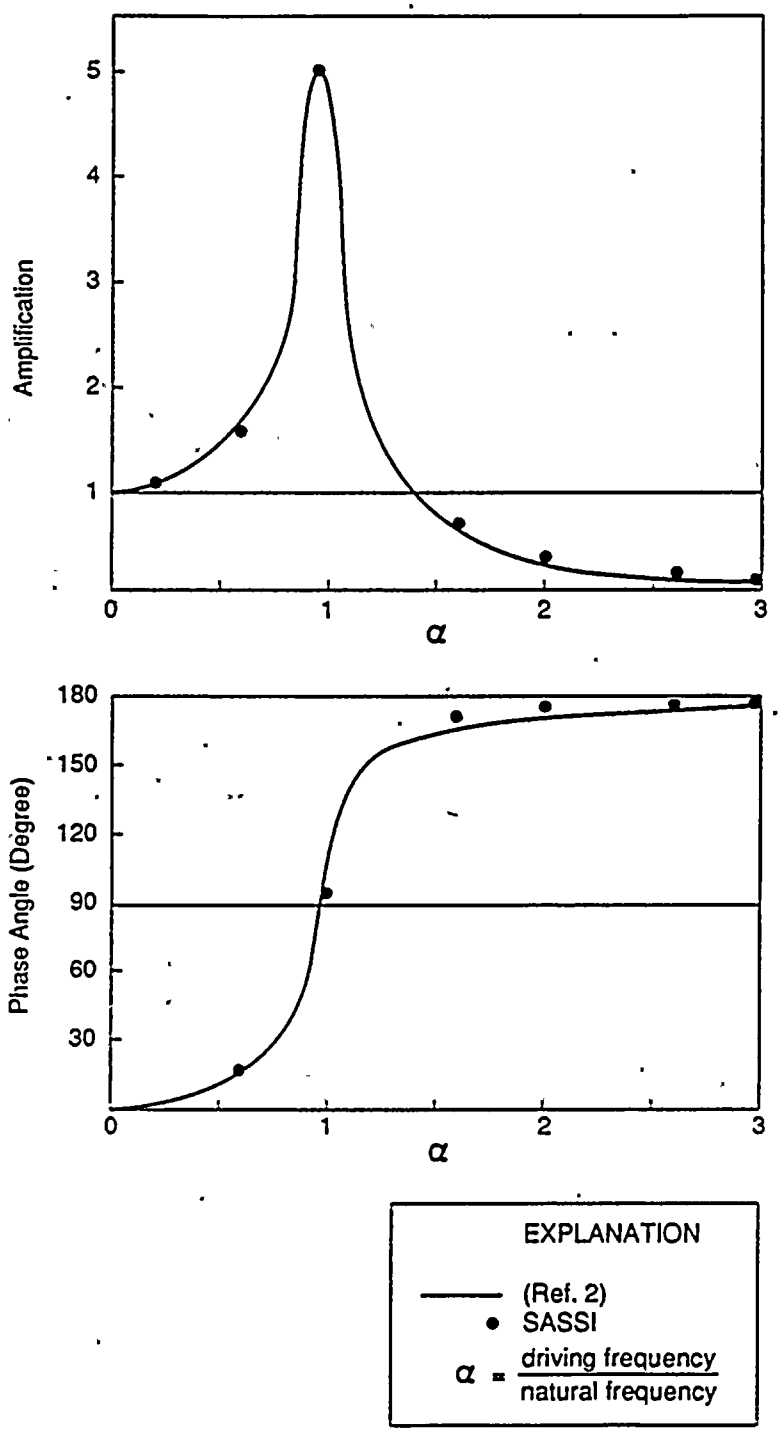

Figure 4.11-1. Comparison of Results for Case 1 (Spring Element)

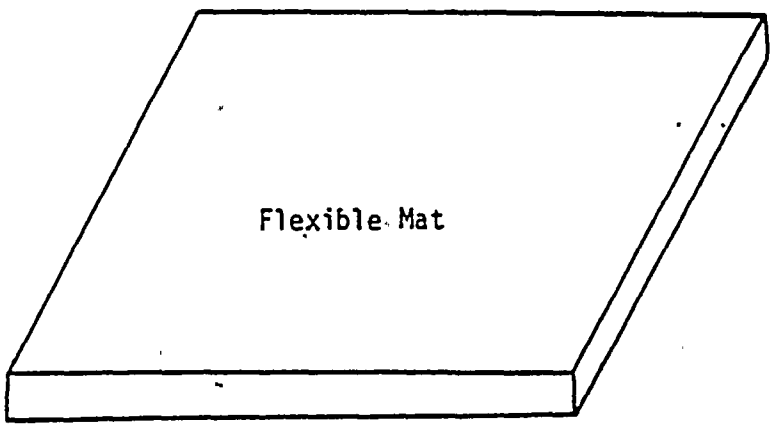

Figure 4.12.1. Flexible Mat Model

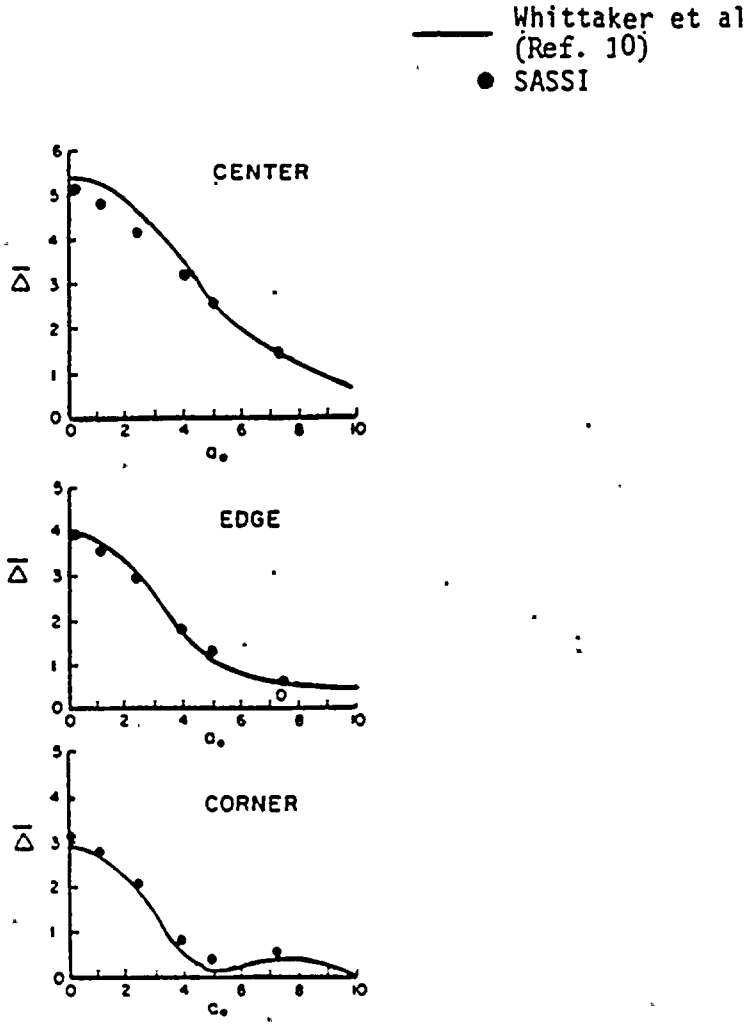

Figure 4.12-2. Normalized Displacement Due to Uniform Vertical Load, Case 1

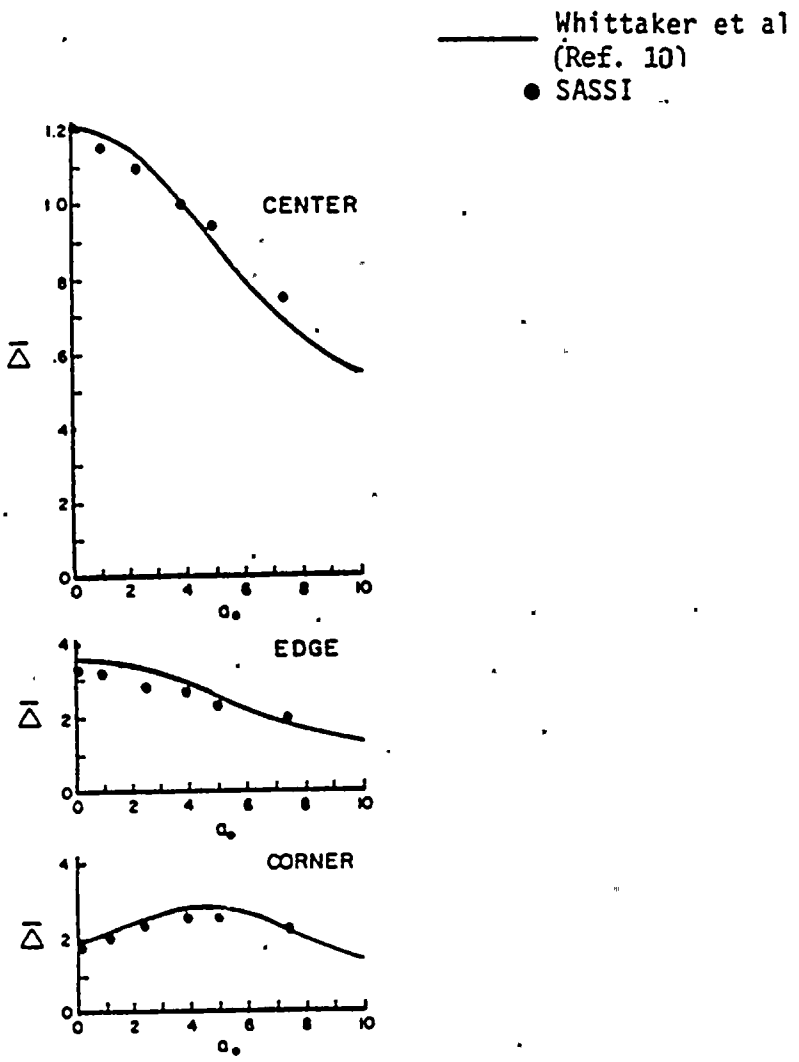

Figure 4.12-3. Normalized Displacement Due to Center Vertical Point Load (Case 2)

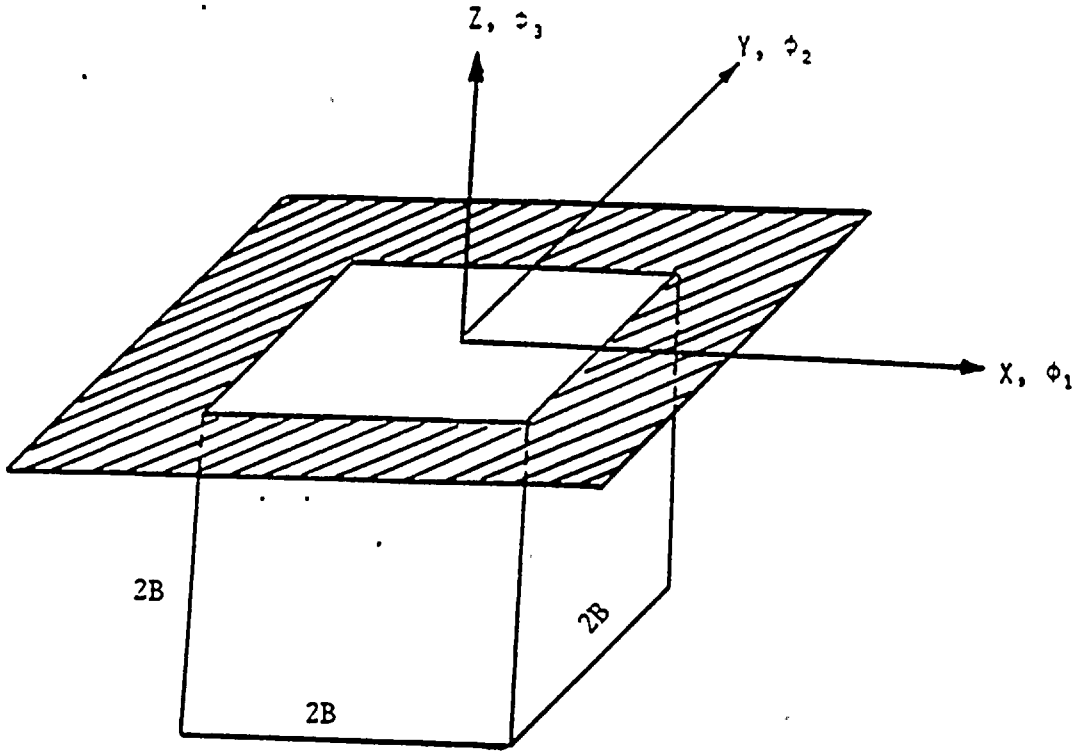

30x30x30 ft

Foundation:

Rigid massless cube, fully embedded

Halfspace:

Shear Wave Velocity	V_S = 900 ft/sec
Poisson's Ratio	ν = 1/3
Density	γ = 128.68 pcf
Material Damping	β = .0

Figure 4.13-1. Soil-Foundation System

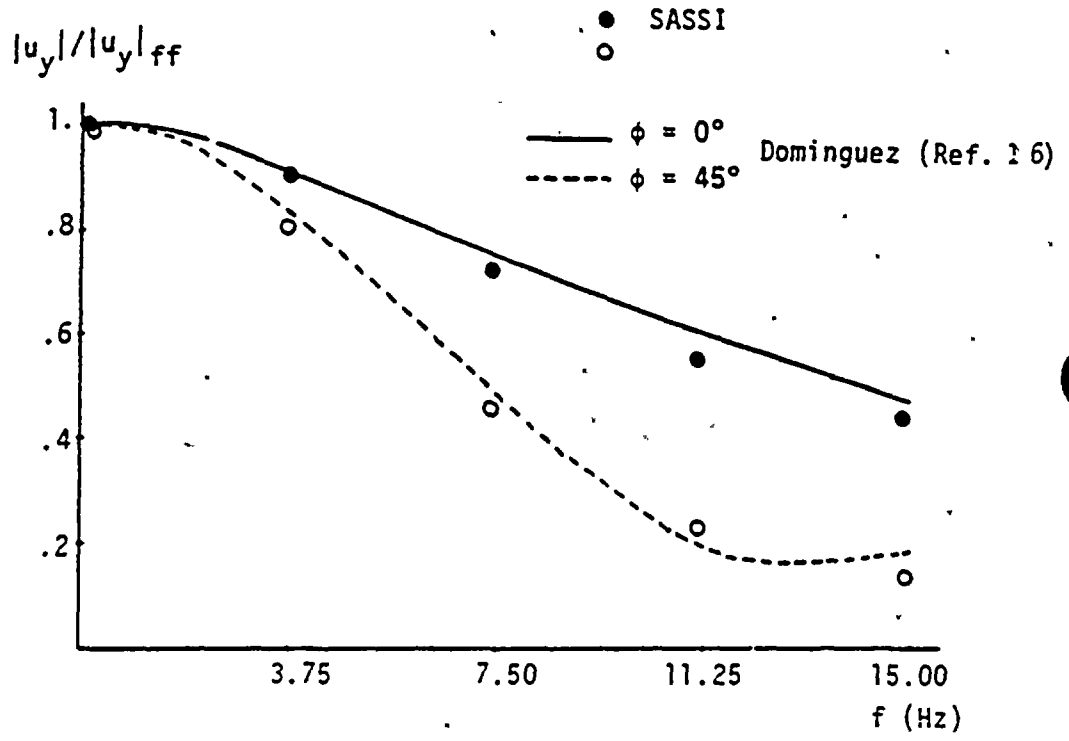

Figure 4.13-2. Horizontal Translation - SH Wave

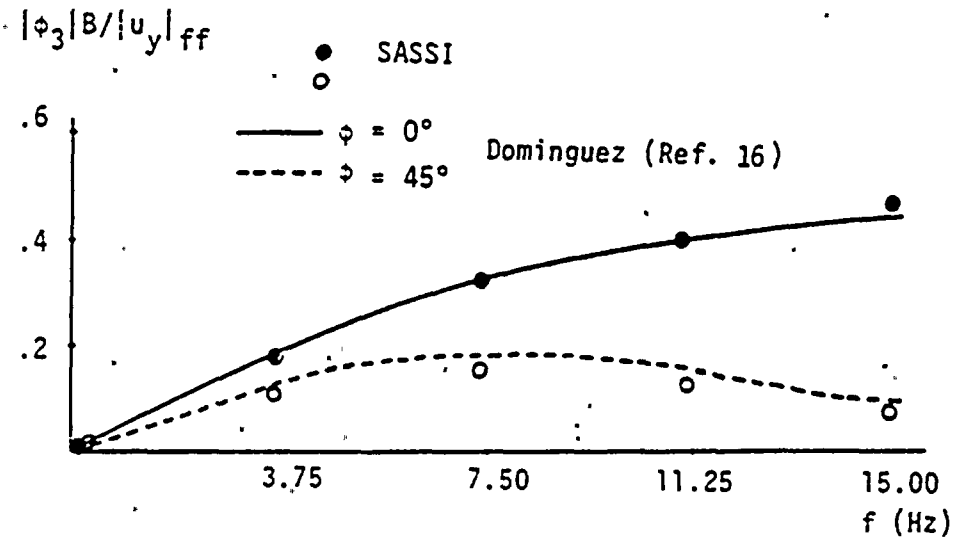

Figure 4.13-3. Torsional Motion - SH Wave

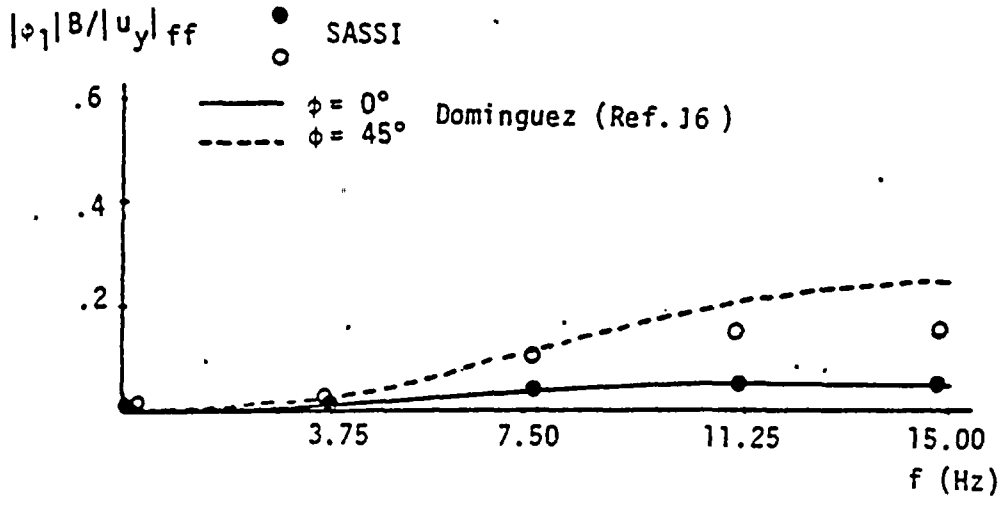

Figure 4.13-4. Rocking Motion - SH Wave

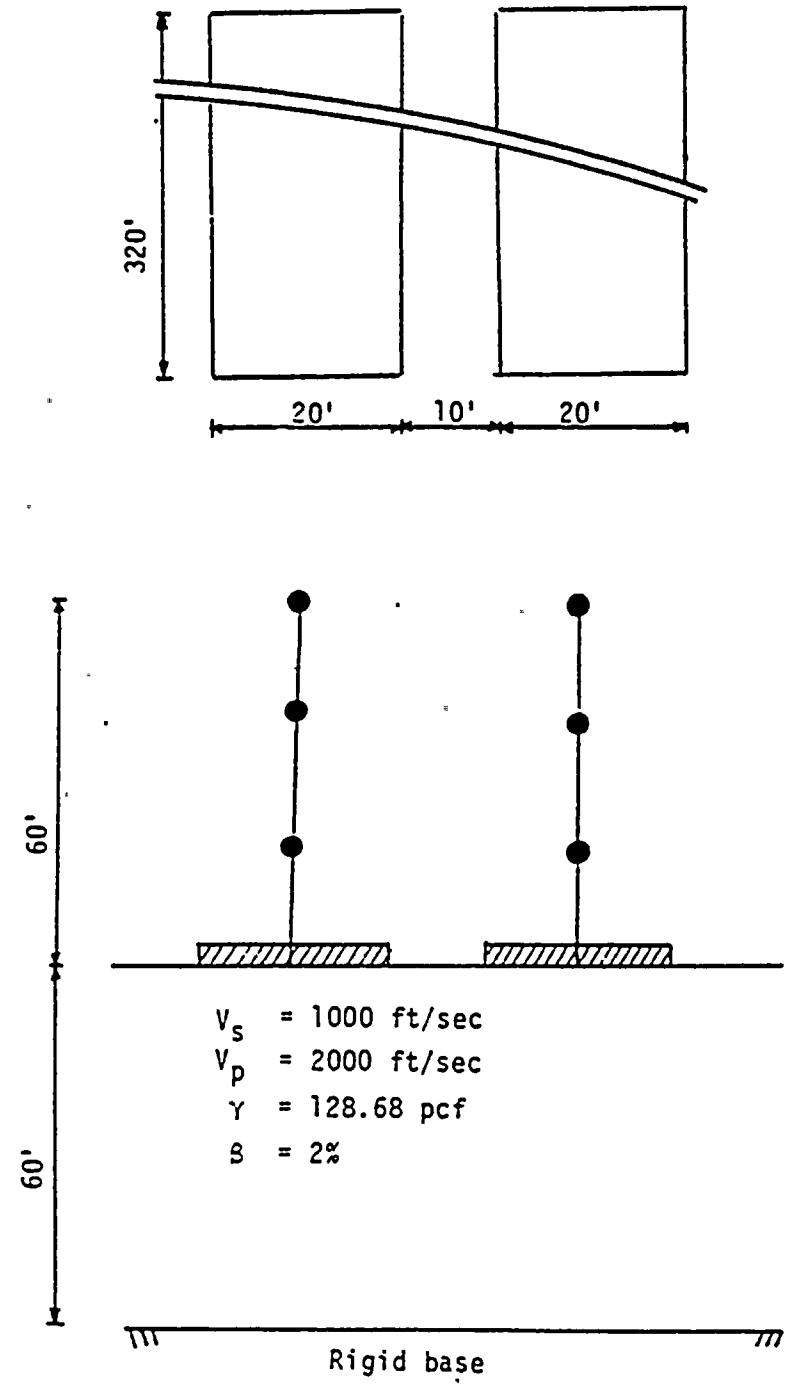

Figure 4.14-1. SASSI 3-D Model of Two Structure Systems

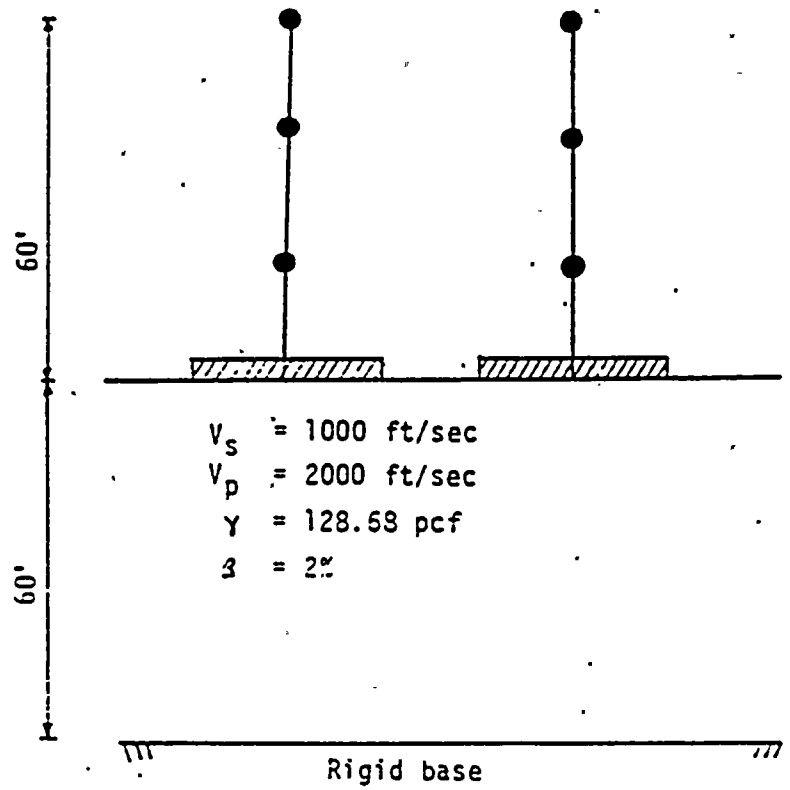

Figure 4.14-2. SASSI 2-D Model of Two Structure Systems

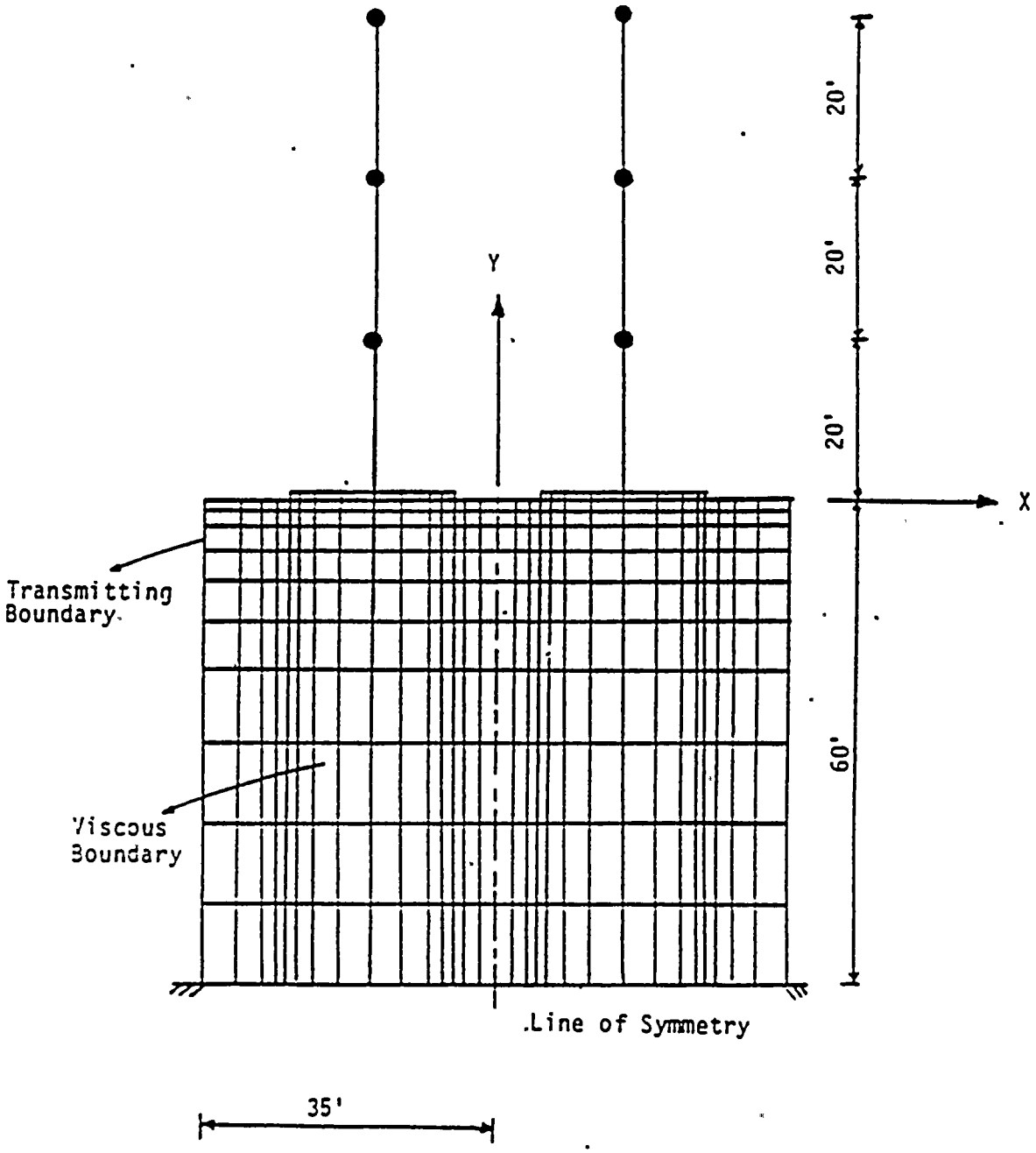

Figure 4.14-3. FLUSH Model of Two Structure System

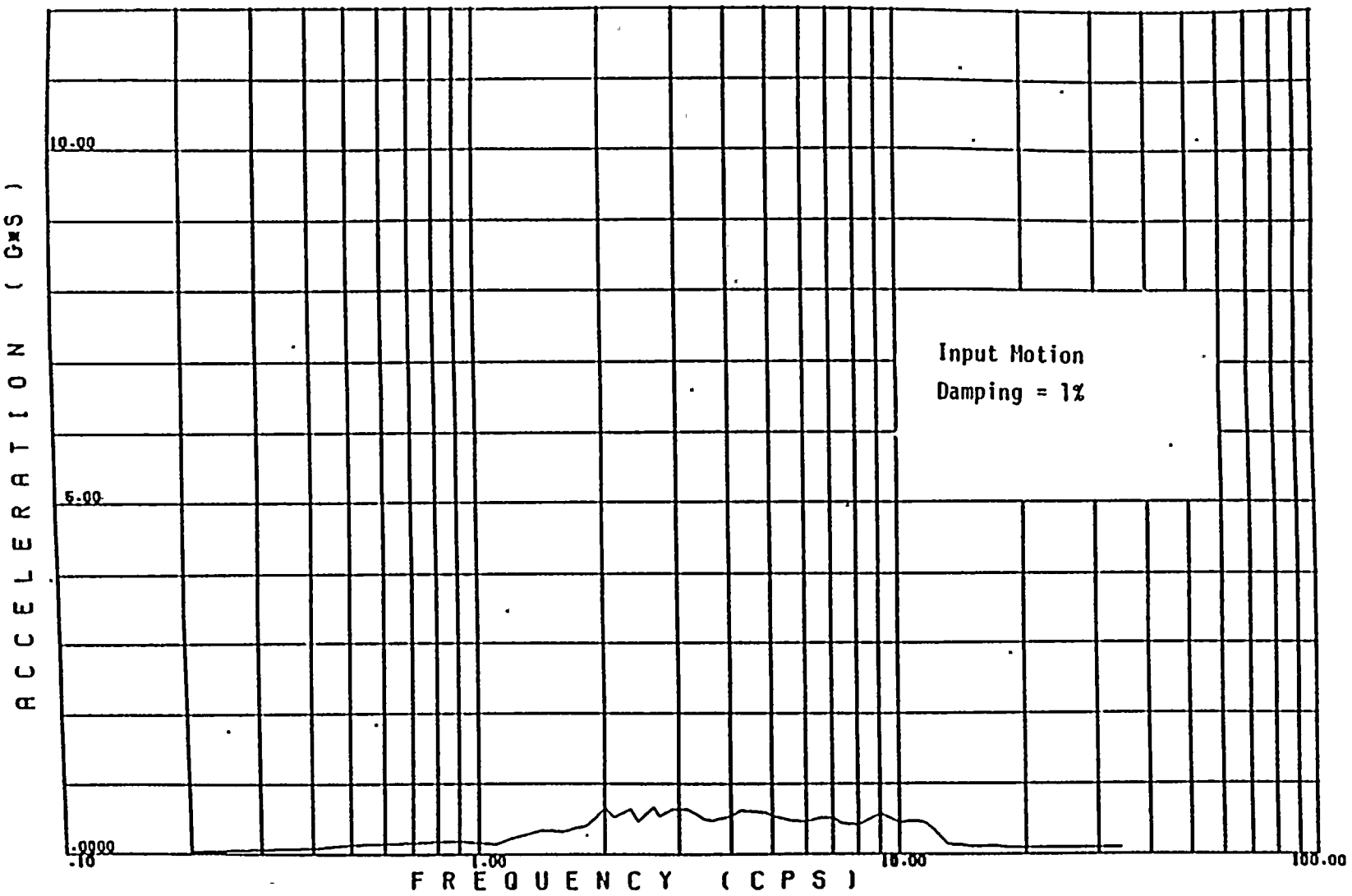

Figure 4.14-4. Absolute Acceleration Response Spectrum of Input Motion

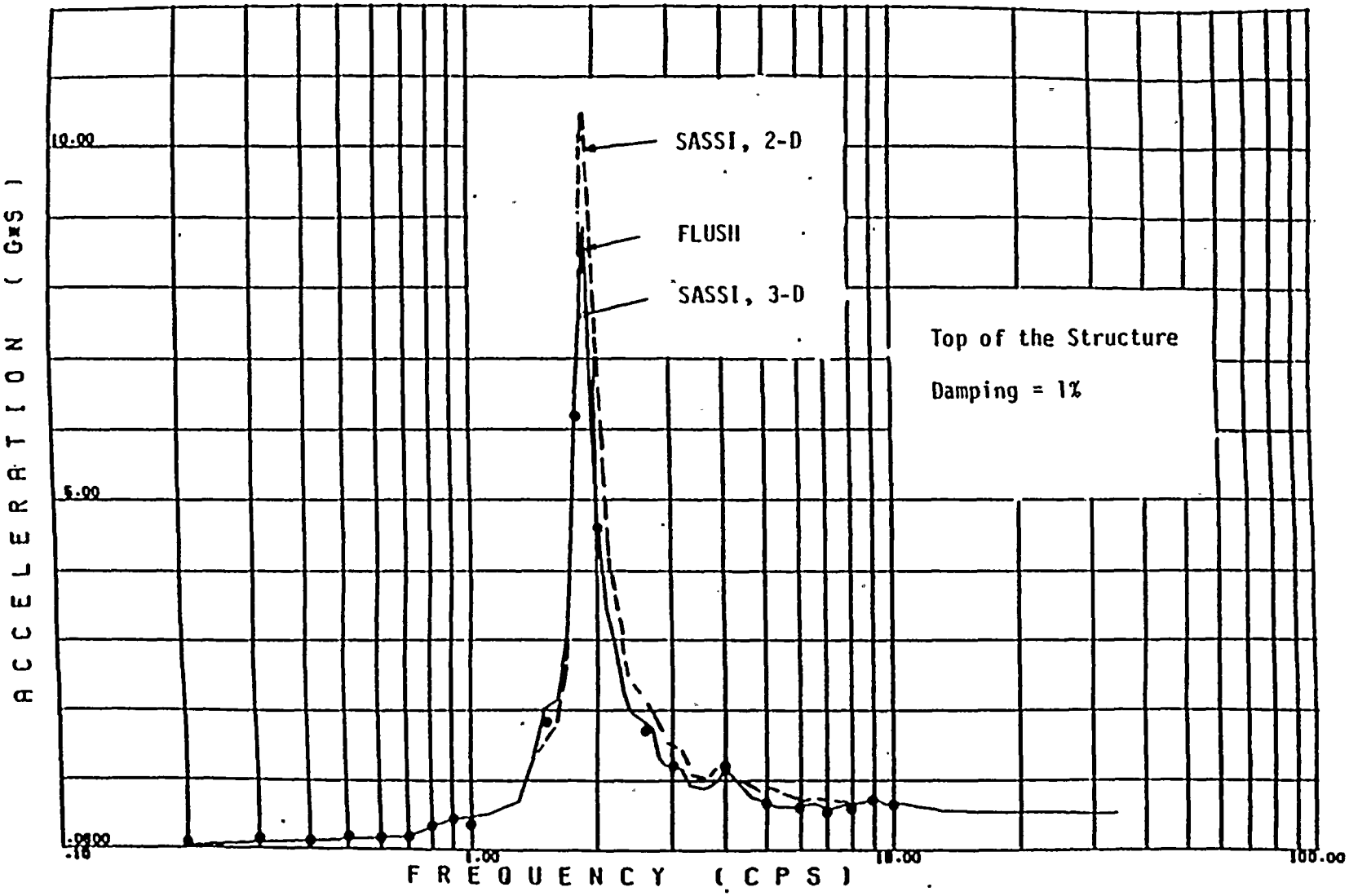

Figure 4.14-5. Absolute Acceleration Response Spectrum at the Top of the Structure

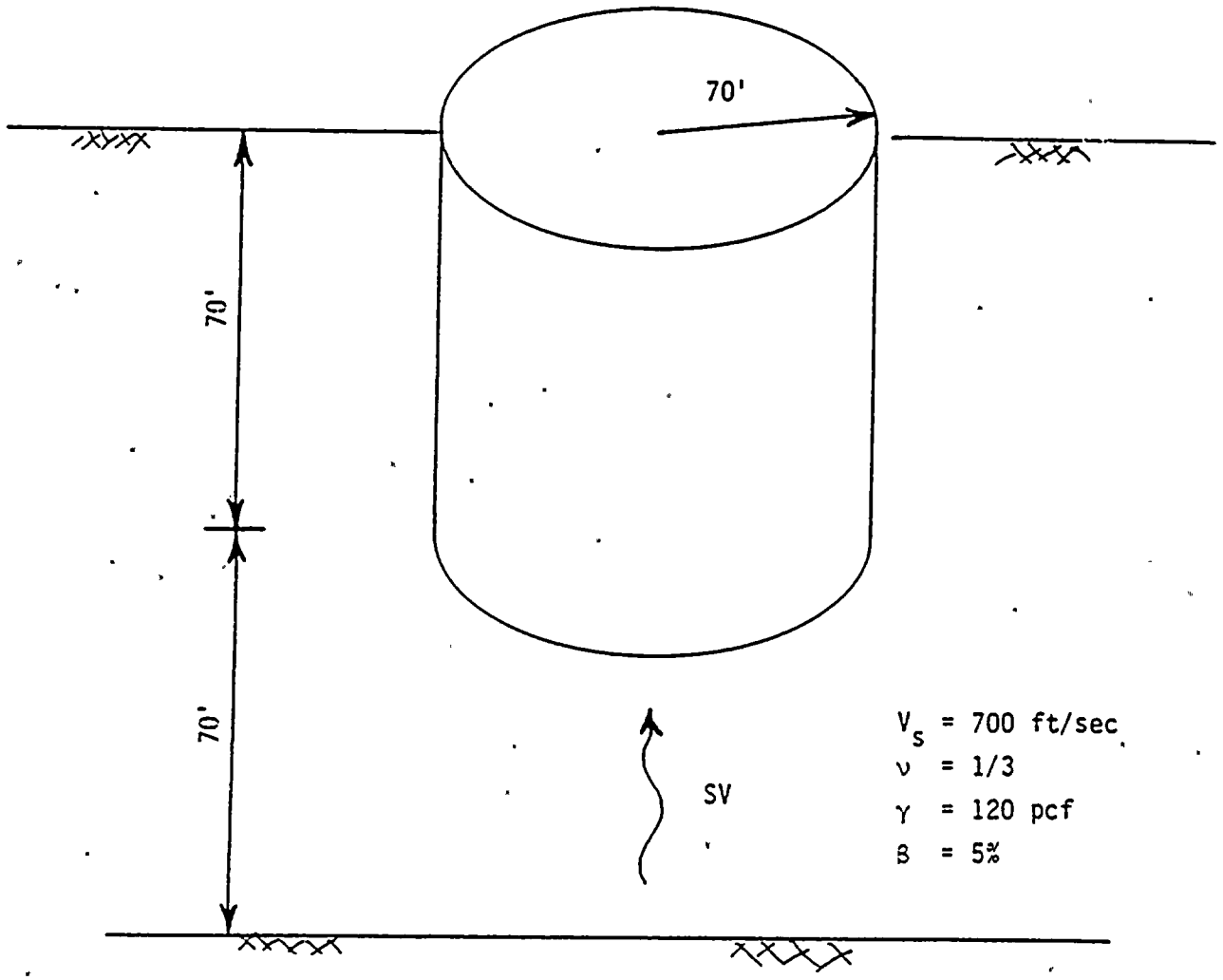

Figure 4.15-1. Embedded Rigid Cylinder Model

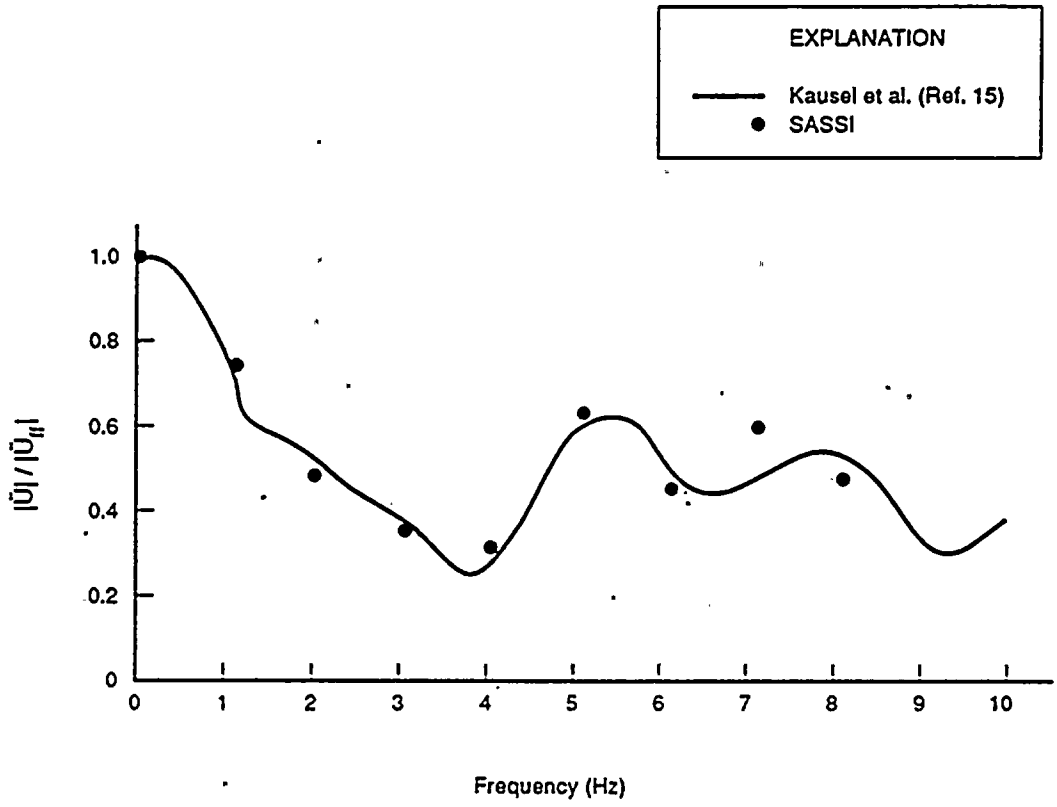

Figure 4.15-2. Normalized Translation Response to the Foundation

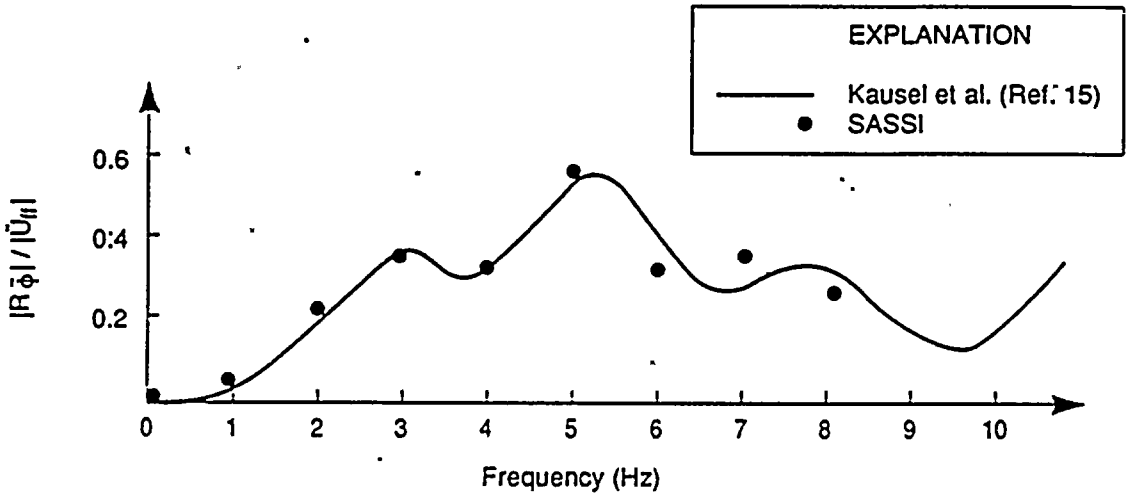

Figure 4.15-3. Normalized Rocking Response of the Foundation

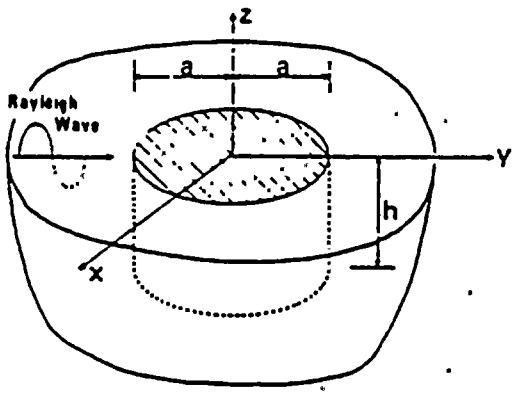

Foundation:

Rigid Massless Cylinder, Fully Embedded

a = 65 ft, h = 32.5 ft

Halfspace:

Shear Wave Velocity	V_S = 2000 ft/sec
Poisson's Ratio	ν = .25
Density	γ = 128.68 pcf
Material Damping	β = .0

Figure 4.16-1. Soil-Foundation System

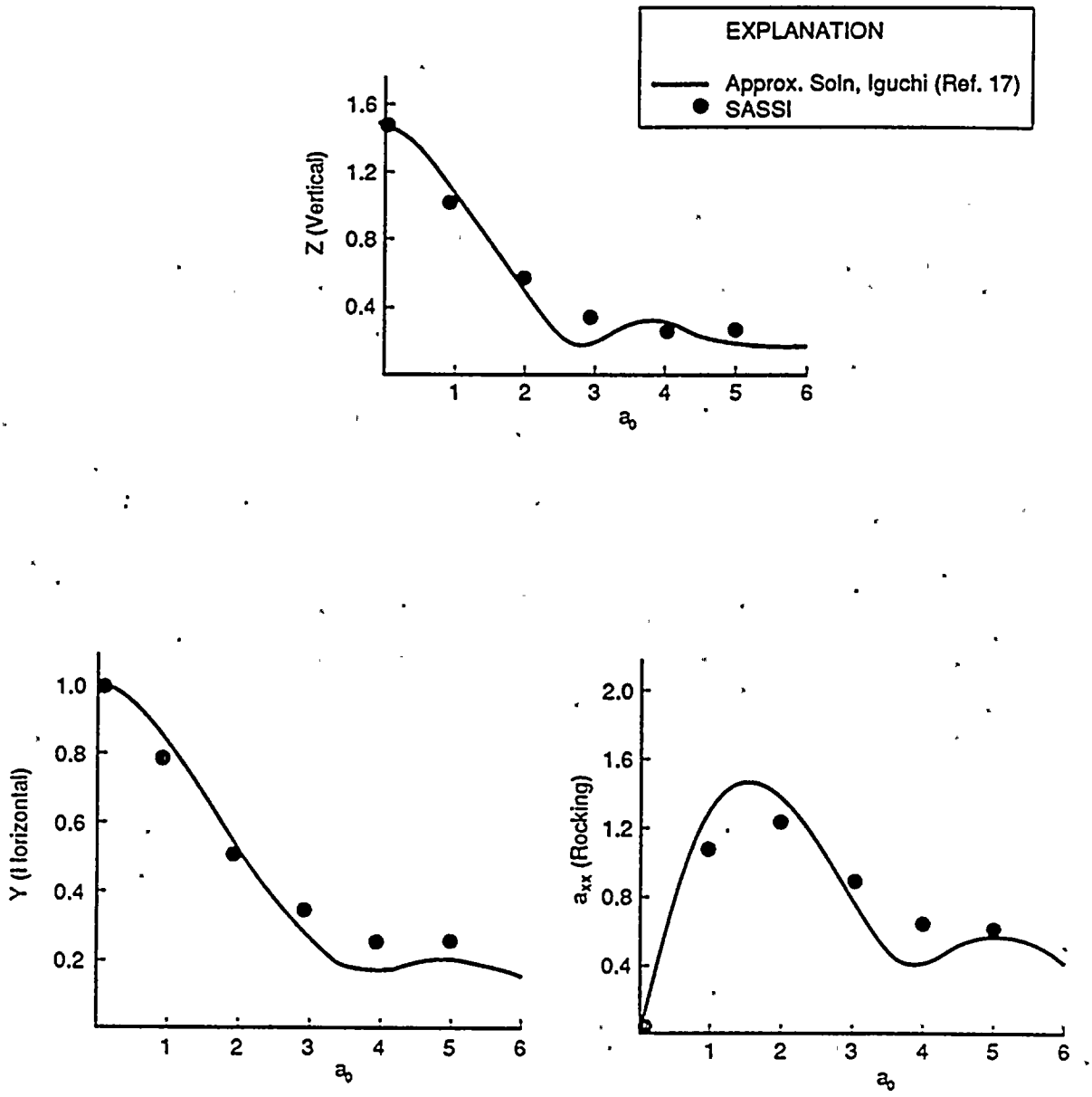

Figure 4.16-2. Vertical, Horizontal, and Rocking Motions

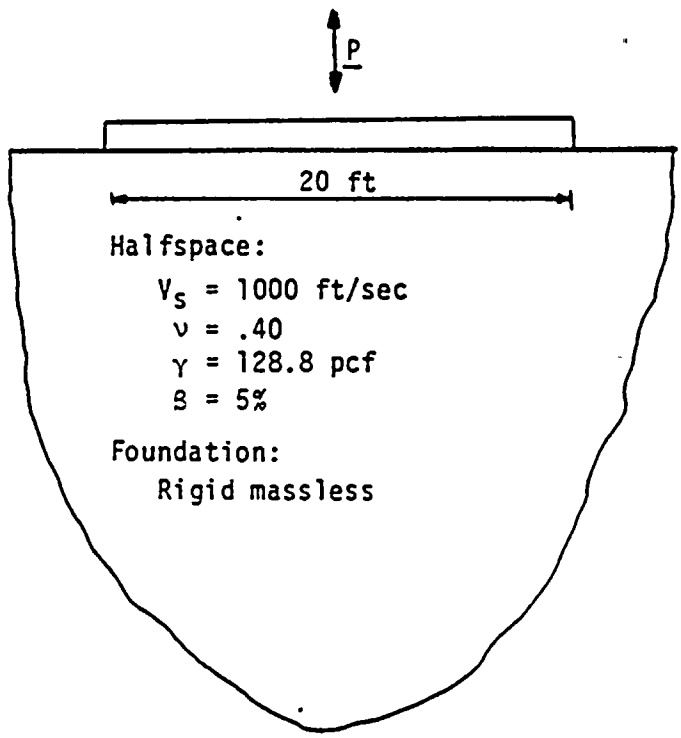

Figure 4.17-1. SASSI 2-D Model for Case 1 (Halfspace)

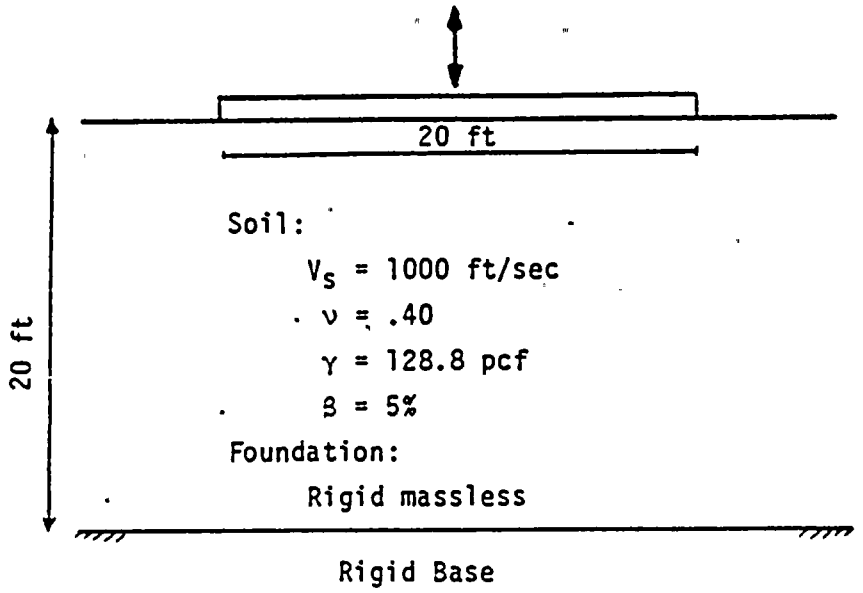

Figure 4.17-2. SASSI 2-D Model for Case 2 (Layered System)

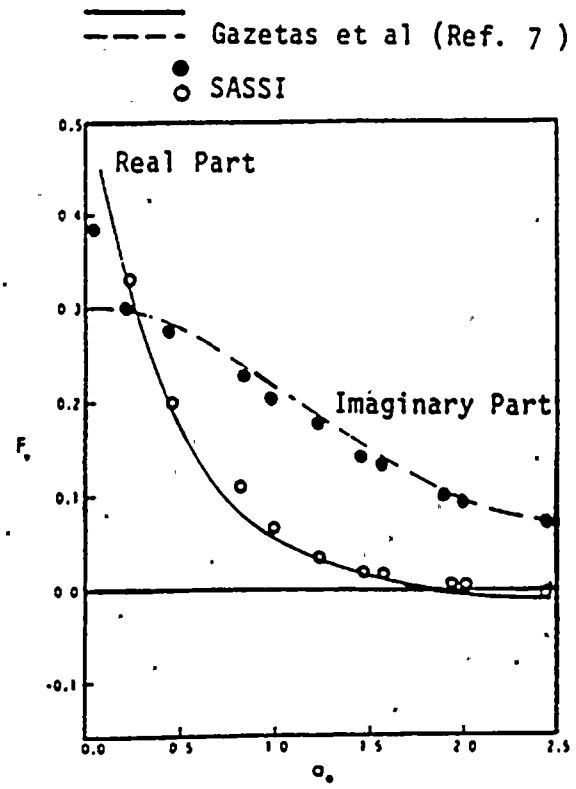

Figure 4.17-3. Vertical Compliance Function for Case 1 (Halfspace)

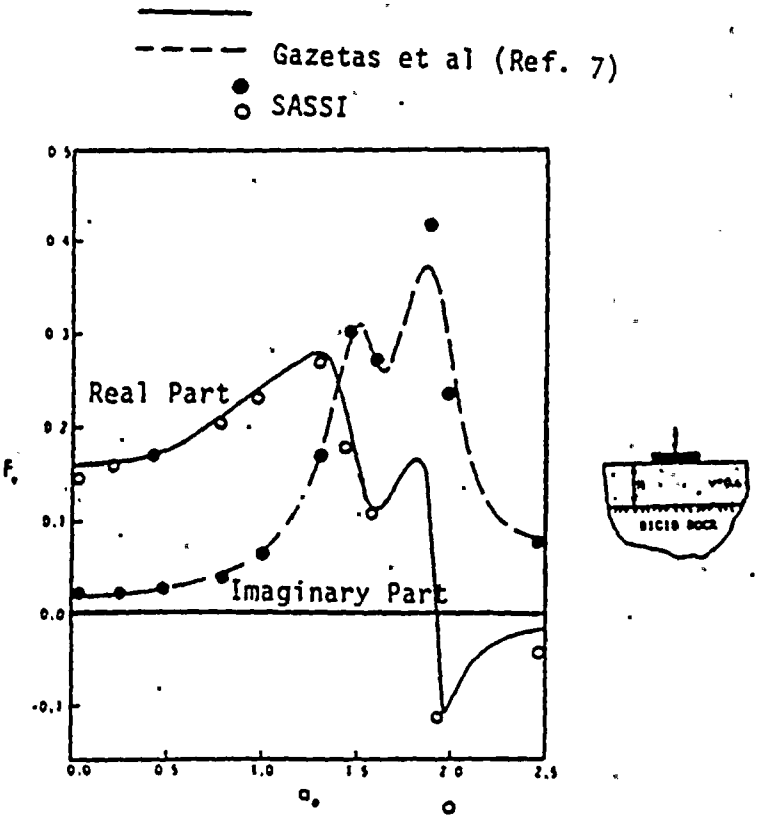

Figure 4.17-4. Vertical Compliance Function for Case 2 (Layered System)

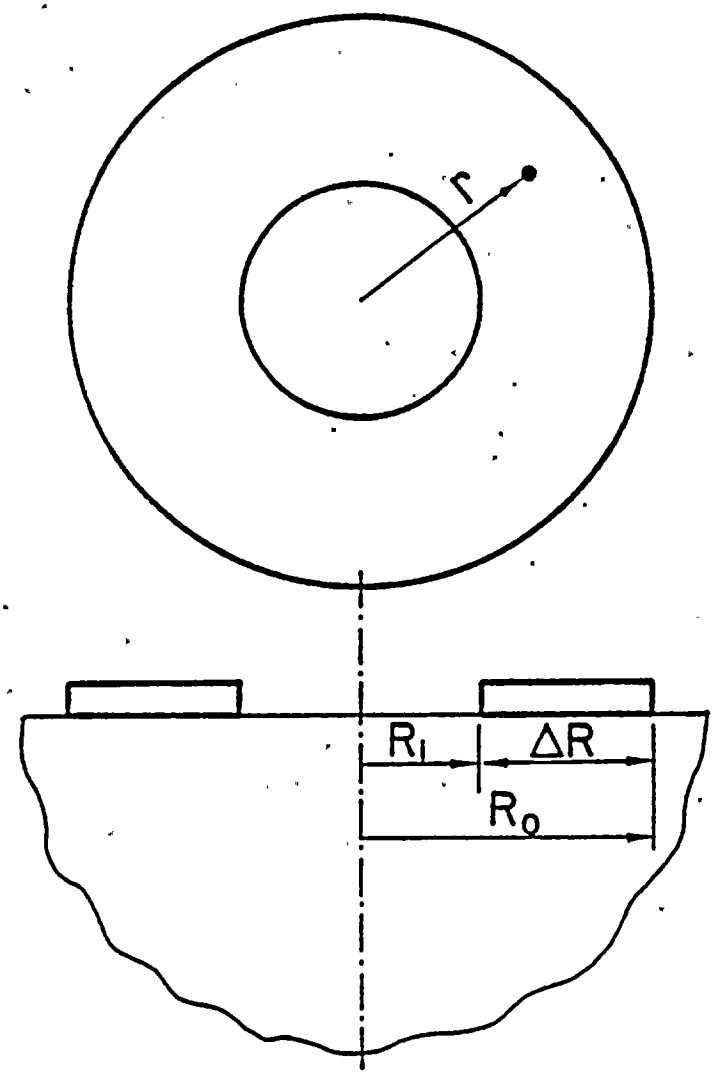

Foundation:

Rigid, Massless Ring

R_o = 100 ft, ΔR = 10 ft

Halfspace:

V_s = 1000 ft/sec

V_p = 2000 ft/sec

γ = 128.8 pcf

β = .0

Figure 4.18-1. Foundation Model

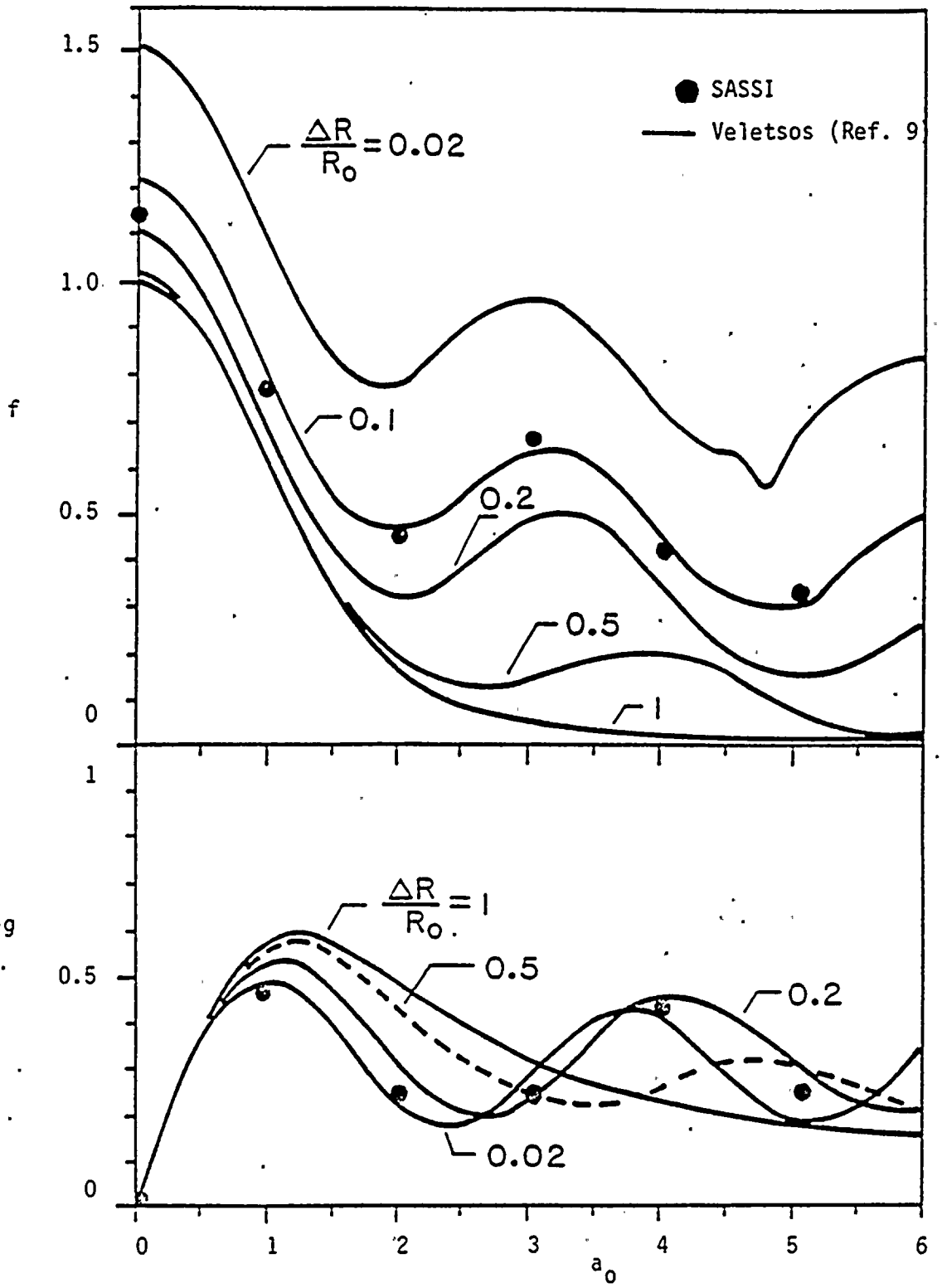

Figure 4.18-2. Flexibility Coefficients

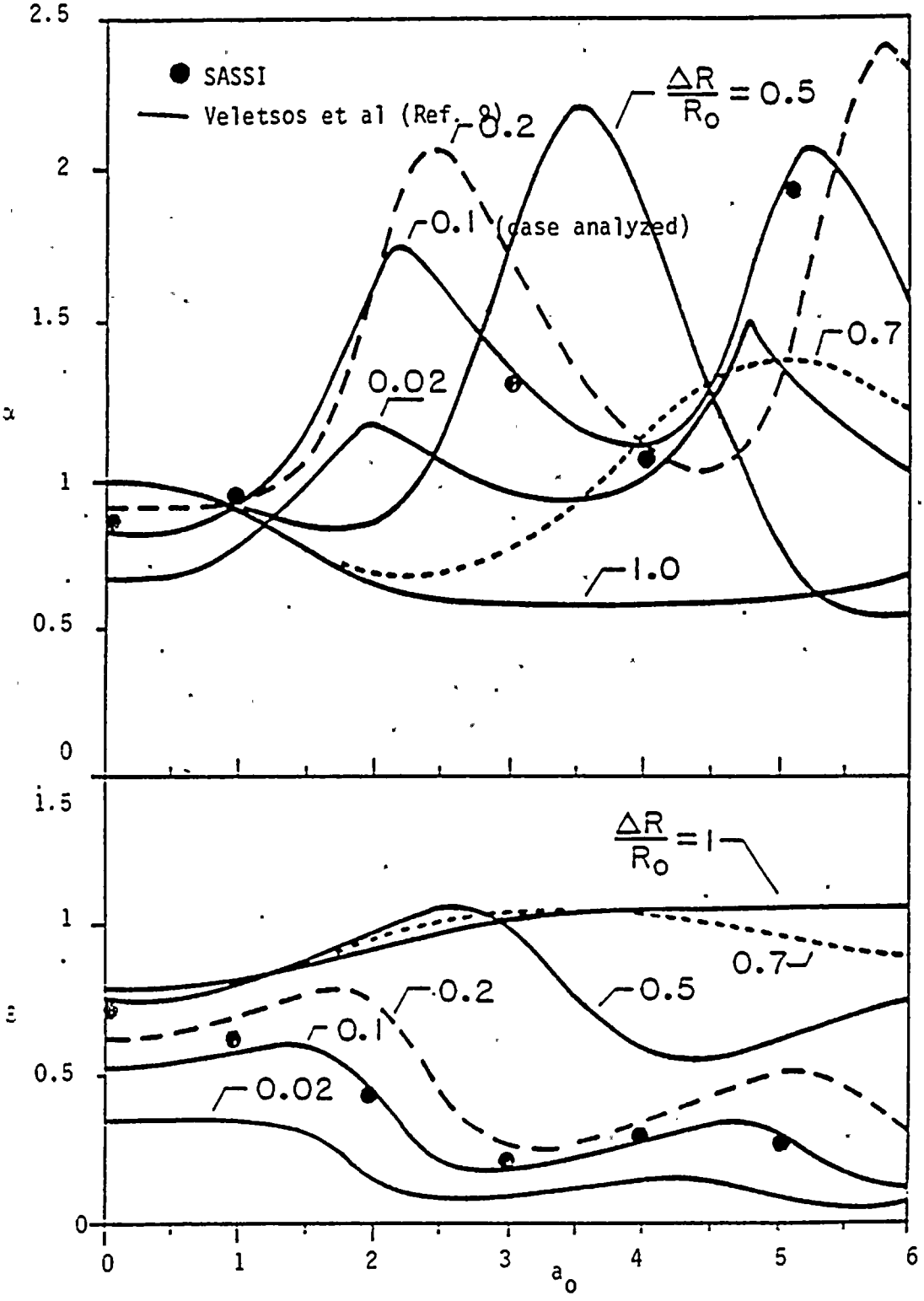

Figure 4.18-3. Stiffness and Damping Coefficients

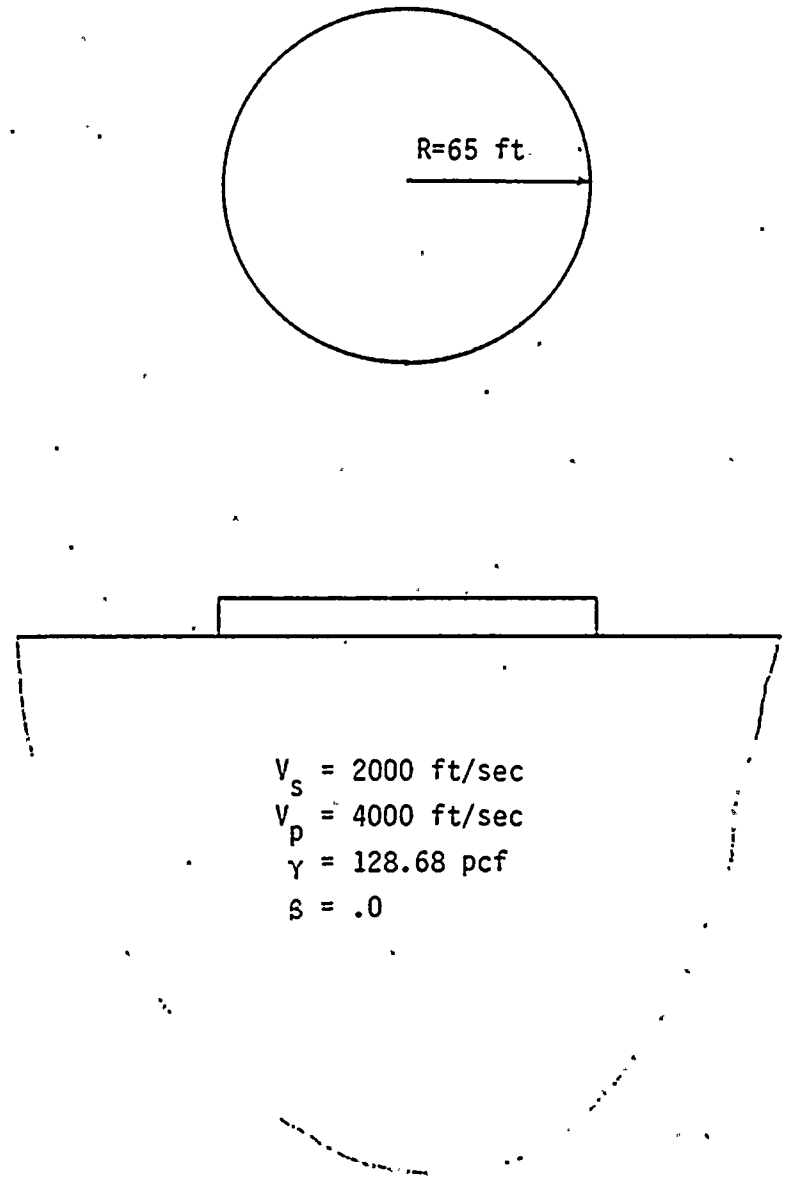

Figure 4.19-1. Foundation Configuration

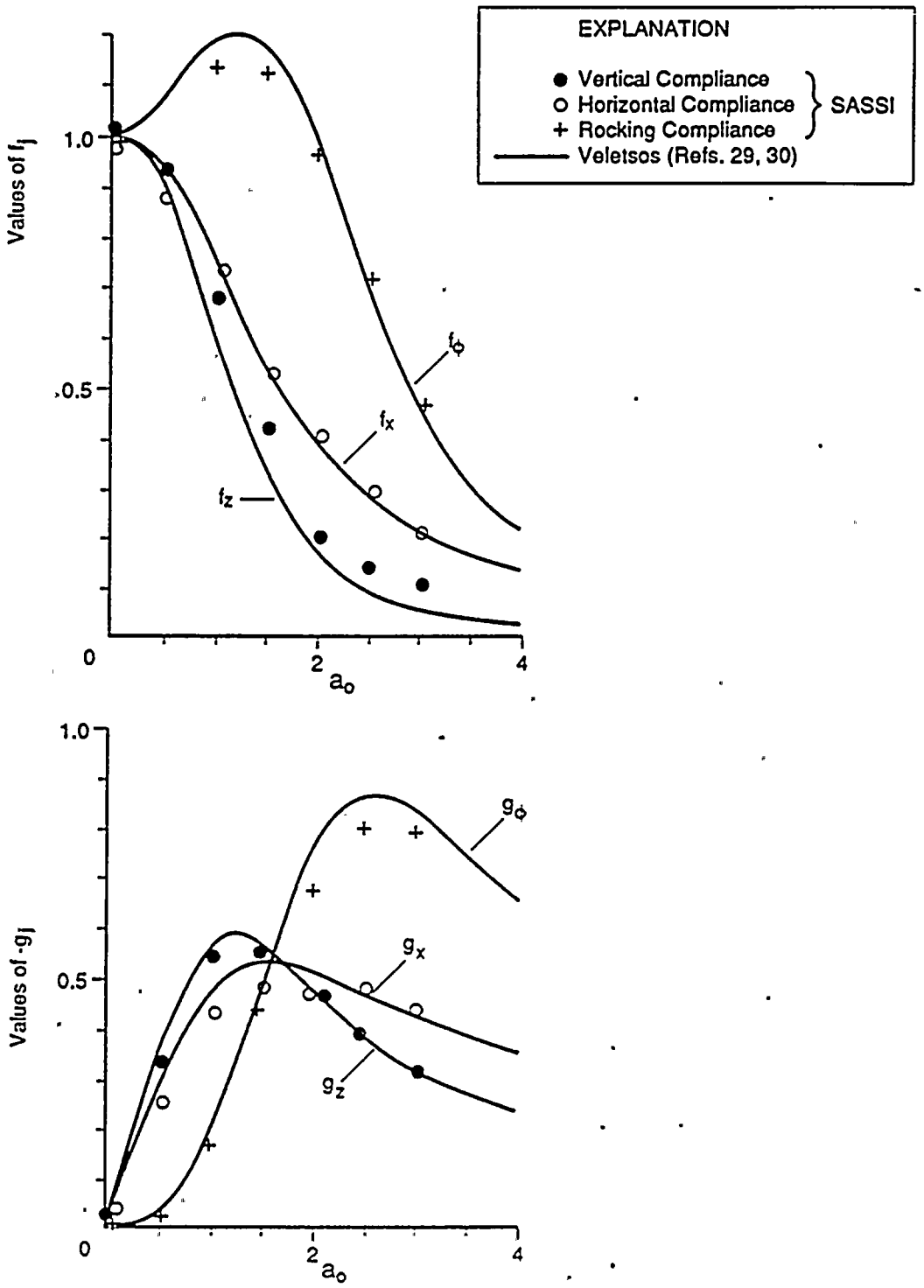

Figure 4.19-2. Vertical, Horizontal, and Rocking Compliance

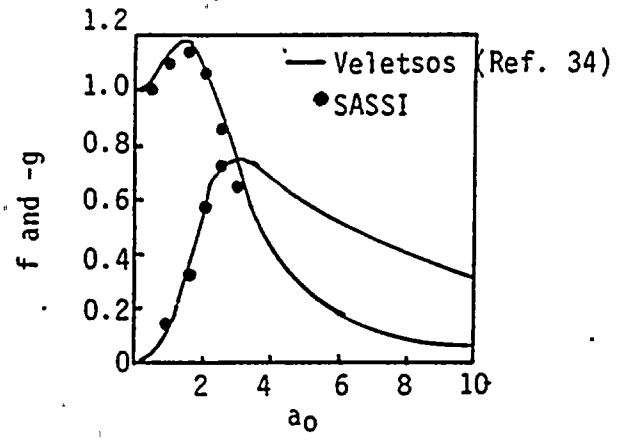

Figure 4.19-3. Torsional Compliance Functions

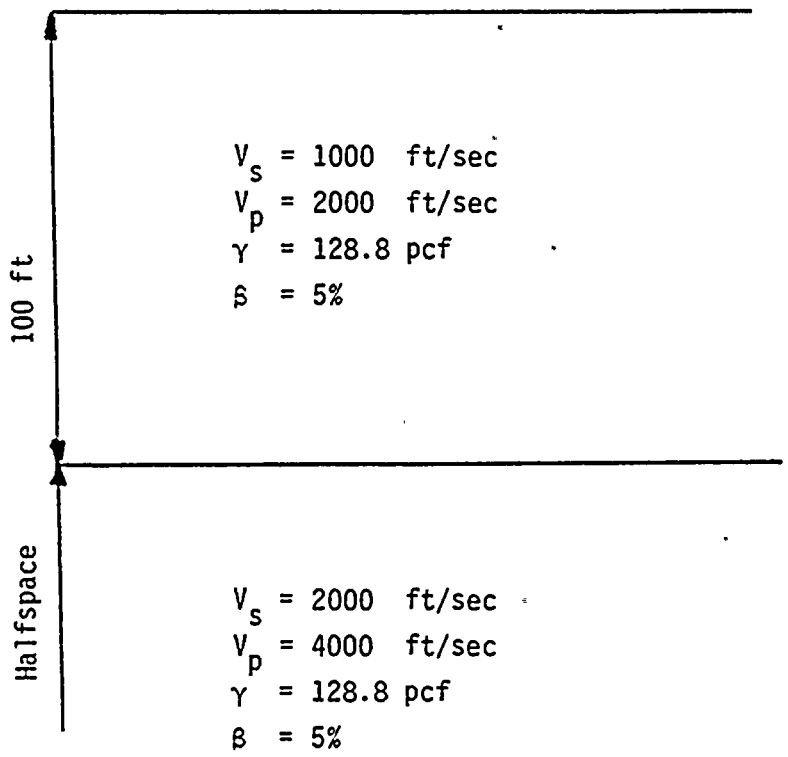

Figure 4.20-1. Free-Field Soil Layered Systems

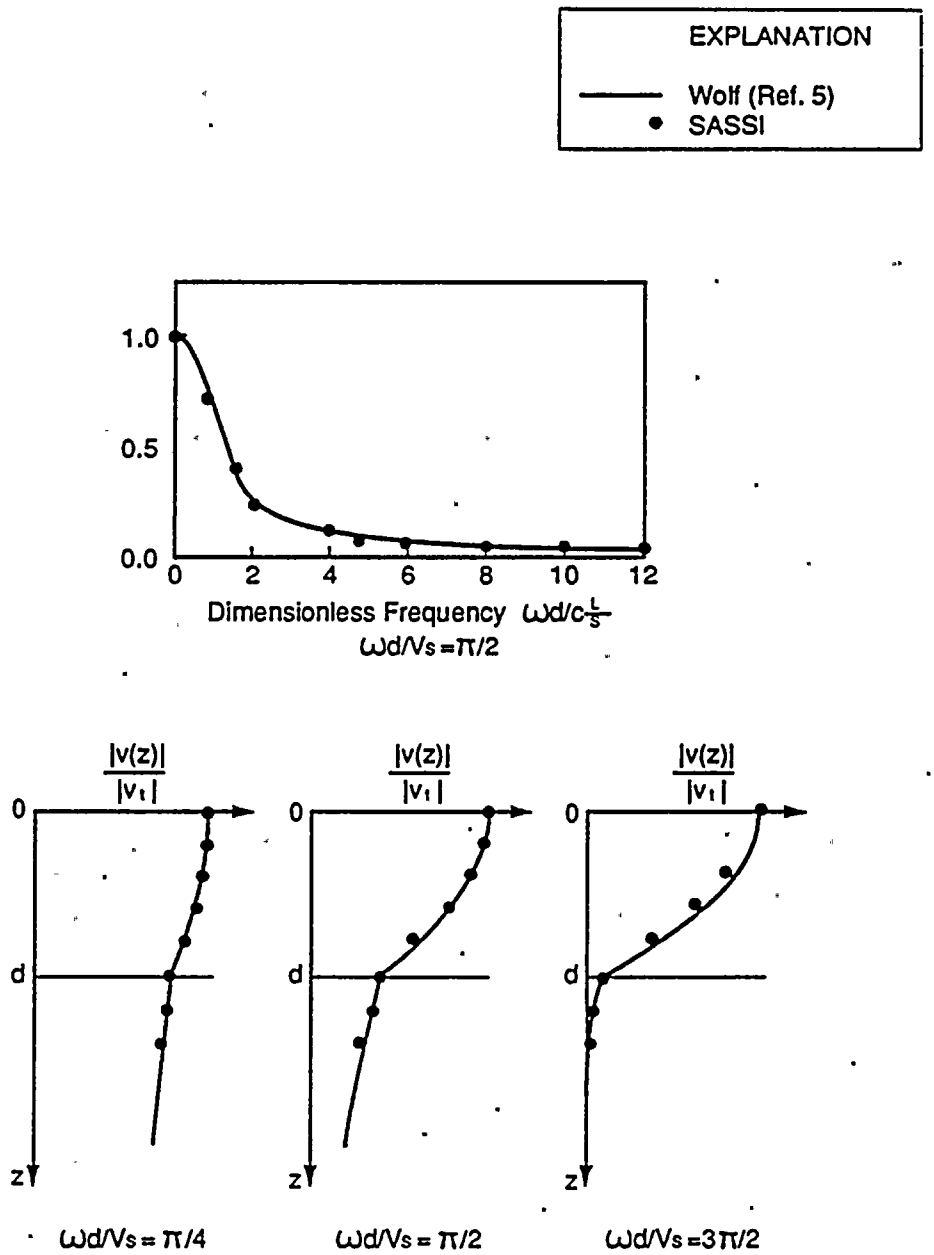

Figure 4.20-2. Love Wave Results

5. CONCLUSIONS

Based on the comparisons of SASSI analysis results with the benchmark solutions for each of the 20 validation test problems with test cases described in this report, it is concluded that the SASSI analysis capabilities as identified in tables in Section 3.2 have been validated. Thus the program is considered valid for applications to SSI analysis involving those analysis capabilities tested in this validation report.

6. REFERENCES

1. Lysmer, J., Tabatabaie-Raissi, M., Tajirian, F., Vahdani, S., and Ostadan, F.,."SASSI - A System for Analysis of Soil-Structure Interaction," Report No. UCB/GT/81-02, Geotechnical Engineering, University of California, Berkeley, CA, April 1981.

2. Timoshenko, S., Young, D. H., Weaver, W., "Vibration Problems in Engineering, "4th Edition, John Wiley & Sons, 1974.

3. Meirovitch, L., "Analytical Methods in Vibrations," The McMillan Company, 1967.

4. Schnabel, P. B., Lysmer, J. and Seed, H. B., "SHAKE - A Computer Program for Earthquake Response Analysis of Horizontally Layered Sites," Report No. EERC 72-12, Earthquake Engineering Research Center, University of California, Berkeley, CA, 1972.

5. Wolf, J. P., and Obernhuber, P., "Free-Field Response from Inclined SH-Waves and Love-Waves," Earthquake Engineering and Structural Dynamics," Vol. 10, pp. 823-845, 1982.

6. Luco, J. E., "Impedance Functions for a Rigid Foundation on a Layered Medium," Nuclear Engineering and Design, 31, 204-217, 1974.

7. Gazetas, G. and Roesset, J. M., "Vertical Vibration of Machine Foundation," Journal of the Geotechnical Engineering Division, ASCE, Vol. 105, No. GT12, December 1979.

8. Iguchi, M. and Luco, J. E., "Dynamic Response of Flexible Rectangular Foundations on an Elastic Halfspace," Journal of Earthquake Engineering and Structural Dynamics, 1981, Vol. 9, pp. 239-249.

9. Veletsos, A. S. and Tang, Y., "Vertical Vibration of Ring Foundations," Structural Report at Rice, Report No. 32, Dept. of Civil Engineering, Rice University, Houston, Texas, July 1985.

10. Whittaker, W. L., Christiano, P., "Dynamic Response of Plate on Elastic Halfspace," Journal of Engineering Mechanics Division, Vol. 108, No. EM1, pp. 133-154, February 1982.

11. Wong, H. L. and Luco, J. E., "Dynamic Interaction Between Rigid Foundations in a Layered Halfspace." Soil Dynamics and Earthquake Engineering, Vol. 5, No. 3, 1986.

12. Wong, H. L. and Luco, J. E., "Dynamic Response of Rectangular Foundations to Obliquely Incident Seismic Waves," Journal of Earthquake Engineering and Structural Dynamics, Vol. 6, pp. 3-16, 1978.

13. Wong, H. L. and Luco, J. E., "Tables of Impedance Functions and Input Motions for Rectangular Foundations," Report No. CE78-15, Dept. of Applied Mechanics and Engineering Science, University of California, San Diego, 1978.

14. Day, S. M., "Finite Element Analysis of Seismic Scattering Problem," Ph. D. Dissertation, University of California, San Diego, 1977.

15. Kausel, E., Whitman, R. V., Morray, J. P., Elsabee, F., "The Spring Method for Embedded Foundations," Nuclear Engineering and Design 48, pp. 377-392, 1978.

16. Dominguez, J., Roesset, J. M., "Response of Embedded Foundations to Travelling Waves," Publication No. R78-24, M.I.T., Dept. of Civil Engineering, Constructed Facilities Div., Cambridge, Massachusetts, 1978.

17. Iguchi, M., "Seismic Response of Cylindrical Embedded Foundations to Rayleigh Wave," Proc. of 6th Japan Earthquake Engineering Symposium, pp. 1729-1736, 1982.

18. Lysmer, J., "Vertical Motion of Rigid Footings," U.S. Army Engineer Waterways Experiment Station, Corps of Engineers, Vicksburg, Mississippi, 1965.

19. Tanaka, H., Ohta, T., Uchiyama, S., "Experimental and Analytical Studies of a Deeply Embedded Reactor Building Model Considering Soil-Structure Interaction (Part II)," 6th SMiRT Conference, Paris, France, 1981.

20. BC-TOP-4A, "Seismic Analysis of Structures and Equipment for Nuclear Power Plants," Rev. 3, November 1974, Bechtel Power Corporation, San Francisco, California.

21. Luco, J. E., "Vibration of a Rigid Disc on a Layered Visco-Elastic Medium," Nuclear Engineering and Design 36, pp. 325-340, 1976.

22. Computer Program CE917 (Version B5-6), Modal Analysis, Bechtel Power Corporation, San Francisco, California.

23. Computer Program CE933 (FASS), (Version A1-1), Fourier Analysis of Soil-Structure System, Bechtel Power Corporation, San Francisco, California.

24. Seed, H. B. and Lysmer, J., "Analysis of Soil-Structure Interaction Effects During Earthquakes for the Diablo Canyon Nuclear Power Station," a report submitted to Pacific Gas & Electric Company, 1978.

25. Computer Program CLASSIF: Validation Report Prepared for PG&E by Bechtel Power Corporation, San Francisco, CA, June 1988.

26. Lysmer, J., Udaka T., Chan-Feng, T. and Seed, H. B., "FLUSH - A Computer Program for Approximate 3-D Analysis of Soil-Structure Interaction Problems, "EERC Report No. 75-30, University of California, Berkeley, November 1975.

27. Dominguez, J., "Dynamic Stiffness of Rectangular Foundations," MIT Research Report R78-20, August, 1978.

28. Luco, J. E., and R. A. Westmann, "Dynamic Response of a Rigid Footing Bonded to an Elastic Halfspace," ASME, Journal of Applied Mechanics, June, 1972.

29. Veletsos, A. S., and Y. T. Wei, "Lateral and Rocking Vibration of Footings," ASCE, Journal of Soil Mechanics and Foundations Divisions, September, 1971.

30. Veletsos, A. S., and B. Verbic, "Basic Response Functions for Elastic Foundations," ASCE, Journal of the Engineering Mechanics Division, April, 1974.

31. Computer Program CE928 (DATAN), Probabilistic Data Analysis, Bechtel Power Corporation, San Francisco, California.

32. Roark, R. J., Young, W. C. (1982), "Formulas for Stress and Strain," Fifth Edition, McGrow Hill.

33. Computer Program SASSI, Theoretical Manual, Prepared for PG&E as apart of DCPP-LTSP-SSI Study, Bechtel Power Corp., San Francisco, CA, June 1988.

34. Veletsos, A. S., and Nair, V.V.D., "Torsional Vibration of Viscoelastic Foundation," ASCE, Journal Geotechnical Engineering, Vol. 100, No. GT3, March 1974.